

Exploitation of a novel heterologous expression system for characterisation of fungal secondary metabolites

Elena Geib

M.Sc. (Chemical Biology), Friedrich Schiller University Jena, 2014

B.Sc. (Biochemistry), Friedrich Schiller University Jena, 2011

Thesis submitted to the School of Life Sciences, University of Nottingham, for
the degree of Doctor of Philosophy.

May 2018

Oh what a thing to do
And it was all yellow

Table of contents

Table of contents	III
Abstract	1
Introduction	4
Fungal secondary metabolism.....	5
Fungal polyketide synthases.....	6
Non-ribosomal peptide synthetases.....	7
Terpene synthases and DMATs	9
Hybrid enzymes.....	10
NRPS-like enzymes.....	11
Regulation of secondary metabolism	13
Global regulators	13
Gene cluster specific transcription factors	14
Intra- and inter-species communication	15
Awakening silent gene cluster.....	17
Fungal expression systems for secondary metabolites.....	19
Selection of the heterologous host	19
Promoter selection for heterologous expression	21
Influencing production rates.....	22
Introduction of foreign genes and gene clusters.....	23
Genus <i>Aspergillus</i>	25
Secondary metabolites from <i>Aspergillus terreus</i>	26
Aims of this study	28
Publications	31
Terrein biosynthesis in <i>Aspergillus terreus</i> and its impact on phytotoxicity.....	32
A new high-performance heterologous fungal expression system based on regulatory elements from the <i>Aspergillus terreus</i> terrein gene cluster	33
A non-canonical melanin biosynthesis pathway protects <i>Aspergillus terreus</i> conidia from environmental stress	34

Comment on: "Melanisation of <i>Aspergillus terreus</i> - Is Butyrolactone I Involved in the Regulation of Both DOPA and DHN Types of Pigments in Submerged Culture? Microorganisms 2017, 5, 22"	35
ATNT: an enhanced system for expression of polycistronic secondary metabolite gene clusters in <i>Aspergillus niger</i>	36
Hybrid <i>in silico/in vitro</i> target fishing to assign function to “orphan” compounds of food origin - the case of the fungal metabolite atromentin.....	37
Cross-chemistry leads to product diversity from atromentin synthetases in aspergilli from section <i>Nigri</i>	38
Genomic and metabolic diversity in <i>Aspergillus</i> section <i>Terrei</i>	39
Recombinant expression and characterisation of NRPS-like enzymes from <i>Aspergillus</i> species section <i>Terrei</i>	40
Methodology	41
<i>In vitro</i> recombination	41
Heterologous expression in <i>A. niger</i> and <i>A. oryzae</i> and use of a TetOn system.....	42
URA-blaster and self-splicing viral peptides	42
Purification of proteins and <i>in vitro</i> metabolite production	43
Extraction and purification of secondary metabolites	44
Discussion	46
General achievements	46
Non-reducing (NR)-PKS of SAT-KS-AT-PT-ACP-ACP-TE type in aspergilli	46
Elucidation of terrein biosynthesis in <i>A. terreus</i>	47
Function of terrein	49
Utilisation of TerR to drive heterologous gene expression in <i>A. niger</i>	50
Construction of a TerR-based expression system	50
Successful application of the heterologous expression system in natural product research	51
Asp-Melanin: a novel type of melanin produced by <i>A. terreus</i>	52
Identification of genes involved in melanin production in <i>A. terreus</i>	52
Asp- Melanin - A novel type of melanin?	53
Melanin as virulence determinant	54
Distribution of Aps-Melanin in aspergilli from section <i>Terrei</i>	55

Cross-Chemistry in heterologous secondary metabolite production.....	56
Aspergilli as heterologous hosts.....	56
Cross-chemistry during atromentin production and general implications	57
Characterisation of NRPS-like enzymes from aspergilli section <i>Terrei</i>	59
Refinement of the TerR/ <i>PterA</i> expression system toolbox	61
Strain refinement	61
Extended toolbox of plasmids for fast and easy generation of expression constructs	64
Identification of biological targets of fungal secondary metabolites	65
Summary and outlook	66
References	69
Conference contributions	82
Awards	83
Acknowledgement.....	84

Abstract

Aspergillus species have a great impact on economy and human health. These filamentous ascomycetes are known to cause food and feed spoilage and can act as pathogens of plants and humans. Besides these detrimental effects, several *Aspergillus* species have been exploited for food production and as producers of bioactive metabolites, organic acids and proteins. The study presented here focusses on *Aspergillus terreus*, which combines most of the features described above. *A. terreus* is used for production of the primary metabolite itaconic acid and the natural product lovastatin. It has been described as cause of disease on potato plants and is an emerging pathogen of humans. Investigation of the interaction of *A. terreus* with immune cells showed that acidification of phagolysosomes in macrophages is not inhibited by *A. terreus* as observed with other *Aspergillus* species. Since inhibition of acidification has been attributed to dihydroxynaphthalene (DHN)-melanin in *Aspergillus* conidia, a different type of melanin in *A. terreus* conidia was expected.

A search for the origin of the pigment in *A. terreus* conidia resulted in the serendipitous identification of the biosynthesis gene cluster responsible for the production of terrein with the polyketide synthase TerA as key biosynthetic enzyme. Further characterisation revealed that terrein production is induced under environmental conditions like those found in the rhizosphere. Combined with its biological activities, terrein can be assumed to increase the fitness of *A. terreus* in the environment. Terrein is produced in large quantities and production depends on the activity of the transcriptional regulator TerR. Binding sites for TerR were found in all promoter regions of the terrein biosynthesis gene cluster, which led to the generation of heterologous expression systems in *Aspergillus niger* and *Aspergillus oryzae* using genetic elements from the *A. terreus* terrein biosynthesis gene cluster. Expression platform strains were generated that contained the *terR* gene either under a sugar- or doxycycline-inducible promoter. Then a gene of interest cloned under control of the *terA* promoter is highly transcribed by binding of TerR. Thereby, the doxycycline-dependent TetOn-*terR* system provides fine-tunable gene expression, which makes it suitable for the production of metabolites toxic to the producer. Furthermore, the use of viral self-splicing peptide sequences was successfully used to express fungal secondary metabolite biosynthesis genes from a polycistronic messenger. Therefore, the heterologous expression systems were subsequently exploited to study secondary metabolism in *A. terreus* and related species.

This system essentially contributed to the identification of the true origin of the pigment in *A. terreus* conidia. This new type of melanin called Asp-melanin derives from the metabolite aspulvinone E that is produced by a non-ribosomal peptide synthetase- (NRPS)-like enzyme and is oxidised and activated for polymerisation by a tyrosinase. The pathway was successfully reconstituted in the heterologous expression system and, furthermore, under *in vitro* conditions. This Asp-melanin protects conidia from UV-radiation and reduces the attraction of soil amoeba,

resulting in reduced phagocytosis rates. Subsequent studies revealed that Asp-melanin is common to species from section *Terrei* and is a discriminator from other *Aspergillus* sections. However, species less closely related to *A. terreus* show either no pigment biosynthesis pathway, a combination of the DHN-melanin and Asp-melanin pathway or a DHN-melanin pathway that has lost its transcriptional activation. Therefore, the lack of a functional DHN-melanin pathway accompanied by the evolution of the Asp-melanin pathway appears to describe a specific environmental adaptation of species from *Terrei*.

The discovery of the contribution of an NRPS-like enzyme to pigment formation in *A. terreus* resulted in further interest in this class of enzymes. NRPS-like enzymes with a domain structure of adenylation, thiolation and thioesterase domain generally use two identical aromatic α -keto acids as substrates that get condensed under the formation of different interconnecting core structures such as bis-indolylquinones, terphenylquinones, dioxolanones or furanones with different substitution patterns. While it is known that core structure formation is specifically catalysed by the thioesterase domain, product-predictive sequence patterns had not been identified. Studies were undertaken to convert a furanone forming aspulvinone E synthetase into a quinone forming atromentin synthetase but approaches by site-directed mutagenesis failed. This indicated that the exchange of individual amino acids is not sufficient to re-direct the chemistry of a thioesterase domain. Domain-swapping experiments successfully converted an aspulvinone E synthetase into an atromentin synthetase, but only when the donor thioesterase domain derived from a phylogenetic closely related species. The reason for this was later identified by a detailed phylogenetic analysis of atromentin synthetases from basidio- and ascomycetes which showed that the phylogenetic origin of a species results in greater sequence differences than caused by differences in the chemistry of the thioesterase domain of an NRPS-like enzyme. Therefore, it can be assumed that a prototype of an NRPS-like enzyme may have been present in a common ancestor of basidio- and ascomycetes, but evolution of NRPS-like enzymes forming a specific metabolite occurred independent in the two fungal lineages.

Unexpectedly, expression of NRPS-like enzymes producing quinone core structures resulted in different metabolites when expressed in *A. niger* compared to *A. oryzae*. Detailed analyses on the expression of atromentin synthetases in *A. niger* revealed that the formation of the quinone structure of atromentin is re-directed towards the formation of atrofuranic acid with a furanic acid core. Further analyses showed that this cross-chemistry enforced by the physiology of the producer is not limited to *A. niger*, but also observed in the black fungus *Aspergillus brasiliensis* from section *Nigri* that contains an intrinsic atromentin/atrofuranic acid synthetase. As this cross-chemistry seems to apply to all quinone core structures that were attempted to be produced in *A. niger*, host physiology may significantly influence product formation. While this broadens the spectrum of metabolites that can be obtained from NRPS-like enzymes, it may be recommended to use at least two different expression platforms with different physiology

when investigating the metabolites produced from previously uncharacterised secondary metabolite producing enzymes.

Further genome analyses from *Aspergillus* species from section *Terrei* revealed that a large number of NRPS-like enzymes with a C-terminal thioesterase domain is present in this section. Therefore, heterologous expression systems were used to obtain insights into the spectrum of metabolites produced in this section. NRPS-like enzymes were grouped into families and individual members selected for heterologous gene expression and product analysis. These analyses confirmed the broad spectrum of NRPS-like-derived metabolites in this section, but also revealed that attributing individual enzymes to specific families and to define structure-predicting sequences in the thioesterase domain requires the characterisation of additional enzymes, especially of those from outside of the genus *Aspergillus*. However, this study identified a putative phenylbutyrolactone IIa and a polyporic acid synthetase. Both enzymes had not previously been described from ascomycetes. It will be interesting to see whether phenylbutyrolactone IIa has similar quorum sensing effects on the producer *Aspergillus ambiguus* as observed for butyrolactone I on *A. terreus*. Furthermore, polyporic acid, a metabolite related to atromentin, has previously only been known from basidiomycetes. This study indicates that polyporic acid might also be produced by ascomycetes and provides the first example of a putative polyporic acid synthetase from any fungal source.

Finally, it was of interest to obtain ideas on how these secondary metabolites could be further exploited. Therefore, an *in silico* target fishing approach was tested using atromentin as a model compound. This *in silico* modelling proposed a weak estrogenic activity on human estrogen receptors and a strong inhibitory function on 17- β -hydroxysteroid dehydrogenase as potential targets. Subsequent *in vitro* experiments were able to confirm the estrogenic activity of atromentin, which indicates that an *in silico* target fishing approach accompanied with *in vitro* experiments is suitable for target prediction and further exploitation of metabolites deriving from NRPS-like enzymes.

Introduction

Fungi have contributed significantly to shaping life on earth. Phylogenetic analyses indicate that fungi evolved from a common eukaryotic ancestor a billion years ago (Doolittle *et al.*, 1996; Berbee, James and Strullu-Derrien, 2017). Contradictory, recently discovered fossils suggest that fungi have been present for more than 2.4 billion years and have made their first appearance during the Great Oxidation Event (Bengtson *et al.*, 2017). Whereas the exact timing of fungal evolution is still a matter of scientific debate, one fact is indisputable: Fungi have been successful ever since. They evolved quickly and can be isolated from nearly all environmental niches. Fungi such as the Glomeromycetes are assumed to have allowed plants to colonise land by forming a symbiotic interaction with plant roots, the so-called arbuscular mycorrhiza (Bonfante and Requena, 2011). In this interaction the fungal partner delivers inorganic compounds such as phosphorus and nitrogen sources to the plant, whereby the plant partner provides carbohydrates from photosynthesis and CO₂ fixation (van der Heijden *et al.*, 2015). Furthermore, fungi are important saprophytes in soil decaying dead organic matter (Benocci *et al.*, 2017), which is essential for the carbon flux in the environment.

While fungi supported the evolution of foliar plants, some fungi specialised as plant pathogens, causing severe pre- and post-harvest losses of crops (Dean *et al.*, 2012). Acting as a successful pathogen requires the escape from the plant immune defence, the ability to penetrate plant tissues and the successful acquisition of nutrients from the host. For this purpose, fungi adopted and evolved a diverse set of secondary metabolites. These natural products may modulate the plant immune response as shown for jasmonic acid produced by *Fusarium oxysporum* (Miersch, Bohlmann and Wasternack, 1999), support epithelial penetration such as the DHN-melanin in appressoria of *Magnaporthe grisea* (Thines, Anke and Weber, 2004) or foster nutrient supply by causing plant necrosis such as phenguignaric acid from *Guignardia bidwellii* (Molitor *et al.*, 2012). Furthermore, besides an obvious contribution to pathogenicity, several mycotoxins such as patulin, deoxynivalenol or aflatoxins are produced by fungal plant pathogens that are responsible for enormous post-harvest losses of crops (Morales *et al.*, 2007; Pusztahelyi, Holb and Pócsi, 2015).

Some fungi also developed strategies to successfully infect and colonise humans such as *Cryptococcus neoformans*, *Candida albicans*, *Pneumocystis jirovecii* or *Aspergillus fumigatus* to mention only a few (May *et al.*, 2016; Mayer, Wilson and Hube, 2013; Köhler, Casadevall and Perfect, 2014). For the filamentous fungal pathogens, it has been shown that secondary metabolites play an important role in pathogenesis such as gliotoxin from *A. fumigatus* that has toxic effects on phagocytic cells such as macrophages and neutrophilic granulocytes (Scharf, Heinekamp and Brakhage, 2014).

While this brief summary may give the impression that secondary metabolites play a crucial role in chemical warfare in nature, there are also several examples of fungal natural products exploited in medicine with beneficial effects for human life. One of the best-known examples is the antibiotic penicillin, which was discovered about 100 years ago. Its use in treatment of bacterial infections has saved millions of lives since (Bud, 2007). Other drugs include immunomodulatory compounds such as cyclosporin (Dittmann *et al.*, 1994) or the cholesterol lowering drug lovastatin and its analogues (Huang *et al.*, 2017).

In fact, for a long time secondary metabolites were the most important source for new pharmaceuticals. Even today a significant number of newly launched drugs are natural products or derived thereof (Butler, 2004). Nature was by far more inventive in evolving new lead structures over the millions of years than chemists could have ever been in the last hundred years. Considering the number of fungal natural products discovered so far and the potential encoded in fungal genomes, which yet needs to be fully explored, it can be assumed that fungi are treasure chests for the discovery of a multitude of novel drugs with promising biological activities. In light of evolution of multi-drug resistant bacteria or the increasing incidences of cancer, new therapeutics are vastly needed.

The great variety of natural products derives from a set of key biosynthetic enzymes that use a surprisingly limited set of different substrates for biosynthesis of the metabolite core structure, which frequently gets modified by additional enzymes that may be arranged on genomic level in a biosynthetic gene cluster. Core structures of secondary metabolites are generally formed by key biosynthetic enzymes that belong to the groups of polyketide synthases, non-ribosomal peptide synthetase, terpene synthases, non-ribosomal peptides synthetase-like enzymes or combinations thereof. A short introduction on these different classes of enzymes will be given in subsequent sections.

Fungal secondary metabolism

Secondary metabolites (SM) or natural products are generally low molecular weight substances produced by plants or microbes, like bacteria or fungi. They are not directly involved in energy and carbon metabolism, developmental or reproductive processes. Therefore, secondary metabolites are not necessary for survival and growth under laboratory conditions but provide the producing species with an evolutionary advantage in its natural habitat.

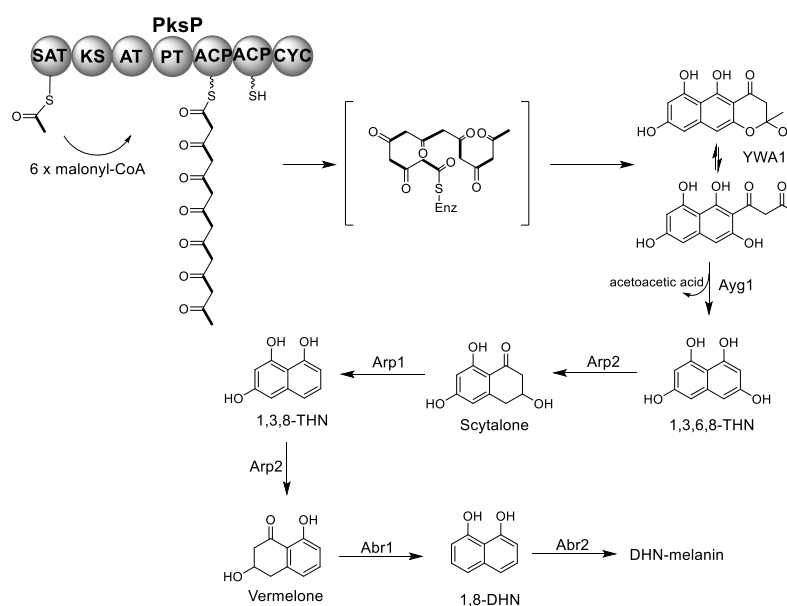
The systematic investigation of fungal natural products began as early as 1923 by Harold Raistrick (Raistrick, 1950), but research in this field was widely neglected before the discovery and, most importantly, the utilisation of penicillin by the middle of the 1940s. This resulted in a particular interest on the discovery of novel fungal SMs by pharmaceutical industries. However, at that early time screenings were mainly based on classical approaches of bioactivity-guided isolation of natural products and elucidation of structure and function

of the most abundant small metabolites. Since then, research on secondary metabolites evolved remarkably. While it may already be difficult to isolate a specific compound, and elucidate its structure, it is even more challenging to understand the underlying mechanisms of its biosynthesis. This difficulty was at least partially relieved with sequencing of the first fungal genomes in the late 1990s, which contributed to the knowledge on the molecular machineries involved in the biosynthesis of natural products.

Interestingly, although fungal secondary metabolites possess extremely versatile structures, their building blocks are limited and mainly consist of acetyl-CoA (respectively malonyl-CoA), amino acids and/or isoprene units. Consequently, one approach to classify SMs is either by characterising their building blocks or by identifying the key enzymes producing a metabolite's core scaffold.

Fungal polyketide synthases

Polyketide synthases (PKS) generally use acetyl-CoA or a short-chain fatty acid as starter and elongate the carbon chain by using malonyl-CoA extender units that undergo a decarboxylative Claisen condensation to produce polyketides (Hertweck, 2009). Malonyl-CoA is formed by the carboxylation of acetyl-CoA by the acetyl-CoA carboxylase. While the condensation of the starter unit and the malonyl-CoA extender unit is catalysed by a so-called ketosynthase domain (KS), a fungal PKS requires at least three additional domains: an acyl-transferase domain (AT), a product template domain (PT) and an acyl-carrier protein domain (ACP) (Scheme 1) (Helfrich, Reiter and Piel, 2014). These four domains form the minimal set of domains of a fungal non-reducing type I PKS. Optional modules for β -keto processing of the growing polyketide chain consist of ketoreductase (KR), dehydratase (DH) and enoyl-reductase (ER) domains. Furthermore, *in situ* methylation by a methyl transferase domain (MT) is possible.



Scheme 1: Example for the biosynthesis of a polyketide by an iterative, non-reducing polyketide synthase with subsequent modifications towards the final metabolite. The PKS PksP (or Alb1) from *Aspergillus fumigatus* produces the heptaketide YWA1 by elongating acetyl-CoA with 6 units of malonyl-CoA (Watanabe *et al.*, 2000). Ayl1 shortens YWA1 to the pentaketide 1,3,6,8-tetrahydroxynaphthalene (1,3,6,8-THN) (Fujii *et al.*, 2004). This is followed by successive reduction steps catalysed by Arp2 and dehydration by Arp1 and Abr1. This results in the formation of 1,8-dihydroxynaphthalene (1,8-DHN). In a final step the copper-dependent laccase Abr2 polymerises 1,8-DHN into the insoluble DHN-melanin (Pihet *et al.*, 2009). 1,3,8-THN = 1,3,8-trihydroxynaphthalene.

Even though knowledge on the biosynthetic steps of each module is increasing, the prediction of the final product of a fungal iterative type I PKS remains elusive. Due to the iterative, but not mandatory use of each module the predictions need to be based on KS or PT phylogeny (Helfrich, Reiter and Piel, 2014) and are error-prone. Two enzymes with an identical set and order of domains may form two completely distinct products.

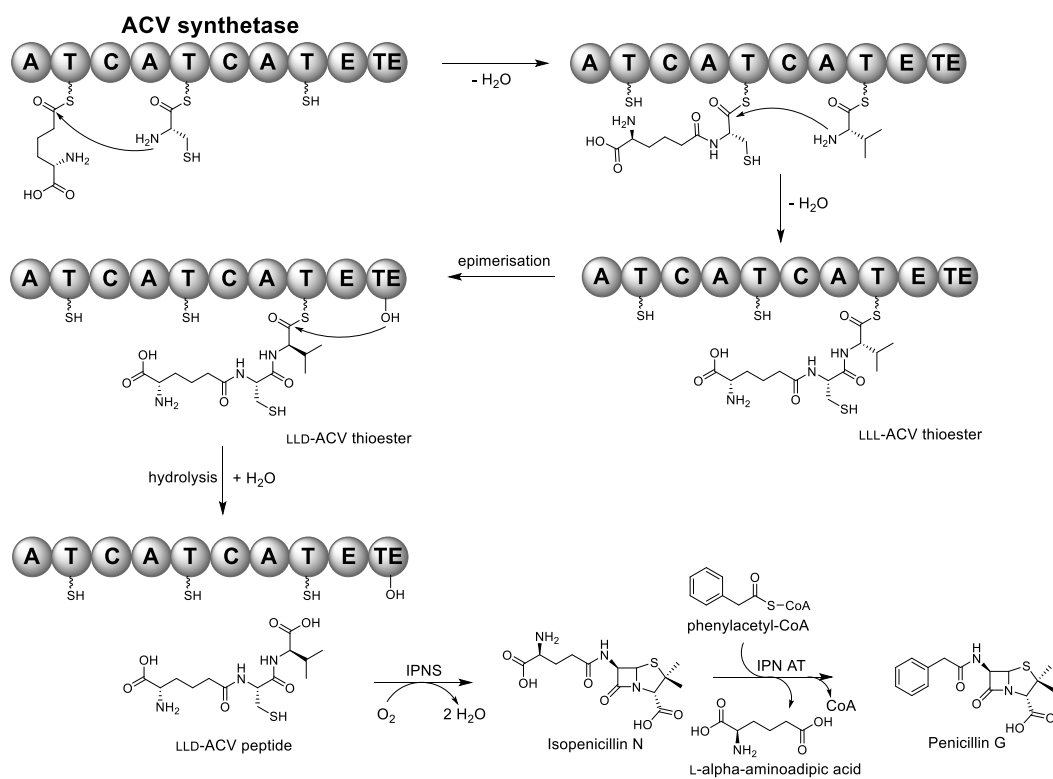
Non-ribosomal peptide synthetases

Small peptides are not necessarily formed by ribosomes, they might also be biosynthesised by non-ribosomal peptide synthetases (NRPS). Unlike ribosomes, NRPS do not need messenger RNA, but follow a collinearity rule (Süssmuth and Mainz, 2017). The order in which amino acids are incorporated is determined by the enzyme design. NRPS enzymes are arranged in modules, whereby the typical module architecture is adenylation (A), thiolation (T), and condensation (C) domain, whereby the T-domain is also called peptidyl carrier protein (PCP) (Scheme 2). Often a thioesterase (TE) domain can be found at the end of the protein (Weissman, 2015).

The selection of the substrate is carried out by the A domain. Its binding pocket has a high specificity for a certain building block. Bioinformatics tools have been developed to use sequence patterns to predict the type of amino acid or related substance that is selected (Strieker, Tanović and Marahiel, 2010; Röttig *et al.*, 2011). Remarkably, the range of known substrates is not limited to proteinogenic amino acids, but also highly modified amino acids, D-amino acids or even keto acids might be used as bio bricks (Walsh, O'Brien and Khosla, 2013). Additionally, the A-domain activates the substrate by forming an aminoacyl-AMP derivative using ATP. After activation the substrate is transferred to the neighbouring T-domain forming a covalently bound thioester.

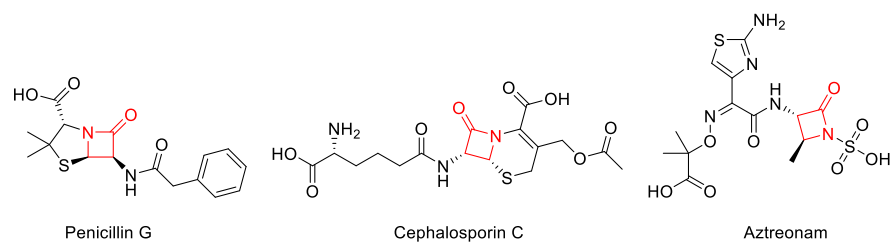
The T-domain with its flexible phosphopantethein linker shuttles the first substrate to the condensation domain, at which a new amid or ester bond is formed with the second substrate that had been selected by the second A-domain (Scheme 2). By this mechanism the growing peptide chain walks along the multi-modular NRPS until it reaches the termination module. In many cases a TE-domain catalyses the release of the nascent peptide chain by nucleophilic attack of water (hydrolysis) or an amino group (aminolysis), resulting in either linear products or macrocycles (Hur, Vickery and Burkart, 2012).

Products of NRPS range from 3 to 25 amino acids. The larger peptides are frequently obtained by dividing the biosynthetic machinery into several smaller proteins, iterative use of single modules or domains and cyclisation or coupling of identical peptide blocks.



Scheme 2: Example for a natural product biosynthetic pathway via a non-ribosomal peptide synthetase. The first step of the biosynthesis of fungal β -lactam antibiotics (penicillin and cephalosporin) is catalysed by the ACV synthetase. The first peptide bond is formed between L- α -aminoadipic acid and L-cysteine. L-valine is linked as third amino acids. The epimerisation module (E) of the NRPS works on the LLL-ACV thioester converting L-valine into its D-form. The LLD-ACV tripeptide is hydrolysed by the thioesterase domain (TE). The isopenicillin N-synthase (IPNS) mediates the oxidative cyclisation step. The isopenicillin N acyltransferase (IPN AT) subsequently exchanges L- α -aminoadipic acid with phenyl acetic acid forming penicillin G (Hamed *et al.*, 2013). A – adenylation domain, T – thiolation domain, C – condensation domain.

Several fungal NRPS products have become famous because of their biological activity and have made their way into medical applications. The best examples are β -lactam antibiotics such as cephalosporins or penicillins which are highly complex NRPS derived structures (Scheme 3). Interestingly, not only fungi but also bacteria are able to produce β -lactam structures as monobactams. In this respect, a semisynthetic version of a monobactam produced by *Chromobacterium violaceum* is marketed as aztreonam (Scheme 3) (Sykes and Bonner, 1985).



Scheme 3: Structures of fungal and bacterial β -lactam antibiotics. The β -lactam ring is highlighted in red.

Other NRPS-derived products can also be harmful to humans or depict virulence determinants during human or plant infections. Examples are the roquefortin from *Penicillium spp.*, gliotoxin from *Aspergillus fumigatus* or HC-toxin from *Cochliobolus carbonum* (Soukup, Keller and Wiemann, 2016). Furthermore, most fungal siderophores such as ferricrocin are produced via NRPS and are essential for a successful iron acquisition in the environment and during infection processes (Haas, 2014).

Terpene synthases and DMATs

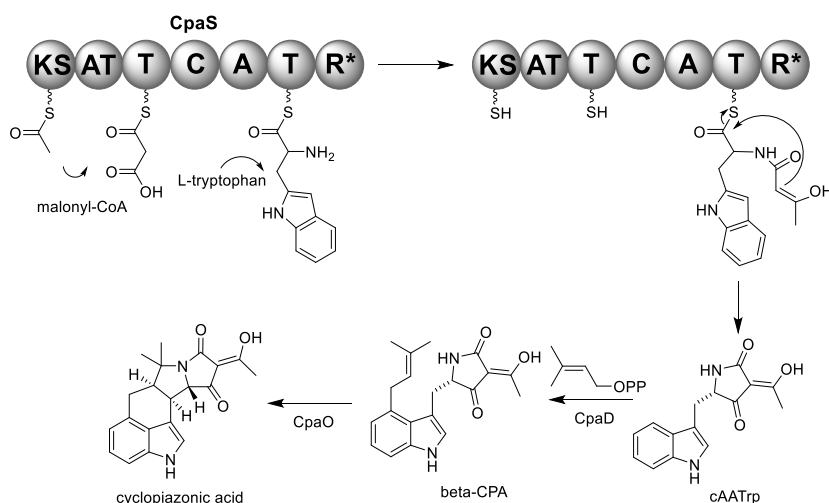
The class of terpenoids consists of terpenes, indole alkaloids and further modified terpenoids. These metabolites are produced by terpene synthases or dimethylallyltryptophan synthases (DMATs). Precursors derive from the primary metabolic mevalonate pathway: dimethylallyl pyrophosphate (DMAPP) and its isomer isopentenyl pyrophosphate. As the name implies, DMATs can transfer DMAPP to L-tryptophan to form indole alkaloids. However, some DMATs are flexible towards the aromatic acceptor compound used. Therefore, other prenylated substances might be the derived product. Furthermore, even when transferred to a tryptophan, the prenylated amino acid is often not the final product, but a precursor for further complex biosynthetic steps. In this respect, ergotamine biosynthesis starts with the condensation of tryptophan with DMAPP by a DMATs catalysed reaction. Further modifications lead to lysergic acid which is a substrate of an NRPS adding three additional amino acids. After further complex enzymatic reactions and spontaneous modifications the final product, ergotamine is released (Gerhards *et al.*, 2014). DMATs are also involved in the biosynthesis of α -cyclopiazoic acid (Scheme 4) or terrequinone A (Scheme 5). Pathways for those compounds are shown in the hybrid enzyme and NRPS-like enzyme sections, respectively.

Higher terpenes derive from oligo-isoprenyl pyrophosphate precursors, e.g. geranyl pyrophosphate or farnesyl pyrophosphate. Here, a condensation of DMAPP with one or more isopentenyl pyrophosphate units is performed. According to the precursor used, terpenes are classified into different groups: monoterpenes, which derive from geranyl pyrophosphate, sesquiterpenes, coming from farnesyl pyrophosphate and diterpenes from geranylgeranyl pyrophosphate (Schmidt-Dannert, 2015). Terpenes do not exclusively

belong to the secondary metabolism, as some primary products such as steroids (triterpenes) share the same biosynthetic origin (Keller, Turner and Bennett, 2005).

Hybrid enzymes

Megasyntases like PKS or NRPS cannot only work individually on different steps of the biosynthesis of natural products but are sometimes also found as hybrid enzymes containing domains of both types of enzymes. Therefore, these enzymes are called PKS-NRPS hybrids. Examples for fungal PKS-NRPS products are cytochalasins, pseurotin A, isoflavipucine and cyclopiazonic acid (Scheme 4). (Boettger and Hertweck, 2013; Gressler *et al.*, 2011). Often these compounds process biological activities like the disruption of actin-filaments, immunosuppression or cytotoxicity. α -Cyclopiazonic acid is a neurotoxin, inhibiting the Ca^{2+} -ATPase at a nanomolar range. It consists of a polyketide, an amino acid and an isoprenoid moiety. The unusual reductase domain at the end of the PKS-NRPS enzyme catalyses a Dieckmann cyclisation forming the tetramic acid core (Scheme 4) (Liu and Walsh, 2009).



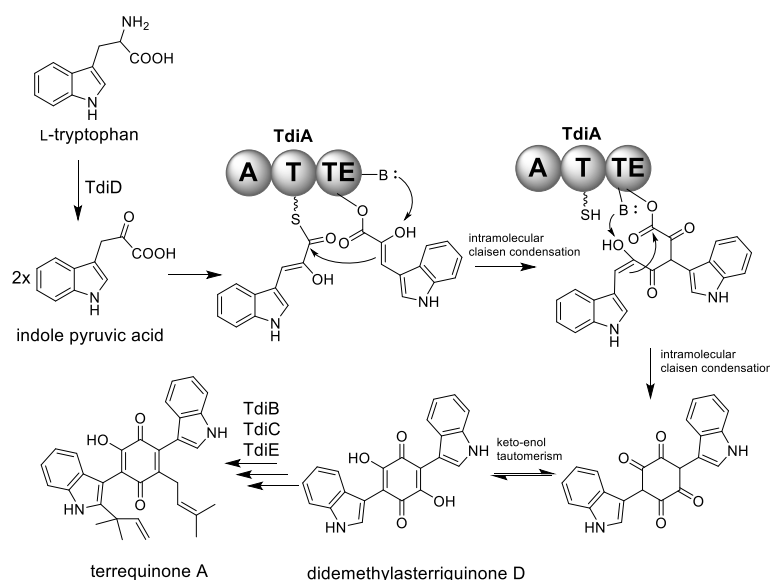
Scheme 4: Example of the biosynthesis of a PKS-NRPS hybrid product. α -Cyclopiazoic acid is produced by three enzymes. CpaS, which is a PKS-NRPS hybrid with a set of three PKS domains: KS – ketosynthase, AT – acyltransferase and T – thiolation or acyl carrier protein domain, followed by four NRPS domains: C – condensation, A – adenylation, T – thiolation and R* - a non-canonical reductase domain. The PKS unit produces an enzyme-bound acetoacetyl unit. The following A domain of the NRPS part selects L-tryptophan and a peptide bond is formed via the C domain. The R* domain finally catalyses a Dieckmann-type cyclisation and releases the cyclo-acetotacetyl-L-tryptophan (cAATrp). Regio selective prenylation is mediated by the dimethylallyltransferase CpaD yielding β -cyclopiazonic acid. Final tailoring of the metabolite is performed by the flavoprotein oxidocyclase CpaO (Liu and Walsh, 2009).

Until late 2015 it was believed that only hybrids of the PKS-NRPS type exist in the fungal world. Yun *et al.* elucidated the biosynthesis of tenuazonic acid in which the TeA synthetase 1 (TAS1) has the unusual domain structure: C-A-T-KS. It was experimentally proven that

the ketosynthase domain is essential for elongation, cyclisation and product release, characterising TAS1 as an NRPS-PKS hybrid (Yun, Motoyama and Osada, 2015).

NRPS-like enzymes

Non-ribosomal peptide synthetase-like enzymes (NRPS-likes) were ignored until a decade ago, as they had been assumed to be dysfunctional or of auxiliary function (Bok *et al.*, 2006). The domain structure of these enzymes resembles that of true NRPS enzymes with the key difference that they lack a canonical condensation domain. As a result, the corresponding genes were considered fragmented and genetic junk. Consequently, it took until 2007 for the first report of an NRPS-like enzyme that forms a product, which was characterised as terrequinone A from *Aspergillus nidulans* (Scheme 5) (Schneider *et al.*, 2007; Balibar, Howard-Jones and Walsh, 2007).

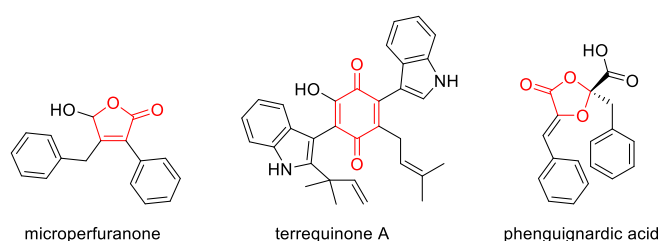


Scheme 5: Biosynthesis of a product of an NRPS-like enzyme of the A-T-TE type. The terrequinone A synthetase (TdiA) loads two molecules of L-tryptophan-derived indole pyruvic acid. Two intramolecular Claisen condensations mediated by the TE-domain release didemethylasterriquinone D (Schneider *et al.*, 2007). The intermediate is further modified by the prenyltransferase TdiB (Schneider, Weber and Hoffmeister, 2008) and the oxidoreductase TdiC. The function of TdiE remains elusive and is not strictly necessary for terrequinone A formation. However, the highest yield of terrequinone A is only produced in the presence of all three tailoring enzymes (Balibar, Howard-Jones and Walsh, 2007). A – adenylation, T – thiolation and TE - thioesterase domain.

Today, two different types of NRPS-like enzymes have been identified: type I NRPS-like enzymes that possess an adenylation (A), thiolation (T) and thioesterase (TE) (A-T-TE) domain structure, and type II NRPS-like enzymes that consist of an adenylation, thiolation and reductase (R) (A-T-R) domain structure. Especially type I NRPS-like enzymes containing a TE-domain have been in focus of recent research activities and an increasing number of metabolites deriving from these enzymes has been identified. This type of NRPS-like enzymes generally uses two molecules of the same α -ketoacid as substrate and catalyses

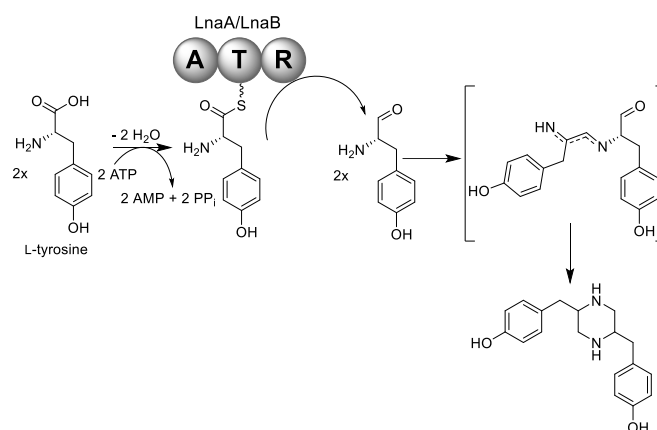
the formation of novel C-C- σ bonds. Due to the special, not yet fully understood chemistry of the thioesterase domain these NRPS-like enzymes are self-sufficient, which means they are not only able to form a product, but also able to release the metabolite without the aid of auxiliary enzymes.

The structural diversity of NRPS-like products is high, at least three distinct core structures are known to be formed: furanones, dihydroxyquinones and dioxolanones (Scheme 6). A furanone moiety is, for example, found in microperfuraneone, a natural product of *A. nidulans* (Yeh *et al.*, 2012). Terrequinone A features a quinone core (Balibar, Howard-Jones and Walsh, 2007). The aforementioned phenguignardic acid, which was first reported from *Guignardia bidwelli* (Molitor *et al.*, 2012), revealed its NRPS-like origin after the identification of the *pgnA* gene product from *A. terreus* (Sun, Guo and Wang, 2016) and features a dioxolanone core.



Scheme 6: Metabolites produced by NRPS-like enzymes. The core structures furanone, quinone and dioxolanone are highlighted in red.

In contrast to the first type of NRPS-like enzymes, enzymes of the A-T-R type cannot form novel chemical bonds, but only reduce their substrates. These enzymes can activate and reduce aryl-acids to aryl-aldehydes. This mechanism allows the terminal reduction of polyketides and seems to be used throughout the fungal kingdom but was first reported for a cryptic gene cluster of *Aspergillus terreus* (Wang, Beissner and Zhao, 2014). Besides the reduction of polyketides, NRPS-like enzymes of this type can also reduce amino acids, as shown for L-tyrosine that is reduced by LnaA/LnaB from *Aspergillus flavus* (Forseth *et al.*, 2013). The resulting amino aldehyde is highly reactive and reacts spontaneously to the dimeric structure of a piperazine (Scheme 7). In general, these A-T-R NRPS-like enzymes are hard to characterise due to the difficulty of substrate prediction and the problem that products formed are frequently highly reactive and unstable.



Scheme 7: Biosynthesis of a product formed by an NRPS-like enzyme of the A-T-R type. The NRPS-like enzymes LnaA and/ or LnaB of the reducing NRPS-like type activate L-tyrosine under energy consumption and reduce it to a reactive aldehyde. A dimeric imine is formed spontaneously or via an enzyme-bound intermediate. The NRPS-like enzyme cyclises and reduces the intermediate to the final piperazine product (Forseth *et al.*, 2013). A – adenylation domain, T – thiolation domain, R – reductase domain.

Regulation of secondary metabolism

Biosynthesis of secondary metabolites is a highly energy consuming process for the producing organism as ATP, reducing equivalents and metabolites are withdrawn from primary metabolism. Therefore, it has been assumed that secondary metabolites are produced to increase the environmental fitness of the producing organism (Spiteller, 2015b). However, to give an advantage rather than a disadvantage due to the uncontrolled waste of energy and building blocks specific regulatory mechanisms are essential. Biosynthesis of secondary metabolites can be controlled at different levels, which might be dominating or interconnected.

Global regulators

During life in the environment a fungus is challenged with a vast variety of different conditions. These can derive from the competition for nutrients with other microbes and changes in the availability of macro-nutrients such as carbon and nitrogen sources. Furthermore, micro-nutrients such as zinc or iron may become limited. To react to these changing conditions, global transcription factors orchestrate fungal metabolism including the formation of secondary metabolites.

A wide range of environmental stimuli and their responding transcription factors or protein complexes have been characterised, including AreA as a sensor of nitrogen availability, CreA as a sensor for fermentable sugar sources, PacC as a pH response element, CBC in combination with HapX as a sensor for the redox status and/or iron levels in the cells by, the velvet complex for reacting to varying light intensity and the SAGA/ADA complex that

seems to sense and regulate interactions with other microorganisms (Macheleidt *et al.*, 2016; Brakhage, 2013).

For some specific examples evidence has been provided that global transcription factors influence the formation of secondary metabolites. An example is the biosynthesis of the fruit rot toxin isoflavipucin produced by *Aspergillus terreus* that is only synthesised in the absence of glucose. CreA acts as a dominant repressor and inhibits the expression of the cluster genes even, as mentioned below, when the biosynthesis gene cluster specific transcription factor is overexpressed (Gressler *et al.*, 2011). Furthermore, the nitrogen metabolite regulators AreA and AreB in *Fusarium fujikuroi* are essential for the regulation of gibberellic acid productions, which is only produced under nitrogen starvation (Michielse *et al.*, 2014).

Gene cluster specific transcription factors

While global regulators play an important role in the regulation of secondary metabolism, the induction of their biosynthesis is by far more complex and controlled on several additional levels. Genes necessary for the biosynthesis of a fungal secondary metabolite are often clustered, which means that they are located in direct proximity and expression of genes is co-regulated. Within the boundaries of these gene clusters, not only the genes encoding for one or more of the biosynthetic key enzymes (PKS, NRPS, terpene cyclases/DMATS, NRPS-like or hybrids), but also genes for biosynthesis of building blocks and for decoration of the maturing product might be found. To assist an efficient production, genes for transporters and self-resistance conferring genes against the final secondary metabolite can be included as well (Süssmuth and Mainz, 2017). These gene cluster resemble bacterial operon structures, but each gene requires its own promoter.

For about half of the currently identified biosynthesis gene clusters a specific transcription factor has been identified that ensures the simultaneous expression of all genes within a cluster under inducing conditions (Macheleidt *et al.*, 2016). Therefore, these transcription factors are generally highly specific and have multiple binding sites in the upstream region of the associated cluster genes.

In addition, there is increasing evidence for a cross-talk between different gene clusters, in which a transcription factor encoded by one cluster can regulate gene expression of another biosynthetic gene cluster (BGC) located at a different chromosomal locus or even on a different chromosome. The first example of such a cross-talk was described for the silent *inp* BGC on chromosome II and the *afo* BGC on chromosome VIII in *A. nidulans* (Bergmann *et al.*, 2010). Both gene clusters contain a cluster-specific transcription factor, ScpR and AfoA, which are involved in controlling expression of the cluster genes. Unexpectedly, when *scpR* was overexpressed under control of the inducible *alcA* promoter, Bergmann *et al.* detected the polyketide asperfuranone as product of the *afo* gene cluster rather than the *inp* BGC

metabolite that is formed from the two NRPS enzymes within this cluster (Chiang *et al.*, 2009). These results were further supported by transcriptional analysis. Interestingly, this regulation was unilateral as AfoA only controlled its own asperfuranone cluster. Unfortunately, SrpC was not sufficient to activate all genes necessary for product formation from the *inp* BCG, which hindered the identification of the product formed by this cluster. It took another six years and serial promoter exchanges to finally link the *inp* gene cluster to fellutamide B biosynthesis (Yeh *et al.*, 2016).

As mentioned above, a well-studied example of the interaction of global and cluster-specific transcription factors is the biosynthesis of isoflavipucine/dihydroisoflavipucine by *Aspergillus terreus*. The gene cluster contains a specific transcriptional activator, which is essential for product formation. However, expression of this cluster-specific transcription factor by the glucose-inducible strong *gpdA* promoter did not lead to product formation (Gressler *et al.*, 2011). Using an elaborate, multidisciplinary approach it was finally shown that the global carbon catabolite repressor CreA overruled pathway-specific activating signals as well as the stimulatory effect mediated by the pH responsive transcription factor PacC. By choosing an alternative glucose independent promoter from arginine metabolism (*PagaA*) for activation of the cluster-specific TF the cluster was finally activated and structure and biosynthesis of isoflavipucine and dihydroflavipucine were successfully elucidated (Gressler *et al.*, 2011).

Intra- and inter-species communication

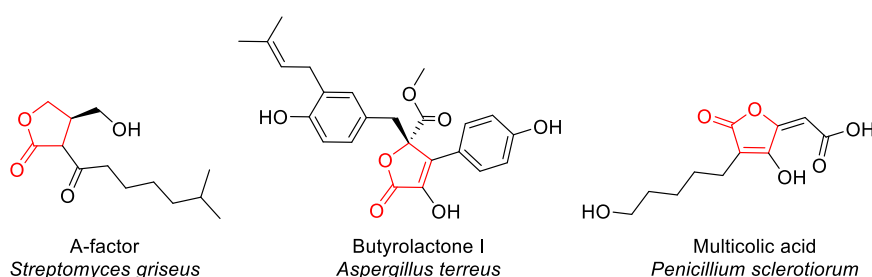
In nature fungi are often found in a complex community of microbes or in interaction with higher organisms such as plants or animals. Due to these biotic interactions, the ecological context can shape the fungal secondary metabolism. Induction of secondary metabolite biosynthesis can either result from the direct physical interaction of microorganisms or from communication by specific metabolites.

When the two soil-dwelling microorganisms *A. nidulans* and *Streptomyces hygroscopicus* are in physical contact, the fungal partner starts to produce various polyketides, including orsellinic acid and its dimer lecanoric acid (Schroeckh *et al.*, 2009). Orsellinic acid is an abundant molecule in fungal secondary metabolism and often associated with lichens (Mosbach, 1969), but despite its high abundance, the polyketide synthase involved in its biosynthesis has remained unknown. However, a co-cultivation approach of *A. nidulans* and *S. hygroscopicus* accompanied by microarray analyses eventually led to the identification of the corresponding gene locus (Schroeckh *et al.*, 2009).

In bacteria a communication mechanism called quorum sensing has been well investigated. Quorum sensing is the process of behavioural changes according to population density and relies on small diffusible metabolites. When a certain threshold in the local population density is exceeded and sensed by accumulation of the chemical signal, these changes in

behaviour can include biofilm formation, production and secretion of virulence factors or bioluminescence (Miller and Bassler, 2001). All these responses are generally a result of synchronised gene expression in bacteria. In actinomycetes γ -butyrolactones such as the A-factor have been identified as active quorum sensing molecules, coordinating differentiation and antibiotic production (Takano, 2006).

While quorum sensing has hardly been studied in fungal species, many fungi produce similar compounds known as butyrolactones, which are hypothesised to have an influence on secondary metabolite production (Scheme 8). In this respect, the industrially important ascomycete *Aspergillus terreus* produces butyrolactone I. Addition of butyrolactone I to cultures of *A. terreus* auto-stimulates its own biosynthesis and in parallel activates lovastatin production (Schimmel, Coffman and Parsons, 1998). However, the biosynthesis of bacterial and fungal butyrolactones follows completely different pathways (Kato *et al.*, 2007; Nitta *et al.*, 1983). In *Penicillium sclerotiorum* another γ -butyrolactone, multicolic acid (Scheme 8), with quorum sensing properties was reported. The addition of culture extracts containing multicolic acid and its derivatives to new cultures resulted in an increased production of the secondary metabolite sclerotiorin (Raina, Odell and Keshavarz, 2010).



Scheme 8: Structures of bacterial and fungal γ -butyrolactones. The γ -butyrolactone moiety is highlighted in red.

Probably the best studied example of fungal quorum sensing molecule is the effect of the isoprenoid farnesol on *Candida albicans*. In low cell densities and in the presence of environmental stimuli such as alkaline pH, serum albumin, elevated temperature or plastic surfaces *C. albicans* grows as filamentous hyphae. However, despite the presence of the external stimuli *C. albicans* undergoes a phenotypical switch towards its yeast form at high cell densities. This process is mediated by increasing concentrations of farnesol (Hornby *et al.*, 2001). *C. albicans* is a commensal and pathogen of humans. Biofilms on medical devices are particularly hard to treat and eradicate, due to their resistance against antimicrobials. While farnesol can inhibit the formation of biofilms (Ramage *et al.*, 2002), it was also shown to have a crucial function on mature biofilms of deep-seated infections. The addition or production of farnesol supports the dispersal of the fungus by releasing individual yeast cells (Albuquerque and Casadevall, 2012). Conversely, tyrosol triggers a filamentation of the yeast cells (Mallick and Bennett, 2013). Recently, a quorum sensing system has also been reported in *Cryptococcus neoformans* that is based on the small, diffusible peptide Qsp1

(Homer *et al.*, 2016). Tackling quorum sensing systems is one highly promising target of developing new weapons against bacterial pathogens and potentially also against fungi. However, as the quorum sensing mechanism in fungi is only partially understood, there is still the need for more systematic research to find effective molecules to fight infections.

Up to now it remains unclear if there is a common quorum sensing system in eukaryotes or if there is a general principle which can be found in several fungal species. On the one hand, the well investigated organisms *C. albicans* and *C. neoformans* do not contain genes that can be attributed to the formation of classical secondary metabolites. Therefore, these organisms may have developed specific molecules for measuring cell density. However, taking into account that γ -butyrolactones also show quorum sensing effects indicates that eukaryotic organisms have developed a wide variety of different mechanisms to measure cell density, which might have an impact on secondary metabolism.

Awakening silent gene cluster

Since the beginning of natural product chemistry and the systematic examination of fungal secondary metabolites in 1923, an unimaginable number of metabolites had been elucidated. Many of those metabolites are derivatives from the same core structure, but overall thousands of highly diverse core structures have been identified. It was always a driving force to find new compounds with interesting biological activities that can be exploited for human benefit.

One of the classical and intuitive approaches to induce secondary metabolite production is by triggering global changes of the fungal transcriptome by applying different stress factors or alternating the chemical and nutritional conditions. These effects are generally pleiotropic, and the outcome cannot be predicted and more than one biosynthetic pathway can be activated during such a procedure. Therefore, no deeper understanding or knowledge about the regulation of a specific biosynthesis gene cluster is necessary or obtained. However, the protocols are easy to scale up or can be transferred to phylogenetically distinct organism. Thus, pleiotropic approaches can be incorporated in high-throughput screening methods for drug discovery (Rutledge and Challis, 2015).

Applying different growth conditions peaked in the One Strain Many Compounds (OSMAC) theory (Bode *et al.*, 2002). One organism is cultured in a range of diverse growth media with changes in the composition of carbon or nitrogen sources and pH. Moreover, cultivation conditions such as temperature, steady or submerged culture, light or dark can be varied. By comparison of culture extracts it becomes obvious that the metabolite profile shows dramatic changes. With these efforts of mimicking certain natural triggers activating a biosynthetic pathway, researchers tried to overcome the fact that many gene cluster remain silent under laboratory conditions. As an example, for a successful mimicry, the addition of soil extract

to *Clostridium cellulolyticum* cultures resulted in the production of closthioamid, the first known secondary metabolite from a strictly anaerobic bacterium (Lincke *et al.*, 2010).

Another untargeted approach is the addition of chromatin modifiers. Small molecules classified as histone deacetylase or DNA methyltransferase inhibitors inhibit the deactivation or methylation of chromatin regions. This epigenetic perturbation can lead to the production of not yet described natural products as demonstrated for *Aspergillus niger* with the production of a novel compound called nygerone A (Henrikson *et al.*, 2009).

With the ever-growing amount of sequencing data and the establishment of protocols for fungal manipulation, another level of pleiotropic interference became possible: overexpression or silencing of global regulators. For the model species *Aspergillus* several major regulators for secondary metabolism have been described by now, for example McrA (multicluster regulator A) controls at least 10 gene cluster in *A. nidulans* (Oakley *et al.*, 2017). Even more impact has been attributed to the methyltransferase LaeA, which has been discovered by its impact on the sterigmatocystin and gliotoxin biosynthesis. After more than ten years of research multiple interaction partners of LaeA are now known. Together they form the velvet complex. Via its hub protein VeA developmental processes, secondary metabolism and virulence are interlinked (Sarikaya-Bayram *et al.*, 2015). It was shown that LaeA controls approximately 50 % of the secondary metabolite gene cluster in *Aspergillus flavus*, *Aspergillus fumigatus* and *A. nidulans* (Bok and Keller, 2004).

In the post-genomic era, it is possible to analyse fungal genomes for their potential for secondary metabolism. Several bioinformatics tools for so-called genome mining are available. Freely accessible online tools for detection and prediction are antiSMASH (antibiotics and secondary metabolite analysis shell) (Blin *et al.*, 2017) and SMURF (secondary metabolite unique regions finder) (Khaldi *et al.*, 2010). Sequence similarities are used to identify biosynthetic core genes and adjacent cluster genes. As mentioned above, approximately half of the known fungal biosynthesis gene clusters contain a cluster specific transcription factor. This fact is used for promoter-based prediction of biosynthesis gene cluster by the CASSIS suite (Wolf *et al.*, 2016). With this information a much more concise and targeted approach is possible.

Cluster-specific transcription factors are one key target for activating silent gene clusters. Replacement of the promoter of the transcription factor by a readily inducible or constitutively active promoter can result in activation of the complete biosynthesis gene cluster. However, as discussed in the cluster-specific transcription factor section, global transcription factors might overrule even this method, as shown for isoflavipucic acid biosynthesis (Gressler *et al.*, 2011).

If the cluster activation by overproduction of a cluster specific transcription factor fails or the cluster even does not encode or possess a specific transcription factor, a promoter

exchange of every gene belonging to a putative cluster is another strategy. Yeh *et al.* demonstrated the applicability of this approach by serial promoter exchange of six cluster genes. Two pairs of genes shared one bidirectional promoter each, so that a total of four transformation steps and marker recycling phases were necessary. Finally, fellutamide B, a potent protease inhibitor, could be identified (Yeh *et al.*, 2016). Interestingly, a cluster specific regulator called ScpR was identified and overexpressed in a study undertaken by the groups of Brakhage and Hertweck (Bergmann *et al.*, 2010). In this case the overexpression of *scpR* only activated some, but not all cluster genes. As a result, no natural product was identified, validating the method of individual promoter exchanges as complicated and time consuming but valuable.

However, prediction of biosynthetic genes, complete clusters and their boundaries opened a new avenue for highly targeted heterologous approaches, e.g. heterologous expression of core biosynthetic genes or whole clusters. Especially for fungal species which are difficult to cultivate under standard conditions, heterologous expression might be the route of choice for secondary metabolite discovery.

Fungal expression systems for secondary metabolites

To link a secondary metabolite core gene with the production of a certain metabolite and to exclude the support by additional enzymes or cross-talks between gene clusters, a heterologous expression approach is a useful technique. Hereby, a gene from a donor organism is placed under the control of a promoter of choice, preferably a constitutively active or inducible promoter. It was shown that the addition of a terminator sequence, artificial or native, may increase the production rates as it inhibits the read through into adjacent genes (Curran *et al.*, 2015). Often this construct is assembled as a so-called expression plasmid and propagated in *E. coli*. Alternatively, a PCR-based approach for assembly of expression cassettes is possible. These expression constructs are then transferred into a suitable host strain.

Selection of the heterologous host

The choice of the heterologous host is of paramount importance. Bacterial expression hosts are difficult to use for expression of eukaryotic genes as some biosynthetic enzymes such as PKS, NRPS or NRPS-like enzymes need activation to their phosphopantetheinylated *holo* form. In addition, cytochrome P450 oxidoreductases need matching redox partners. Even more, as eukaryotic genes are frequently interrupted by intron sequences, only cDNA sequences can be used for cloning. In case the inducing conditions are unknown, cDNA needs to be generated as synthetic genes. To a certain degree strain optimisation is possible and there are examples in which *E. coli* was successfully used to produce fungal natural products like 6-methylsalicylic acid from *Penicillium patulum* (Kealey *et al.*, 1998).

A very basic fungal host for heterologous expression of SM genes is *Saccharomyces cerevisiae*. This yeast was used to produce valuable plant-derived natural products such as artemisinin (Ro *et al.*, 2006) or opioids (Galanie *et al.*, 2015) and a range of other fungal secondary metabolites. The great advantage of yeast is the highly developed genetic tool box and its fast growth rate. However, even though yeast supports some post-translationally modifications of proteins, not all functions required for activation of secondary metabolite biosynthesis proteins may be present. This might be due to the fact that *S. cerevisiae* does not naturally encode genes for secondary metabolite production in its genome and is not adapted to introduce specific modifications required for the biosynthesis of a given secondary metabolite.

Therefore, for complex approaches to reconstitute complete biosynthesis pathways filamentous fungi are preferred. Some of them have only low demands on the growth condition, are already exploited in biotechnological processes and knowledge on up-scaling and fermentation has already been collected. Nevertheless, some important criteria should be kept in mind: first, the fungal host must be amenable to genetic modification by transformation procedures. A variety of different transformation protocols are available and frequently used methods range from protoplast transformation, *Agrobacterium tumefaciens* mediated transformation or biolistic protocols, to name a few (Li *et al.*, 2017). Furthermore, selection of transformants must be possible either by complementation of auxotrophic markers or resistance mediated selection against antibiotics.

If the main focus of the heterologous gene expression is on the isolation of the secondary metabolite rather than the purification of a heterologously produced protein, it is preferable that the host organism produces only a few or no secondary metabolites by itself. Several challenges might occur through unwanted, native secondary metabolite production in the selected host strain: (i) substrates and building blocks can be withdrawn from the biosynthesis of interest, so the overall yield may be rather low, (ii) cross-talk of enzymes from another biosynthetic pathway might lead to unwanted product modification and (iii) downstream processes such as identification and purification of the metabolite can be hindered by interfering metabolites from the producer strain. If the prerequisite of a marginal secondary metabolism is not fulfilled naturally by the host, it might be advantageous to modify the organism by deleting potentially active secondary metabolite gene cluster in its genome. The Oakley group, for example, utilises an *Aspergillus nidulans* expression strain in which six major biosynthetic gene cluster had been removed (Yeh *et al.*, 2016). The preparation of such a strain is tedious and one might run out of selectable markers. Other expression hosts display significantly less secondary metabolite production under laboratory cultivation conditions and are maybe more suitable to use.

Besides *A. nidulans*, other commonly used host species are *A. niger* or *Aspergillus oryzae*. Both fungi have a long tradition in biotechnological application or food production. Their

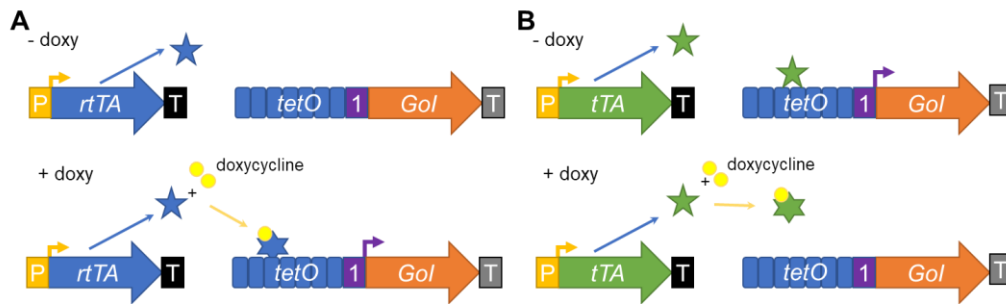
remarkable ability to secrete large amounts of enzymes or small organic acids makes their use particularly advantageous.

Promoter selection for heterologous expression

For gene expression in a eukaryotic host a promoter sequence upstream of the gene of interest is required. The genetic tool box already contains a range of constitutively active or inducible promoters, but there are still new promoters under investigation (Blumhoff *et al.*, 2013) and fine-tuneable systems are developed (Meyer *et al.*, 2011). Constitutively active promoters often derive from primary metabolism, for example the promoter of the glycerinaldehyd-3-phosphate dehydrogenase (*PgpdA*), phosphoglycerate kinase (*PpgkA*) or protein kinase A (*PpkiA*) (Fleissner and Dersch, 2010). For a long time only the strongest promoters had been used for heterologous gene expression, but for establishing complex metabolic fluxes this is not always beneficial (Blumhoff *et al.*, 2013). Primary metabolism-derived, constitutive promoters might also interfere with growth processes or may prohibit fungal growth due to toxic effects elicited by the natural product that is formed. Other promoters are inducible by certain carbon or nitrogen sources and therefore the media composition is crucial for gene expression. Widely used examples for nutrient dependent promoters are the promoter of glucoamylase (*PglaA*), alcohol dehydrogenase I (*PalcA*) or α -amylase (*PamyB*) (Fleissner and Dersch, 2010). The media constraints of these promoters make fermentation processes laborious and cost-intensive because of the use of non-standard nutrients.

On the other hand, there is a demand for inducible promoters and lots of efforts have been made to develop (semi)-synthetic induction systems. In this respect, the prokaryotic TetOn/TetOff system was engineered for eukaryotic organisms. The system depends on the tetracycline transactivator (tTA) or respectively the reverse tetracycline transactivator (rtTA) under the control of a constitutively active promoter (Scheme 9). The gene of interest is placed downstream of multiple copies of the *tetO* response element, whereby a minimal fungal promoter is placed between the transactivator and the operator to allow the fungal transcription machinery to bind (Vogt *et al.*, 2005). For induction of the system the natural inducer tetracycline can be replaced by the chemically more stable doxycycline or the less toxic, high affinity metabolite anhydrotetracycline (Gossen and Bujard, 1993). In a TetOff utilising strain the addition of doxycycline will lead to silencing of the gene of interest. Here, the transactivator will only bind to the *tetO* element if no doxycycline is present in the growth medium (Scheme 9B). Reversely, the gene expression of a TetOn utilising strain will be induced only in the presence of doxycycline, because the reverse transactivator binds doxycycline (Scheme 9A). In this form the rtTA can interact with the *tetO* element and switches gene expression on. It has been shown that this activating response is doxycycline dose dependent (Meyer *et al.*, 2011). As the system initially established for the filamentous fungus *A. niger* showed some genomic instability, further modifications have been made by

searching alternative promoters driving inducer expression. This strategy significantly improved the stable full-length integration into the genome (Wanka *et al.*, 2016).



Scheme 9: Regulation of gene expression by Tet-systems. (A) TetOn system. The reverse transactivator (rtTA) is produced from a constitutive promoter (P). Without doxycycline (doxy) rtTA cannot bind to the seven repeats of the operator binding site (*tetO*). The gene of interest (*GoI*) is not transcribed. The addition of doxycycline leads to binding of doxy to rtTA. The resulting conformational change allows DNA-binding at *tetO*, leading to the transcription of the *GoI*. **(B) TetOff system.** The transactivator tTA is produced from a constitutive promoter (P), binds to the *tetO* elements and facilitates gene expression. The addition of doxycycline leads to a conformational change of tTA that hinders the doxy-bound tTA to bind to *tetO*.

T – terminator. 1 – minimal fungal *gpdA* promoter. (Wanka *et al.*, 2016)

Another metabolic independent and fine-tuneable system relies on the human estrogen receptor (hER α). In *Aspergilli* it was shown that the hER α can migrate in its ligand-bound form into the nucleus and mediate gene expression by interaction with the estrogen response element. The system was proven to be tightly regulate, but linearly inducible with an induction level of up to 300-fold (Pachlinger *et al.*, 2005).

Influencing production rates

A strong induction of the expression rate of heterologous genes accompanied by high production rates of the secondary metabolite are favoured. Not only the strength of the promoter of choice will determine expression levels, but also positioning effects can have a major influence. Expression cassettes randomly integrated into the genome can end up in highly expressed euchromatin regions, or in silent heterochromatin or somewhere inbetween these two extremes. The transcriptional state of the surrounding chromatin region influences the transcription level of the gene of interest. Therefore, targeting loci with known high transcriptional activity for integration of heterologous genes will result in individual transformants showing comparable expression levels (Hansen *et al.*, 2011). However, homologous recombination rates in wild-type filamentous fungi can be very low, so that the number of correct transformants is limited and a tedious screening for accurate integration is necessary. By contrast, undirected gene integration will lead to a higher number of positive transformants, but expression levels of individual transformants might significantly differ and a test for production levels of individual transformants needs to be performed. On the other hand, undirected insertion can also give rise to multi-copy strains, carrying two or more

copies of the same gene. In this case, a continuous increase of gene expression rates is observed when up to six copies are integrated, which might also boost the production level of the protein or metabolite of interest (Verdoes, Punt and van den Hondel, 1995).

Another common problem is the low product titre of secondary metabolites produced by the natural producer. Often these fungi are not amenable to genetic modification or they require challenging culture conditions. Heterologous expression and further strain improvement can overcome this problem and might be a more cost-effective solution than chemical total synthesis especially for metabolites with stereocenters. Enniatin biosynthesis depicts an impressive example in which this principle was applied (Richter *et al.*, 2014). An NRPS gene was taken from *Fusarium oxysporum* and heterologously expressed in *A. niger*. After rational modification of growth medium and culture conditions a 950-fold increase of the production rate was detected. By feeding of precursors a final increase by about 4500-fold was observed. Further studies then used this optimised system for redesigning the NRPS by domain-swapping experiments, which resulted in novel-to-nature secondary metabolites (Zobel *et al.*, 2016).

Introduction of foreign genes and gene clusters

Different strategies have been applied to introduce and express foreign genes in a heterologous host. Either a single gene or a yeast-assembled large expression plasmid containing several genes and regulatory elements can be added to the genome of the recipient. Pseudo-polycistronic approaches in which one promoter controls the expression of multiple genes, which are divided by self-splicing protein sequences and the use of fungal artificial chromosomes have been tested for heterologous production of secondary metabolites. Each method has benefits and limitations.

Adding a single gene is the most intuitive method. The construction of the expression cassette is straightforward: it consists of a promoter, the gene of interest, a terminator and a selection marker. If a targeted integration into a specific locus of the host organism is intended, additional homologous flanking regions need to be added. The size of the resulting plasmid mainly depends on the size of the gene of interest, but in most cases these plasmids can be easily handled in *E. coli*. Fungal transformants grown under inducing conditions will express the target gene, which, in case of a production of a biosynthetic core enzyme directly leads to metabolite production. However, sometimes auxiliary enzymes are needed to enable product identification, as in the case of lovastatin biosynthesis, in which an enoyl reductase acting in *trans* is vital for product release from a polyketide synthase (Campbell and Vederas, 2010).

Pathways of natural product synthesis usually contain more than one enzyme. Therefore, heterologous reconstitution of complete metabolic pathways requires the introduction of multiple genes into the same strain. A stepwise strategy in which expression constructs are

individually assembled for each gene and stepwise transferred into the fungus is one possibility. However, the availability of selection markers and maintaining a large number of different constructs might be an issue. Marker recycling approaches have been developed, but each rescue step takes time and resources (Maruyama and Kitamoto, 2008). Despite these limitations the intermediate product produced by each gene subsequently introduced can be assessed individually as biosynthetic intermediates will accumulate and become amenable to structure elucidation. Therefore, a detailed characterisation of enzyme activities in a biosynthetic pathway is possible.

Whole pathways have been reconstituted on a single plasmid. Due to the size and the necessity of highly efficient homologous recombination during the assembly process, such plasmids are assembled in yeast 2 micron plasmids. Each gene is controlled by an individual promoter, which needs to be unique to avoid miss-assembly during the construction process. The selection of equally strong promoters is essential, and it was shown that not all promoters described have the same induction strength in different *Aspergillus* spp. (Pahirulzaman, Williams and Lazarus, 2012). Wasil *et al.* used this strategy for heterologous expression of the *A. nidulans* aspyridone biosynthesis gene cluster in *A. oryzae*. Although the cluster has been investigated in its native host (Bergmann *et al.*, 2007), the heterologous expression study identified unexpected enzyme functions, detailed pathway insights and novel by-products, showing an intrinsic potential of high diversity in aspyridone biosynthesis (Wasil *et al.*, 2013).

An elegant way to put several pathway genes under the control of a single promoter is the use of self-splicing peptide sequences of viral origin (2A) (Kim *et al.*, 2011). A pioneer study from the Brakhage lab used a combinatorial approach of synthetic genes, PCR amplified genes, yeast-assisted *in vivo* recombination and production of pseudo-polycistronic mRNA for heterologous production of penicillin in *A. nidulans* (Unkles *et al.*, 2014). The study was successful; however, the reported yield of penicillin was rather low.

In another approach, shuttling of fungal gene clusters without previous exogenous DNA modification was reported relying on the construction of fungal artificial chromosomes (FACs) (Bok *et al.*, 2015). The BAC (bacterial artificial chromosome) technology was used and extended by introducing an AMA1 sequence, which allowed an autonomous replication in fungal hosts. The whole genome of *A. terreus* was transferred into more than 7000 FACs resulting in about 20 times genome coverage. Roughly half of the FACs were sequenced from both ends of the insert to map which part of the genome was incorporated and to select, which of the FACs contained sequences of biosynthesis gene clusters. 15 candidate FACs were transformed into *A. nidulans*. Eventually, one new metabolite (terezine D), which was not known to be produced by *A. terreus*, was discovered. In a follow-up study, two additional secondary metabolites from *A. terreus* had been fully elucidated (Clevenger *et al.*, 2017).

Furthermore, the genomes of two additional *Aspergillus* species were converted into FACs and are waiting for detailed analysis.

The conversion of whole genomes into FACs and the identification of biosynthesis genes containing FACs seems to be a tremendous amount of work. However, this approach is scalable and compatible with automatization and might indeed be a novel highway for identification of unknown secondary metabolites. Nevertheless, it can be assumed that a fair proportion of gene clusters will remain silent. This might be due to the lack of transcriptional induction in the heterologous host. Therefore, the induction of gene clusters solely relies on the capability of a host such as *A. nidulans* to activate these clusters.

Genus *Aspergillus*

A special focus of this work lies on members of the genus *Aspergillus*. Especially the secondary metabolism of members of the section *Terrei* is studied in detail, and two different *Aspergillus* species have been selected as hosts for heterologous gene expression.

Several well-known and -characterised species belong to the genus *Aspergillus*. Some of them are detrimental to humans such as the opportunistic pathogens *Aspergillus fumigatus* and *Aspergillus terreus*. Other species like *Aspergillus flavus* cause post-harvest losses of peanuts and other crops by contaminating them with mycotoxins. *Aspergillus nidulans* is one of the most intensely studied model organisms of filamentous fungi. *Aspergillus niger* and *Aspergillus oryzae* have biotechnological applications and are potent microbial cell factories used for bulk production of organic acids or large-scale enzyme production (Yang, Lübeck and Lübeck, 2017; Liu *et al.*, 2014). Both latter species are generally recognised as safe (GRAS), because of their use in food production. This has been the case for *A. oryzae* for more than 2000 years (Goldman and Osmani, 2007).

However, Aspergilli are highly diverse, and the phylogenetic relationship might be similar to man and fish. They are ubiquitously found as saprophytes colonising various habitats from outdoor to indoor environments (Paulussen *et al.*, 2017). We are constantly inhaling their conidia, which are the asexual reproduction forms. They are produced on conidiophores, also called the Aspergillum, a structure which gave the name to the genus, and appearance differs significantly between members with more distant relationships (de Vries *et al.*, 2017). Mature conidia can easily become airborne. Inhaled conidia may cause allergic reactions in immunocompetent humans but are normally cleared by the immune system. In immunocompromised patients some species can actively invade the lung tissue causing invasive bronchopulmonary aspergillosis. The most frequent cause of aspergillosis is *A. fumigatus* (Latgé, 1999). This fungus is well adapted for growth within a host and many virulence determinants for nutrient acquisition as well as for protection from the immune system have been identified (van de Veerdonk *et al.*, 2017). Among these virulence

determinants are secondary metabolites like gliotoxin, siderophores and DHN-melanin (Sugui *et al.*, 2007; Schrettl *et al.*, 2004).

The biosynthesis of DHN-melanin starts with the polyketide synthase PksP/Alb1 and has already been introduced in the polyketide section. The polymerised melanin has a crucial function in cell wall integrity as in the absence of DHN-melanin the conidia surface appears smooth, because the rough rodlet layer cannot properly attach. This has been shown to result in reduced virulence in a murine infection model (Pihet *et al.*, 2009). Comparative genome analyses have revealed that orthologues of the pigment pathway gene are present in most of the Pezizomycotina, including the Aspergilli (Eisenman and Casadevall, 2012; Baker, 2008).

Aspergilli are not only united in their Aspergillum structure, but also their potential to produce secondary metabolites. Since sequencing of genomes became affordable, it is obvious that genomes of aspergilli possess a multitude of biosynthesis genes and gene clusters, vastly exceeding the number of characterised natural products (Sanchez *et al.*, 2012). For decades, the secondary metabolism of aspergilli has remained a booming research subject. A substance of high commercial value is lovastatin, a polyketide produced by *A. terreus*. The capability of inhibiting the HMG-CoA reductase makes lovastatin a cholesterol-lowering pharmaceutical and it was the first statin approved as a drug. Other natural products are virulence determinants or toxic to humans. Despite an excessive library of secondary metabolites produced by aspergilli, there is still some work to do: linking molecules to gene clusters or tackling the remaining orphan biosynthesis genes.

Secondary metabolites from *Aspergillus terreus*

As mentioned later, one major aim of this work was to study the secondary metabolism of aspergilli from the section *Terrei* in more detail. However, up to now only the genome publicly available from a species of this section is the one of *A. terreus*. Secondary metabolites produced by *A. terreus* have been of scientific interest since 1935 (Raistrick and Smith, 1935). However, linking of biosynthesis gene clusters to natural products started with a pioneer study in cloning of a PKS in 1996 (Fujii *et al.*, 1996), but accelerated greatly after sequencing of the genome. The following table summarises the metabolites and corresponding gene clusters from *A. terreus* identified so far.

As can be seen from Table 1, the discovery of gene clusters or biosynthetic enzymes involved in the production of natural products in *A. terreus* accelerated remarkably since 2012. Especially one group contributed towards the decipherment of the secondary metabolisms of *A. terreus* in a high-throughput manner. The fungal artificial chromosome approach revealed metabolites from gene clusters, which have not been previously characterized in classical deletion studies. However, despite these analyses, secondary metabolism of *A. terreus* is far from being completely understood.

Table 1: Characterised core biosynthesis genes from *Aspergillus terreus*.

Locus	Name	type of key enzyme	compound formed by cluster	reference
ATEG_00145	<i>terA</i>	PKS	terrein	This work
ATEG_00325		PKS-NRPS	isoflavipucine/ dihydroisoflavipucine	(Gressler <i>et al.</i> , 2011)
ATEG_00700	<i>atqA</i>	NRPS-like	Asterrequinone	(Guo <i>et al.</i> , 2013a)
ATEG_02004	<i>apvA</i>	NRPS-like	Aspulvinone H	(Guo <i>et al.</i> , 2013a)
ATEG_02815	<i>btyA</i>	NRPS-like	Butyrolactone I	(Guo <i>et al.</i> , 2013a)
ATEG_03090	<i>atrA_{At}</i>	NRPS-like	atromentin	(Hühner <i>et al.</i> , 2018)
ATEG_03470	<i>ataP</i>	NRPS	Acetylaranotin	(Guo <i>et al.</i> , 2013b)
ATEG_03563	<i>mela</i>	NRPS-like	Asp-melanin	This work
ATEG_03576	<i>valB</i>	NRPS	Valactamide A	(Clevenger <i>et al.</i> , 2017)
ATEG_03574/5	<i>valA</i>	PKS		
ATEG_03629		PKS	primary product (5-methyl orsellinic acid)	(Wang, Beissner and Zhao, 2014)
ATEG_06275	<i>atX</i>	PKS	terreic acid	atX (Fujii <i>et al.</i> , 1996), cluster (Guo <i>et al.</i> , 2014)
ATEG_07659	<i>ateafoG</i>	PKS	asperfuranone	(Chiang <i>et al.</i> , 2013)
ATEG_07661	<i>ateafoE</i>			
ATEG_08427		NRPS	terezine D	(Bok <i>et al.</i> , 2015)
ATEG_08451	<i>gedC</i>	PKS	geodin	(Nielsen <i>et al.</i> , 2013)
ATEG_08899	<i>pgnA</i>	NRPS-like	phenguignardic acid	(Sun, Guo and Wang, 2016)
ATEG_09617	<i>ctvA</i>	PKS	citreoviridin	(Lin, Chiang and Wang, 2016)
ATEG_09961	<i>lovB</i>	PKS	lovastatin	(Kennedy <i>et al.</i> , 1999)
ATEG_09968	<i>lovF</i>			
ATEG_10080	<i>trt4</i>	PKS	terretonin	(Guo <i>et al.</i> , 2012)
ATEG_10305	<i>anaPS</i>	NRPS	azonalenin & asterrelenin	(Guo <i>et al.</i> , 2013a)

In this respect, even within a single species, individual strains may show significant variation in the presence or absence of individual secondary metabolite genes or gene cluster. As an example, an additional gene cluster has been described in *A. terreus* AH-02-30-F7 to be responsible for the biosynthesis of 10,11-dehydrocurvularin, which contains a highly reducing (HR) and a non-reducing (NR) PKS as well as a transcription factor and an MFS transporter (Xu *et al.*, 2013). First reports on this secondary metabolite from a fungal source appeared in 1989 proving the polyketide origin by isotope labelling studies (Arai *et al.*, 1989). Another example of an *A. terreus* biosynthesis gene cluster which is not found in the sequenced strain is the benzomalvin cluster, identified with the FAC strategy from *A. terreus* ATCC 20542 (Clevenger *et al.*, 2017). Clevenger *et al.* claimed that more secondary metabolite gene clusters will be linked to their products by their FAC approach. All the studies listed give a clear impression that the secondary metabolism of *A. terreus* is of great interest, from the 1930's till today.

Aims of this study

The initial aim of this work was the identification of the origin of the pigment present in conidia of *A. terreus*. For this purpose, the following question was raised:

Does a non-reducing polyketide synthase of the SAT-KS-AT-PT-ACP-ACP-TE-type contribute to pigment formation in A. terreus conidia?

Characterisation of deletion mutants in *A. terreus* showed that this was not the case. However, it led to the discovery of the terrein biosynthesis gene cluster in *A. terreus*. Since *A. terreus* produces large quantities of terrein, the next objective was to use genetic elements from the terrein biosynthesis gene cluster for development of a heterologous expression system in *A. niger* with the question:

Is the combination of the transcriptional regulator TerR and its target promoter PterA suitable to drive heterologous gene expression in A. niger?

As a result, it was shown that expression of *terR* did not trigger the induction of secondary metabolite biosynthesis in *A. niger* and it was later confirmed that this is also not the case for *A. oryzae*. In contrast, when genes were introduced under control of *PterA* in the *terR*-expressing *Aspergillus* platform strains, a strong gene expression of the target gene exceeding the one obtained from strong constitutive promoters was observed. Furthermore, high levels of metabolites were recovered from platform strains when genes encoding key enzymes from secondary metabolism were expressed in this system. In conclusion, an expression system was created that is well suited for the investigation of fungal secondary metabolism. The mechanism by which the pigment in *A. terreus* is formed, however, remained unknown. Transcriptional analyses, deletion studies and heterologous expression were used to address the following question:

What is the real origin of the pigment in A. terreus conidia?

Transcription analyses identified genes coding for secondary metabolite biosynthesis enzymes that were specifically induced during the formation of asexual conidia in *A. terreus*. Deletion of the respective genes resulted in conidia colour mutants and implied that two genes are required for pigment formation. One gene was an NRPS-like coding gene, the second gene for a tyrosinase. Heterologous expression in *A. niger* resulted in the identification of aspulvinone E as precursor for the pigment. Aspulvinone E gets oxidised and activated for polymerisation by the tyrosinase. Co-expression of both genes resulted in pigmented *A. niger* mycelium and by using purified enzymes, the pigment biosynthesis was reconstituted *in vitro*. The pigmentation was due to a new type of melanin that was termed Asp-melanin. The propagation of transformants was difficult as the high production rates of aspulvinone E resulted in reduced growth rates and limited conidiation capacity in *A. niger* transformants, which made propagation of transformants difficult. This indicates that the

first generation of the TerR/PterA expression system might not be suitable for the expression of toxic metabolites as no fine-tuneable gene expression was possible. Therefore, the next aim was the refinement of the expression system:

Can the well-regulated TetOn system be used for fine-tuning of terR expression in the coupled expression system of TerR/PterA?

A new expression platform strain (ATNT) was developed in *A. niger* that contained the *terR* gene under control of the TetOn system. Reporter studies showed the tight regulation of the system in absence of the inducer doxycycline and a well-defined activation of target gene expression in dependence of the doxycycline concentration. In addition, gene expression was at least 5 times higher from this coupled system compared to gene expression from direct induction under control of TetOn. In addition, to allow for the simultaneous expression of several biosynthesis genes, the viral self-splicing peptide sequence P2A from porcine teschovirus-1 was tested for the production of individual proteins from a polycistronic messenger RNA. This allowed the successful reconstitution of Asp-melanin biosynthesis from a single transcript with correct subcellular localisation of the respective proteins. Asp-melanin had not been previously identified from any other species. Therefore, the following aim was to confirm the existence of this biosynthesis pathway in *Aspergillus* species from section *Terrei* and the question was addressed:

Is Asp-melanin common to section Terrei and can it be used to distinguish this Aspergillus section from others?

This investigation was made possible by a collaboration with Mikael Anderesen at the DTU Denmark. His group is involved in genome sequencing of 350 *Aspergillus* species and the genome assemblies of six new species from section *Terrei* were available. Analyses from heterologous expressions revealed that a functional copy of an aspulvinone E synthetase involved in Asp-melanin formation is conserved in section *Terrei*, whereby some members in this section either contained no pigment biosynthesis pathway at all, an inactivated dihydroxynaphthalene (DHN)-melanin pathway or genes from both melanin biosynthesis pathways. This indicated that the loss of the DNH-melanin pathway accompanied by the evolution of Asp-melanin biosynthesis is a typical feature in section *Terrei*. Further analyses of the novel genomes from section *Terrei* implied that NRPS-like coding genes are overrepresented in these fungi. Therefore, an aim was to characterise the portfolio of NRPS-like enzymes by addressing the question:

Is it possible to group NRPS-like enzymes into distinct families to predict the metabolite produced?

To answer this question, NRPS-like enzymes from *Aspergillus* species were grouped into families based on sequence and available gene cluster information, whereby the best cut-off values were unknown, because the number of already characterised enzymes was very low.

Several members of different families were expressed in the heterologous expression systems and metabolite analyses indicated that some family predictions indeed resulted in the production of identical metabolites, whereas in other families predictions were not reliable. While metabolite characterisation resulted in the identification of previously undescribed compounds from *Aspergillus* species, analyses also revealed that the previously selected cut-off values were too crude for precise family prediction. Therefore, information on additional enzymes will be required to set these values more precisely. However, the thioesterase domain in NRPS-like enzymes is responsible for core structure formation from the condensation of two aromatic α -keto acids and one aim of this work was to identify sequence patterns that direct the chemistry of this domain. The question addressed was:

Is site-directed mutagenesis of individual amino acids sufficient to convert a furanone core-forming aspulvinone E synthetase into a quinone core-forming atromentin synthetase?

It turned out that this is not sufficient, since site directed mutagenesis resulted in inactivation of the aspulvinone E synthetase. However, domain swapping and subsequent gene expression in the heterologous expression platforms revealed that the exchange of the entire thioesterase domain converts an aspulvinone E into an atromentin synthetase. Interestingly, these experiments were only successful when the thioesterase domain derived from an atromentin synthetase from the same species, but not from a different fungal genus. Moreover, these experiments identified an unexpected cross-chemistry on quinone-producing synthetases during heterologous expression in *A. niger*. Thereby, this cross-chemistry, which resulted in yet undescribed metabolites such as atrofuranic acid, was not limited to *A. niger*, but also occurred in the related species *Aspergillus brasiliensis* that contains an intrinsic atromentin synthetase. This points towards a much broader spectrum of metabolites produced from NRPS-like enzymes than previously assumed and product formation is strongly dependent on the physiology of the producing organism. The identification of the large number of different metabolites produced from NRPS-like enzymes finally resulted in the question:

Is it possible to predict a target of an NRPS-like enzyme-derived metabolite that makes it a suitable candidate for pharmaceutical exploitation?

In a collaborative project, the metabolite atromentin was selected as candidate for an *in silico* target fishing approach. Thereby, databases of protein structures with and without bound inhibitor or substrate were used as templates to model atromentin into the active or alternative binding site of the proteins. By this means, atromentin was predicted to possess weak estrogenic activity, which was subsequently confirmed by *in vitro* assays. Furthermore, the human 17- β -hydroxysteroid dehydrogenase was identified as a potential target with a proposed strong inhibitory activity. This study indicated the suitability of *in silico* models for target fishing to direct subsequent *in vitro* and *in vivo* experiments for target valuation.

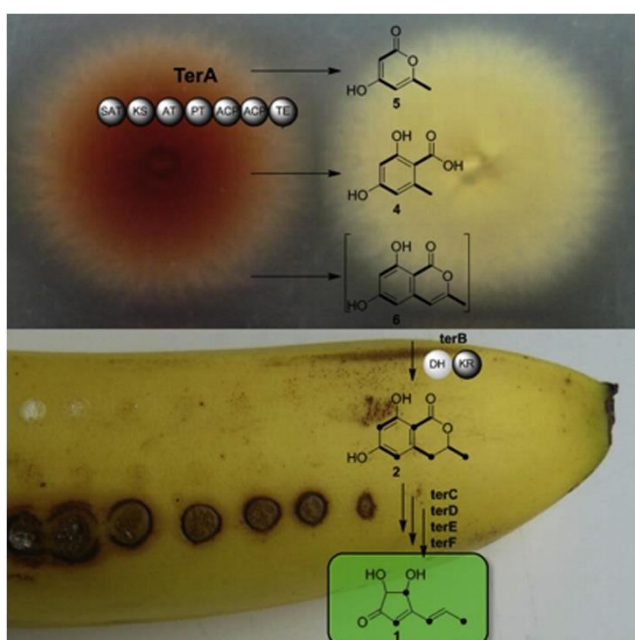
Publications

- Zaehle, C., Gressler, M., Shelest, E., **Geib, E.**, Hertweck, C., and Brock, M., (2014). Terrein biosynthesis in *Aspergillus terreus* and its impact on phytotoxicity. *Chem. Biol.* 21, 719-31
- Gressler, M., Hortschansky, P., **Geib, E.**, and Brock, M. (2015). A new high-performance heterologous fungal expression system based on regulatory elements from the *Aspergillus terreus* terrein gene cluster. *Front Microbiol* 6, 184
- Geib, E.**, Gressler, M., Viediernikova, I., Hillmann, F., Jacobsen, I.D., Nietzsche, S., Hertweck, C., and Brock, M. (2016). A non-canonical melanin biosynthesis pathway protects *Aspergillus terreus* conidia from environmental stress. *Cell Chem Biol* 23, 587-97
- Geib, E.**, and Brock, M. (2017). Comment on: "Melanisation of *Aspergillus terreus*-Is Butyrolactone I Involved in the Regulation of Both DOPA and DHN Types of Pigments in Submerged Culture? *Microorganisms* 2017, 5, 22". *Microorganisms* 2017, 5, 34
- Geib, E.**, and Brock, M. (2017). ATNT: an enhanced system for expression of polycistronic secondary metabolite gene clusters in *Aspergillus niger*. *Fungal Biol Biotechnol* 4, 13
- Dellafiora, L., Aichinger G., **Geib, E.**, Sánchez-Barrionuevo, L., Brock, M., Cánovas, D., Dall'Asta, C., and Marko, D. (2018). Hybrid *in silico/in vitro* target fishing to assign function to "orphan" compounds of food origin – the case of the fungal metabolite atromentin. *Food Chem*; 270, 61-69
- Geib, E.**, Baldeweg, F., Doerfer, M., Nett, M., and Brock, M. Cross-chemistry leads to product diversity from atromentin synthetases in aspergilli from section *Nigri*. *Cell Chem Biol*, accepted
- Theobald, S., Vesth, T. C., **Geib, E.**, Nybo, J. L., Frisvad, J. C., Larsen, T. O., Salamov, A., Riley, R., Lyhne, E. K., Kogle, M. E., Barry, K., Clum, A., Chen, C., Nolan, M., Sandor, L., Kuo, A., Lipzen, A., Magnuson, J. K., Simmons, B. A., Mortensen, U. H., Grigoriev, I. V., Brock, M., Baker, S. E, and Andersen, M. R. Genomic and metabolic diversity in *Aspergillus* section *Terrei*, in preparation
- Geib, E.**, Theobald, S., Andersen, M. R. and Brock, M. Recombinant expression and characterisation of NRPS-like enzymes from *Aspergillus* species section *Terrei*, in preparation

Terrein biosynthesis in *Aspergillus terreus* and its impact on phytotoxicity

Christoph Zaehle, Markus Gressler, Ekatarina Shelest, **Elena Geib**, Christian Hertweck and Matthias Brock

(2014) *Chemical Biology*; 21, 719-31



Summary of the manuscript: This manuscript describes the identification of the terrein biosynthesis gene cluster from the filamentous fungus *Aspergillus terreus*. Expression analysis and gene deletions provided insights into biosynthesis of the secondary metabolite terrein and enabled isolation of key intermediates. First analyses of the biological activity of terrein revealed that it might act as a phytotoxin that could increase the fitness of *A. terreus* while growing in the rhizosphere and on decaying organic

matter.

Contribution: 15% of practical work.

Extraction, isolation and identification of secondary metabolites produced by terrein biosynthesis gene cluster deletion mutants. This work contributed essentially to proposing a pathway for terrein biosynthesis.

Terrein Biosynthesis in *Aspergillus terreus* and Its Impact on Phytotoxicity

Christoph Zaehle,^{1,5} Markus Gressler,^{2,5} Ekaterina Shelest,³ Elena Geib,¹ Christian Hertweck,^{1,*} and Matthias Brock^{2,4,*}

¹Department of Biomolecular Chemistry, Leibniz Institute for Natural Product Research and Infection Biology (HKI), Beutenbergstrasse 11a, 07745 Jena, Germany

²Research Group Microbial Biochemistry and Physiology, Leibniz Institute for Natural Product Research and Infection Biology (HKI), Beutenbergstrasse 11a, 07745 Jena, Germany

³Research Group Systems Biology/Bioinformatics, Leibniz Institute for Natural Product Research and Infection Biology (HKI), Beutenbergstrasse 11a, 07743 Jena, Germany

⁴Institute for Microbiology, Friedrich-Schiller University, 07743 Jena, Germany

⁵Co-first author

*Correspondence: christian.hertweck@hki-jena.de (C.H.), matthias.brock@hki-jena.de (M.B.)

<http://dx.doi.org/10.1016/j.chembiol.2014.03.010>

SUMMARY

Terrein is a fungal metabolite with ecological, antimicrobial, antiproliferative, and antioxidative activities. Although it is produced by *Aspergillus terreus* as one of its major secondary metabolites, not much is known about its biosynthetic pathway. Here, we describe an unexpected discovery of the terrein biosynthesis gene locus made while we were looking for a PKS gene involved in production of conidia coloration pigments common for Aspergilli. The gene, ATEG_00145, here named *terA*, is essential for terrein biosynthesis and heterologous production of TerA in *Aspergillus niger* revealed an unusual plasticity in the products formed, yielding a mixture of 4-hydroxy-6-methylpyranone, orsellinic acid, and 6,7-dihydroxymellein. Biochemical and molecular genetic analyses indicate a low extension cycle specificity of TerA. Furthermore, 6-hydroxymellein was identified as a key intermediate in terrein biosynthesis. We find that terrein production is highly induced on plant-derived media, that terrein has phytotoxic activity on plant growth, and induces lesions on fruit surfaces.

INTRODUCTION

Aspergillus terreus is a ubiquitous filamentous fungus frequently isolated from soil rhizospheres (He et al., 2004; Wijeratne et al., 2003), decaying organic matter (Reddy and Singh, 2002), and marine environments (Damare et al., 2006). *A. terreus* is able to produce potent lipases (Yadav et al., 1998) and cellulases (Narra et al., 2012) and secretes itaconic acid (Kuenz et al., 2012), which makes this fungus attractive for white biotechnology. In addition, *A. terreus* produces a variety of natural products, most notably the medically important HMG-CoA reductase inhibitor lovastatin (Alberts et al., 1980; Tobert 2003). Additionally, a range of metabolites has been extracted from *A. terreus* cultures, among them

teritrems, citreoveridin, and butyrolactones (Samson et al., 2011). Several gene clusters in *A. terreus* responsible for metabolite production have been analyzed, including lovastatin (Hendrickson et al., 1999), methylsalicylic acid (Fujii et al., 1996), atrochryson (Awakawa et al., 2009), acetylaranotin (Guo et al., 2013), and terretinin (Guo et al., 2012), as well as the gene cluster for the PKS-NRPS hybrid metabolite isoflavipucine/dihydroisoflavipucine (Gressler et al., 2011). The latter belongs to the family of fruit rot toxins, implying that *A. terreus* could have specifically adapted to the decay of plant organic matter.

However, the origin of the conidia pigment in *A. terreus* remains to be elucidated. All Aspergilli analyzed so far employ a polyketide synthase to produce naphthopyrone precursors. *A. terreus* neither produces naphthopyrone (Slesiona et al., 2012) nor contains the highly conserved naphthopyrone synthase (Ahuja et al., 2012). This points to a separation of *A. terreus* from other *Aspergillus* species in terms of secondary metabolite production.

This is also highlighted by the fact that *A. terreus* is the only *Aspergillus* species producing terrein as one of its major secondary metabolites (Yin et al., 2013). Terrein was first described approximately 80 years ago (Raistrick and Smith, 1935), and its structure was elucidated in the 1950s (Barton and Miller 1955; Grove 1954). However, a series of recent studies revealed the ecological importance of terrein as an inhibitor of plant growth (Phattanawasin et al., 2007). Furthermore, a number of important biological activities have been attributed to terrein, such as antimicrobial, antiproliferative, and antioxidative activities, among others (Arakawa et al., 2008; Demasi et al., 2010; Lee et al., 2010; Liao et al., 2012; Park et al., 2004).

Considering the great interest in terrein functions, it is striking that so little is known about its biosynthesis. Classical stable-isotope-labeling experiments revealed that terrein biosynthesis involves the condensation of five acetate units, whereas the molecular formula of C₈H₁₀O₃ implied that it is composed of four acetate units only (Birch et al., 1965). It was proposed that the cyclopentanone ring derived from an oxidative decarboxylation with ring contraction of a dihydroisocoumarin (Hill et al., 1981). However, experimental support for this model has been lacking, and to date, the molecular basis for terrein biosynthesis has remained elusive.

Here, we report the serendipitous discovery of the terrein biosynthesis gene locus while searching for polyketide synthases that might be responsible for the pigmentation of *A. terreus* conidia. Through targeted mutations, heterologous expression of the terrein PKS, and analyses of pathway intermediates, we not only discovered the hydroxylated dihydroisocoumarin, which was predicted as a terrein precursor, but also found that the terrein PKS produces a variety of products. Finally, we describe that terrein and congeners exert a phytotoxic effect on radish seeds and fruits.

RESULTS

The PKS ATEG_00145 Is Uniquely Positioned in *Aspergillus* PKS Phylogeny

The color of asexual conidia of *Aspergillus* derives from polyketides that generally originate from the precursor naphthopyrone (Jørgensen et al., 2011; Langfelder et al., 1998; Mayorga and Timberlake, 1992; Watanabe et al., 1999). All these PKSs share the following in common: (1) they are nonreducing (NR), and (2) their domain structure shows tandem ACP domains (Fujii et al., 2001). Interestingly, in *A. terreus* no PKS with close homology to naphthopyrone synthases was identified (Slesiona et al., 2012). However, BLAST analyses revealed two PKSs with the same modular organization, namely, ATEG_00145 and ATEG_07500. To analyze the phylogenetic relation of these *A. terreus* PKSs with other nonreducing fungal PKS, a phylogenetic tree based on the ketosynthase (KS) domains was constructed. This analysis included naphthopyrone synthases, putative melanin, and orsellinic acid synthases. NRPS-PKS hybrids served as an outgroup (Figure 1). Whereas ATEG_07500 appeared at least very distantly related to naphthopyrone synthases, we found that ATEG_00145 does not belong to any of the selected groups of PKSs and seems unique for *A. terreus*. However, because neither ATEG_00145 nor ATEG_07500 closely clustered with naphthopyrone synthases, a contribution in conidia pigmentation remained in question.

ATEG_00145 and ATEG_07500 Do Not Contribute to Conidia Coloration

Deletion mutants of ATEG_00145 and ATEG_07500 were generated in *A. terreus* SBUG844 Δ akuB (Gressler et al., 2011) to investigate their contribution to the development of the conidia color. When the resulting transformants, Δ 00145 and Δ 07500, were tested on various media for conidia pigmentation, none of the mutants showed a difference in comparison to the wild-type (as exemplified in Figure 2A). However, when grown on phosphate-buffered Sabouraud agar plates, the mutant Δ 00145 completely lacked a typical secreted red pigment observed by all other strains (Figure 2B). Additionally, cultivation in liquid potato dextrose broth (PDB) resulted in a red culture broth with the wild-type and Δ 07500 mutant, but not with Δ 00145.

The Metabolic Profile of ATEG_00145 Deletion Mutant Lacks Terrein

To investigate the impact of ATEG_00145 on metabolite production, we cultivated the parental strain and Δ 00145 on various media, such as glucose containing *Aspergillus* minimal medium (AMM), YPD, Sabouraud (Sab), and PDB. Culture supernatants

were extracted with ethylacetate and were analyzed by liquid chromatography-tandem mass spectrometry (LC-MS/MS) (Figures 2C–2F). On AMM, no significant differences were observed. In contrast, YPD and PDB wild-type extracts contained a highly complex mixture of metabolites that largely lacked in the mutant. Furthermore, although the metabolic profile from Sabouraud medium showed a lower complexity than those from YPD and PDB, a major metabolite at 7.5 min (1) with an apparent molecular mass of 154 Da was completely absent from the mutant. This indicates that the deleted polyketide synthase ATEG_00145 is responsible for the production of various metabolites. However, because (1) was detected in significant amounts from all complex media, we isolated and purified the metabolite by crystallization. High-resolution mass determination revealed a molecular formula of C₈H₁₂O₃ indicative for the metabolite terrein. Comparing nuclear magnetic resonance (NMR) data with reported spectroscopic data (Hill et al., 1981) unequivocally confirmed this assumption. Therefore, we denoted the polyketide synthase encoded at locus ATEG_00145 TerA.

ORFs *terA*–*terJ* Constitute the Terrein Biosynthesis Gene Cluster

To confirm expression of *terA* in complex media and to analyze the genes coregulated with *terA*, we monitored expression of 25 genes (ATEG_00126–ATEG_00150) by semiquantitative RT-PCR analyses. Transcripts were analyzed after 36 and 48 hr from AMM (as negative control), YPD, Sab, and PDB media (Figure 3A). Expression of ATEG_00126 to ATEG_00134 and ATEG_00146 to ATEG_00150 did not correlate with expression of *terA* (ATEG_00145). Thus, these genes were excluded as constituents of a putative terrein biosynthesis gene cluster. In contrast, all genes spanning a region from ATEG_00135 to ATEG_00144 were coexpressed with ATEG_00145 and seemed to constitute the terrein biosynthesis gene locus (Figure 3B). The corresponding genes were denoted as *terA*–*J*, and a putative transcriptional regulator was termed *terR*.

To verify their specific contribution, all genes, except those of the MFS transporters (*terG* and *terJ*), were deleted in strain SBUG844 Δ akuB (Gressler et al., 2011). Gene deletions were confirmed by Southern blot analyses (Figure S1 available online), and mutants were cultivated on PDB medium to monitor medium coloration, metabolite profiles, and terrein production level (Figure 4). As expected, the *terA* mutant did not produce any detectable levels of terrein, and most of the prominent metabolites found in the wild-type extract were absent. A similar profile was detected for the Δ *terR* mutant, implying that transcription of the gene cluster strictly depends on this putative transcription factor. Additionally, mutants Δ *terB*, Δ *terC*, Δ *terD*, Δ *terE*, and Δ *terF* did not produce terrein. However, several metabolites accumulated in culture broth of mutants, some of which could also be detected in wild-type extract (1–5 in Figure 4B). Interestingly, although unable to produce terrein, the mutants Δ *terD* and Δ *terE* especially showed an enhanced coloration of the medium, implying that the colored substance does not depend on terrein production but seems to derive from TerA-derived intermediates. Although *terH* and *terI* were clearly coexpressed with *terA* (Figure 3A), both mutants still produced terrein, though the amount in relation to the biomass was reduced. In conclusion, TerA to TerF directly contribute to terrein synthesis with

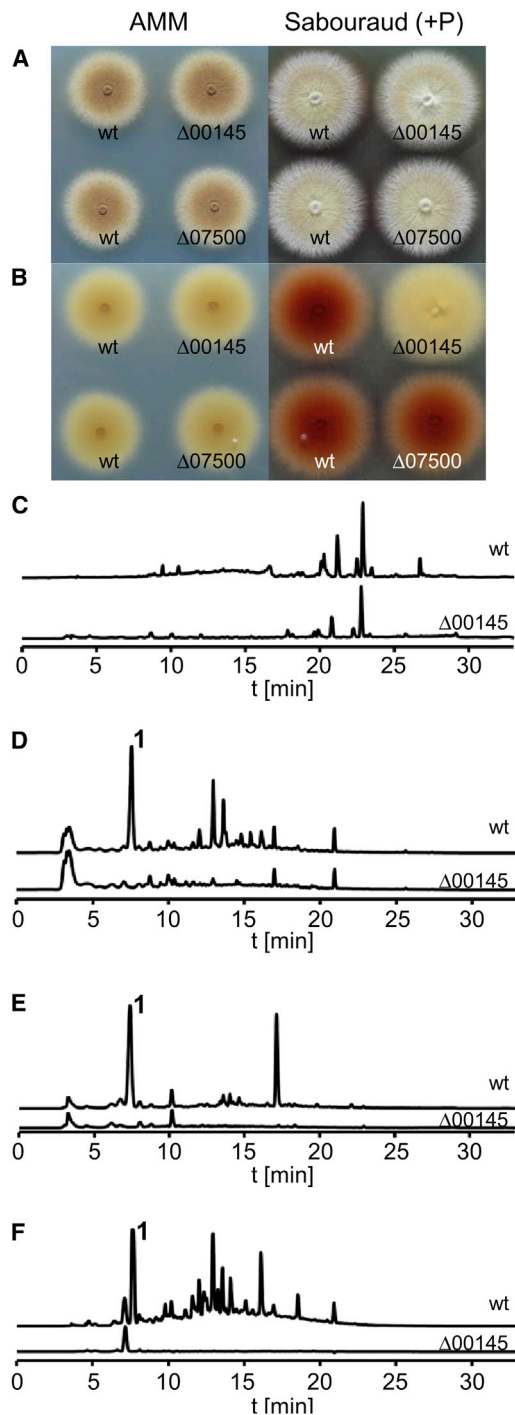


Figure 2. Phenotypic Characterization of ATEG_00145 and 07500 Deletion Mutants and Metabolic Profiling of $\Delta 00145$ in Comparison to the Parental Strain SBUG844 $\Delta akuB$

(A and B) Colony morphology of wild-type and deletion mutants on solid AMM and Sabouraud medium in (A) top and (B) bottom views. The $\Delta 00145$ mutant lacks the typical red pigmentation on Sabouraud medium.

(C–F) HPLC profiles (UV 254 nm) of culture extracts from strain $\Delta akuB$ (upper profiles) and $\Delta 00145$ mutant (lower profiles) cultivated on (C) AMM, (D) YPD, (E) Sab, and (F) PDB. “1” denotes the major metabolite terrein, which is lacking in the deletion mutant.

See also Figure S1.

TerR as an essential regulator, whereas TerH and TerI are dispensable. Therefore, the “minimal” gene cluster required for the synthesis of terrein spans the region from *terR*–*terA* and most likely uses one of the two MFS transporters (*terG* or *terJ*) for efficient secretion of metabolites.

6-hydroxymellein Is the Key Biosynthetic Precursor of Terrein

The accumulation of several metabolites in the mutants $\Delta terB$ to $\Delta terF$ implied the accumulation of putative terrein precursor molecules. Indeed, when culture broth extracts from $\Delta terC$, $\Delta terD$, $\Delta terE$, or $\Delta terF$ were added to the culture medium of the $\Delta terA$ mutant, terrein (**1**) biosynthesis was restored (Figure 5A). However, $\Delta terB$ extracts did not restore terrein formation. Thus, metabolites (**3**) and (**4**) (Figure 4B), which are also produced by $\Delta terB$, are not pathway intermediates, but are rather shunt or side products. To identify a true terrein precursor, we fractionated the $\Delta terC$ extract. We collected eight fractions by preparative high-performance liquid chromatography (HPLC) that baseline separated the major peaks (Figure 5B), including the major metabolite (**2**), and added these fractions to the $\Delta terA$ mutant. Interestingly, only fraction VII consisting of metabolite (**2**) restored terrein synthesis. Its characterization by high-resolution mass spectrometry (HR-MS) and NMR revealed a molecular mass of 194 Da and the molecular formula $C_{10}H_{10}O_4$. Structure elucidation by one-dimensional and two-dimensional NMR revealed the identity of **2** with 6-hydroxymellein (6-HM), a postulated intermediate en route to terrein (Hill et al., 1981).

To unequivocally prove that 6-HM (**2**) is an immediate terrein precursor, we added $[1-^{13}C]$ -glucose to the $\Delta terC$ culture medium (2×100 ml cultures) and isolated 4 mg of labeled 6-HM (**2**). ^{13}C -NMR analysis revealed the expected ^{13}C -labeling pattern of an isocoumarin derivative with polyketide origin (Figure 5B). Next, we added labeled 6-hydroxymellein to the $\Delta terA$ mutant and succeeded in isolating ^{13}C -labeled terrein (Figure 5B). NMR experiments revealed two adjacent nonlabeled carbon atoms in the cyclopentanone ring of terrein (Figure S6), which is completely in line with the model involving the loss of carbon atoms during ring contraction of 6-HM (**2**) (Hill et al., 1981; Zamir and Chin, 1982).

Recombinant TerA Produces Polyketides of Different Chain Length

Because TerA is a NR-PKS, we assumed that 6-hydroxy-2,3-dehydromellein was the product of TerA. Therefore, we heterologously expressed *terA* in *Aspergillus niger* FGSC A1144. To test for suitable promoters, β -galactosidase fusions (Gressler et al., 2011) with *Aspergillus nidulans* glyceraldehyde-3-phosphate dehydrogenase (*PgpdA*) promoter and the *Aspergillus oryzae* α -amylase promoter (*PamyB*) were analyzed. Although *PgpdA* was constitutively active under all conditions, the *PamyB* allowed inducible expression on AMM and YM medium but was not induced on casamino acids (Figure S3). Thus, *PamyB* was selected to construct a promoter fusion with *terA* for heterologous expression in *A. niger*.

Transformants with different integration numbers were screened for metabolite profiles on casamino acids and AMM. Unexpectedly, instead of a single metabolite, three new metabolites that were absent from the parental *A. niger* strain were

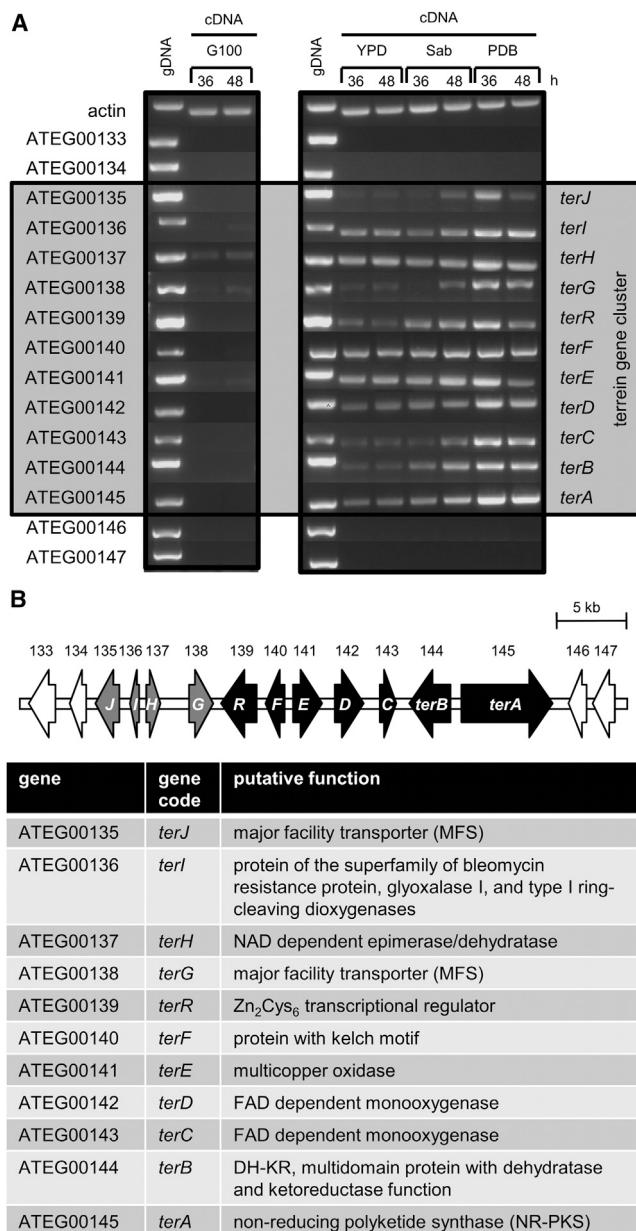


Figure 3. Expression Analysis of the Putative Terrein Synthesis Locus and Gene Annotations

(A) Semiquantitative PCR analysis of ATEG_00133–ATEG_00147 from actin-normalized cDNA generated from mycelium grown for 36 and 48 hr on AMM (G100), YPD, Sab, and PDB medium. Genes from ATEG_00135–00145 (*terJ*–*terA*) show the same expression pattern and form a putative terrein synthesis cluster.

(B) Genome map of the terrein gene cluster (filled arrows). Putative functional domains of the encoded proteins are listed.

detected in the transformants on glucose minimal medium (Figures 5C and 5D), but not on casamino acids (data not shown). HR-MS analyses revealed that compound **4**, the most abundant metabolite, has a molecular mass of 168 Da (C₈H₈O₄). For congeners **3** and **5**, masses of 210 Da (C₁₀H₁₀O₅) and 126 Da (C₆H₆O₃) were inferred. Interestingly, the two major metabolites

(**3** and **4**) showed the same retention time and UV spectra as metabolites (**3** and **4**) of the $\Delta terB$ mutant (Figure 4A), which did not restore terrein production (Figure 5A). Purification of the three metabolites with subsequent NMR-based structure elucidation revealed the structures of orsellinic acid (OA) for **4**, 6,7-dihydroxymellein (6,7-DHM) for **3**, and 4-hydroxy-6-methylpyranone (4-HMP) for the minor metabolite **5**. OA (**4**) and 4-HMP (**5**) represent typical products of an NR-PKS. In contrast, 6,7-DHM (**3**) lacks the expected double bond of 6-hydroxy-2,3-dehydromellein and has a hydroxyl-group on position C7, although there is no oxygenase domain within TerA.

Although 6,7-DHM (**3**) is closely related to 6-HM (**2**) and had been identified from different cluster mutants ($\Delta terB$ – $\Delta terI$; Figure 4A), feeding of complete culture extracts from *A. niger* transformants or their purified metabolites did not restore terrein production in the $\Delta terA$ mutant strain (data not shown). Thus, we assumed that the unexpected hydroxylation at C7 was nonspecifically introduced by the host, thus hampering uptake of the compounds and/or its further conversion to terrein.

To test this hypothesis, we supplemented AMM media with 6-HM (**2**) and inoculated them with either *A. terreus* or *A. niger* wild-type strains. Subsequent analyses of culture extracts revealed metabolites corresponding to hydroxylated forms of 6-HM, among them 6,7-DHM (Figure S4). Thus, this particular hydroxylation takes place in the absence of terrein biosynthesis enzymes. Consequently, recombinant expression of *terA* in *A. niger* yields 6-HM, which is subsequently converted into 6,7-DHM by unspecific enzymes in the heterologous host.

TerA Is Exclusively Primed with Acyl-CoA Starter Units

TerA is an unusual NR-PKS that produces polyketides of different chain length. This may be rationalized by the loading of starter units of different chain lengths or by a different number of elongation cycles. The first scenario would require a “relaxed” specificity of the starter acyl transferase (SAT) domain that may not only load acetyl-CoA but may also load other short-chain acyl-CoA starter units. In SAT domains, a catalytic diad formed by a conserved cysteine and histidine residue initiates the loading process (Crawford et al., 2006). However, inspection of the annotated protein sequence of TerA revealed no conserved cysteine in the N-terminal region. Further analysis of the proposed open reading frame (ORF) revealed an unusual large intron sequence of 223 bp. To rule out an incorrect intron prediction, we generated cDNA from *A. terreus* and sequenced the 5' region. Indeed, our analysis revealed that the intron only spanned a region of 49 bp (accession KF647874). The resulting corrected SAT domain contained the expected cysteine residue (Figure S5). This indicates that an acyl-CoA unit is loaded, but it gave no direct clue on the kind of acyl-CoA ester utilized. Because OA (**4**) was one of the products of TerA, we investigated a possible increase in product specificity by exchanging the TerA SAT domain with that of the orsellinic acid synthase OrsA from *A. nidulans* (Sanchez et al., 2010; Schroeckh et al., 2009). Yet *A. niger* expressing the SAT_{OrsA}:*terA* construct completely lacked synthesis of both 6,7-DHM (**3**) and OA (**4**) (data not shown). This finding suggests that the OrsA SAT domain and TerA are not compatible, although both PKS produce at least one common polyketide.

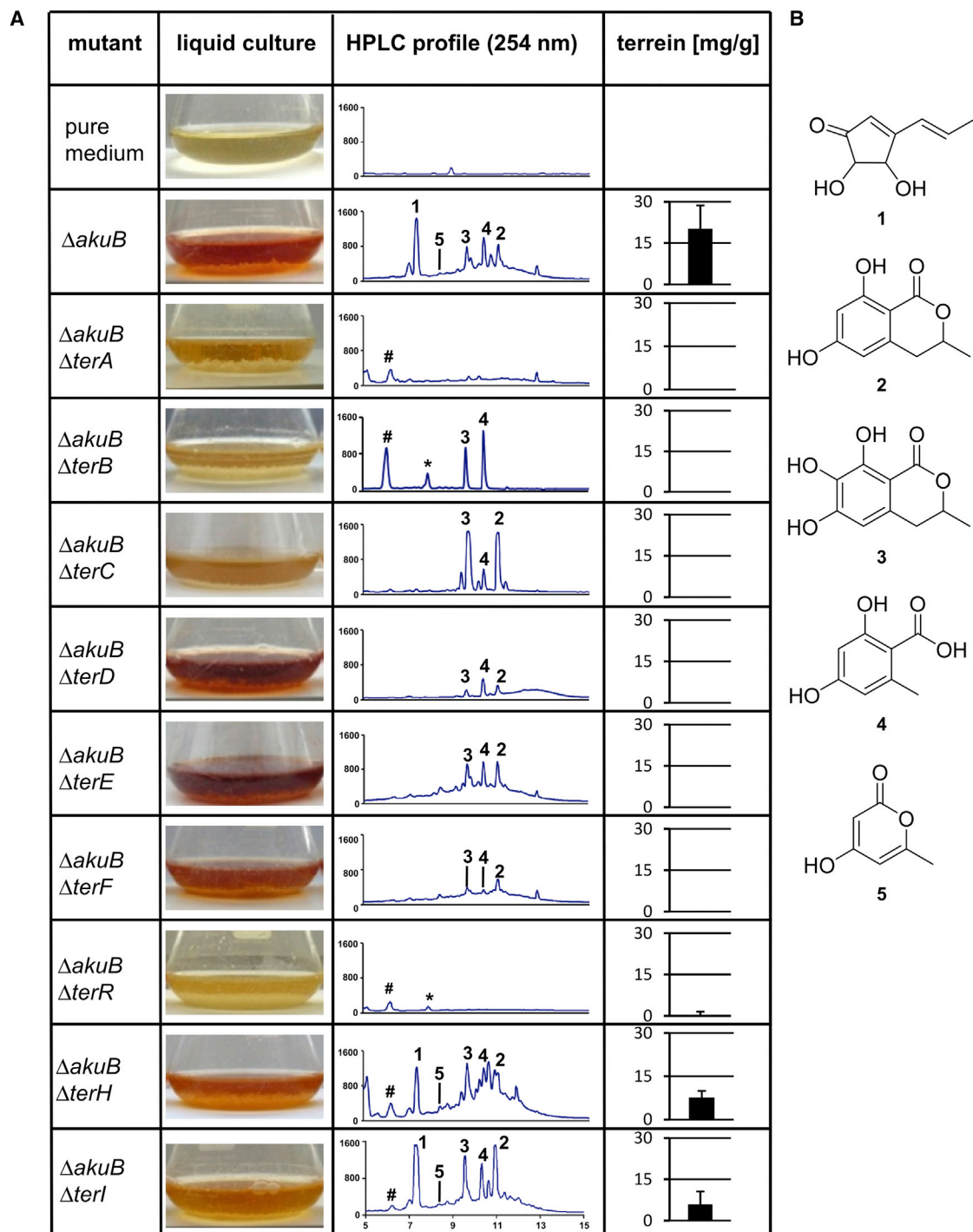


Figure 4. Metabolic Profiling and Terrein Quantification from Terrein Cluster Deletion Mutants

(A) Photographs of cultures were taken after 72 hr of growth in PDB medium at 30°C (column 2). Metabolite profiles of culture supernatants from control, wild-type, and mutants recorded at 254 nm (column 3). Specific terrein (**1**) concentrations per gram of mycelial dry weight were determined from three independent cultures (column 4). The metabolite peaks annotated with # (156 Da; molecular formula $C_7H_7O_4$) and * (154 Da; molecular formula $C_7H_6O_4$) are present in all mutants at varying extent and not related to terrein biosynthesis. Error bars denoted \pm SD.

(B) Structures of metabolites representing the numbered peaks in the HPLC profile: terrein (**1**), 6-hydroxymellein (**2**), 6,7-dihydroxymellein (**3**), orsellinic acid (**4**), and 4-hydroxy-6-methylpyrone (**5**).

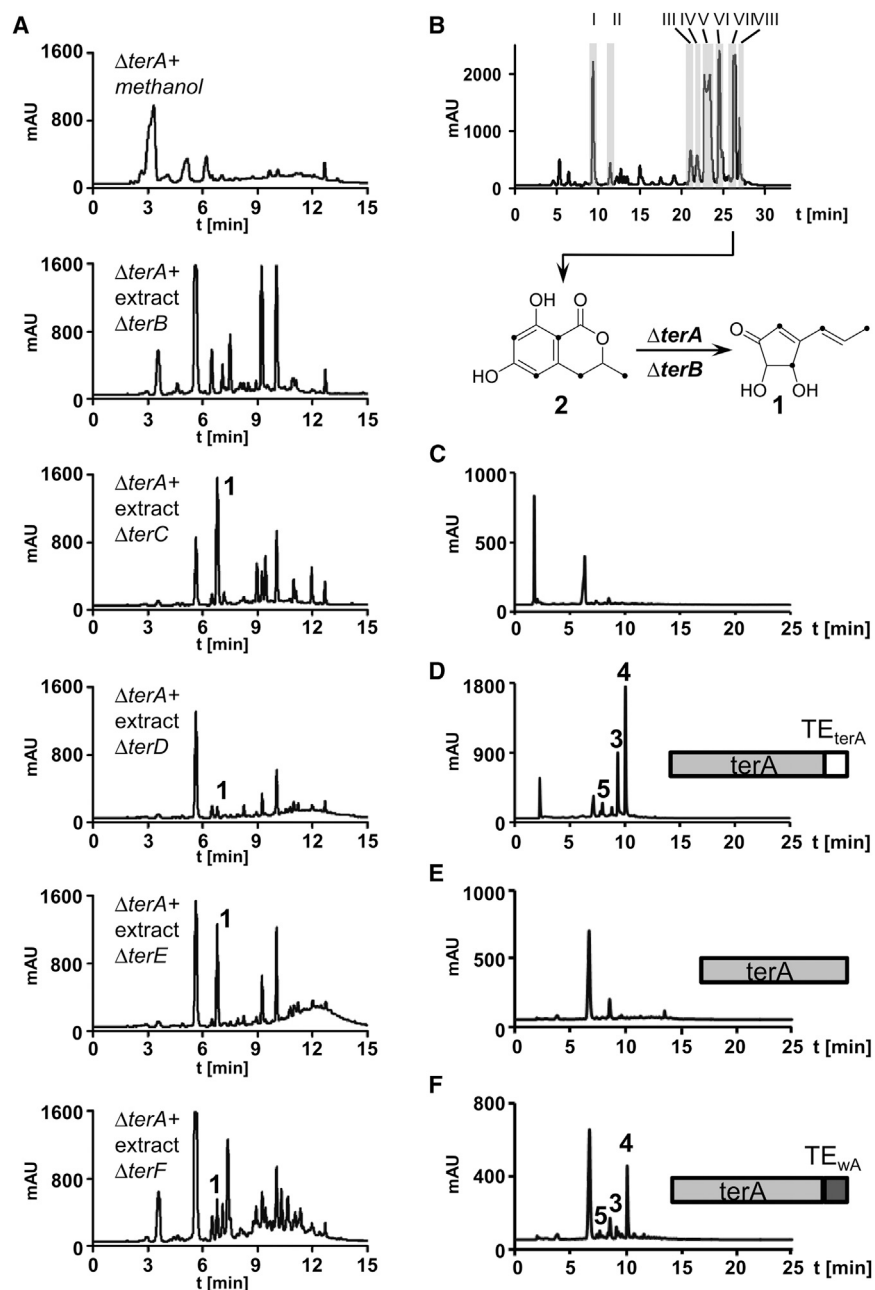


Figure 5. HPLC Profiles of Culture Supernatants from Cross-Feeding Experiments and from Recombinant *A. niger* Strains Expressing Different Modified *terA* Gene Versions

(A) HPLC profiles (UV 254 nm) of culture extracts from *A. terreus* $\Delta terA$ with or without cross-feeding of extracts from other cluster mutants. Feeding of $\Delta terB$ cannot restore terrenin production, whereas extracts from $\Delta terC$ to F lead to varying amounts of terrenin.

(B) Fractionation of the $\Delta terC$ crude extract by preparative HPLC and collection of the major peaks in separate fractions. Isolated fractions were used to supplement the medium of the $\Delta terA$ mutant. Fraction VII restored terrenin production and was identified as 6-hydroxmellein (2). When the $\Delta terC$ mutant was supplemented with [$1-^{13}C$]-glucose, NMR analysis revealed ^{13}C -labeled carbon atoms (marked with black dots) in 6-hydroxmellein that were reidentified in terrenin (see also Figure S6).

(C–F) HPLC profiles of culture extracts from *A. niger* wild-type (C), *A. niger* expressing the native *terA* gene (D), the truncated *terA* gene that lacks the TE domain (E), and the *terA* gene with the native TE domain substituted by the TE domain from *A. nidulans* *wA*. Numbers denote metabolites OA (4), 6,7-DHM (3), and 4-HMP (5). Metabolite peaks not annotated by numbers are also present in *A. niger* wild-type extracts and therefore are not related to *terA* expression. Note that metabolites (3, 4, and 5) were not observed in UV spectra from the truncated *terA* version but were detectable by mass spectrometry (see also Figures S2 and S3).

We next tested alternative PKS priming. First, we added [$1-^{13}C$]-acetate to the culture broth of *A. niger* A1144_*PamyB:terA* and analyzed the labeling pattern of the metabolites. Analysis confirmed the condensation of three acetyl units in 4-HMP (5), four acetyl-units in OA (4), and five acetyl-units in 6,7-DHM (3). Although the incorporation rate in 6,7-DHM (3) was rather weak, the labeling pattern was already confirmed by addition of labeled [$1-^{13}C$]-glucose to the *A. terreus* *terC* mutant (Figure 5B). These data indicated that, in principle, all three metabolites derived from acetyl-CoA units. Nonetheless, we could not exclude that short-chain fatty acids served as starter units to generate the products of different chain length. Thus, we added [$1,2,3,4-^{13}C$]-3-hydroxybutyrate as an alternative starter

unit to *A. niger* A1144_*PamyB:terA* and investigated the labeling pattern in 6,7-DHM (3). Analysis by ^{13}C -NMR revealed 6,7-DHM with an equal distribution of ^{13}C on all carbon atoms, indicating that 3-hydroxybutyrate was cleaved into acetyl units prior to chain elongation and thus did not specifically serve as a starter unit (data not shown). We additionally tested for a relaxed specificity of the SAT domain by adding the *N*-acetyl-cysteamine-esters of butyrate, 3-hydroxybutyrate, 3-hydroxypentanoate, and 3-hydroxyhexanoate. LC-MS/MS analysis neither revealed metabolites with altered or extended carbon skeleton nor an altered relative quantity of one of the three metabolites (data not shown). From these results, we conclude that TerA only utilizes acetyl-CoA starter and malonyl-CoA extender units, and the metabolites of different chain length seem to derive from low extension cycle specificity.

Interestingly, in all experiments, we exclusively detected the reduced 6,7-DHM (3) rather than a 6,7-dihydroxy-2,3-dehydromellein. This implies that, independent from the gene cluster, *A. niger* enzymes reduce 6,7-hydroxy-2,3-dehydromellein to 6,7-DHM (3). Similarly, this reduction also seems to occur nonspecifically in *A. terreus*, because all cluster mutants, except

the $\Delta terA$ and the $\Delta terR$ strain, accumulated 6,7-DHM (**3**) or 6-HM (**2**). However, the cluster also contains a putative ketoreductase (TerB) that may be essential for the correct timing of this reduction step during terrein production, but coexpression of *terB* together with *terA* in *A. niger* resulted in the same product pattern as observed for the strain solely expressing *terA* (data not shown).

The TerA Thioesterase Domain Is Exchangeable without Alteration of Product Formation

Bioinformatics and labeling studies imply that different numbers of elongation cycles are responsible for the different chain lengths of the TerA products. Thioesterase (TE) domains have been shown to contribute to chain length specificity and product release (Watanabe and Ebizuka, 2004). In the *A. nidulans* naphthopyrone synthase WA, the TE domain acts as a Claisen cyclase involved in closure of the “B-ring” in the heptaketide naphthopyrone that is also the sole product of this PKS (Fuji et al., 2001). When deleted, ring closure occurs via nonenzymatic lactonization, resulting in an isocoumarin heptaketide. In contrast, PKS1 from *Colletotrichum lagenarium* produces the tetraketide OA (10%), the pentaketides α -acetylorsellinic acid (25%), tetrahydroxynaphthalene (50%), and the hexaketide 2-acetyl-1,3,6,8-tetrahydroxynaphthalene (15%) (Watanabe and Ebizuka, 2004). Removal of the TE domain resulted in >95% production of an isocoumarin hexaketide. Thus, it was concluded that PKS1 generally produces a hexaketide but that the Claisen cyclase domain interferes with chain growth (Watanabe and Ebizuka, 2004), which could also be true for TerA. Thus, two different constructs were generated: (1) a truncated version of TerA lacking the TE domain (called *terA* Δ TE) and (2) a construct in which the C-terminal part next to the phosphopantetheine binding site was replaced by the TE domain from *A. nidulans* WA (called *terA*:TE_{WA}). Both constructs were produced in *A. niger*, and Southern blot analyses confirmed complete genomic integration of the *terA* Δ TE construct. Whereas the HPLC profile did not reveal production of any prominent product (Figure 5E), molecular masses of OA (**4**) and 6,7-DHM (**3**) were still detected by high-resolution mass spectrometry. In contrast, the exchange of the TE domain in the *terA*:TE_{WA} construct reduced the total amount of OA and DHM, but both metabolites were produced in significant amounts and in similar ratios as seen from the native TerA protein (compare Figures 5D and 5F). Thus, we cannot attribute the formation of different polyketides specifically to the TerA TE domain. We conclude that the thioesterase domain in TerA is of general importance for the efficient release of polyketides. Furthermore, the thioesterase domain of TerA is exchangeable, but at least by using a WA-type Claisen cyclase, the same polyketides are produced. Thus, TerA behaves different to PKS1 from *Colletotrichum lagenarium* and WA from *A. nidulans*.

The Terrein Pathway Produces Phytotoxic Compounds

Although terrein (**1**) is likely the major product of the cluster, OA (**3**) and 6,7-DHM (**4**) that both cannot be converted to terrein, were also present in substantial quantities in *A. terreus* wild-type and mutant strains. As we noted high terrein production rates on potato dextrose broth, we assumed that under natural conditions biologic activities of terrein might be associated with plant inter-

actions. Therefore, we investigated the phytotoxic potential of terrein and TerA-derived metabolites.

First, we investigated the phytotoxic effect of terrein on radish (*Raphanus sativus*) seeds in a range between 1 and 100 μ g/ml. As shown in Figures 6A and 6B, terrein inhibits root and shoot elongation in a concentration-dependent manner. Whereas 100 μ g/ml nearly completely abolished seed germination, 1 μ g/ml only showed a very weak inhibitory effect. Because 25 μ g/ml resulted in approximately 50% reduced root elongation after 5 days of incubation, purified OA (**4**), 6-HM (**2**), and 6,7-DHM (**3**) were also tested at 25 μ g/ml. As shown in Figure 6C, OA (**4**) and 6-HM (**2**) did not inhibit root elongation. 6,7-DHM (**3**) showed a low, but not substantial, inhibition at the applied concentration.

In a second series of biological activity assays, we investigated the ability of terrein and TerA-derived metabolites to cause lesions on fruit surfaces, which has not been tested before. Terrein was highly effective in causing surface lesions, with the highest activity on bananas (2.5–5 μ g effective concentration), but was also effective on other fruits, such as pears (12.5 μ g effective concentration; Figure 6D). However, when OA (**4**), 6-HM (**2**), and 6,7-DHM (**3**) were tested in the banana-surface assay, none of the metabolites generated lesions at concentrations of up to 50 μ g (Figure 6E). These experiments indicate that transformation of primary metabolites from TerA into terrein is required to harm fruit surfaces and may support the nutrient acquisition of *A. terreus* in its natural habitat.

DISCUSSION

In this study, the molecular basis for terrein biosynthesis in *A. terreus* was elucidated. The discovery of this gene cluster was unexpected, because we were initially searching for secondary metabolites responsible for coloration of asexual conidia. In all related *Aspergillus* species, the conidia color is naphthopyrone derived (Langfelder et al., 1998; Watanabe et al., 1999) and essential to inhibit phagolysosome acidification and allows for escape from macrophages (Slesiona et al., 2012; Thywißen et al., 2011). As putative candidates for conidial pigment synthesis in *A. terreus*, we selected two nonreducing polyketide synthases that revealed the same domain structure (SAT-KS-AT-PT-ACP-ACP-TE) as naphthopyrone synthases. When deleted, both mutants showed normal coloration of conidia, and phylogenetic analyses revealed that, despite the same domain structure, none of the two PKSs clustered with PKSs for which products had been described. Especially the ketoreductase domain of ATEG_00145 (subsequently denoted as TerA) formed a distinct phylogenetic branch. This observation was in agreement with a recent study, in which aromatic PKSs from *Aspergilli* were phylogenetically investigated, and ATEG_00145 (TerA) could not be explicitly assigned to any particular clade (Ahuja et al., 2012).

We showed that the *terA* gene encodes for a functional polyketide synthase. When *terA* was expressed in *A. niger*, it produced the triketide 4-hydroxy-6-methylpyranone (**5**), the tetraketide orsellinic acid (**4**), and a pentaketide, which is 6,7-dihydroxymellein (**3**). Although these products were also identified from *A. terreus* wild-type and some of the cluster mutants, the production of 6,7-DHM (**3**) especially did not fit to the domain structure of a NR-PKS. Subsequent analyses revealed that the

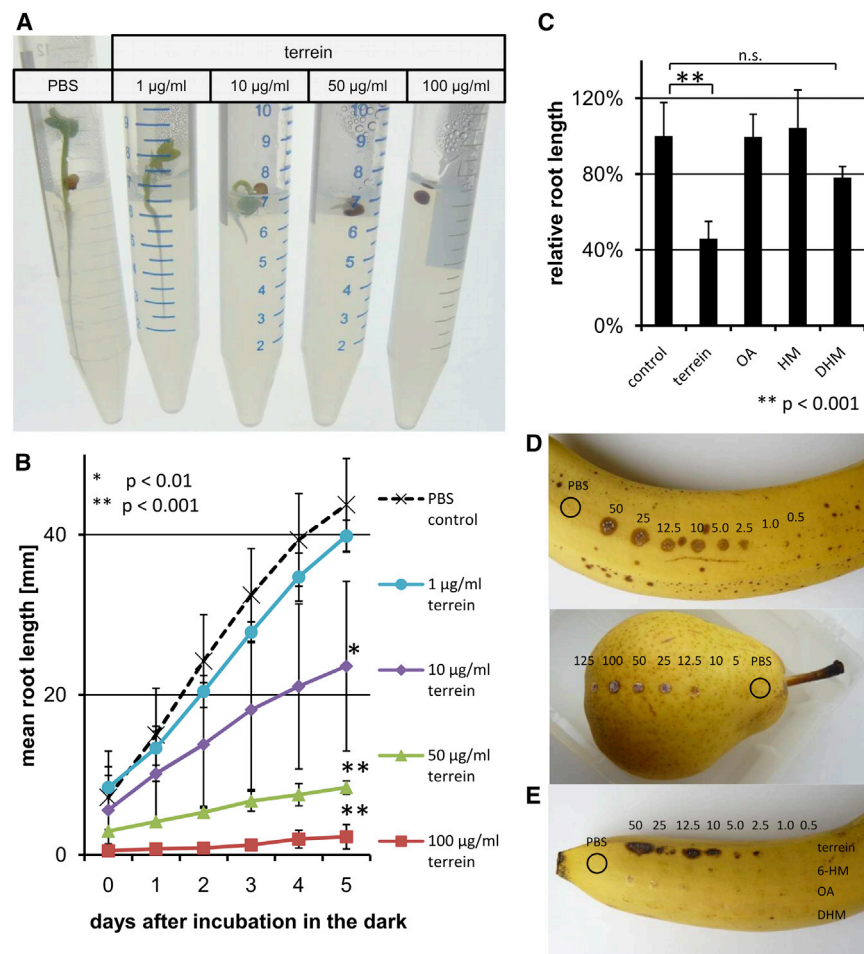


Figure 6. Effect of Terrein and Terrein Cluster Metabolites on Radish Seed Germination and Fruit-Surface Damage

(A) Root growth inhibition by terrenin. Terrein was added in concentrations of 0 (PBS), 1, 10, 50, and 100 µg/ml. Pictures were taken 2 days after incubation in the light.

(B) Graphical presentation of time response analysis of root growth inhibition. Each data point represents the average values from three independent experiments each containing 12 individual seedlings. Error bars represent \pm SD. Significance against control was calculated by the two-tailed t test.

(C) Root length determination of radish seedlings at day 5 in light in the presence of 25 µg/ml terrenin, OA, 6-HM (HM), and 6,7-DHM (DHM). The assay was carried out four times with at least ten individual seedlings. Significance was calculated by the two-tailed t test. Error bars represent \pm SD.

(D) Surface damage of bananas and pears inoculated with 0.5 to 50 µg and 5 to 125 µg terrenin, respectively, and incubated at room temperature. PBS was used as control. Pictures were taken at days 4 and 6.

(E) Banana surface damage by 0.5 to 50 µg terrenin, orsellinic acid (OA), 6-hydroxymellein (HM), or 6,7-dihydroxymellein (DHM). PBS + 0.1% Tween 80 served as control.

hydroxylation at position 7 of 6,7-DHM (**3**) occurs independent from TerA, implying that a derivative of 6-HM (**6** or **2**) rather than of 6,7-DHM (**3**) is the pentaketide produced by TerA. In this respect, one would have expected that 2,3-dehydro-6-HM (**6**) is produced because of a lacking ketoreductase domain in TerA. Indeed, this product was identified by an independent investigation (Ahuja et al., 2012), in which different NR-PKS were expressed in an *A. nidulans* strain deleted for several intrinsic secondary metabolite gene clusters. Thus, although 2,3-dehydro-6-HM (**6**), rather than 6-HM (**2**), is the pentaketide produced by TerA, 6-HM restored terrenin production in the *terA* and *terB* mutants and acts as a direct precursor for terrenin as shown by feeding studies with ^{13}C -labeled 6-HM (**2**). In contrast, triketide (**5**) and tetraketide (**4**) did not serve as precursors for terrenin in any of the mutants. Thus, we were interested in the reason for the low chain-length specificity of TerA, especially because we discovered that the recombinant PKS produced the tetraketide (**4**), rather than the pentaketide (**3**), as major product.

For other PKSs, such as the norsolorinic acid synthase, it was shown that the SAT domain accepts various starter units (Crawford et al., 2006), resulting in products of different chain length, whereby under natural conditions the main substrate is provided by a coregulated fatty acid synthase (Brown et al., 1996; Watanabe et al., 1996). In contrast, our feeding studies showed that in TerA the low specificity for a product with a specific chain

length is independent from the utilization of alternative starter units. A respective SAT-domain-independent mechanism has previously been described for PKS1 from *C. lagenarium* (Crawford et al., 2006), in which the TE domain causes low product specificity. In *C. lagenarium*, the deletion of the TE domain strongly altered the product spectrum in the direction of the product with the highest chain length (Watanabe and Ebizuka, 2004). This is unusual, because in other polyketide synthases, such as the naphthopyrone synthase WA from *A. nidulans*, the TE domain is important for product chemistry but does not direct chain-length specificity (Fujii et al., 2001). In the case of TerA, neither deletion nor exchange of the TE domain altered the product spectrum, but a TE domain was essentially required for high product yields. This implies that the TE domain is not directly involved in chain-length determination but is essential for efficient product release and thus overall activity of the PKS.

These data suggest that the low specificity is a trait inherent to the KS and likely the product template (PT) domain. This PT domain limits the pocket size and thus the possible substrate chain length and substrate orientation prior to the cyclization step (Crawford et al., 2009). It is remarkable that the KS domain of TerA did not fall into any KS clades in the phylogenetic tree. Thus, this part of the PKS may indeed cause the low product specificity. In this context, it should also be noted that fungal HR-PKS have been shown to produce polyketides of different chain lengths when taken out of the biosynthetic context (Kennedy et al., 1999). It is very conceivable that accessory enzyme contribute to the fidelity of the PKS.

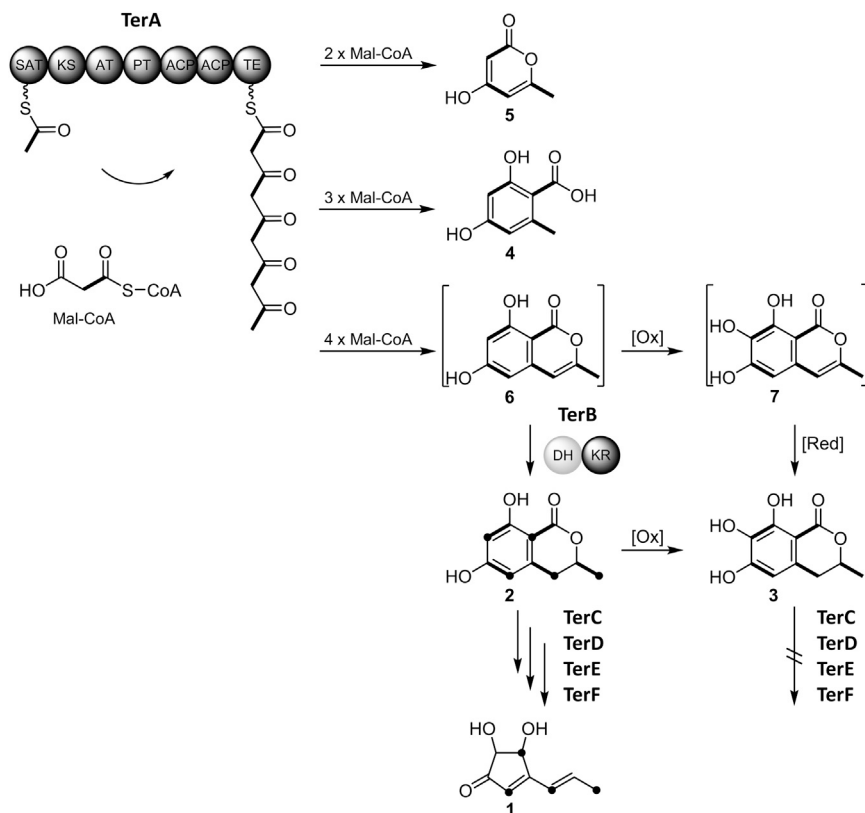


Figure 7. Proposed Scheme for Terrein Biosynthesis

Initially, TerA produces compounds **5** (4-HMP), **4** (OA), and **6** (2,3-dehydro-6-HM) by condensing acetyl-CoA with two, three, or four malonyl-CoA units. Only 6-HM serves as precursor for terrein production. For a detailed explanation of the figure, refer to the discussion section and also see Figure S4.

Terrein has been described to exhibit antibacterial, antifungal, anti-inflammatory, antioxidant, antiproliferative, and proapoptotic properties (Arakawa et al., 2008; Lee et al., 2010; Park et al., 2004; Porameesanaporn et al., 2013). However, according to the high expression levels on the plant-derived PDB medium (>1.1 g/l without further optimization), we focused on possible phytotoxic effects. Previous studies showed that terrein (**1**) and 6-HM (**6**) inhibit root and shoot growth of *Mimosa pigra* and *Echinochloa crus-galli* (Phattanawasin et al., 2007). Similarly, in our studies, terrein (**1**), but not 6-HM (**6**), showed a concentration-dependent germination inhibition of radish seedlings. On the contrary, 6-HM

In this study, we showed that TerA generates 2,3-dehydro-6-HM (**6**) as a precursor of terrein (Figure 7). The timing of hydroxylation at position C7 and hydrogenation between C2 and C3 appears important. When both reactions are performed on 2,3-dehydro-6-HM (**6**), 6,7-DHM (**3**) is formed, which is not converted into terrein in any of the mutants. However, the hydrogenation of 2,3-dehydro-6-HM (**6**) to 6-HM (**2**) yields an appropriate pathway intermediate for the $\Delta terA$ and $\Delta terB$ strains. Thus, we conclude that the specific reduction of 2,3-dehydro-6-HM (**6**) to 6-HM (**2**) without hydroxylation at position C7 is performed by TerB, which is in agreement with an *N*-terminal PKS dehydratase domain that could open and close the lactone ring to enable the C-terminal ketoreductase domain the hydrogenation at positions C2 and C3. However, because 6,7-DHM (**3**) is also found in the $\Delta terB$ strain, unspecific ketoreductases may also perform this reduction on a substrate hydroxylated at position C7.

Although our analyses revealed that *terC*, *terD*, *terE*, and *terF* are essential for terrein production, it remains difficult to assign a specific function to each of the enzymes. One can assume that at least two additional monooxygenase reactions are required. One reaction could involve the hydroxylation at position C9 (Zamir and Chin, 1982) to set the stage for the subsequent decarboxylation at the lactone ring. Another hydroxylation would be required at position C7 or C5 (Hill et al., 1981) to allow for the ring contraction. Because *terC*, *terD*, and *terE* encode either FAD-dependent monooxygenases or multicopper oxidases, all three enzymes are putative candidates for these reactions. Despite many attempts, potential downstream products evaded isolation and structure elucidation because of their instability and/or reactivity.

(**2**) inhibits pollen development in *Arabidopsis thaliana* (Shimada et al., 2002). We also found that terrein, but none of the other compounds produced, causes lesions on fruit surfaces. Thus, in its natural habitat terrein may be specifically required during the interaction with plants and may trigger release of nutrients from the interaction partners. However, various intermediates of terrein synthesis display different beneficial or phytotoxic effects on plant cells, which may explain the high diversity of products released during terrein synthesis.

SIGNIFICANCE

Aspergillus terreus is an important fungus that plays a pivotal role in biotechnology, not only for the production of enzymes and fine chemicals but also for pharmaceutically relevant compounds. Moreover, *A. terreus* has been implicated in various diseases and is regarded as an emerging fungal pathogen. Thus, detailed knowledge about its biosynthetic potential is essential to improve metabolite production and to identify and study potential risk factors. Terrein is a famous, characteristic *A. terreus* metabolite that is endowed with a variety of biological activities, such as antimicrobial and antiproliferative activities. Yet little is known about terrein biosynthesis, and the genes involved remain fully unknown. In this study we unveil the molecular basis for the biosynthesis of this important natural product and gain insights into regulation and mechanisms of the terrein pathway. The identified terrein PKS is unusual as it yields three compounds of different sizes and shapes. Functional and mutational analyses contribute to a better understanding of terrein

assembly. Most notably, we identify a key intermediate of the terrein pathway and unequivocally show that it is transformed into the rearranged polyketide metabolite. Beyond biosynthetic studies, we also report an additional role—which has been overlooked thus far—for terrein, in which it forms lesions on fruit surfaces. This finding is particularly noteworthy as terrein biosynthesis is upregulated in organic media that may mimic the natural habitat. Taken together, our studies not only shed light on the biosynthesis of an important fungal metabolite but may also unveil an additional role for the terrein pathway in environmental competition and phytotoxin production.

EXPERIMENTAL PROCEDURES

Reconstruction of the Phylogenetic Tree

Protein sequences of known and predicted PKSs belonging to pigment biosynthesis pathways and the orsellinic acid clade were collected from the National Center for Biotechnology Information. KS domains from fungal NRPS/PKS hybrids were used as an outgroup. The KS domains were extracted and aligned with Muscle, and the tree was inferred with the neighbor-joining (NJ) method using the Phylip package, with the number of bootstrap trials set to 1,000. Numbers at the nodes indicate the bootstrap support for each clade.

Strains, Cultivation Conditions, and Metabolite Extraction

All strains and mutants used and generated in this study are listed in the [Supplemental Experimental Procedures](#). Minimal media are based on *Aspergillus* minimal medium (AMM; <http://www.fgsc.net/methods/anidmed.html>). The following media were used: AMM (containing 100 mM glucose as standard medium), AMM-CA1% (nitrate and glucose replaced by 1% casamino acids), YPD (20 g/l peptone, 20 g/l glucose, and 10 g/l yeast extract), Sabouraud (Sigma Aldrich; buffered in solid media with sodium phosphate buffer [pH 6.5] to a final concentration of 150 mM), potato dextrose broth (PDB; Sigma Aldrich), and yeast extract/malt extract medium (YM; 5 g/l peptone, 3 g/l malt extract, and 3 g/l yeast extract). Liquid cultures were inoculated with a final concentration of 1×10^6 conidia/ml and incubated at 30°C and 200 rpm. When required, plates were supplemented with 140 µg/ml hygromycin B (Roth) or 0.1 µg/ml pyriithiamine (Sigma Aldrich). Conidia were harvested from solid media in water and filtered over 40 µm cell strainers (VWR). Culture broth was extracted by adding 50 ml ethylacetate to 50 ml broth, and the extraction was repeated once. Evaporated residues were solved in 1 ml methanol and filtered. Standard extract analyses were performed on an Agilent 1100 series HPLC-DAD system coupled with a MSD trap (Agilent Technologies) operating in alternating ionization mode (Gressler et al., 2011).

Generation of Deletion Mutants in *A. terreus*

For generation of deletion mutants, *A. terreus* SBUG844/ Δ akuB (Gressler et al., 2011) was used as the parental strain. Briefly, between 0.5 and 1.3 kbp 5'- and 3'-flanking regions were amplified from genomic DNA and fused with the pyriithiamine resistance cassette *ptrA* (Fleck and Brock, 2010). *A. terreus* was transformed by protoplast fusion and regenerated on osmotically balanced medium with pyriithiamine as a selection marker. Transformants deriving from single-haploid conidia were analyzed by Southern hybridization with digoxigenin-labeled probes directed against upstream- or downstream-flanking regions (Figure S1) (Gressler et al., 2011). For details on oligonucleotides used for fragment amplification and generation of labeled probes, refer to the [Supplemental Experimental Procedures](#).

Generation of β -galactosidase Reporter Strains

Details on oligonucleotides and cloning strategies are found in the [Supplemental Experimental Procedures](#). Briefly, the *A. nidulans* glyceraldehyde-3-phosphate dehydrogenase promoter (*AnPgpdA*, locus ANID_08209.1) amplified from genomic DNA of *A. nidulans* FGSC A4 or the *A. oryzae* α -amylase B promoter (*PamyB* from *A. oryzae* FGSC A815; Kanemori et al.,

1999) was used to generate *lacZ* reporter strains in *A. niger* FGSC A1144. For selection of transformants, the *ptrA* resistance cassette (Fleck and Brock, 2010) was included in the reporter constructs. Transformation of *A. niger* FGSC A1144 and Southern hybridization (Figure S3) was performed as described previously (Gressler et al., 2011).

Generation of *terA*, *terA* Δ TE, and *terA*:TE_{wA} Expression Strains in *A. niger* A1144

Expression of *terA*, *terA* Δ TE, and *terA*:TE_{wA} was controlled by the *A. oryzae* *amyB* promoter as described above. All constructs were additionally fused with terminator sequences to avoid run-through events during transcription. Either the *ptrA* or the *hph* resistance cassette was used as a selection marker for *A. niger* A1144 transformation. Transformants were checked by PCR and Southern hybridization to confirm the complete integration of the constructs (Figure S2). For details concerning oligonucleotides used for fragment amplification, cloning strategies, and generation of labeled probes, refer to the [Supplemental Experimental Procedures](#).

Semiquantitative PCR on Terrein Cluster Genes

RNA from *A. terreus* SBUG844 grown for 36 and 48 hr on AMM, Sabouraud, YPD, and PDB media was isolated using TRIzol (Bioline). After DNase treatment, cDNA was generated using anchored oligo-dT primers, and cDNA amounts were normalized against the actin gene (Gressler et al., 2011). Oligonucleotides P61–P114 ([Supplemental Experimental Procedures](#)) were used for semiquantitative PCR analyses on ATEG_00126–00150. Genomic DNA from SBUG844 was used as a positive control during PCR amplifications.

β -galactosidase Assay

As described above, β -galactosidase assays were performed on cell-free extracts from *A. niger* transformants harboring *lacZ* fusion constructs. Mycelia were harvested from cultures grown for 48 hr in AMM, YM, or AMM-CA1% media at 30°C. Mycelia were ground to a fine powder under liquid nitrogen and resuspended in 50 mM MOPS buffer (pH 7.5) with 2 mM MgCl₂ and 10 mM β -mercaptoethanol. After centrifugation at 21,000 \times g, the supernatant was used for β -galactosidase assays as described (Gressler et al., 2011).

Isolation and Structure Elucidation of Metabolites

Purified terrein was obtained by recrystallization from crude extracts with ethylacetate (Demasi et al., 2010). Details for the isolation of 6-hydroxymellein, 6,7-dihydroxymellein, orsellinic acid, and 4-hydroxy-6-methylpyrone by solid-phase extraction and preparative HPLC are provided in the [Supplemental Experimental Procedures](#). High-resolution electrospray ionisation mass spectrometry (HR-ESI/MS) was carried out on an Accela UPLC-system combined with an Exactive mass spectrometer (Thermo Scientific) operating in positive ionization mode. Separation was carried out on a Betasil C18 column (2.1 \times 150 mm; 3 µm; Thermo Scientific) using water (solvent A) and acetonitrile (solvent B), each containing 0.1% formic acid, as binary solvent system. A flow rate of 250 µl/min and the following gradient was used: 0–1 min = 5% B, 1–16 min = 5%–98% B, 16–19 min = 98% B, and 19–20 min = 98%–5% B. NMR spectra were recorded on a Bruker Avance III 500 and a Bruker Avance III 600 spectrometer (Bruker BioSpin GmbH) equipped with a cryoprobe head using DMSO-*d*₆ and methanol-*d*₄ as solvents and internal standards.

Quantification of Terrein

Extraction of 50 ml cultures with ethylacetate was performed as described above, and 80 ml of extracts were evaporated under reduced pressure, solved in 1 ml methanol, and diluted in a ratio of 1:20. Each sample was applied to an Agilent 1260 modular HPLC system (Agilent Technologies) equipped with DAD. As the stationary phase, a bifunctional-phenylpropyl-modified C18 column (Macherey-Nagel Sphinx RP, 4.0 \times 250 mm; 5 µm) with a binary solvent system consisting of methanol (solvent B) and water containing 0.1% formic acid (solvent A) was used. The following gradient with a flow rate of 0.8 ml/min was applied: 0.5 min = 10% B, 0.5–20 min = 10%–70% B, 20–25 min = 70%–100% B, 25–28 min = 100% B, and 28–33 min = 100%–10% B. Quantification was performed from a calibration curve of known terrein concentrations. For dry-weight correlation the mycelia from the cultures were dried for 48 hr at 37°C and balanced. From these values, the terrein concentrations per gram

of dried mycelium were calculated. All quantifications were carried out in biological triplicates and technical duplicates.

Metabolite Supplementation Experiments

A. niger strains were cultivated for 48 hr on AMM, and *A. terreus* wild-type and mutant strains were cultivated for 72 hr on PDB medium. In precursor feeding experiments, media were supplemented with unlabeled SNAC derivatives of 3-hydroxy butyric acid, 3-hydroxy pentanoic acid, 3-hydroxy hexanoic, and labeled [1,2,3,4-¹³C] 3-hydroxy butyric acid (Cortecnet). Cultures of *A. niger* A1144_PamyB:terA were supplemented at 0 hr and after 24 hr with 2.5 mM of the respective molecules (solved in DMSO). For labeling of terrein, *A. terreus* SBUG844 was cultivated for 72 hr at 30°C in a 4 l Biostat B-DCU II fermenter (Sartorius Stedim Biotech) in PDB medium supplemented with 5 mM [1-¹³C] sodium acetate (Cortecnet). The culture was constantly stirred at 500 rpm, and air was sparged at 2 l/min. Labeled molecules were isolated from *A. terreus* strain SBUG844ΔakuBΔterC cultivated in 100 ml PDB medium supplemented with 1 g [1-¹³C]-D-glucose (Cortecnet). In cross-feedings, 100 μl culture extracts from the deletion mutants ΔterB, ΔterC, ΔterD, ΔterE, and ΔterF were added to cultures of SBUG844ΔakuBΔterA. After 72 hr, culture supernatants were extracted and applied to LC-MS/MS, preparative HPLC, and NMR analysis as described.

Root Growth Inhibition and Fruit Surface Spot Dilution Assays

Details on root growth inhibition are provided in the [Supplemental Experimental Procedures](#). Briefly, single sanitized radish seeds were transferred to 15 ml tubes with 7 ml of modified solid Hoagland medium and overlaid with 500 μl medium. Tested compounds were terrein, OA, 6,7-DHM, and 6-HM that were added to sterile media in final concentrations of 100, 50, 25, 10, or 1 μg/ml. Tubes were incubated for 3 days in the dark (1 day, 4°C; 2 days 20°C) and finally exposed to a constant 12 hr light/dark rhythm, at which time root and hypocotyl length were determined on a daily basis. Triplicates with 12 biological replicates were tested. To test the effect on fruit surfaces, organic bananas (type Bio) or pears were cleaned with water, and 5 μl of the metabolites OA, 6-HM, 6,7-DHM, and terrein (solved in PBS with 0.1% Tween 20; range: 2.5 mg/ml to 1 μg/ml) were applied. Photographs were taken after 2 and 7 days of incubation at room temperature in the dark.

Statistical Analysis

Error bars in figures represent SD (±SD). Statistical analyses were performed by applying the two-tailed Student's *t* test. Data were denoted as significantly different with *p* values ≤ 0.01 (*) or ≤ 0.001 (**).

ACCESSION NUMBERS

The DDBJ/EMBL/GenBank nucleotide sequence database accession number for the 5' coding region spanning intron 1 of the *terA* gene (locus ATEG_00145) reported in this paper is KF647874.

SUPPLEMENTAL INFORMATION

Supplemental Information includes Supplemental Experimental Procedures and six figures and can be found with this article online at <http://dx.doi.org/10.1016/j.chembiol.2014.03.010>.

AUTHOR CONTRIBUTIONS

C.Z. isolated and characterized metabolites, analyzed data, and contributed in writing the manuscript; M.G. constructed mutants, performed biological activity tests, analyzed transcription profiles, and contributed in writing the manuscript; E.S. performed phylogenetic analyses; E.G. contributed in metabolite isolation and structure elucidation; and C.H. and M.B. designed the study, interpreted data, and wrote the manuscript.

ACKNOWLEDGMENTS

We acknowledge M. Cyrulies for assistance in large-scale fermentations, A. Perner for high-resolution mass spectrometry, D. Heine for SNAC-ester syn-

thesis, and H. Heinecke for NMR measurements. This work was financially supported by Deutsche Forschungsgemeinschaft (BR 2216/4-1) and internal funding from the Hans-Knöll Institute. For questions about natural product chemistry/biochemistry, contact C.H., and for questions about molecular biology/microbiology, contact M.B.

Received: January 31, 2014

Revised: March 19, 2014

Accepted: March 26, 2014

Published: May 8, 2014

REFERENCES

- Ahuja, M., Chiang, Y.M., Chang, S.L., Praseuth, M.B., Entwistle, R., Sanchez, J.F., Lo, H.C., Yeh, H.H., Oakley, B.R., and Wang, C.C. (2012). Illuminating the diversity of aromatic polyketide synthases in *Aspergillus nidulans*. *J. Am. Chem. Soc.* *134*, 8212–8221.
- Alberts, A.W., Chen, J., Kuron, G., Hunt, V., Huff, J., Hoffman, C., Rothrock, J., Lopez, M., Joshua, H., Harris, E., et al. (1980). Mevinolin: a highly potent competitive inhibitor of hydroxymethylglutaryl-coenzyme A reductase and a cholesterol-lowering agent. *Proc. Natl. Acad. Sci. USA* *77*, 3957–3961.
- Arakawa, M., Someno, T., Kawada, M., and Ikeda, D. (2008). A new terrein glucoside, a novel inhibitor of angiogenin secretion in tumor angiogenesis. *J. Antibiot.* *61*, 442–448.
- Awakawa, T., Yokota, K., Funa, N., Doi, F., Mori, N., Watanabe, H., and Horinouchi, S. (2009). Physically discrete beta-lactamase-type thioesterase catalyzes product release in atrochryson synthesis by iterative type I polyketide synthase. *Chem. Biol.* *16*, 613–623.
- Barton, D.H.R., and Miller, E. (1955). The constitution and stereochemistry of terrein. *J. Chem. Soc.* *0*, 1028–1029.
- Birch, A.J., Cassera, A., and Jones, A.R. (1965). The biosynthesis of terrein. *Chem. Commun. (Camb.)* *9*, 167–168.
- Brown, D.W., Adams, T.H., and Keller, N.P. (1996). *Aspergillus* has distinct fatty acid synthases for primary and secondary metabolism. *Proc. Natl. Acad. Sci. USA* *93*, 14873–14877.
- Crawford, J.M., Dancy, B.C., Hill, E.A., Udway, D.W., and Townsend, C.A. (2006). Identification of a starter unit acyl-carrier protein transacylase domain in an iterative type I polyketide synthase. *Proc. Natl. Acad. Sci. USA* *103*, 16728–16733.
- Crawford, J.M., Korman, T.P., Labonte, J.W., Vagstad, A.L., Hill, E.A., Kamari-Bidkorpeh, O., Tsai, S.C., and Townsend, C.A. (2009). Structural basis for biosynthetic programming of fungal aromatic polyketide cyclization. *Nature* *461*, 1139–1143.
- Damare, S., Raghukumar, C., and Raghukumar, S. (2006). Fungi in deep-sea sediments of the Central Indian Basin. *Deep-Sea Res. Oceanogr.*, *1*, 14–27.
- Demasi, M., Felicio, A.L., Pacheco, A.O., Leite, H.G., Lima, C., and Andrade, L.H. (2010). Studies on terrein as a new class of proteasome inhibitors. *J. Braz. Chem. Soc.* *21*, 299–305.
- Fleck, C.B., and Brock, M. (2010). *Aspergillus fumigatus* catalytic glucokinase and hexokinase: expression analysis and importance for germination, growth, and conidiation. *Eukaryot. Cell* *9*, 1120–1135.
- Fujii, I., Ono, Y., Tada, H., Gomi, K., Ebizuka, Y., and Sankawa, U. (1996). Cloning of the polyketide synthase gene *atX* from *Aspergillus terreus* and its identification as the 6-methylsalicylic acid synthase gene by heterologous expression. *Mol. Gen. Genet.* *253*, 1–10.
- Fujii, I., Watanabe, A., Sankawa, U., and Ebizuka, Y. (2001). Identification of Claisen cyclase domain in fungal polyketide synthase WA, a naphthopyrone synthase of *Aspergillus nidulans*. *Chem. Biol.* *8*, 189–197.
- Gressler, M., Zaehle, C., Scherlach, K., Hertweck, C., and Brock, M. (2011). Multifactorial induction of an orphan PKS-NRPS gene cluster in *Aspergillus terreus*. *Chem. Biol.* *18*, 198–209.
- Grove, J.F. (1954). The structure of terrein. *J. Chem. Soc.* *0*, 4693–4694.
- Guo, C.J., Knox, B.P., Chiang, Y.M., Lo, H.C., Sanchez, J.F., Lee, K.H., Oakley, B.R., Bruno, K.S., and Wang, C.C. (2012). Molecular genetic

- characterization of a cluster in *A. terreus* for biosynthesis of the meroterpenoid terretonin. *Org. Lett.* **14**, 5684–5687.
- Guo, C.J., Yeh, H.H., Chiang, Y.M., Sanchez, J.F., Chang, S.L., Bruno, K.S., and Wang, C.C. (2013). Biosynthetic pathway for the epipolythiodioxopiperazine acetylaranotin in *Aspergillus terreus* revealed by genome-based deletion analysis. *J. Am. Chem. Soc.* **135**, 7205–7213.
- He, J., Wijeratne, E.M., Bashyal, B.P., Zhan, J., Seliga, C.J., Liu, M.X., Pierson, E.E., Pierson, L.S., 3rd, VanEtten, H.D., and Gunatilaka, A.A. (2004). Cytotoxic and other metabolites of *Aspergillus* inhabiting the rhizosphere of Sonoran desert plants. *J. Nat. Prod.* **67**, 1985–1991.
- Hendrickson, L., Davis, C.R., Roach, C., Nguyen, D.K., Aldrich, T., McAda, P.C., and Reeves, C.D. (1999). Lovastatin biosynthesis in *Aspergillus terreus*: characterization of blocked mutants, enzyme activities and a multifunctional polyketide synthase gene. *Chem. Biol.* **6**, 429–439.
- Hill, R.A., Carter, R.H., and Staunton, J. (1981). Biosynthesis of fungal metabolites. Terrein, a metabolite of *Aspergillus terreus* Thom. *J. Chem. Soc., Perkin Trans. 1*, 2570–2576.
- Jørgensen, T.R., Park, J., Arentshorst, M., van Welzen, A.M., Lamers, G., Vankuyk, P.A., Damveld, R.A., van den Hondel, C.A., Nielsen, K.F., Frisvad, J.C., and Ram, A.F. (2011). The molecular and genetic basis of conidial pigmentation in *Aspergillus niger*. *Fungal Genet. Biol.* **48**, 544–553.
- Kanemori, Y., Gomi, K., Kitamoto, K., Kumagai, C., and Tamura, G. (1999). Insertion analysis of putative functional elements in the promoter region of the *Aspergillus oryzae* Taka-amylase A gene (*amyB*) using a heterologous *Aspergillus nidulans amdS-lacZ* fusion gene system. *Biosci. Biotechnol. Biochem.* **63**, 180–183.
- Kennedy, J., Auclair, K., Kendrew, S.G., Park, C., Vederas, J.C., and Hutchinson, C.R. (1999). Modulation of polyketide synthase activity by accessory proteins during lovastatin biosynthesis. *Science* **284**, 1368–1372.
- Kuenz, A., Gallenmüller, Y., Wille, T., and Vorlop, K.D. (2012). Microbial production of itaconic acid: developing a stable platform for high product concentrations. *Appl. Microbiol. Biotechnol.* **96**, 1209–1216.
- Langfelder, K., Jahn, B., Gehringer, H., Schmidt, A., Wanner, G., and Brakhage, A.A. (1998). Identification of a polyketide synthase gene (*pkpP*) of *Aspergillus fumigatus* involved in conidial pigment biosynthesis and virulence. *Med. Microbiol. Immunol. (Berl.)* **187**, 79–89.
- Lee, Y.H., Lee, N.H., Bhattarai, G., Oh, Y.T., Yu, M.K., Yoo, I.D., Jhee, E.C., and Yi, H.K. (2010). Enhancement of osteoblast biocompatibility on titanium surface with Terrein treatment. *Cell Biochem. Funct.* **28**, 678–685.
- Liao, W.Y., Shen, C.N., Lin, L.H., Yang, Y.L., Han, H.Y., Chen, J.W., Kuo, S.C., Wu, S.H., and Liaw, C.C. (2012). Asperjinone, a nor-neolignan, and terrein, a suppressor of ABCG2-expressing breast cancer cells, from thermophilic *Aspergillus terreus*. *J. Nat. Prod.* **75**, 630–635.
- Mayorga, M.E., and Timberlake, W.E. (1992). The developmentally regulated *Aspergillus nidulans wA* gene encodes a polypeptide homologous to polyketide and fatty acid synthases. *Mol. Gen. Genet.* **235**, 205–212.
- Narra, M., Dixit, G., Divecha, J., Madamwar, D., and Shah, A.R. (2012). Production of cellulases by solid state fermentation with *Aspergillus terreus* and enzymatic hydrolysis of mild alkali-treated rice straw. *Bioresour. Technol.* **121**, 355–361.
- Park, S.H., Kim, D.S., Kim, W.G., Ryoo, I.J., Lee, D.H., Huh, C.H., Youn, S.W., Yoo, I.D., and Park, K.C. (2004). Terrein: a new melanogenesis inhibitor and its mechanism. *Cell. Mol. Life Sci.* **61**, 2878–2885.
- Phattanawasin, P., Pojchanakom, K., Sotanaphun, U., Piyapolrungraj, N., and Zungsontiporn, S. (2007). Weed growth inhibitors from *Aspergillus fischeri* TISTR 3272. *Nat. Prod. Res.* **21**, 1286–1291.
- Porameesanaporn, Y., Uthaisang-Tanechpongthamb, W., Jarintanan, F., Jongrungruangchok, S., and Thanomsub Wongsatayanon, B. (2013). Terrein induces apoptosis in HeLa human cervical carcinoma cells through p53 and ERK regulation. *Oncol. Rep.* **29**, 1600–1608.
- Raistrick, H., and Smith, G. (1935). Studies in the biochemistry of micro-organisms: The metabolic products of *Aspergillus terreus* Thom. A new mould metabolic product-terrein. *Biochem. J.* **29**, 606–611.
- Reddy, C.S., and Singh, R.P. (2002). Enhanced production of itaconic acid from corn starch and market refuse fruits by genetically manipulated *Aspergillus terreus* SKR10. *Bioresour. Technol.* **85**, 69–71.
- Samson, R.A., Peterson, S.W., Frisvad, J.C., and Varga, J. (2011). New species in *Aspergillus* section *Terrei*. *Stud. Mycol.* **69**, 39–55.
- Sanchez, J.F., Chiang, Y.M., Szewczyk, E., Davidson, A.D., Ahuja, M., Elizabeth Oakley, C., Woo Bok, J., Keller, N., Oakley, B.R., and Wang, C.C. (2010). Molecular genetic analysis of the orsellinic acid/F9775 gene cluster of *Aspergillus nidulans*. *Mol. Biosyst.* **6**, 587–593.
- Schroeckh, V., Scherlach, K., Nützmann, H.W., Shelest, E., Schmidt-Heck, W., Schuemann, J., Martin, K., Hertweck, C., and Brakhage, A.A. (2009). Intimate bacterial-fungal interaction triggers biosynthesis of archetypal polyketides in *Aspergillus nidulans*. *Proc. Natl. Acad. Sci. USA* **106**, 14558–14563.
- Shimada, A., Kusano, M., Takeuchi, S., Fujioka, S., Inokuchi, T., and Kimura, Y. (2002). Aspterric acid and 6-hydroxymellein, inhibitors of pollen development in *Arabidopsis thaliana*, produced by *Aspergillus terreus*. *Z. Naturforsch., C, J. Biosci.* **57**, 459–464.
- Slesiona, S., Gressler, M., Mihan, M., Zaehle, C., Schaller, M., Barz, D., Hube, B., Jacobsen, I.D., and Brock, M. (2012). Persistence versus escape: *Aspergillus terreus* and *Aspergillus fumigatus* employ different strategies during interactions with macrophages. *PLoS ONE* **7**, e31223.
- Thywißen, A., Heinekamp, T., Dahse, H.M., Schmalder-Ripcke, J., Nietzsche, S., Zipfel, P.F., and Brakhage, A.A. (2011). Conidial dihydroxynaphthalene melanin of the human pathogenic fungus *Aspergillus fumigatus* interferes with the host endocytosis pathway. *Front. Microbiol.* **2**, 96.
- Tobert, J.A. (2003). Lovastatin and beyond: the history of the HMG-CoA reductase inhibitors. *Nat. Rev. Drug Discov.* **2**, 517–526.
- Watanabe, A., and Ebizuka, Y. (2004). Unprecedented mechanism of chain length determination in fungal aromatic polyketide synthases. *Chem. Biol.* **11**, 1101–1106.
- Watanabe, C.M., Wilson, D., Linz, J.E., and Townsend, C.A. (1996). Demonstration of the catalytic roles and evidence for the physical association of type I fatty acid synthases and a polyketide synthase in the biosynthesis of aflatoxin B1. *Chem. Biol.* **3**, 463–469.
- Watanabe, A., Fujii, I., Sankawa, U., Mayorga, M.E., Timberlake, W.E., and Ebizuka, Y. (1999). Re-identification of *Aspergillus nidulans wA* gene to code for a polyketide synthase of naphthopyrone. *Tetrahedron Lett.* **40**, 91–94.
- Wijeratne, E.M., Turbyville, T.J., Zhang, Z., Bigelow, D., Pierson, L.S., 3rd, VanEtten, H.D., Whitesell, L., Canfield, L.M., and Gunatilaka, A.A. (2003). Cytotoxic constituents of *Aspergillus terreus* from the rhizosphere of *Opuntia versicolor* of the Sonoran Desert. *J. Nat. Prod.* **66**, 1567–1573.
- Yadav, R.P., Saxena, R.K., Gupta, R., and Davidson, W.S. (1998). Purification and characterization of a regiospecific lipase from *Aspergillus terreus*. *Biotechnol. Appl. Biochem.* **28**, 243–249.
- Yin, Y., Xu, B., Li, Z., and Zhang, B. (2013). Enhanced production of (+)-terrein in fed-batch cultivation of *Aspergillus terreus* strain PF26 with sodium citrate. *World J. Microbiol. Biotechnol.* **29**, 441–446.
- Zamir, L.O., and Chin, C.C. (1982). Aromatic origin of cyclopentenoid metabolites. *Bioorg. Chem.* **11**, 338–349.

Chemistry & Biology, Volume 21

Supplemental Information

Terrein Biosynthesis in *Aspergillus terreus*

and Its Impact on Phytotoxicity

**Christoph Zaehle, Markus Gressler, Ekaterina Shelest, Elena Geib, Christian Hertweck,
and Matthias Brock**

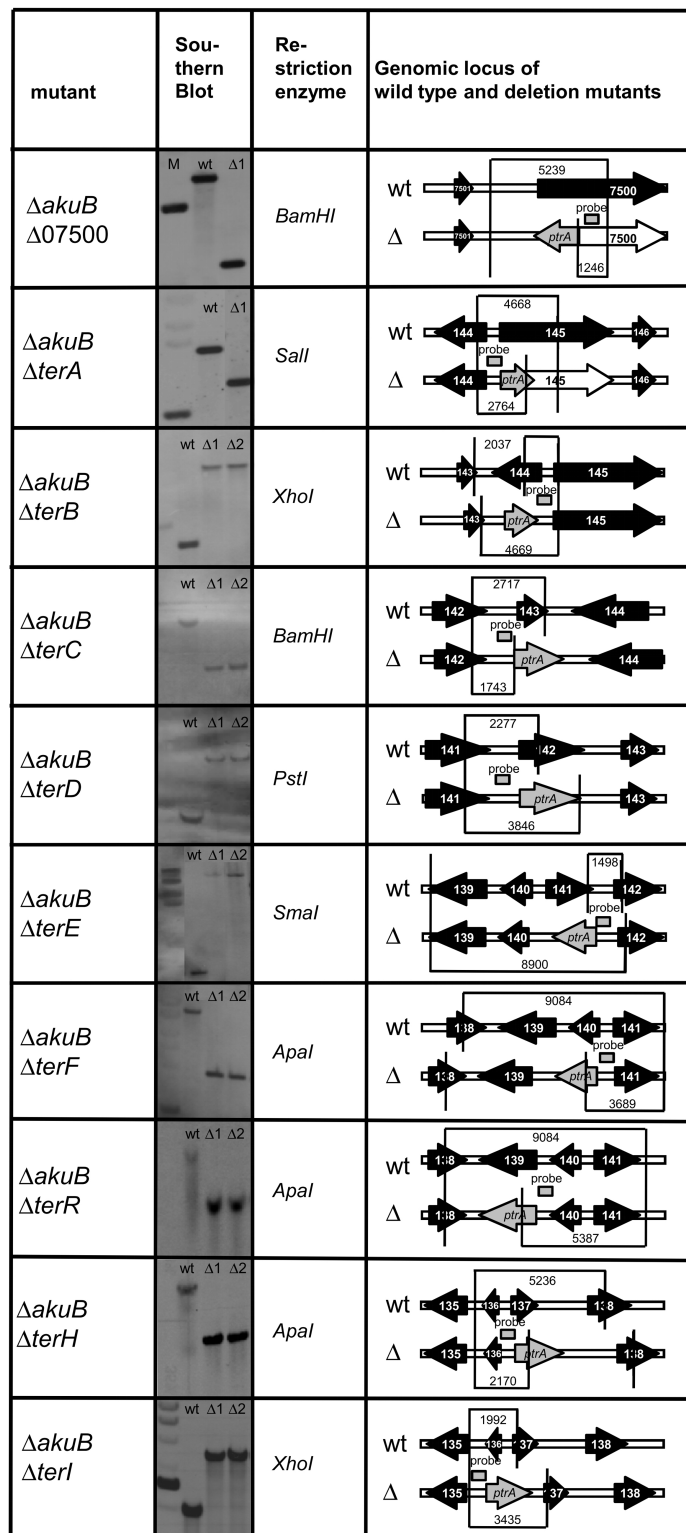


Figure S1: Southern blot analyses of ATEG07500 and terrein gene cluster deletion mutants. Homologous integration of the deletion cassettes was confirmed by Southern blot analysis by comparing wild type (\DeltaakuB , wt) and mutant fragments ($\Delta 1$, $\Delta 2$). The respective restriction enzymes are indicated. Hybridization was performed with digoxigenin-labeled probes. M indicates a molecular size marker. The expected fragment sizes (in bp) are denoted by connected lines. Arrows indicate open reading frames and grey bars the areas of probe hybridization. This figure is supplemental to Figure 2.

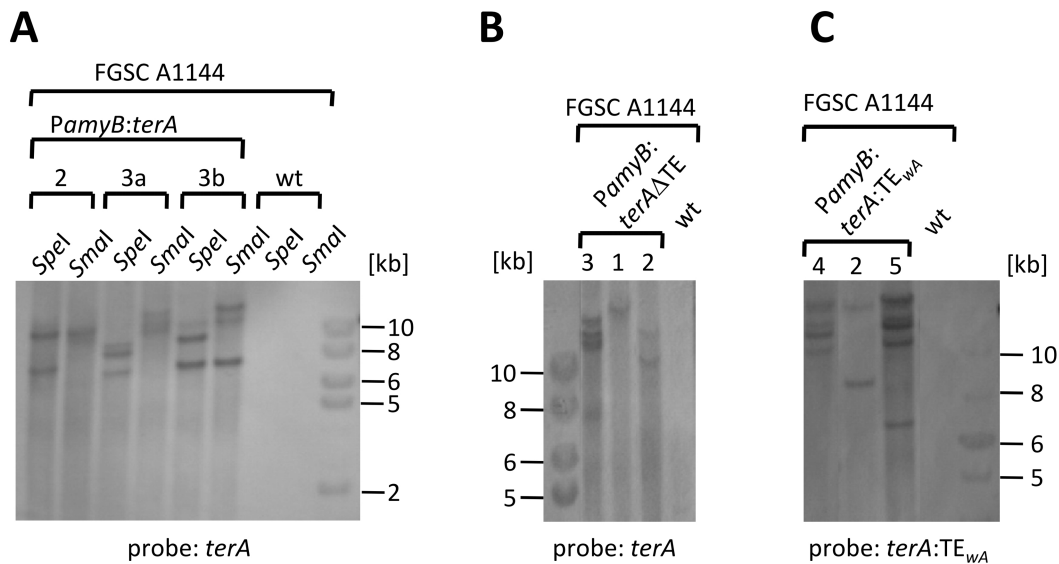


Figure S2: Southern blot analyses of *A. niger* FGSC A1144 transformants. All genes are expressed under control of the *A. oryzae amyB* promoter. For names and sequences of oligonucleotides used for generation of labeled probes refer to the table of oligonucleotides. **(A)** Southern blot of transformants expressing the native *terA* gene. Genomic DNA was either digested with *SmaI* or *SpeI*. The probe was amplified with P 101/104. Double (2) and triple (3a, 3b) integrations of the *PamyB:terA* construct are shown. **(B)** Southern blot of transformants expressing *terA* without TE-domain. Genomic DNA was digested with *KpnI*. The probe was amplified with P 52/54. Single (1), double (2) and triple (3) integrations of the *PamyB:terA* Δ TE construct are shown. **(C)** Southern blot of transformants overexpressing *terA*, from which the natural TE-domain was replaced with that from *A. nidulans wA*. Genomic DNA was digested with *KpnI*. The probe was amplified with P 58/101. Two (2), four (4) and five (5) integrations of the *PamyB:terA:TE_{wA}* construct are shown. This figure is supplemental to Figure 5.

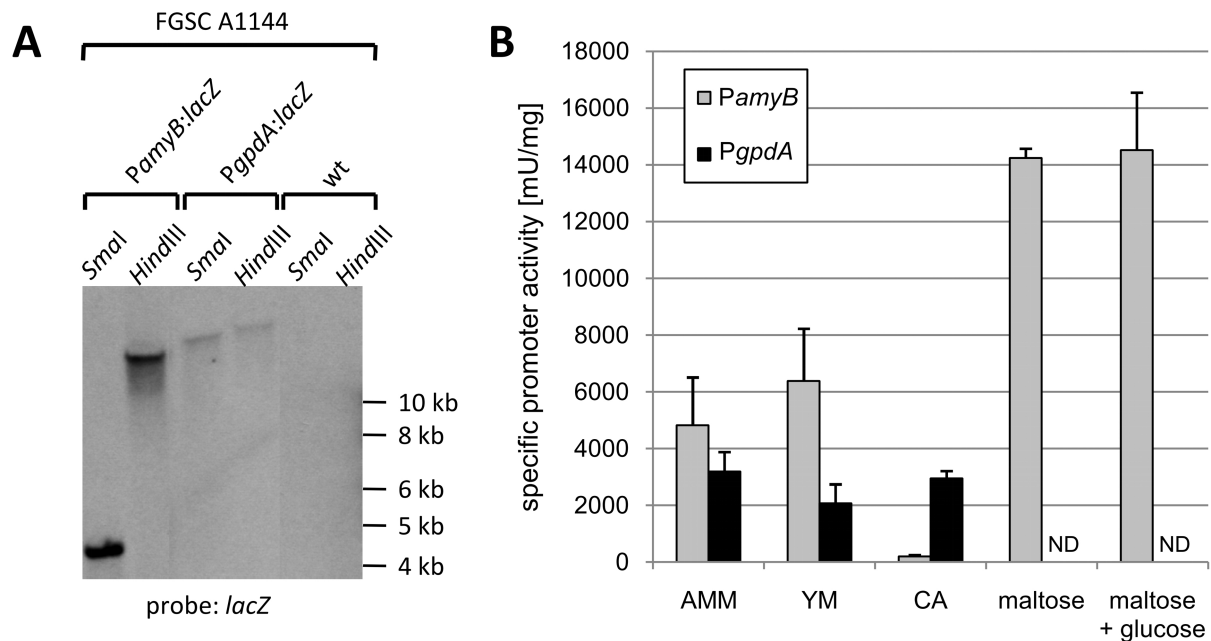


Figure S3: Southern blot analysis and promoter activity of *A. niger* A1144 *lacZ* reporter strains. (A) Southern blot analysis. Single copy integrations of *PamyB:lacZ* and *PgpdA:lacZ* were identified. Genomic DNA of the parental wild type (wt) revealed no signal when hybridized with a probe directed against the *lacZ* gene (amplified with oligonucleotides P53/54). (B) *PamyB* (grey bars) and *PgpdA* (black bars) activity determination by β -galactosidase activity detection from cell-free extracts. Mycelia were grown for 48 h on AMM with glucose, yeast malt extract (YM) and casamino acid (CA) containing media. The *PamyB* reporter strain was additionally tested on AMM with maltose in the presence and absence of glucose. Experiments were performed on biological triplicates. The glyceraldehyde-3-phosphate promoter (*PgpdA*) is constitutively active. The α -amylase promoter (*PamyB*) requires the presence of sugars and is not induced on CA. Strongest induction of *PamyB* is observed on maltose and glucose addition does not reduce the promoter activity. ND = not determined. Error bars denoted \pm SD. This figure is supplemental to Figure 5.

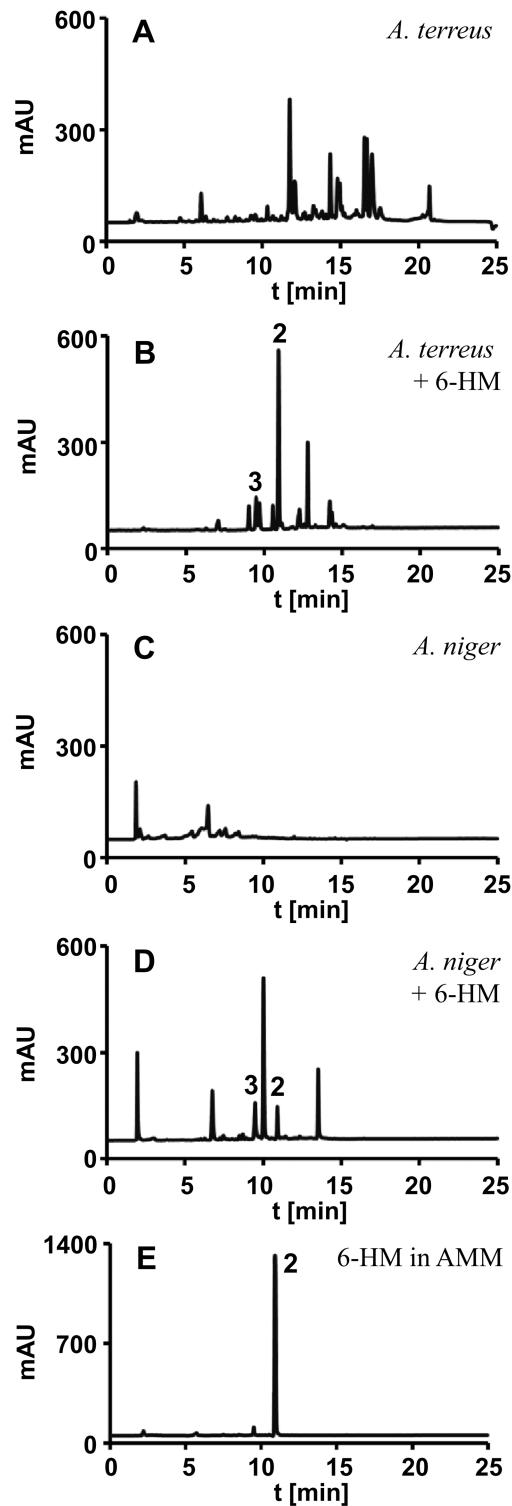


Figure S4: HPLC metabolite profiles of *A. terreus* SBUG844 and *A. niger* FGSC A1144 extracts. Extracts from *A. terreus* and *A. niger* without (A, C) or with (B, D) supplementation of 6-hydroxymellein (6-HM = compound 2). Both fungi hydroxylate and biotransform compound 2 into other metabolites such as compound 3 (6,7-dihydroxymellein). Compound 2 remains stable when incubated in sterile culture medium AMM (E). This figure is supplemental to Figure 7.

Supplemental Figure S5
Zaehle et al.

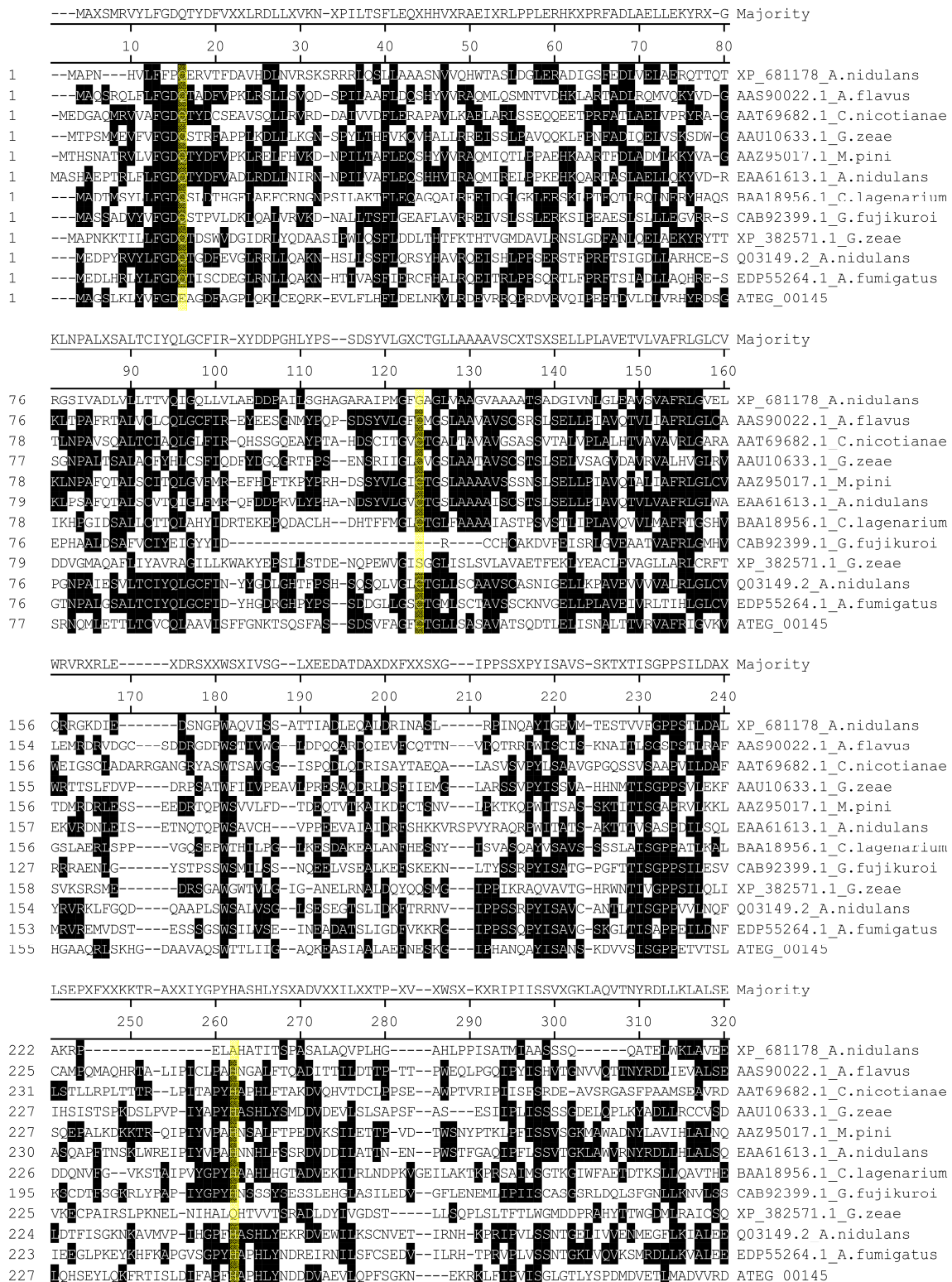
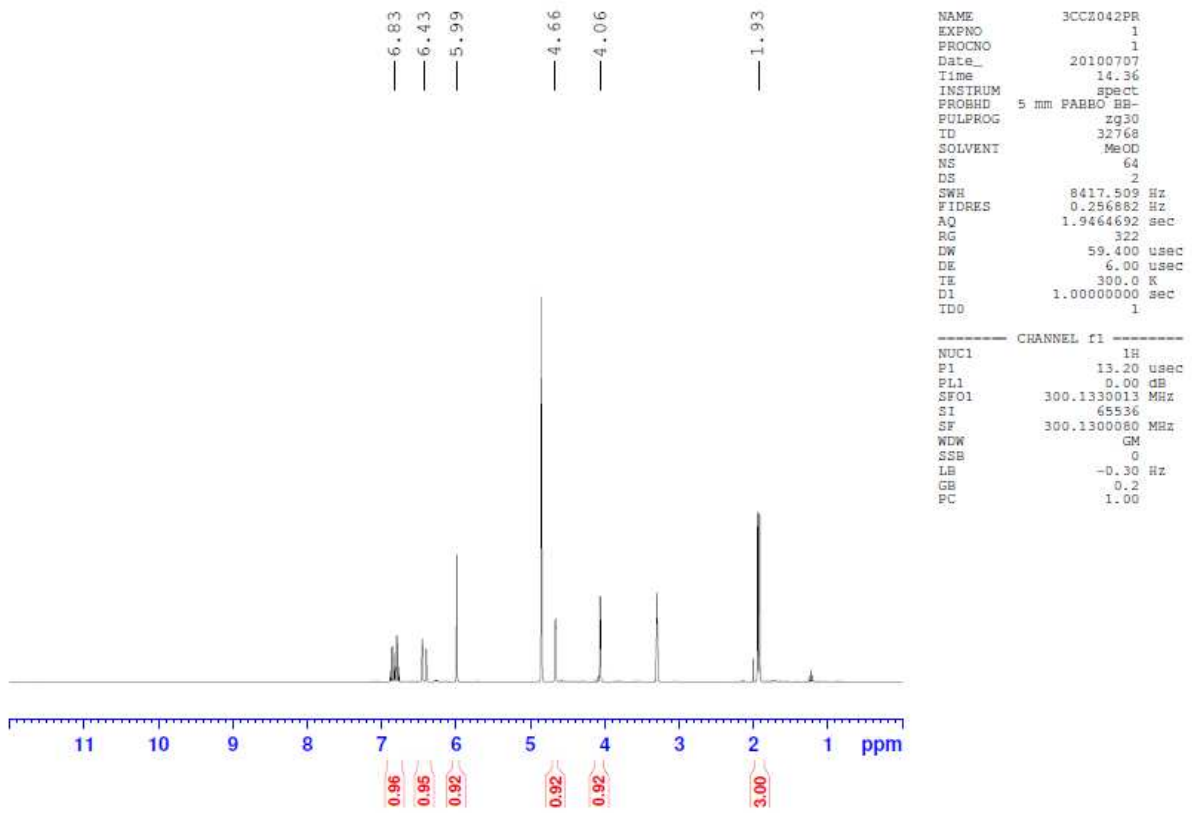


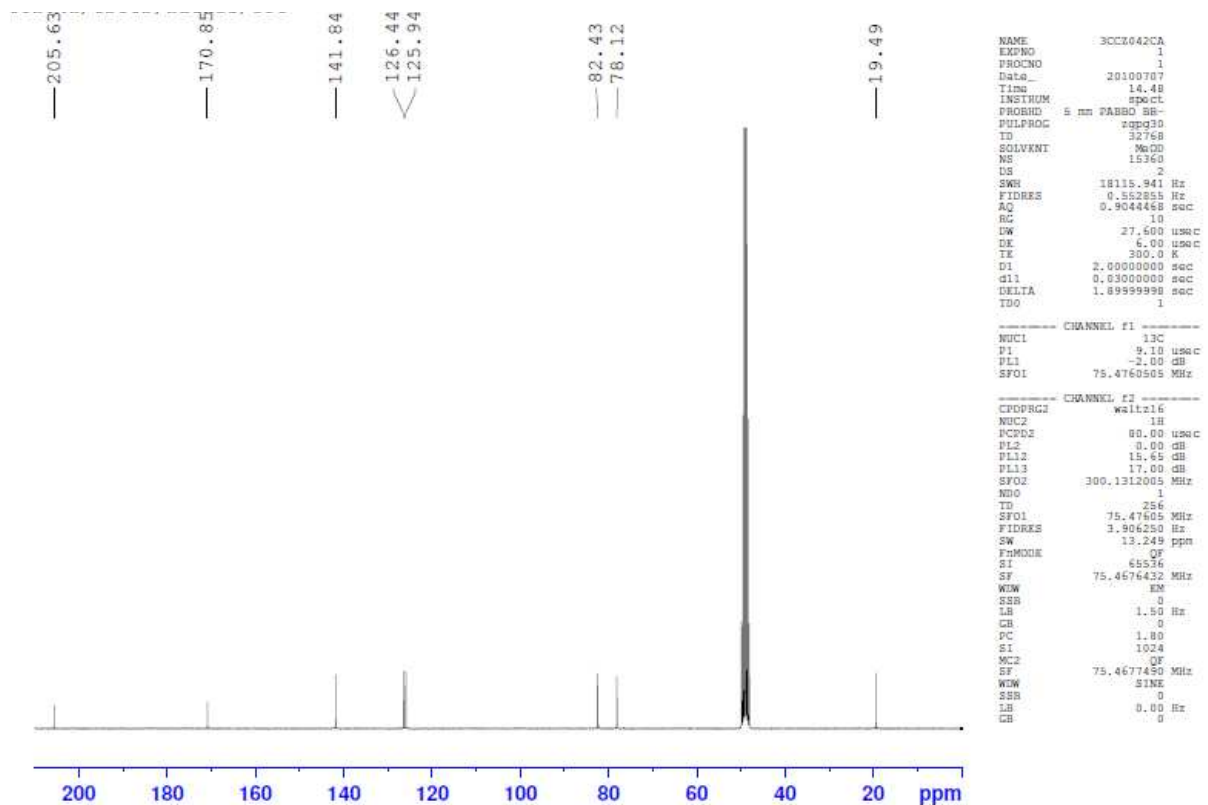
Figure S5: Protein alignment of the *A. terreus* PKS *terA* starter acyl transferase (SAT) unit with sequences from other characterized fungal PKS's. Sequences were aligned using ClustelW algorithm (Megalign DNAsar Lasergene Vers.7.2.1). Areas marked in black indicate identical amino acids. The potential SAT domain contains the proposed catalytic triad (yellow boxes) with the essential Cys¹²⁴. This figure is supplemental to Figure 1.

Supplemental Figure S6
Zaehle et al.

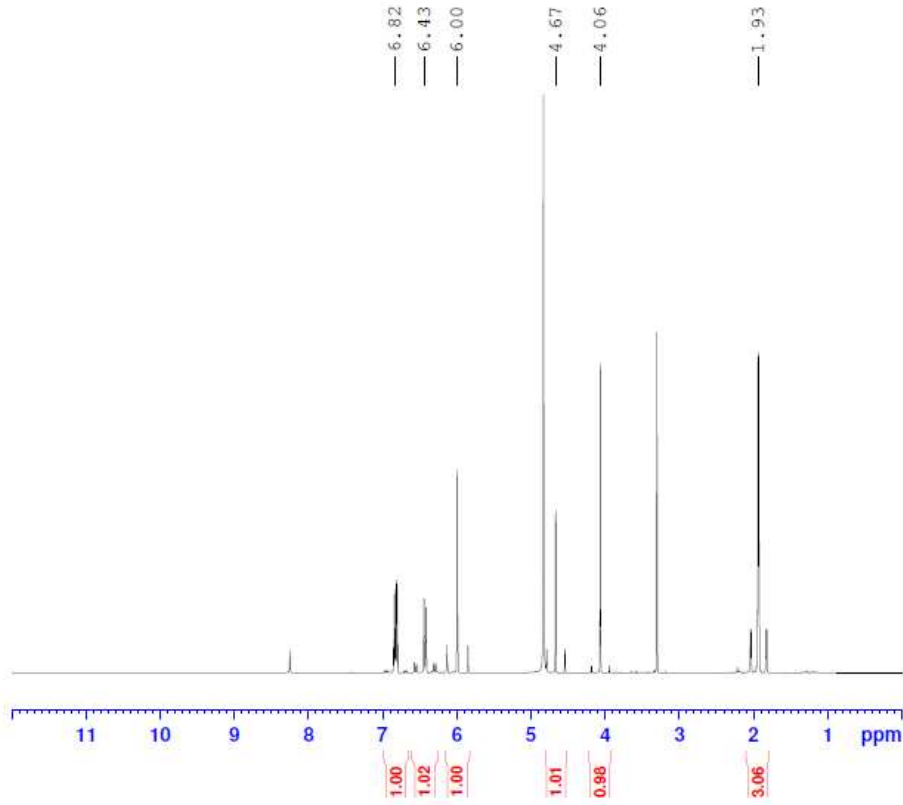
A



B



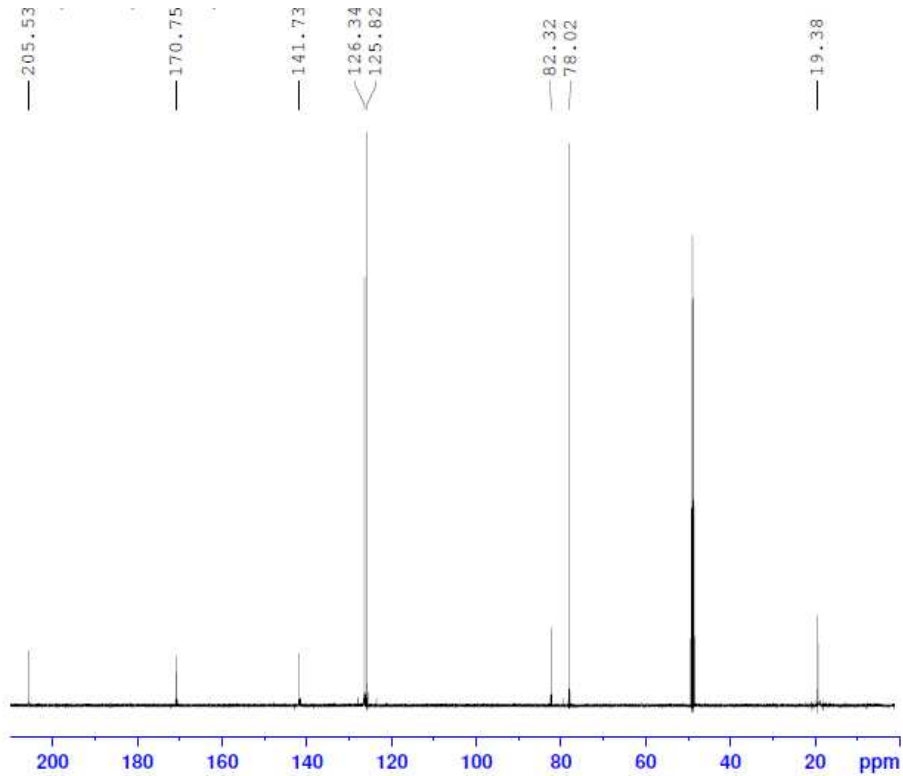
C



```
NAME      6CMG082MU
EXPNO     1
PROCNO    1
Date_     20130116
Time      9.18
INSTRUM   spect
PROBHD    5 mm CPTCI 1H-
PULPROG   zg30
TD         65536
SOLVENT   MeOD
NS         256
DS         2
SWH       12019.230 Hz
FIDRES    0.183399 Hz
AQ        2.7263477 sec
RG         36
DW        41.600 usec
DE        6.50 usec
TE        300.1 K
D1        1.00000000 sec
ID0       1

----- CHANNEL f1 -----
NUC1      1H
P1        8.00 usec
PL1       4.00 dB
PL1W      5.00000000 W
SFO1      600.2754024 MHz
SI        262144
SF        600.2700212 MHz
WDW       EM
SSB       0
LB        0.30 Hz
GB        0
PC        1.00
```

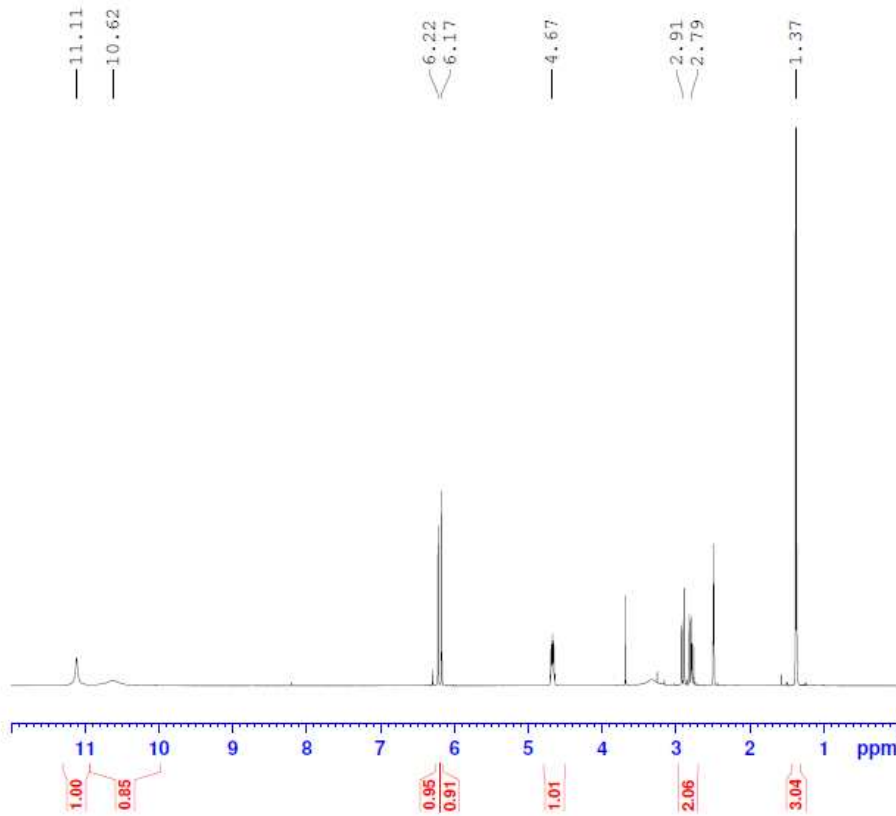
D



```
NAME      6CMG082MU
EXPNO     50
PROCNO    1
Date_     20130116
Time      9.35
INSTRUM   spect
PROBHD    5 mm CPTCI 1H-
PULPROG   zg1q30
TD         65400
SOLVENT   MeOD
NS         354
DS         2
SWH       36231.883 Hz
FIDRES    0.554004 Hz
AQ        0.9025700 sec
RG         1.6
DW        13.800 usec
DE        6.50 usec
TE        300.1 K
D1        2.00000000 sec
D11       0.03000000 sec
ID0       1

----- CHANNEL f1 -----
NUC1      13C
P1        14.00 usec
PL1       0.00 dB
PL1W      75.60778046 W
SFO1      150.9561246 MHz

----- CHANNEL f2 -----
CPDPRG2   waltz16
NUC2      1H
PCPD2     100.00 usec
PL2       4.00 dB
PL12      26.00 dB
PL2W      5.00000000 W
SFO2      600.2748022 MHz
SI        131072
SF        150.9378187 MHz
WDW       EM
SSB       0
LB        0.30 Hz
GB        0
PC        1.00
```

E

```

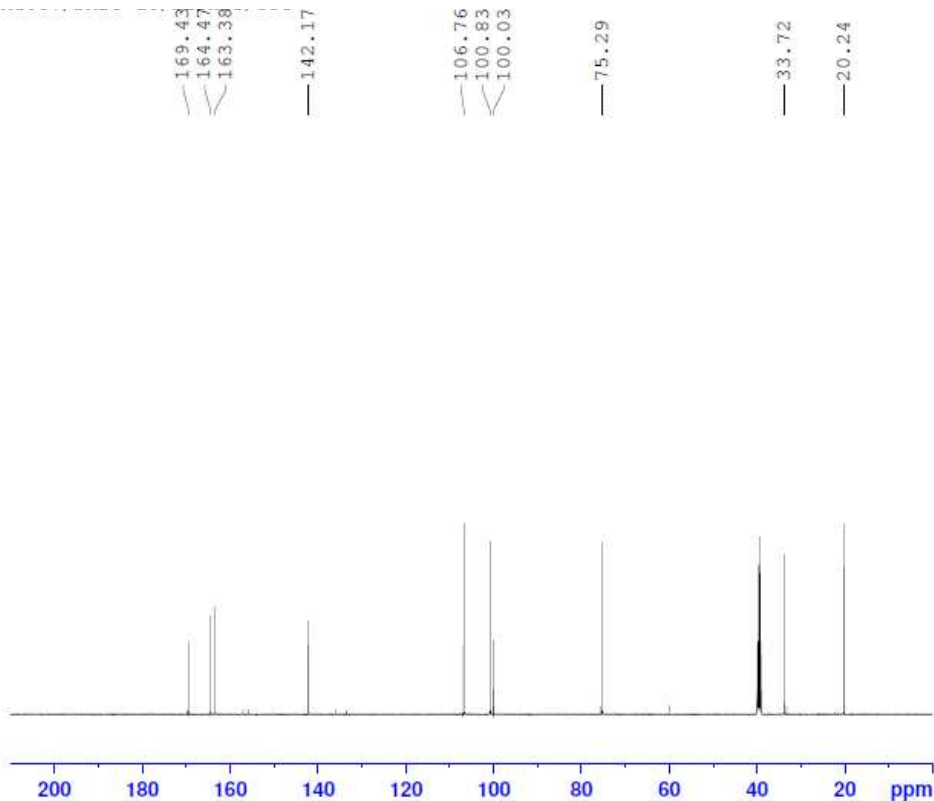
NAME      SCMG087PR
EXPNO     1
PROCNO    1
Date_     20130130
Time      10.48
INSTRUM   spect
PROBHD    5 mm PABBO BB-
PULPROG   zg30
TD         65536
SOLVENT   DMSO
NS         16
DS         2
SWH        10000.000 Hz
FIDRES     0.152588 Hz
AQ         3.2768500 sec
RG         181
DW         50.000 usec
DE         6.50 usec
TE         300.0 K
D1         1.00000000 sec
ID0        1

```

```

----- CHANNEL f1 -----
NUC1      1H
P1        14.00 usec
PL1       5.50 dB
PL1W      7.71660900 W
SFO1      500.3045027 MHz
SI        131072
SF        500.3000097 MHz
WDW       EM
SSB       0
LB        0.30 Hz
GB        0
PC        1.00

```

F

```

NAME      SCMG087CA
EXPNO     1
PROCNO    1
Date_     20130130
Time      7.41
INSTRUM   spect
PROBHD    5 mm PABBO BB-
PULPROG   zgpg30
TD         19996
SOLVENT   DMSO
NS         2994
DS         4
SWH        29761.904 Hz
FIDRES     1.488393 Hz
AQ         0.3358228 sec
RG         2050
DW         16.800 usec
DE         6.50 usec
TE         300.0 K
D1         3.00000000 sec
D11        0.03000000 sec
D12        0.00002000 sec
D20        10.00000000 sec
ID0        1

```

```

----- CHANNEL f1 -----
NUC1      13C
P1        13.00 usec
P12       2000.00 usec
P24       500.00 usec
PL1       3.30 dB
PL1W      44.17614746 W
SFO1      125.8150021 MHz
SFO2      9.18 MHz
SFO3      9.18 MHz
SPNAM2    Crp60comp.4
SPNAM3    Crp60, 0.5, 20.1
SFOAL2    0.500
SFOALS    0.500
SPOFFS2   0.00 Hz
SPOFFS3   0.00 Hz

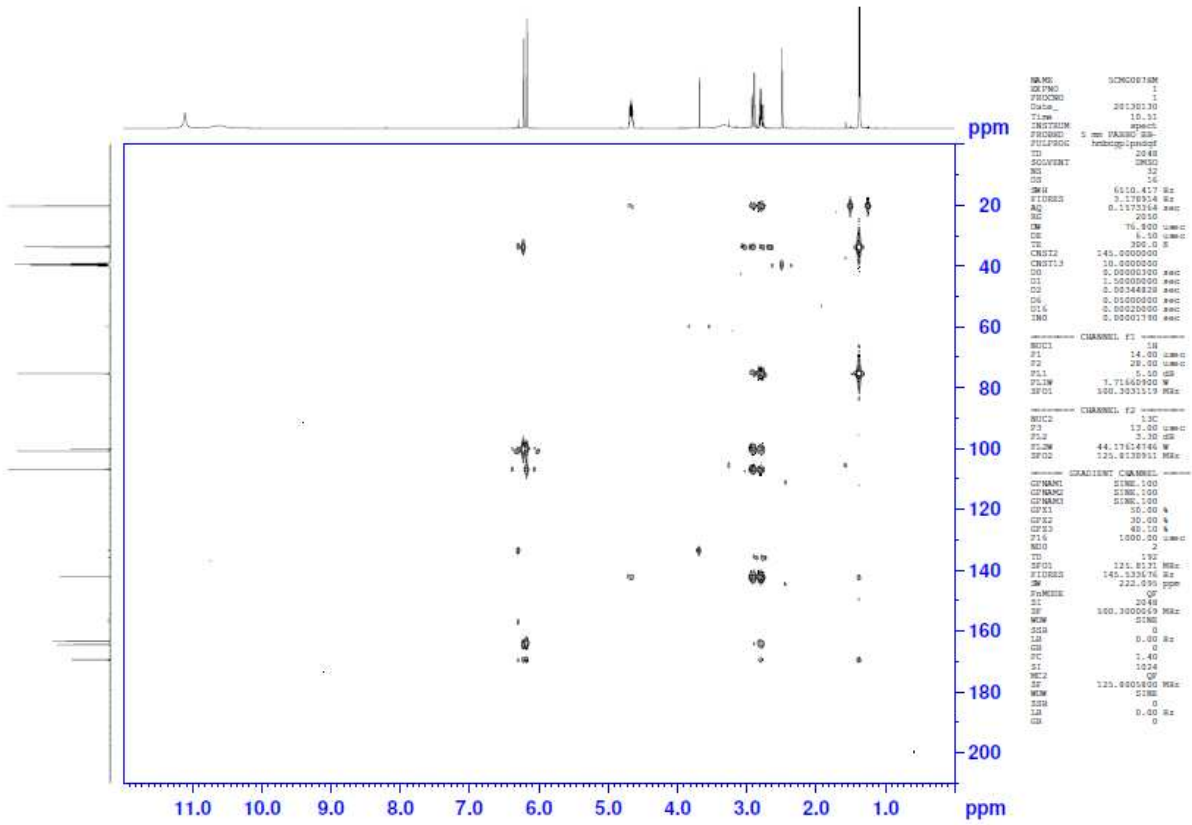
```

```

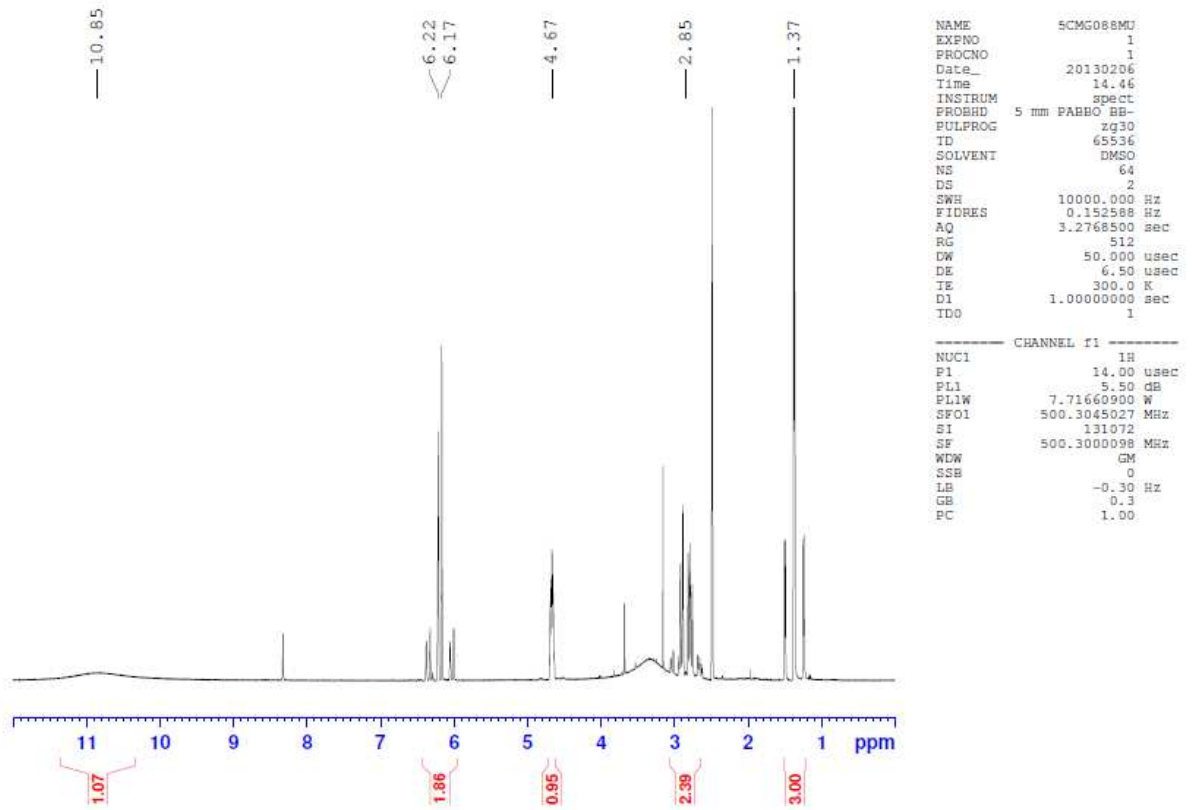
----- CHANNEL f2 -----
CPOPRG2   waltz16
NUC2      1H
PCPD2     100.00 usec
PL2       5.50 dB
PL12      22.58 dB
PL2W      7.71660900 W
PL1W      0.15115638 W
SFO2      500.3020012 MHz
SI        262144
SF        125.8005984 MHz
WDW       EM
SSB       0
LB        1.00 Hz
GB        0
PC        1.40

```

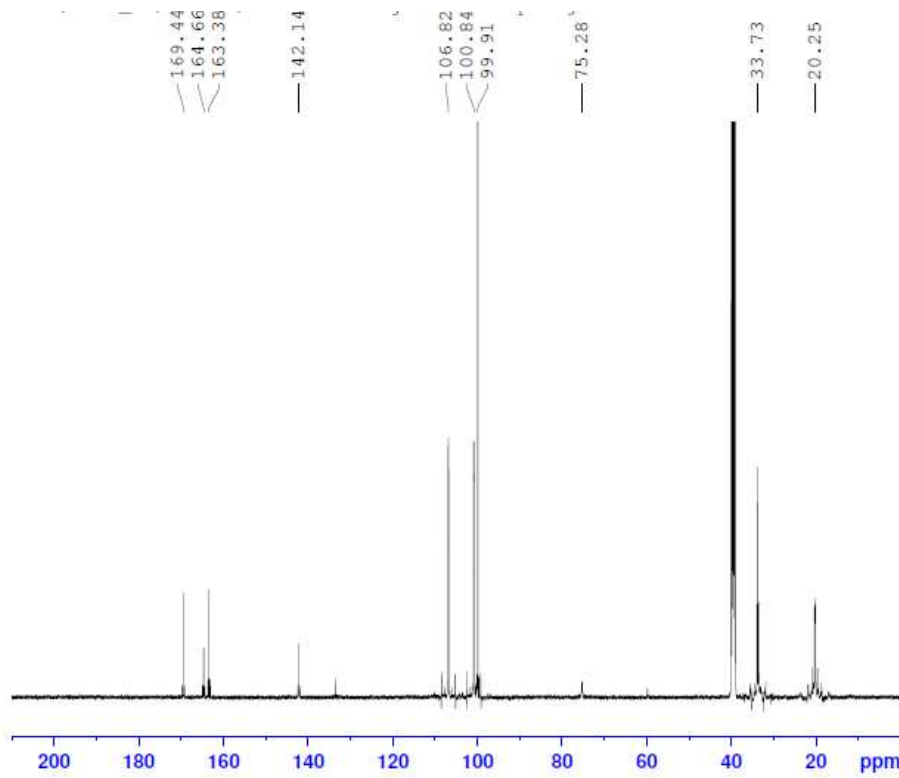
G



H



I

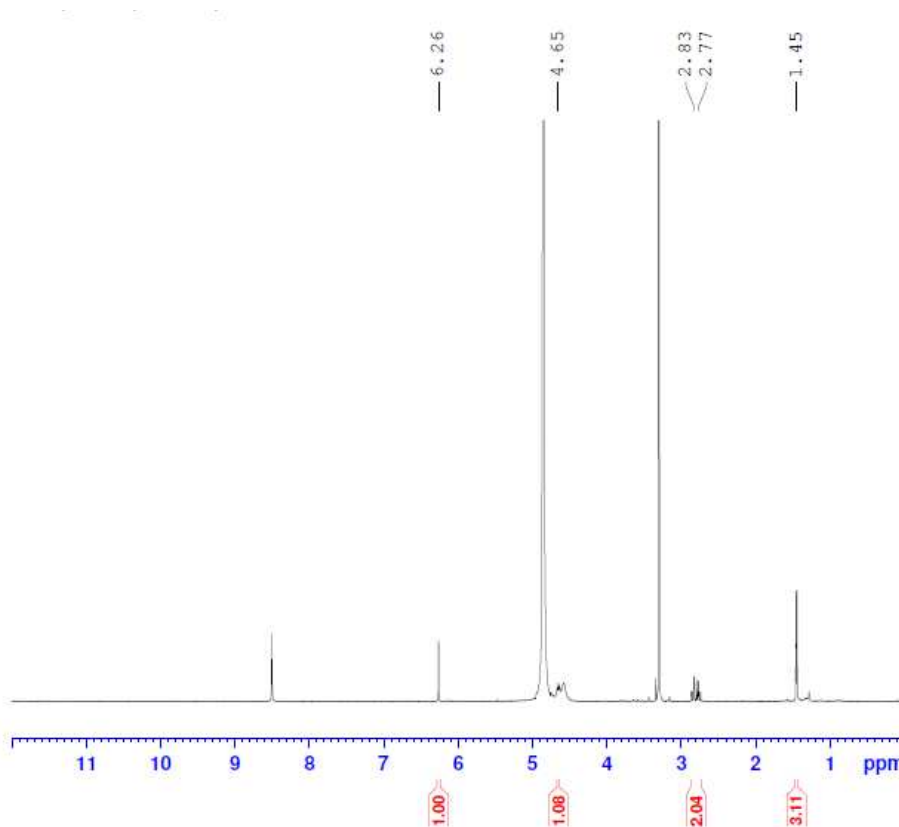


```
NAME          5CMG088MU
EXPNO         2
PROCNO        1
Date_         20130206
Time          14.58
INSTRUM       spect
PROBHD        5 mm FAPBO BB-
PULPROG       zg1q30
TD            65536
SOLVENT       DMSO
NS            9019
DS            4
SWH           29761.904 Hz
FIDRES        0.454131 Hz
AQ            1.1010548 sec
RG            2050
DW            16.800 usec
DE            6.50 usec
TE            300.1 K
D1            5.00000000 sec
D11           0.03000000 sec
TD0           1

----- CHANNEL f1 -----
NUC1          13C
P1            13.00 usec
PL1           3.30 dB
PL1W          44.17614745 W
SFO1          125.8143731 MHz

----- CHANNEL f2 -----
CPDPRG2       waltz16
NUC2          1H
PCPD2         100.00 usec
PL2           5.50 dB
PL12          22.58 dB
PLW           7.71660900 W
PL12W         0.15115638 W
SFO2          500.3075045 MHz
SI            32768
SF            125.8005978 MHz
WDW           EM
SSB           0
LB            1.00 Hz
GB            0
PC            1.40
```

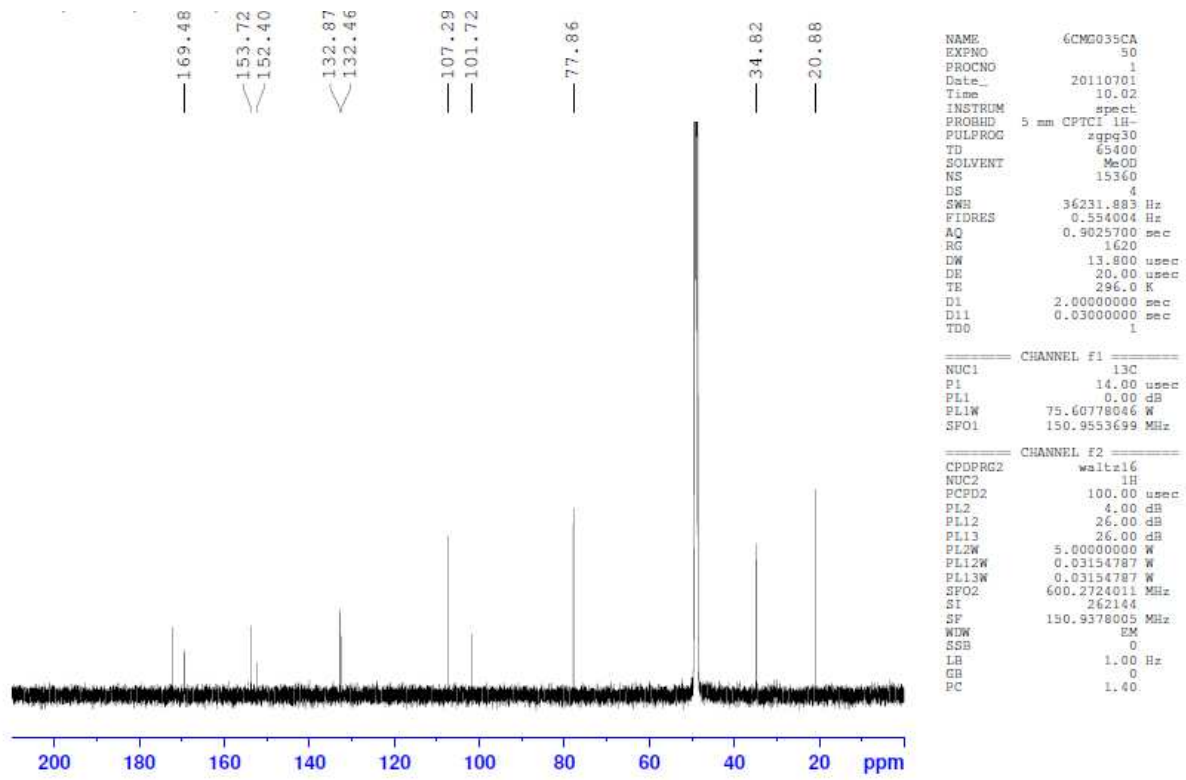
J



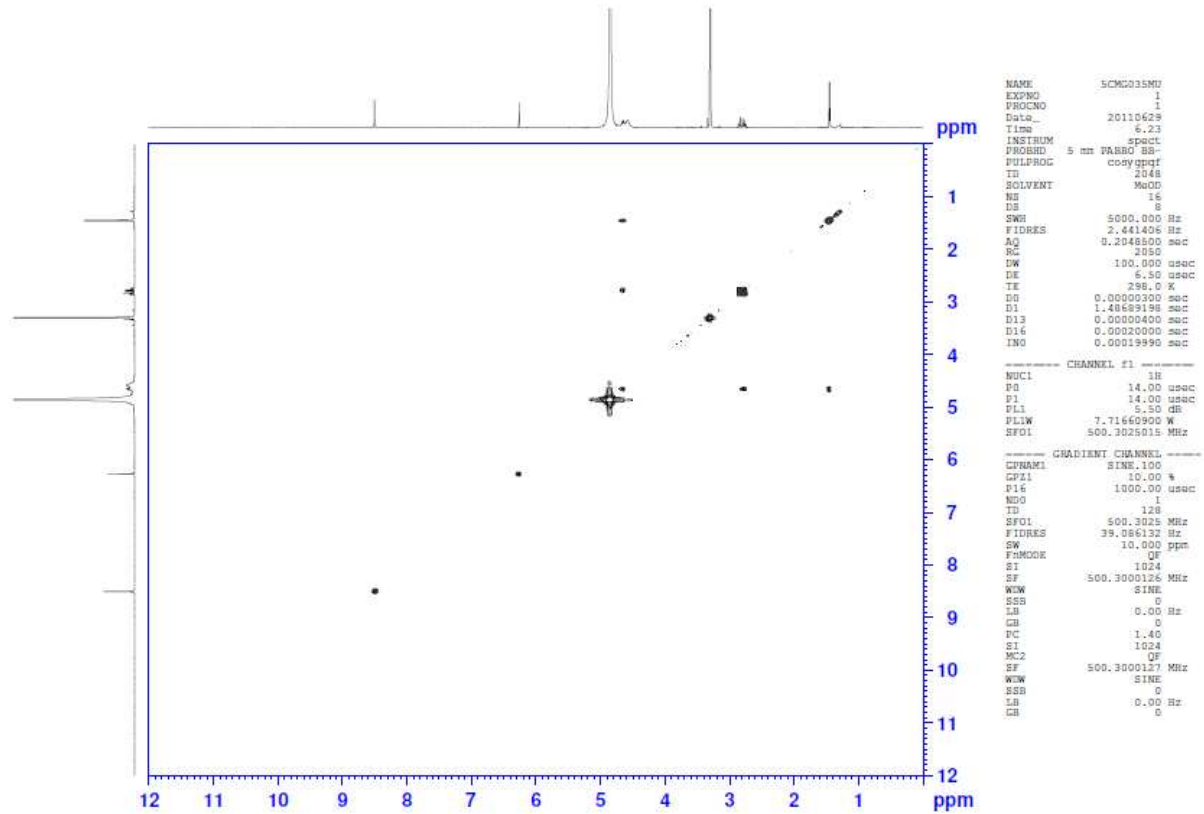
```
NAME          5CMG035PR
EXPNO         1
PROCNO        1
Date_         20110628
Time          14.24
INSTRUM       spect
PROBHD        5 mm FAPBO BB-
PULPROG       zg30
TD            65536
SOLVENT       MeOD
NS            128
DS            2
SWH           10000.000 Hz
FIDRES        0.152588 Hz
AQ            3.2768500 sec
RG            812
DW            50.000 usec
DE            6.50 usec
TE            298.0 K
D1            1.00000000 sec
TD0           1

----- CHANNEL f1 -----
NUC1          1H
P1            14.00 usec
PL1           5.50 dB
PL1W          7.71660900 W
SFO1          500.3045027 MHz
SI            131072
SF            500.3000153 MHz
WDW           EM
SSB           0
LB            0.30 Hz
GB            0
PC            1.00
```

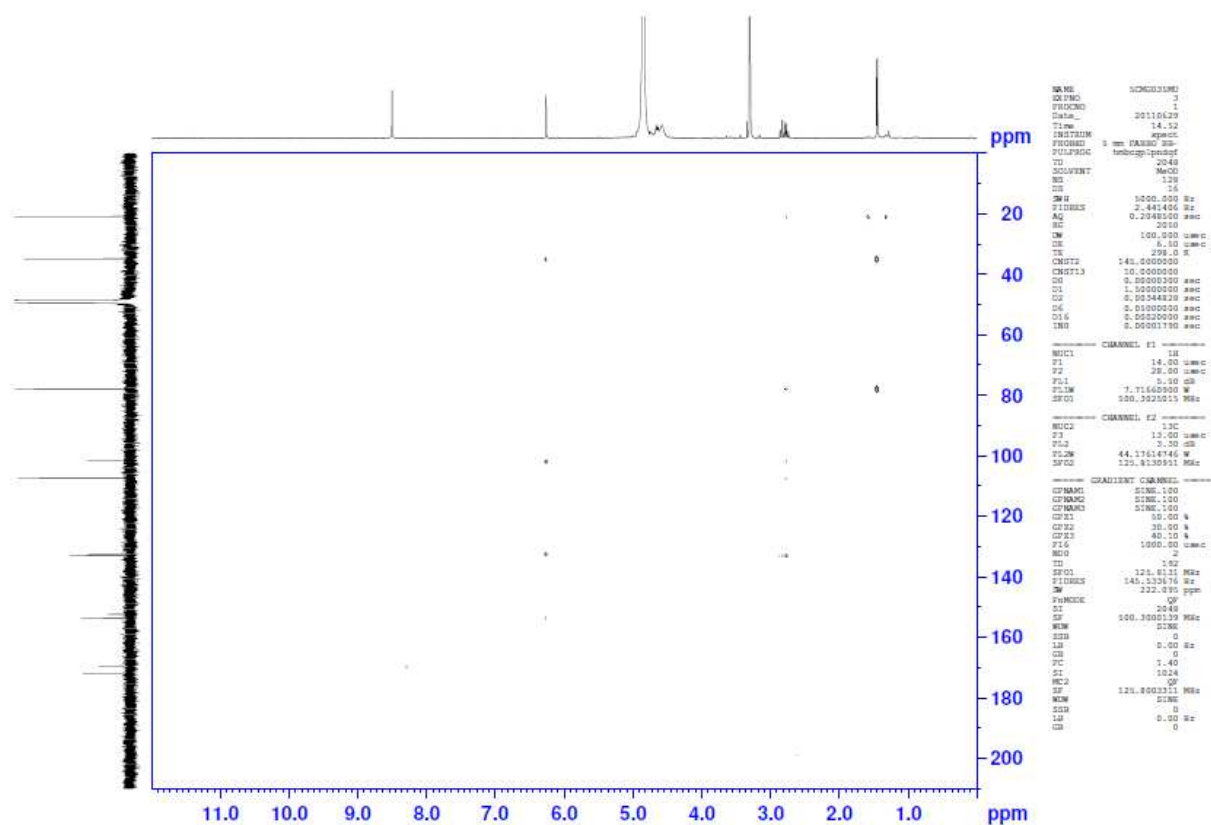
K



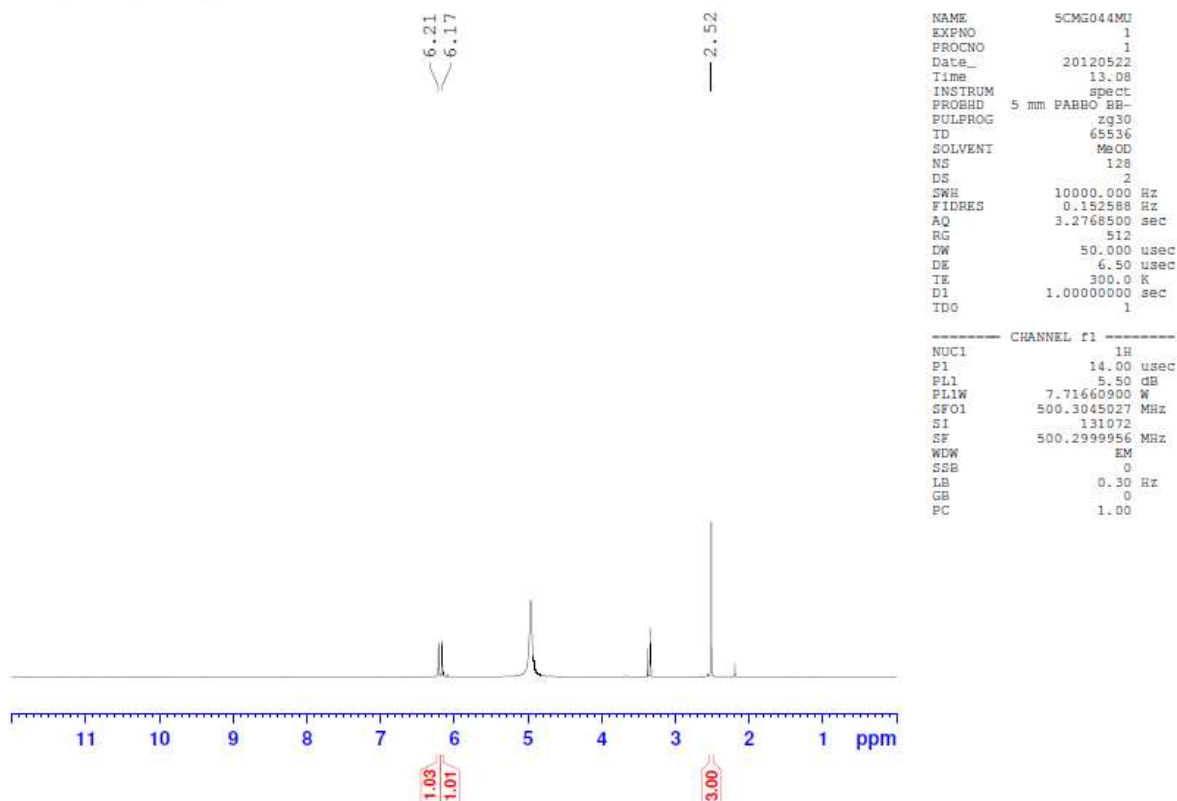
L



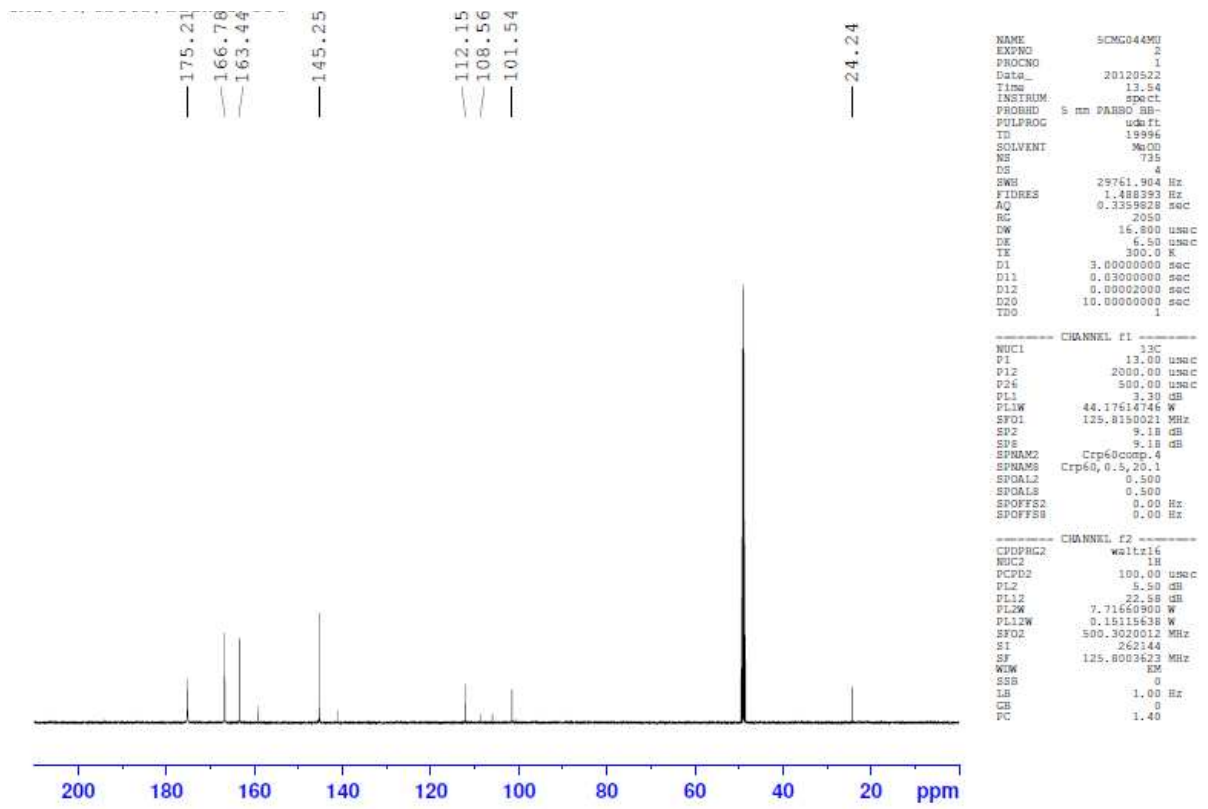
M



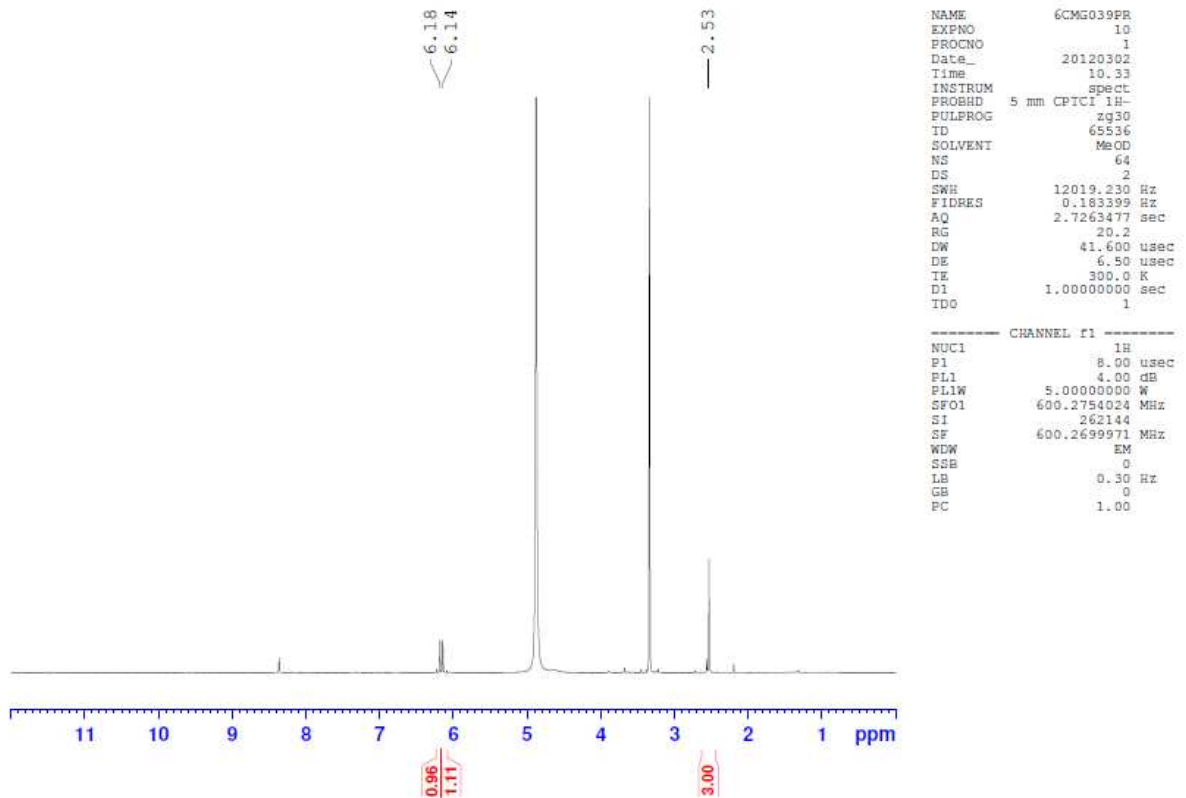
N



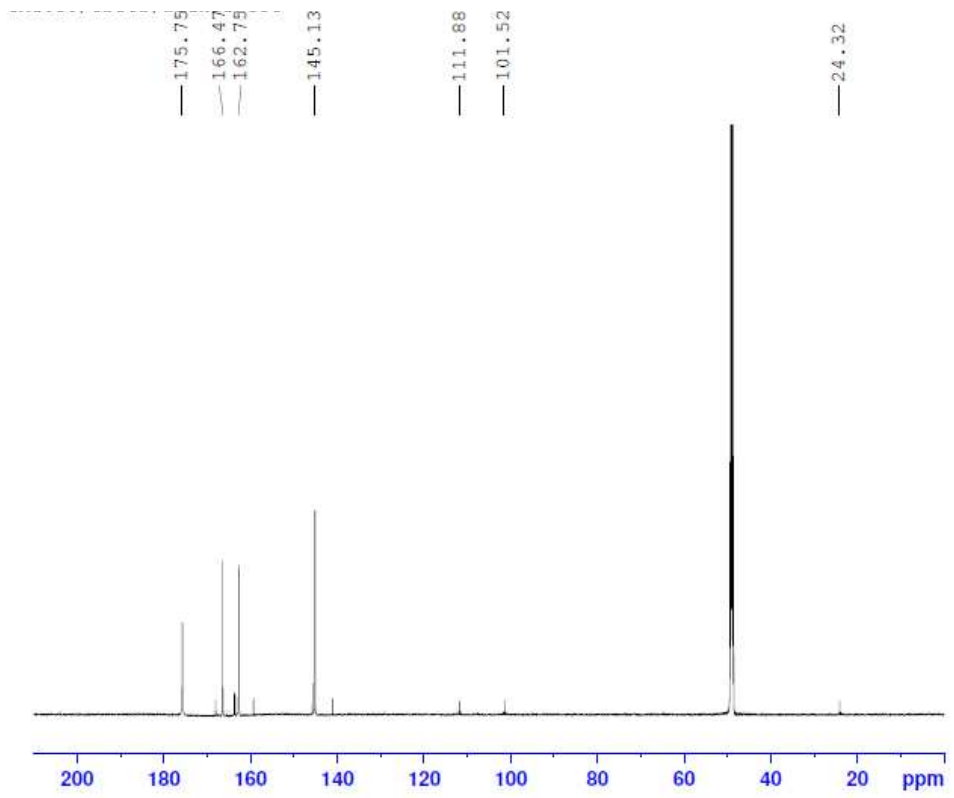
O



P



Q



```

NAME          5CMG039CA
EXPNO         50
PROCNO        1
Date_         20120301
Time          21.08
INSTRUM       spect
PROBHD        5 mm CP1CI 1H-
PULPROG       zgpg30
TD            23860
SOLVENT       MeOD
NS            12288
DS            4
SWH           36231.883 Hz
FIDRES        1.518520 Hz
AQ            0.5292180 sec
RG            2050
DW            13.800 usec
DE            20.00 usec
TE            300.1 K
D1            3.00000000 sec
D11           0.03000000 sec
D12           0.00002000 sec
D20           10.00000000 sec
TD0           1
  
```

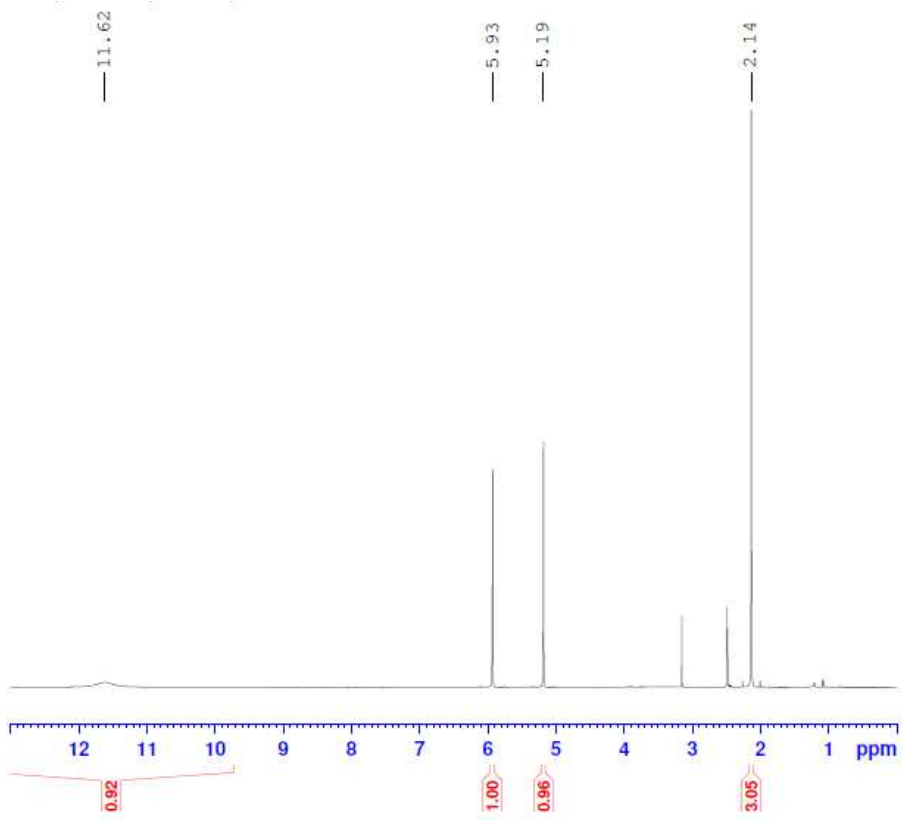
```

----- CHANNEL f1 -----
NUC1          13C
P1            14.00 usec
PL1           0.00 dB
PL1W          75.60778046 W
SFO1          150.9533699 MHz
SF2           5.24 dB
SFS           5.24 dB
SFRAM2        Crp60comp.4
SFRAMS        Crp60, 0.5, 20.1
SFOAL2        0.500
SFOALS        0.500
SFOFFS2       0.00 Hz
SFOFFS8       0.00 Hz
  
```

```

----- CHANNEL f2 -----
CPDPRG2      waltz16
NUC2          1H
PCPD2        100.00 usec
PL2           4.00 dB
PL12         26.00 dB
PL12W        5.00000000 W
PL12Z        0.03154787 W
SFO2         600.2724011 MHz
SI           262144
SF           150.9378004 MHz
WFW          EM
SSB           0
LB            3.00 Hz
GB            0
PC            1.40
  
```

R



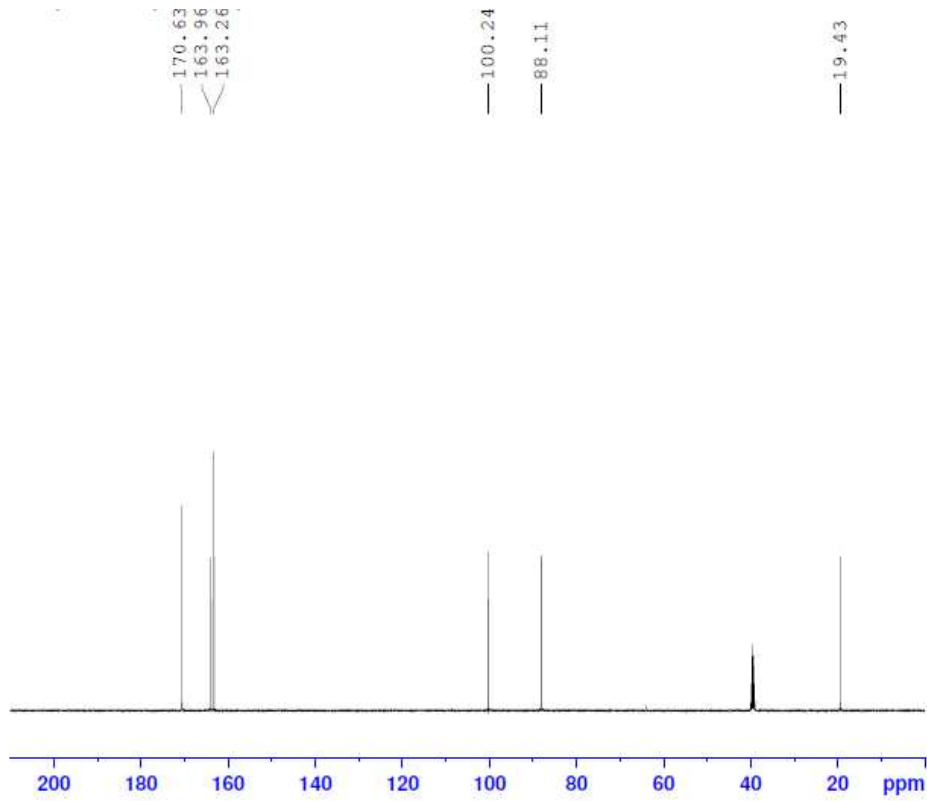
```

NAME          5CMG079PR
EXPNO         2
PROCNO        1
Date_         20120914
Time          11.46
INSTRUM       spect
PROBHD        5 mm PARBO BB-
PULPROG       zg30
TD            65536
SOLVENT       DMSO
NS            128
DS            2
SWH           10000.000 Hz
FIDRES        0.152588 Hz
AQ            3.2768500 sec
RG            512
DW            50.000 usec
DE            6.50 usec
TE            298.0 K
D1            1.00000000 sec
TD0           1
  
```

```

----- CHANNEL f1 -----
NUC1          1H
P1            14.00 usec
PL1           5.50 dB
PL1W          7.71660900 W
SFO1          500.3045027 MHz
SI           131072
SF           500.3000099 MHz
WFW          EM
SSB           0
LB            0.30 Hz
GB            0
PC            1.00
  
```

S



```

NAME      SCMG079CA
EXPNO     2
PROCNO    1
Date_     20120914
Time      12.57
INSTRUM   spect
PROBHD    5 mm PABBO BB-
PULPROG   zgpg30
TD         65536
FIDRES    0.488393
AQ         0.3359828
RG         2050
DW         16.800
DE         6.50
TE         298.0
D1         3.0000000
D11        0.0300000
D12        0.0000200
D20        10.0000000
ID0        1
  
```

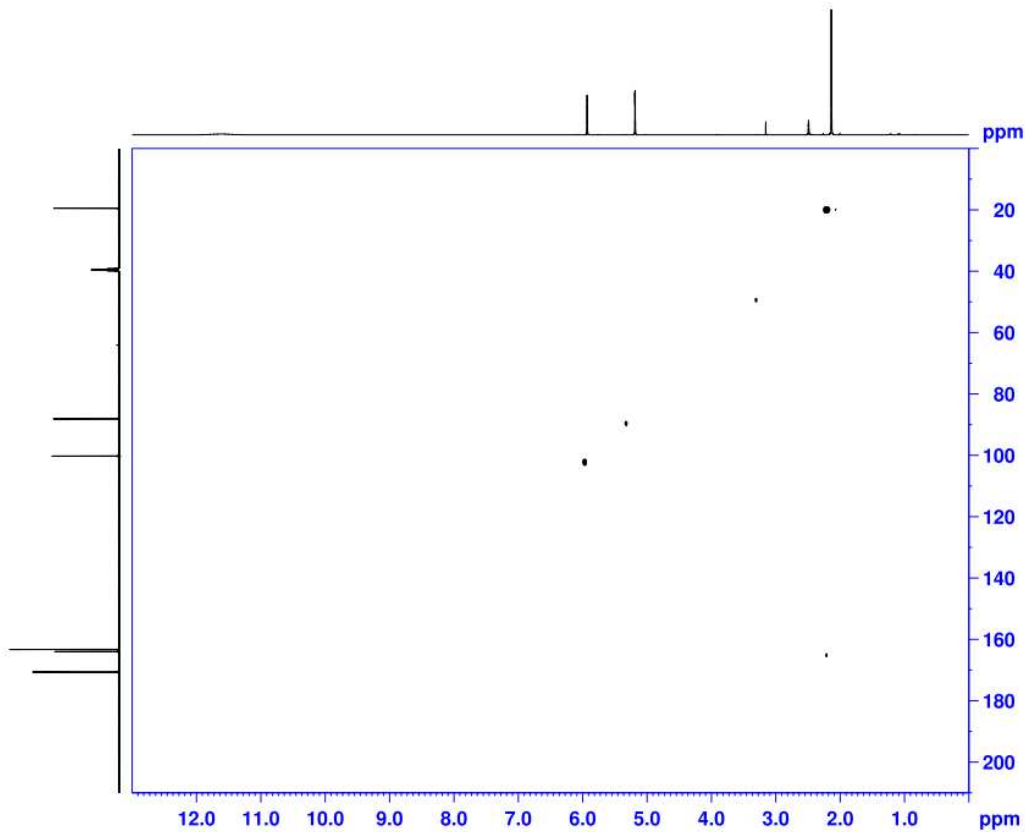
```

CHANNEL f1
NUC1       13C
P1         13.00
P2         2000.00
P3         500.00
PL1        3.30
PL2        44.17614746
PL3        9.18
SFO1       125.8150021
SFO2       9.18
SFO3       9.18
SFO4       Crp60comp.4
SFO5       Crp60,0.5,20.1
SFO6       0.500
SFO7       0.500
SFO8       0.00
SFO9       0.00
  
```

```

CHANNEL f2
CPDPRG2   waltz16
NUC1       1H
PCPD2     100.00
PL2        5.50
PL12       22.58
PL12W      7.7164980
PL12W      0.15115636
SFO1       500.3020012
SFO2       262144
SFO3       125.805917
SFO4       EM
SFO5       0
SFO6       0
SFO7       1.00
SFO8       0
SFO9       1.40
  
```

T



```

NAME      SCMG079MD
EXPNO     1
PROCNO    1
Date_     20120913
Time      14.04
INSTRUM   spect
PROBHD    5 mm PABBO BB-
PULPROG   zgpg30
TD         1624
SOLVENT   MeqD
NS         16
DS         16
SWH        3501.401
FIDRES     0.419327
AQ         0.146272
RG         3858
DW         142.000
DE         6.50
TE         298.0
D1         0.0000000
D11        0.0000000
D12        0.00178571
D13        0.0000000
D14        0.0000000
D15        0.0002000
D20        0.0000000
ID0        2
ZGPTNS    0.0000000
  
```

```

CHANNEL f1
NUC1       1H
P1         14.00
P2         28.00
P3         1000.00
PL1        5.50
PL12       7.7164980
SFO1       500.3017511
  
```

```

CHANNEL f2
CPDPRG2   gqzg
NUC1       13C
P1         13.00
P2         20.00
P3         75.00
PL1        3.30
PL12       41.17614746
PL12W      1.3274840
SFO1       125.8124861
SFO2       125.8124861
  
```

```

GRADIENT CHANNEL
OPRAME1   SINE.100
OPRAME2   SINE.100
GPR1      80.00
GPR2      80.10
F16       1000.00
MOD        2
TD         162
SFO1       125.8125
SFO2       124.511938
SFO3       199.800
PULPROG   Echo-antiecho
SI         1624
SF         500.3001455
SFO1       125.8125
SFO2       124.511938
SFO3       199.800
SFO4       125.803467
SFO5       2
SFO6       0.00
SFO7       0
SFO8       0
SFO9       0
  
```

Figure S6: ^1H -NMR, ^{13}C -NMR, COSY and HMBC spectra. The spectra were recorded for structure elucidation of terrein, 6-hydroxymellein, 6,7-hydroxymellein, orsellinic acid, hydroxymethylpyrone and for identification of biosynthetic routes from stable isotope labeling. In all experiments DMSO- d_6 or methanol- d_4 was used as solvent and internal standard. This Figure is supplemental to Figure 4.

- (A) ^1H -NMR spectrum of terrein (1) in methanol- d_4 recorded at 300 MHz.
- (B) ^{13}C -NMR spectrum of terrein (1) in methanol- d_4 recorded at 75 MHz.
- (C) ^1H -NMR spectrum of terrein (1) in methanol- d_4 from stable isotope labeling experiments with $[1-^{13}\text{C}]$ -glucose recorded at 600 MHz.
- (D) ^{13}C -NMR spectrum of terrein (1) in methanol- d_4 from stable isotope labeling experiments with $[1-^{13}\text{C}]$ -glucose recorded at 150 MHz.
- (E) ^1H -NMR spectrum of 6-hydroxymellein (2) in DMSO- d_6 recorded at 500 MHz.
- (F) ^{13}C -NMR spectrum of 6-hydroxymellein (2) in DMSO- d_6 recorded at 125 MHz.
- (G) HMBC spectrum of 6-hydroxymellein (2) in DMSO- d_6 .
- (H) ^1H -NMR spectrum of 6-hydroxymellein (2) in DMSO- d_6 from stable isotope labeling experiments with $[1-^{13}\text{C}]$ -glucose recorded at 500 MHz.
- (I) ^{13}C -NMR spectrum of 6-hydroxymellein (2) in DMSO- d_6 from stable isotope labeling experiments with $[1-^{13}\text{C}]$ -glucose recorded at 150 MHz.
- (J) ^1H -NMR spectrum of 6,7-dihydroxymellein (3) in methanol- d_4 recorded at 500 MHz.
- (K) ^{13}C -NMR spectrum of 6,7-dihydroxymellein (3) in methanol- d_4 recorded at 125 MHz.
- (L) COSY spectrum of 6,7-dihydroxymellein (3) in methanol- d_4 .
- (M) HMBC spectrum of 6,7-dihydroxymellein (3) in methanol- d_4 .
- (N) ^1H -NMR spectrum of orsellinic acid (4) in methanol- d_4 recorded at 500 MHz.
- (O) ^{13}C -NMR spectrum of orsellinic acid (4) in methanol- d_4 recorded at 125 MHz.
- (P) ^1H -NMR spectrum of orsellinic acid (4) in methanol- d_4 from stable isotope labeling experiments with $[1-^{13}\text{C}]$ -acetate recorded at 600 MHz.
- (Q) ^{13}C -NMR spectrum of orsellinic acid (4) in methanol- d_4 from stable isotope labeling experiments with $[1-^{13}\text{C}]$ -acetate recorded at 150 MHz.
- (R) ^1H -NMR spectrum of 4-hydroxy-6-methylpyrone (5) in DMSO- d_6 from stable isotope labeling experiments with $[2-^{13}\text{C}]$ -acetate recorded at 500 MHz.
- (S) ^{13}C -NMR spectrum of 4-hydroxy-6-methylpyrone (5) in DMSO- d_6 from stable isotope labeling experiments with $[2-^{13}\text{C}]$ -acetate recorded at 150 MHz.
- (T) HMBC spectrum of 4-hydroxy-6-methylpyrone (5) in DMSO- d_6 .

Supplemental experimental procedures

Strains and oligonucleotides

Details on wild-type isolates and strains constructed in this study are listed in the table of strains presented below. Similarly, all oligonucleotides used for generation of deletion mutants, reporter strains and analytical methods are listed in the table of oligonucleotides used in this study.

Table: Genotypes of strains used in this study.

Strain	Genotype	Reference
FGSC A1156 (NIH2624)	wild type	FGSC; Kansas City, USA
SBUG844	wild type	HKI; Jena, Germany
FGSC A1144	wild type	FGSC; Kansas City, USA
SBUG844 Δ <i>akuB</i>	Δ <i>akuB::hph</i>	Gressler <i>et. al.</i> 2011
SBUG844 Δ <i>akuB</i> Δ 07500	Δ <i>akuB::hph</i> ; Δ 7500:: <i>ptrA</i>	This study
SBUG844 Δ <i>akuB</i> Δ <i>terA</i>	Δ <i>akuB::hph</i> ; Δ <i>terA::ptrA</i>	This study
SBUG844 Δ <i>akuB</i> Δ <i>terB</i>	Δ <i>akuB::hph</i> ; Δ <i>terB::ptrA</i>	This study
SBUG844 Δ <i>akuB</i> Δ <i>terC</i>	Δ <i>akuB::hph</i> ; Δ <i>terC::ptrA</i>	This study
SBUG844 Δ <i>akuB</i> Δ <i>terD</i>	Δ <i>akuB::hph</i> ; Δ <i>terD::ptrA</i>	This study
SBUG844 Δ <i>akuB</i> Δ <i>terE</i>	Δ <i>akuB::hph</i> ; Δ <i>terE::ptrA</i>	This study
SBUG844 Δ <i>akuB</i> Δ <i>terF</i>	Δ <i>akuB::hph</i> ; Δ <i>terF::ptrA</i>	This study
SBUG844 Δ <i>akuB</i> Δ <i>terH</i>	Δ <i>akuB::hph</i> ; Δ <i>terH::ptrA</i>	This study
SBUG844 Δ <i>akuB</i> Δ <i>terI</i>	Δ <i>akuB::hph</i> ; Δ <i>terI::ptrA</i>	This study
SBUG844 Δ <i>akuB</i> Δ <i>terR</i>	Δ <i>akuB::hph</i> ; Δ <i>terR::ptrA</i>	This study
A1144_ <i>PamyB::lacZ</i>	<i>ptrA</i> , <i>PamyB::lacZ::trpC</i> ^T	This study
A1144_ <i>PgpdA::lacZ</i>	<i>ptrA</i> , <i>PgpdA::lacZ::trpC</i> ^T	This study
A1144_ <i>PamyB::terA</i>	<i>ptrA</i> , <i>PamyB::terA::terA</i> ^T	This study
A1144_ <i>PamyB::terA</i> Δ TE	<i>hph</i> , <i>PamyB::terA</i> ₁₋₅₅₄₂ :: <i>terA</i> ^T	This study
A1144_ <i>PamyB::terA</i> :TE _{wA}	<i>hph</i> , <i>PamyB::terA</i> ₁₋₅₇₀₃ : <i>wA</i> ₅₈₅₃₋₆₈₁₉ :: <i>wA</i> ^T	This study

Table: Oligonucleotides used in this study.

No.	Name	5'-3' sequence
P1	SmaI_07500up_f	CCCGGGTAACGACAACGATGAACG
P2	NotI_07500up_r	CTCCTGGCGGCCGCACGATTCCAATATGAGGTCC
P3	NotI_07500in_f	GAATCGTGCGGCCGCCAGGAGGATGCATCATAC
P4	SmaI_07500in_r	CCCGGGATAGGAATGGAATAGTCG
P5	KpnI_00145up_f	GGTACCTCCCTTGCTACCAGAC
P6	NotI_00145up_r	CCATCAGCGGCCGCATCCGTCCGATATAAATACG
P7	NotI_00145in_f	GACGGATGCGGCCGCTGATGGTTTCTGTCTGTG
P8	KpnI_00145in_r	GGTACCACCAGGTCATTTCCGGAAGG
P9	BglII_00144up_for	AGATCTCTCTTGGAGGGAAACTTG
P10	NotI_00144in_rev	CGTAGCGGCCGCGATTGCCACGTATCC
P11	NotI_00144in_for	GCAATCGCGGCCGCTACGGTCCGGTTC
P12	BglII_00144dn_rev	AGATCTAACCTCGCTGTCTTCC
P13	KpnI_00143up_for	GGTACCGAGTGGCTACATAAATGAAC
P14	NotI_00143up_rev	GTGCTGCGGCCGCCAGGAGCAAAGATGTGTG
P15	NotI_00143in_for	CTCCTGGCGGCCGCAGCACATTTACGGGATC
P16	KpnI_00143dn_rev	GGTACCCTTTCGGCTGACCTGG
P17	HindIII_00142up_for	AAGCTTGAAGAACAACACTAGATGTTACC
P18	NotI_00142in_rev	CTGCCGCGGCCGCAGTCAACTCCGTATTGTGC
P19	NotI_00142in_for	GTTGACTGCGGCCGCGGCAGATATTTCCAAGG
P20	HindIII_00142dn_rev	AAGCTTCGATTTATGCCATTCGTG
P21	HindIII_00141up_for	AAGCTTGTCTCTGATAACCGGATAGC
P22	NotI_00141in_rev	CTCCGGCGGCCGCTTTTCTTCAACAATGAGAGG
P23	NotI_00141in_for	GAAAAGCGGCCGCCGGAGTCTTTGGAAGG
P24	HindIII_00141dn_rev	AAGCTTGTGGTAGACTGATGGGAAG
P25	BglII_00140up_for	AGATCTACAGGAAACACCTGCTCC
P26	NotI_00140in_rev	TAGATGCGGCCGCACCAATTGAGTAGCGTG
P27	NotI_00140in_for	TTGGTGCGGCCGCATCTATCGGGACATGTTG
P28	BglII_00140dn_rev	AGATCTATGCCGTGCTGATAAAATG
P29	KpnI_00139up_for	GGTACCTGGCAAGGCAATTCTGGTG
P30	NotI_00139in_rev	GCTCTCGCGGCCGCACAGCGGACTTTCTTCG

P31	NotI_00139in_for	GCTGTGCGGCCGCGAGAGCGAAATATGATGC
P32	KpnI_00139dn_rev	GGTACCACTTGTCGATCATTCTTTGAAC
P33	SacI_00137up_for	GAGCTCAGGGAGACAACGACC
P34	NotI_00137in_rev	CATGTTTGCGGCCGCACTCGGTAGCCCAG
P35	NotI_00137in_for	CGAGTGCGGCCGCAAACATGACCCTAGCAAG
P36	SacI_00137dn_rev	GAGCTCGGAAATATGCAGGGTC
P37	SmaI_00136up_for	CCCGGGTTCGAAATAGAGG
P38	NotI_00136in_rev	TCCGAGCGGCCGCAAATCTAGCCATGTTG
P39	NotI_00136in_for	GATTTGCGGCCGCTCGGAACCTCTGGCAAC
P40	SmaI_00136dn_rev	CCCGGGAATAGTATGCTGTGATTG
P41	NotI_AnPgpA_for	GCGGCCGCTCACCAAAAAGTCAGACG
P42	BamHI_AnPgpA_rev	GGATCCCATTGTGATGTCTGCTCAAGC
P43	NotI_AoPamyB_for	GCGGCCGCTACTTAAAAATCGATCTCGCAG
P44	BamHI_AoPamyB_rev	GGATCCCATAAATGCCTTCTGTGGGGTT
P45	LacZ_up_down	GGCGTTACCCAACCTTAATCGC
P46	LacZ_mitte_up	CTCATCCATGACCTGACCATG
P47	SpeI_00145OE_for	ACTAGTGCTGGATCATTGAAGCTGTATG
P48	SwaI_00145OEdn_rev	ATTTAAATGAGCCGTGAACTGTATGAC
P49	SpeI_AnPgpA_rev	ACTAGTCATTGTGATGTCTGCTCAAGC
P50	SpeI_AoPamyB_rev	ACTAGTCATAAATGCCTTCTGTGGGGTT
P51	terA+STOP1_r	CAACACCTCAAATGGCCAACCTTGCCCTG
P52	EcoRV_00145_for	GATATCGGCATGGATGTGCGTG
P53	TterA_forSTOP1_f	GTTGGCCATTTGAGGTGTTGGATCGATGTTTG
P54	terA+STOP1_r	CAACACCTCAAATGGCCAACCTTGCCCTG
P55	terA+TEwA_r	GGAGAATGGAGGTTGCAGGTCGGGTC
P56	wA_TE_forTerA_f	GCAACCTCCATTCTCCTCCAAGGAAACC
P57	SwaI_wATerm_rev	ATTTAAATCTGCCAGACACTCTATGACG
P58	AN_8209_r13	CTGTTCGTTGAAGGGAAGAGG
P59	act_Ater_for	CCATCGAGAAGTCTTATGAGC
P60	act_Ater_rev	GGACAGGGAAGCCAGAATGG
P61	At00126_for1	GCTGTCATCATCACTATGATCG
P62	At00126_rev1	CAGGAGCTGATGGCAACC
P63	At00127_for1	CCAAGCCTTCCTCCTTCG

P64	At00127_rev1	CTAACAATCGTATAAACCGTGG
P65	At00128_for1	CCAGCATCTAAAGCCTACC
P66	At00128_rev1	CTACAAAGGTCCCGTCACC
P67	At00129_for1	GCTCGTCCAATTCCTCGTG
P68	At00129_rev1	CCATAATCGGTTGCAAGACC
P69	At00130_for1	GACCTCCAAGCCTTTCACG
P70	At00130_rev1	GAAATTATCCTACGGCCAGC
P71	At00131_for1	GTGCTTCGAACTGAACAACG
P72	At00131_rev1	GGTATACTCGTGATGTTATTACC
P73	At00132_for1	GACGGAAAGAATACCCAACC
P74	At00132_rev1	GTCGTTCTTGAAATCCTCATCG
P75	At00133_for1	GATCACACTAACACCTACAGC
P76	At00133_rev1	GGATCCTCCCACAACTCC
P77	At00134_for1	GATCGCCAATCTCTGTACTCC
P78	At00134_rev1	CATCAAGGTAGCACAAAGTTAGG
P79	At00135_for1	GAATGGATATCGCTGGATGC
P80	At00135_rev1	CCAAGGCATCACTATTATCGAC
P81	At00136_rev1	GTCCAAACGATCCAAGGTGG
P82	At00136_for1	GGTCTTACAGCTTCTCCTACC
P83	At00137_for1	CGTCTATTCTGCACTCAAAGC
P84	At00137_rev1	CTGTCCTCAAAGCTCGTCC
P85	At00138_for1	GTGGCTTTCCTATCCTCG
P86	At00138_rev1	CTCTTCCACTTGAGTCCTGG
P87	At00139_for1	CAAGAAGAAGCATGTGGTACC
P88	At00139_rev1	GATGGCCAACACAGCTTGG
P89	At00140_for1	CCTACACAAACATCACCTACG
P90	At00140_rev1	GGAACGTCTGAACGACTGG
P91	At00141_for1	GATTACGAGACCACGGTGC
P92	At00141_rev1	GATAGCCTTCCAAAGACTCC
P93	At00142_for1	CAGACGTGCTGATTAACTGG
P94	At00142_rev1	CACAATGACCTCGATCAAGC
P95	At00143_for1	GTACGCAAGTCGCTGTTTGG
P96	At00143_rev1	CACCTCGTCGTACTTGTCC

P97	At00144_for1	GTATTCCTCTTACCTGTCAGC
P98	At00144_rev1	CACAGGTTGTTTCAGTCTAGC
P99	At00144_for2	CGATGAATGTCAGCCTGAGC
P100	At00144_rev2	GATCAAAGGCAAATATACGTACC
P101	At00145_for1	CGAAGCTATGGATGGGTTCC
P102	At00145_rev1	GGTAGAAGGAATAGAGTCTTGG
P103	At00145_for2	GGAATCGAAGGTGTTGCTGC
P104	At00145_rev2	CCTATCAACTTCTCCCATCC
P105	At00146_for1	CTTCAACGAATGCTACCACTG
P106	At00146_rev1	GCAGCTTCTGTCTCGCAGG
P107	At00147_for1	GTATTTATGTCCGATCGGTTTGG
P108	At00147_rev1	CAGGAGGTGGTGATGAATCC
P109	At00148_for1	CGACGAGAACCTCATGTTCC
P110	At00148_rev1	CGTAAGTATCCCACACCACG
P111	At00149_for1	GATGGTTCAGGACGTTAATCG
P112	At00149_rev1	GCTTGCGTTGGATCGTTTCG
P113	At00150_for1	GTCGATACGGTACGAACTGG
P114	At00150_rev1	GGACTTTTCGAGCGTCTGG
P115	ptrA_for	ATGTCTCCTCCAGCTGCCATC
P116	ptrA_rev	CGGGTAGTGAGTCATTTAC

Construction of deletion mutants in *A. terreus* SBUG844

All *A. terreus* deletion mutants were generated in the genetic background of strain SBUG844 Δ *akuB*. Due to close proximity to other genes ATEG00145 (*terA*) and ATEG07500 were only partially deleted by replacing the first 1.7 or 1.9 kb of the coding region with the resistance marker. For ATEG00144 (*terB*), ATEG00143 (*terC*), ATEG00142 (*terD*), ATEG00141 (*terE*), ATEG00140 (*terF*), ATEG00139 (*terR*), ATEG00137 (*terH*), and ATEG00136 (*terI*) the complete coding region was replaced. All deletion constructs consisted of a 500 – 1150 bp upstream and a 750 - 1250 bp downstream flanking region separated by the *ptrA* resistance marker. Flanking regions were amplified from *A. terreus* genomic DNA using Phusion Hot Start II DNA Polymerase (Thermo Scientific) and oligonucleotides P1 to P40 listed in the table of oligonucleotides. PCR-fragments were gel purified, mixed, and fused by PCR in the presence of flanking oligonucleotides generating *NotI* restriction sites

separating the up- and downstream flanks. PCR products were cloned into pJET1.2, excised with restriction enzymes (Thermo Scientific) according to supplemental table below and subcloned into plasmid pUC19. After restriction with *NotI*, the *NotI* restricted *ptrA* cassette from plasmid *ptrA*-pJET1 (Fleck and Brock, 2010) was inserted. Deletion cassettes were separated from the vector backbone by restriction digest, gel purified, and used for transformation (Gressler et al, 2011). For Southern blot analyses (Figure S1) specific digoxigenin labeled probes were amplified with oligonucleotides P3/4 for ATEG07500 and P5/6, P9/10, P13/14, P17/18, P23/24, P25/26, P29/30, P33/34, and P37/38 for *terA* – *terF*, *terR*, *terH* and *terI*, and used for hybridization and band detection as described in the manufacturer’s protocol (Roche Diagnostics).

Table: Oligonucleotides, fragments sizes, and restriction enzymes used for the construction of deletion cassettes and for generating labeled probes. For oligonucleotide sequences also refer to Table “Oligonucleotides used in this study”.

Gene	Flanking region	Fragment size (bp)	Oligo-nucleotides	Restriction enzymes (excision of the deletion cassette)	Name of plasmid	Oligonucleotides used for digoxigenin-labeled probes
ATEG07500	up	1093	P1/2	<i>SmaI/XhoI</i>	ptrA_07500up+dn-pUC19	P3/4
	down	861	P3/4			
ATEG00145 (<i>terA</i>)	up	1104	P5/6	<i>KpnI</i>	ptrA_00145up+dn-pUC19	P5/6
	down	1012	P7/8			
ATEG00144 (<i>terB</i>)	up	912	P9/10	<i>BglII/BamHI</i>	ptrA_00144up+dn-pUC19	P9/10
	down	1237	P11/12			
ATEG00143 (<i>terC</i>)	up	1139	P13/14	<i>KpnI</i>	ptrA_00143up+dn-pUC19	P13/14
	down	937	P15/16			
ATEG00142 (<i>terD</i>)	up	997	P17/18	<i>HindIII</i>	ptrA_00142up+dn-pUC19	P17/18
	down	1038	P19/20			
ATEG00141 (<i>terE</i>)	up	949	P21/22	<i>HindIII</i>	ptrA_00141up+dn-pUC19	P23/24
	down	993	P23/24			
ATEG00140 (<i>terF</i>)	up	838	P25/26	<i>BglII/BamHI</i>	ptrA_00140up+dn-pUC19	P25/26
	down	1049	P27/28			
ATEG00139 (<i>terR</i>)	up	776	P29/30	<i>KpnI</i>	ptrA_00139up+dn-pUC19	P29/30
	down	958	P31/32			
ATEG00137 (<i>terH</i>)	up	586	P33/34	<i>PstI/XhoI</i>	ptrA_00137up+dn-pUC19	P33/34
	down	1086	P35/36			
ATEG00136 (<i>terI</i>)	up	518	P37/38	<i>SmaI</i>	ptrA_00136up+dn-pUC19	P39/40
	down	766	P39/40			

Construction of promoter:*lacZ* fusion strains in *A. niger* A1144

The *A. nidulans* glyceraldehyde-3-phosphate dehydrogenase promoter (AnP*gpdA*, locus ANID_08209.1) was amplified with oligonucleotides P41/42 from genomic DNA of *A. nidulans* FGSC A4 (1344 bp) and the *A. oryzae* α -amylase B promoter (*PamyB*) (Kanemori et al, 1999) from genomic DNA of *A. oryzae* FGSC A815 (1019 bp) with oligonucleotides P43/44. PCR-fragments were cloned into pJET1.2/blunt (Thermo Scientific) and excised by *Bam*HI and *Not*I restriction. Plasmid *lacZ-trpCT*-pJET1.2 (Gressler et al, 2011) restricted with the same enzymes allowing ligation of the promoters 5' to the *Escherichia coli lacZ* gene, which resulted in plasmids AnP*gpdA-lacZ-trpCT*-pJET1.2 and *PamyB-lacZ-trpCT*-pJET1.2. Finally, plasmids were linearized with *Not*I to insert the *ptrA* cassette. The resulting plasmids (1-20 μ g) were used to transform protoplasts of strain *A. niger* A1144. Mycelium was grown for 16 h in YM (yeast extract, malt extract, peptone), harvested by filtration, and incubated for 1 h in YAT buffer (0.6 M KCl in 50 mM maleic acid, pH 5.5) in the presence of 5 mg/ml Yatalase (Takara) and 5 mg/ml Lysing enzyme from *Trichoderma harzianum* (Sigma Aldrich). Protoplasts from this procedure were washed and used for transformation as described (Gressler et al, 2011). Transformants were checked for integration numbers by Southern blot with a digoxigenin labeled probes (oligonucleotides P45/46) directed against the *lacZ* gene (Figure S3).

Construction of *A. niger* A1144 strains expressing *terA*, *terA* Δ TE and *terA*:TE_{wA}

Different versions of the *terA* gene (*terA*, *terA* Δ TE and *terA*:TE_{wA}) were recombinantly expressed in *A. niger* under control of the *amyB* promoter and termination control by the *terA* terminator sequence. *PamyB* was amplified from genomic DNA of *A. oryzae* FGSC A815 (1019 bp) with P43/50, and *terA* including its terminator (*terA*+T) from genomic DNA of *A. terreus* FGSC A1156 (NIH 2624) with P47/48. Fragments were cloned into pJET1.2/blunt. Both plasmids were restricted with *Not*I/*Spe*I, which released *PamyB* and allowed fusion with the *terA* gene. The plasmid was linearized with *Not*I and the *ptrA* cassette was integrated yielding *ptrA_PamyB:terA*-pJET1.2. To generate versions with different C-terminal domains, the N-terminal domains of *terA* together with *PamyB* were excised by *Eco*RV, *Not*I, *Swa*I triple digest and the *Eco*RV/*Not*I-fragment was inserted into the *Eco*RV/*Not*I restricted vector *hph* (*Kpn*I)-pJET1.2 containing the *hph* resistance cassette. The resulting plasmid *hph_PamyB:terA_N*-pJET1.2 enabled the construction of *terA* versions with various different terminal domains via *Eco*RV restriction and ligation. To generate a construct lacking the thioesterase domain, a 1444 bp fragment of *terA* excluding the TE domain was

amplified with oligonucleotides P51/52, and 357 bp *terA* terminator sequence (*terA*^T) with oligonucleotides P53/54. Both fragments were fused by PCR generating a stop codon at the location of the original TE domain (*terA*ΔTE:*terA*^T). The fragment was cloned into pJET1.2/blunt, excised by *EcoRV/SwaI* and cloned into the *EcoRV* digested *hph_PamyB:terA_N-pJET1.2* to gain *hph_PamyB:terA*ΔTE_pJET1.2. To replace the *terA* TE domain by the thioesterase/ Claisen cyclase domain (TE/CYC) of *A. nidulans* *wA*, 1606 bp of *terA* excluding the TE domain was amplified with oligonucleotides P52/55 and the 1321 bp *wA* TE/CYC with its terminators (*wA*^T) was amplified with oligonucleotides P56/57 from genomic DNA of *A. nidulans* FGSC A4. Fragments were fused by PCR and the resulting fragment *terA:TE_{wA}*, was cloned into pJET1.2/blunt. After *EcoRV/SwaI* restriction the fusion construct was cloned into the *EcoRV* digested *hph_PamyB:terA_N-pJET1.2* to yield *hph_PamyB:terA:TE_{wA}-pJET1.2*. All constructs were used for transformation of *A. niger* A1144 as described above. Transformants were screened by Southern blot analysis (Figure S2) using digoxigenin labeled probes directed against the natural or modified *terA* gene. Probes were amplified with oligonucleotides P101/104 (*terA*), P52/54 (*terA*ΔTE), and P58/101 (*terA:TE_{wA}*), respectively.

Semi-quantitative PCR on terrein cluster genes

SBUG844 was cultivated in AMM, Sabouraud, YPD and PDB for 36 and 48 h. Mycelia were harvested, ground under liquid nitrogen and RNA was extracted using TRIsure (Bioline). RNA was treated with DNase using the DNA-free kit (Invitrogen) and transcribed into single stranded cDNA using Superscript Reverse Transcriptase III (Invitrogen) and anchored oligo(dT) primers. Semi-quantitative PCR was performed in a SpeedCycler (Analytik Jena) using GoTaq polymerase (Promega) and combinations of oligonucleotides P59 - P114 (Table "Oligonucleotides used in this study"). All cDNA samples were normalized against the actin gene that was amplified with oligonucleotides P59/60. Genomic DNA from SBUG844 served as positive control.

Isolation and structure elucidation of 6-hydroxymellein, 6,7-dihydroxymellein, orsellinic acid and 4-hydroxy-6-methylpyrone

For metabolite extraction from liquid cultures fluid-fluid extraction of culture broth with ethylacetate was performed. The organic phase was collected and concentrated under reduced pressure. Standard analyses of extracts from mutants and wild type were performed on an Agilent 1100 series HPLC-DAD system coupled with a MSD trap (Agilent

Technologies) operating in alternating ionization mode. As stationary phase a bifunctional phenylpropyl modified C₁₈ column (Macherey-Nagel Sphinx RP, 4.0 × 250 mm; 5 μm) with a binary solvent system consisting of solvent A (water + 0.1% formic acid) and solvent B (acetonitrile) was used. The following gradient with a flow rate of 0.8 mL/min was applied: 0.5 min, 10% B; 0.5 - 20 min, 10% - 70% B; 20 - 25 min, 70% - 100% B; 25 - 28 min, 100% B; 28 - 33 min, 100% - 10% B. For preparative purification of metabolites, the crude ethylacetate extract was subjected to solid phase extraction. Dried extracts were suspended in 20% methanol and applied to prefilled cartridges (Macherey-Nagel) containing 2000 mg of an octadecyl modified silica gel and elution was performed by a stepwise gradient consisting of: water, methanol/water (20:80, 40:60, 60:40, 80:20), and 100% methanol. For further purification of orsellinic acid and 6,7-dihydroxymellein, fractions enriched by solid phase extraction were applied to preparative HPLC using an Agilent 1260 modular HPLC system (Agilent Technologies) equipped with DAD and an automatic fraction collector. The Zorbax Eclipse Plus C₁₈ column (9.4 × 250 mm; 5 μm) was equilibrated with 90% solvent A and 10% solvent C (methanol) with a flow rate of 4 mL/min. The following gradient was applied: 1 min, 10% C; 1 - 22.5 min, 10% - 51% C; 22.5 - 40 min, 51% - 55% C; 40 - 42.5 min, 55% - 90% C; 42.5 - 43.75 min, 90% - 100% C; 43.75 - 55 min, 100% C; 55 - 57 min, 100% - 10% C. To purify 6-hydroxymellein the same HPLC system equipped with a Zorbax Eclipse XDB C₈ column (9.4 × 250 mm; 5 μm) was used with a binary solvent system consisting of solvent A and solvent C. The following gradient was applied: 1 min, 10% C; 1 - 22.5 min, 10% - 51% C; 22.5 - 40 min, 51% - 55% C; 40 - 42.5 min, 55% - 90% C; 42.5 - 43.75 min, 90% - 100% C; 43.75 - 55 min, 100% C; 55 - 57 min, 100% - 10% C. Metabolites were analyzed by NMR as depicted in Figure S6.

Root growth inhibition assay

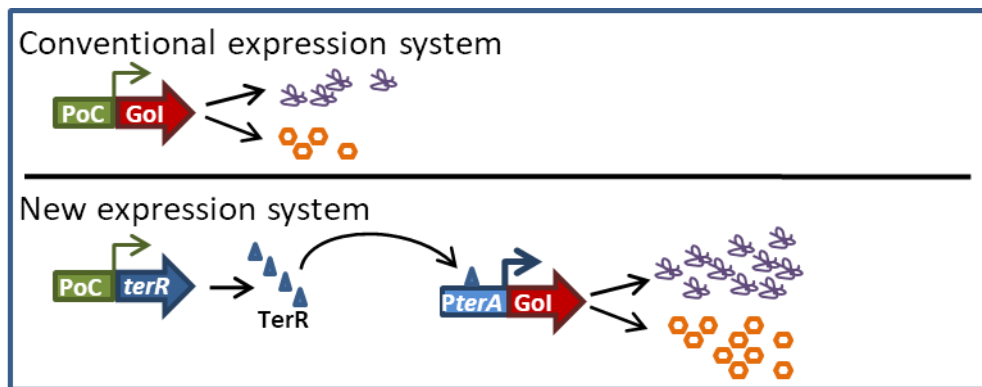
Radish seeds type Kiepenkerl "Riesenbutter" (Bruno Nebelung, Everswinkel) were sanitized in 70% ethanol (2 × 5 min), followed by 0.1% sodium hypochlorite (2 × 10 min) and washing in distilled water (3 × 2 min). 7 ml of modified Hoagland medium (0.5 g/l MES, 10 g/l sucrose, 2.5 mM Ca(NO₃)₂ × 4 H₂O, 0.5 mM MgSO₄ × 6 H₂O, 2.5 mM KNO₃, 0.5 mM (NH₄)₂PO₄, 5 μM Na₂EDTA, 5 μM FeCl₃ × 6 H₂O, 1 × Hutner's trace elements solution; pH 5.7; solidified with 0.8 % LE agarose (Biozym, Hessisch Oldendorf, Germany)) were transferred to a 15 ml tube. A single seed was added and overlaid with 500 μl medium. Tested compounds were solved in PBS (terrein; OA; 6,7-DHM), or 20% methanol in PBS (6-HM) and added to sterile media in final concentrations of 100, 50, 25, 10, or 1 μg/mL. After

planting tubes were loosely sealed with a screw-cap and incubated for three days in the dark (one day, 4°C; two days 20°C) and finally exposed to a constant 12 h light/dark rhythm for five additional days. Root and hypocotyl length were determined on a daily basis after the darkness period. Each condition was tested three times and contained twelve biological replicates.

A new high-performance heterologous fungal expression system based on regulatory elements from the *Aspergillus terreus* terrein gene cluster

Markus Gressler, Peter Hortschansky, **Elena Geib**, and Matthias Brock

(2015) *Frontiers in Microbiology*; 6, 184



Summary of the manuscript: This manuscript describes the characterisation of regulatory elements from the terrein biosynthesis gene cluster and their use in heterologous gene expression. The terrein biosynthesis gene cluster regulator TerR is responsible for cluster gene induction and specific TerR binding sites were identified and characterised for their binding properties. Since TerR is highly specific for the promoters of the terrein biosynthesis genes and strongly activates these promoters, a combination of TerR and the *terA* promoter were selected for the construction of a novel expression system. The system was tested by transcriptional analyses, reporter assays and for its suitability to produce a range of different secondary metabolites. This enabled the identification of the product lecanoric acid from the *orsA* gene of *Aspergillus nidulans*.

Contribution: 15% contribution of practical work.

cDNA analysis of transcriptional regulator gene expression from inducing and non-inducing conditions in the heterologous expression system. Isolation and structure elucidation of lecanoric acid from an *Aspergillus niger* strain heterologously expressing the *orsA* gene from *Aspergillus nidulans*.

A new high-performance heterologous fungal expression system based on regulatory elements from the *Aspergillus terreus* terrein gene cluster

Markus Gressler¹, Peter Hortschansky², Elena Geib¹ and Matthias Brock^{1,3*}

¹ Microbial Biochemistry and Physiology, Leibniz Institute for Natural Product Research and Infection Biology, Hans Knoell Institute, Jena, Germany, ² Molecular and Applied Microbiology, Leibniz Institute for Natural Product Research and Infection Biology, Hans Knoell Institute, Jena, Germany, ³ Institute for Microbiology, Friedrich Schiller University, Jena, Germany

OPEN ACCESS

Edited by:

Ana Lúcia Leitão,
Universidade Nova de Lisboa,
Portugal

Reviewed by:

Wolfgang Buckel,
Philipps-Universität Marburg,
Germany
Peter Punt,
TNO, Netherlands

*Correspondence:

Matthias Brock,
Microbial Biochemistry
and Physiology,
Leibniz Institute for Natural Product
Research and Infection Biology,
Hans Knoell Institute,
Beutenbergstr. 11a, 07745 Jena,
Germany
matthias.brock@hki-jena.de

Specialty section:

This article was submitted to Microbial Physiology and Metabolism, a section of the journal *Frontiers in Microbiology*

Received: 19 December 2014

Paper pending published:
26 January 2015

Accepted: 19 February 2015

Published: 16 March 2015

Citation:

Gressler M, Hortschansky P, Geib E and Brock M (2015) A new high-performance heterologous fungal expression system based on regulatory elements from the *Aspergillus terreus* terrein gene cluster. *Front. Microbiol.* 6:184. doi: 10.3389/fmicb.2015.00184

Recently, the *Aspergillus terreus* terrein gene cluster was identified and selected for development of a new heterologous expression system. The cluster encodes the specific transcription factor TerR that is indispensable for terrein cluster induction. To identify TerR binding sites, different recombinant versions of the TerR DNA-binding domain were analyzed for specific motif recognition. The high affinity consensus motif TCGGHHWYHCGGH was identified from genes required for terrein production and binding site mutations confirmed their essential contribution to gene expression in *A. terreus*. A combination of TerR with its *terA* target promoter was tested as recombinant expression system in the heterologous host *Aspergillus niger*. TerR mediated target promoter activation was directly dependent on its transcription level. Therefore, *terR* was expressed under control of the regulatable amylase promoter *PamyB* and the resulting activation of the *terA* target promoter was compared with activation levels obtained from direct expression of reporters from the strong *gpdA* control promoter. Here, the coupled system outcompeted the direct expression system. When the coupled system was used for heterologous polyketide synthase expression high metabolite levels were produced. Additionally, expression of the *Aspergillus nidulans* polyketide synthase gene *orsA* revealed lecanoric acid rather than orsellinic acid as major polyketide synthase product. Domain swapping experiments assigned this depside formation from orsellinic acid to the OrsA thioesterase domain. These experiments confirm the suitability of the expression system especially for high-level metabolite production in heterologous hosts.

Keywords: *Aspergillus niger*, secondary metabolites, transcription factor, DNA-binding motif, reporter strains, thioesterase domain

Introduction

Aspergillus terreus is a filamentous ascomycete of biotechnological and medical importance, since it produces the primary metabolite itaconic acid (Calam et al., 1939; Klement and Buchs, 2013) and the HMG-CoA reductase inhibitor lovastatin (Alberts et al., 1980; Hutchinson et al., 2000). Besides that, *A. terreus* can cause life-threatening invasive

aspergillosis in immunocompromised patients (Slesiona et al., 2012b), which makes its use in biotechnological applications limited. In previous analyses we searched for secondary metabolite gene clusters that are involved in pigment formation of *A. terreus* conidia (Zaehle et al., 2014). This was of interest, since preliminary analyses suggested that the pigment in *A. terreus* differs from that found in other related *Aspergillus* species (Slesiona et al., 2012a). Coincidentally, we identified the gene cluster producing the metabolite terrein (Zaehle et al., 2014). Terrein is a metabolite with various biological activities, but its phytotoxic potential appears to be at least one of its natural functions and may increase competitiveness of *A. terreus* in the environment (Zaehle et al., 2014).

Interestingly, terrein (Figure 1A) is produced in large quantities, since short-term cultivation in simple potato dextrose broth resulted in more than 1 g of terrein per liter (Zaehle et al., 2014) and even higher yields have been described for cultivation under more optimized conditions (Xu et al., 2012; Yin et al., 2012). This implies that genes from the terrein gene cluster may be expressed at very high levels.

The terrein cluster contains seven genes responsible for terrein biosynthesis (*terA-F*, *terR*), whereby *terA* encodes a non-reducing polyketide synthase (PKS) that produces polyketides of different chain length namely 2,3-dehydro-6-hydroxymellein (C10), orsellinic acid (C8), and 4-hydroxy-6-methylpyrone (C6). The subsequent formation of the cyclopentenoic structure of terrein is proposed to derive from an oxidative ring contraction of the isocoumarinic precursor 2,3-dehydro-6-hydroxymellein. While the terrein gene cluster contains further co-regulated genes, these genes might be dispensible (*terH*, *terI*), because deletion only reduces the final terrein production level or are involved in metabolite export (*terG*, *terJ*) (Zaehle et al., 2014). Importantly, the gene cluster encodes its own transcriptional activator at locus tag ATEG_00139, which is called TerR. TerR is a transcriptional activator with a GAL4-type Zn₂Cys₆ zinc binuclear cluster DNA-binding domain. This type of DNA-binding domain is very common in fungi and is the most common type of DNA-binding domains in transcriptional regulators of secondary metabolite gene clusters from filamentous fungi such as GliZ for gliotoxin biosynthesis from *Aspergillus fumigatus* (Bok et al., 2006), AflR for aflatoxin biosynthesis from *Aspergillus nidulans* and *Aspergillus flavus* (Yu et al., 1996) or ApdR for aspyridone biosynthesis from *A. nidulans* (Bergmann et al., 2007). A genomic deletion of *terR* resulted in complete loss of terrein production, suggesting that this transcription factor essentially contributes to cluster expression (Zaehle et al., 2014). However, neither the DNA binding sites recognized by TerR, nor the signals leading to TerR activation have been identified so far. However, if TerR is sufficient to drive expression of cluster genes, we assumed that a combination of TerR together with promoters from its cluster could enable the development of a new heterologous expression system.

Several filamentous fungi have been used for the recombinant production of proteins, among them especially fungi of industrial importance with GRAS status (generally regarded as safe) such as *Aspergillus niger*, *Aspergillus oryzae*, *Trichoderma reesei*, *Acremonium chrysogenum*, and *Penicillium chrysogenum*

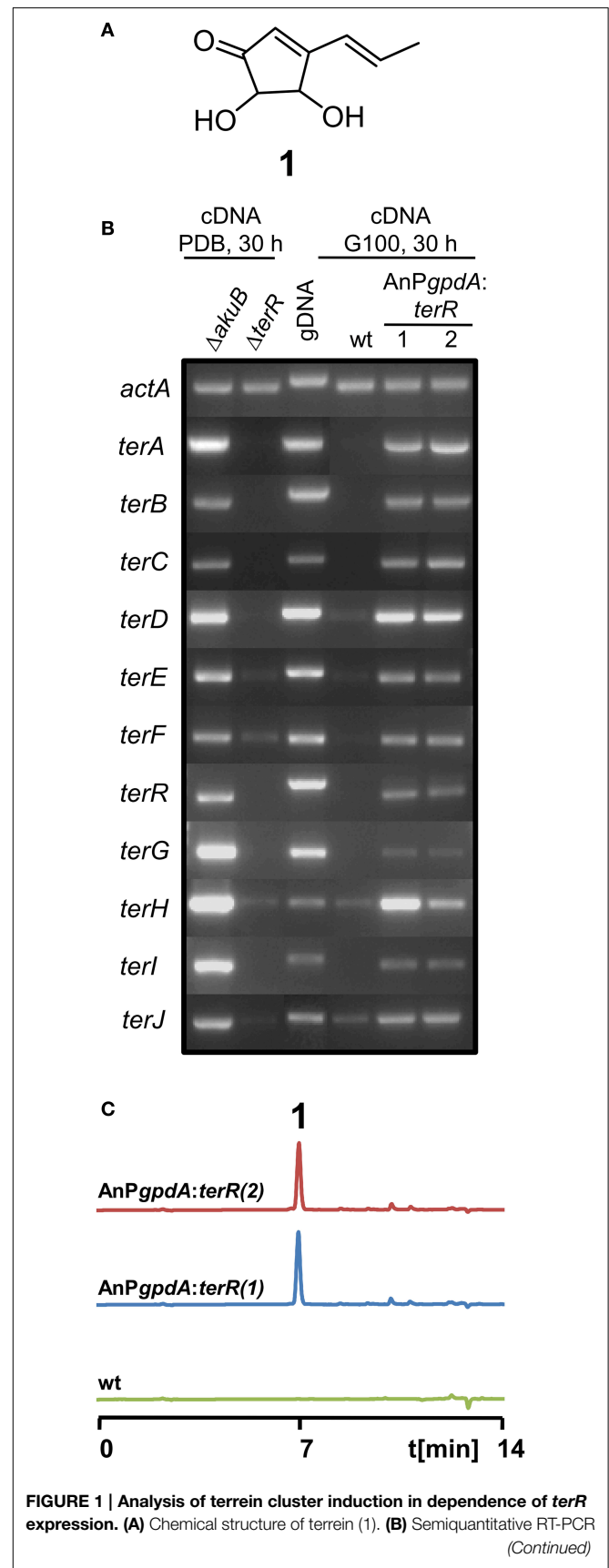


FIGURE 1 | Analysis of terrein cluster induction in dependence of *terR* expression. (A) Chemical structure of terrein (1). (B) Semi-quantitative RT-PCR analysis of gene expression. (C) HPLC analysis of terrein production. (Continued)

FIGURE 1 | Continued

on terrein cluster genes (*terA–terJ*) normalized against *actA* transcript levels. Under naturally inducing conditions (PDB) all genes from the cluster are expressed in *A. terreus* SBUG844 Δ *akuB* (parental strain for gene deletions), but not in a Δ *terR* mutant. The wild-type SBUG844 shows no cluster expression under non-inducing conditions (G100), whereas strains constitutively expressing *terR* under the *A. nidulans* *gpdA* promoter (AnP*gpdA:terR* No. 1 and 2) induce the cluster. **(C)** HPLC analysis of G100 culture extracts from wild type (wt) and *terR* overexpressing strains AnP*gpdA:terR* No. 1 and 2. The metabolite peak for terrein is denoted by “1.”

(Sharma et al., 2009). Several post-transcriptional bottlenecks have been reported to limit the production of proteins. These may consist of incorrect protein folding and subsequent degradation, low secretion efficiency, extracellular degradation or hyperglycosylation and several attempts have been made to overcome these limitations (Ward, 2012). However, filamentous fungi have not only been used for protein production, but are also used for the production of lignofuels or metabolic intermediates such as citric acid and the production of secondary metabolites such as antibiotics and other therapeutically useful compounds (Lubertozzi and Keasling, 2009). Despite specific limitations in all expression systems including the codon-adaptation of the target gene and RNA stability, the initial high-level expression of a target gene is the first key step for high production rates.

In general, a strong promoter is used to drive gene expression. In this respect, expression systems frequently rely on endogenous promoters from primary metabolism that are either constitutively active or can be regulated by applying specific inducing or repressing conditions. Examples are alcohol and aldehyde dehydrogenase (*alcA*; *aldA*), glucoamylase (*glaA*), (Taka) amylase (*amyA*; *amyB*), glyceraldehyde-3-phosphate dehydrogenase (*gpdA*), sucrose (*sucA*), acetamidase (*amdS*), endoxylanase (*exlA*), superoxide dismutase (*sodA*), or cellobiohydrolase I (*cbhl*) (Sharma et al., 2009; Fleissner and Dersch, 2010). Additionally, multiple integrations of an expression construct frequently increases the overall transcription of the target gene, but a linear increase is mainly limited to the first 5–6 copies (Verdoes et al., 1993). Due to these limitations, an inducible system with a promoter that is strongly activated and produces high transcript levels already in single-copy is generally favored.

Interestingly, although high secondary metabolite production rates have been described for several fungal species, information on the use of the involved regulatory elements to drive recombinant gene expression is limited. To analyze, whether elements from the *A. terreus* terrein cluster might be suitable for such a new recombinant expression system, we first analyzed, whether TerR is sufficient to drive terrein cluster expression and identified the respective DNA binding sites. With this knowledge, elements from the cluster were tested by reporter gene expression for their performance in the heterologous host *A. niger*. Finally, the expression system was used to heterologously produce secondary metabolites from *A. terreus* and *A. nidulans* in *A. niger*.

Materials and Methods

Strains and Culture Conditions

Strains used in this study are summarized in Table S1. For maintenance and during transformation procedures, all *Aspergillus* strains (*A. nidulans* wild type FGSC A4, *A. terreus* SBUG844 and its derivatives and all *A. niger* FGSC A1144 derivatives) were cultivated for 4 days at 37 or 30°C on solid *Aspergillus* minimal media (AMM) containing 2% agar (<http://www.fgsc.net/methods/anidmed.html>). When required, either hygromycin B (140 µg/ml, Carl Roth GmbH; Germany), pyrithiamine hydrobromide (0.1 µg/ml) or phleomycin (80 µg/ml) (both Sigma Aldrich; Germany) were added. Conidia were harvested in sterile water from solid media and filtered over 40 µm cell strainers (VWR; Germany). Liquid cultures were generally used in a 50 ml scale and were inoculated with 1×10^6 conidia per ml. Cultures were incubated at 30°C for 48–72 h as specified in the respective experiments. The following liquid media were used: AMM with 100 mM glucose (AMM-G100) or 1% casamino acids (AMM-CA1%), potato dextrose broth (PDB, Sigma Aldrich), and yeast/malt extract medium (YM, 5 g/l peptone, 3 g/l yeast extract, 3 g/l malt extract).

Bacterial Expression and Purification of TerR Polypeptides for SPR Analysis

All oligonucleotides used in this study are listed in Table S2. The gene sequences encoding for TerR residues 1–153 (TerR_{1–153}), 43–138 (TerR_{43–138}), and 35–138 (TerR_{35–138}) were amplified by PCR from cDNA of *A. terreus* wild-type strain SBUG844 that was cultivated for 48 h at 30°C on PDB medium. The following oligonucleotides introducing 5'-*Nde*I and 3'-*Hind*III restriction sites were used: P1/2 for TerR_{1–153}, P3/4 for TerR_{43–138}, and P5/4 for TerR_{35–138}. The fragments were cloned into the pET-29a vector (Novagen; Germany). TerR polypeptides were produced by autoinduction in *E. coli* Rosetta2 (DE3) cells grown at 26°C in 1-l Overnight Express Instant TB Medium (Novagen) in the presence of 1 mM Zn(OAc)₂. Fifteen to twenty grams wet cells were collected by centrifugation, resuspended in 200 ml lysis buffer (20 mM HEPES, 150 mM NaCl, 10 µM Zn(OAc)₂, 5 mM β-Mercaptoethanol, 1 mM AEBSF, pH 7.5) and disrupted using an Emulsiflex C5 high pressure homogenizer (Avestin; Germany). Cleared cellular extracts were loaded on a SP Sepharose HP (GE Healthcare; Germany) column and eluted with a salt gradient up to 1 M NaCl. Pooled fractions containing TerR_{1–153}, TerR_{43–138}, or TerR_{35–138} were adjusted to 150 mM NaCl and applied on a Cellufine Sulfate (Millipore; Germany) column that was equilibrated with 20 mM HEPES, 150 mM NaCl, 10 µM Zn(OAc)₂, 5 mM β-Mercaptoethanol, pH 7.5, followed by elution with a gradient to 1 M NaCl. Peak fractions were concentrated with an Amicon Ultra-15 10K centrifugal filter device and purified to homogeneity by size exclusion chromatography on a Superdex 75 prep grade column (GE Healthcare) by using 20 mM HEPES, 150 mM NaCl, 10 µM Zn(OAc)₂, pH 7.5 as running buffer. TerR proteins were stored in 50% v/v glycerol at –20°C. The absolute molecular mass of TerR_{35–138} was determined by static light scattering experiments on a miniDawn TREOS monitor in series with an Optilab T-rEX differential refractometer

(Wyatt Technology Europe; Germany). TerR_{35–138} was chromatographed on a Superdex 200 10/300 GL column (GE Healthcare) and molar mass was calculated using ASTRA 6 software (Wyatt Technology Europe).

Surface Plasmon Resonance Measurements

Real-time analyses were performed on a Biacore 2000 system (GE Healthcare) at 25°C. DNA duplexes were produced by annealing complementary 18 bp oligonucleotides using a 5-fold molar excess of the non-biotinylated oligonucleotide. The dsDNA was injected on flow cells of a streptavidin (Sigma Aldrich)-coated CM3 sensor chip at a flow rate of 10 µl/min until the calculated amount of DNA that gives a maximum TerR binding capacity of 50 RU had been bound. TerR proteins were injected in running buffer (10 mM HEPES pH 7.4, containing 150 mM NaCl, 0.005% (v/v) surfactant P20, 5 mM β-Mercaptoethanol and 1 µM ZnCl₂) at concentrations from 12.5 to 6400 nM. Sample injection and dissociation times were set to 60 and 120 s at a flow rate of 30 µl/min. Refractive index errors due to bulk solvent effects were corrected with responses from DNA-free flow cell 1 as well as subtracting blank injections. Kinetic raw data were processed and globally fitted with Scrubber 2.0c (BioLogic Software) using a 1:1 interaction model including a mass transport term.

Genetic Manipulation of *A. niger* and *A. terreus*

All strains generated in this study are listed in Table S1. The number of genomic integrations of all constructs generated in this study was determined by Southern blot analyses with digoxigenin labeled probes. Blots were developed by chemoluminescence imaging using CDP-star as recommended by the manufacturer (Roche; Germany). For details on specific strain constructions refer to supplementary experimental procedures. In brief, all *A. terreus terR* expression constructs were amplified from genomic DNA of *A. terreus* SBUG844. The constructs either contained the native *terR* promoter or the *terR* promoter was replaced by the *A. nidulans gpdA* or the *A. oryzae amyB* promoter. The *terR* terminator sequence was maintained in all constructs. Either the pyrithiamine (*ptrA*) or hygromycin B (*hph*) resistance cassette was used as a selectable marker in transformations of *A. terreus* SBUG844, *A. niger* FGSC A1144, or *A. niger* FGSC A1144_ *PterA:lacZ*. Transformations were performed as previously described (Zaehle et al., 2014). For β-galactosidase producing reporter strains the *lacZ* gene from *E. coli* was fused with different promoters. The following promoters were used: The *A. nidulans gpdA* promoter, the *A. terreus terA* promoter in unidirectional (*PterA*) and bidirectional (*PterA/B*) orientation, the *A. terreus terC* promoter and the mutant versions *PterCm1* and *PterCm2*, in which the putative TerR binding site “BS4” was exchanged or mutated. Fusion constructs were cloned into plasmids containing either the *ptrA* or *hph* resistance cassette and used for transformation *A. terreus* SBUG844, *A. niger* FGSC A1144, or *A. niger* FGSC A1144_ *PamyB:terR* (P2 strain). For analysis of the bidirectional *terA/B* promoter a second reporter gene was required and a synthetic codon-optimized *tdTomato* gene coding for a red fluorescent protein was selected (gene accession KP100262). The *lacZ* and *tdTomato* genes were fused

in both orientations with *PterA/B* and cloned in plasmids containing the *hph* resistance cassette. These reporter plasmids were used for transformation of *A. niger* FGSC A1144 or *A. niger* FGSC A1144_ *PamyB:terR* (P2 strain).

Expression of *terA* and *orsA* in *A. niger* P2 Strain and Construction of the Expression Plasmid SM-Xpress

For expression of the *A. terreus terA* gene and the *A. nidulans orsA* gene in the *A. niger* P2 strain (containing the *PamyB:terR* construct), the *terA* promoter was either fused to the *terA* or *orsA* gene, whereas the respective natural terminator sequences were maintained. The fusion constructs were ligated into an *hph* containing vector and used for transformation of the *A. niger* P2 strain. To ease heterologous expression of polyketide synthases in the *A. niger* P2 strain the expression plasmid SM-Xpress was constructed. A plasmid containing the phleomycin (*ble*) resistance cassette (AnP*gpdA:ble:trpC^T*) was linearized with *EcoRI*. A 786 bp fragment of the *A. terreus terA* promoter was amplified with oligonucleotides P6/7 and fused with a 363 bp *trpC* terminator (*trpC^T*) from *A. terreus* (P8/9) and cloned into the *EcoRV* site of the linearized vector by *in vitro* recombination using the InFusion HD Cloning Kit (Clontech laboratories; Germany). Thus, the resulting plasmid “SM-Xpress” contains a phleomycin resistance cassette as selection marker and the fusion of *PterA* and *trpC^T*, which are separated by a *NcoI* site. This vector was used for domain swapping experiments of the *A. nidulans orsA* gene, in which the TE domain of OrsA was replaced by the TE domain from TerA. The *orsA* gene except its TE domain and the TE domain from *terA* were PCR amplified and fused with the *NcoI* restricted plasmid SM-Xpress *via in vitro* recombination. Plasmids were used for transformation of FGSC A1144_ *PamyB:terR* (P2).

Metabolite Extraction

To analyze cultures for secondary metabolite production, culture broth was extracted with an equal volume of ethylacetate and the procedure was repeated once. Both fractions were combined and evaporated under reduced pressure. Evaporated residues were solved in 1 ml methanol and filtered. Standard metabolite analyses were performed on an Agilent 1100 series HPLC-DAD system coupled with a MSD trap (Agilent Technologies; Germany) operating in alternating ionization mode as previously described (Gressler et al., 2011).

Quantification of Orsellinic Acid

To quantify metabolite production levels from the direct and the coupled expression system orsellinic acid from the TerA PKS was selected. Metabolites were analyzed on an analytical Shimadzu HPLC system equipped with a DAD type SPD-M20A using a Zorbax Eclipse XDB C8 column (4.5 × 150 mm; 5 µm) with H₂O + 0.1% formic acid (buffer A) and methanol (buffer B) as solvents. The following gradient was applied: 0–0.5 min = 10% B; 0.5–12 min from 10 to 90% B; 12–14 min from 90 to 100% B; 14–17 min = 100% B; 17–18 min from 100 to 10% B; 18–21 min = 10% B. A standard curve was generated using defined concentrations of purified orsellinic acid (range from

3.9 to 250 $\mu\text{g/ml}$). Cultures were cultivated for 48 h at 30°C and 200 rpm in AMM-G100+Gln50 liquid medium. Mycelium was collected for dry weight determination and culture supernatants were extracted twice with ethylacetate. Extracts were evaporated, solved in 1 ml methanol and filtered. Different dilutions from each sample in a total volume of 10 μl were loaded to the columns. Peak areas for orsellinic acid at 254 nm were quantified and production levels were calculated against the dry weight biomass.

RNA Isolation, cDNA Synthesis and Semiquantitative PCR

A. terreus SBUG844 and *A. niger* FGSC A1144 strains were cultivated for 30 or 48 h in PDB, AMM-G100, YM and AMM-CA1% media. Mycelia were ground under liquid nitrogen and RNA was isolated by the RiboPure RNA purification kit (Thermo Scientific; Germany). Residual genomic DNA was removed by the DNA-free kit (Thermo Scientific) and cDNA was synthesized by the Revert Aid Reverse Transcriptase (Thermo Scientific) using anchored oligo dT primers. Semiquantitative PCR was performed as described (Zaehle et al., 2014) previously using oligonucleotides P10–P35. Transcripts were normalized against the actin gene (*actA*, ATEG_06973) for *A. terreus* strains and against the glyceraldehyde-3-phosphate dehydrogenase gene (*gpdA*, *est_fge1_pm_C_70216*) for *A. niger* strains.

Determination of β -Galactosidase Activity and tdTomato Fluorescence Intensity

β -Galactosidase activity was determined as previously described (Gressler et al., 2011). In brief, mycelia from *A. niger* strains containing *lacZ* fusion constructs were harvested from cultures grown for 48 h at 30°C in PDB, AMM, YM, or AMM-CA1% media. Mycelia were ground under liquid nitrogen and resuspended in 50 mM MOPS buffer (pH 7.5) with 2 mM MgCl_2 and 10 mM β -mercaptoethanol. After centrifugation at 21,000 \times g supernatants were used for determination of β -galactosidase activity using *o*-nitrophenyl- β -galactoside as substrate (Gressler et al., 2011). To detect the fluorescence intensity of *A. niger* transformants containing *tdTomato* fusion constructs, cell-free extracts were prepared as described above. After determination of protein concentrations by the Bradford assay (BioRad; Germany) protein concentrations were adjusted to 2.0, 1.0, and 0.5 mg/ml. 200 μl of the dilutions were transferred to a black flat-bottom 96 well plate (Nunc; Germany) and analyzed in a microplate reader (FLUOstar Omega, BMG Labtech; Germany). Plates were shaken for 1 min in double orbital mode and emission was detected at 590 nm using an excitation wavelength of 544 nm (50 flashes/well, top reading, gain 2000). The parental *A. niger* strains A1144 and P2 that contained no *tdTomato* gene served as negative controls and were subtracted from the fluorescence values of reporter strains. Specific activities were expressed as fluorescence units per mg protein. To calculate relative expression levels, fluorescence intensities (FI) of reporter strains were normalized against fluorescence intensities of an *A. niger* strain expressing the *tdTomato* gene under control of the *A. nidulans gpdA* promoter using the following formula: Relative fluorescence intensity (rFI) [%] = $(\text{FI}_{\text{reporter strain}} - \text{FI}_{\text{P2}}) / (\text{FI}_{\text{AnPgdA}} - \text{FI}_{\text{WT}})$. All

assays were performed in biological and technical triplicates from at least three individual transformants.

Accession Numbers

The DDBJ/EMBL/GenBank nucleotide sequence database accession number for the *Aspergillus* codon-optimized *tdTomato* gene reported in this paper is KP100262.

Results and Discussion

The Transcription Factor TerR is Essential for Expression of Terrein Cluster Genes

Previously, we have shown that *A. terreus* produces large quantities of the metabolite terrein (Figure 1A) and we discovered that the responsible gene cluster contains its own transcription factor TerR, which is encoded at locus tag ATEG_00139 (Zaehle et al., 2014). Gene deletion analysis revealed that TerR is indispensable for terrein production in *A. terreus*, since *terR* deletion resulted in complete loss of terrein production during cultivation on inducing potato dextrose broth (PDB) (Zaehle et al., 2014). To confirm that TerR is directly involved in the activation of the gene cluster, comparative semiquantitative RT-PCR analyses between *A. terreus* wild type and *terR* mutant (ΔterR) were performed. Under inducing conditions, all genes from the cluster spanning the region from *terA* – *terJ* (locus tags ATEG_00145—ATEG_00135) were actively transcribed in the wild type (Figure 1B). While all analyzed genes were strictly dependent on TerR for induction, *terE*, *F* and *H* showed some background expression in the ΔterR background. Thus, TerR seems to act as a transcriptional activator with special importance for transcription of the key polyketide synthase *TerA*, which shares a bi-directional promoter with the *terB* gene. Interestingly, among the 11 genes spanning the cluster, six of them (*terA/B*; *terE/F*, and *terH/I*) share bi-directional promoters, implying that either multiple putative TerR binding sites are found in these promoters or that single binding sites can activate expression in both directions. However, the control of gene expression from bi-directional promoters is frequently found in fungal secondary metabolite gene clusters. As examples, in the aflatoxin gene cluster from *Aspergillus parasiticus* 12 out of 25 genes share a bi-directional promoter (Yu et al., 2004) and in the gliotoxin gene cluster from *Aspergillus fumigatus* (Forseth et al., 2011) 8 out of 12 genes are controlled by shared promoter sequences. Furthermore, similar to our results on TerR-dependency for terrein cluster activation, the Zn_2Cys_6 binuclear transcription factor *gliZ* from the gliotoxin cluster is essential for activation of cluster genes (Bok et al., 2006).

TerR is Sufficient for Activation of Terrein Cluster Genes

In *A. terreus* terrein is only produced under specific environmental conditions, suggesting that transcription and activation of *terR* is itself under the control of other transcription factors that mediate environmental signals toward terrein production. Thus, to analyze, whether TerR production under non-inducing conditions is sufficient to stimulate terrein production in *A. terreus*, we aimed in the exchange of the native *terR* promoter against the constitutively active *gpdA* promoter from *Aspergillus*

nidulans (Punt et al., 1990). The resulting *PgpdA:terR* fusion construct was used to transform an *A. terreus* wild-type strain. Indeed, when transformants were grown on complete glucose minimal medium, which is a repressive condition for terrein production in *A. terreus*, semiquantitative RT-PCR revealed induction of all cluster genes and high amounts of terrein were produced (Figures 1B,C). Thus, *terR* expression in *A. terreus* wild type is strictly dependent on specific inducing signals, but once expressed, TerR is sufficient to induce all genes required for terrein production. Similarly, the transcription factors ApdR (Bergmann et al., 2007), AfR (Liu and Chu, 1998), and GliZ (Bok et al., 2006) have been shown to induce expression of the respective cluster when overproduced in the homologous host. Therefore, our data indicate that promoter elements of the terrein cluster contain specific DNA binding sites that are recognized by TerR.

The TerR Zinc Binuclear Cluster DNA-Binding Domain has a Monomeric Structure

Since TerR was able to induce all genes required for terrein synthesis, we expected that conserved DNA binding sites are present in the promoter regions of genes spanning the terrein cluster. TerR belongs to the family of transcriptional activators with a GAL4-type Zn₂Cys₆ zinc binuclear cluster DNA-binding domain. This type of transcription factors is one of the most abundant transcriptional regulators present in fungi and involved in the regulation of primary and secondary metabolic processes (MacPherson et al., 2006). Their DNA-binding domain is generally located at the N-terminus of the protein and is sufficient to recognize its target sequence (Todd et al., 1998). Additionally, most GAL4-type transcription factors contain a coiled-coil domain near the N-terminus that is involved in dimerization and results in the recognition of consensus repeats (Fitzgerald et al., 2006). Interestingly, no coiled-coil domain is detected in the N-terminus of TerR, instead RADAR (Rapid Automatic Detection and Alignment of Repeats in protein sequences) analysis (Heger and Holm, 2000) detected an unusual amino acid repeat at positions 97–111 and 121–135 with unknown function. Thus, for analysis of the TerR subunit composition and identification of DNA-binding sites we first selected an N-terminal peptide of 153 amino acids (TerR_{1–153}) that was cloned into an expression vector with or without N-terminal His-tag. Unfortunately, regardless the peptide version (tagged or untagged) and the purification procedure, we were unable to obtain a monodispersed protein fraction and MALDI-TOF MS/MS analysis showed co-purification of N- and C-terminal degradation products (Figure 2B). A similar phenomenon was observed during purification of the transcriptional activator AlcR of the ethanol utilization pathway in *A. nidulans* (Felenbok et al., 1988; Cahuzac et al., 2001). An AlcR_{1–197} fragment enclosing the DNA-binding domain could not be purified to homogeneity (Lenouvel et al., 1997). Therefore, we truncated the TerR domain to a TerR_{35–138} fragment (Figure 2A). This protein fragment was purified to >98% homogeneity as judged by SDS-gel electrophoresis (Figure 2B) and analytical size exclusion chromatography. Multiangel static light scattering analysis revealed a molar mass of 11.65 kDa (Figure 2C), demonstrating that the

purified protein exclusively consisted of monomers in solution (theoretical molar mass of 11.35 kDa). Thus, besides the transcriptional activator AlcR, TerR seems to form another example of GAL4-type transcription factors with monomeric solution structure.

TerR Recognizes CGG Direct Repeat Consensus Sequences in the Terrein Cluster

To identify putative TerR binding sites in the terrein gene cluster an *in silico* prediction of candidates constituting regulatory DNA motifs was performed on the intergenic regions of *terA–terJ* (Figure 3A) using the SCOPE motif finder suite (Chakravarty et al., 2007). A SPACER bipartite motif with the direct CGG half-site repeat consensus 5'-CGGHHBNCGG-3' (Figure 3Q) was identified that was present in all promoter regions of the cluster, with the exception of *terG*, *terI*, and *terH*, whereby the latter genes were dispensable for terrein production (Zaehle et al., 2014). Interestingly, the intergenic region that acts as a bidirectional promoter of *terA* and *terB* contained three putative binding sites that were annotated as BS1, BS2, and BS3 (Figure 3A). To analyze recognition of these binding sites by the TerR_{35–138} fragment, protein: DNA real-time surface plasmon resonance (SPR) biosensor interaction analyses were performed. For this purpose, oligonucleotides with a four-nucleotide overhang at the 5'-CGG half-site and a three-nucleotide overhang at the 3'-CGG half-site were deduced. Biotinylated oligonucleotides were hybridized with complementary unbiotinylated anti-strands and immobilized on streptavidin-coated CM3 sensor chips to give a maximum response (R_{\max}) of 50 resonance units (RU) when bound by a single monomeric TerR_{35–138} domain. Kinetic SPR binding responses of TerR_{35–138} to BS1-BS3 fitted with K_D -values ranging between 0.5 and 0.7 μ M. Interestingly, while steady state binding analysis showed that only one monomer binds to the BS1 sequence (Figure 3B, Table 1), BS2 and BS3 revealed that a significant fraction of DNA duplexes were bound by two monomers at these binding sites (Figures 3C,F).

To analyze the specificity for the predicted motif, BS2 was selected for mutations in the first and second CGG half-sites. Mutation of the 5'-CGG to CAA led to a predominant loss of TerR_{35–138} binding (Figure 3D). In contrast, mutation of the 3'-CGG to CAA altered the K_D from 536 to 363 nM, but simultaneously reduced the number of TerR_{35–138} units that bind to the sequence (Figure 3E). While 1.6 monomers bound to the native sequence, only 0.95 monomers were found to bind at the mutated sequence. A similar phenomenon was observed when the second CGG half-site was mutated in BS7 (Figures 3M,N, Table 1). This implies that the 5'-CGG half-site is required for high affinity binding, whereas the 3'-CGG half-site attracts a second monomer to the motif. To confirm this assumption and to define a consensus sequence, we tested all other binding sites that were predicted by SCOPE using SPR analysis (Figure 3). Indeed, all predicted binding sites were recognized by TerR_{35–138}, whereby K_D values ranged from 26 nM to 1.5 μ M with either a tendency to bind only one or two TerR_{35–138} fragments. In this respect, binding of a second monomer seems to be favored when the last nucleotide of the five base pair spacer is a thymidine (BS2,

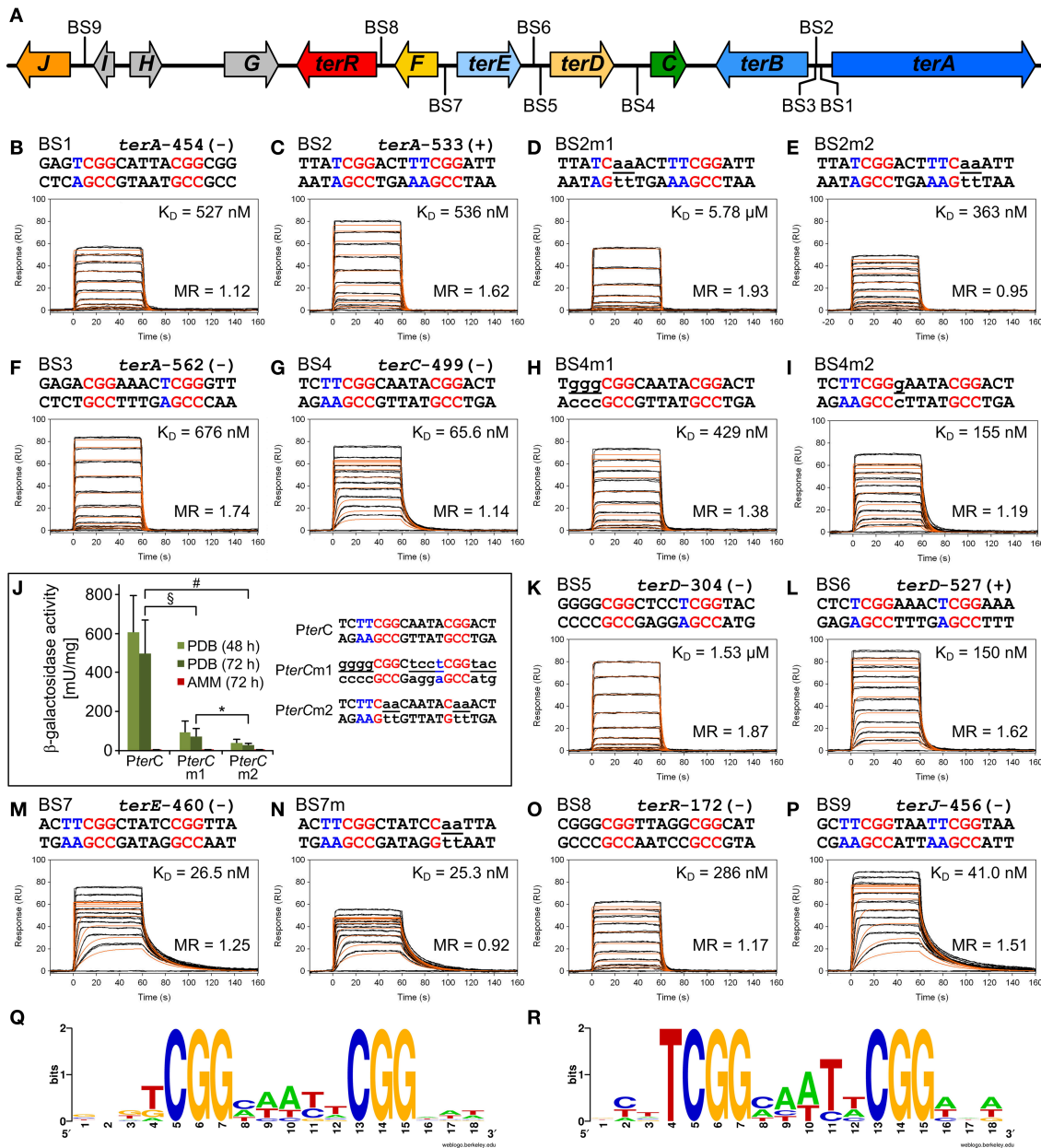


FIGURE 3 | *In vitro* TerR binding to a consensus motif identified in promoters of the *A. terreus* terrein biosynthesis gene cluster and *in vivo* verification of *in vitro* data. (A) Schematic presentation of the terrein gene cluster. Intergenic positions of the consensus TerR-binding motif identified by the SCOPE motif finder suite (Q) are annotated with BS1–9. (B–I, K–P) Real-time *in vitro* SPR interaction analysis of TerR_{35–138} with DNA containing the predicted natural or mutated (denoted by the letter “m”) binding sites from promoters of terrein cluster genes. Sequences of DNA duplexes used for SPR analysis are shown on top of the sensorgrams. Numbers represent the CGG direct repeat motif positions relative to the start of the open reading frame. CGG half-sites and 5′-flanking thymidines are highlighted in red and blue. Substituted nucleotides relative to the wild-type sequence are underlined and shown in lowercase letters. TerR_{35–138} binding responses from triplicate injections of different concentrations (black lines) are overlaid with the best fit derived from a 1:1 interaction model including a mass transport

term (red lines). Dissociation constants (K_D) are plotted inside the sensorgrams. For details on the specific binding motifs refer to the main text. (J) *In vivo* verification of the PterC binding motif BS4. PterC:*lacZ* reporter strains were grown for 48 and 72 h on PDB or for 72 h on AMM and β -galactosidase activity was determined. Highest activity is observed with the native *terC* promoter (PterC), whereas activity is significantly reduced by replacement of the native binding site (BS4) against the low affinity BS5 from the *terD* promoter (PterCm1) or when the two CGG half-sites of BS4 are replaced by CAA triplets (PterCm2). No activity for any reporter is detected on AMM. Statistical significance ($p < 0.01$) was calculated by the student’s unpaired *t*-test using data from at least three independent transformants measured in biological triplicates. Error bars represent SEM. §PterC vs. PterCm1; #PterC vs. PterCm2; *PterCm1 vs. PterCm2, all significances for PDB, but not AMM. (R) WebLogo sequence consensus motif of the experimentally mapped high affinity TerR binding sites BS1, BS2, BS4, BS6, BS7, and BS9.

TABLE 1 | Dissociation constants and stoichiometry of analyzed TerR_{35–138}:DNA interactions

DNA duplex (Binding site)	Mw duplex (Da)	DNA bound (RU)	R _{max} calculated* (RU)	R _{max} measured (RU)	molar ratio TerR:DNA	K _D
BS1	11405	52.4	52.1	58.5 ± 0.5	1.12	527 ± 3 nM
BS2	11401	51.6	51.3	82.9 ± 0.1	1.62	536 ± 3 nM
BS2m1	11399	54.7	54.5	105.2 ± 0.7	1.93	5.78 ± 0.06 μM
BS2m2	11339	51.2	51.0	48.4 ± 0.8	0.95	363 ± 2 nM
BS3	11403	52.0	51.8	90.3 ± 0.1	1.74	676 ± 3 nM
BS4	11403	55.9	55.9	63.6 ± 0.1	1.14	65.6 ± 0.6 nM
BS4m1	11404	53.1	52.8	72.8 ± 0.1	1.38	429 ± 2 nM
BS4m2	11403	52.9	52.7	62.6 ± 0.1	1.19	155 ± 1 nM
BS5	11408	52.9	52.6	98.6 ± 0.1	1.87	1.53 ± 0.06 μM
BS6	11403	52.3	52.1	84.6 ± 0.1	1.62	150 ± 1 nM
BS7	11403	50.1	49.9	62.3 ± 0.1	1.25	26.5 ± 0.3 nM
BS7m	11401	52.4	52.2	48.2 ± 0.1	0.92	25.3 ± 0.2 nM
BS8	11406	52.1	51.8	60.4 ± 0.1	1.17	286 ± 2 nM
BS9	11402	51.7	51.5	77.8 ± 0.2	1.51	41.0 ± 0.4 nM

*R_{max} calculated = 11350 (Mw TerR_{35–138})/Mw DNA × DNA bound.

TABLE 2 | Dissociation constants and stoichiometry of analyzed TerR_{43–138}:DNA interactions.

DNA duplex (Binding site)	Mw duplex (Da)	DNA bound (RU)	R _{max} calculated* (RU)	R _{max} measured (RU)	Molar ratio TerR:DNA	K _D
BS2	11401	56.3	50.5	52.4 ± 0.2	1.04	3.73 ± 0.03 μM
BS4	11403	58.5	52.4	45.9 ± 0.1	0.88	1.07 ± 0.06 μM
BS4m1	11404	57.7	51.7	49.3 ± 0.3	0.95	9.3 ± 1 μM
BS4m2	11403	58.0	52.0	45.9 ± 0.1	0.88	1.37 ± 0.05 μM
BS6	11403	57.3	51.3	43.4 ± 0.1	0.85	2.05 ± 0.09 μM
BS7	11403	60.0	53.8	48.9 ± 0.1	0.91	591 ± 2 nM
BS8	11406	60.9	54.6	58.0 ± 1.0	1.06	17.2 ± 0.5 μM
BS9	11402	59.6	53.4	49.3 ± 0.1	0.92	820 ± 4 nM

*R_{max} calculated = 10218 (Mw TerR_{43–138})/Mw DNA × DNA bound.

(ATEG_00143, **Figure 3A**), which is no longer expressed when *terR* is deleted (**Figure 1B**). Thus, we were interested, whether the *in vitro* binding properties of the predicted binding sites reflect promoter activation *in vivo*. To address this question, we generated three reporter constructs. The first construct contained the native *terC* promoter fused with the *E. coli lacZ* gene (*PterC:lacZ*). For the second construct, BS4 from the *terC* promoter was exchanged with BS5 and also fused with the *lacZ* gene resulting in *PterCm1:lacZ*. BS5 is one of two binding sites in the intergenic region of *terD* (ATEG_00142), which showed a 23 times reduced TerR_{35–138} binding affinity *in vitro*, but a tendency for binding two monomers (**Figure 3K**). Finally, for the last construct, the two CGG half-sites of BS4 were replaced by CAA in *PterC* and fused to the *lacZ* gene resulting in *PterCm2:lacZ*. These mutations in both CGG half-sites were assumed to lead to a complete loss of binding site recognition. The *A. terreus* wild-type strain was transformed with the three constructs and several independent transformants with single genomic integrations were selected for analysis of β-galactosidase activity under inducing and non-inducing conditions (**Figure 3J**). As expected, none of the transformants revealed β-galactosidase activity when

cells were grown under non-inducing conditions (AMM). In contrast, activity significantly increased, when cells were grown on PDB medium. Here, β-galactosidase activity was at least 6 times higher from strains containing the native BS4 site compared to strains containing the less affined BS5 site (*PterCm1*). Moreover, compared to the native promoter, the conversion of both CCG half-sites to CAA (*PterCm2*) reduced promoter activity by a factor 17. Thus, the binding sites predicted from *in silico* and *in vitro* analyses are indeed important for promoter activation by TerR and *in vitro* parameters reflect the *in vivo* situation.

TerR Activates the *terA* Promoter in the Heterologous Host *A. niger*, but Requires a Promoter Exchange

In order to generate a heterologous expression system using regulatory elements from the terrein gene cluster, we selected the filamentous fungus *A. niger*, which is frequently used in biotechnological applications (Sharma et al., 2009). Here, an analysis was required that tested the possibility of TerR mediated induction of terrein cluster promoters in the heterologous host. Thus, to

analyze, whether TerR is sufficient to activate *terA* in *A. niger*, different β -galactosidase reporter strains were generated (Figure 4 and Figure S1). First, the promoter of *terA* (*PterA*), which contained the three DNA binding sites BS1-3 was fused with the *E. coli lacZ* gene and transferred to *A. niger*. After cultivation on different media, β -galactosidase activity hardly exceeded the background level, indicating that the *terA* promoter is not recognized by *A. niger* transcription factors that are present under the applied conditions (Figure 4A and Figure S3). Unfortunately, when *terR* under its native promoter was additionally introduced into the *PterA:lacZ* strain, again no β -galactosidase activity was detected (Figure S3). This indicated that either (i) TerR is not able to activate the *terA* promoter in the heterologous system or that (ii) the native promoter of TerR is not recognized in *A. niger*. To test these assumptions, we analyzed the expression of *terR* by semiquantitative PCR. Indeed, no *terR* transcript

was detected, which confirms that specific regulatory elements from *A. terreus* are required to drive activation of *terR* expression (Figure S3). However, to show that TerR can also activate the *terA* promoter in a heterologous host, *terR* was fused with the constitutively active glyceraldehyde-3-phosphate dehydrogenase promoter (*PgpdA*) from *A. nidulans* and the resulting *PgpdA:terR* construct was introduced into the *A. niger* strain with the *PterA:lacZ* reporter. Indeed, a strong β -galactosidase activity was detected, which confirmed the specific recognition of *terA* promoter elements by TerR even in a heterologous system (Figure 4A). Additionally, β -galactosidase activity doubled in a strain that contained two copies of the *PgpdA:terR* constructs, indicating that TerR levels are the rate limiting step in *terA* promoter activation (Figure 4A). In conclusion, the native *terR* promoter is not stimulated and transcribed in *A. niger*, but when TerR is produced under control of an active promoter, this

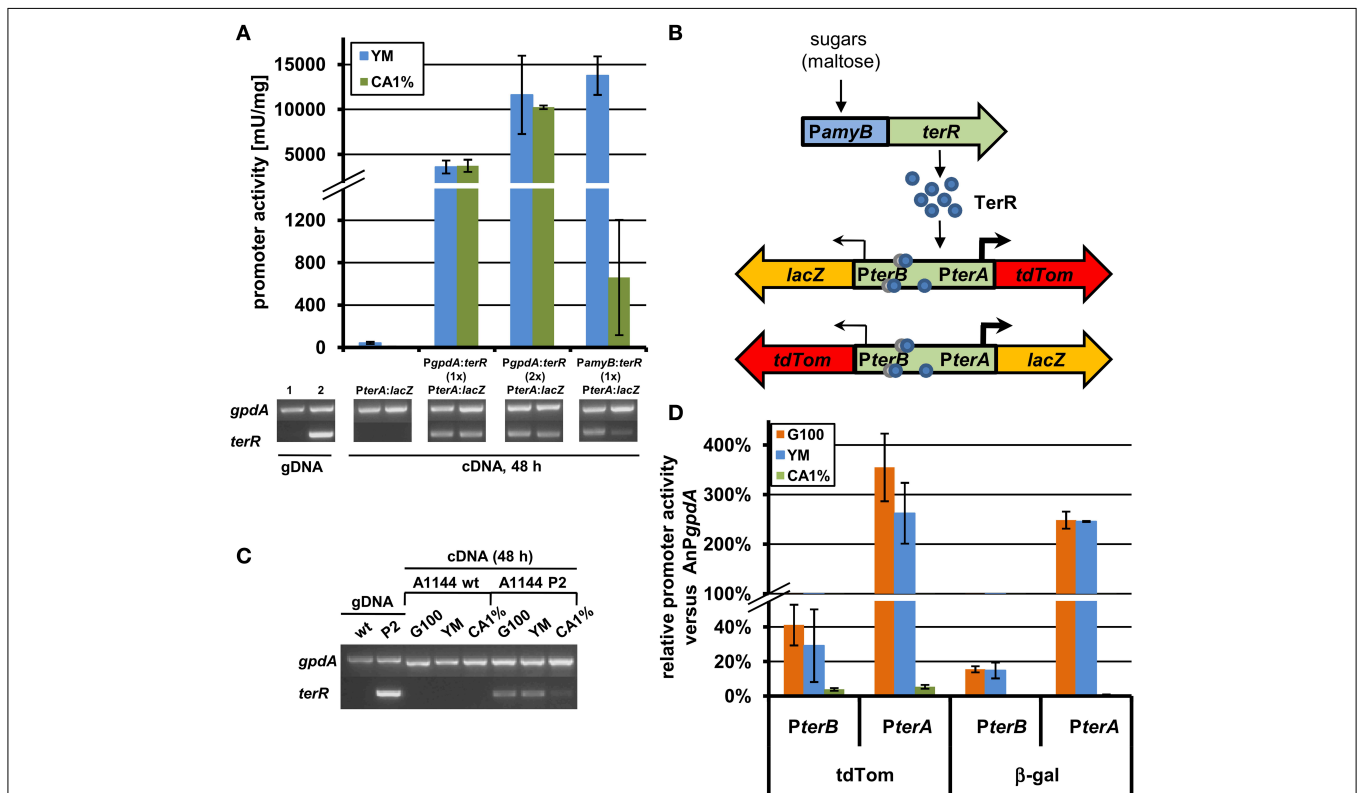


FIGURE 4 | Analysis of recombinant *terR* and *terA* expression in *A. niger* by semiquantitative RT-PCR, LacZ, and *tdTomato* reporter activity. (A) Semiquantitative RT-PCR (lower panels) and β -galactosidase activity (upper panel) of *A. niger* A1144_ *PterA:lacZ* either without *terR* or co-expressing the *terR* gene under control of the *A. nidulans* *gpdA* promoter (*PgpdA:terR*, *PterA:lacZ*; with one (1x) or two (2x) copies of *PgpdA:terR*) or the *A. oryzae* *amyB* promoter (*PamyB:terR*, *PterA:lacZ*). Expression of *terA* requires *terR* co-expression and is dependent on *terR* expression levels. *A. niger* *gpdA* was used as reference gene in semiquantitative RT-PCR analyses. Lane 1, control genomic DNA (gDNA) of *A. niger* *PterA:lacZ*; Lane 2, control gDNA of *A. niger* *PamyB:terR*, *PterA:lacZ*. (B) Scheme of the *terR* dependent expression system using the bi-directional promoter of *terA* and *terB*. After sugars induced expression of *terR*, the TerR protein (blue circles) recognizes the three bindings sites in the bi-directional *terA/B* promoter and

activates the expression of reporter genes (*lacZ* and *tdTomato*) presumably in different strength (indicated by arrows). (C) Semiquantitative RT-PCR analysis of wild type *A. niger* A1144 and A1144_ *PamyB:terR* (P2) expressing *terR* under control of the *amyB* promoter. *terR* is strongly expressed on *PamyB* inducing media (G100 and YM), but hardly detectable on CA1% medium. (D) Relative promoter activity of *PterA* and *PterB* from the reporter system described in (C). The parental strain P2 and the reporter strains P2_ *PterA:lacZ*_ *PterB:tdTom* and P2_ *PterB:lacZ*_ *PterA:tdTom* were cultivated for 48 h on G100, YM and CA1% and β -galactosidase activity and fluorescence intensity from cell-free extracts were determined. All values were normalized against reporter activities from the *A. nidulans* *gpdA* promoter (AnPgpdA: *lacZ* and AnPgpdA: *tdTom*) that were used as 100% reference values. Each experiment was carried out with three independent mutants in biological and technical triplicates.

transcription factor is sufficient to stimulate expression of *terA* also in the heterologous system.

Control of *terR* Expression Under the Inducible *amyB* Promoter Allows Regulated Gene Expression from the Bi-Directional *terA/B* Promoter

Experiments in Section “TerR Activates the *terA* Promoter in the Heterologous Host *A. niger*, but Requires a Promoter Exchange” revealed that control of *terR* expression under the *gpdA* promoter leads to constitutive activation of the *terA* promoter. In order to regulate expression, the *amyB* promoter was selected, since it was previously shown to be highly active in the presence of maltose or glucose, but only shows low background activity on sugar-free media such as 1% casamino acids (CA medium) (Ward, 2012; Zaehle et al., 2014). Indeed when the *A. niger* strain carrying the *PterA:lacZ* reporter was transformed with a *PamyB:terR* construct, high β -galactosidase activity was obtained when cells were cultivated on maltose containing YM medium, whereas activity after cultivation in CA medium was approximately 20 times lower (Figure 4A). This was also reflected by *terR* expression levels that were highly abundant on YM medium, but hardly detected on CA medium (Figure 4A). This again confirms that high *terR* expression levels are crucial for strong activation of target promoters. This also indicates that expression from promoters of the terrein cluster can be regulated by modifying the production level of the TerR regulator.

The selected terrein cluster promoter is assumed to depict a bi-directional promoter, because it separates the reading frames of *terA* and *terB* that are transcribed in opposite directions as already described in Section “The Transcription Factor TerR is Essential for Expression of Terrein Cluster Genes.” Interestingly, it has been shown that in the bi-directional promoters of penicillin biosynthesis from *A. nidulans* (*acvA/ipnA*) (Brakhage, 1997) and cephalosporin biosynthesis from *Acremonium chrysogenum* (*pcbAB/pcbC*) (Menne et al., 1994) transcription rate is favored in one direction. To test transcriptional activation from the *terA/B* promoter, the *lacZ* gene and a codon-optimized tdTomato gene encoding a red fluorescent protein were selected as reporters in both reading directions (Figure 4B). An *A. niger* strain carrying a single copy of the *PamyB:terR* construct (P2 strain) that shows the expected expression pattern of *terR* under inducing and non-inducing conditions (Figure 4C), was used as recipient strain for the different reporter constructs. Four to eight single copy transformants from each construct were analyzed in a pre-screening approach to test for variations in the expression pattern due to positioning effects (Minetoki et al., 1998; Liu et al., 2003; Blumhoff et al., 2013). All transformants revealed a similar tendency of expression levels ($\pm 25\%$ from average). Therefore, three independent transformants were selected from each construct and strains were cultivated in biological triplicates for determination of the average promoter activation rate in comparison to the *gpdA* control promoter. Selected transformants with single copy integration were grown on glucose, YM or CA medium and screened for β -galactosidase activity and fluorescence intensity from cell-free extracts. All measurements were background corrected against extracts from an

A. niger strain without reporter integration. Reporter activities were normalized against activities obtained from expression of the respective reporters under control of the *A. nidulans* *gpdA* promoter (Figure 4D).

Results from both reporters show that (i) *terA/B* promoter activity in both directions is strongly induced on glucose and YM medium, whereas activity remained near background values when cells were grown on non-inducing CA medium. (ii) Reporter activity in direction of the *terA* gene exceeded that of the *gpdA* promoter by up to three times, whereas activity in *terB* direction only reached 20–40% of the control value. Thus, transcription in the direction of the polyketide synthase gene *terA* exceeds that of *terB* by 8–14-fold. Additionally, the relative accumulation of TdTomato was slightly higher than that of the β -galactosidase, which could be due to increased stability of the codon-optimized TdTomato gene. In conclusion, these results indicate that *terA/B* promoter activation is directly dependent on the level of the TerR regulator.

Previous approaches to develop high-level expression systems used strongly expressed and, preferentially, inducible promoter elements for direct control of target gene expression. Examples are the thiamine promoter (*PthiA*) for expression in *A. oryzae* (Shoji et al., 2005), the xylose induced *xylI* promoter in *A. chrysogenum* (Blatzer et al., 2014), synthetic promoters containing the human estrogen receptor (hER α) response elements in *A. nidulans* and *A. niger* (Pachlinger et al., 2005) or the *Escherichia coli* tetracycline resistance operon (Tet-on system) in *A. fumigatus* and *A. niger* (Vogt et al., 2005; Meyer et al., 2011). Here, we identified that the activity of the artificial promoter that controls *terR* expression is amplified via TerR-dependent activation of the *terA* promoter. This assumption derives from the following observation: In previous studies we have shown that the *gpdA* and *amyB* promoter display similar activation levels on G100 medium (Zaehle et al., 2014). Thus, in case there is no signal amplification, reporter activity from the coupled system should be equivalent to *PgpdA*-driven activity. However, the analyses performed here show that reporter activity increased by a factor >2 when *PamyB* controls *terR* expression and the reporter is under *terA* control. Therefore, the coupled system of terrein cluster elements leads to an amplification of the strength of the promoter that is used to regulate *terR* expression. We assume that activity of promoters that are even stronger than *PamyB* could be amplified in our new coupled system. Although it might be expected that a saturation of the *terA* promoter may occur at a specific TerR level, this could either be compensated by increasing the number of *terR* binding sites in the *terA* promoter or by adding additional copies of the fusion of *PterA* with the gene of interest. However, a preliminary analysis of multicopy integrants with the *PterA:lacZ* construct revealed that expression levels run into saturation at approximately five integrations.

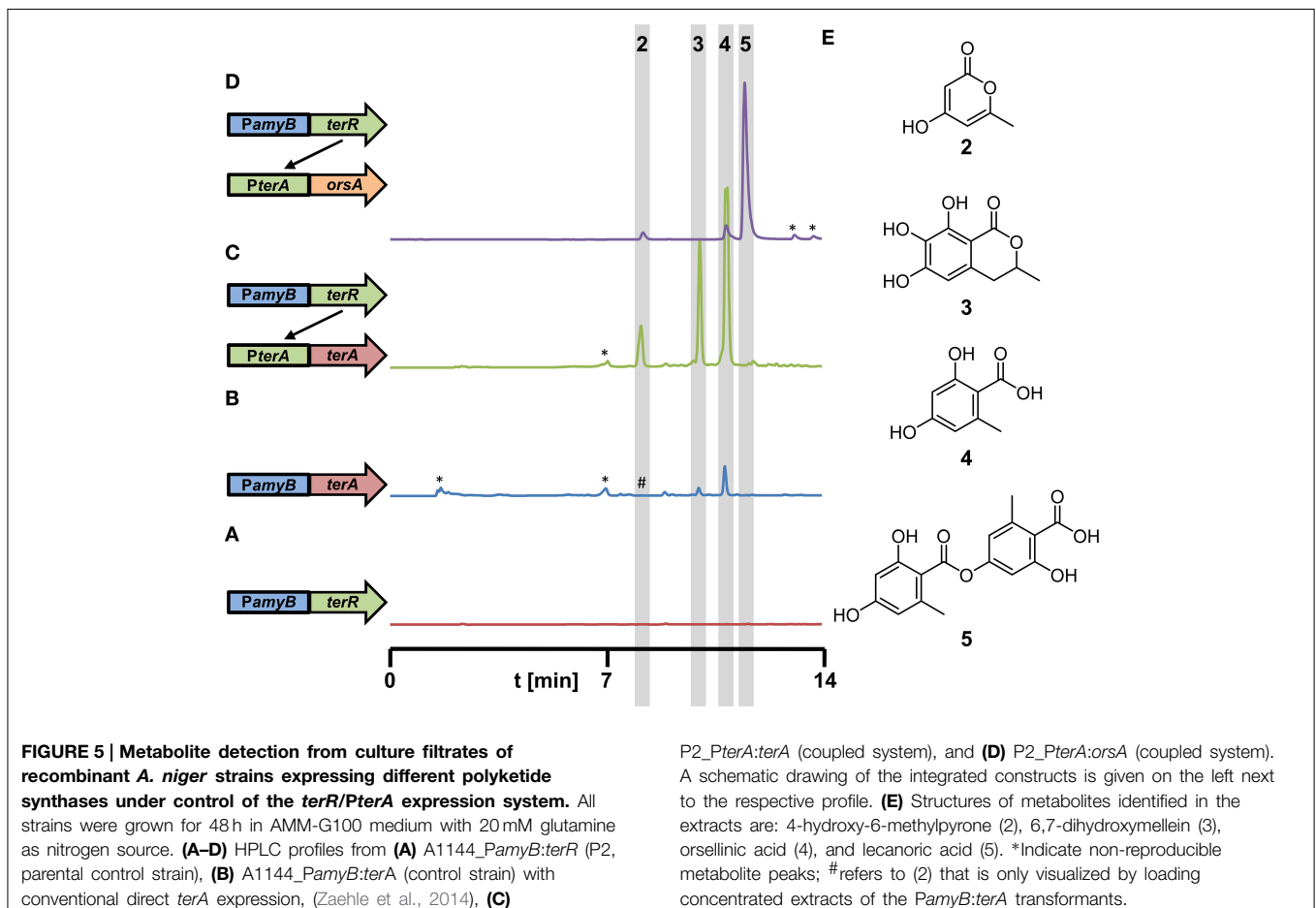
The *PamyB:terR/PterA* System is Suitable for High-Level Heterologous Secondary Metabolite Production

Due to the high reporter activities obtained from the *terA* promoter in combination with the *PamyB:terR* control element, we were interested in the use of this system for the heterologous

production of secondary metabolites. In a previous study, we expressed the terrein synthase gene *terA* under direct control of the *amyB* promoter in *A. niger* (Zaehle et al., 2014). Sufficient quantities of the TerA metabolites orsellinic acid (4), 6,7-dihydroxymellein (3) and 4-hydroxy-6-methylpyrone (2) were produced (for molecular structures refer to **Figure 5E**). However, we assumed that metabolite production in the heterologous system could strongly exceed the quantity of metabolites compared to the previous construct. To confirm this hypothesis, the P2 strain with the single copy of the *PamyB:terR* integration was transformed with the *A. terreus terA* gene under control of its native *terA* promoter. Transformants were cultivated in glucose minimal medium, which was selected since HPLC profiles of the P2 strain showed no significant background metabolite production under this condition (**Figure 5A**). The metabolic profile of transformants was directly compared with that of a *PamyB:terA* strain that was cultivated under the same conditions (**Figures 5B,C**). Indeed, although all three metabolites were detected in similar ratios as detected from the *PamyB:terA* strain, the amount of metabolites produced by the new expression system strongly exceeded that of the former strain. In order to quantify the increase of metabolite production in the coupled system, we selected three *PamyB:terA* single copy and three *PamyB:terA* double copy integrants in the *A. niger*

A1144 genetic background (Zaehle et al., 2014) and four single copy and two double copy *PterA:terA* integrants from the P2 strain. Transformants were cultivated in AMM-G100+Gln50 for 48 h, supernatants were extracted and orsellinic acid concentration was quantified by HPLC and normalized against the mycelial dry weight (Figure S4). Although production rates varied among independent transformants, the single and double copy strains with the *PamyB:terA* construct produced on average 0.37 (± 0.19) and 0.43 (± 0.13) mg orsellinic acid per gram of dried mycelium. Single copy *PterA:terA* integrants produced on average 1.16 (± 0.64) and double copy integrants 3.20 (± 1.69) mg of orsellinic acid per gram of dried mycelium. This results in an approximated 3-fold increase in the coupled expression system for single copy and a 7.5-fold increase for the double copy integrants in comparison to the direct expression system under control of the *amyB* promoter. Although increases in production rates may be metabolite dependent, these results reflect the increased transcription rate from the coupled expression system as shown in **Figure 4D** and confirms the suitability of the system for heterologous expression.

In another approach, we selected the *orsA* PKS gene from *A. nidulans* for heterologous expression in *A. niger*. Previous analyses have shown that the *orsA* gene is induced during the cocultivation of *A. nidulans* with the bacterium



Streptomyces hygroscopicus (Schroeckh et al., 2009). Structure elucidation of the metabolites produced by OrsA required a 14 liter cocultivation of both organisms to obtain sufficient amounts of metabolites. Interestingly, orsellinic acid and lecanoric acid, a depside of two orsellinic acid molecules, were identified. However, it remained unclear, which of the two products is the major metabolite produced by OrsA and whether OrsA is directly performing the transesterification of two orsellinic acid molecules (Schroeckh et al., 2009). Therefore, we generated a *PterA:orsA* construct that was transferred into the *A. niger* P2 strain and single copy integrants were tested for product formation in 50 ml culture scale. Ethylacetate extracts revealed one major and two minor metabolites (Figure 5D) that were identified by HRESI-MS as lecanoric acid (5), orsellinic acid (4) and 4-hydroxy-6-methylpyrone (2) and the identity was confirmed by reference against known standards and ^1H and ^{13}C NMR spectra of purified lecanoric acid (Figure S5 and supplementary experimental procedures). Since lecanoric acid was by far the most prominent metabolite produced by all independent transformants, it can be assumed that the thioesterase (TE)-domain of OrsA performs the transesterification of the *p*-hydroxyl-group of one orsellinic acid molecule with the carboxyl-group of a second molecule rather than releasing orsellinic acid by simple hydrolysis. A similar mechanism of depside formation from orsellinic acid-derived metabolites might be present in lichen-forming fungi in which lecanoric acid and derivatives thereof constitute major secondary metabolites (Parrot et al., 2015). However, whether the involved polyketide synthases perform depside formations has not yet been characterized in detail (Armaleo et al., 2011).

A New Expression Vector Enables Rapid Cloning and Modification of Secondary Metabolite Genes

In order to ease the use of the heterologous expression system, we constructed a plasmid that allows rapid generation of expression constructs called SM-Xpress. For this purpose, we used a plasmid with a phleomycin resistance cassette in which the *ble* gene was controlled by the *A. nidulans gpdA* promoter. Subsequently, the 786 bp *terA* promoter and a 363 bp fragment of the *A. terreus trpC* terminator were amplified by PCR and integrated into the plasmid by *in vitro* recombination. This resulted in plasmid “SM-Xpress” that contained a *NcoI* restriction site that separated promoter and terminator and allowed insertion of the gene of interest by restriction ligation or *in vitro* recombination (Figure 6A). Resulting overexpression plasmids are suitable for direct transformation of the *A. niger* P2 strain that contains the *PamyB:terR* construct.

To test this system, we went back to the *orsA* gene from *A. nidulans*. As stated in Section “The *PamyB:terR/PterA* System is Suitable for High-Level Heterologous Secondary Metabolite Production,” OrsA predominantly produced lecanoric acid and we hypothesized that the depside formation from two orsellinic acid molecules is mediated by the thioesterase domain (TE) of this enzyme. In general, TE domains are important for product release, but can also perform an interketide esterification (cross-coupling) between the carboxyl-function of the polyketide and an alcohol, whereby in a recent example of melleolide formation in *Armillaria mellea* the hydroxyl group derives from a

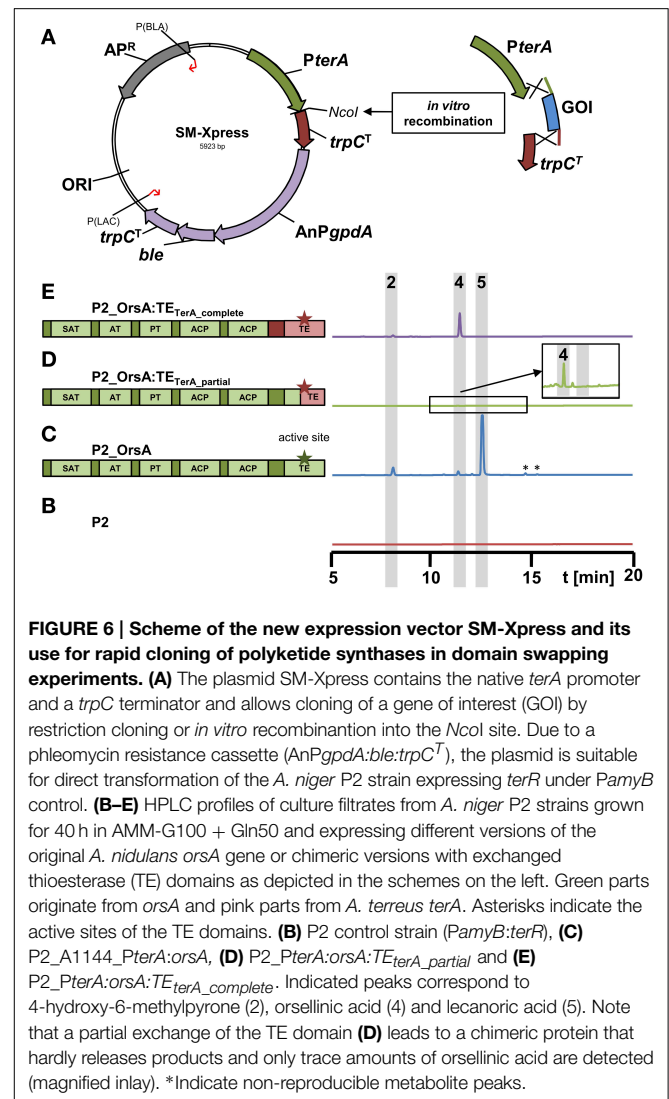


FIGURE 6 | Scheme of the new expression vector SM-Xpress and its use for rapid cloning of polyketide synthases in domain swapping experiments. (A) The plasmid SM-Xpress contains the native *terA* promoter and a *trpC* terminator and allows cloning of a gene of interest (GOI) by restriction cloning or *in vitro* recombination into the *NcoI* site. Due to a phleomycin resistance cassette (*AnPgpda:ble:trpCT*), the plasmid is suitable for direct transformation of the *A. niger* P2 strain expressing *terR* under *PamyB* control. **(B–E)** HPLC profiles of culture filtrates from *A. niger* P2 strains grown for 40 h in AMM-G100 + Gln50 and expressing different versions of the original *A. nidulans orsA* gene or chimeric versions with exchanged thioesterase (TE) domains as depicted in the schemes on the left. Green parts originate from *orsA* and pink parts from *A. terreus terA*. Asterisks indicate the active sites of the TE domains. **(B)** P2 control strain (*PamyB:terR*), **(C)** P2_A1144_PterA:orsA, **(D)** P2_PterA:orsA:TEterA_partial and **(E)** P2_PterA:orsA:TEterA_complete. Indicated peaks correspond to 4-hydroxy-6-methylpyrone (2), orsellinic acid (4) and lecanoric acid (5). Note that a partial exchange of the TE domain **(D)** leads to a chimeric protein that hardly releases products and only trace amounts of orsellinic acid are detected (magnified inset). *Indicate non-reproducible metabolite peaks.

sesquiterpene (Lackner et al., 2013). To confirm that the depside formation in lecanoric acid is specific for the OrsA TE domain, we performed an *in vitro* recombination between the *orsA* gene lacking its TE domain and the TE domain from *A. terreus terA* that only releases monomers of its products (Figures 5C,D and Zaehle et al., 2014). In this approach, two different fusions were made: (i) the complete TE domain starting directly 3' of ACP2 was removed from *orsA* and fused with the complete TE domain of *terA* (*orsA:TEterA_complete*; Figure 6E). (ii) The TE domain from *orsA* was exchanged at a conserved region of the active site of the TE domain (*orsA:TEterA_partial*; Figure 6D). The *A. niger* P2 strain was transformed with the fusion constructs and transformants were analyzed for their metabolic profile (Figures 6B–E). The partial exchange of the active site only resulted in trace amounts of orsellinic acid (Figure 6D), indicating that this exchange led to loss of function of the TE domain. Additionally, it indicates that a functional TE domain is required for product release. This is in agreement with other investigations that showed that TE domains are required for efficient product

release from PKS enzymes, whereby the specific product release mechanism is mainly directed by the TE domain (Du and Lou, 2010; Xu et al., 2013).

In contrast to the chimeric protein with partial exchange of the TE domain at the active site, *A. niger* transformants expressing the chimeric *orsA* with the complete *terA* domain exclusively produced orsellinic acid in high yields and lecanoric acid was no longer detected (Figure 6E). Due to these results we provide the first experimental evidence that the depside formation in lecanoric acid is attributed to the TE domain of *orsA*. This opens a new avenue for domain swapping experiments, in which the *orsA* TE domain could be used for fusions with other polyketide synthases to generate new depsides. Furthermore, these results not only confirm the suitability of our expression system for rapid analysis of products formed from secondary metabolite gene clusters, but also shows that the system provides a tool for rapid combinatory domain swapping experiments.

Conclusions and Outlook

In this study we confirmed specificity of the transcriptional activator TerR from the terrein gene cluster for its target promoters. Furthermore, we were able to identify DNA-binding motifs recognized by TerR. Interestingly, TerR predominantly binds as a monomer to a single CGG half-site, but a second CGG motif that is separated by a five nucleotide spacer can be bound by a second monomer. High affinity sites with tendency for binding of two monomers are characterized by the consensus motif TCG-GHHWYHCGGH. At least one site with this high affinity motif is present in all promoters of genes required for terrein synthesis. Interestingly, no high-affinity consensus motifs are detected in *terG*, *terH*, and *terI* that are dispensable for terrein production, but show the same TerR dependent regulation pattern. Thus, single half-site motifs may be present in these promoters, but these are difficult to predict by bioinformational methods. On the contrary, the *terA* promoter contains three CGG direct repeat motifs and especially expression of the *terA* gene is strongly activated by TerR. The *terC* promoter contains only a single, but high affinity binding motif and its expression level is much lower than that from *terA*. Therefore, the number and probably also the distance of the motifs relative to the transcriptional start point appear important for high-level transcriptional activation. To confirm

this assumption, future studies will replace all binding sites in the *terA* promoter by motifs from other promoters (such as BS6 and BS7). Furthermore, the number of binding sites will be increased to analyze the effect on the promoter activation potential.

Although there might be space for further optimization of the system, heterologous expression analyses in *A. niger* clearly showed that a combination of TerR with its *terA* target promoter is highly efficient and leads to an amplification of the expression level of the promoter that controls *terR* expression. Thus, additional promoters will be used to control *terR* expression to analyze the maximum amplification rates that can be obtained. Another important aspect is the transfer of the system to other fungi of industrial importance. While preliminary analyses showed that the system also works in other *Aspergillus* species, we will study the functionality of the system in yeasts such as *Saccharomyces cerevisiae* and various Basidiomycetes that are amenable to genetic modifications.

Last but not least, our proof of principle studies for heterologous expression of secondary metabolite genes by the TerR/*PterA* coupled system demonstrate an easy and rapid method for production of secondary metabolites. The vector SM-Xpress allows fast cloning of genes and eases domain swapping experiments. By this approach, we were able to show that the TE domain of OrsA performs a depside formation and future studies will use this domain for generating chimera with other polyketide synthases.

Acknowledgments

We greatly acknowledge Sylke Fricke for assistance in cloning and purification of TerR DNA-binding domains, Daniela Hildebrandt for assistance in cloning of fungal reporter constructs, Andrea Perner for HR-MS and Heike Heinecke for recording ¹H- and ¹³C-NMR spectra of secondary metabolites. This work was supported by grant BR 2216/4-1 from the German Science Foundation (DFG) and internal funding from the Hans-Knoell-Institute (HKI).

Supplementary Material

The Supplementary Material for this article can be found online at: <http://www.frontiersin.org/journal/10.3389/fmicb.2015.00184/abstract>

References

- Alberts, A. W., Chen, J., Kuron, G., Hunt, V., Huff, J., Hoffman, C., et al. (1980). Mevinolin: a highly potent competitive inhibitor of hydroxymethylglutaryl-coenzyme A reductase and a cholesterol-lowering agent. *Proc. Natl. Acad. Sci. U.S.A.* 77, 3957–3961. doi: 10.1073/pnas.77.7.3957
- Armaleo, D., Sun, X., and Culberson, C. (2011). Insights from the first putative biosynthetic gene cluster for a lichen depside and depsidone. *Mycologia* 103, 741–754. doi: 10.3852/10-335
- Bergmann, S., Schumann, J., Scherlach, K., Lange, C., Brakhage, A. A., and Hertweck, C. (2007). Genomics-driven discovery of PKS-NRPS hybrid metabolites from *Aspergillus nidulans*. *Nat. Chem. Biol.* 3, 213–217. doi: 10.1038/nchem-bio869
- Blatzer, M., Gsaller, F., Abt, B., Schrettl, M., Specht, T., and Haas, H. (2014). An endogenous promoter for conditional gene expression in *Acremonium chrysogenum*: the xylan and xylose inducible promoter *xyI1(P)*. *J. Biotechnol.* 169, 82–86. doi: 10.1016/j.jbiotec.2013.11.003
- Blumhoff, M., Steiger, M. G., Marx, H., Mattanovich, D., and Sauer, M. (2013). Six novel constitutive promoters for metabolic engineering of *Aspergillus niger*. *Appl. Microbiol. Biotechnol.* 97, 259–267. doi: 10.1007/s00253-012-4207-9
- Bok, J. W., Chung, D., Balajee, S. A., Marr, K. A., Andes, D., Nielsen, K. F., et al. (2006). GliZ, a transcriptional regulator of gliotoxin biosynthesis, contributes to *Aspergillus fumigatus* virulence. *Infect. Immun.* 74, 6761–6768. doi: 10.1128/IAI.00780-06
- Brakhage, A. A. (1997). Molecular regulation of penicillin biosynthesis in *Aspergillus (Emericella) nidulans*. *FEMS Microbiol. Lett.* 148, 1–10. doi: 10.1111/j.1574-6968.1997.tb10258.x

- Cahuzac, B., Cerdan, R., Felenbok, B., and Guittet, E. (2001). The solution structure of an AlcR-DNA complex sheds light onto the unique tight and monomeric DNA binding of a Zn(2)Cys(6) protein. *Structure* 9, 827–836. doi: 10.1016/S0969-2126(01)00640-2
- Calam, C. T., Oxford, A. E., and Raistrick, H. (1939). Studies in the biochemistry of micro-organisms: itaconic acid, a metabolic product of a strain of *Aspergillus terreus* Thom. *Biochem. J.* 33, 1488–1495.
- Chakravarty, A., Carlson, J. M., Khetani, R. S., and Gross, R. H. (2007). A novel ensemble learning method for *de novo* computational identification of DNA binding sites. *BMC Bioinform.* 8:249. doi: 10.1186/1471-2105-8-249
- Du, L., and Lou, L. (2010). PKS and NRPS release mechanisms. *Nat. Prod. Rep.* 27, 255–278. doi: 10.1039/b912037h
- Felenbok, B., Sequeval, D., Mathieu, M., Sibley, S., Gwynne, D. I., and Davies, R. W. (1988). The ethanol regulon in *Aspergillus nidulans*: characterization and sequence of the positive regulatory gene *alcR*. *Gene* 73, 385–396. doi: 10.1016/0378-1119(88)90503-3
- Fitzgerald, M. X., Rojas, J. R., Kim, J. M., Kohlhaw, G. B., and Marmorstein, R. (2006). Structure of a Leu3-DNA complex: recognition of everted CGG half-sites by a Zn2Cys6 binuclear cluster protein. *Structure* 14, 725–735. doi: 10.1016/j.str.2005.11.025
- Fleissner, A., and Dersch, P. (2010). Expression and export: recombinant protein production systems for *Aspergillus*. *Appl. Microbiol. Biotechnol.* 87, 1255–1270. doi: 10.1007/s00253-010-2672-6
- Forstner, R. R., Fox, E. M., Chung, D., Howlett, B. J., Keller, N. P., and Schroeder, F. C. (2011). Identification of cryptic products of the gliotoxin gene cluster using NMR-based comparative metabolomics and a model for gliotoxin biosynthesis. *J. Am. Chem. Soc.* 133, 9678–9681. doi: 10.1021/ja2029987
- Gressler, M., Zaehle, C., Scherlach, K., Hertweck, C., and Brock, M. (2011). Multifactorial induction of an orphan PKS-NRPS gene cluster in *Aspergillus terreus*. *Chem. Biol.* 18, 198–209. doi: 10.1016/j.chembiol.2010.12.011
- Heger, A., and Holm, L. (2000). Rapid automatic detection and alignment of repeats in protein sequences. *Proteins* 41, 224–237. doi: 10.1002/1097-0134(20001101)41:2<224::AID-PROT70>3.0.CO;2-Z
- Hutchinson, C. R., Kennedy, J., Park, C., Kendrew, S., Auclair, K., and Vederas, J. (2000). Aspects of the biosynthesis of non-aromatic fungal polyketides by iterative polyketide synthases. *Antonie Van Leeuwenhoek* 78, 287–295. doi: 10.1023/A:1010294330190
- Klement, T., and Buchs, J. (2013). Itaconic acid—a biotechnological process in change. *Bioresour. Technol.* 135, 422–431. doi: 10.1016/j.biortech.2012.11.141
- Lackner, G., Bohnert, M., Wick, J., and Hoffmeister, D. (2013). Assembly of melleotide antibiotics involves a polyketide synthase with cross-coupling activity. *Chem. Biol.* 20, 1101–1106. doi: 10.1016/j.chembiol.2013.07.009
- Lenouvel, F., Nikolaev, I., and Felenbok, B. (1997). *In vitro* recognition of specific DNA targets by AlcR, a zinc binuclear cluster activator different from the other proteins of this class. *J. Biol. Chem.* 272, 15521–15526. doi: 10.1074/jbc.272.24.15521
- Liu, B. H., and Chu, F. S. (1998). Regulation of *afIR* and its product, AfIR, associated with aflatoxin biosynthesis. *Appl. Environ. Microbiol.* 64, 3718–3723.
- Liu, L., Liu, J., Qiu, R. X., Zhu, X. G., Dong, Z. Y., and Tang, G. M. (2003). Improving heterologous gene expression in *Aspergillus niger* by introducing multiple copies of protein-binding sequence containing CCAAT to the promoter. *Lett. Appl. Microbiol.* 36, 358–361. doi: 10.1046/j.1472-765X.2003.01321.x
- Lubertozzi, D., and Keasling, J. D. (2009). Developing *Aspergillus* as a host for heterologous expression. *Biotechnol. Adv.* 27, 53–75. doi: 10.1016/j.biotechadv.2008.09.001
- MacPherson, S., Laroche, M., and Turcotte, B. (2006). A fungal family of transcriptional regulators: the zinc cluster proteins. *Microbiol. Mol. Biol. Rev.* 70, 583–604. doi: 10.1128/MMBR.00015-06
- Menne, S., Walz, M., and Kuck, U. (1994). Expression studies with the bidirectional *pcbAB-pcbC* promoter region from *Acremonium chrysogenum* using reporter gene fusions. *Appl. Microbiol. Biotechnol.* 42, 57–66. doi: 10.1007/BF00170225
- Meyer, V., Wanka, F., Van Gent, J., Arentshorst, M., Van Den Hondel, C. A., and Ram, A. F. (2011). Fungal gene expression on demand: an inducible, tunable, and metabolism-independent expression system for *Aspergillus niger*. *Appl. Environ. Microbiol.* 77, 2975–2983. doi: 10.1128/AEM.02740-10
- Minetoki, T., Kumagai, C., Gomi, K., Kitamoto, K., and Takahashi, K. (1998). Improvement of promoter activity by the introduction of multiple copies of the conserved region III sequence, involved in the efficient expression of *Aspergillus oryzae* amylase-encoding genes. *Appl. Microbiol. Biotechnol.* 50, 459–467. doi: 10.1007/s002530051321
- Nikolaev, I., Cochet, M. F., Lenouvel, F., and Felenbok, B. (1999). A single amino acid, outside the AlcR zinc binuclear cluster, is involved in DNA binding and in transcriptional regulation of the *alc* genes in *Aspergillus nidulans*. *Mol. Microbiol.* 31, 1115–1124. doi: 10.1046/j.1365-2958.1999.01250.x
- Pachlinger, R., Mitterbauer, R., Adam, G., and Strauss, J. (2005). Metabolically independent and accurately adjustable *Aspergillus* sp. expression system. *Appl. Environ. Microbiol.* 71, 672–678. doi: 10.1128/AEM.71.2.672-678.2005
- Parrot, D., Peresse, T., Hitti, E., Carrie, D., Grube, M., and Tomasi, S. (2015). Qualitative and spatial metabolite profiling of lichens by a LC-MS approach combined with optimised extraction. *Phytochem. Anal.* 26, 23–33. doi: 10.1002/pca.2532
- Punt, P. J., Dingemans, M. A., Kuyvenhoven, A., Soede, R. D., Pouwels, P. H., and Van Den Hondel, C. A. (1990). Functional elements in the promoter region of the *Aspergillus nidulans* *gpdA* gene encoding glyceraldehyde-3-phosphate dehydrogenase. *Gene* 93, 101–109. doi: 10.1016/0378-1119(90)90142-E
- Schroeckh, V., Scherlach, K., Nutzmann, H. W., Shelest, E., Schmidt-Heck, W., Schuemann, J., et al. (2009). Intimate bacterial-fungal interaction triggers biosynthesis of archetypal polyketides in *Aspergillus nidulans*. *Proc. Natl. Acad. Sci. U.S.A.* 106, 14558–14563. doi: 10.1073/pnas.0901870106
- Sharma, R., Katoch, M., Srivastava, P. S., and Qazi, G. N. (2009). Approaches for refining heterologous protein production in filamentous fungi. *World J. Microbiol. Biotechnol.* 25, 2083–2094. doi: 10.1007/s11274-009-0128-x
- Shoji, J. Y., Maruyama, J., Arioka, M., and Kitamoto, K. (2005). Development of *Aspergillus oryzae* *thiA* promoter as a tool for molecular biological studies. *FEMS Microbiol. Lett.* 244, 41–46. doi: 10.1016/j.femsle.2005.01.014
- Slesiona, S., Gressler, M., Mihlan, M., Zaehle, C., Schaller, M., Barz, D., et al. (2012a). Persistence versus escape: *Aspergillus terreus* and *Aspergillus fumigatus* employ different strategies during interactions with macrophages. *PLoS ONE* 7:e31223. doi: 10.1371/journal.pone.0031223
- Slesiona, S., Ibrahim-Granet, O., Olias, P., Brock, M., and Jacobsen, I. D. (2012b). Murine infection models for *Aspergillus terreus* pulmonary aspergillosis reveal long-term persistence of conidia and liver degeneration. *J. Infect. Dis.* 205, 1268–1277. doi: 10.1093/infdis/jis193
- Todd, R. B., Andrianopoulos, A., Davis, M. A., and Hynes, M. J. (1998). FacB, the *Aspergillus nidulans* activator of acetate utilization genes, binds dissimilar DNA sequences. *Embo J.* 17, 2042–2054. doi: 10.1093/emboj/17.7.2042
- Verdoes, J. C., Punt, P. J., Schrickx, J. M., Van Verseveld, H. W., Stouthamer, A. H., and Van Den Hondel, C. A. (1993). Glucoamylase overexpression in *Aspergillus niger*: molecular genetic analysis of strains containing multiple copies of the *glaA* gene. *Transgenic Res.* 2, 84–92. doi: 10.1007/BF01969381
- Vogt, K., Bhabhra, R., Rhodes, J. C., and Askew, D. S. (2005). Doxycycline-regulated gene expression in the opportunistic fungal pathogen *Aspergillus fumigatus*. *BMC Microbiol.* 5:1. doi: 10.1186/1471-2180-5-1
- Ward, O. P. (2012). Production of recombinant proteins by filamentous fungi. *Biotechnol. Adv.* 30, 1119–1139. doi: 10.1016/j.biotechadv.2011.09.012
- Xu, B., Yin, Y., Zhang, F., Li, Z., and Wang, L. (2012). Operating conditions optimization for (+)-terrein production in a stirred bioreactor by *Aspergillus terreus* strain PF-26 from marine sponge *Phakellia fusca*. *Bioprocess Biosyst. Eng.* 35, 1651–1655. doi: 10.1007/s00449-012-0735-z
- Xu, Y., Espinosa-Artiles, P., Schubert, V., Xu, Y. M., Zhang, W., Lin, M., et al. (2013). Characterization of the biosynthetic genes for 10,11-dehydrocurvularin, a heat shock response-modulating anticancer fungal polyketide from *Aspergillus terreus*. *Appl. Environ. Microbiol.* 79, 2038–2047. doi: 10.1128/AEM.03334-12
- Yin, Y., Xu, B., Li, Z., and Zhang, B. (2012). Enhanced production of (+)-terrein in fed-batch cultivation of *Aspergillus terreus* strain PF26 with sodium citrate. *World J. Microbiol. Biotechnol.* 29, 441–446. doi: 10.1007/s11274-012-1196-x

- Yu, J., Chang, P. K., Ehrlich, K. C., Cary, J. W., Bhatnagar, D., Cleveland, T. E., et al. (2004). Clustered pathway genes in aflatoxin biosynthesis. *Appl. Environ. Microbiol.* 70, 1253–1262. doi: 10.1128/AEM.70.3.1253-1262.2004
- Yu, J. H., Butchko, R. A., Fernandes, M., Keller, N. P., Leonard, T. J., and Adams, T. H. (1996). Conservation of structure and function of the aflatoxin regulatory gene *aflR* from *Aspergillus nidulans* and *A. flavus*. *Curr. Genet.* 29, 549–555. doi: 10.1007/BF02426959
- Zaehle, C., Gressler, M., Shelest, E., Geib, E., Hertweck, C., and Brock, M. (2014). Terrein biosynthesis in *Aspergillus terreus* and its impact on phytotoxicity. *Chem. Biol.* 21, 719–731. doi: 10.1016/j.chembiol.2014.03.010

Conflict of Interest Statement: The authors declare that the research was conducted in the absence of any commercial or financial relationships that could be construed as a potential conflict of interest.

Copyright © 2015 Gressler, Hortschansky, Geib and Brock. This is an open-access article distributed under the terms of the Creative Commons Attribution License (CC BY). The use, distribution or reproduction in other forums is permitted, provided the original author(s) or licensor are credited and that the original publication in this journal is cited, in accordance with accepted academic practice. No use, distribution or reproduction is permitted which does not comply with these terms.

Supplementary Material

A new high-performance heterologous fungal expression system based on regulatory elements from the *Aspergillus terreus* terrein gene cluster

Markus Gressler¹, Peter Hortschansky², Elena Geib¹ and Matthias Brock^{1,3*}

¹ Microbial Biochemistry and Physiology, Leibniz Institute for Natural Product Research and Infection Biology, -Hans Knoell Institute-, Beutenbergstr. 11a, 07745 Jena, Germany

² Molecular and Applied Microbiology, Leibniz Institute for Natural Product Research and Infection Biology, -Hans Knoell Institute-, Beutenbergstr. 11a, 07745 Jena, Germany

³ Institute for Microbiology, Friedrich Schiller University, 07743 Jena, Germany

* **Correspondence:** Matthias Brock, Microbial Biochemistry and Physiology, Leibniz Institute for Natural Product Research and Infection Biology, -Hans Knoell Institute-, Beutenbergstr. 11a, 07745 Jena, Germany, Matthias.brock@hki-jena.de

1. Supplementary Experimental Procedures

1.1 Generation of the β -galactosidase reporter strain *A. niger* A1144_PterA:lacZ

For all PCR reactions the high-fidelity proofreading Phusion polymerase was used (Thermo Biosciences). To generate an *A. niger* β -galactosidase reporter strain that expresses the *E. coli lacZ* gene under control of the *A. terreus terA* promoter (PterA; 1220 bp), the promoter fragment was amplified from genomic DNA of *A. terreus* SBUG844 with oligonucleotides P36/37, cloned in the pJET1.2 vector (Thermo Biosciences) and subcloned into the *NotI/BamHI* digested plasmid *lacZ:trpCT*-pJET1.2 (Gressler et al., 2011). The plasmid was linearized by *NotI* digestion and the *ptrA*-cassette from plasmid *ptrA*-pJET1 (Fleck and Brock, 2010) was inserted. The plasmid was used for transformation of *A. niger* A1144 resulting in A1144_PterA:lacZ. Transformants with two genomic integrations of the construct were selected for downstream investigations.

1.2 Expression of *terR* in *A. niger* A1144, *A. niger* A1144_PterA:lacZ and overexpression in *A. terreus* SBUG844

For expression of *terR* under control of its native promoter, the region spanning the promoter, coding sequence and its terminator (*terR*+P+T; 4130 bp) was amplified with oligonucleotides P38/39 from genomic DNA of *A. terreus* SBUG844 and cloned into pJET1.2. The plasmid was linearized by *NotI* digestion and the *hph* resistance cassette from *hph*-pCRIV (Fleck and Brock, 2010) was inserted. The resulting vector *hph_PterR:terR*_pJET1.2 was used for transformation of A1144_PterA:lacZ.

For overexpression of *terR*, the coding region of *terR* (ATEG_00139) together with its terminator (3032 bp) was amplified from genomic DNA of *A. terreus* SBUG844 with oligonucleotides P40/39 and cloned into the pJET1.2 vector resulting in plasmid 00139+T-pJET1.2. The promoter of the glyceraldehyde-3-phosphate dehydrogenase from *A. nidulans* (AnPgpda; 1336 bp) and the α -amylase B promoter from *A. oryzae* (AoPamyB; 1019 bp) were amplified with oligonucleotides P41/42 from genomic DNA of *A. nidulans* FGSC A4 gDNA and with oligonucleotides P43/44 from genomic DNA of *A. oryzae* FGSC A815, respectively. Fragments were subcloned into pJET1.2, excised by *BamHI/NotI* restriction and subcloned into plasmid 00139+T-

pJET1.2. The *hph* resistance cassette from *hph*-pCRIV (Fleck and Brock, 2010) was inserted into the *NotI*-linearized vectors. The resulting plasmids *hph*_AnPgpdA:*terR*_pJET1.2 and *hph*_AoPamyB:*terR*_pJET1.2 were used for transformation of *A. niger* A1144_*PterA*:*lacZ*, *A. niger* A1144_*PterA*:*lacZ* or *A. terreus* SBUG844 as specified in the respective experiments. For transformation of *A. niger* A1144, the *hph* cassette of plasmid *hph*_AoPamyB:*terR*_pJET1.2 was replaced by the *ptrA* resistance cassette. Transformants were analyzed by Southern blot and strains that contained single or double integrations of the constructs were selected as specified.

1.3 Construction of *PterC*:*lacZ* and *PterC*_{m1/2}:*lacZ* reporter strains in *A. terreus* SBUG844

All sequences of the *terC* promoter were amplified from genomic DNA of *A. terreus* SBUG844. To generate the *PterC*:*lacZ* reporter, the promoter (*PterC*; 1203 bp) was amplified with oligonucleotides P45/46. To exchange the putative “BS4” by “BS5” (*PterC*_{m1}) the upstream and downstream promoter fragments adjacent to “BS4” were amplified with oligonucleotides P45/47 and P48/46, gel purified and fused by overlap-PCR using the flanking oligonucleotides P45/46 generating the *PterC*_{m1} fragment. After subcloning into pJET1.2, the native and mutated *PterC* fragments were excised by *NotI*/*BamHI* restriction and ligated into the *NotI*/*BamHI* digested plasmid *lacZ*:*trpC*^T-pJET1.2 (Gressler et al., 2011). The plasmids were linearized with *NotI* and the *ptrA* resistance cassette was inserted. To delete the two CGG half-sites of “BS4” in *PterC* (*PterC*_{m2}), a 928 bp fragment of the *terC* promoter was excised by *StuI*/*SmaI* restriction from plasmid *ptrA*_PterC:*lacZ*:*trpC*^T-pJET1.2. Two fragments containing the mutated half-sites were amplified with oligonucleotides P49/50 and P51/52 and inserted into the *StuI*/*SmaI* restricted vector by *in vitro* recombination using the InFusion Kit HD cloning kit (Clonotech laboratories). All three reporter plasmids were used for transformation of *A. terreus* SBUG844 resulting in strains SBUG844_*PterC*:*lacZ*, SBUG844_*PterC*_{m1}:*lacZ* and SBUG844_*PterC*_{m2}:*lacZ*. Independent transformants with single copy integration of the respective construct were randomly selected for further investigations.

1.4 Generation of reporter strains to investigate the bi-directionality of the *terA/B* promoter

The *tdTomato* gene (1445 bp) was amplified from *tdTom*-pUC57 with oligonucleotides P53/54 and cloned into pJET1.2. The *tdTomato* gene was excised by *NotI*/*BamHI* restriction and ligated into the *NotI*/*BamHI* restricted plasmid *lacZ*:*trpC*^T-pJET1.2. The resulting plasmid *tdTom*:*lacZ*:*trpC*^T-pJET1.2 was linearized with *NotI* and the *hph* resistance cassette was inserted. The *BamHI* restriction site between the *lacZ* and *tdTomato* gene enabled the subsequent insertion of the bi-directional *terA/B* promoter in both orientations. For this purpose, the 783 bp intergenic region between *terA* and *terB* was amplified with oligonucleotides P55/56 from genomic DNA of *A. terreus* SBUG844 resulting in terminal *BglIII* restriction sites at the 5'- and 3'-flank. The fragment was cloned into pJET1.2, excised with *BglIII* ligated into the *BamHI* restricted plasmid *hph*_tdTomato:*lacZ*:*trpC*^T-pJET1.2. Orientation of the promoter was checked by PCR and plasmids containing the promoter in both orientations were used for transformation of A1144_*PamyB*:*terR* (P2). Depending on the orientation of the promoter this resulted in strains *A. niger* A1144_*AoPamyB*:*terR*_PterA:*lacZ*_PterB:*tdTom* and *A. niger* A1144_*AoPamyB*:*terR*_PterB:*lacZ*_PterA:*tdTom*. Independent transformants with single copy integration of the respective construct were selected for further investigations.

1.5 Generation of reference reporter strains *A. niger* A1144_AnPgpdA:*lacZ* and A1144_AnPgpdA:*tdTom*

To generate the β -galactosidase reference reporter strains, the *gpdA* promoter from *A. nidulans* was excised from AnPgpdA-JET1.2 by *BglIII*/*HindIII* restriction and was cloned into the *BamHI*/*HindIII* restricted vector *lacZ*:*trpC*^T-pJET1.2. After restriction with *NotI* the *ptrA* resistance

cassette was introduced. To generate the fluorescent tdTomato reference reporter strain, the *tdTomato* gene (1437 bp) was excised with *BglII/HindIII* from *tdTom-pUC57* and cloned into *AnPgpDA-JET1.2*. The plasmid *AnPgpDA:tdTom-pJET1.2* was linearized with *NotI* and the *hph* resistance cassette was inserted. Both plasmids were used for transformation of the *A. niger* A1144 wild type. Independent transformants with single copy integration of the respective constructs were selected as reference strains.

1.6 Heterologous expression of polyketide synthase genes in P2

For heterologous expression of the *terA* gene (ATEG_00145) the entire coding region including its promoter and terminator sequence were amplified with oligonucleotides P57/56 (7676 bp) from genomic DNA of *A. terreus* SBUG844. The fragment was ligated into pJET1.2/blunt. The plasmid was linearized with *NotI* and the *hph* resistance cassette was inserted. The resulting plasmid *PterA:terA:terA^T_hph_pJET1.2* was used for transformation of *A1144_PamyB:terR* (P2). For heterologous expression of the *orsA* gene (AN7909) under control of the *terA* promoter the coding region of *orsA* together with its terminator was amplified from genomic DNA of *A. nidulans* FGSC A4 using oligonucleotides P58/59 (6707 bp). The *terA* promoter was amplified from genomic DNA of *A. terreus* SBUG844 with oligonucleotides P60/61 (776 bp). The promoter and the *orsA* fragments were fused and introduced into the *EcoRV* digested *hph-pCRIV* vector (Zaehle et al., 2014) by *in vitro* recombination using the InFusion HD Cloning Kit (Clontech Laboratories). The resulting plasmid *PterA:orsA:orsA^T_hph_pCRIV* was used for transformation of *A1144_PamyB:terR* (P2). For heterologous expression of the *orsA* gene with a domain swapping of the thioesterase domain from *terA*, two different constructs were generated, since the starting position of thioesterase domains has not been well defined yet. The *orsA* gene (AN7909) without its sequence coding for the TE domain was amplified from genomic DNA of *A. nidulans* FGSC A4 using either oligonucleotides P62/63 (5873 bp) or P62/64 (5389 bp). In accordance, the sequence coding for the TE domain from *terA* (ATEG_00145) was amplified from genomic DNA of *A. terreus* SBUG844 with either oligonucleotides P65/66 (597 bp) or P67/66 (1126 bp). The expression vector *PterA:trpC^T_AnPgpDA:ble:trpC^T_pUC19* (SM Xpress) was linearized with *NcoI* and the fragments were ligated by *in vitro* recombination using the InFusion HD Cloning Kit (Clontech). The resulting plasmids contained the *orsA* gene with TE domain from *terA* under transcriptional control of the *terA* promoter and were used for transformation of *A. niger* *A1144_PamyB:terR* (P2). Transformants with single copy integrations of the constructs were selected for metabolite identification.

2. Supplementary Figures and Tables

2.1 Supplementary Tables

Table S1. Wild type strains and mutants from this study

Strain	Genotype	Reference
FGSC A1144	wild type	FGSC; Kansas City; USA
FGSC A4	wild type	FGSC; Kansas City; USA
SBUG844	wild type	JMRC, HKI; Jena; Germany
SBUG844 Δ <i>akuB</i>	Δ <i>akuB</i> :: <i>hph</i>	Gressler <i>et al.</i> , 2011
SBUG844 Δ <i>akuB</i> Δ <i>terR</i>	Δ <i>akuB</i> :: <i>hph</i> ; Δ <i>terR</i> :: <i>ptrA</i>	Zaehle <i>et al.</i> , 2014
SBUG844_ <i>AnPgpdA</i> : <i>terR</i>	<i>hph</i> , <i>AnPgpdA</i> : <i>terR</i> : <i>terR</i> ^T	This study.
SBUG844_ <i>PterC</i> : <i>lacZ</i>	<i>ptrA</i> , <i>PterC</i> : <i>lacZ</i> : <i>trpC</i> ^T	This study.
SBUG844_ <i>PterCm1</i> : <i>lacZ</i>	<i>ptrA</i> , <i>PterCm1</i> : <i>lacZ</i> : <i>trpC</i> ^T	This study.
SBUG844_ <i>PterCm2</i> : <i>lacZ</i>	<i>ptrA</i> , <i>PterCm2</i> : <i>lacZ</i> : <i>trpC</i> ^T	This study.
FGSC A1144_ <i>PterA</i> : <i>lacZ</i>	<i>ptrA</i> , <i>PterA</i> : <i>lacZ</i> : <i>trpC</i> ^T	This study.
FGSC A1144_ <i>PterA</i> : <i>lacZ</i> _ <i>PterR</i> : <i>terR</i>	<i>ptrA</i> , <i>PterA</i> : <i>lacZ</i> : <i>trpC</i> ^T ; <i>hph</i> , <i>PterR</i> : <i>terR</i> : <i>terR</i> ^T	This study.
FGSC A1144_ <i>PterA</i> : <i>lacZ</i> _ <i>AnPgpdA</i> : <i>terR</i>	<i>ptrA</i> , <i>PterA</i> : <i>lacZ</i> : <i>trpC</i> ^T ; <i>hph</i> , <i>AnPgpdA</i> : <i>terR</i> : <i>terR</i> ^T	This study.
FGSC A1144_ <i>PterA</i> : <i>lacZ</i> _ <i>AoPamyB</i> : <i>terR</i>	<i>ptrA</i> , <i>PterA</i> : <i>lacZ</i> : <i>trpC</i> ^T ; <i>hph</i> , <i>AoPamyB</i> : <i>terR</i> : <i>terR</i> ^T	This study.
FGSC A1144_ <i>AoPamyB</i> : <i>terR</i>	<i>ptrA</i> , <i>AoPamyB</i> : <i>terR</i> : <i>terR</i> ^T	This study.
FGSC A1144 <i>AoPamyB</i> : <i>terR</i> _ <i>PterA</i> : <i>lacZ</i> _ <i>PterB</i> : <i>tdTom</i>	<i>ptrA</i> , <i>AoPamyB</i> : <i>terR</i> : <i>terR</i> ^T ; <i>hph</i> , <i>PterA</i> : <i>lacZ</i> : <i>trpC</i> ^T , <i>PterB</i> : <i>tdTom</i>	This study.
FGSC A1144 <i>AoPamyB</i> : <i>terR</i> _ <i>PterB</i> : <i>lacZ</i> _ <i>PterA</i> : <i>tdTom</i>	<i>ptrA</i> , <i>AoPamyB</i> : <i>terR</i> : <i>terR</i> ^T ; <i>hph</i> , <i>PterB</i> : <i>lacZ</i> : <i>trpC</i> ^T , <i>PterA</i> : <i>tdTom</i>	This study.
FGSC A1144_ <i>AnPgpdA</i> : <i>lacZ</i>	<i>ptrA</i> , <i>AnPgpdA</i> : <i>lacZ</i> : <i>trpC</i> ^T	This study.
FGSC A1144_ <i>AnPgpdA</i> : <i>tdTom</i>	<i>hph</i> , <i>AnPgpdA</i> : <i>tdTom</i>	This study.
FGSC A1144_ <i>AoPamyB</i> : <i>terR</i> _ <i>PterA</i> : <i>terA</i>	<i>ptrA</i> , <i>AoPamyB</i> : <i>terR</i> : <i>terR</i> ^T ; <i>hph</i> , <i>PterA</i> : <i>terA</i> : <i>terA</i> ^T	This study.

FGSC A1144_AoPamyB:terR_PterA:orsA	<i>ptrA</i> , AoPamyB:terR:terR ^T ; <i>hph</i> , PterA:orsA:orsA ^T	This study.
FGSC A1144 AoPamyB:terR_PterA:orsA:TE _{terA} partial:trpC ^T	<i>ptrA</i> , AoPamyB:terR:terR ^T ; <i>hph</i> , PterA:orsA:TE _{terA} partial:trpC ^T	This study.
FGSC A1144 AoPamyB:terR_PterA:orsA:TE _{terA} complete:trpC ^T	<i>ptrA</i> , AoPamyB:terR:terR ^T ; <i>hph</i> , PterA:orsA:TE _{terA} complete:trpC ^T	This study.
BL21(DE3) Rosetta2	<i>fhuA2</i> [<i>lon</i>] <i>ompT gal</i> (λ DE3) [<i>dcm</i>] Δ <i>hdsS</i> λ DE3 = λ <i>sBamHIo</i> Δ <i>EcoRI-B</i> <i>int::(lacI::PlacUV5::T7 gene1)</i> <i>i21</i> Δ <i>nin5</i> with plasmid pRARE2	Novagen, Germany
BL21(DE3)_PlacZ:terR ₁₋₁₅₃	BL21(DE3) Rosetta2 genotype with PlacZ:terR ₁₋₁₅₃ -pET29a	This study.
BL21(DE3)_PlacZ:terR ₃₅₋₁₃₈	BL21(DE3) Rosetta2 genotype with PlacZ:terR ₃₅₋₁₃₈ -pET29a	This study.
BL21(DE3)_PlacZ:terR ₄₃₋₁₃₈	BL21(DE3) Rosetta2 genotype with PlacZ:terR ₄₃₋₁₃₈ -pET29a	This study.

Table S2. Oligonucleotides used in this study.

No.	name	5'-3' sequence
P1	terR_NdeI_f	catatgttcgccgaacttaacgcaaag
P2	terR_Hind_r	aagcttagctatgccggtcatttg
P3	Nde_shortTerR_f	catatgtctcggcgagaggtg
P4	Bam_shortTerR_r	ggatcctcagcccgcattccggaacc
P5	TerR35-138_f	catatgtcttctgtccgaaaaagaagtg
P6	EcoRI_PterA_for	gacggccagtgaattcgatcctctctgatattgtcg
P7	NcoI_PterA_rev	ccatgggtctgtgatgagaagttg
P8	NcoI_TrpCT_for	atcacagccatggcagcagtgattcaatctgaacc
P9	EcoRI_TrpCT_rev	taccgagctcgaattcagtgagggttgagtacgag
P10	At00135_for1	gaatggatcgcctggatgc
P11	At00135_rev1	ccaaggeatcactattatcgac
P12	At00136_rev1	gtccaaacgatccaaggtgg
P13	At00136_for1	ggtcttacagcttctctacc
P14	At00137_for1	cgtctattctgcactcaaagc
P15	At00137_rev1	ctgtcctcaaagctcgtcc
P16	At00138_for1	gtggcttctcctatcctcg
P17	At00138_rev1	ctctccacttgagtcctgg
P18	At00139_for1	caagaagaagcatgtgtacc
P19	At00139_rev1	gatggccaacacagcttgg
P20	At00140_for1	cctacacaaacatcacctacg
P21	At00140_rev1	ggaacgtctgaacgactgg
P22	At00141_for1	gattacgagaccacggtgc
P23	At00141_rev1	gatagccttcaaagactcc
P24	At00142_for1	cagacgtgctgattaactgg
P25	At00142_rev1	cacaatgacctcgatcaagc
P26	At00143_for1	gtacgcaagtcgctgtttgg
P27	At00143_rev1	cacctcgtcgtactgtcc
P28	At00144_for2	cgatgaatgtcagcctgagc
P29	At00144_rev2	gatcaaaggcaaatacgtacc
P30	At00145_for2	ggaatcgaaggtgtgctgc
P31	At00145_rev2	cctatcaacttctccatcc
P32	act_Ater_for	ccatcgagaagtcttatgagc
P33	act_Ater_rev	ggacagggaagccagaatgg
P34	Anig_gpdA_for	caagttcggcatcggtgagg
P35	Anig_gpdA_rev	ccactcgttgcgtaccagg
P36	NotI_P00145_f	gcgccgcaatattgtgtgcgagaacc
P37	BglII_P00145_r	agatctcatggtgctgtgatgagaagtttg
P38	NotI_00140in_for	ttggtcggccgcatctatcgggacatgttg
P39	SwaI00139OE_rev	atttaaatcatgtagtcaggttgc
P40	BamHI_00139OE_f	ggatccttcgccgaacttaacgcaaagg

P41	NotI_AnPgpdA_for	gcggccgctcaccacaaaagtcagacg
P42	BamHI_AnPgpdA_rev	ggatcccattgtgatgtctgctcaagc
P43	NotI_AoPamyB_for	gcggccgctacttaaaaatcgatctcgag
P44	BamHI_AoPamyB_rev	ggatcccataaatgccttctgtggggtt
P45	NotI_P00143_for	gcggccgcatgtggaagattagtgg
P46	BamHI_P00143_rev	ggatcccattgtatgccaggagcaaag
P47	SwitchBS4-5_rev	ggcggctcctcgggtacagcgaatgcacgccaccccggtagc
P48	SwitchBS4-5new_f	ccgaggagccgccccaggaatggaatccggcctccg
P49	StuI_PterCmut3_f	cgtcatacaccaggccttcttcttccatagagg
P50	BSdel_PterCmut3_r	caacaatacaaaactcgggaatgcacgccacc
P51	BSdel_PterCmut3_f	gagtttgtattgtgaagaggtcaatggaaatccggcctc
P52	SmaI_PterCmut3_r	catgtatgccagcccgggccaggactaggctcaagg
P53	BamHI_tdTom_for	ggatccatggtctccaagggtgagg
P54	NotI_tdTom_rev	gcggccgcctactgttagagctcgtccatac
P55	BglII_P00145_rev	agatctcatggtgctgtgatgagaagtttg
P56	BglII_P00144_rev	agatctcatgatcctctctctgatattg
P57	SwaI_00145OEdn_rev	atttaaatgagccgtgaactgtatgac
P58	SATorsA_for	atggctccaaatcacgttctttttcc
P59	pCRIV-TorsA_r	gccagtgtgatggatcgcaaccctgattatccggttaaag
P60	SATorsA_PterA_r	gtgatttggagccatggtgctgtgatgagaagtttg
P61	pCRIV-PterA_f	gcgaattctgcagatgctgtgtctggtatgtgc
P62	PterA_orsA_for	catcacagcaccatggctccaaatcacgttctt
P63	orsA_forTE-S_r	gcccgcggaccaaccgcc
P64	orsA_forTE-L_r	cgagtccatacccaccgag
P65	orsA_TE(terA)S_f	ggttggtccgcccgggtattttggcgtatgcggtg
P66	trpCT_TETerA_rev	atcactgctccatggtcatgcaccgatcaagcgate
P67	orsA_TE(terA)L_f	gtgggtatggactcgttgatgtcacttaccatcactgg
P68	LacZ_up_down	ggcgttaccacacttaategc
P69	LacZ_mitte_up	ctcatccatgacctgacctg
P70	tdTom_in_for1	ggtcacgagttcgagatcgagg
P71	tdTom_in_rev1	gggtagtcctcgttgtgg
P72	SATorsA_for	atggctccaaatcacgttctttttcc
P73	terA_SATorsA_r	gttggggaagcggccggacatgccaacgacggcaatg
P74	terA+STOP1_r	caacacctcaaatggccaaccttgctg
P75	EcoRV_00145_for	gatatcggcatggatgtgcgtg

2.2 Supplementary Figures

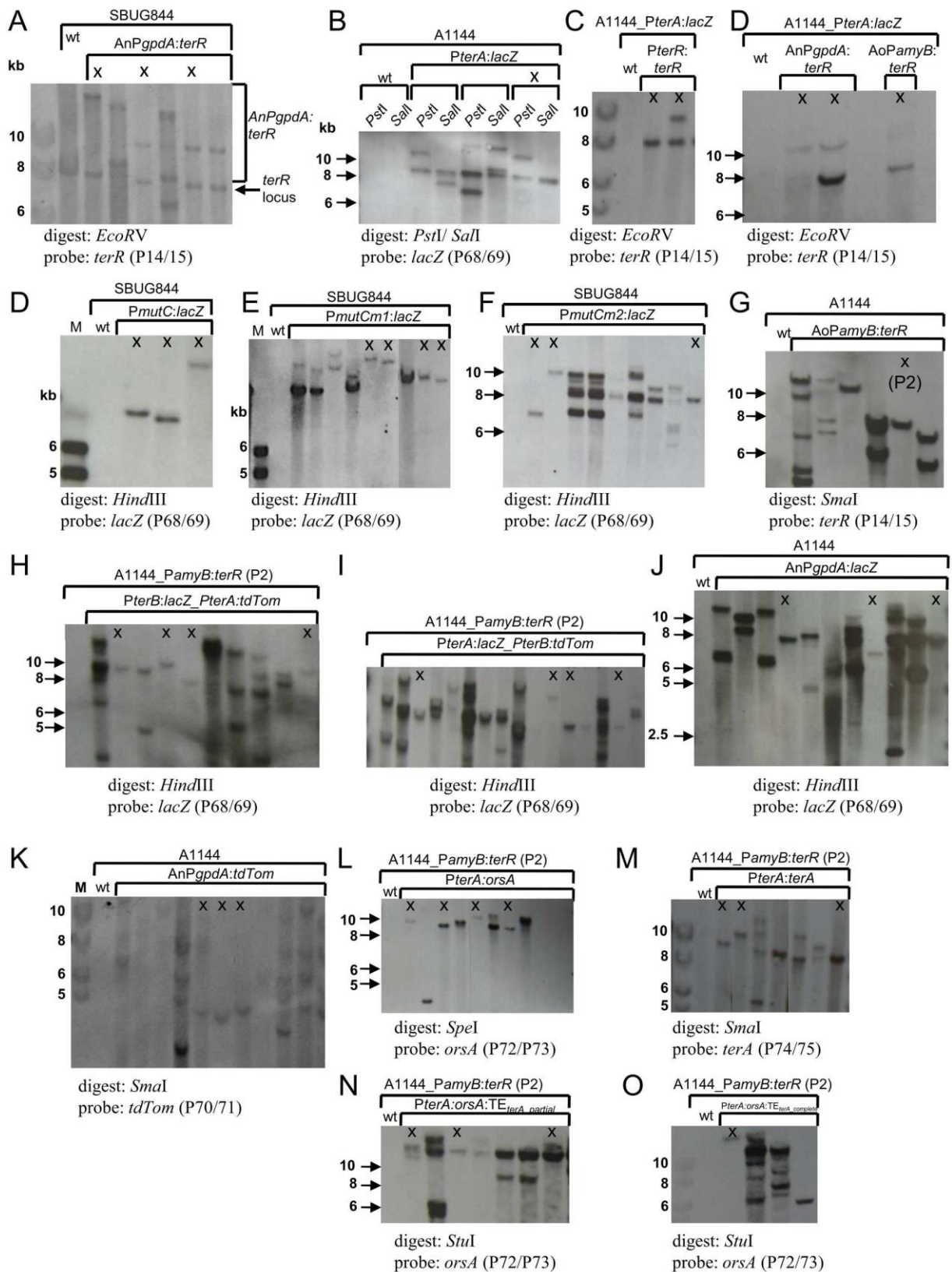


Figure S1. Southern Blot analyses for *A. terreus* and *A. niger* mutants generated in this study. Genomic DNA of parental strains and transformants was restricted with indicated enzymes, blotted on nylon membranes and hybridized with the indicated digoxigenin-labeled probes. Primer pairs used for generation of probes are indicated in brackets and sequences are found in Table S2. Signals were detected by using anti-digoxigenin FAB-fragments conjugated with alkaline phosphatase and the CDP star chemiluminescent substrate (Roche). Strains marked by “X” have been investigated in more detail as described in the main manuscript text. **(A)** Overexpression of *terR* in SBUG844 under control of the *A. nidulans gpdA* promoter. In selected transformants the original *terR* locus (signal at 8125 bp) is not affected. **(B)** Southern blot of the β -galactosidase reporter strain A1144_ *PterA:lacZ* in the *A. niger* FGSC A1144 background. The selected transformant contains two integrations as revealed from the *PstI* digest. **(C)** Integration of *terR* under its native promoter (*PterR*) in the genome of β -galactosidase reporter strain A1144_ *PterA:lacZ*. A strain with single and with double integration was selected. **(D-F)** Southern blot of the β -galactosidase reporter strains A1144_ *PterC:lacZ*, A1144_ *PterCm1:lacZ*, and A1144_ *PterCm2:lacZ*. Single copy integrants were selected for determination of reporter activity. **(G)** Southern blot of *A. niger* strains expressing *terR* under control of the *A. oryzae amyB* promoter. The strain P2 was selected for heterologous metabolite production and analysis of transcriptional activity from the bi-directional *terA/B* promoter. **(H-I)** Southern blot of transformants expressing the *lacZ* and *tdTomato* gene under control of the bi-directional *terA/B* promoter. Constructs are done in both directions. The P2 strain serves as genetic background. **(J)** Southern blot of *A. niger* reference strains (A1144_ *AnPgpdA:lacZ*) expressing the *lacZ* under control of the *A. nidulans gpdA* promoter. **(K)** Southern blot of *A. niger* reference strains (A1144_ *AnPgpdA:tdTom*) expressing the *tdTomato* gene under control of the *A. nidulans gpdA* promoter. **(L)** Southern blot of the P2 strain with integration of the *PterA:orsA* fusion (P2_ *PterA:orsA*). **(M)** Southern blot of the P2 strain with integration of the *terA* gene under control of its native *terA* promoter (P2_ *PterA:terA*) **(N-O)** Southern blot of chimera fusions of *orsA* with partial (N; P2_ *PterA:orsA:TE_{terA}_partial*) and full-length replacement (P2_ *PterA:orsA:TE_{terA}_complete*) of the *orsA* thioesterase domain for expression in *A. niger* P2.

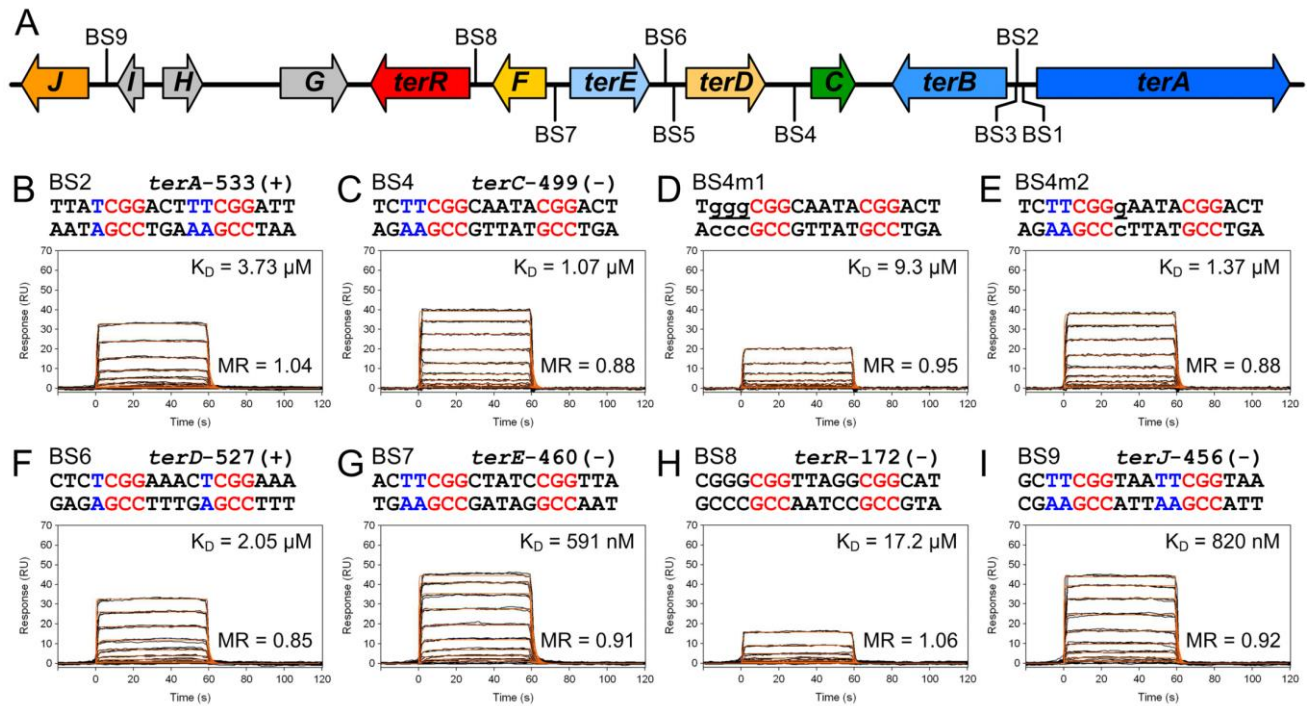


Figure S2. Real-time *in vitro* SPR interaction analysis of TerR₄₃₋₁₃₈ with selected predicted native or mutated TerR DNA-binding sites. The TerR₄₃₋₁₃₈ fragment lacks an *N*-terminal basic stretch present in the TerR₃₅₋₁₃₈ fragment. Intergenic positions of the consensus TerR-binding motif identified by the SCOPE motif finder suite. Sequences of DNA duplexes used for SPR analysis are shown on top of the sensorgrams. CGG half-sites and 5'-flanking thymidines are highlighted in red and blue. Substituted nucleotides relative to the wild-type sequence are underlined and shown in lowercase letters. TerR₄₃₋₁₃₈ binding responses from triplicate injections of different concentrations (black lines) are overlaid with the best fit derived from a 1:1 interaction model including a mass transport term (red lines). Dissociation constants (K_D) and protein:DNA molar ratios (MR) are plotted inside the sensorgrams. For more details refer to Figure 3 and section "A Basic Stretch at the TerR *N*-terminus Promotes High Affinity DNA Binding" of the main manuscript text.

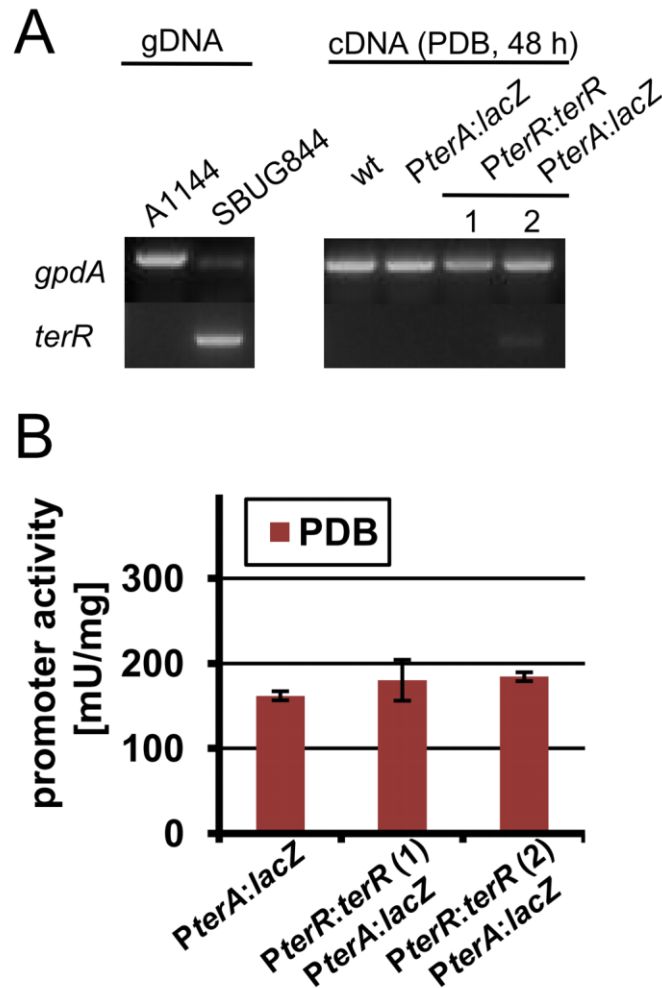


Figure S3. Semiquantitative RT-PCR analysis and β -galactosidase activity of *A. niger* strains A1144_PterA:lacZ and A1144_PterA:lacZ_PterR:terR. Strains were grown for 48 h in PDB medium. **(A)** Semi-quantitative PCR analysis. Left panel: genomic DNA from *A. niger* A1144 and *A. terreus* SBUG844 wild-type strains as template for control amplification of the *A. niger gpdA* and *A. terreus terR* gene. Right panel: Analysis of cDNA from *A. niger* wild type strain and strains containing only the *PterA:lacZ* reporter construct or the reporter together with *terR* under its native promoter in single (1) or double (2) integration. Under its native promoter, no *terR* transcript is observed. **(B)** Determination of β -galactosidase activity. Strains shown in (A) were analyzed for reporter activity. A low background activity is observed that does not increase in reporter strains that contain the *terR* gene under its native promoter regardless of the number of integrations (1 or 2).

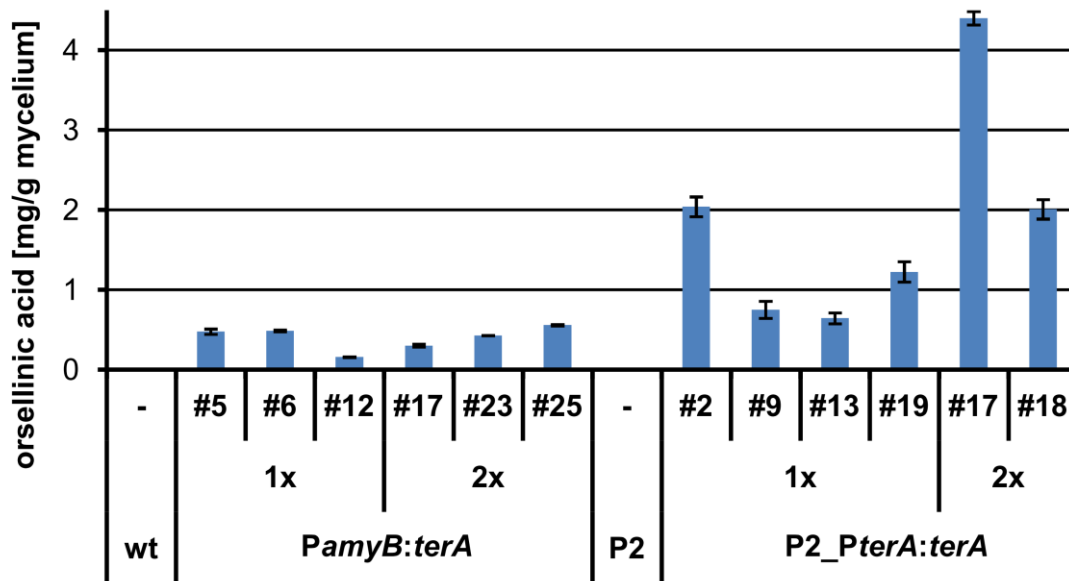
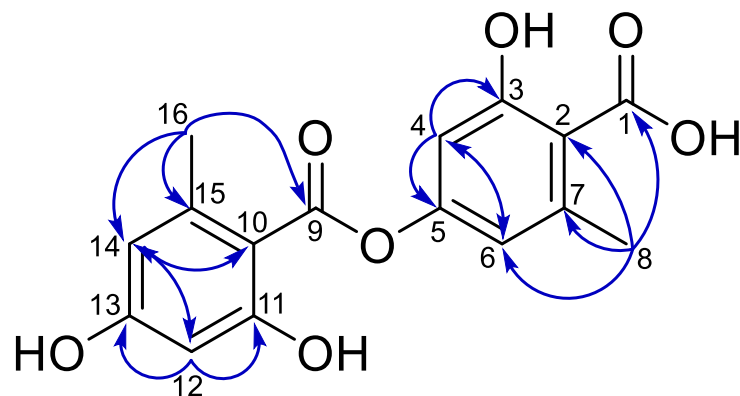


Figure S4. Quantification of orsellinic acid. Orsellinic acid was quantified from culture supernatants of *A. niger* strains expressing the *terA* gene under control of the *amyB* promoter (A1144_*PamyB:terA*) or the *terA* promoter (A1144_P2_*PterA:terA*). The parental strains A1144 (wt) and A1144_P2 (P2) served as controls. All strains were cultivated for 48 h in AMM-G100+Gln50 liquid media. Several transformants (numbers indicated by “#”) with single (1×) and double integration (2×) were analyzed. Orsellinic acid production rates are given in milligram per gram of dried mycelium.



	δ ^1H in ppm (J/Hz)	δ ^{13}C in ppm
1		171.7
2		112.1
3		162.9
4	6.09, d, (2.39)	102.6
5		159.5
6	6.22, d, (2.03)	110.6
7		141.7
8	2.39, s	22.4
9		167.9
10		118.8
11		158.8
12	6.20, d, (2.11)	104.5
13		153.4
14	6.48, d, (1.78)	113.2
15		138.1
16	2.25, s	19.6

Figure S5. Structure elucidation of lecanoric acid by ^1H NMR and ^{13}C NMR. Blue arrows at the structure indicate key heteronuclear multiple bond correlation. Chemical shifts deduced from ^1H NMR and ^{13}C NMR data measured in DMSO- d_6 are shown in the table.

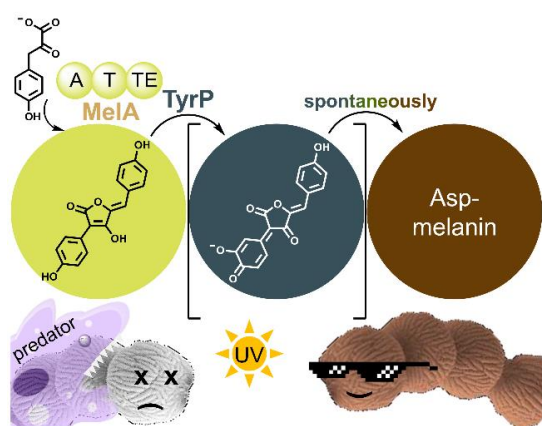
S3. Supplementary References

- Fleck, C.B., and Brock, M. (2010). *Aspergillus fumigatus* catalytic glucokinase and hexokinase: expression analysis and importance for germination, growth, and conidiation. *Eukaryot Cell* 9, 1120-1135.
- Gressler, M., Zaehle, C., Scherlach, K., Hertweck, C., and Brock, M. (2011). Multifactorial induction of an orphan PKS-NRPS gene cluster in *Aspergillus terreus*. *Chem Biol* 18, 198-209.
- Zaehle, C., Gressler, M., Shelest, E., Geib, E., Hertweck, C., and Brock, M. (2014). Terrein biosynthesis in *Aspergillus terreus* and its impact on phytotoxicity. *Chem Biol* 21, 719-731.

A non-canonical melanin biosynthesis pathway protects *Aspergillus terreus* conidia from environmental stress

Elena Geib, Markus Gressler, Iuliia Viediernikova, Falk Hillmann, Ilse D. Jacobsen, Sandor Nietzsche, Christian Hertweck, and Matthias Brock

(2016) Cell Chemical Biology; 23, 587-97



Summary of the manuscript: The manuscript describes a novel and yet undescribed pigment biosynthesis pathway present in *A. terreus* conidia. In contrast to other ascomycetes investigated so far, *A. terreus* does not produce a dihydroxynaphthalene-melanin, but the unique Asp-melanin. In this work the genes responsible for pigment biosynthesis were identified, pigment gene deletion mutants generated and studied for their environmental fitness. Even more, precursor metabolites

were isolated from deletion mutants and from heterologous gene expression. Gene expression approaches also enabled the heterologous reconstruction of pigment biosynthesis and *in vitro* pigment biosynthesis was performed by using purified enzymes. Analyses of reaction intermediates allowed to propose the pathway for the biosynthesis of Asp-melanin.

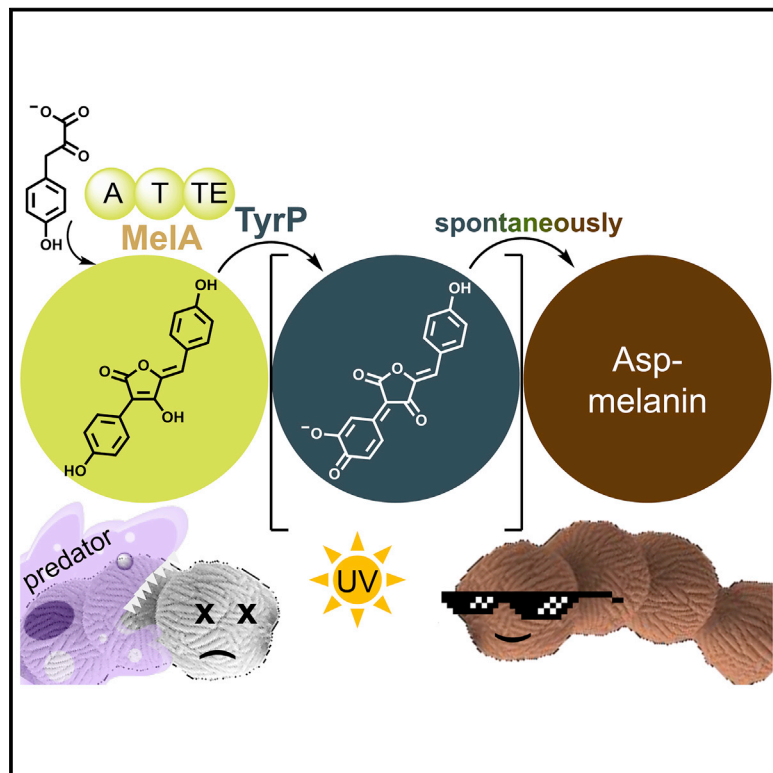
Contribution: 80% contribution of practical work, major contribution to manuscript preparation.

Expression analysis of secondary metabolite biosynthesis gene clusters induced during conidiation, generation of gene deletion mutants, complemented strains and overexpression strains. Isolation, structure elucidation and identification of aspulvinone E and Asp-melanin biosynthesis precursor metabolites. Prediction of the pigment biosynthesis pathway. 5'-RACE transcriptional start point determination of the *tyrP* gene and recombinant expression and purification of TyrP including glycosylation studies, subcellular localisation studies by fluorescence microscopy on fusion proteins. *In vitro* reconstitution of pigment formation from purified TyrP and MelA enzymes, phenotypic characterisation (UV, oxidative stress, pH) of *A. terreus* wild type and pigment mutants.

Cell Chemical Biology

A Non-canonical Melanin Biosynthesis Pathway Protects *Aspergillus terreus* Conidia from Environmental Stress

Graphical Abstract



Authors

Elena Geib, Markus Gressler, Iuliia Viediarnikova, ..., Sandor Nietzsche, Christian Hertweck, Matthias Brock

Correspondence

matthias.brock@nottingham.ac.uk

In Brief

Geib et al. show that conidia of *Aspergillus terreus* produce an uncommon type of melanin by an NRPS-like enzyme. Aspulvinone E derives as precursor and is polymerized by the tyrosinase TyrP. The melanin specifically supports adaptation to the environment.

Highlights

- *Aspergillus terreus* produces a novel type of melanin
- Pigment synthesis was reconstituted heterologously in vivo and in vitro
- An NRPS-like enzyme produces a substrate for tyrosinase-mediated polymerization
- The pigment protects conidia from biotic and abiotic stress factors

A Non-canonical Melanin Biosynthesis Pathway Protects *Aspergillus terreus* Conidia from Environmental Stress

Elena Geib,^{1,5} Markus Gressler,¹ Iuliia Viediernikova,² Falk Hillmann,² Ilse D. Jacobsen,^{3,7} Sandor Nietzsche,⁶ Christian Hertweck,⁴ and Matthias Brock^{1,5,7,*}

¹Microbial Biochemistry and Physiology

²Junior Research Group Evolution of Microbial Interactions

³Microbial Immunology

⁴Biomolecular Chemistry

Leibniz Institute for Natural Product Research and Infection Biology, Hans Knoell Institute, Beutenbergstr. 11a, 07745 Jena, Germany

⁵Fungal Genetics and Biology Group, School of Life Sciences, University of Nottingham, University Park, Nottingham NG7 2RD, UK

⁶Electron Microscopic Centre, University Hospital of the Friedrich Schiller University Jena, Ziegelmühlenweg 1, 07443 Jena, Germany

⁷Institute for Microbiology, Friedrich Schiller University, 07743 Jena, Germany

*Correspondence: matthias.brock@nottingham.ac.uk

<http://dx.doi.org/10.1016/j.chembiol.2016.03.014>

SUMMARY

Melanins are ubiquitous pigments found in all kingdoms of life. Most organisms use them for protection from environmental stress, although some fungi employ melanins as virulence determinants. The human pathogenic fungus *Aspergillus fumigatus* and related Ascomycetes produce dihydroxynaphthalene- (DHN) melanin in their spores, the conidia, and use it to inhibit phagolysosome acidification. However, biosynthetic origin of melanin in a related fungus, *Aspergillus terreus*, has remained a mystery because *A. terreus* lacks genes for synthesis of DHN-melanin. Here we identify genes coding for an unusual NRPS-like enzyme (MelA) and a tyrosinase (TyrP) that *A. terreus* expressed under conidiation conditions. We demonstrate that MelA produces aspulvinone E, which is activated for polymerization by TyrP. Functional studies reveal that this new pigment, Asp-melanin, confers resistance against UV light and hampers phagocytosis by soil amoeba. Unexpectedly, Asp-melanin does not inhibit acidification of phagolysosomes, thus likely contributing specifically to survival of *A. terreus* conidia in acidic environments.

INTRODUCTION

Melanin pigments are found in all kingdoms of life and are known to protect from various environmental stress factors such as UV light or ionizing radiation, and oxidative and other harsh environmental conditions (Eisenman and Casadevall, 2012). In fungi, the production of melanin is very common and frequently associated with virulence. In the phytopathogen *Magnaporthe oryzae* melanization is essential to withstand the high turgor pressure in appressoria during plant infection (Howard and Valent, 1996). In *Cryptococcus* species increased expression of melanin syn-

thesis genes is directly associated with increased virulence (Ngamskulrunroj et al., 2011), and in *Aspergillus fumigatus* and *Penicillium marneffei* melanin increases survival in phagolysosomes, supports hydrophobin attachment to the surface of conidia, and increases oxidative stress resistance (Jahn et al., 2000; Thywissen et al., 2011; Woo et al., 2010).

Two types of melanin are dominant in fungal species. As commonly found in mammals, some fungi produce melanin from exogenous L-3,4-dihydroxyphenylalanine (L-DOPA) or tyrosine (Eisenman and Casadevall, 2012). The second and more common type of fungal melanins results from a polyketide synthase-derived naphthopyrone, which produces a dihydroxynaphthalene- (DHN) melanin. Especially in *Aspergillus* species, this naphthopyrone synthase is highly conserved and mediates the inhibition of phagolysosome acidification after phagocytosis of conidia.

Aspergillus terreus forms an exception among Aspergilli as it lacks this highly conserved naphthopyrone synthase (Zaehle et al., 2014; Gressler et al., 2015b). As a consequence, *A. terreus* conidia are unable to inhibit acidification of phagolysosomes in macrophages, which results in the persistence of resting, but viable, conidia in phagolysosomes (Slesiona et al., 2012a). Nevertheless, conidia of *A. terreus* display a cinnamon-brown color, indicating that a pigment is produced for protection from biotic and abiotic stress factors. However, pigment formation does not require tyrosine or L-DOPA supplementation, which implies that the pigment does not follow the melanin synthesis pathway as described for *Cryptococcus* species (Eisenman and Casadevall, 2012).

Recent investigations on secondary metabolite gene clusters indicated that a non-ribosomal peptide synthetase (NRPS)-like enzyme could be involved in *A. terreus* pigment production (Guo et al., 2015). Here, we report the discovery and characterization of the enzymes and intermediates involved in *A. terreus* pigment synthesis, and analyze the contribution of the pigment to environmental protection and virulence. Furthermore, we heterologously reconstituted pigment biosynthesis in *Aspergillus niger* and produced the pigment in vitro from purified enzymes. Results confirm an exceptional pigment biosynthetic pathway

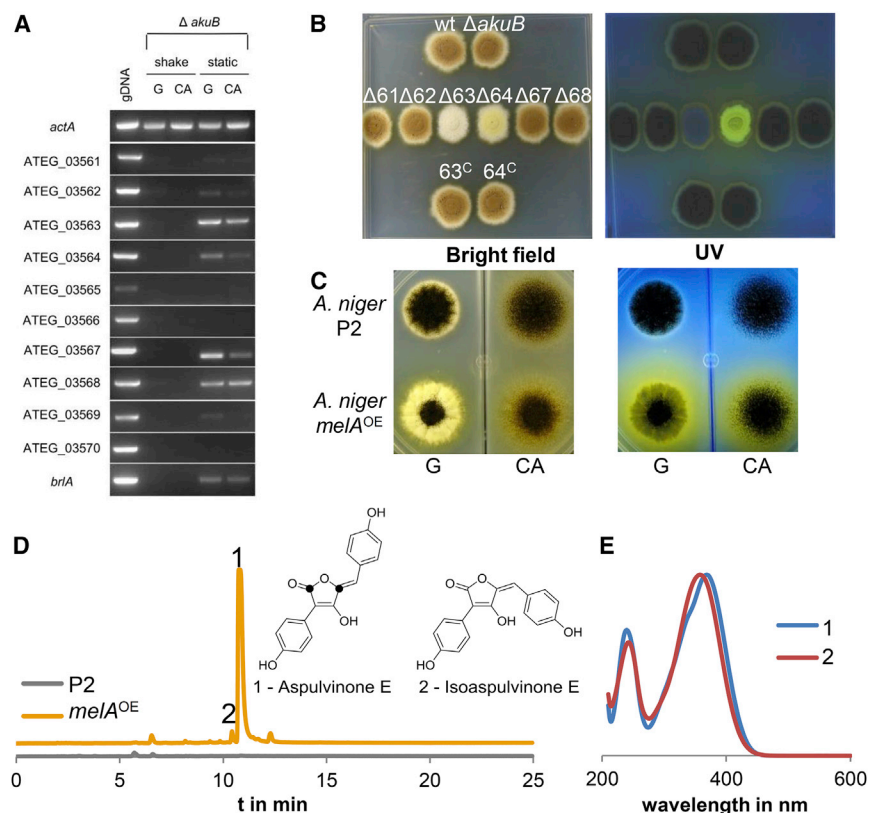


Figure 1. Cluster Analysis of Conidiation-Induced Genes and Heterologous Expression of *melA*

(A) Semi-quantitative PCR on genes of locus tags ATEG_03561 to ATEG_03570. cDNA was isolated from 48-hr shake flask (shake) or 72-hr conidiating (static) cultures from either glucose (G) or casamino acids (CA) media. Actin (*actA*) and *briA* served as controls.

(B) Phenotype of deletion mutants of genes (ATEG_035XX) induced under conidiating conditions as shown in (A). Under UV light the $\Delta tyrP$ mutant is fluorescent.

(C) Comparison of an *A. niger* strain expressing the *melA* gene (*melA*^{OE}) with the parental strain P2 on inducing glucose (G) and non-inducing casamino acids (CA) media.

(D) Metabolite extraction from P2 and *melA*^{OE} from the culture broth of glucose medium. A dominant aspulvinone E (1) and a minor isoaspulvinone E peak (2) are visible. Feeding of [¹³C]tyrosine leads to the production of aspulvinone E exclusively labeled at positions 2 and 5 in the furanone ring (see also Figure S1B).

(E) UV-visible spectra of aspulvinone E (1) and isoaspulvinone E (2).

in conidia of the ascomycete *A. terreus* that is related to pigment biosynthesis in some basidiomycetes.

RESULTS

MelA and *TyrP* Are Required for Conidia Pigmentation in *A. terreus*

We screened for secondary metabolite cluster induction during conidiation and eventually investigated the expression of all genes at locus tags ATEG_03561 to ATEG_03570 by semi-quantitative RT-PCR to identify genes that may form a pigment synthesis cluster. The *briA* gene, known from other *Aspergilli* to regulate conidiation (Park and Yu, 2012), was selected as positive control (Figure 1A). Genes at locus tags ATEG_03561–03564 and ATEG_03567–03569 showed the same expression pattern as *briA*, whereby especially *melA* at locus tag ATEG_03563 and the neighboring gene ATEG_03564, subsequently called *tyrP*, and the two genes at loci ATEG_03567 and 03568 showed the highest expression levels (Figure 1A). To analyze the contribution of expressed genes on pigment formation, we generated the respective deletion mutants (Figures 1B and S1A) in an *A. terreus* strain with a $\Delta akuB$ background that supports increased homologous integration rates (Gressler et al., 2011). Deletion of *melA* (ATEG_03563) and *tyrP* (ATEG_03564) resulted in white and bright fluorescent yellow conidia, respectively (Figure 1B), while none of the other mutants were affected in conidiation or pigment formation. Therefore, we hypothesized that only the NRPS-like *MelA* and the putative tyrosinase *TyrP* are required for conidia pigment synthesis.

The corrected sequence contains no intron and can be found under Genbank: KU530117. The *melA* cDNA with or without a sequence coding for an N-terminal histidine affinity tag (His-tag) was used for transformation of *A. niger* in a recently developed high-level expression system (Gressler et al., 2015a). Regeneration of transformants on glucose (reflecting inducing condition) resulted in bright-yellow fluorescent colonies with low numbers of conidia. Phenotypically normal colonies were obtained under non-inducing conditions (Figure 1C). High-performance liquid chromatography (HPLC) analyses of culture supernatants of *melA*^{OE} strains revealed two peaks (Figure 1D) with identical UV-visible profiles (Figure 1E) and molecular masses of $m/z = 295.0611$ ($[M-H]^-$) that were absent from the parental strain. This mass was in agreement with that of aspulvinone E (Ojima et al., 1973) with a theoretical m/z of 295.0606 ($[M-H]^-$). Furthermore, nuclear magnetic resonance (NMR) shifts (Figure S1B) were in agreement with previous reports (Gao et al., 2013). One peak was identified as aspulvinone E and the second peak as its UV-convertible isomer isoaspulvinone E (Gao et al., 2013) as confirmed by UV irradiation of the isolated compounds (Figure S1C). The structure of aspulvinone E implied an origin from deaminated tyrosine, and exogenous addition of tyrosine increased aspulvinone E contents in a concentration-dependent manner (Figure S1D). Therefore, 2-¹³C-labeled L-tyrosine was added, and molecular mass analysis of purified aspulvinone E indicated an exclusive labeling of two carbon atoms at defined positions (Figure 1D) as confirmed by ¹³C-NMR analysis (Figure S1B).

MelA Produces Aspulvinone E and Isoaspulvinone from Tyrosine

We sequenced the full-length *melA* cDNA and identified an incorrect intron

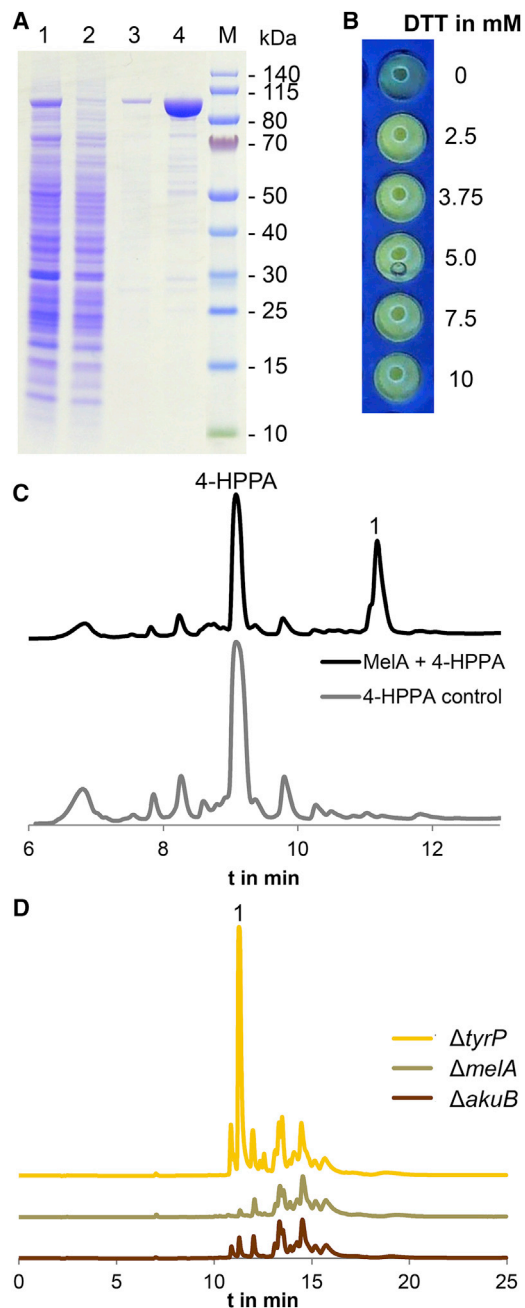


Figure 2. Purification and Characterization of Recombinant MelA
 (A) Purification of MelA from *A. niger* his_{melA}^{OE}. 1, cell-free extract; 2, flow-through from Ni-NTA Sepharose; 3, wash fraction; 4, elution; M, molecular mass marker.
 (B) In vitro reaction of MelA in the presence of different DTT concentrations.
 (C) Identification of aspulvinone E from an in vitro reaction of MelA with 4-hydroxyphenylpyruvate (4-HPPA) (see also Figure S2).
 (D) Analysis of conidia extractions from *A. terreus* parental strain and pigment mutants. Aspulvinone E is detected only from the Δ tyrP strain.

MelA Produces Aspulvinone E In Vitro

For in vitro synthesis of aspulvinone E, a His-tagged MelA version was purified via affinity chromatography on Ni-Sepharose to about 95% purity (Figure 2A). In vitro analyses indicated

that a slightly alkaline pH, 4-hydroxyphenylpyruvate (4-HPPA) concentrations below 10 mM, and the presence of DTT appeared favorable for aspulvinone E formation (Figure 2B). To confirm the identity of aspulvinone E and to test the substrate specificity of MelA, we extracted upscaled reactions with either 4-HPPA or phenylpyruvate as substrates and subjected them to high-resolution electrospray ionization mass spectrometry (HR-ESI MS) HPLC analyses. Results confirmed that aspulvinone E derives from 4-HPPA (Figure 2C). No product was detected from phenylpyruvate (Figure S2). These results suggest high substrate specificity of MelA, indicate a requirement for reducing conditions, and show that no additional enzymes are involved in the formation of aspulvinone E from 4-HPPA.

Identification of the tyrP Coding Region

The *A. terreus* tyrP deletion mutant produced yellow fluorescent conidia, and metabolite extraction from conidia identified aspulvinone E (Figure 2D). Domain analyses revealed that TyrP contains a tyrosinase motif, indicating that TyrP might perform hydroxylation of aspulvinone E with subsequent oxidation as typical for this kind of enzymes (Halaoui et al., 2006). While it was possible to amplify cDNA from the predicted 3'-coding region of the tyrP gene, no full-length product of the predicted open reading frame (ORF) was obtained. Subsequent cDNA sequencing revealed that the predicted ATG start codon was located within an intron sequence (Figure 3A), and a 5'-RACE (rapid amplification of cDNA ends) was performed. The newly derived coding region was used for a BLAST analysis against fungal proteins, and a class of tyrosinase-like proteins with more than 50% identity to TyrP was detected from *Penicillium* species such as *Penicillium expansum* (Genbank: KGO48648), *Penicillium camemberti* (Genbank: CRL30472), or *Penicillium italicum* (Genbank: KGO71193). All sequences revealed a common export signal sequence at the N-terminus. Resulting from these analyses, a PCR fragment spanning the proposed entire tyrP region was successfully amplified (Genbank: KU530118). Thus, after removal of three intron sequences (Figure 3A), the tyrP ORF codes for a protein of 356 amino acids of which the first 19 amino acids encode a putative signal sequence for cellular export as predicted by SignalP (Petersen et al., 2011).

TyrP Induces Pigment Formation from Aspulvinone E during Heterologous Expression

The new full-length cDNA of tyrP was expressed with a C-terminal His-tag sequence in the *A. niger* P2 strain with or without melA-expressing background. P2 transformants only receiving the tyrP gene did not show an altered phenotype. In addition, melA-expressing *A. niger* transformants regained the ability to produce larger quantities of conidia, which might be due to a detoxification of aspulvinone E, and, most strikingly, formed a dark-brown colored mycelium (Figure 3B). To attribute pigment formation to TyrP activity, we point inoculated an aspulvinone E-expressing *A. niger* strain and surrounded it with tyrP-expressing transformants (Figure 3C). All tyrP-expressing strains displayed a dark-brown to black non-extractable zone where mycelia of the melA- and the tyrP-expressing strains converged (Figure 3C). Observation under UV light revealed that aspulvinone E fluorescence was absent from the intersection zone, while an aspulvinone E diffusion zone remained between

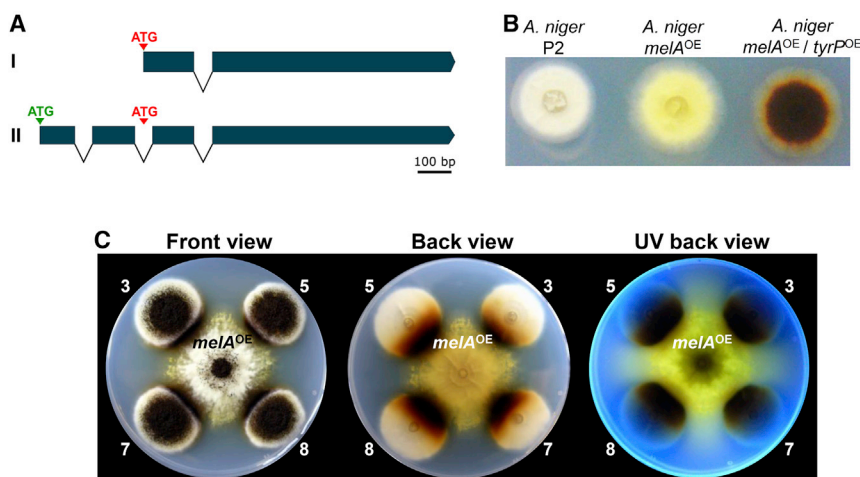


Figure 3. Reidentification of the *tyrP* Gene and In Vivo Pigment Formation

(A) Scheme of the *tyrP* gene as previously annotated (I) and its corrected version (II). Red ATG denotes the misannotated and green ATG the experimentally verified start codon. (B) Expression of full-length *tyrP* (*tyrP*^{OE}) in the *melA*-expressing background (*melA*^{OE}) resulting in dark-brown mycelium. (C) Co-cultivation of *tyrP*^{OE} strains with the *melA*^{OE} strain. Plates are shown in visible light as front and back view and under UV illumination in back view. Aspulvinone E produced by *melA*^{OE} is converted into the dark-brown pigment. Numbers denote independent transformants.

colonies (Figure 3C). These analyses indicate that MelA and TyrP jointly produce the *A. terreus* pigment.

Purification of Recombinant TyrP

For in vitro pigment production, we aimed at purification of TyrP. Culture supernatant was collected from the *A. niger* P2 transformant *tyrP*₇ (Figures 3C and S3), concentrated at least 100-fold, and tested for pigment formation in white microplates. No activity with aspulvinone E was observed, implying that despite its N-terminal signal sequence TyrP is not an extracellular enzyme. On the contrary, cell-free extracts incubated with aspulvinone E led to a time-dependent change in coloration and eventual disappearance of the aspulvinone E fluorescence. Although the *tyrP* gene was cloned to express a C-terminally His-tagged product, chromatography on Ni-Sepharose did not result in a homogeneous protein band at the expected molecular mass of about 41 kDa. The majority of enzymatic activity eluted at the washing step. However, the N-terminal signal sequence pointed to an import into the ER with subsequent glycosylation in the Golgi. Therefore, purification via concanavalin A (Con A) agarose was performed. Strong binding of TyrP to the column was observed, and up to 1.5 M α -methylglucopyranoside was required to efficiently elute tyrosinase activity from the column. Pooled protein fractions were concentrated, desalted, and subjected to chromatography on Ni-Sepharose, which resulted in a major prominent band at about 55 kDa according to SDS-PAGE analyses (Figure 4A).

Glycosylation and Subcellular Localization of TyrP

Despite its apparent molecular mass of 55 kDa rather than the calculated 41 kDa, mass analysis of a tryptic digest confirmed the identity of the TyrP protein. To confirm that this mass shift was due to glycosylation, we performed periodic acid-Schiff (PAS) staining of the native and denatured protein before and after deglycosylation was performed (Figure 4B). The native protein strongly stained with PAS, whereas the denatured deglycosylated protein only stained with Coomassie and revealed a mass shift of about 15 kDa (Figure 4C). Deglycosylation of the native protein was incomplete and yielded a pattern of fully and partially deglycosylated proteins. We additionally purified a

full-length and N-terminally truncated TyrP version from *Escherichia coli*. The deglycosylated TyrP protein matched with the N-terminally truncated version from *E. coli*, indicating that the signal sequence was removed during ER import (Figure 4C). To further confirm that glycosylation was not host dependent, we produced the His-tagged version of TyrP in *A. terreus*. As deduced from SDS-PAGE analyses and activity determinations, the TyrP amounts from production in *A. terreus* were lower than those from the heterologous expression system in *A. niger*. However, TyrP produced in *A. terreus* revealed the same apparent molecular masses before and after deglycosylation as the protein from *A. niger* (Figure 4C).

To study the subcellular localization of TyrP, we produced a fusion with the red fluorescent protein tdTomato in the *A. niger* P2 strain. The resulting reporter strains produced brown mycelium in the interaction zone with *melA*^{OE} (Figure 4D), confirming the catalytic activity of the fusion protein. Microscopic analyses clearly indicated a subcellular localization in granular organelles, which correlates with the predicted localization in the ER or Golgi apparatus (Figure 4E).

Biochemical Characterization of TyrP

Purified TyrP converted aspulvinone E via a blue and a greenish-brown intermediate into a dark-brown pigment (Video S1). Phenylthiourea (PTU) is a known inhibitor of phenol oxidases and tyrosinases (Buitrago et al., 2014; Hall and Orlow, 2005); and approximately 2 mM PTU were required to block TyrP activity (Video S1 and Figure 5A). Despite a strict copper dependence of tyrosinases (Ramsden and Riley, 2014), EDTA at concentrations of up to 10 mM had no inhibiting effect on enzymatic activity (not shown). The enzyme remained active in a pH range of 4–8, but showed highest activity at pH 5–7 (Figure 5C). Interestingly, while the aspulvinone E synthetase MelA required DTT for activity in vitro, TyrP activity was completely inhibited in the presence of 1–2 mM DTT (Figure 5B). This sensitivity against reducing agents correlates with the subcellular localization in the ER and Golgi that are oxidative environments (Csala et al., 2012).

Identification of TyrP Reaction Intermediates

For analysis of intermediates, TyrP reactions with aspulvinone E were extracted at different time points, evaporated, dissolved in

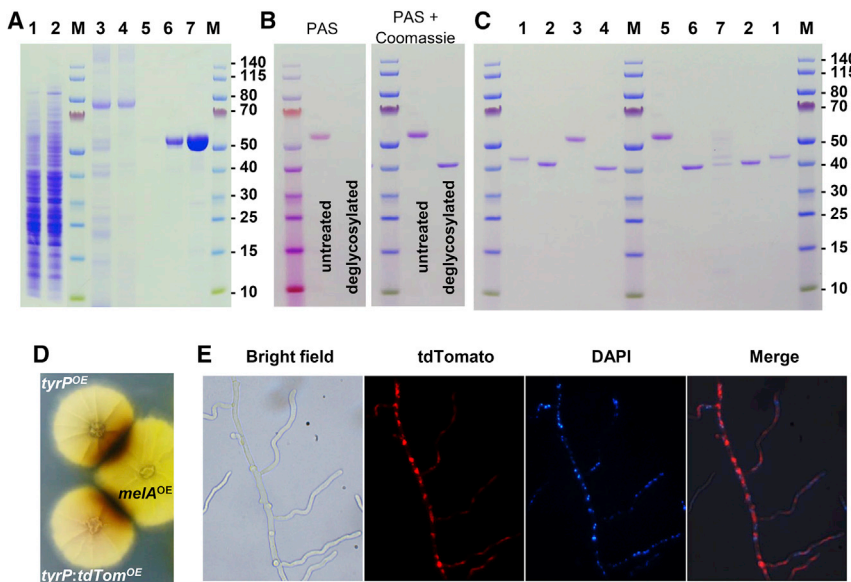


Figure 4. Purification, Glycosylation, and Localization of TyrP

(A) SDS-PAGE analysis of TyrP purified from *A. niger tyrP^{OE}*. 1, cell-free extract; 2, ConA column flow-through; 3, elution from ConA column; 4, flow-through from Ni-Sepharose; 5, wash fraction; 6 and 7, elution and concentrate from Ni-Sepharose column; M, molecular mass marker.

(B) Left panel: PAS glyco stain of purified untreated and deglycosylated TyrP. Right panel: additional Coomassie stain.

(C) Deglycosylation analysis of TyrP produced in *A. terreus* and *A. niger* in comparison with recombinant full-length and truncated TyrP from *E. coli*. 1, full-length TyrP *E. coli*; 2, truncated TyrP from *E. coli*; 3, TyrP from *A. terreus*; 4, deglycosylated TyrP from *A. terreus*; 5, TyrP from *A. niger*; 6, deglycosylated TyrP from *A. niger*; 7, native deglycosylation of TyrP from *A. niger*; M, molecular mass marker.

(D) Pigmented zone formed *A. niger tyrP^{OE}* and the *tyrP:tdTom^{OE}* fusion strain in vicinity of *melA^{OE}*.

(E) Localization studies of the TyrP-tdTomato fusion in *A. niger* under 200 \times magnification. Bright field, tdTomato fluorescence, DAPI stain, and merge are shown.

methanol, and immediately subjected to liquid chromatography-mass spectrometry (LC-MS). Peaks for aspulvinone E rapidly declined and new peaks appeared that varied in intensity depending on time of extraction (Figures 5D and 5E). Since two aromatic moieties are present in aspulvinone E, the tyrosinase should perform hydroxylations of both aromatic moieties (Figure 5F). Consistent with this hypothesis, the mass of mono-hydroxylated aspulvinone E was detected at two different retention times (Figure 5G). Further structure assignments were not possible due to instability of the compounds. Taking the reaction mechanisms of the di-copper center of tyrosinases into account, all modifications start with a hydroxylation in the *ortho* position to the existing hydroxyl group. Its oxidation and deprotonation results in a delocalized hydroxyquinone methide anion that coincides with the blue color initially observed in the TyrP reaction (Figure 5C and Video S1). Due to the high reactivity of methides and *ortho*-diquinones (Gill and Steglich, 1987) a polymer starts to form spontaneously, which we termed Asp-melanin.

Impact of the Conidial Pigment on Surface Structures and Biotic and Abiotic Stress Resistance

In *A. fumigatus* conidia the loss of the conidial pigment reduces the attachment of surface hydrophobins (Jahn et al., 2000). Therefore, we compared the surface structure of the parental *A. terreus* \DeltaakuB with the $\Delta melA$ and $\Delta tyrP$ mutants by scanning (SEM) and transmission electron microscopy (TEM) (Figure 6A). Scanning electron microscopy revealed a protein coating on the surface of conidia from all strains. However, TEM revealed a dark zone at the outer cell wall of conidia in the wild-type and the *tyrP* mutant that was lacking from the *melA* strain.

Resistance of *A. fumigatus* against oxidative and UV stress depends on naphthopyrone-derived pigments (Jahn et al., 2000; Figures S3B and S3D), but no difference in oxidative stress resistance of color mutants was observed for *A. terreus* (Figure S3A). However, pigmentation also had a protective effect on UV resis-

tance of *A. terreus* (Figures 6B and S3C). We then investigated the effect of pH during prolonged incubation of conidia at elevated temperature. Although the $\Delta tyrP$ mutant showed a slightly reduced long-term survival compared with the $\Delta melA$ mutant and the parental strain, no significant differences in pH-dependent survival were observed (Figure 6C). Nevertheless, it should be noted that *A. terreus* conidia showed highest survival rates at pH 4 but were less viable when incubated at pH 7.0. In contrast, conidia of other Aspergilli survived at neutral pH but were inactivated under acidic conditions (Figure 6D). Furthermore, no significant differences were observed when mutants were tested in a chicken embryo infection model (Jacobsen et al., 2010), indicating that the pigment is of minor importance for virulence at least in this model system (Figure 6E). Interestingly, when tested in a phagocytosis assay with the soil amoeba *Dictyostelium discoideum* a slight, but significant reduction in phagocytosis rate was observed for the wild-type compared with the pigment mutants (Figure 6F), although all strains were eventually found in acidified phagolysosomes. In summary, the pigment from *A. terreus* protects to some extent against UV light and reduces phagocytosis by amoeba.

DISCUSSION

It has been generally assumed that filamentous Ascomycetes produce DHN-melanin to protect conidia from environmental stresses (Braga et al., 2015). Our studies show that the pigment in *A. terreus* conidia is unrelated to DHN-melanin. It also differs from classical eumelanins that are formed from L-DOPA. Formation of eumelanins in fungi such as Cryptococci relies on precursor provision from the host (Eisenman et al., 2007). In contrast, the pigment in *A. terreus* is synthesized from 4-HPPA, which is converted to aspulvinone E. The biosynthesis of this Asp-melanin precursor is performed by an unusual non-ribosomal peptide synthetase-like enzyme (MelA) with a tri-domain structure consisting of an adenylation (A), thiolation (T),

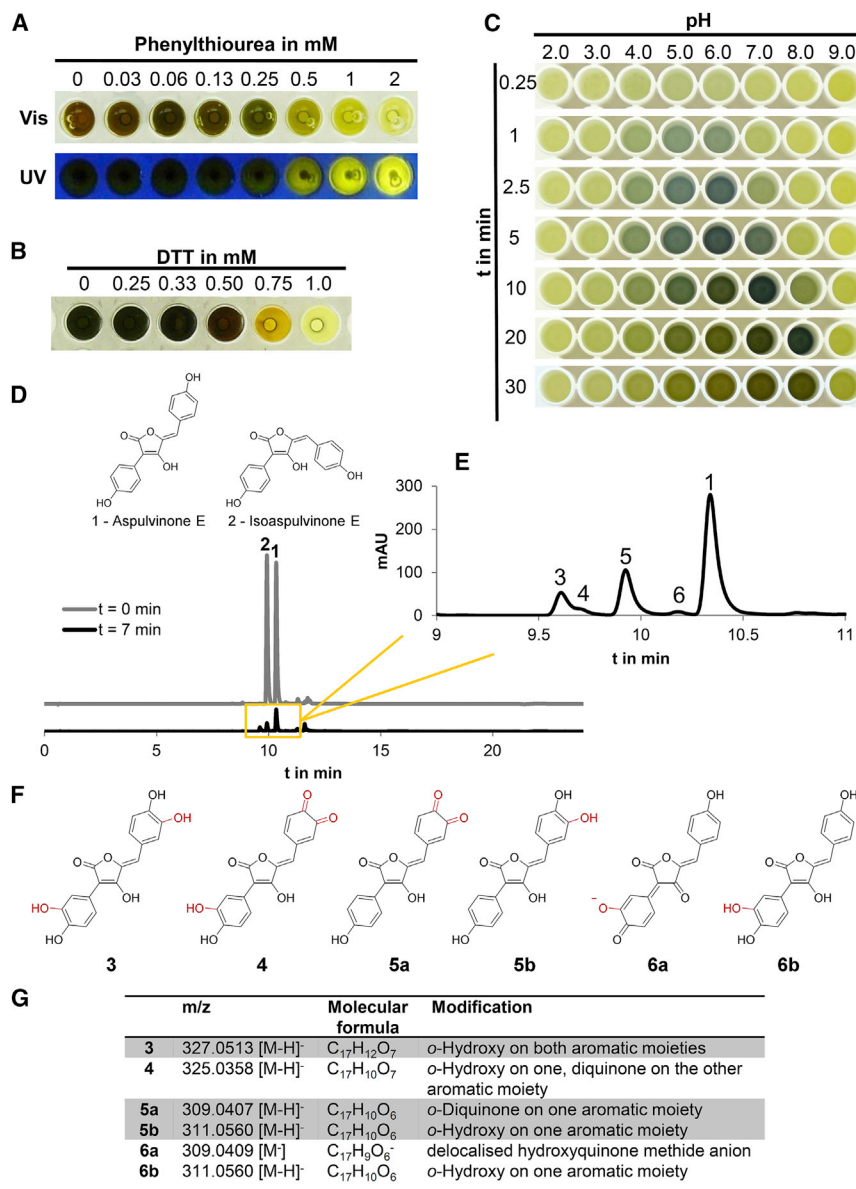


Figure 5. Biochemical Characterization of TyrP and Its Reaction Products

(A) Inhibition of TyrP by different concentrations of phenylthiourea. Brown pigment formation and lack of UV fluorescence from aspulvinone E indicate TyrP activity. (B) Inhibition of TyrP by different concentrations of DTT. (C) pH-dependent activity of TyrP in time lapse. (D) HPLC analysis of TyrP reaction intermediates. Aspulvinone E (1) and isoaspulvinone (2) from 0 min are rapidly converted. (E–G) Magnification of the HPLC profile of the TyrP reaction after 7 min (E), with annotation of underlying structures and substitutions compared with aspulvinone E in red (F) and corresponding masses (G).

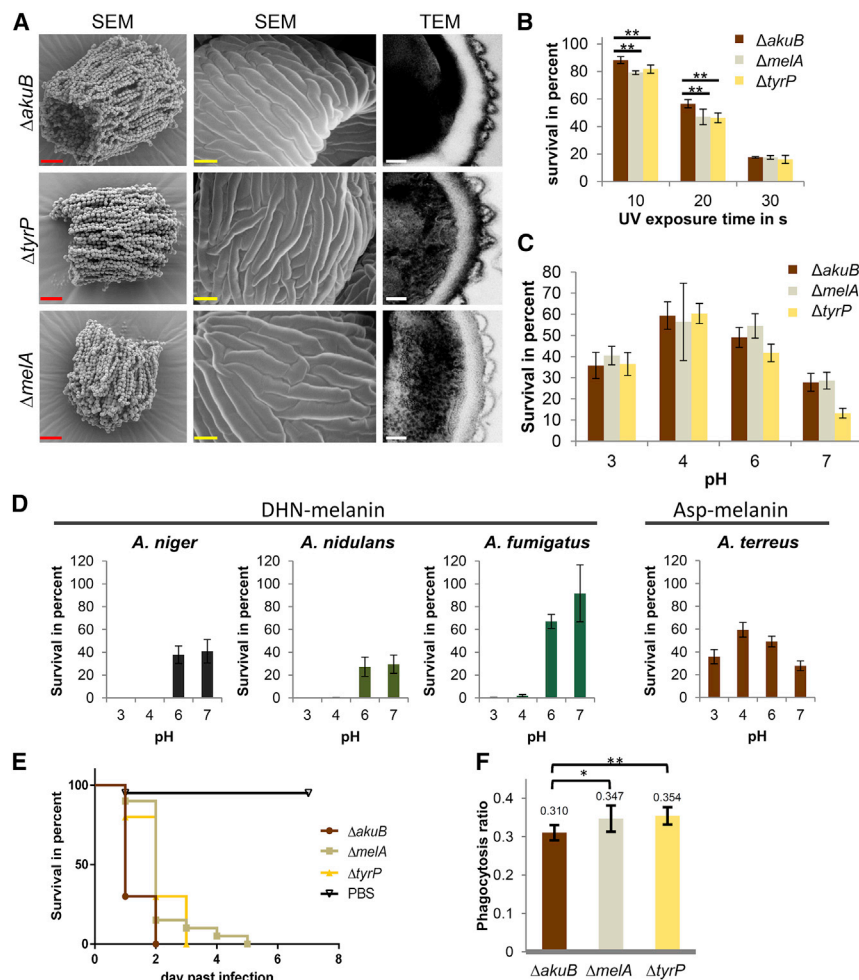
a terphenylquinone intermediate, which is oxidatively cleaved and lactonized and may become decarboxylated (Schuffler et al., 2011; Figure 7B); second (Pauly et al., 2014), a direct aldol condensation of two building blocks in which a single new C-C-σ bond is formed. This is followed by decarboxylation and lactonization (Figure 7C). However, different substitution patterns of the furanone core structures indicate diverging biosynthetic pathways not yet understood in detail. The furanone of aspulvinone E is substituted at positions 3 and 5, whereas it is substituted at positions 3 and 4 in ral-furanone B or 4 and 5 in xenofuranone B and allantofuranone.

Structures of aspulvinones from *A. terreus* have been known since the 1970s (Ojima et al., 1973), and various models of biosynthetic pathways have been proposed. Seto (1979) suggested a biosynthetic pathway involving atromentin as intermediate (Figure 7B), whereas Guo et al. (2015) hypothesized a direct furanone formation (Figure 7C). However, neither hypothesis was supported by experimental data.

Recent analyses aimed at defining fingerprint motifs of the thioesterase domains that distinguish between quinone and furanone synthesis (Braesel et al., 2015). It has been assumed that quinone formation is directed by an asparagine residue present in a motif of the TE domain where it is followed by a double proline. The primary structure of MelA contains exactly this amino acid pattern, indicating a quinone product. In contrast, the labeling pattern observed from feeding [2-¹³C] tyrosine to *meA*^{OE} opposes this. The oxidative cleavage of an atromentin intermediate followed by internal ester formation would result in a randomized labeling at three positions of the molecule (Figure 7B), but only two intensified carbon signals were found in ¹³C-NMR spectra of aspulvinone E (Figure 1E). Moreover, the quinone reaction pathway requires a

and thioesterase (TE) domain, but lacking the condensation domain that is typical for true NRPS enzymes (Schneider et al., 2007). Some NRPS-like enzymes containing a reduction rather than a thioesterase domain have been shown to perform substrate reduction without condensation (Wang et al., 2014). However, thioesterase-containing NRPS-like enzymes mediate the condensation of two identical aromatic α-keto acids, and two major classes of compounds are produced: terphenylquinones and furanones (Figure 7A) (Schneider et al., 2007; Balibar et al., 2007; Pauly et al., 2014; Braesel et al., 2015; Schuffler et al., 2011; Brachmann et al., 2006).

The core motif of terphenylquinones is formed by two symmetric nucleophilic attacks of the C3 of one α-keto acid at the C1 of the other and vice versa, resulting in two new C-C-σ bonds. For formation of the butenolide core structure of furanones, two divergent biosynthesis routes are possible: first, generation of



second enzyme for oxidative opening of the terphenylquinone core, but in vitro biosynthesis of aspulvinone E was independent of auxiliary oxidases. Taken together, all experiments support a biosynthesis pathway as shown in Figure 7C. Further studies are under way to analyze the amino acids that orchestrate reactions leading to either quinone or furanone core structures.

Natural products similar to the structure of aspulvinone E have been reported from basidiomycetes, such as pulvinic acid derivatives like xerocomic acid in various members of the boletes (Gill and Steglich, 1987). Notably, these compounds are produced via terphenylquinone intermediates and therefore their biosynthesis significantly differs from aspulvinone E. Xerocomic and variegatic acid are monomeric compounds that give the typical yellow to red color to some boletes mushrooms (Gill and Steglich, 1987). Bruising and exposing these pigments to oxygen causes a blueing of the flesh due to the formation of delocalized hydroxyquinone methide anions (Gill and Steglich, 1987). A blue reaction intermediate was also found in the reaction of TyrP with aspulvinone E. Tyrosinases typically perform an *ortho*-hydroxylation of a monohydroxylated aromatic moiety followed by an oxidation leading to *ortho*-diquinones. Using high-resolution MS the masses of such modified aspulvinone E derivatives

were identified. Among these reaction intermediates we also identified a blue-colored delocalized hydroxyquinone methide anion (Figure 5F, structure 6a) with a marked absorption maximum at 596 nm. This anion and the *ortho*-diquinones are highly reactive intermediates that undergo autopolymerizations leading to the brown pigment of the conidia. Interestingly, the basidiomycete *Xerocomus badius* seems to be able to suppress such a polymerization process by producing badiones. This pigment is formed from two xerocomic acids that undergo a Diels-Alder reaction after oxidation to the diquinone without further polymerization.

One of the most striking questions is the reason for the lack of a DHN-melanin pigment in *A. terreus*. All our analyses indicate that a naphthopyrone-based pigment has superior protective effects compared with the aspulvinone E-derived pigment from *A. terreus*. While the *A. terreus* Asp-melanin mediates UV protection, it is not protective against oxidative stress. Non-pigmented conidia reveal the same virulence as the pigmented wild-type. The *A. terreus* pigment is also not involved in surface attachment of the hydrophobin layer but slightly reduces phagocytosis of conidia by amoeba. However, conidia end up in acidified phagolysosomes of macrophages (Slesiona et al., 2012a) and *D. discoideum* as revealed from positive lysotracker

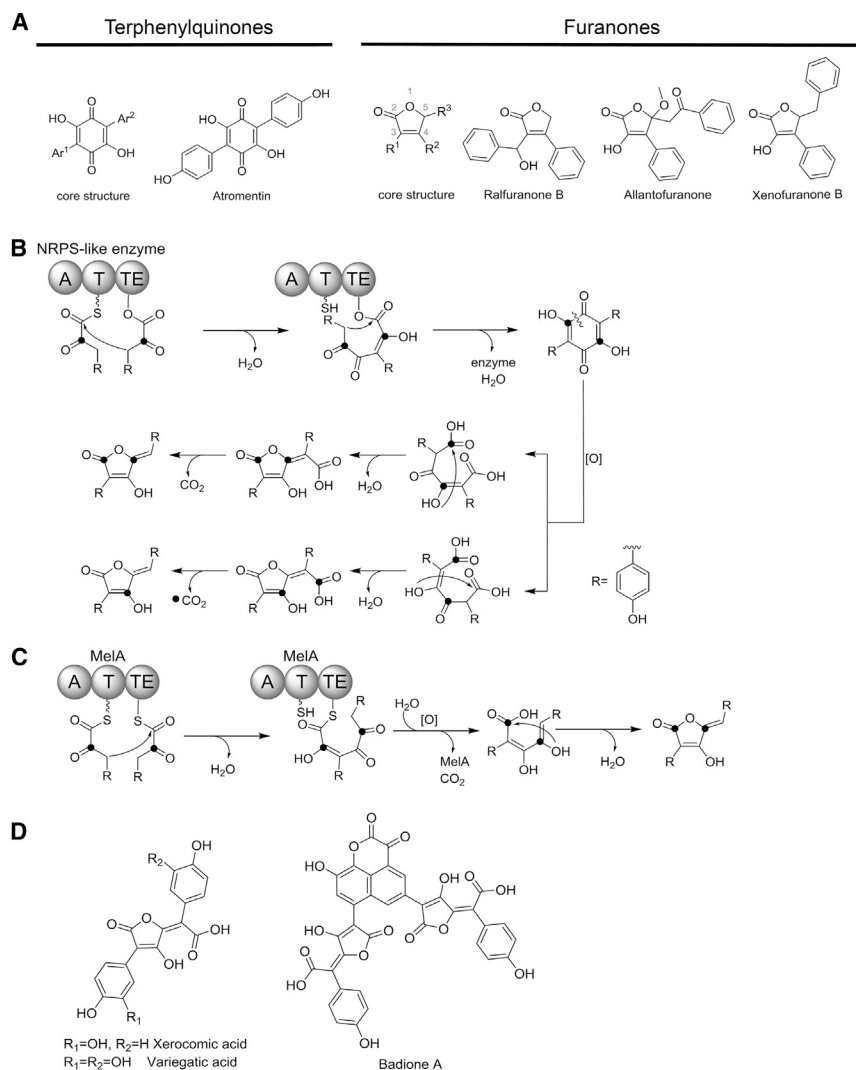


Figure 7. Different NRPS-like Enzyme-Derived Metabolites and Divergent Pathways for Biosynthesis of Aspulvinone E

(A) Core structures of terphenylquinones and furanones and selected examples for both classes of metabolites.

(B) Postulated pathway for aspulvinone E biosynthesis via the terphenylquinone atromentin and the resulting labeling pattern when produced from [2-¹³C]tyrosine.

(C) Biosynthesis of aspulvinone E by direct furanone formation. For details of both pathways, refer to the main text.

(D) Structures of xerocomic and variegatic acid and badione A from basidiomycetes.

some melanins protect against oxidative stresses or increase the rigidity of the cell wall. In *Aspergillus* species a polyketide synthase produces a common melanin precursor that is polymerized to a dihydroxynaphthalene- (DHN) melanin. It has been believed that this type of melanin is generally produced by filamentous Ascomycetes. Nevertheless, previous studies suggested that pigment formation in *A. terreus* differs, because typical features of DHN-melanin were missing and no candidate genes for production of the naphthopyrone precursors were detectable. Herein, we identified the genes contributing to the Asp-melanin biosynthesis in *A. terreus* conidia. The pigment is produced from an NRPS-like enzyme and a tyrosinase. The NRPS-like enzyme MelA directly produces the furanone

staining in phagocytosis analyses. The inhibition of phagolysosome acidification, either in macrophages or other predators, may depict a major function of the DHN-melanin in other *Aspergillus* species, but might be detrimental for *A. terreus*. Our analyses showed that *A. terreus* conidia survived best when incubated at pH 4, whereas conidia of *A. fumigatus*, *Aspergillus nidulans*, or *A. niger* were rapidly inactivated at this pH under the applied conditions (Figure 6). Therefore, inhibition of acidification of phagolysosomes and rapid escape are important strategies for the latter species. However, neutral pH was less well tolerated by *A. terreus* conidia. Therefore, to support a long-term persistence within phagolysosomes of predators or macrophages (Slesiona et al., 2012a, 2012b), it appears advantageous for *A. terreus* to avoid the production of a DHN-melanin that would lead to generation of less favored environmental conditions.

SIGNIFICANCE

Bacteria, plants, and vertebrates produce melanin pigments that protect from damage by UV light. Additionally,

aspulvinone E, although its thioesterase domain organization points toward the production of a terphenylquinone precursor. Therefore, additional studies on the specificity of these domains are required. The tyrosinase hydroxylating and oxidizing aspulvinone E is localized in subcellular organelles such as ER or Golgi, where it finds the required oxidizing conditions. However, it remains speculative by which mechanism and in which form the pigment eventually locates in the cell wall of conidia. *A. terreus* Asp-melanin protects from UV stress and reduces phagocytosis by amoeba, but overall appears less protective than DHN-melanin, raising questions about the loss of DHN-melanin. This could be due to the preference of *A. terreus* conidia to persist within acidic environments. Unlike DHN-melanin, the *A. terreus* melanin does not inhibit acidification of phagolysosomes, which results in formation of an ecological niche that allows long-term persistence and dissemination of conidia. Therefore, the pigment produced by a specific species does not necessarily follow its phylogenetic tree rather than the need of an organism for environmental adaptation.

EXPERIMENTAL PROCEDURES

Media and Cultivation Conditions

A. niger strains were cultivated at 28°C–30°C and *A. terreus* strains at 37°C. All media and strains used in this study are listed in Tables S2 and S3. Conidia suspensions were prepared from 2% agar slants of AMM(-N)G50Gln10 medium. When required, selection markers such as hygromycin B (180 µg/ml), phleomycin (80 µg/ml), or pyrithiamine (0.1 µg/ml) were added. Conidia were harvested in water, filtered through 40 µm cell strainers (Greiner), repeatedly washed in water, and counted in a hemocytometer. Liquid cultures were inoculated with 10⁶ conidia/ml. For labeling experiments a 50 ml liquid AMM(-N)G50Gln10 culture of *A. niger melA*^{OE} was supplemented with 50 mg of L-[2-¹³C]tyrosine. For secondary metabolite extractions, strains were grown in liquid medium containing either 50 mM glucose or 2% starch as carbon sources. Surface biofilms for conidiation in liquid cultures were produced by incubation without shaking. *Dictyostelium discoideum* AX2 was grown in cell-culture dishes from frozen spores at 22°C in 1 × HL5 or 0.2 × HL5 medium (Formedium) with 1% (w/v) glucose. Amoeba cell numbers were determined using a CASY TT Cell Counter (OLS Bio).

RNA Isolation, cDNA Synthesis, and Semi-quantitative RT-PCR

Mycelium was ground to a fine powder and total RNA was isolated using the MasterPure RNA isolation kit (Biozym). Traces of genomic DNA (gDNA) were removed with Turbo DNase (Ambion, Thermo Scientific) as confirmed by control PCR on the actin gene (ATEG_06973) (P1/2). cDNA was synthesized using Superscript III Reverse Transcriptase (Thermo Scientific) and anchored oligo(dT) primers as described previously (Zaehle et al., 2014). cDNA levels were normalized against the actin gene and used as a template for amplification of 3' regions from secondary metabolite gene cluster genes using P5-P20 and P87-P90. Oligonucleotides are listed in Table S1. The *brlA* gene (ATEG_5140) (P3/4) served as marker for conidiation.

5'-RACE and Sequence Analyses

5'-RACE was carried out on RNA of *A. terreus* with P50-P55 as described by Scotto-Lavino et al. (2006). PCR products were purified by gel electrophoresis, ligated into pJET 1.2 vectors (Thermo Scientific), and sequenced with P85 and P86. The coding sequence of the *melA* gene was analyzed by sequencing genomic and cDNA with oligonucleotides P9, P10, P68, P82, and P83.

Genetic Manipulation of *A. terreus* and *A. niger* and Transformant Analysis

Protoplast transformation of fungi was carried out as described previously (Gressler et al., 2011, 2015a) using a mixture of lysing enzymes (Sigma) and yatalase (Takara Clontech). Protoplasts were regenerated on 1.2 M sorbitol containing AMM(-N)G50Gln10 medium and the respective selection marker. For purification, transformants were repeatedly streaked on fresh medium. Transformants were checked by diagnostic PCR and Southern blot analyses with digoxigenin-labeled probes (Figure S1). Blots were analyzed by chemoluminescence imaging after incubation with CDP-star (Roche Diagnostics). Gene deletions and complementation were performed in *A. terreus* SBUG844/ Δ *akuB* (Gressler et al., 2011). In brief, 0.5–1 kb upstream and downstream flanks of the gene of interest were PCR amplified and fused by in vitro recombination (InFusion Enzyme Mix, Clontech) with the *ptrA* resistance cassette. Complementation constructs consisted of the entire coding region including the upstream flank and a short terminator sequence, the phleomycin resistance cassette, and a downstream flanking region. Fragments were assembled by in vitro recombination. For heterologous gene expression either the *A. niger* P2 strain (Gressler et al., 2015a) or *A. terreus* SBUG844 was used. The standard SM-Xpress vector (Gressler et al., 2015a) or one of its His-tag versions were used for generation of heterologous expression constructs. The ORFs of the *melA* and *tyrP* gene from *A. terreus* were amplified from cDNA. For TyrP localization studies a fusion with the gene coding for tdTomato (Genbank: KP100262) was generated. Oligonucleotides are listed in Table S1.

Generation of a Modified SM-Xpress Vector Set

The SM-Xpress vector was initially constructed with phleomycin as resistance marker (Gressler et al., 2015a). Here, the spectrum of cloning vectors was broadened by (1) changing the resistance marker and (2) building a vector

for introducing His-tags. In SM-Xpress2 the phleomycin resistance cassette was replaced by the hygromycin resistance gene deleted for an internal *NcoI* restriction site, allowing transformation of strains previously transformed with the SM-Xpress vector. The *his*_{SM-Xpress} vector contains a His-tag sequence that can be used for adding the tag at either the C- or N-terminus of a protein. Details on fragment amplification and cloning strategies are given in Supplemental Experimental Procedures.

Expression of *tyrP* in *E. coli*

For recombinant TyrP production in *E. coli*, either the full-length *tyrP* (P79/P81) or a 5'-truncated version (P80/P81) lacking the sequence coding for a putative export signal sequence was amplified from *A. terreus* cDNA. PCR fragments were fused with a *Bam*HI/*Hind*III restricted modified pET43.1 vector that adds an N-terminal His-tag to the protein (Hortschansky et al., 2007). Plasmids were propagated and reisolated from *E. coli* DH5 α and transferred to *E. coli* BL21(DE3) Rosetta 2 cells (Merck, Novagen) for protein production.

Purification of Recombinant Proteins

For purification, MelA and TyrP were produced with N- or C-terminal His-tag, respectively. For purification of MelA, *A. niger his-melA*^{OE} was grown for 26 hr at 30°C in liquid YM medium. For TyrP purification, *A. niger tyrP*^{OE} was grown for 32 hr at 28°C in AMM(-N) starch 2% Gln 50 medium and *A. terreus tyrP*^{OE} for 40 hr at 37°C in GSMY medium (Table S2), whereby for both species 10 g/l talc powder was added. Gene expression in *E. coli* was induced in Express Instant TB medium (Merck, Novagen). Fungal mycelia were disrupted by grinding under liquid nitrogen, whereas *E. coli* cells were disrupted by sonication. All His-tagged proteins were purified by Ni-chelate chromatography using Ni-Sepharose 6 Fast Flow (GE Healthcare). For purification of TyrP an additional purification step via a Con A agarose (GE Healthcare) column was required. Recombinant TyrP proteins from *E. coli* were purified under denaturing conditions from inclusion bodies. Details on specific buffers and chromatographic conditions are provided in Supplemental Experimental Procedures.

Glycostaining, Deglycosylation, and MALDI-TOF MS Analyses

TyrP (60–100 µg) was desalted against 10 mM Tris-HCl buffer (pH 7.5) (NAP5 column, GE Healthcare), lyophilized, and dissolved in water at defined concentrations. Deglycosylation was performed under native and denaturing conditions using the protein deglycosylation mix as described in the manufacturer's protocol (New England Biolabs). Glycostaining of proteins after SDS-PAGE on a 4%–12% NuPage Bis-Tris gel was performed as described in the technical bulletin of the glycostain detection kit (Sigma-Aldrich). After extensive washings with water to enhance band intensities, the gel was photographed and subsequently stained with Coomassie R350 (PhastGel Blue R, GE Healthcare). For MALDI-TOF MS analyses in-gel tryptic digests were performed virtually as described by Shevchenko et al. (2006) using sequencing-grade modified trypsin (Promega). Peptides were mixed with α -cyano-4-hydroxycinnamic acid, dried on an MTP 800/834 anchor chip target, and analyzed using a Bruker Ultraflex I device (Bruker Daltonics) as described by Teutschbein et al. (2010).

TyrP Localization Studies

A. niger producing the fusion of TyrP and tdTomato was pre-grown for 24 hr on AMM(-N)Starch 2% Gln20 2% agar plates and subsequently surrounded with coverslips coated with medium solidified with 1% agar. Incubation was continued for another 24 hr. Coverslips were placed on an object slide, embedded in mounting solution with DAPI (ProLong Gold Antifade with DAPI, Thermo Scientific), and covered with a large coverslip. Pictures were taken using a GXML3201LED microscope equipped with a GXCAM controlled by GXCapture software (GX microscopes). Overlay images were assembled using GIMP 2 software.

Metabolite Extraction, Analysis, and Structure Elucidation

Metabolites were extracted from mycelium by homogenization in ethyl acetate with an Ultra-Turrax (IKA) at 14,000 rpm. Cell debris was removed by filtration. Culture filtrates were mixed with an equal volume of ethyl acetate and the organic layer collected. Extracts were filtered over anhydrous sodium sulfate and evaporated under reduced pressure, and residues dissolved in methanol. Analytical HPLC (Gressler et al., 2015a) and HR-ESI MS (Zaehle et al., 2014) were carried out as described previously. Semi-preparative isolation of aspulvinones was

performed on an Agilent 1260 series equipped with DAD and quaternary pump as described in [Supplemental Experimental Procedures](#). Purified metabolites were subjected to NMR analyses with DMSO-d₆ as solvent and internal standard. NMR spectra were recorded either on a Bruker Avance III 500 or a Bruker Avance III 600 spectrometer (Bruker BioSpin) equipped with a cryoprobe head.

Aspulvinone E Production and Purification from Recombinant MeIA

Recombinant purified MeIA (10 μg) was mixed in a final volume of 20 μl with different buffers (Tris-HCl [pH 8.0]; potassium phosphate [pH 6.2 or 6.8]; PIPES [pH 7.5]) at a concentration of 100 mM in the presence of 5 mM ATP, 10 mM MgCl₂ and varying concentrations of *p*-hydroxyphenylpyruvate (0–20 mM). Also, DTT in a range of 0–10 mM was added. Activity was analyzed by monitoring aspulvinone E fluorescence on a UV screen at 302 nm. Optimum conditions were identified as 100 mM PIPES (pH 7.5) with 5 mM ATP, 10 mM MgCl₂, 2.5 mM DTT, and 7.5 mM *p*-hydroxyphenylpyruvate. In a 10-ml scale-up, 1 mg of enzyme was incubated with either 7.5 mM *p*-hydroxyphenylpyruvate or 7.5 mM phenylpyruvate. Reactions without enzyme served as controls. After 18 hr at 28°C, reactions were acidified to pH 3 with HCl and repeatedly extracted with ethyl acetate. Extracts were dried under reduced pressure, dissolved in methanol, and analyzed as described above.

TyrP In Vitro Assays and Identification of TyrP Reaction Intermediates

TyrP activity was assessed in 20 μl reactions by observing the time-dependent pigment formation. Potassium phosphate (40 mM) at pH 6.8 in the presence of 1.8 mM aspulvinone E (from 18 mM stock solution in methanol) was used in standard analyses. Inhibitory effects of additives such as DTT, phenylthiourea, or EDTA were tested in a range of 0–10 mM. Aspulvinone E consumption and pigment formation was monitored under UV and visible light at different time points. TyrP reaction intermediates were identified from 1 ml reactions containing 5 μg of TyrP, 0.61 mM aspulvinone E, and 20 mM sodium phosphate buffer (pH 6.8). Samples were extracted at different time points with ethyl acetate, evaporated under reduced pressure, dissolved in methanol, filtered, and directly injected to LC-MS on an Agilent 1260 Infinity system equipped with a quaternary pump, autosampler, diode array detector and a 6120 quadrupole mass spectrometer in negative ionization mode. For separation a Poroshell 120 EC-18, 4.6 × 50-mm, 2.7 μm column was used (Agilent).

Electron Microscopy

For SEM, conidia were collected without liquid suspension and analyzed on an LEO-1530 Gemini field emission scanning electron microscope (Carl Zeiss) at electron energy of 8 keV using the in-lens secondary electron detector and 50,000- to 200,000-fold magnification. For TEM, conidia were harvested in sterile water and prepared for microscopy from suspension. Samples were ultrathin sectioned and analyzed on an EM 900 transmission electron microscope (Zeiss) at 80 kV and magnifications of 3,000–20,000×. Details on sample preparations can be found in [Supplemental Experimental Procedures](#).

UV Sensitivity and Oxidative Stress Resistance of Conidia

Conidia suspensions (100 μl with 3 × 10⁹ conidia/ml) were plated on malt extract agar and irradiated with UV light at 254 nm (100 μW/cm²) for 10–60 s (Sylvania G15T8 germicidal UV-C source). The colony-forming units on control plates were set to 100%. Each strain and time point was analyzed from two independent biological replicates including three technical replicates. Oxidative stress was analyzed by measuring inhibition zones in the presence of different amounts of H₂O₂ as described in [Supplemental Experimental Procedures](#).

Analysis of pH Sensitivity and Conidia Germination

Conidia were adjusted to 6 × 10³/ml in 0.9% NaCl with 0.1% Tween 20 and mixed with an equal volume of Britton-Robinson-Buffer of different pH values (Britton and Robinson, 1931) composed of 0.1 M phosphoric acid, 0.1 M boric acid, and 0.1 M acetic acid. Controls were plated in triplicates directly after mixing conidia with buffers and set as reference. Suspensions were incubated at 37°C for 48 hr with vortex mixing every 24 hr. Aliquots of 100 μl were plated in triplicates on 25 mM MES (pH 6.2)-buffered malt extract agar plates. Colony-forming units were determined after 24 and 48 hr of incubation at 37°C. *A. niger* was incubated at 28°C. *A. terreus* color mutants were tested in biological rep-

licates with technical triplicates, and weighted means were calculated from both datasets. Data from other *Aspergillus* species were collected from technical triplicates. For germination analyses, conidia were labeled with fluorescein isothiocyanate (FITC) as described previously (Ibrahim-Granet et al., 2008). Conidia were incubated for 8 hr in PDB medium in chamber slides and evaluated on an AxioImager fluorescence microscope (Zeiss). Details are provided in [Supplemental Experimental Procedures](#).

Amoeba Phagocytosis Assay and Egg Infection Model

Embryonated chicken eggs were infected on the chorioallantoic membrane with 1 × 10⁶ conidia as described previously (Jacobsen et al., 2010; Slesiona et al., 2012b). Survival rates were evaluated by Kaplan-Meier plots with log-rank test. FITC-labeled conidia were used for confrontation with *D. discoideum* as described previously (Hillmann et al., 2015). After settling of amoeba for 2 hr, LysoTracker red (Fisher Scientific) was added in a final concentration of 100 nM. FITC-stained conidia were added at an MOI of 4. Microscopic images from four biological replicates were taken as tile scans of 675 μm² 1 hr post infection using an LSM 780 Live confocal laser scanning microscope (Zeiss). For each strain, conidia and amoeba were counted using ImageJ software (Schneider et al., 2012). Total counts were 3,248 and 807 (\DeltaakuB), 3,877 and 882 ($\Delta meiA$), and 2,191 and 715 ($\Delta tyrP$) for conidia and amoeba, respectively. Phagocytosis ratio p_r was determined as previously described (Mattern et al., 2015) and defined as $p_r = N_{phag} / (N_{phag} + N_{adh})$ with N_{phag} (phagocytosed conidia) and N_{adh} (amoeba adherent conidia). Statistical analysis was carried out using the Wilcoxon rank-sum test.

ACCESSION NUMBERS

The accession number for the *meIA* sequence reported in this paper is Genbank: KU530117. The accession number for the *tyrP* sequence reported in this paper is Genbank: KU530118.

SUPPLEMENTAL INFORMATION

Supplemental Information includes Supplemental Experimental Procedures, three figures, three tables, and one movie and can be found with this article online at <http://dx.doi.org/10.1016/j.chembiol.2016.03.014>.

AUTHORS CONTRIBUTIONS

E.G., M.G., and M.B. conceived of and designed the experiments. E.G., M.G., I.V., F.H., I.D.D., S.D., and M.B. performed experiments. All authors analyzed the data. E.G. and M.B. wrote the manuscript with contributions from C.H., and revisions were made by all authors.

ACKNOWLEDGMENTS

We are grateful to D. Hildebrandt and F. Meyer for general support in cloning procedures and metabolite analyses, M. Pötsch for setting up MALDI-TOF MS analyses, H. Heinicke for recording NMR spectra, A. Perner for HR-ESI-MS analyses, S. Silva and B. Weber for assistance in the chicken egg infection model, and M. Samalova for valuable advice in sample preparation for fluorescence microscopy.

Received: February 17, 2016

Revised: March 15, 2016

Accepted: March 17, 2016

Published: April 28, 2016

REFERENCES

- Balibar, C.J., Howard-Jones, A.R., and Walsh, C.T. (2007). Terrequinone A biosynthesis through L-tryptophan oxidation, dimerization and bisprenylation. *Nat. Chem. Biol.* 3, 584–592.
- Brachmann, A.O., Forst, S., Furgani, G.M., Fodor, A., and Bode, H.B. (2006). Xenofuranones A and B: phenylpyruvate dimers from *Xenorhabdus szentirmaii*. *J. Nat. Prod.* 69, 1830–1832.

- Braesler, J., Gotze, S., Shah, F., Heine, D., Tauber, J., Hertweck, C., Tunlid, A., Stallforth, P., and Hoffmeister, D. (2015). Three redundant synthetases secure redox-active pigment production in the basidiomycete *Paxillus involutus*. *Chem. Biol.* **22**, 1325–1334.
- Braga, G.U., Rangel, D.E., Fernandes, E.K., Flint, S.D., and Roberts, D.W. (2015). Molecular and physiological effects of environmental UV radiation on fungal conidia. *Curr. Genet.* **61**, 405–425.
- Britton, H.T.S., and Robinson, R.A. (1931). CXCVIII.—Universal buffer solutions and the dissociation constant of veronal. *J. Chem. Soc. (Resumed)*, 1456–1462.
- Buitrago, E., Vuillamy, A., Boumendjel, A., Yi, W., Gellon, G., Hardre, R., Philouze, C., Serratrice, G., Jamet, H., Reglier, M., et al. (2014). Exploring the interaction of N/S compounds with a dicopper center: tyrosinase inhibition and model studies. *Inorg. Chem.* **53**, 12848–12858.
- Csala, M., Kereszturi, E., Mandl, J., and Banhegyi, G. (2012). The endoplasmic reticulum as the extracellular space inside the cell: role in protein folding and glycosylation. *Antioxid. Redox Signal.* **16**, 1100–1108.
- Eisenman, H.C., and Casadevall, A. (2012). Synthesis and assembly of fungal melanin. *Appl. Microbiol. Biotechnol.* **93**, 931–940.
- Eisenman, H.C., Mues, M., Weber, S.E., Frases, S., Chaskes, S., Gerfen, G., and Casadevall, A. (2007). *Cryptococcus neoformans* laccase catalyses melanin synthesis from both D- and L-DOPA. *Microbiology* **153**, 3954–3962.
- Gao, H., Guo, W., Wang, Q., Zhang, L., Zhu, M., Zhu, T., Gu, Q., Wang, W., and Li, D. (2013). Aspulvinones from a mangrove rhizosphere soil-derived fungus *Aspergillus terreus* Gwq-48 with anti-influenza A viral (H1N1) activity. *Bioorg. Med. Chem. Lett.* **23**, 1776–1778.
- Gill, M., and Steglich, W. (1987). Pigments of fungi (*Macromycetes*). *Fortschr. Chem. Org. Naturst.* **51**, 1–317.
- Gressler, M., Zaehle, C., Scherlach, K., Hertweck, C., and Brock, M. (2011). Multifactorial induction of an orphan PKS-NRPS gene cluster in *Aspergillus terreus*. *Chem. Biol.* **18**, 198–209.
- Gressler, M., Hortschansky, P., Geib, E., and Brock, M. (2015a). A new high-performance heterologous fungal expression system based on regulatory elements from the *Aspergillus terreus* terrein gene cluster. *Front. Microbiol.* **6**, 184.
- Gressler, M., Meyer, F., Heine, D., Hortschansky, P., Hertweck, C., and Brock, M. (2015b). Phytotoxin production in *Aspergillus terreus* is regulated by independent environmental signals. *Elife* **4**, e07861.
- Guo, C.-J., Sun, W.-W., Bruno, K.S., Oakley, B.R., Keller, N.P., and Wang, C.C.C. (2015). Spatial regulation of a common precursor from two distinct genes generates metabolite diversity. *Chem. Sci.* **6**, 5913–5921.
- Halaoui, S., Asther, M., Sigoillot, J.C., Hamdi, M., and Lomascolo, A. (2006). Fungal tyrosinases: new prospects in molecular characteristics, bioengineering and biotechnological applications. *J. Appl. Microbiol.* **100**, 219–232.
- Hall, A.M., and Orlow, S.J. (2005). Degradation of tyrosinase induced by phenylthiourea occurs following Golgi maturation. *Pigment Cell Res.* **18**, 122–129.
- Hillmann, F., Novohradská, S., Mattern, D.J., Forberger, T., Heinekamp, T., Westermann, M., Winckler, T., and Brakhage, A.A. (2015). Virulence determinants of the human pathogenic fungus *Aspergillus fumigatus* protect against soil amoeba predation. *Environ. Microbiol.* **17**, 2858–2869.
- Hortschansky, P., Eisendle, M., Al-Abdallah, Q., Schmidt, A.D., Bergmann, S., Thon, M., Kniemeyer, O., Abt, B., Seeber, B., Werner, E.R., et al. (2007). Interaction of HapX with the CCAAT-binding complex—a novel mechanism of gene regulation by iron. *EMBO J.* **26**, 3157–3168.
- Howard, R.J., and Valent, B. (1996). Breaking and entering: host penetration by the fungal rice blast pathogen *Magnaporthe grisea*. *Annu. Rev. Microbiol.* **50**, 491–512.
- Ibrahim-Granet, O., Dubourdeau, M., Latge, J.P., Ave, P., Huerre, M., Brakhage, A.A., and Brock, M. (2008). Methylcitrate synthase from *Aspergillus fumigatus* is essential for manifestation of invasive aspergillosis. *Cell Microbiol.* **10**, 134–148.
- Jacobsen, I.D., Grosse, K., Slesiona, S., Hube, B., Berndt, A., and Brock, M. (2010). Embryonated eggs as an alternative infection model to investigate *Aspergillus fumigatus* virulence. *Infect. Immun.* **78**, 2995–3006.
- Jahn, B., Boukhallouk, F., Lotz, J., Langfelder, K., Wanner, G., and Brakhage, A.A. (2000). Interaction of human phagocytes with pigmentless *Aspergillus conidia*. *Infect. Immun.* **68**, 3736–3739.
- Mattern, D.J., Schoeler, H., Weber, J., Novohradská, S., Kraibooj, K., Dahse, H.M., Hillmann, F., Valiante, V., Figge, M.T., and Brakhage, A.A. (2015). Identification of the antiphagocytic trypacidin gene cluster in the human-pathogenic fungus *Aspergillus fumigatus*. *Appl. Microbiol. Biotechnol.* **99**, 10151–10161.
- Ngamskulrungraj, P., Price, J., Sorrell, T., Perfect, J.R., and Meyer, W. (2011). *Cryptococcus gattii* virulence composite: candidate genes revealed by microarray analysis of high and less virulent Vancouver island outbreak strains. *PLoS One* **6**, e16076.
- Ojima, N., Takenaka, S., and Seto, S. (1973). New butenolides from *Aspergillus terreus*. *Phytochemistry* **12**, 2527–2529.
- Park, H.S., and Yu, J.H. (2012). Genetic control of asexual sporulation in filamentous fungi. *Curr. Opin. Microbiol.* **15**, 669–677.
- Pauly, J., Nett, M., and Hoffmeister, D. (2014). Ralfuranone is produced by an alternative aryl-substituted gamma-lactone biosynthetic route in *Ralstonia solanacearum*. *J. Nat. Prod.* **77**, 1967–1971.
- Petersen, T.N., Brunak, S., von Heijne, G., and Nielsen, H. (2011). SignalP 4.0: discriminating signal peptides from transmembrane regions. *Nat. Methods* **8**, 785–786.
- Ramsden, C.A., and Riley, P.A. (2014). Tyrosinase: the four oxidation states of the active site and their relevance to enzymatic activation, oxidation and inactivation. *Bioorg. Med. Chem.* **22**, 2388–2395.
- Schneider, P., Weber, M., Rosenberger, K., and Hoffmeister, D. (2007). A one-pot chemoenzymatic synthesis for the universal precursor of antidiabetes and antiviral bis-indolylquinones. *Chem. Biol.* **14**, 635–644.
- Schneider, C.A., Rasband, W.S., and Eliceiri, K.W. (2012). NIH Image to ImageJ: 25 years of image analysis. *Nat. Methods* **9**, 671–675.
- Schuffler, A., Liermann, J.C., Opatz, T., and Anke, T. (2011). Elucidation of the biosynthesis and degradation of allantofuranone by isotopic labelling and fermentation of modified precursors. *Chemochem* **12**, 148–154.
- Scotto-Lavino, E., Du, G., and Frohman, M.A. (2006). 5' end cDNA amplification using classic RACE. *Nat. Protoc.* **1**, 2555–2562.
- Seto, S. (1979). Biosynthesis of aspulvinones, metabolites from *Aspergillus terreus*. In *Organic Chemistry*, T. Mukaiyama, ed., pp. A21–A32.
- Shevchenko, A., Tomas, H., Havlis, J., Olsen, J.V., and Mann, M. (2006). In-gel digestion for mass spectrometric characterization of proteins and proteomes. *Nat. Protoc.* **1**, 2856–2860.
- Slesiona, S., Gressler, M., Mihlan, M., Zaehle, C., Schaller, M., Barz, D., Hube, B., Jacobsen, I.D., and Brock, M. (2012a). Persistence versus escape: *Aspergillus terreus* and *Aspergillus fumigatus* employ different strategies during interactions with macrophages. *PLoS One* **7**, e31223.
- Slesiona, S., Ibrahim-Granet, O., Olias, P., Brock, M., and Jacobsen, I.D. (2012b). Murine infection models for *Aspergillus terreus* pulmonary aspergillosis reveal long-term persistence of conidia and liver degeneration. *J. Infect. Dis.* **205**, 1268–1277.
- Teutschbein, J., Albrecht, D., Potsch, M., Guthke, R., Aïmanianda, V., Clavaud, C., Latge, J.P., Brakhage, A.A., and Kniemeyer, O. (2010). Proteome profiling and functional classification of intracellular proteins from conidia of the human-pathogenic mold *Aspergillus fumigatus*. *J. Proteome Res.* **9**, 3427–3442.
- Thywissen, A., Heinekamp, T., Dahse, H.M., Schmalder-Ripcke, J., Nietzsche, S., Zipfel, P.F., and Brakhage, A.A. (2011). Conidial dihydroxynaphthalene melanin of the human pathogenic fungus *Aspergillus fumigatus* interferes with the host endocytosis pathway. *Front. Microbiol.* **2**, 96.
- Wang, M., Beissner, M., and Zhao, H. (2014). Aryl-aldehyde formation in fungal polyketides: discovery and characterization of a distinct biosynthetic mechanism. *Chem. Biol.* **21**, 257–263.
- Woo, P.C., Tam, E.W., Chong, K.T., Cai, J.J., Tung, E.T., Ngan, A.H., Lau, S.K., and Yuen, K.Y. (2010). High diversity of polyketide synthase genes and the melanin biosynthesis gene cluster in *Penicillium mamefei*. *FEBS J.* **277**, 3750–3758.
- Zaehle, C., Gressler, M., Shelest, E., Geib, E., Hertweck, C., and Brock, M. (2014). Terrein biosynthesis in *Aspergillus terreus* and its impact on phytotoxicity. *Chem. Biol.* **21**, 719–731.

Cell Chemical Biology, Volume 23

Supplemental Information

A Non-canonical Melanin Biosynthesis Pathway

Protects *Aspergillus terreus* Conidia

from Environmental Stress

Elena Geib, Markus Gressler, Iuliia Viediarnikova, Falk Hillmann, Ilse D. Jacobsen, Sandor Nietzsche, Christian Hertweck, and Matthias Brock

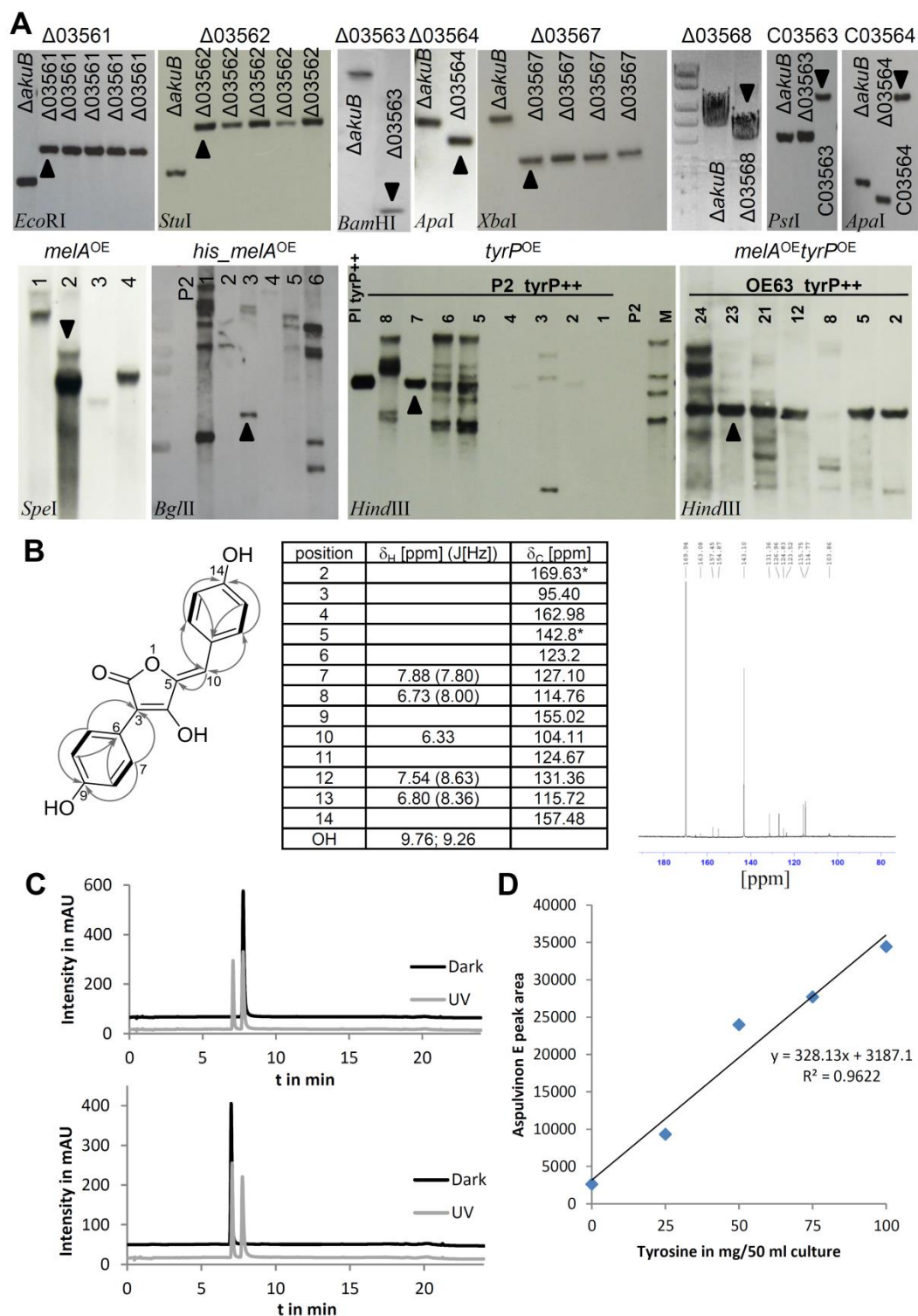


Figure S1: *A. terreus* and *A. niger* transformant analyses and structure elucidation of aspulvinones from *A. niger melA*^{OE}. This figure is supplemental to Fig. 1. (A) Upper row: Southern blot and PCR analyses on gene deletions and complementation in the *A. terreus* \DeltaakuB strain. Locus tags of genes and enzymes used for digestion of genomic DNAs are annotated in the respective picture. Lower row: Southern blot analyses of *A. niger melA* and *tyrP* expressing strains. Strains selected for analyses in this study are labelled with arrowheads. (B) Structure of aspulvinone E with key NMR signals from heteronuclear multiple-bond correlation (grey arrows) and correlation spectroscopy (bold bonds). Chemical shifts and coupling constants are annotated in the table and ¹³C-NMR spectra of the unlabelled and labelled aspulvinone E are presented. (C) HPLC profiles of purified aspulvinone E (upper panel) and isoaspulvinone E (lower panel) before (black) and after (grey) UV radiation. (D) HPLC-based relative quantification of aspulvinone E synthesis in dependence on the tyrosine supplementation of growth media of *A. niger melA*^{OE}.

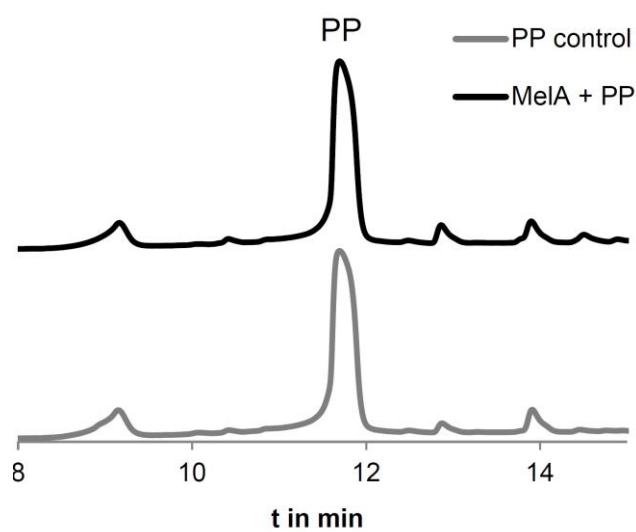


Figure S2: Analysis of MelA reactivity on phenylpyruvate. This figure is supplemental to Fig. 2. A 10 ml reaction with 7.5 mM phenylpyruvate and with (black line) or without (grey line) 1 mg of purified MelA was extracted and subjected to HPLC analysis. No difference between both samples is observed, indicating that MelA does not use phenylpyruvate as substrate.

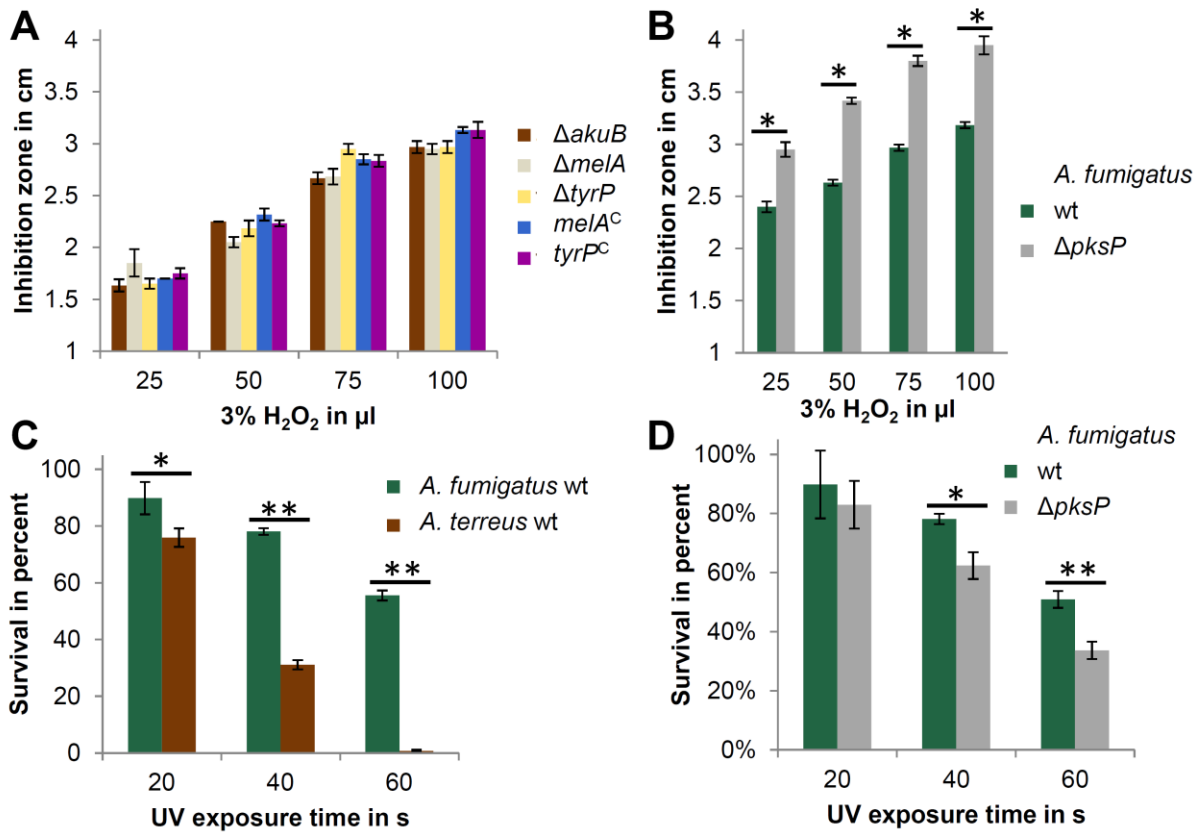


Figure S3: Oxidative and UV stress resistance of *A. terreus* and *A. fumigatus* wild type and mutant strains. This figure is supplemental to Fig. 6. **(A)** Sensitivity of *A. terreus* $\Delta akuB$ wild type, pigment mutants and complemented strains against hydrogen peroxide. No significant differences in diameters of inhibition zones were observed. **(B)** Same analysis as in (A), but with *A. fumigatus* wild type and corresponding white *pksP* mutant. **(C)** Comparison of *A. fumigatus* and *A. terreus* wild type strains (without genetic $\Delta akuB$ background). *A. fumigatus* appears naturally more UV resistant than *A. terreus*. **(D)** UV sensitivity of *A. fumigatus* wild type and corresponding white *pksP* mutant. The wild type shows increased UV protection. All data were collected from biological duplicates performed in technical triplicates. Significance was calculated by student's t-test from weighted means with *= $p < 0.05$ and **= $p < 0.01$. Data are shown as mean \pm SD.

Supplemental video information

Video S1: Recording of the *in vitro* reaction of TyrP with and without tyrosinase inhibitor. This video is supplemental to Fig. 5. A 96-well microplate with total reaction volumes of 20 μ l was used for recording the TyrP reaction in a time-lapse movie. The movie shows for wells. Upper left = aspulvinone E control without TyrP. Upper right = TyrP with 2 mM of the tyrosinase inhibitor phenylthiourea (PTU). Lower left = aspulvinone E with TyrP. Lower right = aspulvinone E with 2 mM PTU and TyrP. Over a total period of 60 min single photographs were taken every 20 s under magnification of a Leica S8APO Binocular equipped with a QImaging MicroPublisher 3.3 RTV camera. Pictures were assembled with Image-Pro Insight (Media Cybernetics Software). Due to technical reasons, the first two min after starting the reaction with TyrP have not been recorded.

Supplemental Tables

Table S1: Oligonucleotides used in this study. This table is supplemental to the experimental procedures and is provided as a separate Excel file.

Table S2: Media used in this study. This table is supplemental to the experimental procedures.

Minimal media	
AMM	6 g/l NaNO ₃ , 0.52 g/l KCl, 0.52 g/l MgSO ₄ × 7 H ₂ O, 1.52 g/l KH ₂ PO ₄ ; 1 ml/l 1000× Hutner's trace elements (Hutner et al., 1950); pH 6.5
G50	50 mM glucose
G100	100 mM glucose
AMM(-N)	0.52 g/l KCl, 0.52 g/l MgSO ₄ × 7 H ₂ O, 1.52 g/l KH ₂ PO ₄ ; 1 ml/l 1000× Hutner's trace elements; pH 6.5
G50Gln20	50 mM glucose and 10 mM glutamine
CA1%	1% casamino acids
Starch2%Gln50	2% starch and 50 mM glutamine
Complex media	
YM	3 g/l yeast extract, 3 g/l malt extract, 5 g/l meat peptone; pH 6.6
GSMY	30 g/l glucose, 2.5 g/l soy bean meal, 0.5 g/l yeast extract, 1 g/l KH ₂ PO ₄ , 1 g/l MgSO ₄ × 7 H ₂ O, 0.5 g/l NaCl, 0.5 g/l CaCl ₂ × 2 H ₂ O, 2 mg /l FeCl ₃ × 2 H ₂ O, 2 mg/l ZnSO ₄ × 7 H ₂ O; pH 5.5
PDB	24 g/l potato dextrose broth, pH 6.5
Malt agar	30 g malt extract, 5 g bacterial peptone, 2% agar

Table S3: Strains used in this study. This table is supplemental to the experimental procedures.

Strain	Genotype	Reference
<i>A. terreus</i> SBUG844		JMRC; HKI; Jena
<i>A. terreus</i> Δ akuB	<i>A. terreus</i> SBUG 844 Δ akuB::hph ^R	Gressler et al., 2011
<i>A. terreus</i> Δ melA	<i>A. terreus</i> SBUG 844 Δ akuB::hph ^R ; Δ melA::ptrA ^R	this study
<i>A. terreus</i> Δ tyrP	<i>A. terreus</i> SBUG 844 Δ akuB::hph ^R ; Δ tyrP::ptrA ^R	this study
<i>A. terreus</i> Δ 03561	<i>A. terreus</i> SBUG 844 Δ akuB::hph ^R ; Δ 03561::ptrA ^R	this study
<i>A. terreus</i> Δ 03562	<i>A. terreus</i> SBUG 844 Δ akuB::hph ^R ; Δ 03562::ptrA ^R	this study
<i>A. terreus</i> Δ 03567	<i>A. terreus</i> SBUG 844 Δ akuB::hph ^R ; Δ 03567::ptrA ^R	this study
<i>A. terreus</i> Δ 03568	<i>A. terreus</i> SBUG 844 Δ akuB::hph ^R ; Δ 03568::ptrA ^R	this study
<i>A. terreus</i> tryP ^{OE}	<i>A. terreus</i> SBUG844; AtPterA:tyrP:AttrpC ^T	this study
<i>A. niger</i> A1144		FGSC; Kansas City; USA
<i>A. niger</i> P2	<i>A. niger</i> A1144 ptrA ^R , AoPamyB:terR:terR ^T	Gressler et al., 2015a
<i>A. niger</i> melA ^{OE}	<i>A. niger</i> A1144 ptrA ^R , AoPamyB:terR:terR ^T ; ble ^R , AtPterA:melA:AttrpC ^T	this study
<i>A. niger</i> his_melA ^{OE}	<i>A. niger</i> A1144 ptrA ^R , AoPamyB:terR:terR ^T ; ble ^R , AtPterA:his_melA:AttrpC ^T	this study
<i>A. niger</i> tyrP ^{OE}	<i>A. niger</i> A1144 ptrA ^R , AoPamyB:terR:terR ^T ; hph ^R , AtPterA:tyrP:AttrpC ^T	this study
<i>A. niger</i> tyrP:tdTom ^{OE}	<i>A. niger</i> A1144 ptrA ^R , AoPamyB:terR:terR ^T ; hph ^R , AtPterA:tyrP:tdTomato:AttrpC ^T	this study
<i>A. niger</i> melA ^{OE} tyrP ^{OE}	<i>A. niger</i> A1144 ptrA ^R , AoPamyB:terR:terR ^T ; ble ^R , AtPterA:melA:AttrpC ^T ; hph ^R , AtPterA:tyrP:AttrpC ^T	this study
<i>A. fumigatus</i> ATCC46645		ATCC; Manassas; USA
<i>A. fumigatus</i> Δ pksP	<i>A. fumigatus</i> ATCC46645 pksP ⁻ (UV mutant)	(Jahn et al., 1997)
<i>A. nidulans</i> SCF1.2	veA1	(Fleck and Brock, 2008)
BL21(DE3) Rosetta2	fhuA2 [lon] ompT gal (λ DE3) [dcm] Δ hsdS λ DE3 = λ sBamHIo Δ EcoRI-B int::(lacI::PlacUV5::T7 gene1) i21 Δ nin5 with plasmid pRARE2	Novagen, Germany
BL21(DE3)_tyrP ⁺⁺	BL21(DE3) Rosetta2 genotype with PT7:tyrP ⁺⁺ - pET43.1H6	this study
BL21(DE3)_tyrP ⁺	BL21(DE3) Rosetta2 genotype with PT7:tyrP ⁺ - pET43.1H6	this study

Supplemental Experimental Procedures

Gene deletion and complementation in *A. terreus*

Gene deletion constructs were generated by PCR amplification of 0.5 – 1 kb upstream and downstream flanks of the gene of interest using Phusion Hot Start II polymerase (Thermo Scientific, Braunschweig, Germany) and genomic DNA from *A. terreus* SBUG844 as template. Oligonucleotides P21-P44 were used for the specific gene deletions and are shown in Table S1. Deletion constructs generally contained the *ptrA* resistance cassette (Fleck and Brock, 2010) and were assembled by *in vitro* recombination (InFusion Enzyme Mix, Clontech, Saint-Germain-en-Laye, France) in a *KpnI*-linearised pUC19 vector by mixing the plasmid with the resistance cassette and the two gene specific flanks. Plasmids were amplified in *E. coli* DH5 α and re-isolated using the NucleoSpin Plasmid (Machery-Nagel, Düren, Germany). Deletion constructs were excised by *KpnI* restriction and used for transformation of the *A. terreus* SBUG844/ Δ *akuB* strain (Gressler et al., 2011). The *mela* deletion was complemented using P29 and P45-47 and *tyrP* deletion with P33 and P48, 49 and P36. Complementation constructs consisted of the entire coding region including the upstream flank and a short terminator sequence, the phleomycin resistance cassette and a downstream flanking region that were assembled by *in vitro* recombination.

Heterologous gene expression in *Aspergillus* species

Cloning of *mela* in SM-Xpress was performed with oligonucleotides P64-P71 and resulted in *A. niger* strain *mela*^{OE}. An *N*-terminally His-tagged MelA was produced with oligonucleotide P72 and P81, the former oligonucleotide containing a His-tag coding sequence. The amplified product was cloned into the SM-Xpress vector. The *tyrP* gene was amplified with P73/74 and cloned into the *NsiI* restricted His_SM-Xpress vector to add a *C*-terminal His-tag. Subsequently, the phleomycin resistance cassette was replaced by the *NotI* restricted *hph* gene that derived from plasmid *hph_pCRIV* (Fleck and Brock, 2010). Constructs were used for transformation of *A. niger* P2, *mela*^{OE} or *A. terreus* SBUG844. For localisation studies of TyrP a *C*-terminal fusion with the red fluorescent protein tdTomato separated by a synthetic peptide linker sequence of 14 amino acids (QSTVPRARDPPVAT: (Mezzanotte et al., 2014)) was performed. The *tyrP* gene was amplified with oligonucleotides P75/76 and tdTomato gene with P77/78. All fragments were fused by *in vitro* recombination and used for transformation of *A. niger* P2 and *A. niger mela*^{OE}.

Generation the SM-Xpress2 and *his*_SM-Xpress cloning vectors

To construct a vector that allows transformation of strains already carrying a SM-Xpress vector construct, the SM-Xpress2 vector was generated that contained the hygromycin B resistance cassette rather than the phleomycin cassette. Cloning of the gene of interest requires linearization with *NcoI* and an internal *NcoI* restriction site in the *hph* gene had to be removed. This was done by overlap PCR using primer pairs P56/57 and P58/59, which resulted in a silent point mutation. Subsequently, the *ble* gene was excised from SM-Xpress by *NotI* restriction and replaced by the mutated *hph* gene by *in vitro* recombination resulting in SM-Xpress2. For generating a vector suitable for production of His-tagged proteins a strategy was selected that allows either *N*- or *C*-terminal tagging of proteins in dependence of the restriction enzyme used for plasmid linearization. The *terA* promoter was amplified with oligonucleotides P60/61, which resulted in a 817 bp fragment with a 5'-overlap to the *EcoRI* restricted pUC19 vector and a His-tag sequence at its 3'-end. The *trpC* terminator was amplified with oligonucleotides P62/63 resulting in a 5'-overlap to the His-tag sequence and a 3' overlap to the resistance cassette. The promoter and terminator sequences were removed from the original SM-Xpress vector by *EcoRI* restriction and replaced by the new fragments *via in vitro* recombination. This resulted in plasmid *his*_SM-Xpress that flanks the His-tag sequence 5' by an *NsiI* and 3' by an *NcoI* restriction site. This allows to tag proteins at the *C*-terminus by insertion of the gene of interest in the *NsiI*, whereas insertion into the *NcoI* restriction site results in a protein with an *N*-terminal His-tag.

Purification of recombinant MelA

For purification of MelA an *A. niger* strain producing MelA with an *N*-terminal His-tag (P2_his-*mela*) was selected. The strain was grown for 26 h at 30°C on 2 × 100 ml YM medium. Mycelium was harvested over filter gaze (Miracloth, Merck, Darmstadt, Germany) and pressed dry. Approximately 4 g mycelium (wet weight) were ground to a fine powder under liquid nitrogen and suspended in buffer A (50 mM Tris-HCl, 150 mM NaCl, 10% glycerine at pH 7.5) supplemented with 20 mM imidazole. Cell debris was removed by 10 min centrifugation at 4°C and 14000 × g. The supernatant was filtered over a 0.45 μ m filter (Sartorius) before applied to a 1 ml Ni-Sepharose FF gravity flow column (Macherey-Nagel) previously equilibrated with the suspension buffer. After washing the column with 6 column volumes of buffer A containing 40 mM imidazole, MelA was eluted in buffer A with 200 mM imidazole. Eluates were concentrated and desalted against buffer A by use of centrifugal filter devices (Millipore, cut-off 30 kDa). Purity of the protein was checked by using Novex NuPAGE 4-12% Bis-Tris gels in a MES buffered running system (Invitrogen/Life Technologies/Thermo Scientific).

Purification of recombinant TyrP from *A. niger* and *A. terreus*

Recombinant TyrP was purified from *A. niger* *tryP*^{OE} and *A. terreus* PterA:*tyrP*⁺⁺ 10. The protein from both sources contained a C-terminal His-tag for purification *via* Ni-Sepharose. In an initial attempt *A. niger tryP*^{OE} was grown for 36 h on AMM(-N)G100Gln50 medium and purification from ground mycelium was performed over Ni-Sepharose as described for purification of MelA from *A. niger*. Unfortunately, most of TyrP activity eluted at the 40 mM imidazole washing step and analysis by SDS PAGE did not allow unambiguously attributing a specific protein band to TyrP activity. Due to indications for a post-translational modification by glycosylation the purification procedure was adapted accordingly. First, enzyme production from *A. niger* was optimised by incubating the production strain for 36 h at 28°C in AMM(-N)50Gln with 2% soluble starch (Difco, Oxford, UK) as carbon source and 10 g/l talc (Sigma, Gillingham, UK). *A. terreus* was cultured for 28 h at 37°C in GSMY medium. From both species approximately 10 g mycelium (wet weight) was ground to a fine powder and suspended in 30 ml buffer B (20 mM Tris/HCl, 200 mM NaCl; pH 7.4). The suspension was centrifuged at 14,000 × g and filtered over 0.45 µm syringe filters. The cell-free extract was loaded on a 2 ml gravity-flow ConA-Sepharose 4B column previously equilibrated with buffer B. The column was washed with 3 column volumes of buffer B followed by 3 column volumes of a stringency wash with buffer B containing 50 mM methyl- α -D-glucopyranoside (Sigma). Elution was performed in buffer B with 1 M methyl- α -D-glucopyranoside. Elution was paused several times for about 15 min to increase elution efficiency (Soper and Aird, 2007). About 28 ml of active fractions were pooled and concentrated using a centrifugal filter device with a 30 kDa cut-off. Concentration of methyl- α -D-glucopyranoside was reduced by diluting the enzyme concentrate in buffer A and the solution was applied to a 1 ml gravity-flow Ni-Sepharose column. The column was washed with 4 column volumes buffer A containing 20 mM imidazole and TyrP was eluted by increasing the imidazole concentration to 200 mM. Enzyme purity was analysed by SDS-PAGE on Novex NuPAGE 4-12% Bis-Tris gels using a MES buffered running system.

Purification of different TyrP versions from *E. coli*

For purification of proteins from *E. coli* Express Instant TB medium (Merck, Novagen) was used. Cultures of 20 ml were inoculated with BL21(DE3) Rosetta 2 cells carrying pET expression vectors with either the full length or truncated version of *tyrP*. *E. coli* cells were incubated at 28°C for 26 h or at 21°C for 40 h with identical results. Samples were disrupted by sonication and soluble and insoluble fractions were analysed for tyrosinase activity and for protein production via SDS-PAGE analysis. Since no activity was detected and the protein was exclusively detected from inclusion bodies, purification was performed under denaturing conditions. Approximately 0.5 g of cells were suspended in buffer A and disrupted by sonication (3 × 2 min continuous sonication at 60% power; Soniprep 150, MSE, London). Insoluble material was collected by centrifugation at 13,000 × g and washed once with buffer A. The pellet was dissolved for 30 min in 2 ml buffer C (50 mM Tris/HCl, 150 mM NaCl, 8 M Urea; pH 7.5). After centrifugation at 13,000 × g for 6 min the supernatant was loaded on a 1 ml Ni-Sepharose and washed with 6 ml buffer C with 20 mM imidazole followed by 5 ml with 40 mM imidazole. Proteins were finally eluted by increasing the imidazole concentration to 200 mM in buffer C. Purification was analysed by SDS-PAGE on Novex NuPAGE 4-12% Bis-Tris gels using a MES buffered running system.

Isolation and characterisation of aspulvinones

Semi-preparative isolation of aspulvinones was performed on an Agilent 1260 series equipped with DAD and quaternary pump as described in the supplemental experimental procedures. Separation was carried out on a C18 column (Zorbax Eclipse XDB-C18, 5 µm, 250 × 9.4 mm, Agilent Technologies, Waldbronn, Germany) using a gradient of solvents A (water + 0.1% formic acid) and B (methanol). The following gradient was applied at a flow rate of 3.5 ml/min: 0 - 0.5 min 45% B, 0.5 - 4 min to 55% B, 4 - 16 min to 62% B, 16 - 19 min to 90% B, 19 - 19.5 min to 100% B holding to 26 min. Regeneration to 45% B from 26 - 30 min. Extracts from *A. terreus* Δ *tyrP* were pre-fractionated using a SPE C18 cartridge (C18_{ec}, Chromabond, Macherey and Nagel). The 60% MeOH portion containing Aspulvinones were used for semi-quantitative HPLC.

H₂O₂ sensitivity

Oxidative stress sensitivity was determined as described previously (Maerker et al., 2005) by the size of inhibition zones formed in the presence of various amounts of H₂O₂. The assay was performed on square 10 × 10 cm petri dishes with 40 ml (AMM(-N)G50Gln10 medium containing 2% agar. Top agar (20 ml) was mixed with 3 × 10⁸ conidia for *A. fumigatus* and 4 × 10⁸ conidia for *A. terreus* and poured on top of the bottom agar. Four holes with 1 cm in diameter were punched and varying amounts of a 3% H₂O₂ solution (25 µl to 100 µl) were added. Plates were incubated for 20 h at 37°C and inhibition zones were measured. All tests were performed in triplicates.

Electron microscopy

For scanning electron microscopy conidia were collected directly from plates. Plates were point inoculated with *A. terreus* strains and incubated for 7 days at 37°C to yield colonies with mature conidiophores. Plates were turned upside down and conidia were transferred directly to the sample holder on an electrically conductive and adhesive tag (Leit-Tab, Plano GmbH, Wetzlar, Germany) by carefully tapping on the back of the plate. Conidia were fixed for 24 h in the vapour of a 1:1 mixture of formaldehyde and glutaraldehyde. A critical point drying was not performed. To avoid surface charging the samples were coated with platinum (thickness approx. 2 nm) by high vacuum evaporation using a BAF 400 D (BALTEC, Liechtenstein). Coated conidia were investigated with a field emission scanning electron microscope LEO-1530 Gemini (Carl Zeiss NTS GmbH, Oberkochen, Germany) at electron energy of 8 keV using the in-lens secondary electron detector and magnifications of 50,000 to 200,000×. For transmission electron microscopy conidia were harvested in sterile water, washed once and the pellet was overlaid with freshly prepared 0.1 M cacodylate buffer (pH 7.2) containing 2.5% glutaraldehyde and fixed for 2.5 h at room temperature. After washing three times with pure cacodylate buffer the pellet was post-fixed for 1 h with 1% osmium tetroxide and dehydration in ascending ethanol series followed by post-staining with uranyl acetate. Subsequently, the pellets were embedded in epoxy resin (Araldite) and ultrathin sectioned using a LKB Ultratome III (LKB, Stockholm, Sweden). After mounting on filmed Cu grids and post-staining with lead citrate the sections were studied in a transmission electron microscope EM 900 (Zeiss, Oberkochen, Germany) at 80 kV and magnifications of 3,000 to 20,000×.

Germination analysis

Fluorescein isothiocyanate (FITC; Sigma) labelled conidia were used for germination analyses. Conidia were adjusted to 10⁶ conidia per ml in PBS with 0.01% Tween. For germination analyses 10 µl of the respective conidia suspension were added to 790 µl PDB medium in four well chamber slides (NUNC, Thermo Scientific) and incubated for 8 h at 37°C and 5% CO₂. Slides were centrifuged at 200 × g and the medium was carefully removed. Conidia were embedded in a mounting solution containing DAPI (ProLong Gold Antifade with DAPI; Invitrogen/Thermo Scientific), incubated over night at 4°C and the number of germinated and non-germinated conidia was counted using an AxioImager fluorescence microscope (Zeiss, Jena, Germany). Experiments were performed in triplicates and approximately 1000 conidia per strain were evaluated.

Supplemental References

- Fleck, C.B., and Brock, M. (2008). Characterization of an acyl-CoA: carboxylate CoA-transferase from *Aspergillus nidulans* involved in propionyl-CoA detoxification. *Mol Microbiol* 68, 642-656.
- Fleck, C.B., and Brock, M. (2010). *Aspergillus fumigatus* catalytic glucokinase and hexokinase: expression analysis and importance for germination, growth, and conidiation. *Eukaryot Cell* 9, 1120-1135.
- Gressler, M., Zaehle, C., Scherlach, K., Hertweck, C., and Brock, M. (2011). Multifactorial induction of an orphan PKS-NRPS gene cluster in *Aspergillus terreus*. *Chem Biol* 18, 198-209.
- Hutner, S.H., Provasoli, L., Schatz, A., and Haskins, C.P. (1950). Some Approaches to the Study of the Role of Metals in the Metabolism of Microorganisms. *Proc Am Phil Soc* 94, 152-170.
- Jahn, B., Koch, A., Schmidt, A., Wanner, G., Gehringer, H., Bhakdi, S., and Brakhage, A.A. (1997). Isolation and characterization of a pigmentless-conidium mutant of *Aspergillus fumigatus* with altered conidial surface and reduced virulence. *Infect Immun* 65, 5110-5117.
- Maerker, C., Rohde, M., Brakhage, A.A., and Brock, M. (2005). Methylcitrate synthase from *Aspergillus fumigatus*. Propionyl-CoA affects polyketide synthesis, growth and morphology of conidia. *FEBS J* 272, 3615-3630.
- Mezzanotte, L., Blankevoort, V., Lowik, C.W., and Kaijzel, E.L. (2014). A novel luciferase fusion protein for highly sensitive optical imaging: from single-cell analysis to *in vivo* whole-body bioluminescence imaging. *Anal Bioanal Chem* 406, 5727-5734.
- Soper, A.S., and Aird, S.D. (2007). Elution of tightly bound solutes from concanavalin A Sepharose. Factors affecting the desorption of cottonmouth venom glycoproteins. *J Chromatogr A* 1154, 308-318.

Table of oligonucleotides used in this study. This table is supplemental to the experimental procedures.

#	name	5' -> 3' sequence	template	function
1	act_Ater_for	CCATCGAGAAGTCTTATGAGC	gDNA, cDNA of <i>A. terreus</i>	semiquantitative RT-PCR
2	act_Ater_rev	GGACAGGGAAGCCAGAATGG	gDNA, cDNA of <i>A. terreus</i>	semiquantitative RT-PCR
3	AT_brlA_cDNA_for	CGACTACATGGATGACTACC	gDNA, cDNA of <i>A. terreus</i>	semiquantitative RT-PCR
4	AT_brlA_cDNA_rev	GGATCTTCAGCTTGGAGC	gDNA, cDNA of <i>A. terreus</i>	semiquantitative RT-PCR
5	At_03561_for	CCATATACCAGCATCTATTGTGC	gDNA, cDNA of <i>A. terreus</i>	semiquantitative RT-PCR
6	At_03561_rev	CACTGCCAGCAACCTTAAGC	gDNA, cDNA of <i>A. terreus</i>	semiquantitative RT-PCR
7	At_03562_for	CGTCTCTCGAGCTTATCTTCC	gDNA, cDNA of <i>A. terreus</i>	semiquantitative RT-PCR
8	At_03562_rev	GGCACAGCACAGATCTCG	gDNA, cDNA of <i>A. terreus</i>	semiquantitative RT-PCR
9	At_NRPS_03563_for	CGACGTTGGCATTGACTCC	gDNA, cDNA of <i>A. terreus</i>	semiquantitative RT-PCR
10	At_NRPS_03563_rev	GCGCATCTTAATGTGTGGAGG	gDNA, cDNA of <i>A. terreus</i>	semiquantitative RT-PCR
11	At_03564_for	CCATGCCTTCGACTACAACC	gDNA, cDNA of <i>A. terreus</i>	semiquantitative RT-PCR
12	At_03564_rev	GGCTCATTAGTTCATACAATGG	gDNA, cDNA of <i>A. terreus</i>	semiquantitative RT-PCR
13	At_03565_for	CGGTGAGTACAGCGAGGC	gDNA, cDNA of <i>A. terreus</i>	semiquantitative RT-PCR
14	At_03565_rev	CGTCTTCAGTCTCACTCGC	gDNA, cDNA of <i>A. terreus</i>	semiquantitative RT-PCR
15	At_03566_for	GCATTGCGTCTCGAATCTGC	gDNA, cDNA of <i>A. terreus</i>	semiquantitative RT-PCR
16	At_03566_rev	CCATCCGCTTCAAAGTCC	gDNA, cDNA of <i>A. terreus</i>	semiquantitative RT-PCR
17	At_03567_for	CTCAGGGTTTCGTCTTGACG	gDNA, cDNA of <i>A. terreus</i>	semiquantitative RT-PCR
18	At_03567_rev	GGCAAGCATGGGATCAAGG	gDNA, cDNA of <i>A. terreus</i>	semiquantitative RT-PCR
19	At_03568_for	GCCTCGACCTGTACTGGC	gDNA, cDNA of <i>A. terreus</i>	semiquantitative RT-PCR
20	At_03568_rev	CCATCCCAACAGCATCATCC	gDNA, cDNA of <i>A. terreus</i>	semiquantitative RT-PCR
21	D_03561_up_fw	ttcgagctcggtACCGGAGTGGTTGCGATGAACC	gDNA of <i>A. terreus</i>	flanking regions for deletion
22	D_03561_up_rv	CGTAATCAAGCGGCGCCTACTCACCTAAGACTCTAGC	gDNA of <i>A. terreus</i>	flanking regions for deletion
23	D_03561_dn_fw	caagaaagacgcggccgcctagccagagtaatgtacg	gDNA of <i>A. terreus</i>	flanking regions for deletion
24	D_03561_dn_rv	GGATCCCCGGGTACCCCTCAGATAATACATCCGAAGG	gDNA of <i>A. terreus</i>	flanking regions for deletion
25	pUC19_KO62up_fw	gtgaattcgagctcggtaccggaacagatcacacgacgag	gDNA of <i>A. terreus</i>	flanking regions for deletion
26	pUC19_KO62up_rv	CGT AAT CAA GCG GCC GCC GAC AGC AGA GCG GTA GGC C	gDNA of <i>A. terreus</i>	flanking regions for deletion
27	pUC19_KO62dn_fw	gtataatacgcggccgcccatacccttgcctat	gDNA of <i>A. terreus</i>	flanking regions for deletion
28	pUC19_KO62dn_rv	CTA GAG GAT CCC CGG GTA CCG GTT TGG TTT TAG TCG TGC A	gDNA of <i>A. terreus</i>	flanking regions for deletion
29	pUC_NRPS03563up_f	gtgaattcgagctcggtACCTTGAATCTGGTCCATACTGTATGTC	cDNA of <i>A. terreus</i>	flanking regions for deletion
30	ptrA_NRPS03563up_r	cgtaatcaagcggccGCGAAATCCCTCAATGTTTCCGGTTC	cDNA of <i>A. terreus</i>	flanking regions for deletion
31	ptrA_NRPS03563dn_f	gtataatacgcggccGCGGTTTGGTTTTAGTCGTGCATC	cDNA of <i>A. terreus</i>	flanking regions for deletion
32	pUC_NRPS03563dn_r	ctagaggatccccgggtACCGGCTCTGATAGCGTCCGCC	cDNA of <i>A. terreus</i>	flanking regions for deletion
33	pUC_TYR03564up_f	gtgaattcgagctcggtACCCCGGCCGAACCATTGAC	cDNA of <i>A. terreus</i>	flanking regions for deletion
34	ptrA_TYR03564up_r	cgtaatcaagcggccGCCGCAGTGAAGTCATCATAGCG	cDNA of <i>A. terreus</i>	flanking regions for deletion
35	ptrA_TYR03564dn_f	gtataatacgcggcCGCCTTCTAGTATAGGAAACGGAG	cDNA of <i>A. terreus</i>	flanking regions for deletion
36	pUC_TYR03564dn_r	ctagaggatccccgggtaccCAGAGAGGAAACCAATAAACC	cDNA of <i>A. terreus</i>	flanking regions for deletion
37	D_03567_Up_fw	ttcgagctcggtACCGTCTGATGATCATATAGTTGATCG	gDNA of <i>A. terreus</i>	flanking regions for deletion
38	D_03567_Up_rv	CGTAATCAAGCGGCGCGGTATCGTTCGGCAGGACATAAG	gDNA of <i>A. terreus</i>	flanking regions for deletion
39	D_03567_dn_fw	aagaaagacgcggccgcctattggaagatgtacgaagg	gDNA of <i>A. terreus</i>	flanking regions for deletion
40	D_03567_dn_rv	GGATCCCCGGGTACCGCATGTATCTAGTGTAAACAGCAGG	gDNA of <i>A. terreus</i>	flanking regions for deletion
41	D_03568_up_fw	ttcgagctcggtACCCGACACACCTAGATTTCC	gDNA of <i>A. terreus</i>	flanking regions for deletion
42	D_03568_up_rv	cgtaatcaagcggccGCCGTAAGTACTGAGCGGCTTTTGC	gDNA of <i>A. terreus</i>	flanking regions for deletion
43	D_03568_dn_fw	aagaaagacgcggccgctctgtctgtgtaatatattgg	gDNA of <i>A. terreus</i>	flanking regions for deletion
44	D_03568_dn_rv	GGATCCCCGGGTACCGGATATTTGTCTGAGAGTCC	gDNA of <i>A. terreus</i>	flanking regions for deletion
45	Comp_03563_P2_rv	TTGTGGTGAGCGGCCGCTTGGCAACAGAATACAGATCTGC	gDNA of <i>A. terreus</i>	complementation construct
46	Comp_03563_Dn_f2	ccctcactcgcggccgctattttgacgttttcgacg	gDNA of <i>A. terreus</i>	complementation construct
47	Comp_03563_Dn_r2	GGATCCCCGGGTACCCCTCGGGTAATTCGACATGG	gDNA of <i>A. terreus</i>	complementation construct

48	Comp_03564_P2_rv	GACTTTTGTGGTGAGCGGCCGCCGTATACTTCAATATACCG	gDNA of <i>A. terreus</i>	complementation construct
49	Comp_03564_dn_fw	ccctcaactcgcgcccgccttctctagtatagaaacg	gDNA of <i>A. terreus</i>	complementation construct
50	tyrP_GSPRT_rv	GGTTCGGGATTGAGCTCG	cDNA of <i>A. terreus</i>	5'-RACE
51	tyrP_GSP1_rv	GCTCGGTAGCATTGAATTCC	cDNA of <i>A. terreus</i>	5'-RACE
52	tyrP_GSP2_rv	GAAAGGGACGTTTTCGGTGC	cDNA of <i>A. terreus</i>	5'-RACE
53	QT_RACE	CCAGTGAGCAGAGTGACGAGGACTCGAGCTCAAGCTTTTTTTTTTTTTTTTT	cDNA of <i>A. terreus</i>	5'-RACE
54	QO_RACE	CCAGTGAGCAGAGTGACG	cDNA of <i>A. terreus</i>	5'-RACE
55	QI_RACE	GAGGACTCGAGCTCAAGC	cDNA of <i>A. terreus</i>	5'-RACE
56	NotI_AnPgpda_for	GCGGCCgctcaccacaaaagtccagacg	hph-Plasmid	mutation of hph resistance gene for SM-Xpress 2
57	hph_mut fw	gcatccatagcctccgcgacc	hph-Plasmid	mutation of hph resistance gene for SM-Xpress 3
58	hph_mut rv	GGAGGCTATGGATGCGATCG	hph-Plasmid	mutation of hph resistance gene for SM-Xpress 4
59	Nothph_up	GCG GCC GCC AGT GTG ATG G	hph-Plasmid	mutation of hph resistance gene for SM-Xpress 5
60	EcoRI_PterA_for	gacggccagtgaattcgatcctctctctgatattgctg	SM-Xpress-Plasmid	construction of Tag_SM-Xpress
61	PterA_tag_rv	ATG GTG ATG ATG ATG CAT GGT GCT GTG ATG AGA AGT TTG	SM-Xpress-Plasmid	construction of Tag_SM-Xpress
62	Tag_trpCT_fw	CAT CAT CAT CAC CAT CAC CA TGGA TAA cagcagtgattcaatctgaac	SM-Xpress-Plasmid	construction of Tag_SM-Xpress
63	EcoRI_TrpCT_rv	TAC CGA GCT CGA ATT CGA GTG AGG GTT GAG TAC GAG	SM-Xpress-Plasmid	construction of Tag_SM-Xpress
64	KpnI_fwnAup_for	gtgaattcagagctc ggtaccgatagtgccgaatgctcaagg	gDNA <i>A. niger</i>	overexpression of <i>melA</i> in <i>A. niger</i> P2
65	fwnAup_rev	GTA CCC GTT TTT GTG TTC GAT TC	gDNA <i>A. niger</i>	overexpression of <i>melA</i> in <i>A. niger</i> P2
66	fwnAup_PterA_for	cacaaaaacgggtacgatcctctctctgatattgctg	SM-Xpress-Plasmid	overexpression of <i>melA</i> in <i>A. niger</i> P2
67	melA_PterA_rev	AAG GCT TGG TTG CAT GGT GCT GTG ATG AGA AGT TTG	SM-Xpress-Plasmid	overexpression of <i>melA</i> in <i>A. niger</i> P2
68	AtmelA_for	ATGCAACCAAGCCTTATTCCTC	gDNA of <i>A. terreus</i>	overexpression of <i>melA</i> in <i>A. niger</i> P2
69	AtmelA_rev	GCG GCC GCC TCG AGA GTT TGA GAA TAT CC	gDNA of <i>A. terreus</i>	overexpression of <i>melA</i> in <i>A. niger</i> P2
70	melA_fwnA_dn_for	tctcgaggcggcggcgaagatctctggaagtcgctc	gDNA of <i>A. niger</i>	overexpression of <i>melA</i> in <i>A. niger</i> P2
71	fwnA_dn_rev	CTA GAG GAT CCC CGG GTA CCC GTG TGA CTG ATG ATA ATT CTC C	gDNA of <i>A. niger</i>	overexpression of <i>melA</i> in <i>A. niger</i> P2
72	PterA_His_MelA_fw	catcacagcaccatgcatcaccatcaccatcaccaaccaagccttattccctc	cDNA of <i>A. terreus</i>	overexpression of <i>his_melA</i> in <i>A. niger</i> P2
73	tyrP++_CTerm_fw	tcacagcaccatgcatggtttctacaggaatctagtcg	cDNA of <i>A. terreus</i>	overexpression of <i>tyrP</i> in <i>A. niger</i> P2 and <i>melA</i> ^{OE}
74	tyrP_SM-X_chis_rv	GAT GGT GAT GAT GCA TGG TAT ATG TAT AAC AAT AAG GAC C	cDNA of <i>A. terreus</i>	overexpression of <i>tyrP</i> in <i>A. niger</i> P2 and <i>melA</i> ^{OE}
75	SM_X_tyrP++ fw	catcacagcaccatggtttctacaggaatctagtcg	cDNA of <i>A. terreus</i>	<i>tyrP:tdTomato</i> fusion construct
76	IF_tyrP_Linkerv	GTCGCGGGCGCGGGGGACGGTGGACTGGGTATATGTATAACAATAAGGAC	cDNA of <i>A. terreus</i>	<i>tyrP:tdTomato</i> fusion construct
77	IF_Linkerv_tdTom fw	ccccgcgcccgcgacccccgcgaccatggtctccaagggtgagg		<i>tyrP:tdTomato</i> fusion construct
78	SM_X_tdTom_rv	ATCACTGCTGCCATGCTACTTGTAGAGCTCGTCCATAC		<i>tyrP:tdTomato</i> fusion construct
79	IF_pET_tyrP++	tcacatagcggatccatggtttctacaggaatctagtcg	cDNA of <i>A. terreus</i>	full length <i>tyrP</i> in <i>E. coli</i>
80	IF_tyrP+_pET	tcacatagcggatccctctgcccagctccgagatg	cDNA of <i>A. terreus</i>	<i>tyrP</i> without signal peptide sequence for <i>E. coli</i>
81	IF_pET_tyrP_rv	gtgcgccgcaagcTTA GGT ATA TGT ATA ACA ATA AGG	cDNA of <i>A. terreus</i>	<i>tyrP</i> expression in <i>E. coli</i>
82	melA_seq1_fw	cctcccgaacaatcgtcc	gDNA, cDNA of <i>A. terreus</i>	sequencing primer for <i>melA</i>
83	melA_seq2_fw	ggacggatggttaagactgg	gDNA, cDNA of <i>A. terreus</i>	sequencing primer for <i>melA</i>
84	melA_rv	TTA CAT GCC CCT CTC AGC AAG	gDNA, cDNA of <i>A. terreus</i>	sequencing primer for <i>melA</i>
85	pJET1.2_for	CGA CTC ACT ATA GGG AGA GCG GC	pJET plasmids containing different sequences	sequencing primer for pJET
86	pJET1.2_rev	AAG AAC ATC GAT TTT CCA TGG CAG	pJET plasmids containing different sequences	sequencing primer for pJET
87	At_03569_for	CCGTTGTGACGTTCAATGCC	gDNA, cDNA of <i>A. terreus</i>	semiquantitative RT-PCR
88	At_03569_rev	CCATATATTCCAGTCCAGG	gDNA, cDNA of <i>A. terreus</i>	semiquantitative RT-PCR
89	At_03570_for	GGAACGGACCTTATTATCCG	gDNA, cDNA of <i>A. terreus</i>	semiquantitative RT-PCR
90	At_03570_rev	CCTCTACCTATCACCTCTTCC	gDNA, cDNA of <i>A. terreus</i>	semiquantitative RT-PCR
91	melA_trypcT_rv	ATC ACT GCT GCC ATG GTT ACA TGC CCC TCT CAG CAA G	cDNA of <i>A. terreus</i>	overexpression of <i>his_melA</i> in <i>A. niger</i> P2

Comment on: "Melanisation of *Aspergillus terreus*-
Is Butyrolactone I Involved in the Regulation of Both
DOPA and DHN Types of Pigments in Submerged Culture?
Microorganisms 2017, 5, 22".

Elena Geib and Matthias Brock (2017).

(2017) Microorganisms; 5, 34

Summary of the manuscript: In response to a recently published manuscript, it needed to be clarified that Asp-melanin biosynthesis in *Aspergillus terreus* is not related to DOPA-melanin formation, but forms a distinct type of melanin. Inhibitor studies clearly showed that *A. terreus* neither responds to inhibitors for DHN- nor DOPA-melanin biosynthesis. Previously published manuscripts that were used for speculations in the commented manuscript relied on data that lacked solvent controls. In this comment article, the effect of the solvents on conidia pigmentation are presented that show that inhibitor studies for the identification of melanin biosynthesis pathways need to be interpreted with care.

Contribution: 100% of practical work, significant contribution to manuscript preparation
Performance of inhibitor and solvent control studies on several *Aspergillus* species.



Comment

Comment on: “Melanisation of *Aspergillus terreus*—Is Butyrolactone I Involved in the Regulation of Both DOPA and DHN Types of Pigments in Submerged Culture? *Microorganisms* 2017, 5, 22”

Elena Geib and Matthias Brock *

Fungal Genetics and Biology, School of Life Sciences, University of Nottingham, University Park, NG72RD Nottingham, UK

* Correspondence: Matthias.brock@nottingham.ac.uk; Tel.: +44 (0)115 951 3230

Received: 23 May 2017; Accepted: 19 June 2017; Published: 21 June 2017

Abstract: A recent article by Palonen et al. describes the effect of butyrolactone I on the expression of a secondary metabolite biosynthesis gene cluster from *Aspergillus terreus* that shows similarities to fusarubin biosynthesis gene clusters from *Fusarium* species. The authors claim that two different types of pigments are formed in *Aspergillus terreus* conidia, whereby one pigment is termed a DOPA-type melanin and the second a DHN-type melanin. Unfortunately, the terminology of the classification of melanin-types requires revision as Asp-melanin present in *A. terreus* conidia is clearly distinct from DOPA-melanins. In addition, some hypotheses in this manuscript are based on questionable data published previously, resulting in incorrect conclusions. Finally, as biochemical data are lacking and metabolite production is only deduced from bioinformatics and transcriptomic data, the production of a second pigment type in *A. terreus* conidia appears highly speculative.

Palonen et al. studied the expression of a newly identified *pgm* gene cluster from *Aspergillus terreus* during growth in submerged culture conditions and in the presence or absence of the quorum sensing metabolite butyrolactone I [1]. Transcriptional analyses revealed that in the presence of butyrolactone I the expression of *pgm* cluster genes increase with cultivation time. Simultaneously, expression of the two genes, *melA* and *tyrP*, responsible for Asp-melanin biosynthesis in *A. terreus* conidia [2] decrease in the presence of butyrolactone I. Since butyrolactone I increases sporulation of *A. terreus* in submerged cultures [3] and the *pgm* gene cluster shows similarity to perithecium pigment biosynthesis gene clusters from *Fusarium* species [1], the authors conclude that besides the well-characterised Asp-melanin, a dihydroxynaphtalene-type melanin (DHN-melanin) might be produced in *A. terreus* conidia. This speculation additionally is based on a manuscript by Pal et al. [4], in which inhibitor studies indicated that *Aspergillus* species simultaneously produce a DHN-melanin and an L-DOPA-melanin as conidia pigments. Unfortunately, the study by Pal et al. [4] lacked an investigation of solvent controls on conidia pigment formation, which would have revealed that inhibitor studies need to be interpreted with care. Kojic acid, an inhibitor of the L-DOPA-melanin pathway, was solved in 70% DMSO and applied to growth media. Analysis of conidia melanisation revealed that most *Aspergillus* species lost colouration in the presence of kojic acid, which led to the conclusion that an L-DOPA-melanin pathway may be involved in pigmentation of conidia [4]. As can be seen in Figure 1 of this letter, DMSO rather than kojic acid is responsible for this loss in pigmentation with the highest effect on *Aspergillus fumigatus*, followed by *Aspergillus nidulans* and *Aspergillus niger*. No effect was observed on *A. terreus*. Similarly, the laccase inhibitor pyrrolidone, which inhibits polymerisation of DHN-melanin precursors, showed a strong effect on *A. fumigatus*, followed by *A. nidulans* and *A. niger*. Again, no effect is observed on *A. terreus*. This indicates that the inhibitory effect caused by kojic acid may eventually be caused by the solvent and does not confirm

an L-DOPA-melanin pathway in *Aspergillus* species. Furthermore, these experiments confirm that *A. terreus* shows no sensitivity against either type of melanin biosynthesis inhibitors, which is in agreement with the novel type of Asp-melanin produced by this fungus.

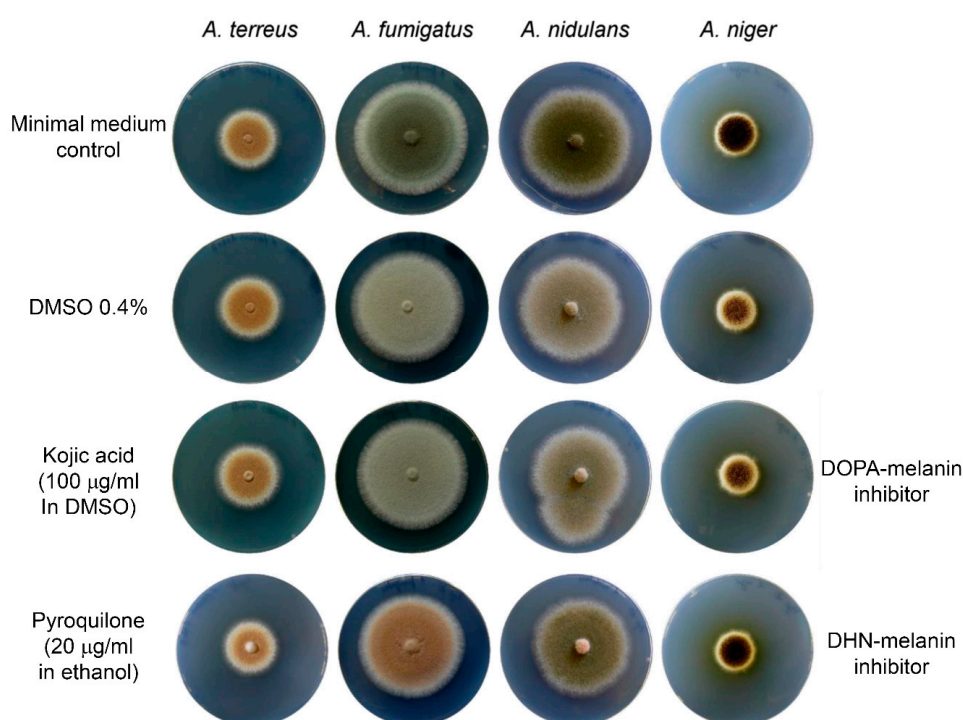


Figure 1. Effect of DMSO, kojic acid and pyroquilonone on conidia pigmentation of different *Aspergillus* species. The following strains were used: *A. terreus* SBUG844 (Jena Microbial Resource Collection, HKI Jena, Germany), *A. fumigatus* CBS144.89 (CBS-KNAW Collection, Utrecht, Netherlands), *A. nidulans* FGSC A4 and *A. niger* FGSC A1144 (FGSC = Fungal Genetics Stock Center, Kansas, USA). All strains were grown in glucose containing minimal media. DMSO strongly affects conidia pigmentation of all *Aspergillus* species except *A. terreus*, which makes the assessment of the effect of kojic acid on conidia pigmentation (solved in DMSO) difficult. The DHN-melanin inhibitor pyroquilonone (solved in ethanol) inhibits pigment polymerisation of *A. fumigatus*, and, at the applied concentration, shows weak effects on *A. nidulans* and *A. niger*, but not *A. terreus*. Growth in the presence of 0.5% ethanol does not affect conidia pigmentation of any strain (not shown).

However, Palonen et al. [1] denote the formation of Asp-melanin in *A. terreus* as a type of DOPA-melanin. The authors base this on the fact that a tyrosinase is involved in its biosynthesis. Unfortunately, we cannot agree with this definition. L-DOPA (L-dihydroxyphenylalanine) is not a precursor of Asp-melanin. 4-Hydroxyphenylpyruvate is the substrate for the NRPS-like enzyme MelA that forms the precursor aspulvinone E [2,5]. The subsequent hydroxylation of aspulvinone E by the tyrosinase TyrP leads to auto-polymerisation of aspulvinone E units [2]. Reaction intermediates have been analysed and no L-DOPA has been detected at any step as precursor molecule [2]. Furthermore, the tyrosinase TyrP does not use L-DOPA as substrate. Therefore, defining Asp-melanin as an L-DOPA-type melanin is not correct, as Asp-melanin is a novel type of melanin pigment not related to either L-DOPA- or DHN-melanin.

As deletion of *melA* results in white conidia [2,5] and in vitro studies with purified MelA and TyrP proteins have reconstituted the Asp-melanin biosynthesis pathway, it can be excluded that an additional DHN-melanin is produced in *A. terreus* conidia, at least, when grown on solid media or as biofilm surface cultures in liquid media. Palonen et al. [1] used a submerged culture condition throughout their studies in which they supplemented the medium artificially with butyrolactone I.

Under these conditions, an increased expression of the *pgm* gene cluster accompanied by a decreasing expression of the Asp-melanin gene cluster was observed. As *pgm* cluster expression further increased at the late stage of fermentation and, furthermore, the culture turned into an increasingly brown colour after nine days of incubation, the authors speculated that a DHN-melanin type pigment deriving from the *pgm* gene cluster might be formed under these cultivation conditions.

However, this speculation has several problems: (i) No analysis of the type or number of spores has been presented. *A. terreus* not only produces conidia from conidiophores, but also accessory conidia, which are generally hyaline. Which types of spores and in which numbers have been produced under these conditions? What colour do they show? By which experiments did the authors exclude that the brownish pigment does not derive from Asp-melanin? Is the brownish colour also observed in a *mela*⁻ mutant? (ii) No data on secondary metabolite profiles have been presented. On which basis other than bioinformatics do the authors base their assumption of a DHN-melanin formed by *A. terreus* under these culture conditions? The authors may be aware that most fungal polyketide synthases (PKS) are iterative and, currently, it appears impossible to predict the number of malonyl-CoA extender units used by such an enzyme. The similarity of a fungal PKS to other PKSs may provide a hint towards its product, but without experimental data it remains purely speculative as to which kind of product is formed.

Interestingly, the authors do not seem to consider that the gene cluster identified in this study may be involved in production of an ascospore pigment. Although butyrolactones are naturally produced by *A. terreus* [3], the conditions with external supplementation of media with butyrolactone I appear rather artificial and may not resemble the natural induction conditions of the *pgm* gene cluster. However, as a quorum sensing molecule butyrolactones cannot be excluded to play a role in sexual reproduction of *A. terreus*. As the *pgm* gene cluster identified here shows highest similarity to gene clusters producing pigments in fungal perithecia—which are sexual reproduction structures of ascomycetes—it is difficult to understand why the authors did not follow this hypothesis further.

In conclusion, while the manuscript by Palonen et al. [1] shows solid transcriptional analyses on the *pgm* gene cluster from *A. terreus*, all hypotheses on the nature of the resulting metabolite are purely speculative and should be taken as such. Furthermore, the definition of Asp-melanin as an L-DOPA type melanin needs revision.

Conflicts of Interest: The authors declare no conflict of interest.

References

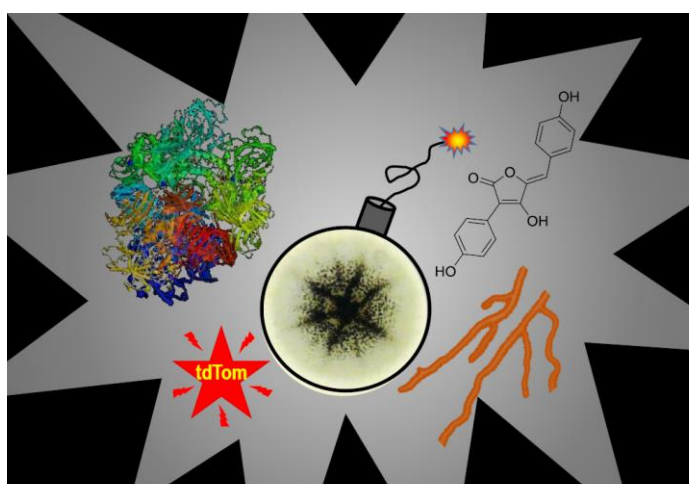
1. Palonen, E.K.; Raina, S.; Brandt, A.; Meriluoto, J.; Keshavarz, T.; Soini, J.T. Melanisation of *Aspergillus terreus*-is butyrolactone I involved in the regulation of both DOPA and DHN types of pigments in submerged culture? *Microorganisms* **2017**, *5*, 22. [CrossRef] [PubMed]
2. Geib, E.; Gressler, M.; Viediernikova, I.; Hillmann, F.; Jacobsen, I.D.; Nietzsche, S.; Hertweck, C.; Brock, M. A non-canonical melanin biosynthesis pathway protects *Aspergillus terreus* conidia from environmental stress. *Cell Chem. Boil.* **2016**, *23*, 587–597. [CrossRef] [PubMed]
3. Schimmel, T.G.; Coffman, A.D.; Parsons, S.J. Effect of butyrolactone I on the producing fungus, *Aspergillus terreus*. *Appl. Environ. Microbiol.* **1998**, *64*, 3707–3712. [PubMed]
4. Pal, A.K.; Gajjar, D.U.; Vasavada, A.R. DOPA and DHN pathway orchestrate melanin synthesis in *Aspergillus* species. *Med. Mycol.* **2014**, *52*, 10–18. [PubMed]
5. Guo, C.J.; Knox, B.P.; Sanchez, J.F.; Chiang, Y.M.; Bruno, K.S.; Wang, C.C. Application of an efficient gene targeting system linking secondary metabolites to their biosynthetic genes in *Aspergillus terreus*. *Organ. Lett.* **2013**, *15*, 3562–3565. [CrossRef] [PubMed]



ATNT: an enhanced system for expression of polycistronic secondary metabolite gene clusters in *Aspergillus niger*

Elena Geib and Matthias Brock

(2017) Fungal Biology and Biotechnology; 4, 13



Summary of the manuscript:

Fungal secondary metabolites are frequently produced from secondary metabolite biosynthesis gene clusters. Their investigation is tedious since lots of individual cloning steps are required for heterologous production of these metabolites. By use of a self-splicing peptide, genes can be combined in transcriptional units.

During translation the proteins get separated and work as individual enzymes. In this manuscript the self-splicing peptide P2A from porcine teschovirus-1 is used to combine genes from Asp-melanin biosynthesis in a transcriptional unit. Analyses reveal that functional enzymes are produced and transported into the correct subcellular compartments. For tight regulation of gene expression, the heterologous expression system was additionally modified by controlling gene expression from the doxycycline dependent TetOn system. This will be of high importance when producing metabolites with antifungal properties.

Contribution: 80% contribution of practical work, major contribution to manuscript preparation.

Generation and validation of the TetOn expression system. Comparison of direct gene expression from TetOn *versus* control from the coupled system in which TetOn controls the expression of the transcriptional activator TerR, which, in turn, controls expression of genes from the *terA* promoter. Cloning of Asp-melanin biosynthesis genes in combination with the fluorescent reporter tdTomato in transcriptional units. Characterisation of product formation, analysis of gene expression, splicing efficiency and subcellular localisation of enzymes.

RESEARCH

Open Access



ATNT: an enhanced system for expression of polycistronic secondary metabolite gene clusters in *Aspergillus niger*

Elena Geib and Matthias Brock^{*}

Abstract

Background: Fungi are treasure chests for yet unexplored natural products. However, exploitation of their real potential remains difficult as a significant proportion of biosynthetic gene clusters appears silent under standard laboratory conditions. Therefore, elucidation of novel products requires gene activation or heterologous expression. For heterologous gene expression, we previously developed an expression platform in *Aspergillus niger* that is based on the transcriptional regulator TerR and its target promoter *PterA*.

Results: In this study, we extended this system by regulating expression of *terR* by the doxycycline inducible Tet-on system. Reporter genes cloned under the control of the target promoter *PterA* remained silent in the absence of doxycycline, but were strongly expressed when doxycycline was added. Reporter quantification revealed that the coupled system results in about five times higher expression rates compared to gene expression under direct control of the Tet-on system. As production of secondary metabolites generally requires the expression of several biosynthetic genes, the suitability of the self-cleaving viral peptide sequence P2A was tested in this optimised expression system. P2A allowed polycistronic expression of genes required for Asp-melanin formation in combination with the gene coding for the red fluorescent protein tdTomato. Gene expression and Asp-melanin formation was prevented in the absence of doxycycline and strongly induced by addition of doxycycline. Fluorescence studies confirmed the correct subcellular localisation of the respective enzymes.

Conclusion: This tightly regulated but strongly inducible expression system enables high level production of secondary metabolites most likely even those with toxic potential. Furthermore, this system is compatible with polycistronic gene expression and, thus, suitable for the discovery of novel natural products.

Keywords: Asp-melanin, P2A, Polycistronic mRNA, Tet-on system, Doxycycline, Terrein biosynthetic gene cluster

Background

Genome mining has revealed that fungal genomes contain a large number of yet unexplored secondary metabolite biosynthetic gene clusters [1]. Due to next generation sequencing approaches the number of available fungal genomes is steadily increasing as can be seen from the growing number of genomes in the 1000 fungal genomes project [2]. Interestingly, even highly related fungal species contain at least a few unique secondary metabolite

biosynthetic gene clusters [3] and it has frequently been observed that more than one metabolite is produced from a single biosynthetic gene cluster [4]. Therefore, the potential of producing metabolites with interesting pharmaceutical characteristics appears nearly unlimited. However, as secondary metabolites are frequently produced in response to distinct biotic or abiotic stress factors [5], a large number of the respective biosynthetic gene clusters remains silent under laboratory conditions and, thus, their products unexplored. To exploit the full potential of fungal secondary metabolite production different strategies have been applied [6, 7].

*Correspondence: Matthias.brock@nottingham.ac.uk
Fungal Genetics and Biology, School of Life Sciences, University of Nottingham, University Park, Nottingham NG7 2RD, UK

One approach that can be directly applied to cultivable fungal species is the addition of epigenetic modifiers [8] or co-cultivation with other microbes, which may result in the specific induction of biosynthetic gene clusters [9]. However, while this strategy may lead to the production of novel metabolites, a direct correlation between biosynthetic gene cluster and metabolite product remains difficult. Another strategy is the overexpression of a transcriptional regulator controlling a specific biosynthetic gene cluster [10]. Unfortunately, not all secondary metabolite biosynthetic gene clusters contain a transcriptional activator in direct proximity to their biosynthetic genes [11], which may hamper this approach. In addition, global transcriptional regulators may overrule the activation from a cluster specific transcription factor as shown for the dihydroisoflavipucine biosynthesis in *Aspergillus terreus* [12]. While this biosynthetic gene cluster contains a specific transcriptional activator that is indispensable for its activation, the activating effect is overruled in the presence of glucose through the carbon catabolite repressor CreA [12].

The strategy of targeted activation of cluster specific transcription factors additionally requires the ability for genetic modification of the natural producer strain and may not be suitable for many fungal species. Therefore, recent approaches used the generation of fungal artificial chromosomes (FAC) to clone and transfer whole fungal gene clusters into genetically amenable fungal expression platform strains [13]. In a previous study, 56 gene cluster containing FACs with yet uncharacterised biosynthetic genes from *Aspergillus wentii*, *Aspergillus aculeatus* and *A. terreus* were transferred to *Aspergillus nidulans*, which resulted in the identification of 17 novel metabolites from 15 different FACs [13]. However, not all gene clusters were successfully activated in the recombinant host, which may be due to the lack of transcriptional activators, repressing conditions or the lack of the correct starter metabolites in the heterologous host.

It has also been shown that induction of secondary metabolite biosynthetic gene clusters in a heterologous host can be achieved by regulating the expression of the global regulator of secondary metabolism LaeA in *Aspergillus* species [14]. In this respect, a transfer of the biosynthetic gene clusters for monacolin K from *Monascus pilosus* and terrequinone A from *A. nidulans* resulted in successful product formation after overexpression of *leaA* in *Aspergillus oryzae* [15]. However, induction of several biosynthetic gene clusters appears independent from LaeA control and a specific transcriptional activator in direct proximity to the biosynthetic gene cluster may be lacking. Therefore, a different strategy for gene activation was successfully applied to *A. nidulans*, in which a serial promoter exchange of each individual gene of a

biosynthetic gene cluster was performed. This strategy resulted in the identification of the proteasome inhibitor fellutamide B and its resistance conferring gene *inpE* [16]. Although successful, this strategy required several rounds of metabolite screening, marker regeneration and subsequent transformation and appears prohibitively time consuming for routine applications.

Due to these challenges it remains difficult to recommend an expression system that allows for high throughput screening for all yet uncharacterised secondary metabolite biosynthetic gene clusters. Heterologous gene expression generally aims for high product yields to elucidate the structure of the metabolite and to analyse its biological activity. A prerequisite for this is the high level expression of target genes, which can be achieved by generating multiple copy integrations, selection of strong promoters or a combination of both [17, 18]. Recently, we introduced a heterologous expression system that uses an *Aspergillus niger* strain as expression platform that contains regulatory elements from *A. terreus* [18]. These regulatory elements consist of the terrein biosynthetic gene cluster specific transcriptional activator TerR and its target promoter *PterA*. When expression of *terR* is controlled by the *A. oryzae* amylase promoter and a reporter gene is expressed under *PterA* control the induction level of the amylase promoter gets amplified through this coupled system [18]. In addition, a SM-Xpress vector has been constructed that allows easy generation of expression plasmids by in vitro recombination with the target gene. This expression system had been successfully applied for the identification of lecanoric acid as product from the *A. nidulans* *orsA* gene [18], has enabled the heterologous in vivo reconstruction of the *A. terreus* Asp-melanin biosynthetic pathway in *A. niger* [19] and was recently successfully used for identification of basidiocin, which is a novel siderophore produced from a non-ribosomal peptide synthetase (NRPS) that is widely distributed among basidiomycetes [20].

Another challenge in heterologous expression of secondary metabolite biosynthetic gene clusters derives from possible toxicity of resulting metabolites. Therefore, a tight regulation of gene expression is favoured as it allows for the formation of fungal biomass prior to induction of the expression of target genes. In this respect a tuneable Tet-on/Tet-off expression system has been adapted for use in *Aspergillus* species [21, 22]. The Tet-on system uses a reverse tetracycline-controlled transactivator that enables titratable induction of gene expression by the addition of the tetracycline derivative doxycycline. In the absence of doxycycline gene expression remains at low background levels, but expression gets strongly induced by addition of doxycycline [21, 22].

As most secondary metabolites are produced from biosynthetic gene clusters, production of the final metabolite generally requires the heterologous expression of more than only one single gene. While a strategy of subsequent transformations with isolated genes accompanied by a marker recycling technique works for clusters comprising only a small number of genes, this procedure is extremely time consuming and probably not suitable for larger clusters containing five or more genes. Therefore, another strategy is the use of self-splicing viral peptide sequences such as the 2A peptide that separates proteins from a polycistronic messenger in different viruses such as the porcine teschovirus-1 (P2A). P2A and similar sequences have been successfully used to separate individual proteins in a range of different eukaryotic organisms [23, 24] among them yeasts such as *Saccharomyces cerevisiae* [25, 26] and *Pichia pastoris* [27]. A recent study also used a 2A peptide in *Trichoderma reesei*, in which the gene coding for the cellobiohydrolase Cel7A from *Penicillium funiculosum* was combined in a single transcript with the eGFP coding gene to ease screening of cellobiohydrolase positive transformants [28]. Importantly, this technique has also been applied for heterologous production of penicillin in the filamentous fungus *A. nidulans* by genetic engineering of a synthetic *Penicillium chrysogenum* penicillin biosynthetic gene cluster [29]. Despite low yields, penicillin K was successfully produced by *A. nidulans* transformants expressing the polycistronic penicillin biosynthetic gene cluster [29], indicating that this strategy is suitable for use in fungal secondary metabolite biosynthesis. The suitability of P2A was further confirmed in a recent study on enniatin biosynthesis in *A. niger*, in which two genes required for enniatin biosynthesis and a luciferase were separated by P2A sequences [30]. While a positioning effect in dependence of the gene order in the polycistronic messenger was observed, all strains produced enniatin and displayed light emission from luciferase activity. Positioning effects were also observed in the cellobiohydrolase expression in *T. reesei* [28] and murine cells [31], indicating that despite polycistronic gene expression the amount of individual proteins may vary depending on the gene order in the expression construct.

Here, we aimed to generate an optimised fungal heterologous expression system by combining the three latter aspects of heterologous secondary metabolite production in *A. niger*: (1) using the expression amplification system of TerR/*PterA* under (2) fine-tuneable control of the Tet-on system for expression of (3) polycistronic mRNA of the Asp-melanin biosynthetic genes combined with a fluorescent reporter to study correct subcellular localisation of enzymes.

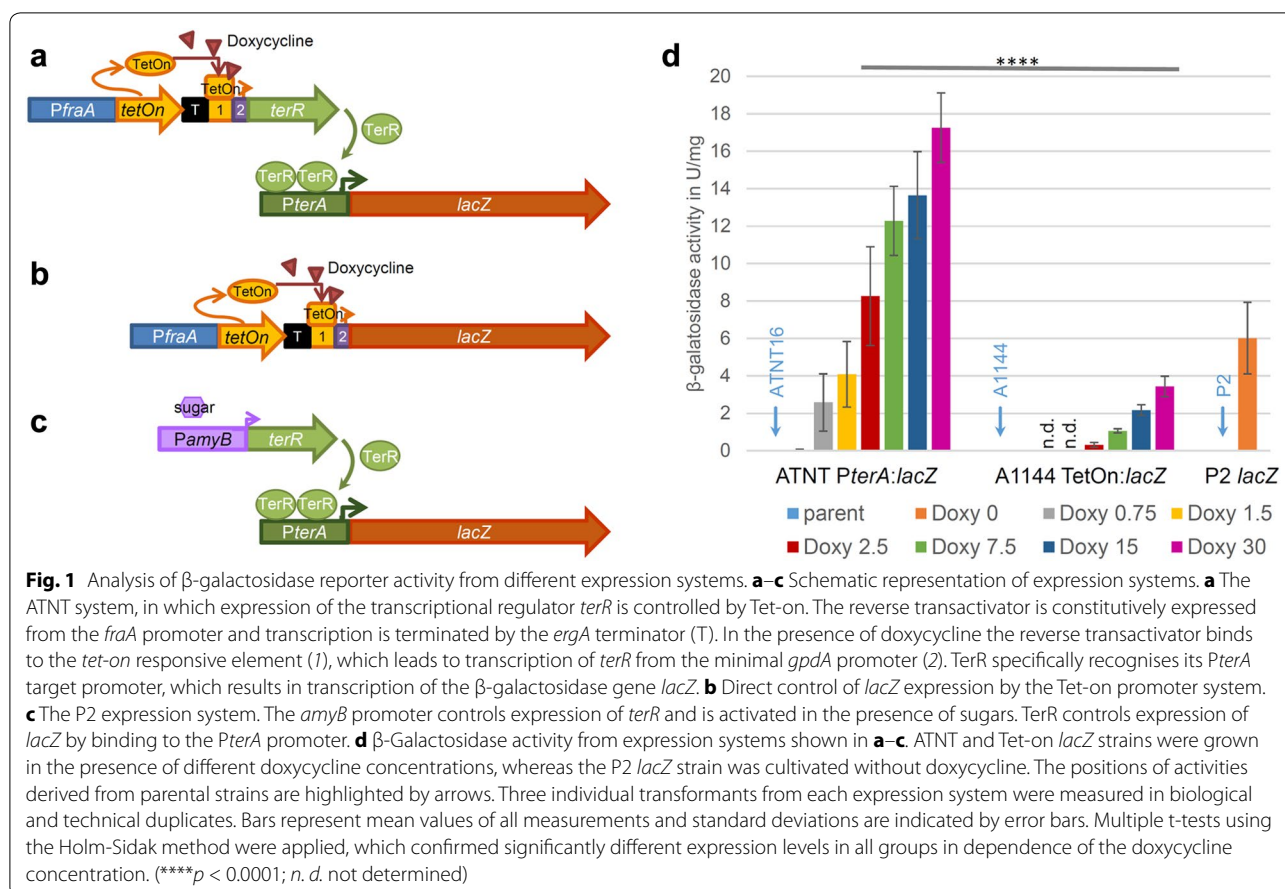
Results

Integration of Tet-on control into the coupled TerR/*PterA* expression system

We previously developed a heterologous expression system in *A. niger* that bases on the transcriptional activator TerR from the *A. terreus* terrein biosynthetic pathway and its *terA* (*PterA*) target promoter [18]. In this combination the induction level of *PterA* directly depends on the transcriptional level of the *terR* gene [18]. Furthermore, the activity of the promoter controlling *terR* expression gets amplified at the target promoter *PterA* as reporter expression in the coupled system was significantly higher than direct expression of reporter genes [18]. In this first version of the expression system, we controlled *terR* expression by either the glyceraldehyde-3-phosphate dehydrogenase promoter *PgpdA* or the amylase promoter *PamyB*. As both of these promoters derive from primary metabolism, their use may interfere with fungal metabolic physiology. In addition, both promoters are difficult to silence and *PamyB* shows significant background activity even when *A. niger* is grown on casamino acids in the absence of any sugars. As this background promoter activity may hamper the production of toxic metabolites, we replaced *PamyB* in the control of *terR* by the reverse tetracycline-controlled transactivator (Fig. 1a) containing the *fraA* promoter sequence for improved cassette stability. The *fraA* gene encodes a putative ribosomal subunit and had been identified from microarray analyses showing a similar expression pattern as the glyceraldehyde-3-phosphate dehydrogenase and is assumed to be constitutively expressed [22]. The Tet-on:*terR* construct was used for transformation of the *A. niger* A1144 strain (Fungal Genetics Stock Center, Kansas, USA) and resulting transformants were analysed for full length single copy integration into the genome (Additional file 1). The resulting expression platform strain ATNT16 (ATNT = **A**1144 **T**et-on:**t**erR) was analysed for its performance in gene expression.

Analysis of β -galactosidase reporter gene expression

To elucidate the performance of the new Tet-on-controlled expression system in *A. niger* ATNT16, we generated β -galactosidase reporter strains. Two different constructs were made that both contained the *lacZ* gene from *Escherichia coli* as reporter. The first construct contained a fusion of *PterA* with the *lacZ* gene (*PterA:lacZ*) for transformation of the ATNT16 strain (Fig. 1a). The second construct contained a fusion of the Tet-on promoter system directly with the *lacZ* gene (Tet-on:*lacZ*) for transformation of the parental *A. niger* strain A1144 (Fig. 1b). This enabled the comparison of doxycycline dependent gene activation in the coupled amplification system of TerR/*PterA* under control of Tet-on against



the direct reporter gene induction by the Tet-on system. After transformation of the respective *A. niger* strains, transformants with a single copy integration of the respective reporter construct were identified by Southern blot analysis (Additional file 2) and three independent transformants from each construct were selected for downstream investigation of reporter activities. In addition, three reporter strains from the original *PamyB*:*terR* expression platform (P2 strain; *terR* gene under control of the amylase promoter) with single copy integration of the *lacZ* gene under control of *PterA* [18] were included (Fig. 1c). This allowed comparison of expression properties of the new ATNT16 expression platform with that of the previous platform strain P2. All strains were cultivated for 24 h on 100 mM glucose containing minimal media with 20 mM glutamine as nitrogen source and 1% talc to avoid the formation of cell pellets [32]. For the Tet-on-containing strains parallel cultures were supplemented with various amounts of doxycycline in a range between 0 and 30 μ g/ml. All strains were cultivated in two biological replicates and β -galactosidase activity was determined from cell-free extracts in technical duplicates (Fig. 1d). The average specific β -galactosidase activity of

the P2 reporter strain on this glucose containing medium was about 6 U/mg, which was in agreement with previous determinations under this growth condition [18]. Both, the ATNT16 reporter strains as well as the Tet-on:*lacZ* strains only revealed very low background activity when cultivated in the absence of doxycycline (< 0.05 U/mg). Addition of doxycycline to the Tet-on:*lacZ* strains resulted in a titratable induction of reporter activity, reaching a maximum of 3.4 U/mg at 30 μ g/ml of doxycycline. The ATNT16 strain with the *PterA*:*lacZ* reporter construct showed significant reporter activity of 2.5 U/mg already at 0.75 μ g/ml, which further increased to 17.3 U/mg at 30 μ g/ml of doxycycline. This latter activity is about five times higher than the maximum activity obtained from the uncoupled system at 30 μ g/ml in which Tet-on directly induces the expression of the target gene. Thus, the ATNT16 expression platform with the *terR* gene under Tet-on control is tightly regulated in the absence of doxycycline and strongly induced by its addition. However, accompanied with high reporter gene expression, biomass formation in the presence of 30 μ g/ml doxycycline in the ATNT16 reporter strains was significantly reduced. This may be due to the high reporter

protein production during initiation of germination and seems independent from high levels of activated transactivator protein as the ATNT16 strain without *lacZ* reporter construct showed no growth defects in the presence of 30 $\mu\text{g}/\text{ml}$ doxycycline and β -galactosidase background activity in the ATNT16 strain did not increase by the addition of different doxycycline concentrations (not shown).

Production of aspulvinone E in the ATNT16 expression platform

Our reporter gene analyses indicated that the Tet-on-controlled *TerR/PterA* system is tightly regulated and allows high level gene expression in the presence of doxycycline. To test whether this also transfers to secondary metabolite production, we used the *melA* gene, which encodes the aspulvinone E synthetase from *A. terreus* [19] under control of *PterA* and transferred this construct into the Tet-on:*terR* strain ATNT16. After selection for single copy integration (Additional file 3), strains were cultivated for 48 h in glucose minimal medium either in the absence or presence of 15 $\mu\text{g}/\text{ml}$ doxycycline. In accordance with a light yellow colour of aspulvinone E, the cultures grown in the presence of doxycycline turned yellow (Fig. 2a) and the main proportion of the coloured substance solved in the ethyl acetate phase during extraction of culture filtrates (Fig. 2b). In contrast, no obvious yellow colouration of the culture or the ethyl acetate phase was observed in the control cultures without doxycycline (Fig. 2a, b). To confirm that aspulvinone E was produced only under inducing conditions samples were analysed by HPLC using reversed phase chromatography on a C_{18} column. As shown in Fig. 2c the induced culture revealed a strong signal for aspulvinone E and a minor signal of its stereoisomer isoaspulvinone E [19]. By contrast, only extremely weak background signals were detected in the control culture. These results are in agreement with the β -galactosidase reporter studies and confirm that (1) metabolite production is suppressed in the absence of doxycycline and (2) high yields of metabolites can be achieved under inducing conditions even in strains only carrying a single copy integration of the gene of interest.

Model gene cluster expression from polycistronic mRNA using the P2A peptide

In the next step we aimed in the expression of multiple genes in the Tet-on-controlled *TerR/PterA* system by engineering polycistronic mRNAs. For a proof-of-concept, the Asp-melanin pathway combined with a fluorescent reporter was used [19]. Asp-melanin is the conidial pigment produced by *A. terreus* and is distinct from the dihydroxynaphthalene melanin found in conidia of other

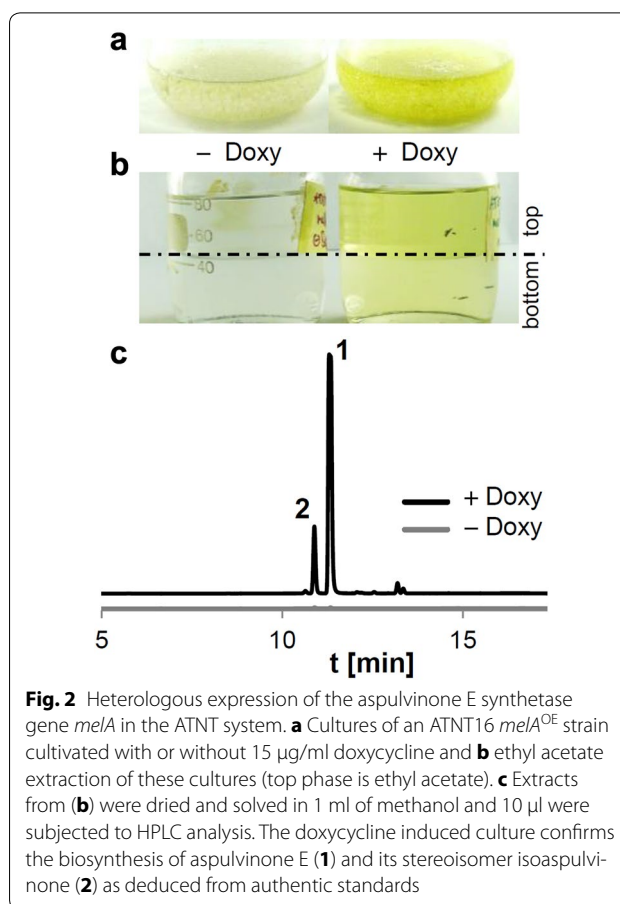


Fig. 2 Heterologous expression of the aspulvinone E synthetase gene *melA* in the ATNT system. **a** Cultures of an ATNT16 *melA*^{OE} strain cultivated with or without 15 $\mu\text{g}/\text{ml}$ doxycycline and **b** ethyl acetate extraction of these cultures (top phase is ethyl acetate). **c** Extracts from (**b**) were dried and solved in 1 ml of methanol and 10 μl were subjected to HPLC analysis. The doxycycline induced culture confirms the biosynthesis of aspulvinone E (**1**) and its stereoisomer isoaspulvinone (**2**) as deduced from authentic standards

Aspergillus species. This melanin pigment does not derive from a naphthopyrone precursor that is produced by a polyketide synthase rather than an aspulvinone E synthetase, which is a non-ribosomal peptide synthetase-like (NRPS-like) protein [19]. This pigment biosynthesis pathway appeared most suitable as: (1) Asp-melanin is produced from only two proteins, which are the aspulvinone E synthetase *MelA* and the tyrosinase *TyrP*; (2) co-expression of individually controlled genes in the *A. niger* P2 strain resulted in brown mycelium due to the formation of Asp-melanin, which is easy to visualise; (3) Asp-melanin formation requires the correct subcellular localisation of both enzymes as *MelA* requires the reducing environment of the cytoplasm and *TyrP* the oxidising environment of Golgi or ER (4) protein localisation and cleavage efficiency can be visualised by using the red fluorescent protein *tdTomato* as a reporter.

For the separation of individual proteins during ribosomal translation, the 22 amino acid 2A peptide (P2A, GSGATNFSLKQAGDVEENPGP) sequence from porcine teschovirus-1 was used [24], whereby codon sequences of individual P2A peptides were varied on DNA level to allow directed in vitro recombination into

the SM-Xpress expression vector that contains the *tera* promoter, the *trpC* terminator sequence and a resistance gene for selection of transformants [18]. Two different polycistronic constructs consisting of the *melA* gene, the *tyrP* gene and the gene coding for tdTomato were generated to test the efficiency of P2A cleavage and protein localisation in the ATNT16 expression platform (Fig. 3a). For the first construct all three genes were separated by a P2A coding sequence (P2A_P2A construct), which was assumed to result in three individual functional proteins under inducing conditions that lead to brown mycelium and a cytoplasmic localisation of tdTomato as this reporter does not contain a subcellular localisation signal. The second construct only contained a single P2A sequence (P2A construct) separating the *melA* and *tyrP* genes, whereby the gene coding for tdTomato was fused

in frame with the *tyrP* gene [19]. Here, we expected the formation of brown mycelium under inducing conditions, but a fluorescence localisation in subcellular organelles of ER and Golgi, which would confirm the correct targeting of TyrP. ATNT16 was transformed with the respective constructs and resulting transformants were analysed by Southern blot analysis (Additional file 4) for single copy integration. For analysis of selected transformants split plates were prepared with glucose minimal medium containing 0 or 10 µg/ml of doxycycline. On these plates the control strain ATNT16 as well as strains containing either the P2A or the P2A_P2A construct were spotted and pictures taken after 72 h of incubation. As shown in Fig. 3b, all strains showed similar growth and conidia formation in the top view of plates. However, the bottom view shows that mycelium of strains

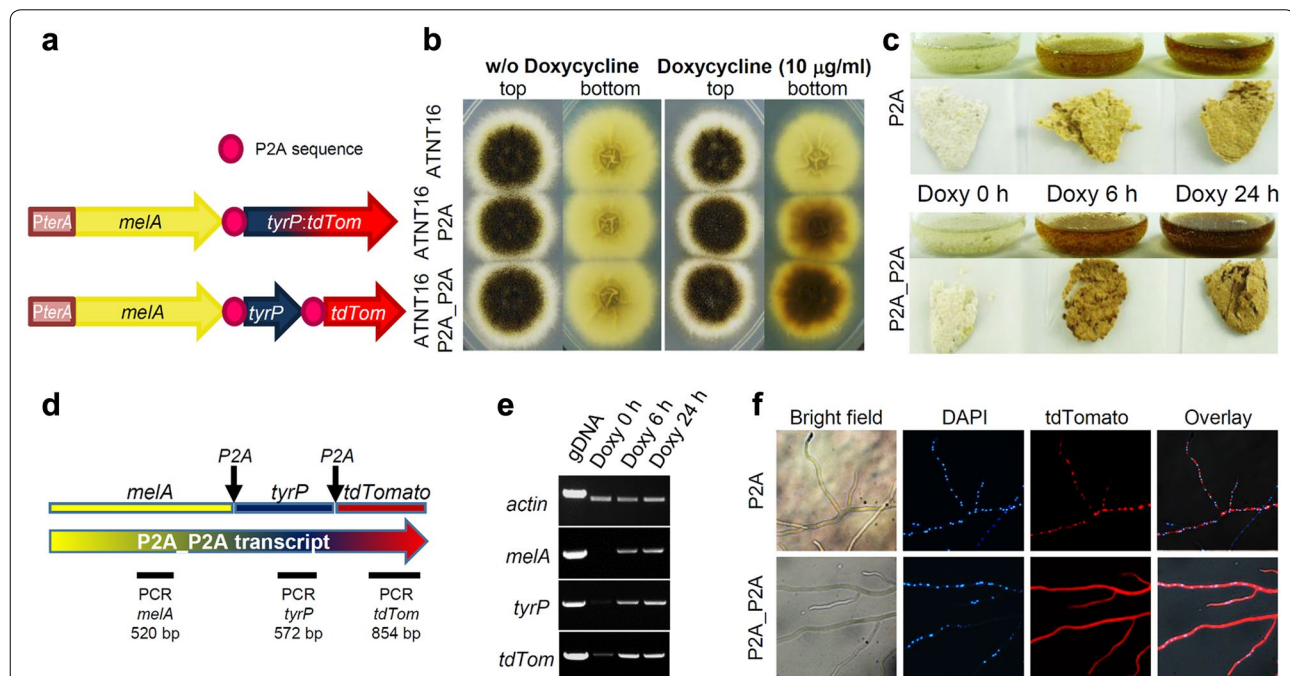


Fig. 3 Asp-melanin formation and subcellular protein localisation from polycistronic gene expression in the ATNT system. **a** Schematic presentation of polycistronic expression constructs separated by P2A sequences. *tyrP:tdTom* denotes an in frame fusion of the *tyrP* gene with the gene coding for the red fluorescent protein tdTomato. **b** Colonies in top and bottom view of the parental strain ATNT16 and strains carrying the expression construct with one or two P2A separations grown in the absence and presence of doxycycline. Addition of doxycycline induces the formation of Asp-melanin, which is indicated by brown colouration of mycelium in the bottom view. **c** Liquid cultures of ATNT16 strains carrying the expression construct with one or two P2A sequences. Mycelium was harvested after 24 h of incubation. Cultures were grown without doxycycline (Doxy 0 h) or were induced with doxycycline for the last 6 h of total incubation time (Doxy 6 h) or for the whole 24 h (Doxy 24 h). A stronger colouration of mycelium is observed when TyrP and tdTomato are separated by an additional P2A peptide. **d** Scheme of the polycistronic P2A_P2A mRNA. Localisation of the individual gene sequences are indicated above and localisation and size of PCR products for verification of transcription are shown below the transcript. **e** Semiquantitative RT-PCR on cDNA derived from cultures in **c**. The actin gene was used for normalisation of cDNA. Amplification from genomic DNA (gDNA) is shown as a control with a decrease in fragment size of the actin gene due to intron splicing. Full length-transcription of the polycistronic messenger is confirmed by PCR products from all genes when grown in the presence of doxycycline. **f** Fluorescence analysis for subcellular localisation of proteins produced from the two polycistronic expression constructs. Nuclei are shown in blue by DAPI staining. Red fluorescence indicates localisation of tdTomato. In the P2A construct the fusion of TyrP with tdTomato reflects a punctuated fluorescence consistent with ER and Golgi. When tdTomato is separated by P2A in the P2A_P2A construct, tdTomato localises to the cytoplasm

with the P2A and the P2A_P2A construct turned dark brown. Similarly, liquid cultures inoculated with conidia of the respective transformants were incubated for a total of 24 h in absence (Doxy 0 h) or presence of 15 µg/ml doxycycline. Thereby, the inducer doxycycline was added either directly at the start of cultivation (Doxy 24 h) or after a pre-cultivation for 18 h to allow for conidia germination and hyphae formation prior to induction resulting in an induction time of 6 h (Doxy 6 h). In the absence of doxycycline mycelia of cultures containing either of the two different constructs remained uncoloured, whereas mycelia turned brown under inducing conditions even when induced for only 6 h (Fig. 3c). Therefore, both constructs produce functional proteins that produce Asp-melanin and regulation of gene expression is active on solid and in liquid media.

Expression of full length polycistronic mRNAs

To confirm that all genes from the polycistronic mRNA were expressed with high efficiency only under inducing conditions, we aimed in semiquantitative RT-PCR analyses on the P2A_P2A transcript. Total RNA was isolated from liquid cultures containing the ATNT strain with the P2A_P2A construct. The cultures were grown for 24 h either without doxycycline or were induced for 6 or 24 h. cDNAs were generated with anchored oligo(dT) primers and cDNA levels from the different cultivation conditions were normalised against the *A. niger* actin gene. Oligonucleotides were deduced that amplify regions of the three individual genes that are contained in the polycistronic transcript (Fig. 3d). As shown in Fig. 3e, in the absence of doxycycline (Doxy 0 h) no amplification was observed on the 5' and middle region of the polycistronic transcript encoding MelA and TyrP and only a weak band was detected for the gene sequence coding for tdTomato. This is in agreement with the low basal expression observed in *lacZ* reporter assays and in analysis of aspulvinone E metabolite production. However, strong induction was observed from both induced cultures (Doxy 6 h and Doxy 24 h) with PCR products on all three gene regions from the polycistronic messenger. This indicates that the full-length mRNA is efficiently transcribed only under doxycycline inducing conditions.

Subcellular localisation of proteins

Colouration of the mycelium indicated functional production and separation of MelA and TyrP and transcript analyses showed that all three genes encoded on the single transcript were efficiently transcribed. However, these analyses did not confirm the correct separation of proteins from the second P2A peptide, which should result in a cytoplasmic localisation of tdTomato, nor confirmed the correct subcellular localisation of any of

the proteins. Therefore, fluorescence microscopy analyses were performed. While the supplementation of liquid media with talc avoids pellet formation, it hampers microscopic analyses of hyphae due to the attached talc particles. On the other hand, individual hyphae are difficult to visualise once fungal pellets are formed. As our analyses showed that Asp-melanin is formed either on liquid or solid media, strains were grown on glucose minimal media containing agar plates and coverslips coated with doxycycline containing glucose minimal media were placed around the colonies. Once hyphae grew on the edges of the coverslips they were removed, embedded in a DAPI-containing mounting solution and analysed by fluorescence microscopy. As shown in Fig. 3f hyphae of the strain containing the single P2A separator, which means a fusion of the *tyrP* gene with the gene coding for the red fluorescent protein tdTomato, exclusively showed red fluorescence in subcellular organelles most likely resembling Golgi and ER [19]. This indicates that TyrP is quantitatively transported into the correct subcellular compartment after P2A cleavage from MelA and a functional TyrP-tdTomato fusion protein is produced. In contrast, hyphae of the strain containing the P2A_P2A construct showed very strong cytoplasmic red fluorescence, indicating that both P2A cleavage sites were correctly recognised and full length tdTomato had been produced. Observation of colonies grown in the absence of doxycycline only revealed DAPI staining of nuclei but no red fluorescence signal (not shown).

Discussion

The aim of this study was the generation of an optimised fine-tuneable expression system in *A. niger* that produces high expression rates when fully induced and which is suitable to express polycistronic genes for recombinant expression of fungal secondary metabolite biosynthetic gene clusters. Previous studies investigated the suitability of *A. niger* as expression platform for the production of secondary metabolites such as the non-ribosomal peptide enniatin [33]. Thereby, the use of the Tet-on expression system combined with optimised fermentation conditions resulted in 4.5 g/l enniatin confirming both, the suitability of the Tet-on system to induce secondary metabolite production and the suitability of *A. niger* as expression platform. Similarly, we have previously shown that a range of different metabolites such as polyketides [18], non-ribosomal peptides [20] and products from NRPS-like enzymes [19] can be successfully produced in *A. niger*.

The combination of our TerR/*PterA*-system with the Tet-on-system resulted in an expression system with exceptionally high transcription rates which are still titratable. The coupling of Tet-on with the highly specific

transcription factor TerR resulted in an amplification of gene expression by more than 5 times compared to direct gene expression from Tet-on. Therefore, even single copy integrations result in high transcript levels, which makes a selection for multi copy integration strains dispensable [17] and reduces adverse effects on growth and physiology caused by multiple random genome integration events. However, as our approach did not target a specific gene locus, some positioning effect from independent single copy integration strains was observed, which is resembled in the standard deviations from β -galactosidase activity determinations.

Another advantage of using the coupled Tet-on controlled TerR/*PterA* expression system compared to direct expression from the Tet-on promoter system is the low concentration of doxycycline required for induction of gene expression. Significant expression rates were already observed at 0.75 μ g/ml doxycycline. This activity from the coupled system was similar to that obtained from the direct Tet-on controlled gene expression at 15 μ g/ml. Low amounts of doxycycline reduce the risk of co-extraction of the inducer when aiming for purification of secondary metabolites. However, as highest expression rates were observed at 15 to 30 μ g doxycycline, these should be used especially when producing toxic metabolites that require significant biomass production prior to high level induction of gene expression. As a proof-of-concept we showed that Asp-melanin is efficiently produced when strains were pre-grown for 18 h and induced by doxycycline for only 6 h.

The tight regulation of the Tet-on controlled TerR/*PterA* expression system combined with its high induction rate makes it also superior to our original *PamyB* controlled TerR/*PterA* expression system, which is constitutively active on sugar containing media [18]. As glucose containing medium is generally used in the regeneration of protoplasts in fungal transformations, the production of toxic natural products may prevent growth of positive transformants. In contrast, regeneration of protoplasts of ATNT16 strain in the absence of doxycycline prevents expression of heterologous genes. In this respect, when we expressed the aspulvinone E synthetase gene *mela* in the *A. niger* P2 strain (*PamyB* control of *terR* expression) we suffered from the reduced ability of fungal colonies to produce conidia [19]. In this study, ATNT16 *mela*^{OE} strains grown in the absence of doxycycline were indistinguishable from the parental control strain, unless induced by doxycycline.

Importantly, the P2A polycistronic gene expression was compatible with our high level expression system. Asp-melanin was efficiently produced from both, the single P2A construct that contained the fusion of TyrP with tdTomato as well as the construct in which all three

proteins were separated by P2A sequences. While we were not able to quantify the production of the insoluble pigment Asp-melanin, the brown colouration of the mycelium in the single P2A construct appeared less pronounced compared to the P2A_P2A construct (Fig. 3b, c). Positioning effects due to the order of genes in the polycistronic messenger as described previously [28, 30] that may in part be due to a drop-off of the ribosome after the translational skipping event [31] cannot account for this difference as the position of the *tyrP* gene was identical in both constructs. Therefore, it is likely that the fusion of TyrP with tdTomato affects activity of the tyrosinase. Nevertheless, this fusion unambiguously showed that the TyrP protein is correctly and quantitatively targeted to the ER and Golgi as (1) TyrP is inactive in the reducing environment of the cytoplasm [19] and therefore needs to be transported to the oxidative environment of Golgi and ER and (2) no cytoplasmic background fluorescence from tdTomato remaining in the cytoplasm was observed. Therefore, the recognition of the *N*-terminal subcellular localisation sequence has not been affected by the proline residue added to TyrP from the P2A peptide [24] when cleaved from the Aspulvinone E synthetase MelA. Whether *C*-terminal localisation sequences such as the peroxisomal PTS1 tripeptide import sequence SKL or AKL, as found in proteins of fungal siderophore biosynthesis [34], may be masked by the *C*-terminal addition of a P2A sequence needs to be tested in future studies.

This study also showed that the second P2A sequence in the P2A_P2A construct is efficiently cleaved as this construct showed extremely bright red fluorescence from the cytoplasm. However, due to the extremely bright fluorescence from this construct, which even leads to a reddish appearance of the edges of colonies on plates, we cannot exclude that some uncleaved protein may still be transported into the ER and Golgi. Nevertheless, due to the high fluorescence intensity from the cytoplasm combined with the high activity of the tyrosinase from the P2A_P2A construct, the majority of P2A peptides has efficiently been cleaved.

Conclusion

The combination of tightly controlled Tet-on induction with the highly specific TerR/*PterA* expression system resulted in a well-regulated fine-tuneable and very strong gene expression. Therefore, the system appears suitable for high-level production of metabolites, even those with antifungal properties. In addition, the system is compatible with the use of self-cleaving peptides such as P2A. Cleavage sites are efficiently recognised and at least *N*-terminal secretion signals seem to remain unaffected. Therefore, this system can be used for the discovery

of metabolites from yet unexplored fungal secondary metabolite biosynthetic gene clusters.

Methods

Media, fungal cultivation and transformation

Conidia suspensions were obtained by growing *Aspergillus niger* strains in slope cultures containing *Aspergillus* minimal medium with 50 mM glucose as carbon and 10 mM glutamine as nitrogen source [19] denoted as GG10 medium. For solid media 2% agar was added. Slopes were incubated for 4 days at 28 °C and overlaid with 6 ml phosphate-buffered saline (PBS) containing 0.01% Tween 20. Conidia were scraped into suspension using sterile cotton swabs. Suspensions were filtered over a 40 µm cell strainer (Greiner BioOne) to remove hyphae and clumps of conidia. After centrifugation the supernatant was discarded, conidia suspended in PBS and conidia concentrations determined using an improved Neubauer chamber. If not indicated otherwise, GG10 liquid cultures were inoculated with 1×10^6 conidia/ml with or without the addition of doxycycline (final concentration 0–30 µg/ml) and incubated at 28 °C on a rotary shaker at 150 rpm. Mycelia and culture supernatants were separated by filtration over Miracloth filter gauze (Merck, Calbiochem). Mycelia were pressed dry between tissue paper and frozen in liquid nitrogen for subsequent analyses. Fungal transformation was performed as described previously [20] with some minor modifications. Mycelia for protoplast formation were generated by inoculating YEPD medium (20 g peptone, 10 g yeast extract, 5 g glucose per litre) with spores of the *A. niger* wild-type strain A1144 (Fungal Genetics Stock Center, Kansas, USA) or the expression platform strain ATNT16. After 22 h mycelia were washed and incubated for 60 min in 90 mM citrate–phosphate buffer pH 7.3 containing 10 mM dithiothreitol. Protoplasts were generated by using 1.3 g/20 ml sterile filtered VitoTaste Pro (Novozymes) in osmotic medium with 0.6 M KCl as osmotic stabiliser. After transformation protoplasts were regenerated on solid GG10 media containing 1.2 M sorbitol and either 40 µg/ml phleomycin, 140 µg/ml hygromycin B or 0.1 µg/ml pyrithiamine as selectable marker. Genomic DNA was isolated using the MasterPure Yeast DNA purification kit (Epicenter).

Generation of the ATNT16 expression platform strain

All oligonucleotides used in this study are listed in Additional file 5: Table 1. All PCR reactions were performed in a SpeedCycler² (Analytic Jena) in 10 µl volumes using either Phusion (fragment cloning, Thermo Scientific) or Phire Hot Start II DNA polymerase (colony PCR, Thermo Scientific) for DNA amplification. PCR fragments and digested plasmids for cloning purposes

were gel purified using the GeneJet Gel Extraction Kit (Thermo Scientific). To generate the *A. niger* ATNT16 strain a plasmid was generated that contained the gene of the transcriptional activator *terR* under control of the Tet-on reverse transactivator system [22]. The construct was cloned into the *HindIII* linearized pUC19-ble [18] vector containing a phleomycin resistance cassette for selection of transformants. The Tet-on system was amplified with oligonucleotides 1 and 2 from plasmid pFW22.1 (kindly provided by V. Meyer, Berlin) and contained overhangs to the *HindIII* site of pUC19-ble. Subsequently, the *terR* gene including its own terminator sequence was amplified with oligonucleotides 3 and 4 from genomic DNA of *Aspergillus terreus* SBUG844 and cloned into the *NcoI* linearized TetOn_ble_pUC19 vector [12]. The 5'-end contained an overhang to the Tet-on system and at the 3'-end to the *HindIII* site of pUC19-ble. Linearized plasmid and gel-purified PCR products were mixed and assembled by in vitro recombination using the InFusion HD cloning kit (Takara/Clontech) resulting in plasmid Tet-on:*terR*_ble_pUC19. The assembled plasmid was amplified in *Escherichia coli* DH5α using Mix & Go competent cells (Zymo Research). Positive clones were selected by colony PCR using oligonucleotides 5 and 6. Plasmids were isolated by use of the NucleoSpin Plasmid Miniprep kit (Macherey-Nagel) and correct assembly was confirmed by restriction analyses. The plasmid was used for transformation of *A. niger* A1144 and phleomycin resistant transformants were checked for single copy integration of the construct by Southern blot analysis using a dig labelled probe amplified with oligonucleotides 7 and 8. Transformant ATNT16 was selected for subsequent studies.

Generation of *lacZ* reporter and aspulvinone E synthetase gene expressing strains

To generate the *lacZ* reporter strains in the ATNT16 background, plasmid *hph_tdTomato:lacZ:trpC^T_pJET1.2* [18] containing the *lacZ* reporter under control of the *terA* promoter and a hygromycin B resistance cassette were used for transformation of ATNT16. A fusion of the Tet-on transactivator with the *lacZ* gene was assembled in the *PstI* restricted pUC19_ *ptrA* plasmid [35] containing the pyrithiamine resistance cassette as selectable marker. Tet-on was amplified from plasmid pFW22.1 with oligonucleotide 9 containing an overhang to the *PstI* site of pUC19_ *ptrA* and oligonucleotide 10. The *lacZ* gene including a *trpC* terminator was amplified from plasmid *hph_tdTomato:lacZ:trpC^T_pJET1.2* with oligonucleotide 11 containing an overhang to the 3'-end of Tet-on and oligonucleotide 12 with overhang to the *PstI* site of pUC19_ *ptrA*. Linearized plasmid and the two gel-purified PCR fragments

were mixed, assembled by in vitro recombination and transferred to *E. coli* as described above. Positive clones were selected by colony PCR using oligonucleotides 13 and 14. Isolated plasmids were checked by restriction analyses and used for transformation of A1144. Genomic DNA of ATNT16 and A1144 transformants was restricted with *Sma*I and analysed by Southern blot with a probe against the *lacZ* gene (oligonucleotides 13 and 14). At least three strains with a single copy integration of the reporter construct were used for expression analyses. For expression of the *A. terreus* aspulvinone E synthetase gene *melA* in the ATNT16 background, plasmid *his_melA-SM-Xpress* [19] was used as it contains a fusion of the *terA* promoter with the *melA* gene. The phleomycin resistance cassette of this plasmid was excised by *Not*I restriction and replaced by the pyrithiamine resistance cassette (*ptrA*) for transformation of ATNT16. Transformants were analysed by Southern blot with a probe against the *melA* gene (oligonucleotides 15 and 16) and strains with single copy integration were selected (Additional file 3).

Generation of model gene cluster expressing strains

Two different polycistronic expression constructs were generated for gene expression in ATNT16. The first construct contained the *melA* gene and a fusion of the *tyrP* gene and the gene coding for tdTomato. The *melA* and *tyrP* genes were separated by a P2A coding sequence. The *melA* gene was amplified from genomic DNA of *A. terreus* SBUG844 with oligonucleotide 17 that contained an overlap to the *Nco*I restricted SM-Xpress2 vector [19] and oligonucleotide 18 with an overhang coding for a the P2A sequence. The gene fusion of *tyrP* with the tdTomato gene was amplified from plasmid *tyrP:tdTomato_SM-Xpress2* [19] with oligonucleotide 19 possessing an overhang to the P2A sequence and oligonucleotide 20 with an overlap to the *Nco*I restricted SM-Xpress2 vector. In the second construct all three genes were separated by P2A sequences. The *melA* gene was amplified with the same oligonucleotides as for the first construct. The *tyrP* gene was amplified from genomic DNA of *A. terreus* SBUG844 with oligonucleotide 19 containing the P2A sequence overhang towards *melA* and oligonucleotide 21 with a P2A sequence overhang towards the tdTomato gene. Finally, the tdTomato gene was amplified from plasmid *tyrP:tdTomato_SM-Xpress2* with oligonucleotide 22 possessing the complementary overhang to the *tyrP* 3' P2A sequence and oligonucleotide 20 with a compatible overhang to the SM-Xpress2 vector. Constructs were assembled by in vitro recombination and transferred to *E. coli* DH5 α . Clones were checked by colony PCR using oligonucleotides 23 and 24 to test for correct gene assembly. Plasmid DNA was isolated and used for transformation

of ATNT16 with hygromycin B as selectable marker. Transformants were analysed by Southern blot with a probe against the *melA* gene (oligonucleotides 15 and 16) and strains with single copy integration were analysed further (Additional file 4).

β -Galactosidase reporter assays

To study β -galactosidase reporter activities, fungi were inoculated at 2×10^6 conidia per ml and grown for 24 h in 100 mM glucose containing minimal media with 20 mM glutamine as nitrogen source and 1% talc to avoid the formation of cell pellets. Mycelia were harvested over Miracloth, pressed dry and frozen in liquid nitrogen. Mycelia were ground to a fine powder under liquid nitrogen and suspended in Z buffer (60 mM Na₂HPO₄, 40 mM NaH₂PO₄, 10 mM KCl, 1 mM MgSO₄, 0.7% β -mercaptoethanol). After centrifugation for 5 min at $16,000 \times g$ and 4 °C the cell-free supernatant was removed and used for determination of β -galactosidase activity as previously described [36] using *o*-nitrophenyl- β -D-galactopyranoside (ONPG; $\epsilon = 3.5 \text{ mM}^{-1} \text{ cm}^{-1}$) as substrate. Protein concentrations were determined by using the Bradford Protein Assay (BioRad) with bovine serum albumin as standard. All spectrophotometric assays were carried out using an Evolution 220 UV-VIS spectrophotometer (ThermoFisher Scientific). From each construct three independent strains were grown in biological duplicates and activity determinations were made in technical duplicates.

Analysis of aspulvinone E production

To test production of aspulvinone E in ATNT16 strains carrying a single copy integration of the *PterA:melA* construct, GG10 medium was inoculated with 1×10^6 conidia/ml and one culture was supplemented with 15 $\mu\text{g/ml}$ of doxycycline, whereas the other was left untreated. Incubation was performed for 48 h at 28 °C on a rotary shaker at 150 rpm. Mycelium was removed by filtration over Miracloth and the culture filtrate was extracted twice with an equal volume of ethyl acetate. After evaporation of the solvent under reduced pressure the residue was solved in 1 ml of methanol and subjected to HPLC analysis using a Dionex UltiMate3000 (ThermoFisher Scientific) and Eclipse XDB-C18 column, 5 μm , $4.6 \times 150 \text{ mm}$ (Agilent) that was kept at 40 °C. A binary solvent system consisting of water acidified with 0.1% formic acid (solvent A) and methanol (solvent B) was applied. The following gradient at a flow rate of 1 ml/min was used: 0–0.5 min 10% B, 0.5–15 min 10–90% B, 15–17 min 90% B, 17–17.5 min 90–100% B, 17.5–22 min 100% B, 22–23 min 100–10% B, 23–25 min 10% B. An authentic sample containing a mixture of aspulvinone E and isoaspulvinone E served as reference.

Semiquantitative RT-PCR analyses

To analyse transcription of genes from the polycistronic messenger RNA of the ATNT16 P2A_P2A strain RNA was isolated using the MasterPure-Yeast RNA Purification Kit (Epicentre) from mycelium cultivated for 24 h in the absence or presence of 15 µg/ml doxycycline or pre-grown for 18 h without doxycycline and further cultivated for 6 h after addition of doxycycline. After a DNase treatment (TURBO DNase; ThermoFisher) RNA was transcribed into cDNA as previously described [19]. For normalisation of cDNA levels in the respective samples, serial dilutions were used for amplification of the *A. niger* actin gene using oligonucleotides 25 and 26. These primers span an intron region, which allows visualisation of a band shift from cDNA compared to genomic DNA (gDNA) and confirms the absence of contaminating gDNA in cDNA samples. For amplification of the *mela* gene oligonucleotides 15 and 16, for *tyrP* oligonucleotides 27 and 28 and for the *tdTomato* gene oligonucleotides 20 and 29 were used. PCRs of 30 cycles were performed in a SpeedCycler² (Analytik Jena) using Phire Hot Start II polymerase (Thermo Scientific).

Fluorescence microscopy

Fluorescence microscopy was performed as described previously [19] with some minor modifications. Strains were spotted on GG10 agar plates and pre-grown at 28 °C for one day, after which GG10 agarose coated coverslips containing 10 µg/ml doxycycline were placed next to the growing colony. 12 to 16 h later the coverslips were removed and placed on an object slide, overlaid with a droplet of mounting solution containing DAPI (ProLong Gold Antifade with DAPI, Thermo Scientific) and covered with a large coverslip. A GXML3201LED microscope (GX microscopes) was used for picture acquisition. Overlays of images were assembled by using the GIMP 2 software.

Statistical analyses

Comparison of expression levels from β-galactosidase activity determinations were analysed using GraphPad Prism (GraphPad Software) by applying multiple t-tests using the Holm-Sidak method, with $\alpha = 0.05$. Each row was analysed individually, without assuming a consistent standard deviation.

Additional files

Additional file 1. Southern blot analyses and plasmid map of construct used for generation of ATNT strains. **(A)** Southern blot for identification of single copy integration strains. A digoxigenin labelled probe was used for hybridisation. Plasmid control and genomic DNA of parental strains and transformants were restricted with *Apal*, which cuts once in the respective plasmid. The transformant used in subsequent analyses is numbered. **(B)** Plasmid map of the transformation construct. Position of oligonucleotides used in this study (P + number) as well as the position of the probe generated for Southern blot analysis and position of the restriction enzyme are

shown. *ble* = bleomycin resistance cassette. TetOn = Tet-on promoter system. *terR* = *terR* gene including its native terminator sequence.

Additional file 2. Southern blot analyses and plasmid maps of constructs used for generation of *lacZ* reporter strains. **(A, C)** Southern blot for identification of single copy integration strains. Digoxigenin labelled probes were used for hybridisation. Transformants used in subsequent analyses are numbered. **(A)** A1144 strains with integration of the *tet-on:lacZ* construct. Plasmid control and genomic DNA of parental strains and transformants were restricted with *AhdI*, which cuts once in the respective plasmid. **(C)** ATNT16 strain transformed with the *PterA:lacZ* construct. Plasmid control and genomic DNA of parental strains and transformants were restricted with *HindIII*, which cuts once in the respective plasmid. **(B, D)** Plasmid maps of the transformation constructs. Position of oligonucleotides used in this study (P + number) as well as the position of the probe generated for Southern blot analyses and position of the restriction enzyme are shown. *ptrA* = pyrithiamine resistance cassette. *hph* = hygromycin resistance cassette. *PterA* = *terA* promoter from *Aspergillus terreus*. *lacZ* = β-galactosidase gene from *Escherichia coli*. *TtrpC* = *trpC* terminator sequence from *Aspergillus terreus*.

Additional file 3. Southern blot analysis and plasmid map of construct used for generation of ATNT *mela* strains. **(A)** Southern blot for identification of single copy integration strains. A digoxigenin labelled probe was used for hybridisation. Plasmid control and genomic DNA of parental strains and transformants were restricted with *BglII*, which cuts once in the respective plasmid. The transformant used in subsequent analyses is numbered. **(B)** Plasmid map of the transformation construct. Position of oligonucleotides used in this study (P + number) as well as the position of the probe generated for Southern blot analysis and position of the restriction enzyme are shown. *ptrA* = pyrithiamine resistance cassette. *PterA* = *terA* promoter from *Aspergillus terreus*. *TtrpC* = *trpC* terminator sequence from *Aspergillus terreus*. *mela* = Aspulvinone E synthetase gene *mela* from *Aspergillus terreus*.

Additional file 4. Southern blot analyses and plasmid maps of constructs used for generation of ATNT16 P2A_P2A and P2A strains. **(A)** Southern blot for identification of single copy integration strains. A digoxigenin labelled probe was used for hybridisation. Plasmid control and genomic DNA of parental strains and transformants were restricted with *XbaI*, which cuts once in the respective plasmids. Transformants used in subsequent analyses are numbered. **(B, C)** Plasmid maps of the transformation constructs. Position of oligonucleotides used in this study (P + number) as well as the position of the probe generated for Southern blot analysis and position of the restriction enzyme are shown. *hph* = hygromycin B resistance cassette. *PterA* = *terA* promoter from *Aspergillus terreus*. *TtrpC* = *trpC* terminator sequence from *Aspergillus terreus*. *mela* = Aspulvinone E synthetase gene *mela* from *Aspergillus terreus*. *tyrP* = tyrosinase gene *tyrP* from *Aspergillus terreus*. *tdTomato* = codon optimised *tdTomato* gene. *tyrP:tdTom* = fusion of *tyrP* and *tdTomato* genes. *P2A* = sequence coding for the 2A peptide from porcine teschovirus-1.

Additional file 5: Table 1. Oligonucleotides used in this study.

Authors' contributions

EG performed experiments and collected data. EG and MB designed the study, analysed data and wrote the manuscript. All authors read and approved the final manuscript.

Acknowledgements

We are grateful to Vera Meyer and Franziska Wanka (Technical University Berlin, Germany) for providing plasmid pFW22.1 containing the Tet-on promoter system.

Availability of data and materials

All main data generated or analysed during this study are included in this published article. Raw data on enzymatic activity determinations and pictures of Southern blots for selection of transformants are available from the corresponding author on reasonable request.

Competing interests

The authors declare that they have no competing interests.

Consent for publication

Not applicable.

Ethics approval and consent to participate

Not applicable.

Funding

This research was supported by the School of Life Sciences of the University of Nottingham. The funding body had no impact on the design of the study and collection, analysis, and interpretation of data and in writing the manuscript.

Publisher's Note

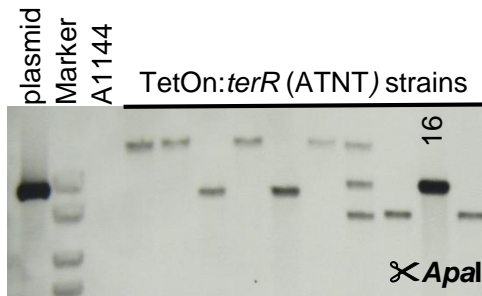
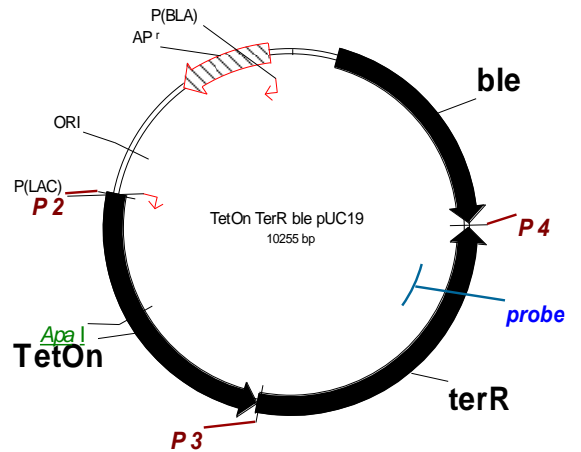
Springer Nature remains neutral with regard to jurisdictional claims in published maps and institutional affiliations.

Received: 16 October 2017 Accepted: 12 December 2017

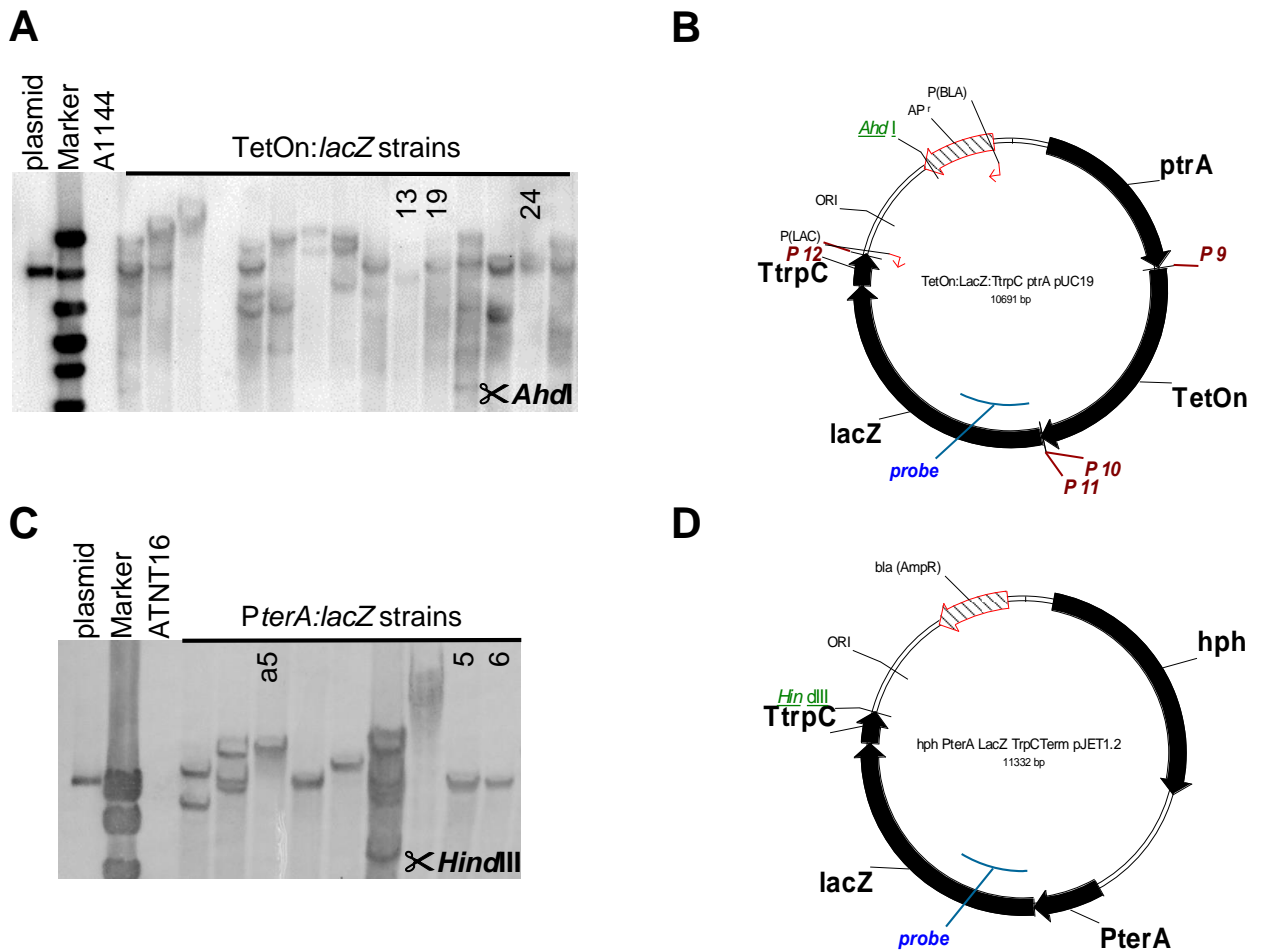
Published online: 19 December 2017

References

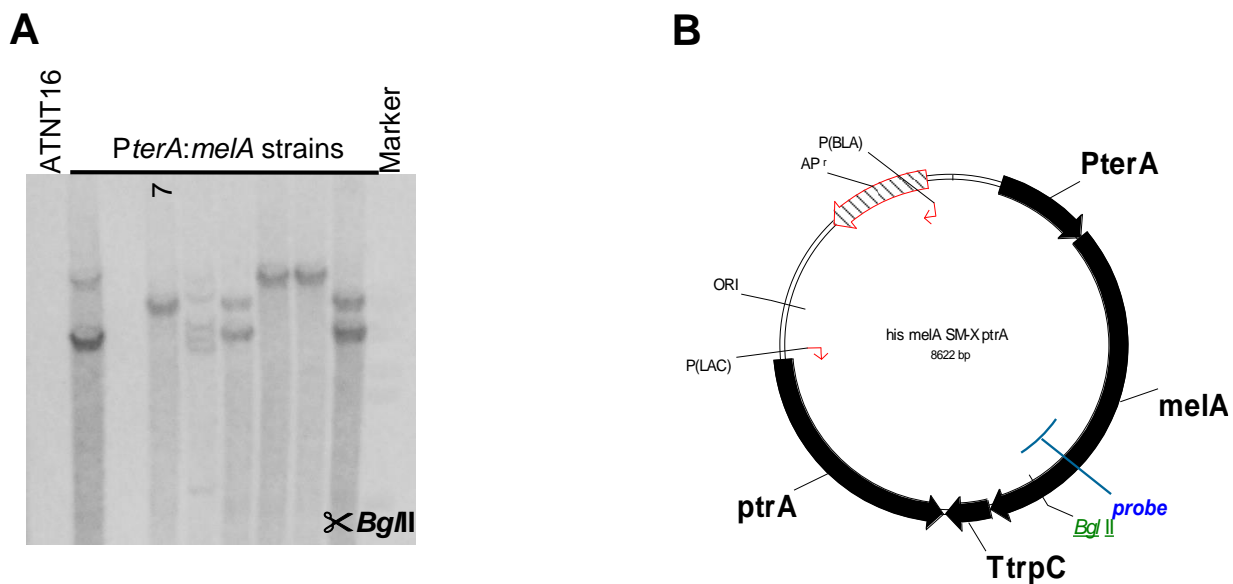
- Bok JW, Hoffmeister D, Maggio-Hall LA, Murillo R, Glasner JD, Keller NP. Genomic mining for *Aspergillus* natural products. *Chem Biol*. 2006;13:31–7.
- Grigoriev IV, Nikitin R, Haridas S, Kuo A, Ohm R, Otilar R, Riley R, Salamov A, Zhao X, Korzeniewski F, et al. MycoCosm portal: gearing up for 1000 fungal genomes. *Nucl Acids Res*. 2014;42:D699–704.
- de Vries RP, Riley R, Wiebenga A, Aguilar-Osorio G, Amillis S, Uchima CA, Anderluh G, Asadollahi M, Askin M, Barry K, et al. Comparative genomics reveals high biological diversity and specific adaptations in the industrially and medically important fungal genus *Aspergillus*. *Genome Biol*. 2017;18:28.
- Wasil Z, Pahirulzaman KAK, Butts C, Simpson TJ, Lazarus CM, Cox RJ. One pathway, many compounds: heterologous expression of a fungal biosynthetic pathway reveals its intrinsic potential for diversity. *Chem Sci*. 2013;4:3845–56.
- Gressler M, Meyer F, Heine D, Hortschansky P, Hertweck C, Brock M. Phytotoxin production in *Aspergillus terreus* is regulated by independent environmental signals. *eLife*. 2015;4:e07861.
- Alberti F, Foster GD, Bailey AM. Natural products from filamentous fungi and production by heterologous expression. *Appl Microbiol Biotechnol*. 2017;101:493–500.
- Anyaogu DC, Mortensen UH. Heterologous production of fungal secondary metabolites in *Aspergilli*. *Front Microbiol*. 2015;6:77.
- Gonzalez-Mendez V, Perez-Bonilla M, Perez-Victoria I, Martin J, Munoz F, Reyes F, Tormo JR, Genilloud O. Multicomponent analysis of the differential induction of secondary metabolite profiles in fungal endophytes. *Molecules*. 2016;21(2):234.
- Netzker T, Fischer J, Weber J, Mattern DJ, König CC, Valiante V, Schroeckh V, Brakhage AA. Microbial communication leading to the activation of silent fungal secondary metabolite gene clusters. *Front Microbiol*. 2015;6:299.
- Brakhage AA, Schroeckh V. Fungal secondary metabolites—strategies to activate silent gene clusters. *Fungal Genet Biol*. 2011;48:15–22.
- Brakhage AA. Regulation of fungal secondary metabolism. *Nat Rev Microbiol*. 2013;11:21–32.
- Gressler M, Zaehle C, Scherlach K, Hertweck C, Brock M. Multifactorial induction of an orphan PKS-NRPS gene cluster in *Aspergillus terreus*. *Chem Biol*. 2011;18:198–209.
- Clevenger KD, Bok JW, Ye R, Miley GP, Verdán MH, Velk T, Chen C, Yang K, Robey MT, Gao P, et al. A scalable platform to identify fungal secondary metabolites and their gene clusters. *Nat Chem Biol*. 2017;13:895–901.
- Bok JW, Keller NP. LaeA, a regulator of secondary metabolism in *Aspergillus* spp. *Eukaryot Cell*. 2004;3:527–35.
- Sakai K, Kinoshita H, Nihira T. Heterologous expression system in *Aspergillus oryzae* for fungal biosynthetic gene clusters of secondary metabolites. *Appl Microbiol Biotechnol*. 2012;93:2011–22.
- Yeh HH, Ahuja M, Chiang YM, Oakley CE, Moore S, Yoon O, Hajovsky H, Bok JW, Keller NP, Wang CC, Oakley BR. Resistance gene-guided genome mining: serial promoter exchanges in *Aspergillus nidulans* reveal the biosynthetic pathway for fellutamide B, a proteasome inhibitor. *ACS Chem Biol*. 2016;11:2275–84.
- Fleissner A, Dersch P. Expression and export: recombinant protein production systems for *Aspergillus*. *Appl Microbiol Biotechnol*. 2010;87:1255–70.
- Gressler M, Hortschansky P, Geib E, Brock M. A new high-performance heterologous fungal expression system based on regulatory elements from the *Aspergillus terreus* terrein gene cluster. *Front Microbiol*. 2015;6:184.
- Geib E, Gressler M, Viedernikova I, Hillmann F, Jacobsen ID, Nietzsche S, Hertweck C, Brock M. A non-canonical melanin biosynthesis pathway protects *Aspergillus terreus* conidia from environmental stress. *Cell Chem Biol*. 2016;23:587–97.
- Brandenburger E, Gressler M, Leonhardt R, Lackner G, Habel A, Hertweck C, Brock M, Hoffmeister D. A highly conserved basidiomycete peptide synthetase produces a trimeric hydroxamate siderophore. *Appl Environ Microbiol*. 2017;83:e01478-17.
- Meyer V, Wanka F, van Gent J, Arentshorst M, van den Hondel CA, Ram AF. Fungal gene expression on demand: an inducible, tunable, and metabolism-independent expression system for *Aspergillus niger*. *Appl Environ Microbiol*. 2011;77:2975–83.
- Wanka F, Cairns T, Boecker S, Berens C, Happel A, Zheng X, Sun J, Krappmann S, Meyer V. Tet-on, or Tet-off, that is the question: advanced conditional gene expression in *Aspergillus*. *Fungal Genet Biol*. 2016;89:72–83.
- Tang X, Liu X, Tao G, Qin M, Yin G, Suo J, Suo X. "Self-cleaving" 2A peptide from porcine teschovirus-1 mediates cleavage of dual fluorescent proteins in transgenic *Eimeria tenella*. *Vet Res*. 2016;47:68.
- Kim JH, Lee SR, Li LH, Park HJ, Park JH, Lee KY, Kim MK, Shin BA, Choi SY. High cleavage efficiency of a 2A peptide derived from porcine teschovirus-1 in human cell lines, zebrafish and mice. *PLoS One*. 2011;6:e18556.
- Beekwilder J, van Rossum HM, Koopman F, Sonntag F, Buchhaupt M, Schrader J, Hall RD, Bosch D, Pronk JT, van Maris AJ, Daran JM. Polycistronic expression of a beta-carotene biosynthetic pathway in *Saccharomyces cerevisiae* coupled to beta-ionone production. *J Biotechnol*. 2014;192(Pt B):383–92.
- Efimova VS, Isaeva LV, Makeeva DS, Rubtsov MA, Novikova LA. Expression of cholesterol hydroxylase/lyase system proteins in yeast *S. cerevisiae* cells as a self-processing polyprotein. *Mol Biotechnol*. 2017;59:394–406.
- de Amorim Araujo J, Ferreira TC, Rubini MR, Duran AG, De Marco JL, de Moraes LM, Torres FA. Coexpression of cellulases in *Pichia pastoris* as a self-processing protein fusion. *AMB Express*. 2015;5:84.
- Subramanian V, Schuster LA, Moore KT, Taylor LE 2nd, Baker JO, Vander Wall TA, Linger JG, Himmel ME, Decker SR. A versatile 2A peptide-based bicistronic protein expressing platform for the industrial cellulase producing fungus, *Trichoderma reesei*. *Biotechnol Biofuels*. 2017;10:34.
- Unkles SE, Valiante V, Mattern DJ, Brakhage AA. Synthetic biology tools for bioprospecting of natural products in eukaryotes. *Chem Biol*. 2014;21:502–8.
- Schuetz T, Meyer V. Polycistronic gene expression in *Aspergillus niger*. *Microb Cell Fact*. 2017;16:162.
- Liu Z, Chen O, Wall JBJ, Zheng M, Zhou Y, Wang L, Ruth Vaseghi H, Qian L, Liu J. Systematic comparison of 2A peptides for cloning multi-genes in a polycistronic vector. *Sci Rep*. 2017;7:2193.
- Drion H, Sommer B, Wittmann C. Morphology engineering of *Aspergillus niger* for improved enzyme production. *Biotechnol Bioeng*. 2010;105:1058–68.
- Richter L, Wanka F, Boecker S, Storm D, Kurt T, Vural O, Sussmuth R, Meyer V. Engineering of *Aspergillus niger* for the production of secondary metabolites. *Fungal Biol Biotechnol*. 2014;1:4.
- Grundlinger M, Yasmin S, Lechner BE, Geley S, Schrettl M, Hynes M, Haas H. Fungal siderophore biosynthesis is partially localized in peroxisomes. *Mol Microbiol*. 2013;88:862–75.
- Fleck CB, Brock M. *Aspergillus fumigatus* catalytic glucokinase and hexokinase: expression analysis and importance for germination, growth, and conidiation. *Eukaryot Cell*. 2010;9:1120–35.
- Ebel F, Schwienbacher M, Beyer J, Heesemann J, Brakhage AA, Brock M. Analysis of the regulation, expression, and localisation of the isocitrate lyase from *Aspergillus fumigatus*, a potential target for antifungal drug development. *Fungal Genet Biol*. 2006;43:476–89.

A**B**

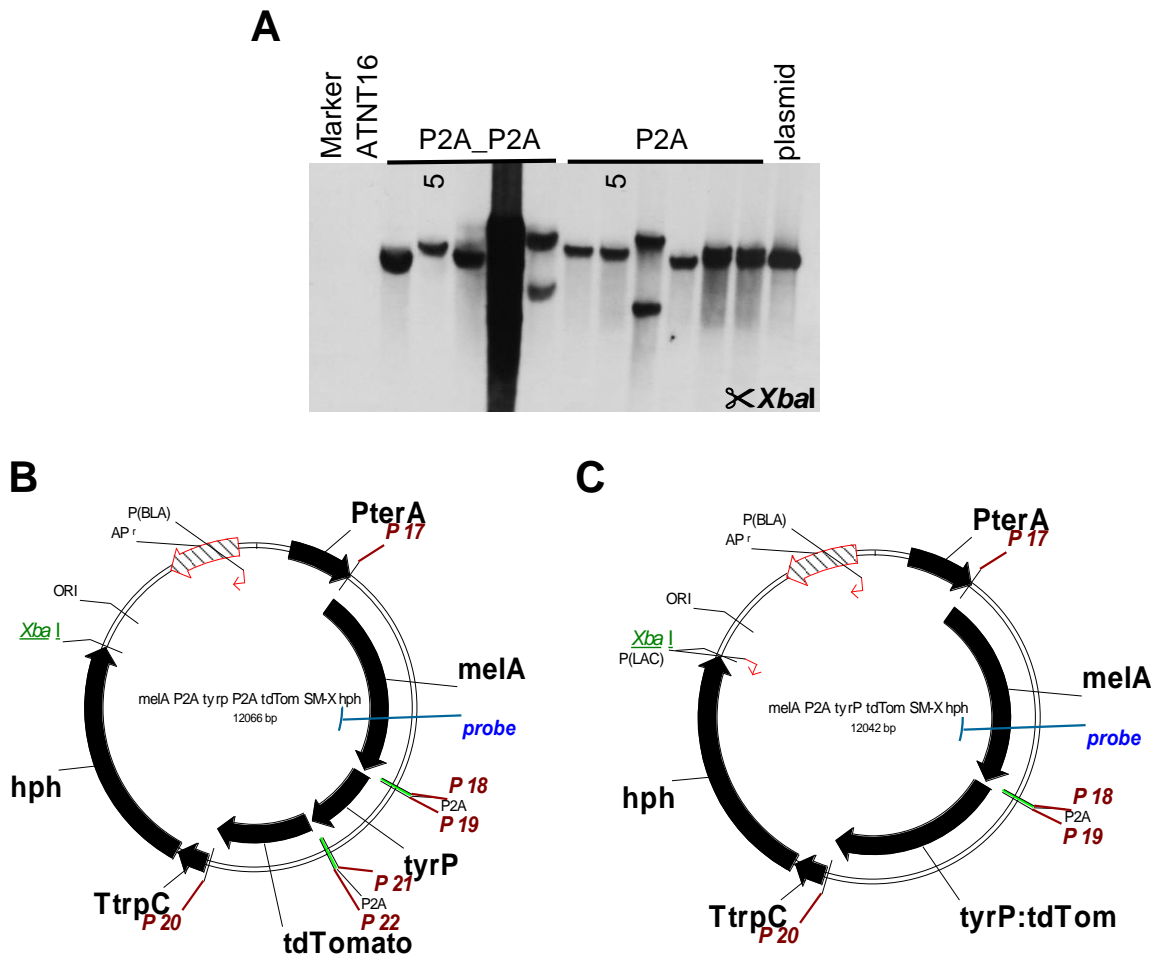
Additional file 1: Southern blot analyses and plasmid map of construct used for generation of ATNT strains. (A) Southern blot for identification of single copy integration strains. A digoxigenin labelled probe was used for hybridisation. Plasmid control and genomic DNA of parental strains and transformants were restricted with *ApaI*, which cuts once in the respective plasmid. The transformant used in subsequent analyses is numbered. (B) Plasmid map of the transformation construct. Position of oligonucleotides used in this study (P + number) as well as the position of the probe generated for Southern blot analysis and position of the restriction enzyme are shown. *ble* = phleomycin resistance cassette. TetOn = Tet-on promoter system. *terR* = *terR* gene including its native terminator sequence.



Additional file 2: Southern blot analyses and plasmid maps of constructs used for generation of *lacZ* reporter strains. (A, C) Southern blot for identification of single copy integration strains. Digoxigenin labelled probes were used for hybridisation. Transformants used in subsequent analyses are numbered. (A) A1144 strains with integration of the *tet-on:lacZ* construct. Plasmid control and genomic DNA of parental strains and transformants were restricted with *AhdI*, which cuts once in the respective plasmid. (C) ATNT16 strain transformed with the *PterA:lacZ* construct. Plasmid control and genomic DNA of parental strains and transformants were restricted with *HindIII*, which cuts once in the respective plasmid. (B, D) Plasmid maps of the transformation constructs. Position of oligonucleotides used in this study (P + number) as well as the position of the probe generated for Southern blot analyses and position of the restriction enzyme are shown. ptrA = pyrithiamine resistance cassette. hph = hygromycin resistance cassette. PterA = *terA* promoter from *Aspergillus terreus*. lacZ = β -galactosidase gene from *Escherichia coli*. TtrpC = *trpC* terminator sequence from *Aspergillus terreus*.



Additional file 3: Southern blot analysis and plasmid map of construct used for generation of ATNT *melA* strains. (A) Southern blot for identification of single copy integration strains. A digoxigenin labelled probe was used for hybridisation. Plasmid control and genomic DNA of parental strains and transformants were restricted with *BglII*, which cuts once in the respective plasmid. The transformant used in subsequent analyses is numbered. (B) Plasmid map of the transformation construct. Position of oligonucleotides used in this study (P + number) as well as the position of the probe generated for Southern blot analysis and position of the restriction enzyme are shown. ptrA = pyrithiamine resistance cassette. PterA = *terA* promoter from *Aspergillus terreus*. TtrpC = *trpC* terminator sequence from *Aspergillus terreus*. melA = Aspulvinone E-synthetase gene *melA* from *Aspergillus terreus*.



Additional file 4: Southern blot analyses and plasmid maps of constructs used for generation of ATNT16 P2A_P2A and P2A strains. (A) Southern blot for identification of single copy integration strains. A digoxigenin labelled probe was used for hybridisation. Plasmid control and genomic DNA of parental strains and transformants were restricted with *Xba*I, which cuts once in the respective plasmids. Transformants used in subsequent analyses are numbered. (B, C) Plasmid maps of the transformation constructs. Position of oligonucleotides used in this study (P + number) as well as the position of the probe generated for Southern blot analysis and position of the restriction enzyme are shown. *hph* = hygromycin B resistance cassette. *PterA* = *terA* promoter from *Aspergillus terreus*. *TtrpC* = *trpC* terminator sequence from *Aspergillus terreus*. *melA* = Aspulvinone E-synthetase gene *melA* from *Aspergillus terreus*. *tyrP* = tyrosinase gene *tyrP* from *Aspergillus terreus*. *td-Tomato* = codon optimised *td-Tomato* gene. *tyrP:td-Tom* = fusion of *tyrP* and *td-Tomato* genes. *P2A* = sequence coding for the 2A peptide from porcine teschovirus-1.

Table 1: Oligonucleotides used in this study.

#	Sequence	Feature
1	CGACCTGCAGGCATGCAAGCTTCCATGGTGTTTAA ACGGTGATGTCT	TetOn_ble_pUC19
2	TGACCATGATTACGCCAAGCTTCCCTCGGCTGGTC	TetOn_ble_pUC19
3	CACCGTTTAAACACCATGTTGCGCCGAACTTAACGC AAAG	TetOn:terR_ble_pUC19
4	GACCTGCAGGCATGCAAGCTTCGCATCACGTCTTG TTATCTGTTG	TetOn:terR_ble_pUC19
5	CAAGAAGAAGCATGTGGTACC	control primer <i>terR</i>
6	GATGGCCAACACAGCTTGG	control primer <i>terR</i>
7	GTCAGCATGCCAACGCTCTC	probe primer <i>terR</i>
8	CCAAGAAAGTCACACAGATCG	probe primer <i>terR</i>
9	TCCTCTAGAGTCGACCTGCAGCCCTCGGCTGGTCT GTCTTAC	TetOn:lacZ_ptrA_pUC19
10	GGTGATGTCTGCTCAAGCG	TetOn:lacZ_ptrA_pUC19
11	TGAGCAGACATCACCATGAGATCCACCATGATTA CGG	TetOn:lacZ_ptrA_pUC19
12	CCAAGCTTGCATGCCTGCAGGAGTGAGGGTTGAG TACGAG	TetOn:lacZ_ptrA_pUC19
13	GGCGTTACCCAACCTTAATCGC	control primer <i>lacZ</i>
14	CTCATCCATGACCTGACCATG	control primer <i>lacZ</i>
15	CGACGTTGGCATTGACTCC	probe primer <i>melA</i>
16	GCGCATCTTAATGTGTGGAGG	probe primer <i>melA</i>
17	CATCACAGCACCATGCATCACCATCACCATCACCA ACCAAGCCTTATTCCCTC	his_melA_P2A_XXX_SM -Xpress
18	CCGGCTTGCTTCAGGAGGCTGAAATTGGTAGCGCC GCTGCCCATGCCCTCTCAGCAAGAG	P2A constructs
19	TCCTGAAGCAAGCCGGTGATGTGGAGGAAAACCC TGGCCCTATGGGTTTCTACAGGAATCTAG	P2A constructs
20	ATCACTGCTGCCATGCTACTTGTAGAGCTCGTCCA TAC	P2A constructs
21	CAGCCTGTTTGAGCAGGGAAAAGTTAGTGGCACC GGAACCGGTATATGTATAACAATAAGGACC	P2A constructs
22	CTGCTCAAACAGGCTGGCGACGTCGAAGAGAATC CCGGTCCCATGGTCTCCAAGGGTGAGG	P2A constructs
23	ACGGACCATAACGCTCTCGCCGGCTATTCTATGGG	colony PCR P2A constructs
24	GAAAGGGACGTTTCGGTGC	colony PCR P2A constructs
25	GCGAGAGGAGAAAGACTGG	RT-PCR actin
26	CAAGCCAGCAAGAATAACCACC	RT-PCR actin
27	CCCATGATATTCTGAAATTCG	RT-PCR <i>tyrP</i>
28	CCTCCTGAGCTATCAGTCG	RT-PCR <i>tryP</i>
29	CCAAGCTCGACATCACCTCC	RT-PCR <i>tdTom</i>

Hybrid *in silico/in vitro* target fishing to assign function to
“orphan” compounds of food origin -
the case of the fungal metabolite atromentin.

Luca Dellafiora, George Aichinger, **Elena Geib**, Leyre Sánchez-Barrionuevo, Matthias Brock, David Cánovas, Chiara Dall’Asta and Doris Marko

(2019) Food Chemistry; 270, 61-69

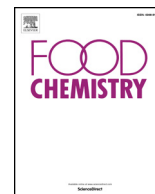


Summary of the manuscript: Atromentin was used as a model compound to identify potential biological targets via a so-called target fishing approach. The procedure relies on a computational screening for activity identification coupled with experimental trials for dose-response characterization. The computational results identified estrogen receptors and 17- β -hydroxysteroid dehydrogenase as potential targets of atromentin, whereby only weak binding to estrogen receptors was proposed. By applying *in vitro* experiments, the weak estrogenic

activity was confirmed, supporting the reliability of the prediction. Although the estrogenic activity appears limited, the inhibition of 17- β -hydroxysteroid dehydrogenase should be investigated further to clarify any possible endocrine disruptive effects caused by atromentin.

Contribution: 10% of practical work, contribution to manuscript preparation

Construction of an atromentin production strain. Extraction, purification and quality analysis of atromentin.



Hybrid *in silico/in vitro* target fishing to assign function to “orphan” compounds of food origin – The case of the fungal metabolite atromentin

Luca Dellafiora^a, Georg Aichinger^b, Elena Geib^c, Leyre Sánchez-Barrionuevo^d, Matthias Brock^c, David Cánovas^d, Chiara Dall'Asta^{a,*}, Doris Marko^b

^a Department of Food and Drug, University of Parma, Via G.P. Usberti 27/A, 43124 Parma, Italy

^b Department of Food Chemistry and Toxicology, Faculty of Chemistry, University of Vienna, Waehringer Str. 38, 1090 Vienna, Austria

^c Fungal Genetics and Biology Groups, School of Life Sciences, University of Nottingham, University Park, NG7 2RD Nottingham, UK

^d Department of Genetics, Faculty of Biology, University of Sevilla, 41012, Spain

ARTICLE INFO

Keywords:

Atromentin
Target fishing
Estrogenic activity
Fungal metabolite
Activity assignment
17- β -Hydroxysteroid dehydrogenase

ABSTRACT

Many small molecules of food origin may effect human health but lack an adequate description of their biological activity. To fill this knowledge gap, a first-line workflow is needed to assign putative functions, rank the endpoints for testing and guide wet-lab experiments. In this framework, the identification of potential biological targets can be used to probe the activity of orphan compounds using a so-called “target fishing” approach. Here, we present a proof of concept study using an *in silico/in vitro* target fishing approach on the fungal secondary metabolite atromentin. The procedure relies on a computational screening for activity identification coupled with experimental trials for dose-response characterization. Computational results identified estrogen receptors and 17- β -hydroxysteroid dehydrogenase as potential targets. Experiments confirmed a weak estrogenic activity, supporting the reliability of the procedure. Despite limited estrogenicity of atromentin, the proposed inhibition of 17- β -hydroxysteroid dehydrogenase should be considered as a source for endocrine disruptive effects.

1. Introduction

Food may be a source of exposure to many xenobiotics with potential biological or toxic activity. Such compounds may be inherently present as food constituents or they may be introduced, either voluntarily or not, along the food production chain (Rather, Koh, Paek, & Lim, 2017). Considering the huge number of compounds occurring in food, an adequate characterization of any possible biological/toxic activity is still lacking for many of them. Nevertheless, the overall identification of bioactive and toxic molecules in food is crucial to advance the current understanding of the effects on human health and well-being. In this respect, the understanding of small molecules profiling and fingerprinting is getting more and more detailed by taking advantage of -omic sciences such as proteomics and metabolomics (e.g. ref. (Scalbert et al., 2014)). However, the assignment of biological properties to such a wide number of molecules is currently challenging, albeit it is the primal step to assess the hazards or benefits to human health. Obviously, the risk assessment of toxicants and the assignment of health claims require the collection of a wealth of evidence including

data on occurrence, exposure, bioavailability, bioaccessibility and both, the chronic and acute effects in living organisms. Nevertheless, the use of upstream methods to preliminarily assign a possible toxic or biological activity to molecules of interest, which is framed into the hazard/activity identification process, may allow a more effective setting up of further experimental investigations. Currently, there is an outbreak of novel molecular scaffolds as a result of the efforts of the international scientific community in discovering new fungal secondary metabolites, which makes the assignment of function an exceptional challenge. Thus, prompt work-flows need to be implemented to support decision making in a timely manner and to plan effective future investigations.

In this framework, the identification of the biological targets along with proposing possible mechanisms of action may be an effective way to probe the activity of orphan compounds (i.e. compounds with poorly characterized activity and/or unknown biological targets). In this regard, the so defined “target fishing” is a consolidated approach in medicinal chemistry to discover unexpected targets for pharmacologically active molecules. Target fishing is commonly applied to investigate the polypharmacology of drugs (Cereto-Massagué et al., 2015;

* Corresponding author.

E-mail addresses: luca.dellafiora@unipr.it (L. Dellafiora), georg.aichinger@univie.ac.at (G. Aichinger), Elena.Geib@nottingham.ac.uk (E. Geib), leyresan@gmail.com (L. Sánchez-Barrionuevo), Matthias.Brock@nottingham.ac.uk (M. Brock), davidc@us.es (D. Cánovas), chiara.dallasta@unipr.it (C. Dall'Asta), doris.marko@univie.ac.at (D. Marko).

<https://doi.org/10.1016/j.foodchem.2018.07.027>

Received 17 March 2018; Received in revised form 21 May 2018; Accepted 2 July 2018

Available online 04 July 2018

0308-8146/© 2018 Elsevier Ltd. All rights reserved.

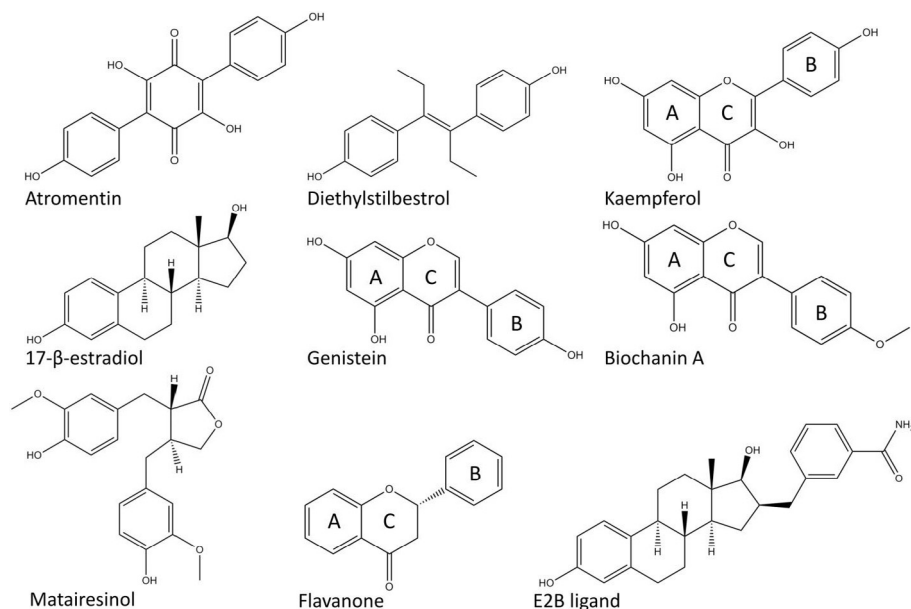


Fig. 1. Structures of the molecules mentioned in the work.

Chaudhari, Tan, Huang, & Zhang, 2017), in off-targets identification, and in drug repositioning (Delavan et al., 2017). Currently, target fishing studies mainly rely on proteomic-, genomic- and computational-based approaches (Jung & Kwon, 2015). In particular, the integrated use of *in silico* simulations and *in vitro* trials already proved to be effective in target fishing studies and in the bioactivity/toxicity assessment of small molecules (Dellafiora, Dall'Asta, & Galaverna, 2018; Scafuri et al., 2017).

In this work, we investigated whether a target fishing approach can also be successfully applied in the field of food chemistry and toxicology by investigating the potential activity of poorly characterized molecules of food origin. A hybrid *in silico/in vitro* workflow is presented composed of ligand-based virtual screening and structure-based molecular modelling studies coupled to experimental trials. Atromentin (Fig. 1), a fungal metabolite from involutin biosynthesis of *Paxillus involutus* (Braesel et al., 2015) with a poorly characterized activity/toxicity (NCBI) was selected as a proof of principle. Atromentin is a low molecular weight fungal pigment precursor with a polyphenolic and benzoquinone structure that can be found in basidiomycetes mushrooms, including some intended for human consumption (Hu & Liu, 2003; Ngoc Quang et al., 2003). More recently, it was also found as a secondary metabolite produced by the ascomycete *Aspergillus terreus* (Hühner, Backhaus, Kraut, & Li, 2018), pointing to a broader distribution among the fungal kingdom. Even though some biological properties have been identified over the years (e.g. anticoagulant, apoptotic and antimicrobial activity) (Brewer, Jen, Jones, & Taylor, 1984; Khanna, Malone, Euler, & Brady, 1965; Kim & Lee, 2009), the body of evidence collected so far is still fragmentary, making atromentin a good candidate for the study proposed. This work identified biological targets of potential concern and possible mechanisms of action, extending the knowledge on atromentin activity and paving the ground for further investigations.

2. Material and methods

2.1. *In silico* modelling

2.1.1. Data collection and ligand-based virtual screening

The atromentin 3D structure was used as a template to investigate a database of compounds with known activity and biological targets, aiming at identifying hits with degrees of physico-chemical similarities.

The database was built using the ligands repository available in the RCSB PDB databank (<https://www.rcsb.org>) (Berman et al., 2000) containing all the ligands bound to the proteins deposited in the databank. In particular, all non-redundant 3D structures of ligands (24,893 entries) were downloaded from the Ligand Expo Download page (<http://ligand-expo.rcsb.org>) in the chemical table file format (*sdf*); last database access in August, 23rd 2017). Considering that atromentin has a molecular weight of 324.3 g/mol, all compounds were pre-filtered taking only those with a molecular weight ranging between 200 and 500 g/mol (15,248 entries were selected). This subset of compounds was used for the ligand-based virtual screening using the FLAP software (<https://www.moldiscovery.com>) (Baroni, Cruciani, Sciabola, Perruccio, & Mason, 2007). The default software setting was used to create the database and virtual screening was performed using the bit string mode to reduce the computation time.

2.1.2. Structure-based molecular modelling

The ligand-based virtual screening aimed at sorting the compounds according to the degree of similarity to atromentin. Notably, structural similarity may allow different compounds to share biological/toxicological endpoints as they may use the common chemical features to interact with the same biological targets (*vide infra*). Therefore, the interaction between atromentin and the biological targets of the best hits, identified by the virtual screening, was thoroughly investigated using a structure-based molecular modelling study. The structure-based study relied on the pharmacophoric analysis of the ligand binding sites and on docking simulations to investigate the molecular details of the ligand-target interaction.

2.1.2.1. Model preparations. The models for the alpha and beta isoforms of the estrogen receptor (ER α and ER β , respectively), the 17- β -hydroxysteroid dehydrogenase (HSD) from *Curvularia lunata* and the human Type I HSD were derived from the crystallographic structures deposited in the RCSB PDB databank (<http://www.rcsb.org>) (Berman et al., 2000) with ID codes 2YJA (Phillips et al., 2011), 3OLL (Möcklinghoff et al., 2010), 4FJ1 (Cassetta et al., 2017) and 3HB5 (Mazumdar et al., 2009), respectively. All protein structures were processed using the Sybyl software, version 8.1 (www.certara.com) and the consistency of atom and bond types was checked as described previously (Dellafiora, Galaverna, Dall'Asta, & Cozzini, 2015). All co-crystallized ligands were removed, except for both 17- β -HSD enzymes

that were computed in the holo form with the NADPH cofactor.

2.1.2.2. Pharmacophoric analysis. The binding site of all models was defined using the Flapsite tool of the software FLAP (Baroni et al., 2007) while the GRID algorithm (Carosati, Sciabola, & Cruciani, 2004) was used to investigate the corresponding pharmacophoric space. The DRY probe was used to describe potential hydrophobic interactions, while the sp2 carbonyl oxygen (O) and the neutral flat amino (N1) probes were used to describe the hydrogen bond acceptor and donor capacity of the target, respectively. All images were obtained using the software PyMol version 1.7 (<http://www.pymol.org>).

2.1.2.3. Docking simulations. The interaction between atromentin and the putative targets was investigated using a docking study. The software GOLD (Genetic Optimization for Ligand Docking) was chosen as it already showed good performances in computing ligand-target interactions and in estimating the activity of ligands (e.g. ref. (Dellafiara, Galaverna, & Dall'Asta, 2017)). In particular, the higher the computational scores, the better the expected capability of ligands to arrange favourably within the ligand binding site. Software setting and docking protocol reported by Ehrlich (Ehrlich et al., 2015) were used. As an exception, the external scoring functions were omitted as the GOLD's internal scoring function GOLDScore succeeded in analysing the reference set of compounds (*vide infra*). Specifically, GOLDScore fitness considers the external (protein-ligand complex) and internal (ligand only) van der Waals energy, protein-ligand hydrogen bond energy and ligand torsional strain energy. In each docking study, the proteins were kept semi-flexible and the polar hydrogen atoms were set free to rotate. The ligands were set fully flexible. The maximum number of poses to generate for each ligand was set at 50. In all models considered, only the pose with the highest GOLDScore fitness was kept for each ligand, according to Dellafiara and co-workers (Dellafiara et al., 2017). Additionally, all analyses were done in triplicate to exclude non-causative scores assignment as GOLD implements a Lamarckian genetic algorithm that may introduce variability in the results.

2.2. In vitro experiments

2.2.1. Chemicals and reagents

Cell culture media and supplements were purchased from GIBCO Invitrogen (Karlsruhe, Germany), Sigma–Aldrich (Schnellendorf, Germany) and SARSTEDT AG & CO (Nuembrecht, Germany). 17- β -estradiol was purchased from Sigma-Aldrich (Schnellendorf, Germany), genistein from Extrasynthese (Genay, France) and ICI 182,780 from Tocris (Bristol, United Kingdom). Atromentin was purified ($\geq 99\%$ by HPLC; Fig. 1S, Supplementing material) from heterologous expression of the *P. involutus invA5* gene in *Aspergillus oryzae* as described below.

2.2.2. Cell culture

The estrogen-sensitive human endometrial adenocarcinoma cell line Ishikawa, expressing ER α and ER β was selected for this study (Vejdovszky, Schmidt, Warth, & Marko, 2016) and purchased from ECACC (Wiltshire, United Kingdom). Cells were cultivated in Minimum Essential Medium (MEM), supplemented with 5% FBS (Fetal Bovine Serum), 1% l-glutamine and 1% penicillin/streptomycin under humidified conditions (37 °C, 5% CO₂). Experiments were performed in cells between passages 5 and 20 with the use of “assay medium”, a phenol red free Dulbecco's Modified Eagle Medium containing the F-12 nutrient solution (DMEM/F-12), supplemented with 5% charcoal-dextran stripped foetal bovine serum to ensure low hormone levels (Fisher Scientific, Braunschweig, Germany). For all assays, the Ishikawa cells were seeded at a density of 15,000 cells/well into a 96 well-plate 24 h before a 48 h incubation. All measurements were conducted as technical triplicates and repeated in at least three independent cellular preparations (biological replicates). Cells were routinely tested for the absence of mycoplasma with the PCR Mycoplasma Test Kit (PanReac

AppliChem, Darmstadt, Germany).

2.2.3. Alkaline phosphatase assay

To evaluate the estrogenic activity, the transcriptional response of cells was evaluated by measuring the catalytic activity of alkaline phosphatase using a spectrophotometric readout (see below). The natural estrogen 17- β -estradiol (1 nM) was tested in parallel as positive control and vehicle solvent (1% DMSO) was used as negative control in accordance to Dellafiara and co-workers (Dellafiara et al., 2018). As an additional control and to confirm that the results of the assay arose from estrogenic stimuli, the most effective concentrations of atromentin was co-incubated with 1 μ M of the high affinity estrogen receptor antagonist ICI 182,780.

The alkaline phosphatase assay was conducted as previously described by Lehmann and co-workers (Lehmann, Wagner, & Metzler, 2006). 15,000 cells/well were seeded in 96-well plates and after 48 h of incubation, they were washed three times with PBS, and lysed thermally at -80 °C for 20 min. Cell lysates were then incubated at room temperature for five minutes, followed by addition of 50 μ l of ALP buffer (5 mM 4-nitrophenylphosphate, 1 M diethanolamine, 0.24 mM MgCl₂, pH 9.8) to each well (5 min). Measurements of absorbance (405 nm) to quantify enzymatic activity were performed every three minutes, for one hour, at 37 °C, on a PerkinElmer Victor^{3V} multiple plate reader. Alkaline phosphatase activity was calculated as the slope of the curve obtained by the measurements over one hour. Final results were normalized to the solvent control.

2.3. Recombinant production and purification of atromentin

A heterologous expression system in *A. oryzae* was developed for recombinant expression of the *P. involutus invA5* atromentin synthetase gene. The expression system bases on the previously described combination of the terrein biosynthesis regulator TerR and its terrein synthase target promoter *PterA* (Gressler, Hortschansky, Geib, & Brock, 2015). A construct containing the *terR* gene under control of the sugar inducible amylase promoter *PamyB* and the pyrithiamine resistance gene *ptrA* (Gressler et al., 2015) was used for transformation of *A. oryzae* RIB40. Strain OP12 containing a single full-length integration of the transcription factor construct was selected as expression platform strain. A synthetic version of the *P. involutus invA5* gene containing an N-terminal His-tag (Braesel et al., 2015) was provided by D. Hoffmeister (Friedrich-Schiller University Jena, Germany) and used as a template for amplification with oligonucleotides *invA5_Sm-X_fw* (5'-CAT CAC AGC ACC ATG GGC AGC AGC CAT CAT CAT CAT C-3') and *invA5_SM-X_rv* (5'-ATC ACT GCT GCC ATG GTT ACA GAC CAC GAG CTT CGA G-3') using Phusion Hot Start II polymerase (Thermo Scientific). The PCR product was fused by *in vitro* recombination with an *NcoI* restricted SM-X vector containing a phleomycin resistance cassette (Gressler et al., 2015) using the InFusion HD cloning kit (Takara). The resulting *invA5* expression plasmid was used for transformation of the OP12 strain and transformants were regenerated in the presence of 30 μ g/ml phleomycin. Independent transformants were screened for atromentin production and strain OP12_InvA5.1 was selected for up-scaled atromentin production. *Aspergillus* minimal medium (Gressler et al., 2015) containing 2% soluble starch as inducing carbon source and 20 mM glutamine as nitrogen source was used. Eight 50 ml cultures were inoculated with 1×10^6 conidia/ml and incubated for 42 h at 28 °C on a rotary shaker. The mycelium was removed by filtration over Miraclot filter gauze (Merck) and the combined culture filtrates were acidified with formic acid (0.2% final concentration). An XAD-16 resin was regenerated in methanol, extensively washed with water and added to the acidified culture filtrate. The mixture was shaken for 10 min at 150 rpm to allow binding of atromentin to the resin. The clear supernatant was discarded and atromentin was eluted by repeated addition of methanol. Purity of atromentin was analysed by HPLC chromatography over an Eclipse XDB-C18 column, 5 μ m, 4.6 \times 150 mm (Agilent) on a Dionex

UltiMate3000 HPLC (Thermo Fisher Scientific) as previously described (Geib & Brock, 2017). No other contaminating metabolite peaks were observed (Supporting materials, Fig. 1S). Purified atromentin (about 120 mg) was dried under reduced pressure and stored as dried compound until further use.

2.4. Statistical analysis

All experiments were performed at least in triplicate ($n \geq 3$; at least three independent biological replicates, each performed as technical triplicates). Data are expressed as the mean \pm standard error mean (SEM). Statistical analysis was performed using the Origin Pro 2016G software. The data was analysed by one-way ANOVA ($\alpha = 0.05$), followed by post hoc Fisher's LSD test ($\alpha = 0.05$).

3. Results and discussion

3.1. Overview of the computational target fishing workflow

The workflow presented in this study aims at assigning function to molecules of interest based on the physico-chemical similarities and mechanistic analogies with already characterized compounds. The rationale behind this approach relies on the principle that similar compounds may compete for the same biological targets. Accordingly, they may have a degree of analogy in initiating specific molecular events, as well as in eliciting similar biological effects (McKinney, Richard, Waller, Newman, & Gerberick, 2000). Once the reliability of the computational performance has been assessed, the *in silico* workflow presented in this study may serve as a first analytical screening tool to identify the possible activity of orphan compounds. In analogy to the hazard identification in the risk assessment process, the activity identification consists in describing qualitatively the biological effects that orphan compounds might have, without proving their actual incidence *in vivo*. Furthermore, when coupled with *in vitro* trials, it may provide activity characterization in terms of dose-effect response and mode of action. The overall workflow of the study is depicted in Fig. 2.

In this work, atromentin was used as a proof of concept. Atromentin 3D structure was used as template for a ligand-based virtual screening querying a database of small molecules with known activity and

already described biological targets. Then, the most similar compounds identified by the screening were inspected for the assigned biological targets prioritizing those related to either human macromolecules or pathways of sound pharmacological interest. Subsequently, the interaction with atromentin was assessed thoroughly at an atomistic level in docking studies. Then, *in vitro* experiments were performed to achieve activity characterization.

3.2. Computational results

3.2.1. Ligand-based virtual screening

The RCSB PDB repository (<http://www.rcsb.org>) (Berman et al., 2000) was used to generate the database of compounds analysed with the ligand-based virtual screening (the results are reported in Table 1S, Supporting material). The PDB archive is a unique worldwide public repository of information about the 3D structure of biological macromolecules. It contains more than 130,000 structures resolved mainly by X-ray crystallography, NMR spectroscopy and cryo-electron microscopy. Many macromolecules are in the bound state and therefore their structures are available along with the structure of more than 20,000 different low molecular weight compounds. The so defined “chemical components” groups a wide number of ligands *sensu stricto* (including enzyme substrates and inhibitors), metal ions and cofactors with known activity and well-described dynamics of target interaction. Using atromentin as a template (324.3 g/mol), all compounds with molecular weight ranging between 200 and 500 g/mol (15,248 entries in total) were used to carry out the ligand-based virtual screening. The screening was done using the FLAP software (see material and method for more details) and the output sorted according to the FLAP “distance score”, which is an overall estimate of the divergence of compounds from the template (atromentin in this case) in terms of physico-chemical properties (the lower the score the more similar the compounds are).

The RCSB PDB archive collects macromolecules from a wealth of organisms from different kingdoms. Therefore, all ligands not associated to either human macromolecules or pathways of sound pharmacological interest were not taken into account. As shown in Table 1S, the best scored compound among those related to human macromolecules was the ligand having PDB ID 1W3. It is a polyphenol-derivative compound in complex with the human carrier transthyretin.

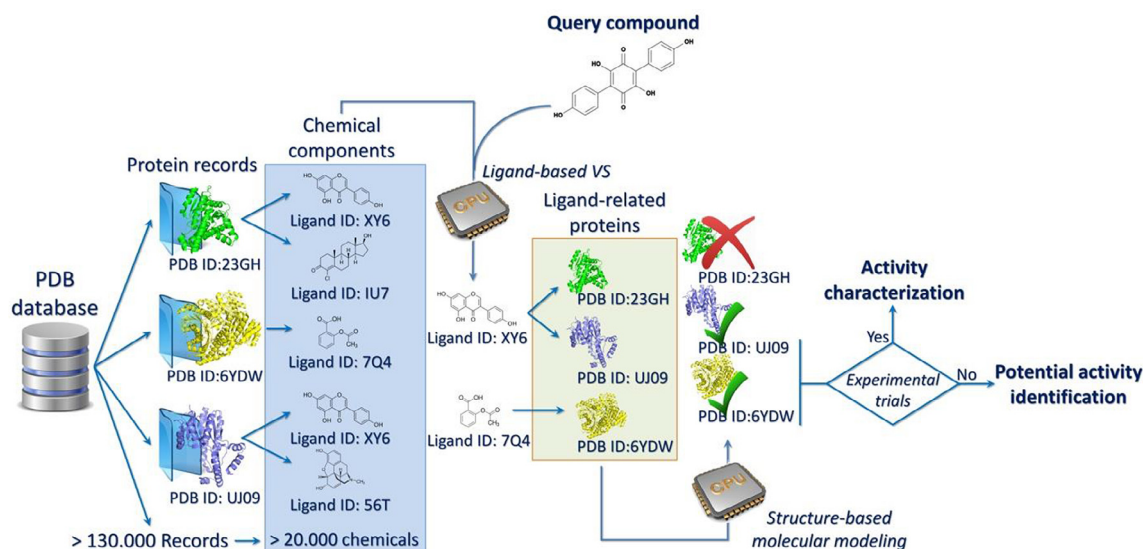


Fig. 2. Schematic representation of the workflow used in the target fishing study. The low-molecular weight compounds belonging to the so called “chemical components” repository of the RCSB PDB archive (<https://www.rcsb.org/>) are accounted for a ligand-based virtual screening study. This first-line screening aims at identifying compounds sharing a degree of physico-chemical similarity with the query compound atromentin. Each low-molecular weight compound occurs as ligand in at least one macromolecule-ligand complex. Therefore, once the most similar compounds are identified, the interaction between the respective macromolecular structures and atromentin is thoroughly investigated with docking studies. The prediction of the atromentin-target interaction may lead to the identification of a potential activity, while the experimental assessment may allow characterization of the biological activity.

However, the interaction between atromentin and transthyretin was not considered for further investigation as the binding to serum transporters can be reasonably expected as non-specific and it cannot be directly related to the onset of biological stimuli. The next most similar compound identified was the polyphenol genistein (PDB ID: GEN) (Fig. 1) found bound to ten protein-ligand complex structures. Among them, the human estrogen receptor isoforms (ER α and ER β) were considered with highest priority to further investigate the possible interaction with atromentin as: i) estrogenic compounds of food origin may be of high relevance for human health; ii) a relevant xenoestrogenic activity might be expected on the basis of the molecular similarity between atromentin and the synthetic estrogen diethylstilbestrol (Fig. 1); iii) the ligand-based screening highlighted a degree of similarity between atromentin and matairesinol (Table 1S), which is a well-described phytoestrogen (Kiyama, 2016). On this basis, the interaction between atromentin and both human ER α and ER β was further investigated in molecular modelling studies.

Moreover, the 17- β -hydroxysteroid dehydrogenase (17- β -HSD) from the fungus *Curvularia lunata* was also found among the proteins in the bound state with genistein. This enzyme can be used in medicinal chemistry studies in preliminary screenings for possible inhibitors of the human 17- β -HSD enzymes (Cassetta et al., 2017). In addition, genistein is also known to inhibit the human Type I 17- β -HSD enzymes (Blomquist, Lima, & Hotchkiss, 2005). Therefore, the interaction between atromentin and the fungal orthologous enzyme as well as the human Type I 17- β -HSD enzyme was assessed *in silico*.

It is worth to mention that many additional targets of interest could have been identified scrolling down the rank list of similar compounds. However, the systematic analysis of all possible targets requires huge computational resources and therefore was not considered in this proof of concept study. Therefore, potential interaction with additional targets not included in this work cannot be ruled out.

3.2.2. Docking studies

On the basis of the virtual screening results, the interaction between atromentin and some potential biological targets was further assessed by docking studies. As shown previously, docking scores may reliably estimate the thermodynamic favours of the host-guest complex formation correlating with the energy of binding, with the inhibitory activity of competitive inhibitors (e.g. Dellafiara et al., 2015;) and with the xenoestrogenic activity of low molecular-weight compounds (Dellafiara et al., 2018; Ehrlich et al., 2015). Nevertheless, a fit-for-purpose validation of procedural performances was done to assess the case-specific reliability. To this end, the capability to successfully compute a set of reference compounds in comparison to a benchmark ligand was tested for each target.

3.2.2.1. Estrogen receptors. The results of docking simulation on both the ER α and ER β are reported in Table 1. The endogenous ligand 17 β -estradiol, the polyphenol genistein and the well-known synthetic estrogen diethylstilbestrol were selected as reference compounds to test the performance of the procedure. Genistein was used as the benchmark for computing the relative activity of compounds. The procedure proved to be reliable as: i) it succeeded in calculating the binding architecture of the reference compounds (Fig. 2S); ii) reference compounds were correctly ranked for their relative potency in comparison to the benchmark compound (Table 1).

Atromentin showed in both ERs a binding architecture resembling that of the other compounds with a marked shape overlapping with the synthetic estrogen diethylstilbestrol (Fig. 3A). However, atromentin recorded the lowest scores among all the compounds tested in both ER isoform models pointing to a worse fitting into the ligand binding site. The pharmacophoric analysis of the ligand pocket and the comparison between the binding pose of atromentin and the mode of binding reported for the ER ligands provided a structural explanation. ER ligands need to interact with the two polar ends of the pocket (formed by

Glu353, Arg394 and His524) and have to satisfy the hydrophobic environment with hydrophobic groups (Spyrakakis & Cozzini, 2009). However, even though the phenolic groups of atromentin may engage the polar ends of the ERs pocket, the central benzoquinone moiety bears 4 polar groups that locally reduce the lipophilic characteristic of the molecule causing hydrophobic/hydrophilic interferences (Fig. 3B).

On the basis of these results, ERs were identified as putative targets of atromentin and a possible estrogenic activity could be expected accordingly. Nevertheless, on account of the low scores recorded in both ER isoform and the non-optimal fitting into the ERs, the interaction with the ERs can be considered as less favoured than that of the benchmark compound analysed. Therefore, a lower efficacy in triggering an ER-dependent stimulus can be expected, as further confirmed *in vitro* (see below).

3.2.2.2. 17- β -HSDs. According to the results of the virtual-screening, the interaction between atromentin and the fungal 17- β -HSD was investigated. In this respect, it has already been reported that the procedure used in this study may successfully estimate the inhibitory activity of competitive inhibitors (Dellafiara et al., 2015). Therefore, it may also succeed in estimating the possible inhibitory activity of atromentin. In order to assess the procedural performance, genistein and the two other polyphenols kaempferol and biochanin A were taken as reference compounds since both the geometry of binding and the inhibitory activity have already been assessed (Cassetta et al., 2017). Genistein was accounted as the benchmark compound. The computed binding geometry of reference compounds was in strong agreement with the crystallographic data collected so far (Fig. 3S). In addition, as shown in Table 2, reference compounds were correctly ranked for the relative activity in comparison to the benchmark compound genistein. On this basis, the procedure could be considered reliable in providing a plausible geometry of binding for atromentin and in estimating its potential relative activity in comparison to genistein.

As shown in Table 2, atromentin recorded a score close to that of genistein pointing to a comparable capability to fit into the enzyme pocket. Concerning the geometries of binding, the crystallographic data collected so far revealed a unique binding pose for genistein and kaempferol with the B ring directed toward the binding site entrance (Fig. 3C). Conversely, biochanin A may have two possible modes of arranging into the binding pocket: one retraces the mode of binding of genistein and kaempferol (the one predicted by the molecular modelling), while the other presents an opposite direction of the B ring that is more embedded into the binding site close to the nicotinamide moiety of the prosthetic group NADPH (Cassetta et al., 2017). This eventually suggests that polyphenols may have alternative modes in arranging within the enzyme binding site. Atromentin retraced the binding mode of genistein keeping the same π - π interaction with the side chain of Tyr212. However, the longer length of the chemical structure of atromentin caused a more pronounced sinking of the aromatic ring towards the bottom of the pocket engaging via hydrogen bond of the side chain of Tyr167 (Fig. 3D). In addition, atromentin satisfied the pharmacophoric fingerprint of the binding site, which consists in a central lipophilic environment with spaces able to receive hydrophilic groups on the two sides. Indeed, the central hydrophobic core of the molecule is embedded in the lipophilic space, while the polar groups are placed in the hydrophilic environment (Fig. 3E). On the basis of these results the interaction between atromentin and the fungal 17- β -HSD can be considered as possible and a certain degree of inhibitory activity can be expected accordingly. It is noteworthy however that the inhibitory activity of genistein towards the fungal enzyme is quite weak and therefore, on the basis of computational scores, a mild activity can be expected also for atromentin.

Subsequently, the interaction between atromentin and the human Type I 17- β -HSD was assessed in account of: i) the positive interaction between atromentin and the fungal orthologous; ii) the similarity found by the virtual screening between atromentin and genistein, which is a

Table 1
Results of docking simulation on ER α and ER β .

Compound	ER α			ER β		
	RCA (%) ^a	ERP ^b	Experimental potency rank ^{c,d}	RCA (%) ^a	ERP ^b	Experimental potency rank ^d
Genistein	100	/	3	100	/	3
17 β -estradiol (E2)	123.39 \pm 0.12	↑	1	113.05 \pm 0.17	↑	2
Diethylstilbestrol	117.23 \pm 0.10	↑	2	113.98 \pm 0.43	↑	1
Atromentin	80.09 \pm 0.23	↓	Untested	65.13 \pm 0.49	↓	Untested

^a RCA (Relative computed activity) indicates the percentage of relative computed activity of compounds in respect to the genistein taken as benchmark (100%; in bold). RCA values express the mean \pm SD of three calculations.

^b ERP (Expected relative potency) indicates the expected potency of compounds based on the computed scores in comparison to that the benchmark compound genistein. The symbols ↓ and ↑ indicate lower and higher activity, respectively.

^c Reference [Sonneveld et al. \(2006\)](#).

^d Reference [Schopfer et al. \(2002\)](#).

known inhibitor of the human Type I 17- β -HSD ([Schuster et al., 2008](#)). Genistein, the strong inhibitor 3-[[9 β ,14 β ,16 α ,17 α]-3,17-dihydroxyestra-1,3,5(10)-trien-16-yl]methyl]benzamide (PDB ID E2B) and flavanone were selected as reference compounds to assess the procedural performance. Genistein was accounted as the benchmark. As seen for the fungal enzyme, the procedure succeeded in calculating the geometry of binding ([Fig. S2](#)) and in ranking the reference compounds in accordance to the inhibitory activity reported so far ([Table 2](#)).

As shown in [Table 2](#), atromentin recorded a score higher than

genistein pointing to an overall better fitting into the pocket. The pharmacophoric fingerprint of the pocket was similar to that of the fungal enzyme (i.e. a central lipophilic environment with hydrophilic regions on the sides), albeit the hydrophilic regions were found to be less extended. The geometry of binding of genistein into the human enzymes has not been resolved yet. However, in accordance to the geometry of binding proposed for polyphenols by Schuster and co-workers ([Schuster et al., 2008](#)), genistein was found contacting via hydrogen bonds Glu284 with the hydroxyl groups on the A ring and the

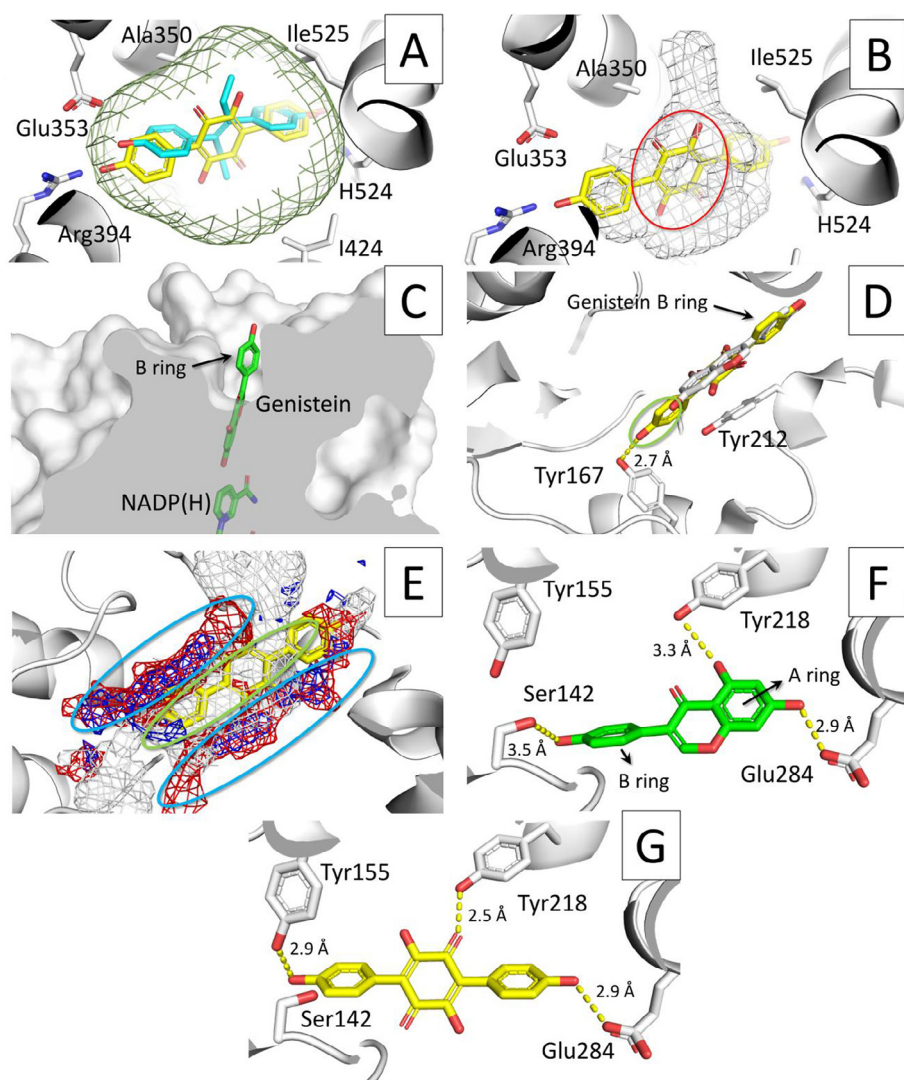


Fig. 3. Binding geometry of atromentin into the ER pocket (A and B), and atromentin and genistein into fungal and human 17- β -HSDs (C–G). Due to the high conservation between ER isoforms, only the interaction with the ER α pocket is shown. Proteins are represented in cartoon (A, B, D–G) or in cut surface (C), while ligands and amino acids side chains are represented in sticks. Hydrogen bonds are indicated with yellow dashed lines. **A.** Binding pose of atromentin (yellow) overlapping diethylstilbestrol (cyan). The green mesh represents the shape of the binding site. **B.** Binding pose of atromentin. The white mesh indicates the hydrophobic environment of the pocket. The red circle highlights the unfavourable arrangement of the polar core of atromentin. **C.** Crystallographic pose of genistein into the fungal enzyme (PDB code 4FJ1; ([Cassetta et al., 2017](#))). **D.** Computational pose of atromentin (yellow) into the fungal enzyme superimposed to the crystallographic pose of genistein (white). The ring indicates the molecular region sinking towards the bottom of the binding site. **E.** Binding pose of atromentin in comparison to the pharmacophoric fingerprint of the binding site. White, red and blue contours identify regions sterically and energetically favourable for hydrophobic, H-bond acceptors and H-bond donor groups, respectively. Blue and green rings indicate the position of the polar and hydrophobic regions of atromentin, respectively. **F.** Computed architecture of genistein. **G.** Computed architecture of atromentin. (For interpretation of the references to colour in this figure legend, the reader is referred to the web version of this article.)

Table 2
Results of docking simulation on 17- β -HSD enzymes from *Curvularia lunata* and *Homo sapiens*.

17- β -HSD <i>Curvularia lunata</i>			
Compound	RCA (%) ^a	ERP ^b	Experimental potency rank ^c
Genistein	100	/	3
Kaempferol	107.71 \pm 0.83	↑	1
Biochanin A	101.82 \pm 0.40	↑	2
Atromentin	99.85 \pm 0.84	↑↓	Untested
Type 1 17- β -HSD <i>Homo sapiens</i>			
Compound	RCA (%) ^a	ERP ^b	Experimental potency rank ^{d,e}
Genistein	100	/	2
E2B ligand	156.93 \pm 0.19	↑	1
Flavanone	85.58 \pm 0.63	↓	3
Atromentin	102.48 \pm 0.18	↑	Untested

^a RCA (Relative computed activity) indicates the percentage of relative computed activity of compounds in respect to the known inhibitor genistein taken as reference (100%; in bold). RCA values express the mean \pm SD of three calculations.

^b ERP (Expected relative potency) indicates the expected potency of compounds based on the computed scores in comparison to that of the known inhibitor genistein taken as benchmark. The symbols ↓ and ↑ indicates lower and higher activity, respectively.

^c Reference Cassetta et al. (2017).

^d Reference Schuster et al. (2008)

^e Reference Laplante, Cadot, Fournier, and Poirier (2008).

Ser142 with the hydroxyl group on the B ring (Fig. 3F). The consistence with the geometry of binding previously reported may strengthen further the reliability of the predicted geometries. Also an additional contact with Tyr218 was found, while the aromatic parts were arranged into the lipophilic environment of the pocket. Similar to genistein, atromentin engaged via hydrogen bonds with Glu284 and Tyr218, but not Ser142. In addition, as seen in the fungal enzyme, the more pronounced sinking into the pocket allowed atromentin to contact Tyr155 via hydrogen bonding (Fig. 3G). Also in this case, the hydrophobic aromatic scaffolds were found to be embedded in the lipophilic environment, while the polar groups were found mainly arranged within a

hydrophilic environment. Therefore, atromentin succeeded in fitting the pharmacophoric requirements of the Type I human 17- β -HSDs pocket.

Taking into account the computational score and the pharmacophoric fitting into the enzyme pocket, the interaction between the human Type I 17- β -HSD enzyme and atromentin can be considered as possible. A degree of inhibitory activity can be hypothesized accordingly. In particular, a higher inhibitory activity than genistein might be hypothesized on the basis of the higher score recorded. It is worth to note that genistein already has a good inhibitory activity towards the human Type I 17- β -HSD in comparison to the other polyphenols tested (Poirier, 2003; Schuster et al., 2008). Notably, the human Type 1 17- β -HSD is a relevant enzyme in human physiology as it plays critical role in balancing the conversion of estrone to 17 β -estradiol and *vice versa* (Mazumdar et al., 2009). Along with the other human isoforms, Type 1 17- β -HSD has been accounted in drug development for the therapeutic treatment of a number of hydroxysteroid-sensitive pathologies (Poirier, 2003). Therefore, the applied workflow identified the possible inhibitory activity towards Type 1 17- β -HSD as an activity to be tested with priority in further studies to deepen the possible biological roles of atromentin.

3.3. Experimental assessment of estrogenic activity

The *in silico* prediction of the possible estrogenic activity of atromentin was supported by an *in vitro* assessment of estrogenicity with a reporter gene assay in Ishikawa cells using the estrogenic impact on alkaline phosphatase expression as read-out. In particular, the dose-response activity of atromentin was assessed at concentrations ranging from 0.05 to 250 μ M and compared to that of the benchmark compound genistein at concentrations ranging from 0.001 to 1 μ M. The activity of the endogenous ligand 17 β -estradiol (1 nM) was taken as a reference. Both atromentin and genistein showed a dose-response effect (Fig. 4A). However, no significant activity for atromentin was detected below 100 μ M, while genistein showed significant response starting from 0.05 μ M ($P < 0.001$). In addition, the estrogen receptor-dependent activity of atromentin was tested by co-incubating the most effective concentration with the ER antagonist ICI 182,780 (1 μ M). As shown in Fig. 4B, the co-incubation was able to significantly suppress the activity of atromentin ($P < 0.001$) supporting the ER-dependent mechanism of action identified by the *in silico* study. On the basis of this result, the

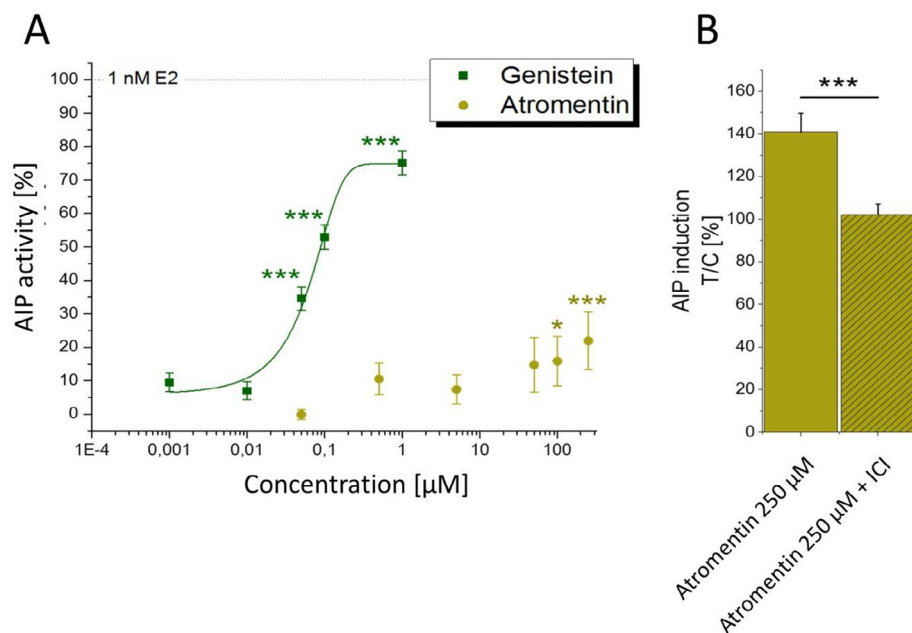


Fig. 4. Estrogenic activity of atromentin assessed *in vitro*. **A.** Estrogenic activity of atromentin in comparison to genistein as measured after 48 h of incubation with the AIP assay in Ishikawa cells. The graph shows the increase of AIP induction as mean values + SEM of at least 4 independent experiments related to the effect of the positive control (1 nM E2), which was set to 100%. Significant differences to the lowest applied concentration of the respective compound were calculated by one-way ANOVA, followed by Fisher's LSD post-hoc testing, and are indicated with “*” ($P < 0.05$), “***” ($P < 0.01$) or “****” ($P < 0.001$). **B.** AIP results for 250 μ M atromentin, incubated with and without 1 μ M ICI 182,780. Results are expressed as means + SEM of at least 4 independent experiments. The significant difference between those results, which proves its ER-dependency of the observed inductive effect, was calculated by Student's *t*-test ($P < 0.001$).

mild estrogenic activity of atromentin *via* the ER-dependent mechanism found *in silico* was confirmed *in vitro*.

4. Conclusions

A target fishing study using ligand-based virtual screening and structure-based analysis, coupled with *in vitro* trials, has been presented. In particular, once the reliability of the computational procedure was assessed, the workflow allowed the identification of potential activities for further testing. However, when coupled with *in vitro* experiments, the procedure may also provide an activity characterization in terms of dose-response effects. The analysis of the orphan fungal secondary metabolite atromentin was selected as a proof of principle. Ligand-based screening identified several putative biological targets and the interaction with some of those relevant for human health had been investigated thoroughly with docking studies. According to the computational results, estrogen receptors and 17- β -HSD were identified as possible relevant targets of atromentin. Therefore, in the framework of activity identification, degrees of estrogenicity via ERs activation and inhibition of 17- β -HSD could be expected. The computational data on estrogenicity were supported by the *in vitro* assessment using an alkaline phosphatase activity assay in Ishikawa cells, which confirmed the weak potency of atromentin. Nevertheless, in spite of the mild activity observed, broader effects on the enzymes that regulate estrogen production cannot be excluded on account of the results obtained for 17- β -HSDs. Therefore, in the light of deepening possible biological/toxic roles of atromentin in living organisms, the effects on estrogen production and regulation, along with those on the estrogen-mediated responses, need to be prioritised for investigation.

In addition, the results collected proved the procedure reliable in assigning biological functions. Accordingly, hybrid *in silico/in vitro* target fishing studies have been shown to be a valuable tool for investigating the unexpected activity of molecules of food origin, as well as for assigning possible biological targets to orphan compounds. Therefore, we propose this approach as a first-line analytical tool to widen the current understanding of the bioactive/toxic composition of food constituents.

Acknowledgements

The study was partially supported by Fondazione Cariparma, under TeachInParma Project. The authors kindly acknowledge Prof. Gabriele Cruciani (University of Perugia, Italy) for the use of FLAP software (<https://www.moldiscovery.com/>) and Prof. Dirk Hoffmeister (Friedrich Schiller University, Jena) for provision of the synthetic version of the *invA5* gene.

Conflict of interest

The authors declare no conflict of interest.

Appendix A. Supplementary data

Supplementary data associated with this article can be found, in the online version, at <https://doi.org/10.1016/j.foodchem.2018.07.027>.

References

Baroni, M., Cruciani, G., Sciabola, S., Perruccio, F., & Mason, J. S. (2007). A common reference framework for analyzing/comparing proteins and ligands. Fingerprints for Ligands and Proteins (FLAP): Theory and application. *Journal of Chemical Information and Modeling*, 47(2), 279–294.

Berman, H. M., Westbrook, J., Feng, Z., Gilliland, G., Bhat, T. N., Weissig, H., ... Bourne, P. E. (2000). The protein data bank. *Nucleic Acids Research*, 28(1), 235–242.

Blomquist, C. H., Lima, P. H., & Hotchkiss, J. R. (2005). Inhibition of 3 α -hydroxysteroid dehydrogenase (3 α -HSD) activity of human lung microsomes by genistein, daidzein, coumestrol and C(18)-, C(19)- and C(21)-hydroxysteroids and ketosteroids. *Steroids*, 70(8), 507–514.

Braesel, J., Götze, S., Shah, F., Heine, D., Tauber, J., Hertweck, C., ... Hoffmeister, D. (2015). Three redundant synthetases secure redox-active pigment production in the basidiomycete *Paxillus involutus*. *Chemistry & Biology*, 22(10), 1325–1334.

Brewer, D., Jen, W. C., Jones, G. A., & Taylor, A. (1984). The antibacterial activity of some naturally occurring 2,5-dihydroxy-1,4-benzoquinones. *Canadian Journal of Microbiology*, 30(8), 1068–1072.

Carosati, E., Sciabola, S., & Cruciani, G. (2004). Hydrogen bonding interactions of covalently bonded fluorine atoms: From crystallographic data to a new angular function in the GRID force field. *Journal of Medicinal Chemistry*, 47(21), 5114–5125.

Cassetta, A., Stojan, J., Krastanova, I., Kristan, K., Brunskole Švegelj, M., Lamba, D., & Lanišnik Rižner, T. (2017). Structural basis for inhibition of 17 β -hydroxysteroid dehydrogenases by phytoestrogens: The case of fungal 17 β -HSDcl. *The Journal of Steroid Biochemistry and Molecular Biology*, 171, 80–93.

Cereto-Massagué, A., Ojeda, M. J., Valls, C., Mulero, M., Pujadas, G., & Garcia-Vallve, S. (2015). Tools for *in silico* target fishing. *Methods*, 71, 98–103.

Chaudhari, R., Tan, Z., Huang, B., & Zhang, S. (2017). Computational polypharmacology: A new paradigm for drug discovery. *Expert Opinion on Drug Discovery*, 12(3), 279–291.

Delavan, B., Roberts, R., Huang, R., Bao, W., Tong, W., & Liu, Z. (2017). Computational drug repositioning for rare diseases in the era of precision medicine. *Drug Discovery Today* in press.

Dellaflora, L., Dall'Asta, C., & Galaverna, G. (2018). Toxicodynamics of mycotoxins in the framework of food risk assessment-an *in silico* perspective. *Toxins*, 10(2), E52.

Dellaflora, L., Galaverna, G., & Dall'Asta, C. (2017). An *in silico* perspective on the toxicodynamic of tetrodotoxin and analogues – A tool for supporting the hazard identification. *Toxicol*, 138, 107–118.

Dellaflora, L., Galaverna, G., Dall'Asta, C., & Cozzini, P. (2015). Hazard identification of cis/trans-zearalenone through the looking-glass. *Food and Chemical Toxicology*, 86, 65–71.

Dellaflora, L., Marchetti, M., Spyrikis, F., Orlandi, V., Campanini, B., Cruciani, G., ... Mozzarelli, A. (2015). Expanding the chemical space of human serine racemase inhibitors. *Biorganic & Medicinal Chemistry Letters*, 25(19), 4297–4303.

Dellaflora, L., Warth, B., Schmidt, V., Del Favero, G., Mikula, H., Fröhlich, J., & Marko, D. (2018). An integrated *in silico/in vitro* approach to assess the xenoestrogenic potential of Alternaria mycotoxins and metabolites. *Food Chemistry*, 248, 253–261.

Ehrlich, V. A., Dellaflora, L., Mollergues, J., Dall'Asta, C., Serrant, P., Marin-Kuan, M., ... Cozzini, P. (2015). Hazard assessment through hybrid *in vitro/in silico* approach: The case of zearalenone. *ALTEX*, 32(4), 275–286.

Geib, E., & Brock, M. (2017). ATNT: An enhanced system for expression of polycistronic secondary metabolite gene clusters in *Aspergillus niger*. *Fungal Biology & Biotechnology*, 4, 13.

Gressler, M., Hortschansky, P., Geib, E., & Brock, M. (2015). A new high-performance heterologous fungal expression system based on regulatory elements from the *Aspergillus terreus* terrein gene cluster. *Frontiers in Microbiology*, 6, 184.

Hu, L., & Liu, J. K. (2003). p-Terphenyls from the basidiomycete *Thelephora aurantiotincta*. *Zeitschrift für Naturforschung*, 58(5–6), 452–454.

Hühner, E., Backhaus, K., Kraut, R., & Li, S. M. (2018). Production of α -keto carboxylic acid dimers in yeast by overexpression of NRPS-like genes from *Aspergillus terreus*. *Applied Microbiology and Biotechnology*, 102(4), 1663–1672.

Jung, H. J., & Kwon, H. J. (2015). Target deconvolution of bioactive small molecules: The heart of chemical biology and drug discovery. *Archives of Pharmacological Research*, 38(9), 1627–1641.

Khanna, J. M., Malone, M. H., Euler, K. L., & Brady, L. R. (1965). Atromentin, anticoagulant from *Hydnellum diabolus*. *Journal of Pharmaceutical Sciences*, 54(7), 1016–1020.

Kim, J. H., & Lee, C. H. (2009). Atromentin-induced apoptosis in human leukemia U937 cells. *Journal of Microbiology and Biotechnology*, 19(9), 946–950.

Kiyama, R. (2016). Biological effects induced by estrogenic activity of lignans. *Trends in Food Science & Technology*, 54, 186–196.

Laplante, Y., Cadot, C., Fournier, M. A., & Poirier, D. (2008). Estradiol and estrone C-16 derivatives as inhibitors of type 1 17 β -hydroxysteroid dehydrogenase: Blocking of ER + breast cancer cell proliferation induced by estrone. *Biorganic & Medicinal Chemistry*, 16(4), 1849–1860.

Lehmann, L., Wagner, J., & Metzler, M. (2006). Estrogenic and clastogenic potential of the mycotoxin alternariol in cultured mammalian cells. *Food and Chemical Toxicology*, 44(3), 398–408.

Mazumdar, M., Fournier, D., Zhu, D. W., Cadot, C., Poirier, D., & Lin, S. X. (2009). Binary and ternary crystal structure analyses of a novel inhibitor with 17 β -HSD type 1: A lead compound for breast cancer therapy. *The Biochemical Journal*, 424(3), 357–366.

McKinney, J. D., Richard, A., Waller, C., Newman, M. C., & Gerberick, F. (2000). The practice of structure activity relationships (SAR) in toxicology. *Toxicological Sciences*, 56(1), 8–17.

Möcklinghoff, S., Rose, R., Carraz, M., Visser, A., Ottmann, C., & Brunsvelde, L. (2010). Synthesis and crystal structure of a phosphorylated estrogen receptor ligand binding domain. *Chembiochem*, 11(16), 2251–2254.

NCBI. PubChem Compound Database (<https://pubchem.ncbi.nlm.nih.gov>) CID=99148; Last database access 7th March 2018.

Ngoc Quang, D., Hashimoto, T., Hitaka, Y., Tanaka, M., Nukada, M., Yamamoto, I., & Asakawa, Y. (2003). Thelephantins D-H: Five p-terphenyl derivatives from the inedible mushroom *Thelephora aurantiotincta*. *Phytochemistry*, 63(8), 919–924.

Phillips, C., Roberts, L., Schade, M., Bazin, R., Bent, A., Davies, N., ... Irving, S. (2011). Design and structure of stapled peptides binding to estrogen receptors. *Journal of the American Chemical Society*, 133(25).

Poirier, D. (2003). Inhibitors of 17 β -hydroxysteroid dehydrogenases. *Current Medicinal Chemistry*, 10, 453–477.

Rather, I. A., Koh, W. Y., Paek, W. K., & Lim, J. (2017). The sources of chemical

- contaminants in food and their health implications. *Frontiers in Pharmacology*, 8, 830.
- Scafuri, B., Varriale, A., Facchiano, A., D'Auria, S., Raggi, M. E., & Marabotti, A. (2017). Binding of mycotoxins to proteins involved in neuronal plasticity: A combined in silico/wet investigation. *Scientific Reports*, 7(1), 15156.
- Scalbert, A., Brennan, L., Manach, C., Andres-Lacueva, C., Dragsted, L. O., Draper, J., ... Wishart, D. S. (2014). The food metabolome: A window over dietary exposure. *The American Journal of Clinical Nutrition*, 99(6), 1286–1308.
- Schopfer, U., Schoeffter, P., Bischoff, S. F., Nozulak, J., Feuerbach, D., & Floersheim, P. (2002). Toward selective ERbeta agonists for central nervous system disorders: Synthesis and characterization of aryl benzthiophenes. *Journal of Medicinal Chemistry*, 45(7), 1399–1401.
- Schuster, D., Nashev, L. G., Kirchmair, J., Laggner, C., Wolber, G., Langer, T., & Odermatt, A. (2008). Discovery of nonsteroidal 17beta-hydroxysteroid dehydrogenase 1 inhibitors by pharmacophore-based screening of virtual compound libraries. *Journal of Medicinal Chemistry*, 51(14), 4188–4199.
- Sonneveld, E., Riteco, J. A., Jansen, H. J., Pieterse, B., Brouwer, A., Schoonen, W. G., & van der Burg, B. (2006). Comparison of in vitro and in vivo screening models for androgenic and estrogenic activities. *Toxicological Sciences*, 89(1), 173–187.
- Spyrakakis, F., & Cozzini, P. (2009). How computational methods try to disclose the estrogen receptor secrecy—modeling the flexibility. *Current Medicinal Chemistry*, 16(23), 2987–3027.
- Vejdovszky, K., Schmidt, V., Warth, B., & Marko, D. (2016). Combinatory estrogenic effects between the isoflavone genistein and the mycotoxins zearalenone and alternariol in vitro. *Molecular Nutrition & Food Research* in press.

Supporting materials

Hybrid *in silico/in vitro* target fishing to assign function to “orphan” compounds of food origin – the case of the fungal metabolite atromentin

Luca Dellafiora¹, Georg Aichinger², Elena Geib³, Leyre Sánchez-Barrionuevo⁴, Matthias Brock³,
David Cánovas⁴, Chiara Dall’Asta¹, Doris Marko²,

¹ Department of Food and Drug, University of Parma, Via G.P. Usberti 27/A, 43124 Parma, Italy

² Department of Food Chemistry and Toxicology, Faculty of Chemistry, University of Vienna,
Währinger Str. 38, 1090 Vienna, Austria

³ Department of Genetics, Faculty of Biology, University of Sevilla, 41012, Spain

⁴ Fungal Genetics and Biology Groups, School of Life Sciences, University of Nottingham,
University Park, NG7 2RD Nottingham, UK

Corresponding author: Chiara Dall’Asta

Department of Food and Drug, University of Parma, Via G.P. Usberti 27/A, 43124
Parma, Italy

Table 1S. Results of the ligand-based virtual screening

Distance score	Ligand ID	Ligand name	Related structure ID	
0.12	1G4	(3S,6S)-3,6-bis(4-hydroxybenzyl)piperazin-2-one	4IPS	Cytochrome P450 from <i>Mycobacterium tuberculosis</i>
0.13	69T	4-(5-((4-hydroxyphenyl)amino)-1H-pyrazol-3-yl)phenol	5IBJ	Cytochrome P450 from <i>M. tuberculosis</i>
0.14	KRA	1-(4-hydroxyphenyl)-4-phenyl-butane-2,3-dione	Record not available	---
0.14	1W3	7-hydroxy-3-[(E)-2-(4-hydroxy-3,5-dimethylphenyl)ethenyl]-4-methyl-2H-chromen-2-one	4KY2	Transthyretin complex from <i>Homo sapiens</i>
0.15	1G7	(3S,6S)-3-(3,4-dihydroxybenzyl)-6-(4-hydroxybenzyl)piperazine-2,5-dione	4IPW	Cytochrome P450 from <i>M. tuberculosis</i>
0.16	GEN	Genistein	5KDA	Aromatic prenyltransferase from <i>Aspergillus terreus</i>
			5AUZ	Death-associated protein kinase 1 from <i>H. sapiens</i>
			5AV4	Death-associated protein kinase 1 from <i>H. sapiens</i>
			<u>4FJ1</u>	<u>17-β-HSD from <i>Curvularia lunata</i></u>
			3KGT	Transthyretin complex from <i>H. sapiens</i>
			3KGU	Transthyretin complex from <i>H. sapiens</i>
			<u>2QA8</u>	<u>ERα from <i>H. sapiens</i></u>
			<u>1X7J</u>	<u>ERβ from <i>H. sapiens</i></u>
			<u>1X7R</u>	<u>ERα from <i>H. sapiens</i></u>
			<u>1QKM</u>	<u>ERβ from <i>H. sapiens</i></u>
0.16	1CQ	4,4'-{3-[(4-hydroxyphenyl)amino]-1H-pyrazole-4,5-diyl}diphenol	4KTL	Cytochrome P450 from <i>M. tuberculosis</i>
0.16	MAX	Matairesinol	2BGM	Secoisolariciresinol Dehydrogenase from <i>Podophyllum peltatum</i>
0.16	RP4	(1R,4R,5R)-1,4,5-trihydroxy-3-(3-phenylsulfanylphenyl)cyclohex-2-ene-1-carboxylic acid	2CJF	Type II dehydroquinase from <i>Streptomyces coelicolor</i>
0.16	64O	N-(4-{{[4'-(carbamoylamino)-6-hydroxybiphenyl-3-yl]oxy}-3,5-dichlorophenyl}propanamide	5HK9	CFTR inhibitory factor from <i>Pseudomonas aeruginosa</i>

Note → The ten top scored ligands are shown. The records related to either relevant macromolecules and pathway of sound pharmacological interest are underlined

Purified atromentin from heterologous *invA5* expression in *Aspergillus oryzae* OP12.

An HPLC analysis was performed to test the purity of atromentin purified from the culture broth of *A. oryzae* OP12. The methanolic fraction was loaded on an Eclipse XDB-C18 column and the absorption spectrum was recorded at 254 nm. As shown in Figure 1S, atromentin elutes at 9.6 min and shows its typical UV/Vis spectrum. Only very minor impurities were observed and based on this analysis the fraction was judged as $\geq 99\%$ pure.

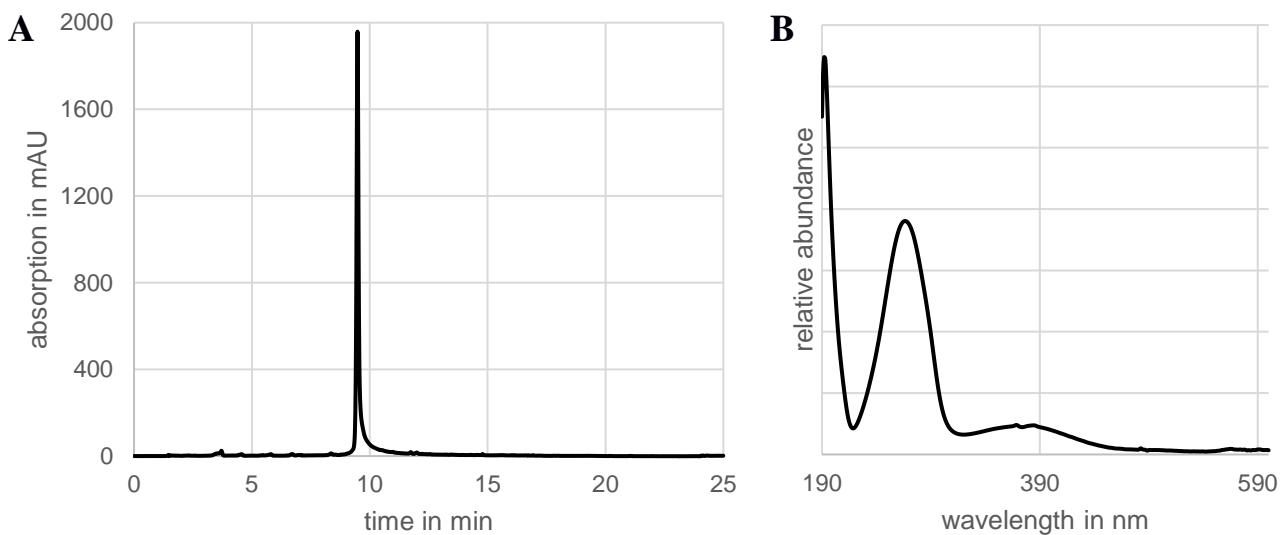


Figure 1S: HPLC analysis of purified atromentin by reverse phase chromatography over an Eclipse XDB-C18 column. (A) Chromatogram recorded at 254 nm. (B) UV/Vis spectrum of atromentin.

Comparison between computational geometries of binding and crystallographic poses of compounds

To check the procedural reliability in predicting the geometries of binding, the computed poses were compared to those obtained in crystallographic studies. As shown in Figure 2S and 3S, all calculated geometries of binding were found to be consistent with the crystallographic poses, confirming the procedural reliability.

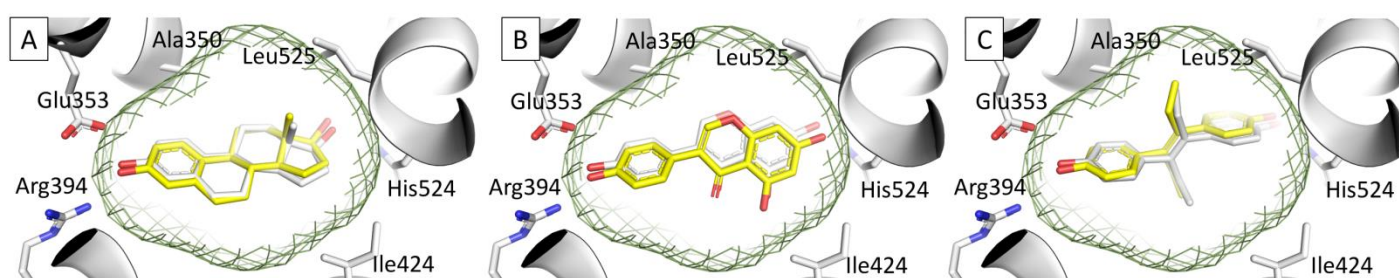


Figure 2S. Comparison between the computational geometries of binding (yellow) and the crystallographic poses (white) of 17 β -estradiol (A), genistein (B) and diethylstilbestrol (C) into the ER ligand binding pocket. All ligands and side chain residues are represented in stick while the protein is shown in cartoon. The green mesh retraces the shape of the binding site. The crystallographic pose of ligands derived from the crystallographic ER α structure with PDB code 2YJA. The PDB codes used for comparison were 2YJA [24], 1X7R [51] and 3ERD [52], respectively.

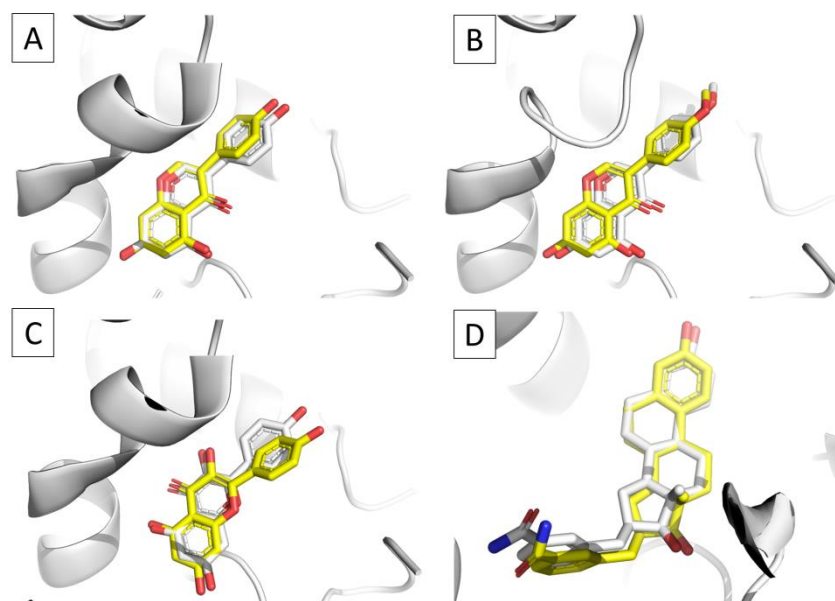


Figure 3S. Comparison between the computational geometries of binding (yellow) and the crystallographic poses (white) of genistein (A), biochanin A (B) and kaempferol (C) into the pocket of 17-β-HSD enzymes from *Curvularia lunata* (A, B and C) or *Homo sapiens* (D). All ligands are shown in sticks while proteins are represented in cartoon. The crystallographic pose of ligands derived from the crystallographic 17-β-HSD structures with PDB codes 4FJ1, 4FJ2, 3QWH [26] and 3HB5 [27], respectively

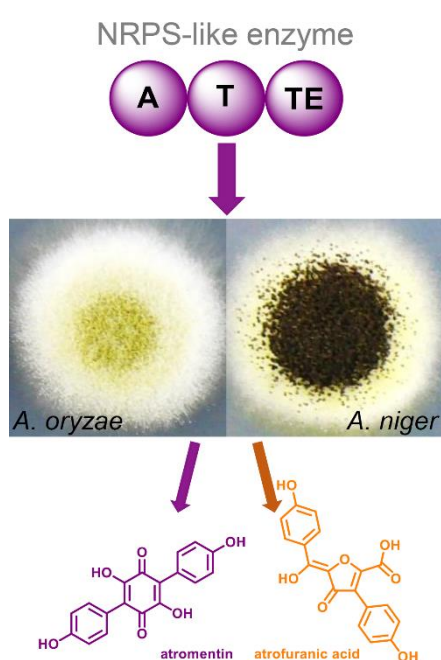
Reference not reported in the main text

51. Manas ES, Xu ZB, Unwalla RJ, Somers WS. Understanding the selectivity of genistein for human estrogen receptor-beta using X-ray crystallography and computational methods. *Structure*. 2004 Dec;12(12):2197-207
52. Shiau AK, Barstad D, Loria PM, Cheng L, Kushner PJ, Agard DA, Greene GL. The structural basis of estrogen receptor/coactivator recognition and the antagonism of this interaction by tamoxifen. *Cell*. 1998 Dec 23;95(7):927-37

Cross-chemistry leads to product diversity from atromentin synthetases in aspergilli from section *Nigri*

Elena Geib, Florian Baldeweg, Maximilian Doerfer, Markus Nett and Matthias Brock

(2018) Cell Chemical Biology, accepted



Summary of the manuscript: NRPS-like enzymes have been neglected for a long time but produce a fascinating variety of different compounds. Little is known about the catalytic properties of this type of secondary metabolite synthetases. Here, we aimed in a deeper understanding of the chemistry performed by thioesterase domains from NRPS-like enzymes. Site-directed mutagenesis led to the identification of essential amino acid residues in aspulvinone E synthetase and domain-swapping experiments converted an aspulvinone E synthetase into an atromentin synthetase. However, a close phylogenetic relationship of enzymes was necessary for successful conversion. Unexpectedly, expression of atromentin

synthetases in *Aspergillus niger* failed to produce atromentin under *in vivo* conditions, but produced the novel compound atrofuranic acid, whereby *in vitro* assays from purified enzymes confirmed atromentin formation. This so-called cross chemistry effect induced by the host physiology was not only observed in *A. niger*, but also in *Aspergillus brasiliensis* from section *Nigri*. In contrast, *Aspergillus oryzae* produced atromentin, indicating that the physiology of expression platform strains influences product formation from NRPS-like enzymes.

Contribution: 75% of practical work, major contribution to manuscript preparation

Generation of expression constructs and strains, site-directed mutagenesis, domain swapping experiments and construction of a URA blaster cassette. Protein purification and *in vitro* assays. Transfer of the heterologous expression system into *Aspergillus oryzae* (OP12). Inactivation of *pyrG* in ATNT16 and OP12. Extraction, purification and analysis of secondary metabolites by HPLC, HR-ESI-MS and NMR.

Cross-chemistry leads to product diversity from atromentin synthetases in *Aspergilli*
from section *Nigri*

Elena Geib¹, Florian Baldeweg², Maximilian Doerfer², Markus Nett³, Matthias Brock^{1#}

¹ Fungal Genetics and Biology, School of Life Sciences, University of Nottingham, University Park, NG7 2RD Nottingham, UK

² Department of Pharmaceutical Microbiology at the Leibniz Institute for Natural Product Research and Infection Biology – Hans Knoell Institute, Friedrich-Schiller-University Jena, Adolf-Reichwein Straße 23a, 07745 Jena, Germany

³ Department of Biochemical and Chemical Engineering, TU Dortmund University, Emil-Figge-Straße 66, 44227 Dortmund, Germany

#Corresponding author:

E-mail: Matthias.brock@nottingham.ac.uk

Phone: +44 (0)115 951 3230

Running title: Cross-chemistry in *Aspergillus niger*

Key words: Atromentin, Aspulvinone E, *Aspergillus oryzae*, NRPS-like, thioesterase

Summary

Nonribosomal peptide synthetase (NRPS)-like enzymes catalyse the non-oxidative homodimerisation of aromatic α -keto acids, but the exact reaction mechanism is unknown. The furanone-forming thioesterase domain of the *Aspergillus terreus* aspulvinone E synthetase MelA displays a predicted quinone-forming motif, whereby its catalytic triad contains an essential cysteine indicating an unusual thioester intermediate. To convert MelA into a quinone-forming atromentin synthetase its thioesterase domain was replaced with that from a *Paxillus involutus* or *A. terreus* atromentin synthetase. Phylogenetic proximity of donor and acceptor seems important as only replacement with the *A. terreus* thioesterase was functional. Heterologous expression of atromentin synthetases in *Aspergillus niger* and *Aspergillus oryzae* revealed host-dependent product formation whereby cross-chemistry directed atromentin biosynthesis in *A. niger* towards atrofuranic acid. Screening of aspergilli from section *Nigri* identified an atromentin synthetase in *Aspergillus brasiliensis* that produced atrofuranic acid in the homologous host. Therefore, cross-chemistry on quinone cores appears common to section *Nigri*.

Introduction

Non-ribosomal peptide synthetase (NRPS)-like enzymes are widespread in the fungal kingdom, and even closely related species seem to contain a large number of non-homologous enzymes. For instance, *Aspergillus terreus* contains 15 NRPS-like genes (van Dijk, Guo and Wang, 2016) and 14 NRPS-like genes are found in *Aspergillus nidulans* (Yeh *et al.*, 2012). Corresponding to other NRPSs, NRPS-like enzymes are composed of several catalytic domains. They feature an adenylation (A), thiolation (T) and thioesterase (TE) or, alternatively, a reductase (R) domain, but lack the condensation domain (C) of prototypical NRPSs (van Dijk, Guo and Wang, 2016). Therefore, rather than forming peptide bonds from individual amino acids, NRPS-like enzymes generally catalyse the condensation of two identical α -keto acids. For a long time, the importance of NRPS-like enzymes in the production of secondary metabolites had been neglected and biochemical information on their catalytic properties were rare (Schneider *et al.*, 2007). However, in recent years it has been shown that NRPS-like enzymes, either alone or embedded in gene clusters, produce metabolites important for fungal development and environmental competition. The first fungal product confirmed to derive from a gene cluster containing an NRPS-like enzyme was terrequinone A (**1**) (for metabolite structures refer to **Fig. 1**) from *Aspergillus nidulans* (Bok *et al.*, 2006; Balibar, Howard-Jones and Walsh, 2007). While the direct contribution of terrequinone A to environmental competition has not been described yet, terrequinone A exhibits cytotoxic activity (He *et al.*, 2004). The γ -butyrolactones from *A. terreus* are also formed by NRPS-like enzymes (Guo *et al.*, 2013) and have been shown to stimulate sporulation in submerged cultures and increase the production of secondary metabolites such as lovastatin (Schimmel *et al.*, 1998). In addition, butyrolactone I (**2**) can scavenge reactive oxygen species and acts as inhibitor of α -glucosidase, which is an important feature for the treatment of type 2 diabetes (Dewi *et al.*, 2012). Aspulvinone E (**3**) is the precursor of the Asp-melanin pigment in *A. terreus* conidia that is

significantly different to the dihydroxynaphthalene melanin found in other *Aspergillus* species (Geib *et al.*, 2016). Another NRPS-like enzyme from *A. terreus* was shown to direct the biosynthesis of phenguignardic acid (**4**) (Sun *et al.*, 2016), which had previously been reported from the grape black rot fungus, *Guignardia bidwelii*, together with the structurally related guignardic acid (**5**) (Molitor *et al.*, 2012; Rodrigues-Heerklotz *et al.*, 2001). These two dioxolanone natural products were demonstrated to cause plant leaf necrosis and might thus act as virulence factors of *G. bidwelii* (Molitor *et al.*, 2012). Furthermore, the ectomycorrhizae-forming basidiomycete *Paxillus involutus* produces atromentin (**6**) that is subsequently converted into involutin (Braesel *et al.*, 2015) and is assumed to contribute to the oxidative degradation of lignocellulose *via* Fenton chemistry by reducing Fe^{3+} to Fe^{2+} (Shah *et al.*, 2015). Atromentin also possesses estrogenic activity and may act as potent inhibitor of 17- β -hydroxysteroid dehydrogenase (Dellafiora *et al.*, 2019). Very recently, an atromentin synthetase has also been identified from *A. terreus* by recombinant expression of the *atrA_{At}* gene in yeast, but the naturally inducing conditions in *A. terreus* have not been identified yet (Hühner *et al.*, 2018). These and other examples show that NRPS-like enzymes are widespread in the fungal kingdom. They direct fungal development and support virulence and nutrition. Furthermore, due to described antitumor and antidiabetic properties, this class of compounds has several interesting pharmaceutical characteristics.

The α -keto acids of the aromatic amino acids phenylalanine, tyrosine and tryptophan provide the major substrates of fungal NRPS-like enzymes (Hühner *et al.*, 2018). This is at least true for all examples mentioned above except for guignardic acid (**5**) for which the molecular basis of its biosynthesis is still unknown. The condensation of aromatic α -keto acids results in a variety of interconnecting core ring structures, which in non-reducing NRPS-like enzymes was proposed to be performed by the thioesterase domain of these enzymes (Balibar *et al.*, 2007; Braesel *et al.*, 2015). While the exact mechanism of product formation by the thioesterase

domain has not been solved yet, Braesel *et al.* suggested that certain sequence motifs could specify the formation of the core ring structures. A motif with a catalytic triad made from serine, asparagine and histidine in combination with a branched-chain aliphatic amino acid and two proline residues was described to be consistent with the formation of a core quinone ring structure as found in atromentin (**6**). In contrast, furanone structures were assumed to be formed by a triad made from serine, aspartate and histidine (Braesel *et al.*, 2015) as found in microperfuranone (**7**) biosynthesis by MicA from *A. nidulans* (Yeh *et al.*, 2012) or ralfuranone B (**8**) biosynthesis by RalA from the bacterium *Ralstonia solanacearum* (Wackler *et al.*, 2011). On the contrary to this prediction, the NRPS-like proteins MelA and ApvA from *A. terreus* form a furanone in aspulvinone E (**3**) and aspulvinone H (**9**) but show a sequence motif similar to that of quinone forming TE-domains except that the serine residue in the catalytic triad is replaced by a cysteine (Geib *et al.*, 2016). As the InvA atromentin synthetases from *P. involutus* and the aspulvinone E synthetase from *A. terreus* both use the substrate *p*-hydroxyphenylpyruvate, our intention was to perform mutation analyses on the *mela* gene to identify the contribution of specific amino acids in product formation. Accordingly, by using expression systems that base on the transcriptional activator TerR from terrein biosynthesis in combination with its *terA* target promoter (Gressler *et al.*, 2015; Geib and Brock, 2017) we expressed different versions of the *mela* and the *invA5* gene and characterised the corresponding products. Additionally, we studied the products formed from the *A. terreus* atromentin synthetase AtrA_{At} in different expression platform strains (Hühner *et al.*, 2018) and determined the products of a yet uncharacterised NRPS-like enzyme from *Aspergillus brasiliensis* with similarity to aspulvinone E and atromentin synthetases.

Results

Mutation of C733S and N760D in the aspulvinone E synthetase MelA from *Aspergillus terreus*

A sequence alignment of thioesterase domains of the aspulvinone E and H synthetases MelA and ApvA from *A. terreus* revealed sequence motifs matching with the predicted sequence motif of quinone core formation as found in the atromentin synthetase InvA5 from *P. involutus* rather than the predicted furanone motif as found in the microperofuranone synthetase MicA (**Fig. 2A**). However, MelA and ApvA that were identified as furanone synthetases both possess a cysteine instead of a serine in the postulated catalytic triad. This suggests that during furanone core structure formation in aspulvinone E (**3**) biosynthesis the intermediate is bound *via* a thioester rather than an oxoester. As MelA activity was found to depend on a reducing environment (Geib *et al.*, 2016), the thiol group was assumed to be essential. To confirm this assumption and to test whether a change of the catalytic triad from a cysteine into a serine alters product formation, a C733S mutation was introduced. The mutated gene was cloned with an *N*-terminal His-tag into the SM-Xpress vector (Gressler *et al.*, 2015) and used for transformation of the *A. niger* expression platform strain P2. No change in the metabolite profile compared to the parental strain was observed with the C733S mutant, although enzyme purification confirmed the production of a full-length protein (**Fig. 2B**). In addition, an *in vitro* assay with native and mutated MelA only revealed product formation with the wild type, but not with the C733S mutant (**Fig. 2C**). This indicates that the cysteine in the thioesterase domain is essential in the formation of aspulvinone E (**3**). We next analysed the importance of asparagine 760 in MelA, which also matches the pattern in quinone, but not furanone core forming enzymes (**Fig. 2A**). Like the C733S mutant, a N760D mutant was generated and expressed in *A. niger*. Again, no metabolite was produced and also the purified enzyme (**Fig. 2B**) did not show product formation (**Fig. 2C**). These results indicate that both amino acids, C733 and N760 essentially contribute to the catalytic mechanism and/or the correct folding of

the thioesterase domain of the aspulvinone E synthetase, but the core motifs predicted to discriminate between quinone and furanone core formation seem to be more complex.

Generation of a chimeric MelA_(A):InvA5_(T-TE) protein

As the mutation of C733 and N760 in MelA inactivated the enzyme, we were interested, whether replacement of the MelA thiolation and thioesterase domains with those from *P. involutus* InvA5 convert the aspulvinone E synthetase into an atromentin synthetase. Previous studies on the aspulvinone H synthetase ApvA from *A. terreus* showed that an exchange of the thiolation and thioesterase domain with that from the butyrolactone IIa (**10**) synthetase BtyA from *A. terreus* successfully converted the enzyme into a butyrolactone synthetase (van Dijk, Guo and Wang, 2016). To produce a chimeric MelA:InvA5 protein highly conserved residues in the stretch between adenylation and thiolation domain were selected for generating the MelA_(A):InvA5_(T-TE) fusion protein. While a full-length protein was successfully re-isolated from *A. niger* (**Fig. 2B**), neither under *in vivo* nor under *in vitro* conditions (**Fig. 2C**) atromentin (**6**) or any other metabolite was detected. This observation led to the following hypotheses: (i) as InvA5 derived from a basidiomycete, it might not properly fold when produced in the ascomycete *A. niger*; (ii) the reaction mechanism discriminating furanone and quinone core formation is also directed by the A domain or (iii) the gene fusion was placed at an incompatible position.

Heterologous expression of the atromentin synthetase *invA5* in *A. niger*

To test the first hypothesis that InvA5 cannot be produced as a functional protein in *A. niger*, we cloned the full-length *invA5* gene including an *N*-terminal His-tag into the SM-Xpress expression vector and transformed several *A. niger* expression platform strains. These included the sugar inducible P2 strain (Gressler *et al.*, 2015) and the doxycycline inducible ATNT16

strain (Geib and Brock, 2017), which both derived from the parental *A. niger* wild type A1144. Furthermore, the sugar inducible expression system was transferred into *A. niger* N402 and the resulting expression platform strain NP4 was also used for *invA5* expression. Transformants produced a bright yellow culture broth under inducing conditions, which was extracted for metabolite analysis. While a single major metabolite peak for atromentin (**6**) was expected, only a very minor peak identical with the retention time and UV/VIS profile of atromentin was observed (**Fig. 3A and Fig. S1**). By contrast, several other major metabolite peaks (**11, 12, 13, X**) were detected with strikingly different retention times compared to atromentin (**6**). However, when InvA5 was purified and subjected to an *in vitro* assay, atromentin (**6**) was the exclusive metabolite produced from the substrate *p*-hydroxyphenylpyruvate (**Fig. 3D**). Furthermore, when a crude cell-free extract of an *invA5* expressing *A. niger* strain was used in an enzymatic assay with 4-hydroxyphenylpyruvate as substrate, traces of **13** were detected as a carry-over from the cell-free extract and atromentin (**6**) was the major metabolite produced (**Fig. S1C**). This confirms that InvA5 is functionally produced in *A. niger*, but under *in vivo* conditions atromentin biosynthesis seems to undergo unexpected modifications that are not observed in cell-free extracts.

Time-dependent metabolite production from *invA5* expression in *A. niger*

While InvA5 was confirmed to act as atromentin synthetase under *in vitro* conditions, several different metabolites were produced in the heterologous host *A. niger* regardless the expression platform strain used. However, peak intensities of individual metabolites strongly varied among the different strains in this screening. Therefore, we selected individual transformants and extracted culture supernatant and mycelium at different time points (**Fig. 3A-B and Fig. S1**). A metabolite at a retention time of 14.99 min (**13**) and with a molecular mass of 340.29 g/mol was dominant at early time points, but its intensity in the culture broth decreased during

prolonged cultivation. However, at 72 h the metabolite again accumulated in the culture supernatant. In agreement, this metabolite was nearly exclusively isolated from the mycelium at 36 and 48 h. Furthermore, at least three other dominant metabolites with molecular masses of 342.30 g/mol (**X**), 312.28 g/mol (**11**) and 138.12 g/mol (**12**) (retention times 3.74 min, 4.88 min and 5.09 min) accumulated during cultivation.

Identification of metabolites from heterologous *invA5* expression in *A. niger*

Metabolite X showed an exact molecular mass of 341.0669 [M-H]⁻ resulting in a sum formula of C₁₈H₁₄O₇. Stability issues prevented the structural elucidation of this compound. In contrast, structures of metabolites with exact masses of *m/z* 339.0514 [M-H]⁻ (**13**) and *m/z* 311.0566 [M-H]⁻ (**11**) as well as that of metabolite (**12**) with an exact mass of *m/z* 137.0232 [M-H]⁻ were elucidated by NMR spectroscopy. Metabolite (**11**) was identified as gyroporin, a known atromentin-derived metabolite in *P. involutus* (Besl *et al.*, 1973). Metabolite (**12**) was identified as *p*-hydroxybenzoic acid (**table S1**).

The molecular formula of the previously undescribed atrofuranic acid (**13**) was determined as C₁₈H₁₂O₇ by high resolution ESI-MS measurement (*m/z* 340.0583), which is consistent with 13 degrees of unsaturation. The ¹H NMR spectrum showed only four signals in the aromatic range. These signals were ascribed to two *p*-substituted benzene residues based on their chemical shifts, splitting, and 2D NMR correlations (**Fig. S2-S4** and **tables S2**). The deduced number of eight aromatic protons together with the molecular formula indicated that **13** must contain four hydroxyl groups with exchangeable protons. Because the treatment of **13** with acetic anhydride in pyridine yielded exclusively a triacetylated product (**14**) (**Fig. S2-S4** and **table S3**), it became evident that one hydroxyl group in **13** is part of a carboxylic acid moiety (Chattaway, 1931). The remaining two oxygen atoms are due to a ketone, which shows a resonance at 180.6 ppm in the ¹³C NMR spectrum, and an ether function, respectively. The

four, yet unassigned signals in the ^{13}C NMR spectrum possess chemical shifts characteristic of sp^2 -hybridized carbons and were thus attributed to two carbon-carbon double bonds. The presence of two benzene rings, two carbonyl groups and two C-C double bonds in **13** left a single degree of unsaturation unassigned, which must be due to another ring structure. Consolidating the above information with the chemical shifts of the respective nuclei as well as data from a heteronuclear multiple bond correlation (HMBC) experiment, the structure of **13** was finally elucidated. As evidenced by the signal doubling in the ^{13}C NMR spectrum, **13** is subject to keto-enol tautomerism and, therefore, exists as a mixture of *E* and *Z* isomers. After feeding *A. niger* cultures with 2- ^{13}C -labelled tyrosine, spectroscopic analysis of isolated **13** revealed four intensified ^{13}C NMR signals (**Fig. S3**) that were in agreement with the proposed structure of atrofuranic acid and its tautomerism.

Metabolite production from atrofuranic acid

To elucidate the interconnection of products formed by heterologous expression of the atromentin synthetase InvA5 in *A. niger*, feeding studies were performed. When atromentin (**6**) was fed to *A. niger* cultures, subsequent product analysis did not provide any evidence for the presence of atrofuranic acid (**13**), metabolite X (**X**), gyroporin (**11**) or *p*-hydroxybenzoic acid (**12**). This indicates that either externally added atromentin (**6**) does not enter *A. niger* or that atromentin (**6**) does not act as precursor for any of these metabolites. Therefore, atrofuranic acid (**13**) was added to *A. niger* ATNT16 cultures and to a control medium (**Fig. 3C**). Analysis of the control revealed the presence of *p*-hydroxybenzoic acid (**12**), indicating that **13** can spontaneously decompose into **12** in the culture broth. However, when *A. niger* cultures supplemented with **13** were extracted, **12** was detected along with metabolite X (**X**) and gyroporin (**11**). This implies that atrofuranic acid (**13**) is the prime metabolite formed by heterologous expression of the *invA5* gene in *A. niger* with all other metabolites deriving from

this compound. Furthermore, metabolite X and gyroporin (**11**) production seems dependent on the presence of *A. niger* cells.

Heterologous *invA5* and *melA* expression in *A. oryzae*

Our data showed that InvA5 was produced as a functional protein in *A. niger*, whereby under *in vivo* conditions a cross-chemistry during product formation resulted in the production of a furanic acid core structure. To investigate whether atromentin (**6**) production is generally directed towards other metabolites in *Aspergillus* species, we introduced the *A. terreus* transcriptional regulator gene *terR* under control of the *PamyB* promoter (Gressler *et al.*, 2015) into the genome of *Aspergillus oryzae* RIB40. The single copy transformant OP12 was selected as *A. oryzae* expression platform strain. Cultivation of OP12 and its parental RIB40 strain in glucose or starch containing minimal medium revealed no significant background production of secondary metabolites in either strain (**Fig.4A**).

To test the general suitability of OP12 to produce metabolites from an NRPS-like enzyme, we first introduced the *A. terreus melA* gene under control of the *terA* promoter. As with *melA* expression in the *A. niger* P2 strain (Geib *et al.*, 2016), production of aspulvinone E (**3**) and its UV-interconvertible isomer isoaspulvinone E (#) was confirmed by HPLC analysis from culture extracts of the OP12 *melA* strain (**Fig. 4A**). Next, we transformed the OP12 strain with the *invA5* expression construct. Transformants secreted a purple metabolite into the solid and liquid growth medium. Analytical HPLC from culture extracts revealed a single metabolite peak matching the retention time and UV spectrum of authentic atromentin (**6**) (**Fig.4B**). This experiment confirmed that cross-chemistry on the benzoquinone core of atromentin (**6**) does not occur in *A. oryzae* and no other metabolites were detected in this expression host. This indicates further that the physiology of *Aspergillus* species used for heterologous gene

expression differs and is important for identification of metabolites from a specific yet uncharacterised gene of interest.

Generation of chimeric proteins by domain fusions from MelA and AtrA_{At}

Analyses showed that InvA5 is functionally expressed in *A. niger* and *A. oryzae*, which indicates that the failure to retrieve a functional chimeric protein from the fusion of MelA with InvA5 was either due to selection of an incorrect protein fusion site or an incompatibility between an *A. terreus* (ascomycete) and *P. involutus* (basidiomycete) enzyme. To test these assumptions further, we fused the MelA protein with the atromentin synthetase AtrA_{At} from *A. terreus* (Hühner *et al.*, 2018) and selected two different fusion sites. The first construct (C1) used the identical fusion site as selected for the fusion of MelA and InvA5 resulting in MelA_(A):AtrA_{At(T-TE)}. In the second construct (C2) we only replaced the thioesterase domain of MelA resulting in the chimeric protein MelA_(A-T):AtrA_{At(TE)}. Both gene fusions as well as the full-length *atrA_{At}* gene were cloned into the tag-SM-Xpress expression plasmid (Geib *et al.*, 2016) for transformation of the *A. oryzae* OP12 and *A. niger* ATNT16 expression platform strains. *A. oryzae* transformants secreted a purple metabolite and HPLC analyses of extracts confirmed the production of atromentin (**6**) from all three constructs (**Fig. 4C**). In contrast, all *A. niger* transformants regardless of the integrated construct produced a yellow culture broth and mycelium under inducing conditions. In agreement, HPLC analyses of mycelium extractions confirmed the production of atrofuranic acid (**13**) (**Fig. 4D**). As functional proteins were produced from both gene fusion strategies, the fusion site selected for generation of the MelA_(A):InvA5_(T-TE) chimeric protein was suitable and unlikely to cause the production of an inactive enzyme. More importantly, this experiment indicated that the thioesterase domain directs the chemistry of an NRPS-like enzyme and a furanone-forming enzyme can be successfully converted into a quinone-forming enzyme by exchange of the TE-domain. To

confirm this assumption, we also produced a fusion protein that contained the A- and T-domain of the atromentin synthetase AtrA_{At} and the TE-domain of MelA. The gene fusion was cloned into the tag-SM-Xpress vector and used for transformation of the *A. oryzae* OP12 and *A. niger* ATNT16 expression platform strains. Culture supernatants turned into a fluorescent yellow indicating the production of aspulvinone E (**3**) and its UV-interconvertible isomer isoaspulvinone E (#) (Geib *et al.*, 2016), which was confirmed by HPLC analysis of culture extracts (**Fig. 4C and D**; construct *atrA_{At}:melA* C2). Therefore, we conclude that a successful replacement of the thioesterase domain of an NRPS-like enzyme depends on the phylogenetic relationship of the fusion partners. Furthermore, while the furanone core containing product aspulvinone E (**3**) is produced in both, *A. niger* and *A. oryzae*, the product formed from atromentin synthetases differs among the two species. While *A. oryzae* produces atromentin (**6**), the major primary metabolite produced in *A. niger* is atrofuranic acid (**13**).

Identification of an atromentin synthetase from *Aspergillus brasiliensis*

As *A. niger* mainly produced atrofuranic acid (**13**) from the expression of atromentin synthetase genes, we were interested in metabolites produced from NRPS-like enzymes in aspergilli from section *Nigri*. For this purpose, we used the MelA protein sequence from *A. terreus* as a template and screened the genome of *Aspergillus brasiliensis* strain CBS101740. A protein with accession number OJJ76880 was identified that when used as a template in BLAST searches against *A. terreus* revealed the best hits with the atromentin synthetase AtrA_{At} (57% identity, 72% similarity; accession AUO29225), the aspulvinone H synthetase ApvA (54% identity, 72% similarity, accession AUO29222) and the aspulvinone E synthetase MelA (55% identity, 72% similarity; accession AND66115). This shows that a simple BLAST analysis of NRPS-like enzymes does not necessarily allow the prediction of the metabolite produced. However, it appeared likely that the *A. brasiliensis* enzyme, subsequently called AbrA,

produces an atromentin-like metabolite, as no cysteine was detected in the active site of the thioesterase domain. To confirm this assumption, the *abra* gene was amplified from genomic DNA of *A. brasiliensis* CBS101740 and cloned into the tag-SM-Xpress expression vector and used for transformation of *A. niger* ATNT16 and *A. oryzae* OP12. In *A. niger*, the culture supernatant and mycelium turned into bright yellow, whereas *A. oryzae* produced a purple compound (**Figure 4E**), indicating that the *A. brasiliensis abra* gene encodes an atromentin synthetase. When extracts were analysed by HPLC, this assumption was confirmed as metabolite X, gyroporin (**11**), *p*-hydroxybenzoic acid (**12**) and atrofuranic acid (**13**) were identified from *A. niger* extracts, whereas a single metabolite peak of atromentin (**6**) was detected from the OP12 strain. Furthermore, atromentin (**6**) was the sole product produced under *in vitro* conditions from purified AbrA (**Fig. S1D**). This shows that atromentin synthetases are common to ascomycetes and more specifically shows that *A. brasiliensis* belonging to the section *Nigri* possesses such an enzyme.

Cross-chemistry on benzoquinones in section *Nigri*

Preliminary trials to identify atromentin from *A. brasiliensis* under some selected cultivation conditions failed (**Fig. S5**). We were, therefore, interested in the fate of atromentin (**6**) biosynthesis when induced in *A. brasiliensis*. Therefore, the atromentin synthetase gene *abra* was cloned under control of the constitutively expressed *Aspergillus nidulans gpdA* promoter and *A. brasiliensis* was transformed using pyrithiamine as selection marker. Positive transformants were cultivated in glucose containing minimal medium and the culture broth and mycelium were extracted and analysed for the metabolite profile. The parental *A. brasiliensis* wild-type strain served as negative control. Unexpectedly, no atromentin (**6**) was identified from transformants, whereas peaks with retention times and UV/Vis spectra of atrofuranic acid (**13**) and *p*-hydroxybenzoic acid (**12**) were detected (**Figure 4F**). Further inspection of the

genomic region surrounding the *abrA* gene identified a putative biosynthesis gene cluster including a predicted hydroxylase, an oxidoreductase, an O-methyltransferase, a monooxygenase, a CYP450 protein, and an MFS transporter (**Figure 4G**). This leads to the speculation that if atromentin is produced under certain growth conditions, it might get instantly converted into a yet unknown metabolite. However, it appears even more likely that atrofuranic acid (**13**) is the precursor molecule for further modification in *A. brasiliensis*. Furthermore, since atrofuranic acid (**13**) was identified from both, *A. niger* and *A. brasiliensis*, cross-chemistry on a benzoquinone core seems not limited to *A. niger* but appears common to *Aspergillus* species from section *Nigri*.

Phylogeny of fungal atromentin synthetases

The identification of *AbrA* from *A. brasiliensis* acting as atromentin synthetase under *in vitro* conditions tempted us to study the phylogenetic relationship of fungal NRPS-like enzymes. The failure to produce a functional chimeric protein from the gene fusion of *MelA* and *InvA5*, but successful fusions between *MelA* and *AtrA_{At}* led to the speculation of a separated phylogeny of atromentin synthetases in ascomycetes and basidiomycetes. Therefore, we extracted the thioesterase domains of all fungal NRPS-like enzymes characterised so far by using InterPro (Finn *et al.*, 2017). Sequences were aligned by Clustal Omega (Sievers and Higgins, 2018) and used to calculate a phylogenetic tree with IQ-Tree (Kalyaanamoorthy *et al.*, 2017) that was plotted with iTOL (Letunic and Bork, 2016). The thioesterase domain from the polyketide synthase *TerA* (Gressler *et al.*, 2015) served as outgroup (**Fig. 5**). More details are provided in the STAR methods. Indeed, atromentin synthetases originating from basidiomycetes (*AtrA* from *Tapinella panuoides*, *InvA5* from *P. involutus* and *GreA* from *Suillus grevillei*) formed a cluster that was distinct from all thioesterase domains from *Aspergillus* species. While the number of NRPS-like enzymes with known products is limited,

a tendency for clustering of enzymes producing the same product also became visible among the *Aspergillus*-derived enzymes, especially aspulvinone E and atromentin synthetases showed a close phylogenetic relationship. This supports the idea that this close phylogenetic relationship enabled the successful generation of functional chimeric proteins. These results additionally imply that atromentin synthetases from basidio- and ascomycetes evolved independently. However, to confirm this assumption, additional enzymes from both families need to be characterised.

Discussion

Although non-reducing NRPS-like enzymes generally only use aromatic α -keto acids as substrates, they are responsible for the formation of a large variety of different natural products. The main interconnecting core structures identified so far are furanones, benzoquinones and dioxolanones, which arise from the action of the C-terminal thioesterase domain. However, due to the limited number of non-reducing NRPS-like enzymes characterised so far, prediction of the thioesterase chemistry by sequence pattern analysis remains difficult. Previous work suggested a catalytic triad made from serine, asparagine and histidine in combination with a branched-chain aliphatic amino acid and two proline residues as indicative for benzoquinone core formation (Braesel *et al.*, 2015). While this may still hold true, more discriminating amino acids seem to be required for core structure prediction. The aspulvinone E synthetases MelA and ApvA also resemble this benzoquinone forming amino acid pattern, but contain an essential cysteine instead of a serine in the catalytic triad. An oxidative environment (Geib *et al.*, 2016) or the exchange of the cysteine by a serine inactivates the aspulvinone E synthetase MelA. This indicates that formation of a substrate thioester is essential for the furanone-forming chemistry of this specific thioesterase. However, other furanone core forming enzymes with a substitution pattern different to that from aspulvinone E (**3**), such as the

microperfuranone (**7**) synthetase MicA from *A. nidulans* (Yeh *et al.*, 2012) also contain a serine rather than a cysteine and, thus, form a substrate oxoester in the active site. Therefore, the substrate thioester formation in aspulvinone E synthetases proceeds differently and depicts an exception in furanone core production rather than the rule. This shows that understanding of the precise chemistry of thioesterase domains from non-reducing NRPS-like enzymes remains limited and more reliable predictions on the core structure formation will require the analysis of a protein crystal structure and the characterisation of additional enzymes for identification of prognostic sequences patterns.

To convert the furanone forming MelA protein into a benzoquinone forming enzyme, domain swapping currently appears as the method of choice, although a close phylogenetic proximity may be a prerequisite for the success of such experiments. Previous studies have shown that the exchange of the thioesterase domain of an *A. terreus* aspulvinone E synthetases with that from an *A. terreus* butyrolactone synthetase successfully converted the enzyme into a butyrolactone IIa synthetase (van Dijk, Guo and Wang, 2016). Our first approach on MelA from *A. terreus* (Geib *et al.*, 2016) in combination with InvA5 from the basidiomycete *P. involutus* (Braesel *et al.*, 2015) failed, whereas a combination with the atromentin synthetase AtrA_{At} from *A. terreus* (Hühner *et al.*, 2018) was successful. This clearly demonstrates that a conversion is possible but may be limited to domain exchanges within species rather than across fungal divisions. In agreement, our phylogenetic analysis indicates a significant distance between NRPS-like enzymes from asco- and basidiomycetes (**Fig. 5**). The identification of an additional atromentin synthetase from *A. brasiliensis* will allow further domain exchange studies to analyse the possibility of successful combinations of NRPS-like enzymes from aspergilli deriving from different sections.

Interestingly, despite functional expression of atromentin synthetases in both *A. niger* and *A. oryzae*, we were surprised to detect only marginal amounts of atromentin in *A. niger*. The fact

that we discovered the yet undescribed metabolite atrofuranic acid (**13**) as well as the metabolites gyroporin (**11**) and *p*-hydroxybenzoic acid (**12**) implies that the physiology of *A. niger* initiates a cross-specificity and cross-chemistry event on the NRPS-like enzyme.

The host-physiology dependent cross-chemistry described here differs from that described for the biosynthesis of the meroterpenoids austinol and dehydroaustinol in *A. nidulans*, in which one biosynthesis gene cluster contains a polyketide synthase producing an orsellinic acid core structure, whereas a second biosynthesis gene clusters is responsible for the prenylation of the polyketide moiety (Lo *et al.*, 2012). In contrast, the production of atrofuranic acid (**13**) and other products observed in *A. niger* is independent from a specific cross-acting biosynthesis gene cluster as *A. niger* does not seem to contain its own intrinsic atromentin synthetase. It also appears unlikely that atromentin (**6**) acts as a precursor molecule for any of the metabolites in *A. niger* as feeding with atromentin (**6**) did not result in the production of atrofuranic acid (**13**). Therefore, atrofuranic acid (**13**) may not derive from an oxidative ring-opening of atromentin (**6**). In contrast, feeding of atrofuranic acid (**13**) resulted in the production of gyroporin (**11**) and metabolite X. Based on the analysis of atrofuranic acid generated from 2-¹³C-labelled L-tyrosine in combination with previous labelling studies performed on atromentin (Gill and Steglich, 1987), we hypothesise the biosynthesis pathway for metabolites produced in *A. niger* as proposed in **Fig. 6**. A re-direction of the chemistry of the thioesterase domain under physiologic condition in *A. niger* gives rise to a dihydrofuroic acid, even though it is unclear whether the proposed reaction occurs with the substrate being tethered to the thioesterase domain as depicted in **Fig. 6**. It would also be conceivable that the re-direction of the thioesterase chemistry promotes the release of a linear intermediate, which is subsequently converted into a dihydrofuroic acid. In any case, dehydration and oxidation would then lead to the formation of atrofuranic acid (**13**). As we did not detect an intermediate without the final hydroxylation, this modification either occurs prior to the final release from the enzyme or

occurs instantly and quantitatively after product release. The speculation on a quantitative hydroxylation in *A. niger* without detection of an intermediate lacking the hydroxylation is also in agreement with previous studies on *A. terreus* terrein biosynthesis. Expression of the terrein synthase gene *terA* in *A. niger* should lead to the production of the polyketide 2,3-dehydro-6-hydroxymellein. However, the modified terrein precursor 6,7-dihydroxymellein was isolated from *A. niger* extracts even without traces of 2,3-dehydro-6-hydroxymellein being detected (Zaehle *et al.*, 2014).

While *p*-hydroxybenzoate seems to spontaneously derive from incubation of atrofuranic acid in the culture broth, the biosynthesis of gyroporin (**11**) might proceed via metabolite X. Thereby, the structure of metabolite X could derive from a Piancatelli-type rearrangement (Piutti and Quartieri, 2013; Verrier *et al.*, 2018), which is subsequently decarboxylated and oxidised to form gyroporin (**11**). Interestingly, if this biosynthetic pathway holds true, it differs from gyroporin (**11**) production as described for *P. involutus* during biosynthesis of involutin (Braesel *et al.*, 2015). In *P. involutus*, atromentin (**6**) acts as precursor for gyroporin (**11**) biosynthesis, in which an oxidative ring contraction of atromentin (**6**) first results in the production of gyrocyanin. Gyrocyenin can then either become converted into involutin or, by a further oxidation event into gyroporin (**6**) (**Fig. 6**). Since atrofuranic acid (**13**) has not been detected in *P. involutus* and, in turn, gyrocyenin was not found in *A. niger* the biosynthesis of gyroporin (**11**) may indeed differ among these organisms. However, the elucidation of the structure of the unstable metabolite X will be a prerequisite to confirm the biosynthesis route of gyroporin (**11**) in *A. niger*.

Despite the cross-chemistry events observed in *A. niger* during the expression of atromentin synthetases, this study confirmed that atromentin synthetases are not limited to basidiomycetes but seem to be widely distributed also among ascomycetes. Nevertheless, it needs to be confirmed that atromentin (**6**) is indeed an intermediate or final metabolite produced in the

original ascomycete hosts. A recent study showed that the NRPS-like enzyme AtrA_{At} from *A. terreus* produces atromentin (**6**) when heterologously expressed in yeast (Hühner *et al.*, 2018), but it needs to be confirmed that atromentin is also produced in *A. terreus*. Similarly, we discovered the atromentin synthetase AbrA from *A. brasiliensis*. When *abrA* was expressed in the *A. oryzae* expression platform, atromentin (**6**) was produced in significant amounts and no other by-products were observed. Not unexpectedly, expression in *A. niger* resulted in the production of *p*-hydroxybenzoic acid (**12**), gyroporin (**11**) and, mainly, atrofuranic acid (**13**). However, most interestingly, when *abrA* was homologously expressed in *A. brasiliensis* atrofuranic acid (**13**) rather than atromentin (**6**) was the major metabolite produced. This suggests that (i) atromentin (**6**) also undergoes cross-chemistry in *A. brasiliensis*, indicating that modifications of benzoquinone core structures are common to *Aspergillus* species of the section *Nigri* and (ii) atromentin (**6**) is unlikely to be a product that can be identified from *A. brasiliensis*. Finally, as *A. brasiliensis* produces atrofuranic acid (**13**), it appears unlikely that the genes forming a putative biosynthesis gene cluster with *abrA* (**Fig. 4G**) act on atromentin (**6**). Additional analyses will be required to identify the respective metabolite(s) produced in *A. brasiliensis*, but the existence of these possibly modifying enzymes also supports the function of non-reducing NRPS-like enzymes to act as producers of core intermediates in secondary metabolite biosynthesis. Further examples for such biosynthesis gene clusters are the formation of Asp-melanin (Geib *et al.*, 2016) and aspulvinone H (**9**) (Guo *et al.*, 2013) from aspulvinone E (**3**), involutin from atromentin (**6**) (Braesel *et al.*, 2015) or terrequinone A (**1**) from didemethylasterriquinone (Schneider *et al.*, 2007; Balibar *et al.*, 2007). Given the fact that NRPS-like enzymes are widespread in fungal genomes and their metabolites have hardly been characterised yet, these enzymes and their accompanying biosynthesis gene clusters provide a treasure chest for metabolites of pharmacological interest. Nevertheless, characterisation of products from NRPS-like enzymes may be hampered by cross-chemistry occurring on

metabolite core structures during heterologous expression. Therefore, it is recommended to use different heterologous expression platforms in parallel to elucidate the true nature of products formed from uncharacterised NRPS-like enzymes.

Significance

While terpenes, polyketides and products from non-ribosomal peptide synthetases (NRPS) are known for a great variety of biological activities, products from NRPS-like enzymes are less well studied. However, metabolites analysed so far show phytotoxic, antiviral, anti-proliferative and anti-diabetic activities making them interesting candidates for further exploitation. NRPS-like enzymes with a C-terminal thioesterase (TE) domain catalyse the condensation of two aromatic α -keto acids by forming connecting indolylquinone, benzoquinone, dioxolanone or furanone core structures, but the exact reaction mechanisms are hardly understood. Current knowledge on sequence patterns in thioesterase domains is too limited for core structure prediction, as the *A. terreus* furanone forming aspulvinone E synthetase MelA was not converted into a quinone forming atromentin synthetase by site-directed mutagenesis. However, mutagenesis experiments confirmed that MelA forms a substrate thioester, which is unprecedented in NRPS-like enzymes. Despite the inability of MelA conversion into an atromentin synthetase by site-directed mutagenesis, this was successfully achieved by domain swapping. Conversion required use of a thioesterase domain from an atromentin synthetase of the same species. This successful reassembly from closely related enzymes may also explain the expansion in the number of NRPS-like enzymes in individual fungal species. Furthermore, this study demonstrated that host physiology in heterologous expression has significant impact on product formation. While atromentin synthetases produce atromentin *in vitro* and in *A. oryzae*, cross-chemistry directs the formation of atrofuranic acid and eventually gyroporin in *A. niger*. This cross-chemistry was not limited

to *A. niger*, but also occurred in *A. brasiliensis*, which contains an intrinsic atromentin synthetase. Therefore, a single enzyme can form different products depending on the physiology of the producer. While this cross-chemistry widens the product portfolio from NRPS-like enzymes, a single expression platform might be insufficient when analysing product formation from yet uncharacterised secondary metabolite biosynthesis genes.

Acknowledgement

We thank Andrea Perner for HR-ESI-MS analysis and Heike Heinecke for recording NMR spectra. We are grateful to the School of Life Sciences of the University of Nottingham for financial support and a scholarship to EG. FB thanks the graduate school Jena School for Microbial Communication (JSMC) for a PhD fellowship.

Author contributions

EG and MB conceived and designed experiments. EG, MB, FB and MD performed experiments. MN, FB and MD analysed NMR data. All authors contributed to writing of the manuscript and approved the final version.

Declaration of conflicts of interest

All authors declare no conflicts of interest

References

Balibar, C.J., Howard-Jones, A.R., and Walsh, C.T. (2007). Terrequinone A biosynthesis through L-tryptophan oxidation, dimerization and bisprenylation. *Nat. Chem. Biol.* 3, 584-

- Besl, H., Bresinsky, A., Steglich, W., and Zipfel, K. (1973). Pilzpigmente, {XVII}. Über Gyrocyanin, das blauende Prinzip des Kornblumenröhrlings (*Gyroporus cyanescens*), und eine oxidative Ringverengung des Atromentins. *Chemische Berichte* 106, 3223-9
- Bok, J.W., Hoffmeister, D., Maggio-Hall, L.A., Murillo, R., Glasner, J.D., and Keller, N.P. (2006). Genomic mining for *Aspergillus* natural products. *Chem. Biol.* 13, 31-7
- Braesel, J., Götze, S., Shah, F., Heine, D., Tauber, J., Hertweck, C., Tunlid, A., Stallforth, P., and Hoffmeister, D. (2015). Three Redundant Synthetases Secure Redox-Active Pigment Production in the Basidiomycete *Paxillus involutus*. *Chem. Biol.* 22, 1325-34
- Brock, M., Darley, D., Textor, S., and Buckel, W. (2001). 2-Methylisocitrate lyases from the bacterium *Escherichia coli* and the filamentous fungus *Aspergillus nidulans*: characterization and comparison of both enzymes. *Eur. J. Biochem.* 268, 3577-86
- Chattaway, F.D. (1931). CCCXLII. - Acetylation in aqueous alkaline solutions. *J. Chem. Soc.* 0, 2495-6
- Dellaflora, L., Aichinger, G., Geib, E., Sánchez, L., Brock, M., Cánovas, D., Dall'Asta, C., Marko, D. (2019). Hybrid *in silico/in vitro* target fishing to assign function to “orphan” compounds of food origin - The case of the fungal metabolite atromentin. *Food Chem.* 270, 61-9
- Dewi, R.T., Tachibana, S., and Darmawan, A. (2012). Antidiabetic and Antioxidative Activities of Butyrolactone I from *Aspergillus terreus* MC751. *International Journal of Biological, Biomolecular, Agricultural, Food and Biotechnological Engineering* 6, 929-34
- Finn, R.D., Attwood, T.K., Babbitt, P.C., Bateman, A., Bork, P., Bridge, A.J., Chang, H., Dosztányi, Z., El-Gebali, S., Fraser, M. et al. (2017). InterPro in 2017 - beyond protein family and domain annotations. *Nucleic Acids Res.* 45, D190-9

- Fleck, C.B., and Brock, M. (2010). *Aspergillus fumigatus* catalytic glucokinase and hexokinase: expression analysis and importance for germination, growth, and conidiation. *Eukaryotic Cell* 9, 1120-35
- Geib, E., Gressler, M., Viediarnikova, I., Hillmann, F., Jacobsen, I.D., Nietzsche, S., Hertweck, C., and Brock, M. (2016). A Non-canonical Melanin Biosynthesis Pathway Protects *Aspergillus terreus* Conidia from Environmental Stress. *Cell Chem Biol* 23, 587-97
- Geib, E., and Brock, M. (2017). ATNT: an enhanced system for expression of polycistronic secondary metabolite gene clusters in *Aspergillus niger*. *Fungal Biol Biotechnol* 4, 13
- Gill, M., and Steglich, W. (1987) Pigments of Fungi (Macromycetes). In: Fortschritte der Chemie organischer Naturstoffe / Progress in the Chemistry of Organic Natural Products. 51, 1-297. Springer
- Gressler, M., Hortschansky, P., Geib, E., and Brock, M. (2015). A new high-performance heterologous fungal expression system based on regulatory elements from the *Aspergillus terreus* terrein gene cluster. *Front Microbiol* 6, 184
- Guo, C., Knox, B.P., Sanchez, J.F., Chiang, Y., Bruno, K.S., and Wang, C.C.C. (2013). Application of an efficient gene targeting system linking secondary metabolites to their biosynthetic genes in *Aspergillus terreus*. *Org. Lett.* 15, 3562-5
- He, J., Wijeratne, E.M.K., Bashyal, B.P., Zhan, J., Seliga, C.J., Liu, M.X., Pierson, E.E., Pierson, L.S., VanEtten, H.D., and Gunatilaka, A.A.L. (2004). Cytotoxic and other metabolites of *Aspergillus* inhabiting the rhizosphere of Sonoran desert plants. *J. Nat. Prod.* 67, 1985-91
- Hoang, D.T., Chernomor, O., von Haeseler, A., Minh, B.Q., Vinh, L.S. (2018). UFBoot2: Improving the ultrafast bootstrap approximation. *Mol. Biol. Evol.* 35,518-22

- Hühner, E., Backhaus, K., Kraut, R., and Li, S. (2018). Production of α -keto carboxylic acid dimers in yeast by overexpression of NRPS-like genes from *Aspergillus terreus*. *Appl. Microbiol. Biotechnol.* 102, 1663-72
- Kalyaanamoorthy, S., Minh, B.Q., Wong, T.K.F., von Haeseler, A., Jermiin, L.S. (2017) ModelFinder: Fast model selection for accurate phylogenetic estimates. *Nat. Methods* 14, 587-9
- Letunic, I. and Bork, P. (2016). Interactive tree of life (iTOL) v3: an online tool for the display and annotation of phylogenetic and other trees. *Nucleic Acids Res.* 44, W242-5
- Lo, H., Entwistle, R., Guo, C., Ahuja, M., Szewczyk, E., Hung, J., Chiang, Y., Oakley, B.R., and Wang, C.C.C. (2012). Two separate gene clusters encode the biosynthetic pathway for the meroterpenoids austinol and dehydroaustinol in *Aspergillus nidulans*. *J. Am. Chem. Soc.* 134, 4709-20
- Molitor, D., Liermann, J.C., Berkelmann-Löhnertz, B., Buckel, I., Opatz, T., and Thines, E. (2012). Phenguignardic acid and guignardic acid, phytotoxic secondary metabolites from *Guignardia bidwellii*. *J. Nat. Prod.* 75, 1265-9
- Piutti, C., and Quartieri, F. (2013). The Piancatelli Rearrangement: New Applications for an Intriguing Reaction. *Molecules* 18, 12290-312
- Rodrigues-Heerklotz, K., Drandarov, K., Heerklotz, J., Hesse, M., and Werner, C. (2001). Guignardic Acid, a Novel Type of Secondary Metabolite Produced by the Endophytic Fungus *Guignardia* sp.: Isolation, Structure Elucidation, and Asymmetric Synthesis. *Helvetica Chimica Acta* 84, 3766-72
- Schimmel, T.G., Coffman, A.D., and Parsons, S.J. (1998). Effect of butyrolactone I on the producing fungus, *Aspergillus terreus*. *Appl. Environ. Microbiol.* 64, 3707-12

- Schneider, P., Weber, M., Rosenberger, K., and Hoffmeister, D. (2007). A one-pot chemoenzymatic synthesis for the universal precursor of antidiabetes and antiviral bis-indolylquinones. *Chem. Biol.* 14, 635-44
- Shah, F., Schwenk, D., Nicolás, C., Persson, P., Hoffmeister, D., and Tunlid, A. (2015). Involutin is an Fe³⁺ reductant secreted by the ectomycorrhizal fungus *Paxillus involutus* during Fenton-based decomposition of organic matter. *Appl. Environ. Microbiol.* 81, 8427-33
- Sievers, F. and Higgins, D.G. (2018). Clustal Omega for making accurate alignments of many protein sequences. *Protein Sci.* 27, 135-45
- Sun, W., Guo, C., and Wang, C.C.C. (2016). Characterization of the product of a nonribosomal peptide synthetase-like (NRPS-like) gene using the doxycycline dependent Tet-on system in *Aspergillus terreus*. *Fungal Genet. Biol.* 89, 84-8
- Wackler, B., Schneider, P., Jacobs, J.M., Pauly, J., Allen, C., Nett, M., and Hoffmeister, D. (2011). Ralfuranone biosynthesis in *Ralstonia solanacearum* suggests functional divergence in the quinone synthetase family of enzymes. *Chem. Biol.* 18, 354-60
- Yeh, H., Chiang, Y., Entwistle, R., Ahuja, M., Lee, K., Bruno, K.S., Wu, T., Oakley, B.R., and Wang, C.C.C. (2012). Molecular genetic analysis reveals that a nonribosomal peptide synthetase-like (NRPS-like) gene in *Aspergillus nidulans* is responsible for microperfuranone biosynthesis. *Appl. Microbiol. Biotechnol.* 96, 739-48
- van Dijk, J.W.A., Guo, C., and Wang, C.C.C. (2016). Engineering Fungal Nonribosomal Peptide Synthetase-like Enzymes by Heterologous Expression and Domain Swapping. *Org. Lett.* 18, 6236-9
- Verrier, C., Moebis-Sanchez, S., Queneau, Y., and Popowycz, F. (2018). The Piancatelli reaction and its variants: recent applications to high added-value chemicals and biomass valorization. *Org. Biomol. Chem.* 16, 676-87

Zaehle, C., Gressler, M., Shelest, E., Geib, E., Hertweck, C., and Brock, M., (2014). Terrein biosynthesis in *Aspergillus terreus* and its impact on phytotoxicity. Chem. Biol. 21, 719-31

Figure legends

Figure 1: Metabolites produced by NRPS-like enzymes.

Figure 2: Characterisation and mutation of the aspulvinone E synthetase MelA. **A:** Partial sequence alignment from thioesterase domains of four NRPS-like enzymes. InvA5 = atromentin synthetase from *P. involutus*, MelA = aspulvinone E synthetase for Asp-melanin biosynthesis from *A. terreus*, ApvA = aspulvinone E synthetase for aspulvinone H biosynthesis from *A. terreus*, MicA = microperfuranone synthetase from *A. nidulans*. The catalytic motif and the proposed fingerprint region directing the core structure formation are highlighted. **B:** SDS-PAGE analysis of wild-type and mutated MelA proteins. **C:** HPLC chromatograms from *in vitro* assays from purified MelA proteins shown in (B) in comparison to authentic standards of aspulvinone E (**3**), the UV-interconvertible isoaspulvinone E (**#**) and atromentin (**6**). The (*) denotes the peak derived from the substrate 4-hydroxyphenylpyruvate. MI – chimeric MelA_(A):InvA5_(T-TE). HPLC runs were recorded at 254 nm.

Figure 3: Analysis of products formed from *invA5* expression in *A. niger* and from purified InvA5. **A and B:** Time dependent extraction of (A) culture filtrates and (B) mycelium from heterologous *invA5* expression in the *A. niger* P2 strain. **C:** Analysis of metabolite formation from atrofuranic acid (**13**). When **13** is incubated for 24 h in sterile culture medium 4-hydroxybenzoic acid (**12**) is formed. In the presence of *A. niger* **13** is additionally transformed into gyroporin (**11**) and metabolite X. **D:** InvA5 purification and HPLC analysis of products formed from an *in vitro* assay. In A, B and C a modified HPLC method (COR_ESIA_25-50) was used to achieve higher peak resolution, whereas method COR_ESIA was used in D. All HPLC runs were recorded at 254 nm. For heterologous expression of atromentin synthetases in *A. niger* strains NP4 and ATNT16 and *in vitro* assay with an *invA5*

expressing *A. niger* cell extract refer to **Fig. S1**. NMR data for structure elucidation of compounds are provided in **tables S1-S3** and **Fig. S2-S3**.

Figure 4: Expression of different NRPS-like enzymes in *A. niger* and *A. oryzae* and product analysis by HPLC. **A:** Background metabolite production in the *A. oryzae* wild-type strain RIB40, the expression platform strain *A. oryzae* OP12 and identification of aspulvinone E (**3**) and its *cis*-isomer isoaspulvinone E (#) from an OP12 strain expressing the *melA* gene from *A. terreus*. **B:** Analysis of a culture extract of an OP12 strain expressing the atromentin synthetase *invA5*. Authentic atromentin (**6**) was run as a reference standard and confirms the production of atromentin (**6**) in *A. oryzae*. **C** and **D:** Analysis of metabolites formed from recombinant production of the atromentin synthetase $AtrA_{At}$ and the chimeric proteins $MelA_{(A)}:AtrA_{At(T-TE)}$ (C1), $MelA_{(A-T)}:AtrA_{At(TE)}$ (C2) and $AtrA_{At(A-T)}:MelA_{(TE)}$ (C2) in *A. oryzae* OP12 and *A. niger* ATNT16. **C:** Culture extracts from *A. oryzae* OP12 with accumulation of atromentin (**6**). **D:** Mycelium extractions from *A. niger* ATNT 16 with accumulation of atrofuranic acid (**13**). In **C** and **D** the construct $AtrA_{At(A-T)}:MelA_{(TE)}$ (C2) produces aspulvinone E (**3**) and isoaspulvinone E (#). **E:** Cultures and HPLC profiles of extracts from heterologous expression of *abrA* from *A. brasiliensis* in ATNT16 and OP12. **F:** Homologous overexpression of *abrA* in *A. brasiliensis* and authentic standards of atrofuranic acid (**13**) and atromentin (**6**). For a metabolite screening on *A. brasiliensis* culture extracts refer to **Fig. S5**. All HPLC runs were recorded at 254 nm. **G:** Putative *abrA* containing biosynthesis gene cluster in *A. brasiliensis*.

Figure 5: Phylogenetic tree of thioesterase domains of NRPS-like enzymes from basidiomycetes and *Aspergillus* species. Bootstrap support is shown at the nodes of the tree and enzyme names and enzymatic activity are provided. The originating organism can be

extracted from the colour coding. Black letters with grey background denote atromentin synthetases from the basidiomycetes *Tapinella panuoides* (AtrA), *P. involutus* (InvA5) and *Suillus grevillei* (GreA). Enzymes in green derive from *A. nidulans*, in brown from *A. terreus* and in red from *A. brasiliensis*. The thioesterase domain of the polyketide synthase TerA from *A. terreus* served as outgroup. For protein accession numbers refer to the STAR methods.

Figure 6: Proposed scheme for metabolite biosynthesis. The predicted biosynthetic pathway of atrofuranic acid (**13**) is supported by molecule labelling derived from feeding 2-¹³C-labelled L-tyrosine. The three C-atoms from the two tyrosine side-chains are numbered in red and blue and the ¹³C-labelled C-atoms are indicated by an additional (*). The purple arrow indicates the formation of atromentin (**6**) at the thioesterase domain of atromentin synthetases, which acts as precursor for gyrocyanin that can be further converted into gyroporin (**11**) and involutin as suggested for *P. involutus*. Orange arrows indicate the formation of atrofuranic acid in *Aspergillus* species from section *Nigri*. A subsequent Piancatelli-type rearrangement and decarboxylation results in the formation of gyroporin (**11**). For NMR-data of atrofuranic acid (**13**) refer to the supporting **Fig. S2-4** and **table S2**.

STAR Methods

Contact for reagents and resource sharing

Further information and reasonable requests for resources and reagents should be directed to and will be fulfilled by the Lead Contact, Matthias Brock (Matthias.brock@nottingham.ac.uk). Requests for fungal strains and plasmids will need a material transfer agreement (MTA), if a use is intended.

Experimental model and subject details

The *A. niger* strain FGSC A1144 (Fungal Genetics Stock Center, Manhattan, Kansas, USA) served as parental wild-type strain for generation of the expression platform strains *A. niger* P2 (Gressler *et al.*, 2015) and ATNT16 (Geib and Brock, 2017). *A. niger* strain N402 (also known as ATCC 64974; American Type Culture Collection, Manassas, Virginia, USA) was used as parental strain for generation of the expression platform strain NP4. *A. oryzae* RIB40 (also known as ATCC 42149, American Type Culture Collection) served as parental strain for generating the expression platform strain OP12. In addition, the *A. brasiliensis* strain CBS 101740 (CBS-KNAW Collection, Utrecht, Netherlands) was used in this study. Genotypes of individual transformants and media compositions are listed in the key resource table or table S5. All *Aspergillus* strains were cultivated at 28 °C. Liquid cultures were agitated on a rotary shaker at 150 rpm.

Method details

Preparation of conidia suspensions and selection of fungal transformants

Conidia suspensions were prepared from agar slopes of AMM(-N)G50Gln10 solidified with 2% agar. Slopes were overlaid with 4 ml of phosphate buffered saline (PBS) containing 0.01% Tween 20 and conidia were collected by scrapping cultures with a cotton swab. For inoculation

of media with a defined amount of conidia, suspensions were filtered through a 40 µm cell strainer (Greiner bio-one), washed once with PBS/Tween and counted by use of an improved Neubauer chamber. For selection of *A. niger* transformants either 140 µg/ml hygromycin B, 40 µg/ml phleomycin or 0.1 µg/ml pyrithiamine were used. For selection of *A. oryzae* transformants either 30 µg/ml phleomycin or 0.1 µg/ml pyrithiamine were added. Transformants from *A. brasiliensis* were selected by media supplementation with 0.1 µg/ml pyrithiamine. For transformation of expression platform strains ATNT16 Δ *pyrG*x24 and OP12_*pyrG*⁻ with deleted or disrupted *pyrG* gene the *pyrG* gene from *A. nidulans* FGSC A4 was used as a selection marker and protoplasts were regenerated on media without addition of 10 mM uridine.

Generation of expression platform strains *A. niger* NP4, *A. oryzae* OP12 and *pyrG*⁻ strains

To generate alternative expression platform strains the wild-type strains *A. niger* N402 and *A. oryzae* RIB40 were selected as parental strains. Both strains were transformed with a *PamyB:terR_ptrA* plasmid (Gressler *et al.*, 2015) that contains the *A. terreus* transcriptional regulator gene *terR* under control of the *A. oryzae* amylase promoter *PamyB* and the *ptrA* gene as pyrithiamine resistance marker for selection of transformants. Resulting transformants were checked by Southern blot analysis for single copy integration of the construct, resulting in the selection of *A. niger* NP4 and *A. oryzae* OP12 as alternative expression platform strains. For using the *pyrG* gene from *A. nidulans* as selectable marker in transformation of the expression platform strains *A. niger* ATNT16 and *A. oryzae* OP12, the intrinsic *pyrG* genes were either deleted or disrupted. For generating an OP12 *pyrG* negative strain 1×10^8 conidia were plated on 50 mM HEPES pH 7.0 buffered AMM(-N)G50Gln10 solid medium containing 20 mM uridine and 2 mg/ml fluoroorotic acid (Melford Biolaboratories). Plates were incubated at 28°C

for 7 days and three individual colonies were recovered. Subsequent plating on media with or without 10 mM uridine confirmed uridine auxotrophy of the strains. Genomic DNA was isolated from one of the strains, the *pyrG* gene amplified and sequenced. Sequencing results with P1+P2 (see table S4 for oligonucleotide sequences) confirmed a deletion of 8 bases at position 583-590bp in the *pyrG* coding region. The strain was termed OP12_Δ*pyrG*. For ATNT16 a *pyrG* deletion cassette was generated by amplifying a 1 kb upstream region with oligonucleotides P3+P4 and a 1 kb downstream region with P5+P6. Oligonucleotides contained overlapping sequences to the *KpnI* restriction site of pUC 19 and to the *NotI* excised *ptrA* gene from plasmid *ptrA_pJET1.2*. The three fragments were assembled with the *KpnI* restricted pUC19 vector by *in vitro* recombination. The deletion fragment was excised by *KpnI* restriction and used for transformation of *A. niger* ATNT16 using pyrithiamine as selection marker. Resulting transformants were repeatedly streaked on pyrithiamine containing plates before tested for uridine auxotrophy. Southern blot analysis confirmed that strain ATNT16Δ*pyrG*x24 contained a *pyrG* deletion without ectopic integrations of the deletion construct and was used as *pyrG* negative ATNT16 strain in subsequent studies.

Generation of a URA-blaster cassette for transformation of *pyrG*- expression platform strains

For transformation of *pyrG* negative fungal expression platform strains a URA-blaster cassette was generated. The cassette consisted of a direct repeat of an 800 bp internal *E. coli prpB* fragment flanking the entire *A. nidulans pyrG* gene including its promoter and terminator region. The direct repeats enable excision of the *pyrG* gene by mitotic recombination allowing the marker to be re-used in subsequent transformation approaches. As recipient plasmid for the URA-blaster cassette the *ble*-gene was excised by *NotI* restriction from plasmid pUC-*ble* (Geib and Brock, 2017) leaving a *NotI* restriction site in the resulting pUC_Δ*ble* plasmid. The direct

repeats of the *prpB* gene with overlaps to the *NotI* restriction site of pUC_NotI and the *A. nidulans pyrG* gene were amplified from plasmid pQE30_*prpB* (Brock *et al.*, 2001) with oligonucleotides P7+P8 and P9+P10. A 1900 bp fragment enclosing the *A. nidulans pyrG* gene was amplified from genomic DNA of *A. nidulans* strain FGSC A4 with oligonucleotides P11+P12. The three PCR fragments were mixed with the *NotI*-restricted pUC_NotI plasmid and the URA-blaster cassette was assembled by *in vitro* recombination using the In-Fusion® HD Cloning System (Takara/Clontech). The URA-blaster was excised by *NotI* restriction and used to replace alternative resistance markers in SM-Xpress plasmids.

Generation of expression constructs for production of NRPS-like and chimeric proteins

All PCR amplifications for gene cloning procedures were carried out by using the Phusion Green Hot Start II High-Fidelity DNA Polymerase (ThermoFisher Scientific) in a SpeedCycler² (Analytik Jena). PCR for generation of the mutated *melA_{C→S}* gene producing the amino acid exchange C733S was performed with oligonucleotide pair P13+P14 and P15+P16. Similarly, PCR for generation of the mutated *melA_{N→D}* producing the amino acid exchange N760D was performed with P13+P17 and P18+P19. The chimeric *melA_A:invA5_{T-TE}* construct was assembled by amplifying the *melA* part with P13+P20 and the *invA5* part with P21+P22. The complete *invA5* gene was amplified with P23+P22. Assembly of the respective amplicons in SM-Xpress plasmids was performed by *in vitro* recombination using the In-Fusion® HD Cloning System (Takara/Clontech). For full-length expression of the *melA* gene in *A. oryzae* OP12, the previously generated plasmid his_*melA*-SM-Xpress (Geib *et al.*, 2016) was used for fungal transformation.

For heterologous expression of the *atrA_{At}* gene and gene fusions of *melA* and *atrA_{At}* in *A. niger* ATNT16Δ*pyrG*x24 and *A. oryzae* OP12*pyrG*⁻, PCR was performed on genomic DNA of *A. terreus* wild-type strains SBUG844 and A1156. The full-length *atrA_{At}* gene was amplified with

oligonucleotides P24+P25 and cloned by *in vitro* recombination into the *his*-SM-Xpress_URA plasmid. For the gene fusion construct *mela*_(A):*atrA*_{At(T-TE)} (C1) the *mela* sequence was amplified with oligonucleotides P26+P27 and the *atrA*_{At} sequence with P28+P25. For the gene fusion construct *mela*_(A-T):*atrA*_{At(TE)} (C2) the *mela* sequence was amplified with oligonucleotides P26+P29 and the *atrA*_{At} sequence with P30+P25. Finally, for the gene fusion construct *atrA*_{At(A-T)}:*mela*_(TE) (C2) the *atrA*_{At} sequence was amplified with oligonucleotides P24+P40 and the *mela* sequence with P41+P42.

For heterologous expression of the *abrA* in *A. niger* and *A. oryzae* expression platform strains the gene was amplified from genomic DNA of *A. brasiliensis* CBS101740 using oligonucleotides P31+P32. The resulting PCR fragment was fused by *in vitro* recombination with plasmid *his*_SM-Xpress_*hph* in which the original phleomycin resistance gene was replaced by the hygromycin B resistance cassette *hph*.

For homologous constitutive expression of the *A. brasiliensis* *abrA* gene in *A. brasiliensis* the gene was placed under control of the *gpdA* promoter from *A. nidulans*. The 992 bp promoter region of the *gpdA* gene was amplified with P33+P34 from genomic DNA of *A. nidulans* strain FGSC A4. The *abrA* gene was amplified from genomic DNA of *A. brasiliensis* CBS101740 with P35+P36. Both amplicons were fused by *in vitro* recombination into the *Hind*III (ThermoFisher Scientific) restricted *ptrA*_pJET1.2 plasmid (Fleck and Brock, 2010).

All assembled plasmids were transferred into and propagated in chemically competent *Escherichia coli* DH5 α (Mix & Go!, Zymo Research). Plasmids were purified using the NucleoSpin Plasmid kit (Macherey and Nagel).

Fungal transformation and transformant analysis

Mycelia for protoplast generation were generated by inoculating YEPD media with $2 - 3 \times 10^6$ conidia/ml of the strain to be transformed. After 22 h mycelium was harvested and incubated

for 1 h at 28°C without agitation in citrate-phosphate buffer pH 7.3 containing 10 mM dithiothreitol. Protoplasts were generated in 20 ml potassium phosphate-buffered (pH 5.8) osmotic medium with 0.6 M potassium chloride as osmotic stabiliser and 1.3 g VinoTaste Pro (Novozymes) and 0.1g lysing enzyme (Sigma-Aldrich). Protoplasts were washed and mixed with the respective plasmids and PEG solution (25% PEG8000, 50 mM CaCl₂, 10 mM Tris/HCl pH 7.5) and incubated for 30 min on ice. After transformation protoplasts were regenerated on AMM(-N)G50Gln10 agar plates containing 1.2 M sorbitol as osmotic stabiliser and the respective selection marker (Geib and Brock, 2017).

Transformants were streaked twice onto AMM(-N)G50Gln10 agar containing the respective selectable marker. Genomic DNA from individual transformants was purified using the MasterPure Yeast DNA kit (Epicenter). Transformants carrying the *PamyB:terR* construct for generation of expression platform strains were checked by Southern Blot analysis for single copy integration. All other transformants carrying specific heterologous gene expression constructs were checked either by Southern Blot or diagnostic PCR using Phire Green Hot Start II DNA Polymerase (ThermoFisher Scientific) and oligonucleotides P37+P38 for NRPS-like enzyme genes and P33+P39 for homologous *abrA* overexpression.

Southern Blot analysis

Southern Blots were performed by restriction of genomic DNA with suitable restriction enzymes, separation on a 0.8% agarose gel and transfer of fragments to a positively charged nylon membrane (Amersham Nylon-Hybond⁺, GE Healthcare). Gene specific probes were amplified with Taq DNA Polymerase (NEB) and labelled by incorporation of digoxigenin-11-dUTP (Roche). Hybridisation was performed over night at 65°C and bands were visualised by subsequent hybridisation with anti-digoxigenin-alkaline phosphatase Fab fragments (Roche) and CDPstar (Roche) as substrate.

Heterologous expression and purification of proteins

All NRPS-like enzymes were cloned with an *N*-terminal His-tag peptide. Protein purification followed a protocol as previously described (Geib *et al.*, 2016). In brief, strains were grown in AMM(-N)Starch2%Gln20Talc for 32 - 40 h at 28 °C under constant shaking at 150 rpm. Mycelium was harvested over Miracloth filter gauze (Merck), rinsed with tap water, pressed dry between paper tissues and frozen in liquid nitrogen. The mycelium was ground under liquid nitrogen to a fine powder, suspended in buffer A (50 mM Tris/HCl pH 7.5, 150 mM NaCl and 10% glycerol) and disrupted further by ultrasonication. The cell-free extract and cell debris were separated by centrifugation at 17 000 × *g* and filtered through a 0.45 µm filter (Sartorius). For purification a 3 ml Ni-Sepharose 6 Fast Flow (GE Healthcare) gravity flow column was used. After application of the cell-free extract, the column was washed with 4 volumes of buffer A supplemented with 20 mM imidazole and eluted with buffer A supplemented with 200 mM imidazole. Proteins were desalted by centrifugal concentration (Amicon 15-Ultra, 30 kDa cut-off, Millipore) and stored in 50% glycerol with 1 mM dithiothreitol at -20°C.

***In vitro* assays**

In vitro product formation from NRPS-like enzymes followed a protocol as previously described (Geib *et al.*, 2016) with some minor modifications. Purified proteins (0.5 – 1 mg) or cell-free extract (600 µl; 6 mg total protein) were mixed in a final volume of 5 ml with PIPES buffer pH 7.5 (100 mM), ATP (10 mM), MgCl₂ (15 mM) and 7.5 mM 4-hydroxyphenylpyruvate. Optionally, 3 mM DTT were added to enzymes containing a cysteine residue in the active site of the thioesterase domain. Assays were incubated for 18 h at 28°C in the dark with gentle agitation. For metabolite extraction assays were acidified to pH 3.5 with HCl and incubated for 10 min on ice. Precipitates were collected by centrifugation. Both, pellet

and supernatant, were extracted separately with ethyl acetate. The organic solvent was evaporated under reduced pressure, the residue solved in methanol and analysed by HPLC as described.

Secondary metabolite analysis

For secondary metabolite analysis liquid cultures of AMM(-N)G50Gln10 (*A. niger*) or AMM(-N)Starch2%Gln20 (*A. oryzae*) were inoculated with 1×10^6 conidia/ml. For metabolite extraction from time dependent incubation AMM(-N)G100Gln20 was used. For induction of heterologous gene expression in *A. niger* ATNT16 strains the medium was additionally supplemented with 10 µg/ml doxycycline. After 36 - 48 h or at specifically indicated time points, cultures were harvested and separated into a cell-free culture filtrate and mycelium. Both fractions were extracted with ethyl acetate. The organic solvent layer was collected, dried over anhydrous sodium sulphate and evaporated under reduced pressure. Residual compounds were solved in methanol and subjected to HPLC analysis using a Dionex UltiMate3000 (ThermoFisher Scientific) and an Eclipse XDB-C18 column (4.6 × 150 mm, 5 µm; Agilent) following a gradient (COR_ESIA) of water + 0.1% formic acid (solvent A) and methanol (solvent B) with a flow rate of 1 ml/min: 0.5 min 10% B, 15 min 90% B, 17 min 90% B, 17.5 min 100% B, 22 min 100% B, 23 min 10% B, 25 min 10% B. For more detailed resolution of metabolites obtained from the time dependent extraction of *A. niger* P2 strains expressing the *invA5* gene a modified gradient (COR_ESIA_25-50) was applied at a flow rate of 1 ml/min: 0.5 min 10% B, 1.5 min 25% B, 12 min 50% B, 14 min 90% B, 15 min 100%B, 18 min 100% B, 20 min 10% B, 24 min 10% B.

High-resolution electrospray ionisation mass spectrometry (HR-ESI-MS) was carried out on an Accela UPLC-system combined with an Exactive mass spectrometer (Thermo Scientific). Separation of individual metabolites was achieved by using a Betasil C18 column (2.1 × 150

mm, 3 μm ; Thermo Scientific) with water + 0.1% formic acid (solvent A) and acetonitrile + 0.1% formic acid (solvent B) as solvents. The following solvent gradient at a flow rate of 250 $\mu\text{l}/\text{min}$ was applied: 1 min 5% B, 16 min 98% B, 19 min 98% B, 20 min 5% B.

Isolation and structure elucidation of natural products

Metabolites from P2 *invA5* or ATNT16 *abrA* culture filtrates were purified over a Zorbax RX-C18 column (9.5 \times 250 mm, 5 μm) using an Agilent 1200 equipped with an auto-sampler, DAD and fraction collector. The following gradient of water + 0.1% TFA (A) and methanol (B) with a flowrate of 1.8 ml/min was applied: 0.5 min 25% B, 2 min 35% B, 20 min 40% B, 23 min 90% B, 25 min 100% B, 31 min 100% B, 34 min 25% B, 36 min 25% B. Peaks were automatically collected using slope and threshold parameters.

The 1D and 2D NMR spectra of **11**, **12**, **13** and **14** were recorded at 300 K on a Bruker Avance III spectrometer (Bruker BioSpin) at 500 and 600 MHz for proton and at 125 and 150 MHz for carbon spectra. DMSO-*d*₆ was used as solvent and internal standard. The solvent signals were referenced to δ_{H} 2.49 ppm and δ_{C} 39.5 ppm.

For final structure elucidation of atrofuranic acid (**13**) an acetylation was performed using the following method: pyridine (14 μl , 173.5 μmol) was added slowly to a suspension of **13** (9.1 mg, 26.8 μmol) in acetic anhydride (821 μl , 90.5 mmol) and stirred on ice for 30 min. The temperature was then raised to room temperature and stirred for another 18 h. After addition of 8 ml water, the mixture was transferred to a CHROMABOND® C₁₈ec-column (0.5 g), washed with 16 ml of water and eluted with 16 ml methanol. After evaporation of the solvent a complete triacetylation of **13** was confirmed by HPLC-MS on an Agilent 1260 HPLC system equipped with a C₁₈ column (Zorbax Eclipse XDB, 150 \times 4.6 mm, 5 μm) and coupled to a 6130 Single Quadrupole mass detector by using the following gradient of CH₃CN in H₂O + 0.1%

TFA: initial holding of 30% CH₃CN for 1 min, then increasing from 30 to 100% CH₃CN in 12 min and terminal holding of 100% CH₃CN for 8 minutes.

To obtain ¹³C-labelled atrofuranic acid (**13**), two 50 ml AMM(-N)G100Gln20 cultures of *A. niger* ATNT16 cultures expressing an atromentin synthetase were supplemented with 2.2 mM 2-¹³C-labelled L-tyrosine and incubated for 48 h at 28°C. Labelled atrofuranic acid (**13**) was extracted with ethyl acetate from *A. niger* mycelium. Extracts were dried under reduced pressure, solved in methanol, purified by HPLC as described above and subjected to NMR analyses.

Phylogenetic tree construction

To analyse the phylogenetic relationship of NRPS-like enzymes the thioesterase domain sequences were extracted by InterPro (Finn *et al.*, 2017) using the alpha/beta hydrolase fold (SSF53474) as template. The following NRPS-like protein sequences were used: AtrA from *Tapinella panuoides* (accession no.: B7STY1); InvA from *P. involutus* (accession no.: A0A0S2E7W7.1); GreA from *Suillus grevillei* (accession no.: I6NXV7.1); MicA from *A. nidulans* (accession no.: Q5B7T4.1); TdiA from *A. nidulans* (accession no.: ABU51602.1); BtyA from *A. terreus* (accession no.: AUO29224.1) AtqA from *A. terreus* (accession no.: XP_001210786.1); PgnA from *A. terreus* (accession no.: XP_001217485.1); ApvA from *A. terreus* (accession no.: XP_001211182.1); AtrA_{At} from *A. terreus* (accession no.: MG384315.1); MelA from *A. terreus* (accession no.: KU530117.1); AbrA from *A. brasiliensis* (JGI protein ID Aspbr1 165333). The thioesterase domain of the polyketide synthase TerA from *A. terreus* (accession no.: Q0D1N9) was used as outgroup. The extracted protein domains were aligned using Clustal Omega (Sievers and Higgins, 2018) and assemblies were used for tree calculations with IQ-Tree by identifying the optimal tree building algorithm resulting in a model with the highest likelihood (Kalyaanamoorthy *et al.*, 2017). Bootstrap support was

calculated by the ultrafast bootstrap approximation UFBoot2 implemented in IQ-Tree (Hoang *et al.*, 2018). The results were plotted by using iTOL (Letunic and Bork, 2016).

Quantification and statistical analysis

Does not apply.

Data and software availability

No datasets or software was generated.

Additional resources

No new website/forum was generated. This study did not include a clinical trial.

Supplementary item titles

Figure S1 - Related to Figure 3: Time dependent extraction of (A) culture filtrates and (B) mycelium from heterologous *invA5* and *abrA* expression in the *A. niger* NP4 strain and *abrA* expression in *A. niger* ATNT16 strain. (C) *In vitro* assay with cell-free extract of an *invA5* expressing *A. niger* strain and 4-hydroxyphenylpyruvate as substrate. Minor amounts of atrofuranic acid (13) derive from the cell extract. Atromentin (6) is produced as the dominating metabolite. (D) *In vitro* assay with purified *AbrA* protein resulting in the production of atromentin (6). HPLC files were recorded with COR_ESIa method at 254 nm.

Figure S2 - Related to Figure 3: ^1H NMR spectrum of **13** (A), ^{13}C -labelled **13** (B) and **14** (C) in $\text{DMSO-}d_6$. D: ^1H , ^1H COSY NMR spectrum of **13** in $\text{DMSO-}d_6$

Figure S3 - Related to Figure 3: ^1H decoupled ^{13}C NMR spectrum of **13** (A), ^{13}C -labelled **13** (B) and **14** (C) in $\text{DMSO-}d_6$

Figure S4 - Related to Figure 3: ^1H , ^{13}C HSQC (red) and HMBC (blue) NMR spectrum of **13** (A), ^{13}C -labelled **13** (B) and **14** (= acetylated **13**) (C) in $\text{DMSO-}d_6$.

Figure S5 - Related to Figure 4: Culture filtrate extracts of *A. brasiliensis* in comparison to authentic atromentin and atrofuranic acid standards

Table S1 - Related to Figure 3: NMR data for **12** in $\text{DMSO-}d_6$. COSY correlations are shown as bold bonds. HMBC correlations are shown as arrows.

Table S2 - Related to Figure 3: NMR data for **13** in $\text{DMSO-}d_6$. COSY correlations are shown as bold bonds. Key HMBC correlations are shown as arrows.

Table S3 - Related to Figure 3: NMR data for **14** in $\text{DMSO-}d_6$. Key HMBC correlations are shown as arrows.

Table S4 - Related to STAR methods: Oligonucleotides used in this study.

Table S5 - Related to STAR methods: Media used in this study.

Figure 1

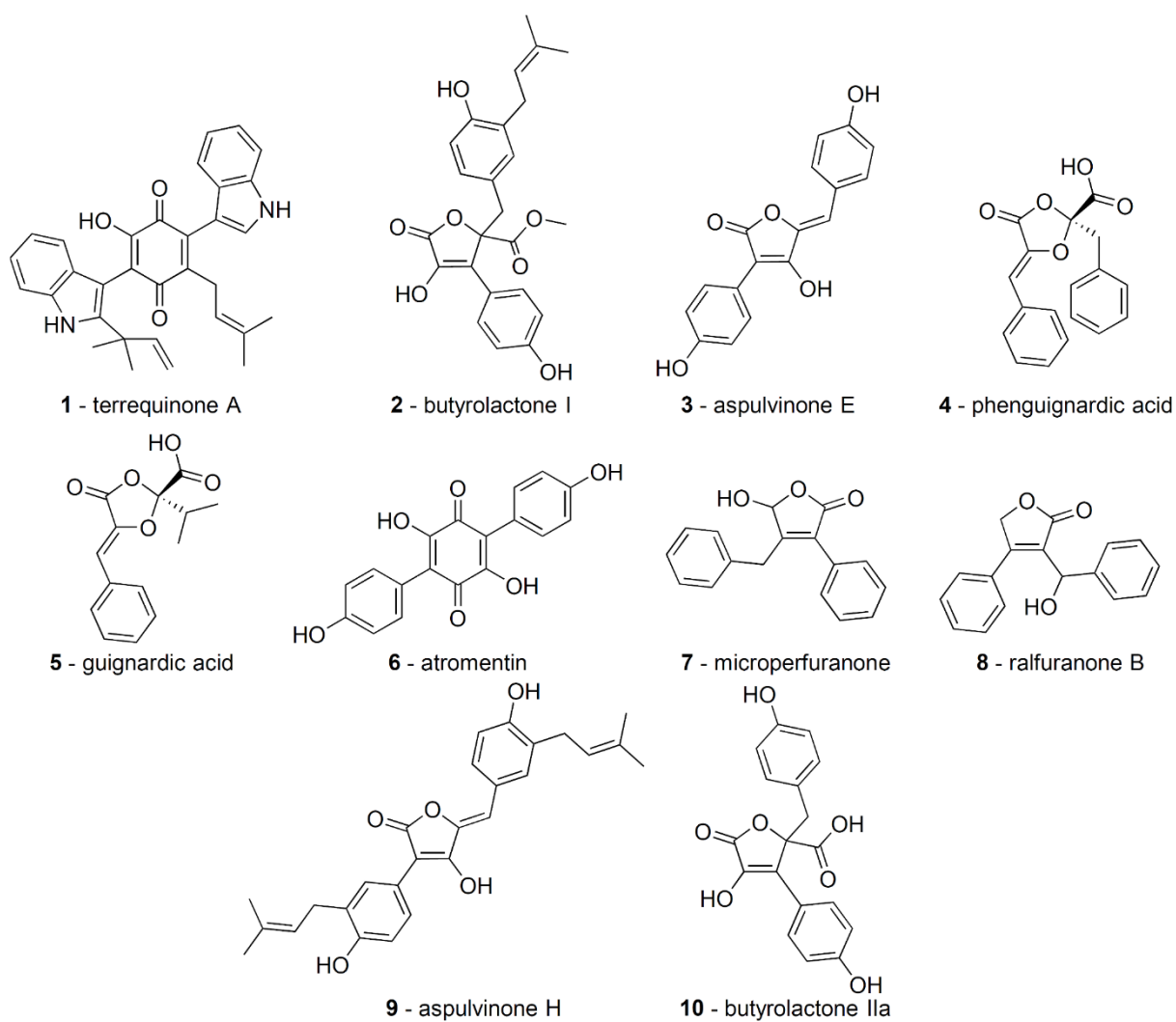


Figure 3

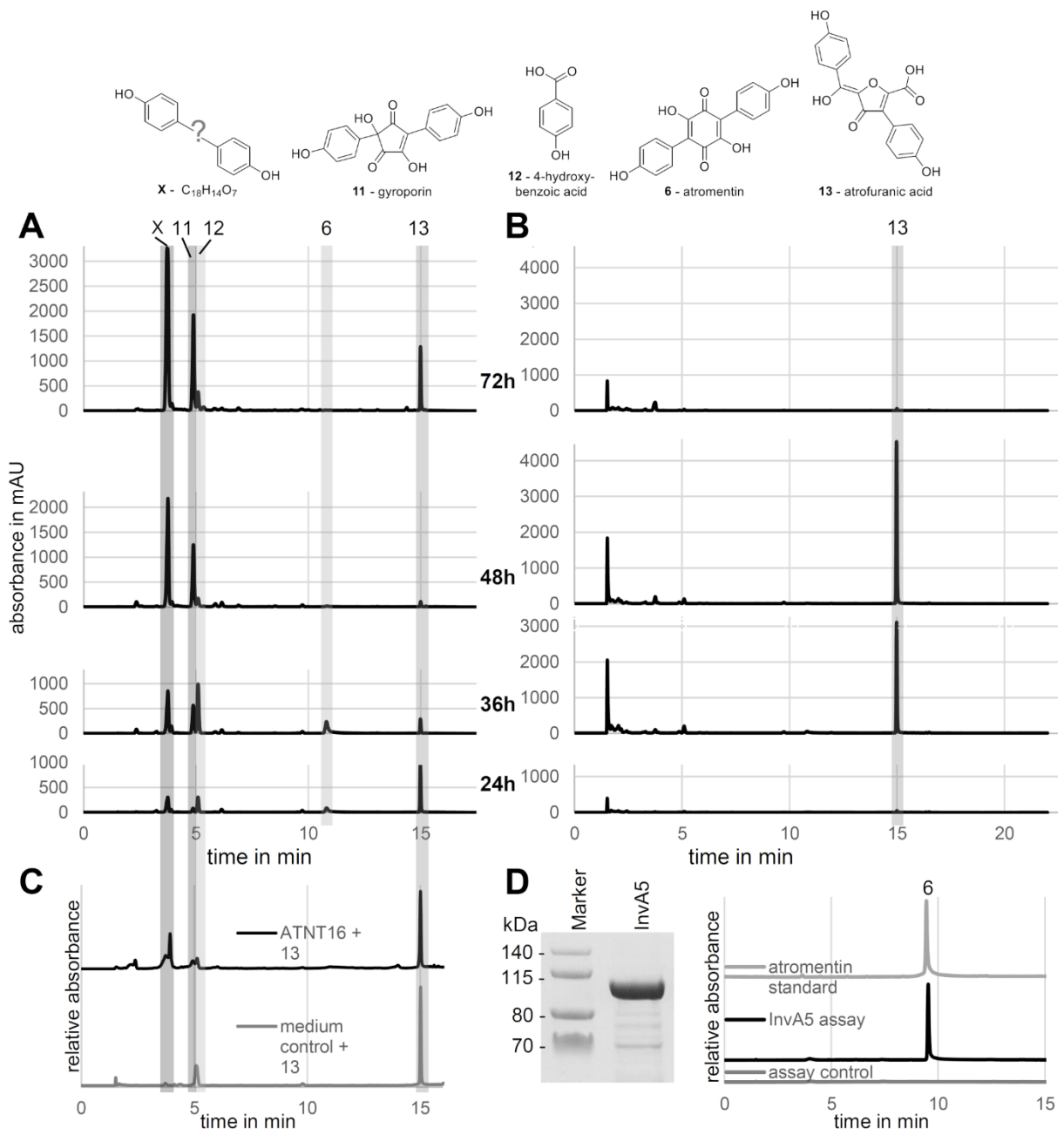


Figure 4

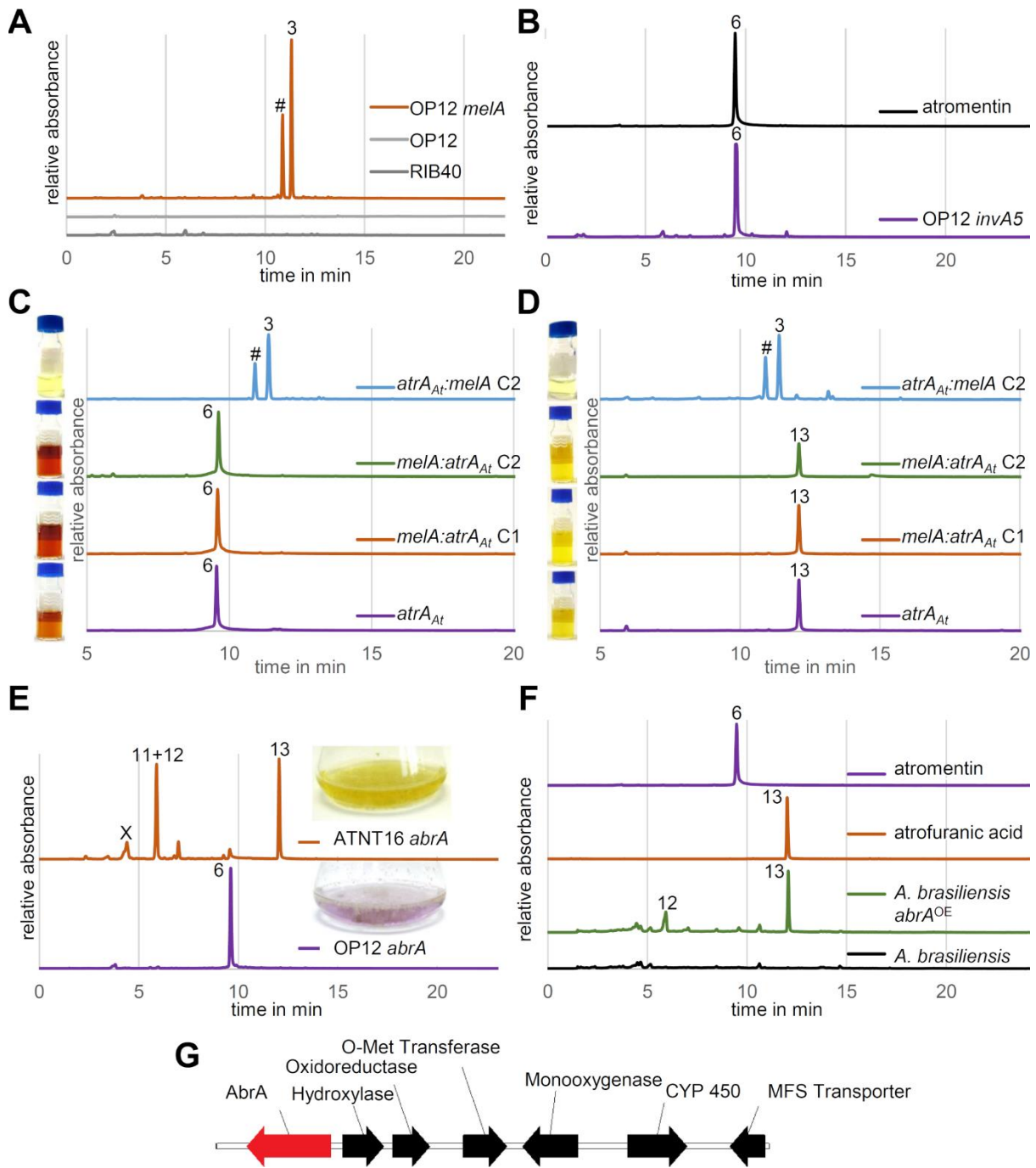


Figure 5

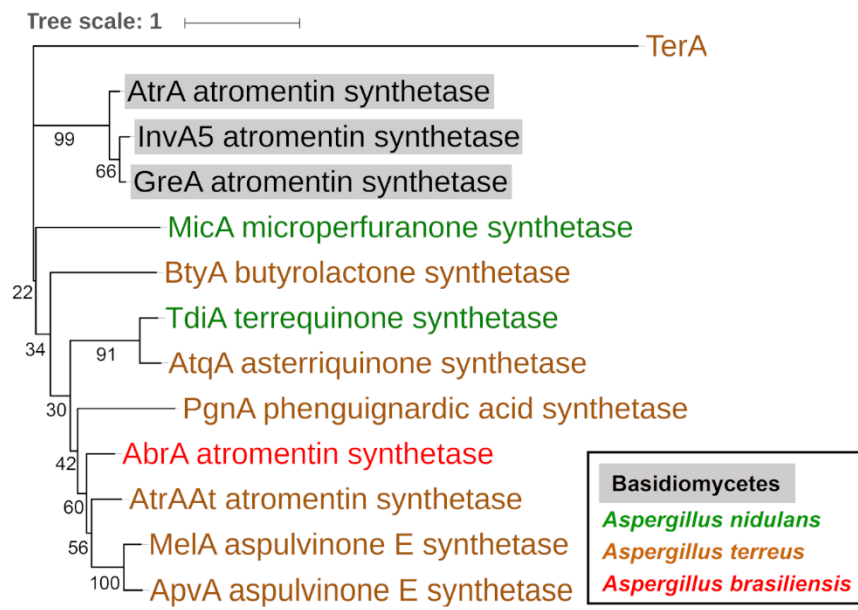
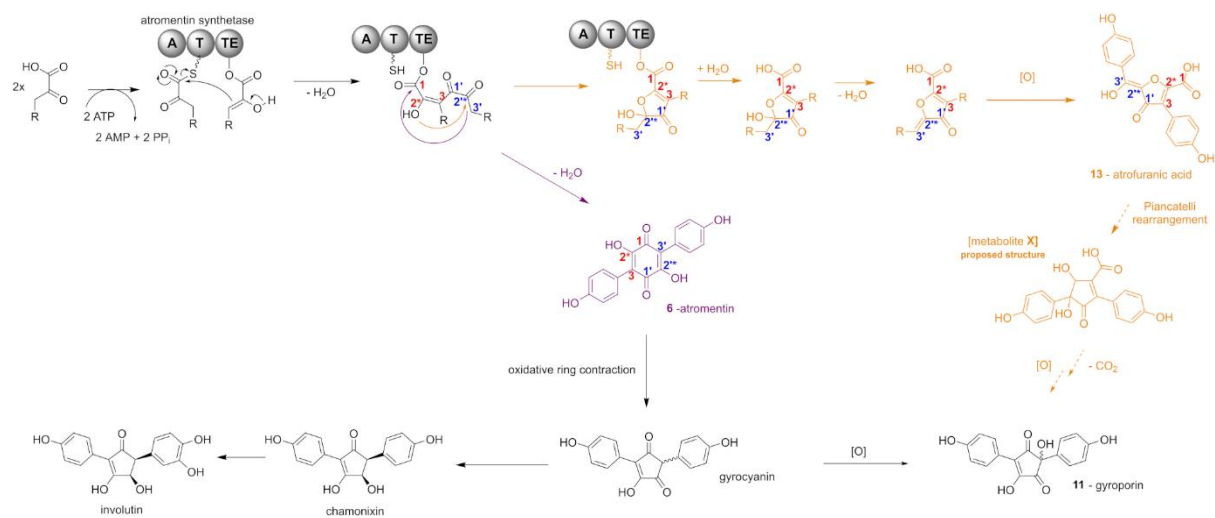
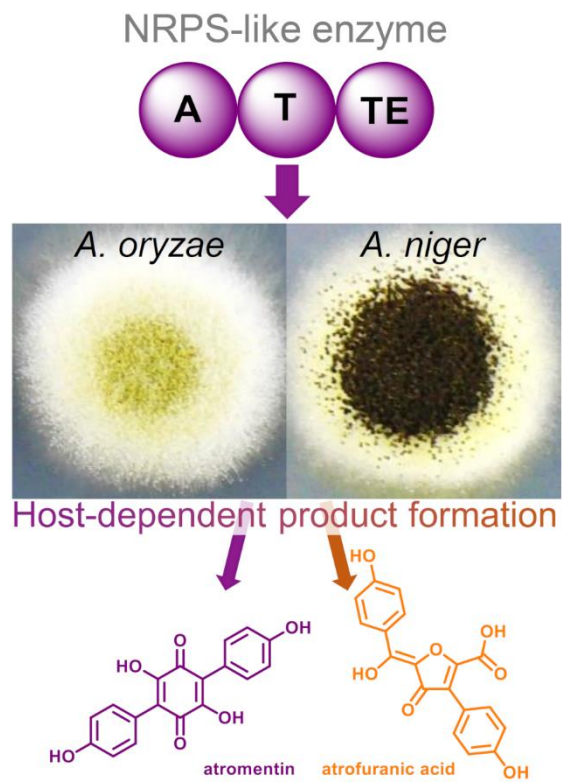


Figure 6



Graphical abstract



eTOC

Geib et al investigated core structure formation by thioesterase domains of fungal NRPS-like enzymes. Exchange of thioesterase domains alters product formation, but requires close phylogenetic relationship of donor and acceptor. Product formation further depends on expression hosts with furanic acid rather than quinone core formation in aspergilli from section *Nigri*.

Highlights

- The product spectrum of NRPS-like enzymes depends on the expression platform
- Cross-chemistry occurs on quinone core structures in aspergilli from section *Nigri*
- Cross-chemistry produces novel metabolites such as atrofuranic acid
- Identification of an atromentin synthetase from *Aspergillus brasiliensis*

KEY RESOURCES TABLE

REAGENT or RESOURCE	SOURCE	IDENTIFIER
Bacterial and Fungal Strains		
<i>E. coli</i> DH5 α	Zymo Research	Zymo 5 α
<i>A. niger</i> A1144 P2 (<i>PamyB:terR_ptrA</i>)	(Gressler <i>et al.</i> , 2015)	N/A
<i>A. niger</i> P2 <i>melA</i> (<i>PterA:melA_ble</i>)	(Geib <i>et al.</i> , 2016)	N/A
<i>A. niger</i> P2 <i>melA</i> _{C\rightarrowS} (<i>PterA:melA</i> _{C\rightarrowS} <i>_ble</i>)	This study	N/A
<i>A. niger</i> P2 <i>melA</i> _{N\rightarrowD} (<i>PterA:melA</i> _{N\rightarrowD} <i>_ble</i>)	This study	N/A
<i>A. niger</i> P2 <i>melA</i> _{A:invA5} _{T-TE} (<i>PterA:melA</i> _{A:invA5} _{T-TE} <i>_ble</i>)	This study	N/A
<i>A. niger</i> ATNT16 (<i>TetOn:terR_ble</i>)	(Geib and Brock, 2017)	N/A
<i>A. niger</i> ATNT16 Δ <i>pyrG</i> _{X24} (<i>TetOn:terR_ble</i> ; Δ <i>pyrG::ptrA</i>)	This study	N/A
<i>A. niger</i> N402	American Type Culture Collection	N402
<i>A. niger</i> N402 NP4 (<i>PamyB:terR_ptrA</i>)	This study	N/A
<i>A. niger</i> NP4 <i>invA5</i> (<i>PterA:invA5_ble</i>)	This study	N/A
<i>A. niger</i> P2 <i>invA5</i> (<i>PterA:invA5_ble</i>)	This study	N/A
<i>A. oryzae</i> RIB40	American Type Culture Collection	RIB40
<i>A. oryzae</i> RIB40 OP12 (<i>PamyB:terR_ptrA</i>)	This study	N/A
<i>A. oryzae</i> RIB40 OP12 _{<i>pyrG</i>} (<i>PamyB:terR_ptrA</i> ; <i>pyrG</i> ⁻)	This study	N/A
<i>A. oryzae</i> OP12 <i>melA</i> (<i>PterA:melA_ble</i>)	This study	N/A
<i>A. oryzae</i> OP12 <i>invA5</i> (<i>PterA:invA5_ble</i>)	This study	N/A
<i>A. brasiliensis</i> CBS101740	CBS-KNAW Collection	CBS101740
<i>A. niger</i> ATNT16 <i>abrA</i> (<i>PterA:abrA_hph</i>)	This study	N/A
<i>A. oryzae</i> OP12 <i>pyrG abrA</i> (<i>PterA:abrA_URA</i>)	This study	N/A
<i>A. brasiliensis</i> OE <i>abrA</i> (<i>PgpdA:abrA_ptrA</i>)	This study	N/A
Chemicals, Peptides, and Recombinant Proteins		
VinoTaste Pro	Novozymes	Free sample
Lysing enzyme from <i>Trichoderma harzianum</i>	Sigma Aldrich	Cat#L1412
DMSO- <i>d</i> ₆	Deutero	Cat#00905-10ml
4-Hydroxylphenylpyruvic acid	Sigma Aldrich	Cat#114286
Taq DNA Polymerase	New England BioLabs	Cat#M0273S
Phusion Green Hot Start II High-Fidelity DNA Polymerase	ThermoFisher Scientific	Cat#F537S
Phire Green Hot Start II DNA Polymerase	ThermoFisher Scientific	Cat#F124L
digoxigenin-11-dUTP	Sigma Aldrich	Cat#11093088910
anti-digoxigenin-alkaline phosphatase Fab fragments	Sigma Aldrich	Cat#11093274910
CDPstar	Sigma Aldrich	Cat#12041677001
Soluble Starch	Fisher Scientific	Cat#DF0178-17-7
Acetic anhydride puriss. p.a., ACS Reag.	Fluka	Cat#45830
Pyridin, EMSURE® ACS Reag.	Merck	Cat#1.09728.0500
Critical Commercial Assays		
In-Fusion® HD Cloning System	Takara/Clontech	Cat#639647
MasterPure Yeast DNA kit	Epicenter	Cat#MPY80200
Mix & Go!	Zymo Research	Cat#T3001
Oligonucleotides		
	See table S4	
Recombinant DNA		
<i>PamyB:terR_ptrA_pUC19</i>	(Gressler <i>et al.</i> , 2015)	N/A
SM-Xpress	(Gressler <i>et al.</i> , 2015)	N/A

<i>his</i> _SM-Xpress	(Geib <i>et al.</i> , 2016)	N/A
<i>his</i> _SM-Xpress_ <i>hph</i>	This study	N/A
<i>PterA:his_melA_ble</i> _SM-Xpress	(Geib <i>et al.</i> , 2016)	N/A
<i>PterA:his_melA_{C→S}_ble</i> _SM-Xpress	This study	N/A
<i>PterA:his_melA_{N→D}_ble</i> _SM-Xpress	This study	N/A
<i>PterA:his_melA_{A:invA5_{T-TE}}_ble</i> _SM-Xpress	This study	N/A
<i>PterA:his_invA5_ble</i> _SM-Xpress	This study	N/A
<i>PterA:abrA_his</i> _SM-Xpress_ <i>hph</i>	This study	N/A
<i>PterA:abrA_his</i> _SM-Xpress_URA blaster	This study	N/A
pJET1.2/blunt (CloneJET)	ThermoFisher Scientific	Cat#K1232
<i>ptrA</i> _pJET1.2	(Fleck and Brock, 2010)	N/A
<i>ble</i> _pUC19	(Geib and Brock, 2017)	N/A
<i>PgpdA:abrA_ptrA</i> _pJET1.2	This study	N/A
Software and Algorithms		
ChemStation version Rev. B. 04. 03 [16]	Agilent	N/A
Chromeleon version 7.2	ThermoFisher Scientific	N/A
TopSpin version 3.5pl7	Bruker BipSpin	www.bruker.com/service/support-upgrades/software-downloads/nmr/free-topspin-processing/free-topspin-download.html
Other		
Dionex UltiMate3000	ThermoFisher Scientific	N/A
Eclipse XDB-C18 (4.6 × 150 mm, 5 μm)	Agilent	N/A
Agilent 1200 HPLC with autosampler, DAD and fraction collector	Agilent	N/A
EASYstrainer 40 μm	Greiner bio-one	Cat#542040
Amersham Nylon-Hybond ⁺	GE Healthcare	Cat#RPN303 B
SpeedCycler ²	Analytik Jena	N/A
Miracloth	VWR	Cat#475855-1
Amicon 15-Ultra, 30 kDa cut-off	Merck	Cat#UFC803 024
CHROMABOND C ₁₈ ec-column (0.5g)	MACHERY-NAGEL	Cat#730014
Bruker Avance III spectrometer 500Mhz	Bruker	N/A
Bruker Avance III spectrometer 600Mhz	Bruker	N/A

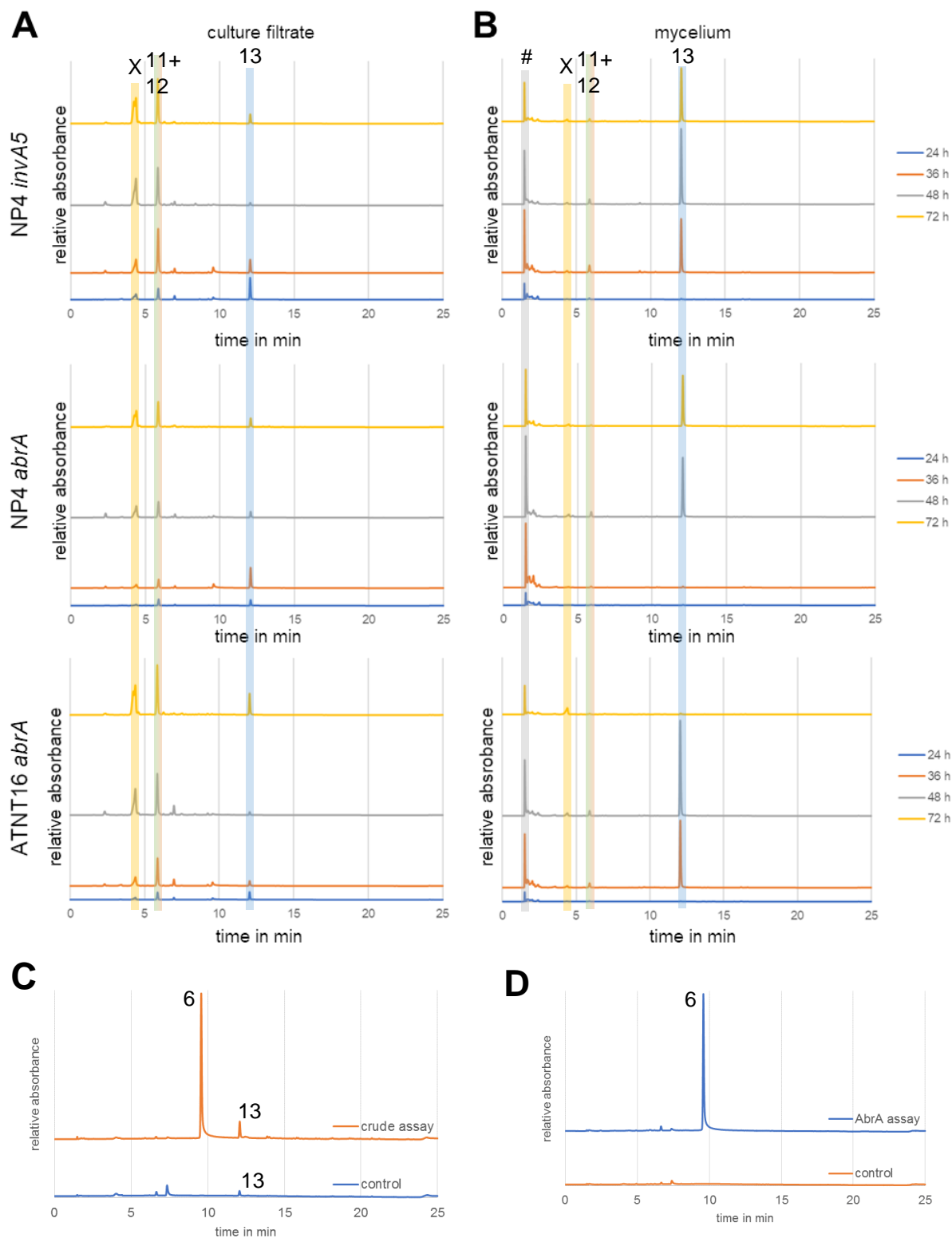


Figure S1 - Related to Figure 3: Time dependent extraction of (A) culture filtrates and (B) mycelium from heterologous *invA5* and *abrA* expression in the *A. niger* NP4 strain and *abrA* expression in *A. niger* ATNT16 strain. (C) *In vitro* assay with cell-free extract of an *invA5* expressing *A. niger* strain and 4-hydroxyphenylpyruvate as substrate. Minor amounts of atrofuranic acid (13) derive from the cell extract. Atromentin (6) is produced as the dominating metabolite. (D) *In vitro* assay with purified AbrA protein resulting in the production of atromentin (6). HPLC files were recorded with COR_ESIa method at 254 nm.

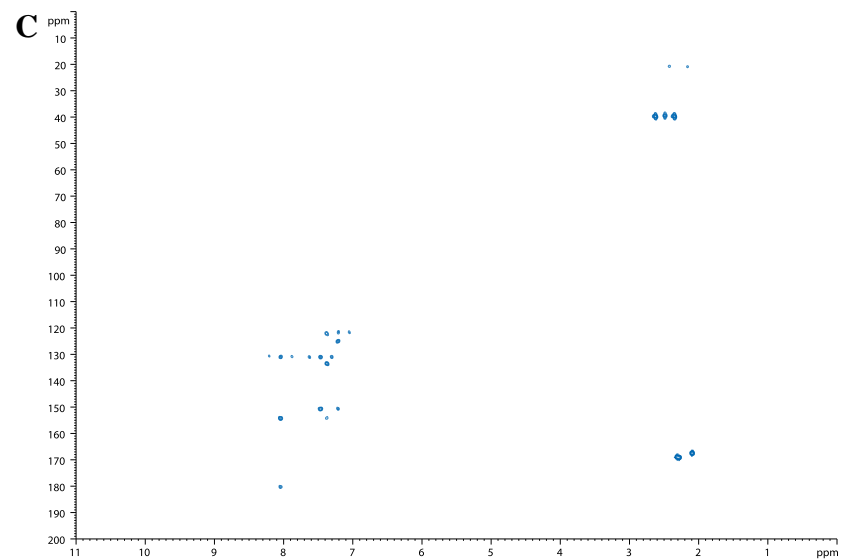
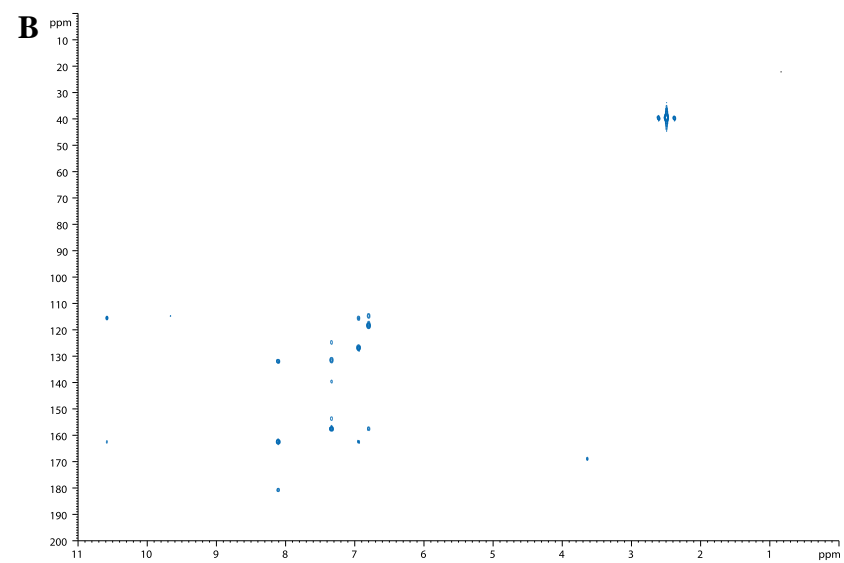
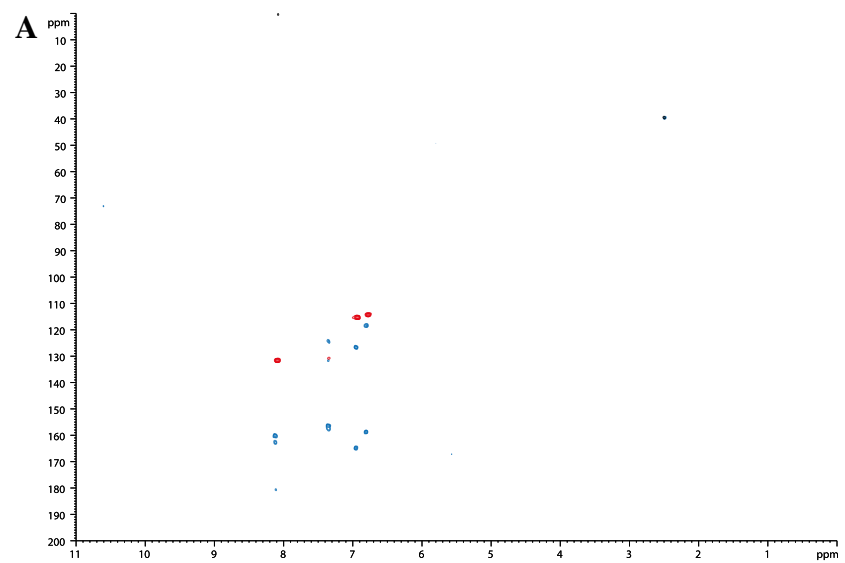


Figure S4 - Related to Figure 3: ^1H , ^{13}C HSQC (red) and HMBC (blue) NMR spectrum of **13** (A), ^{13}C -labelled **13** (B) and **14** (= acetylated **13**) (C) in $\text{DMSO-}d_6$.

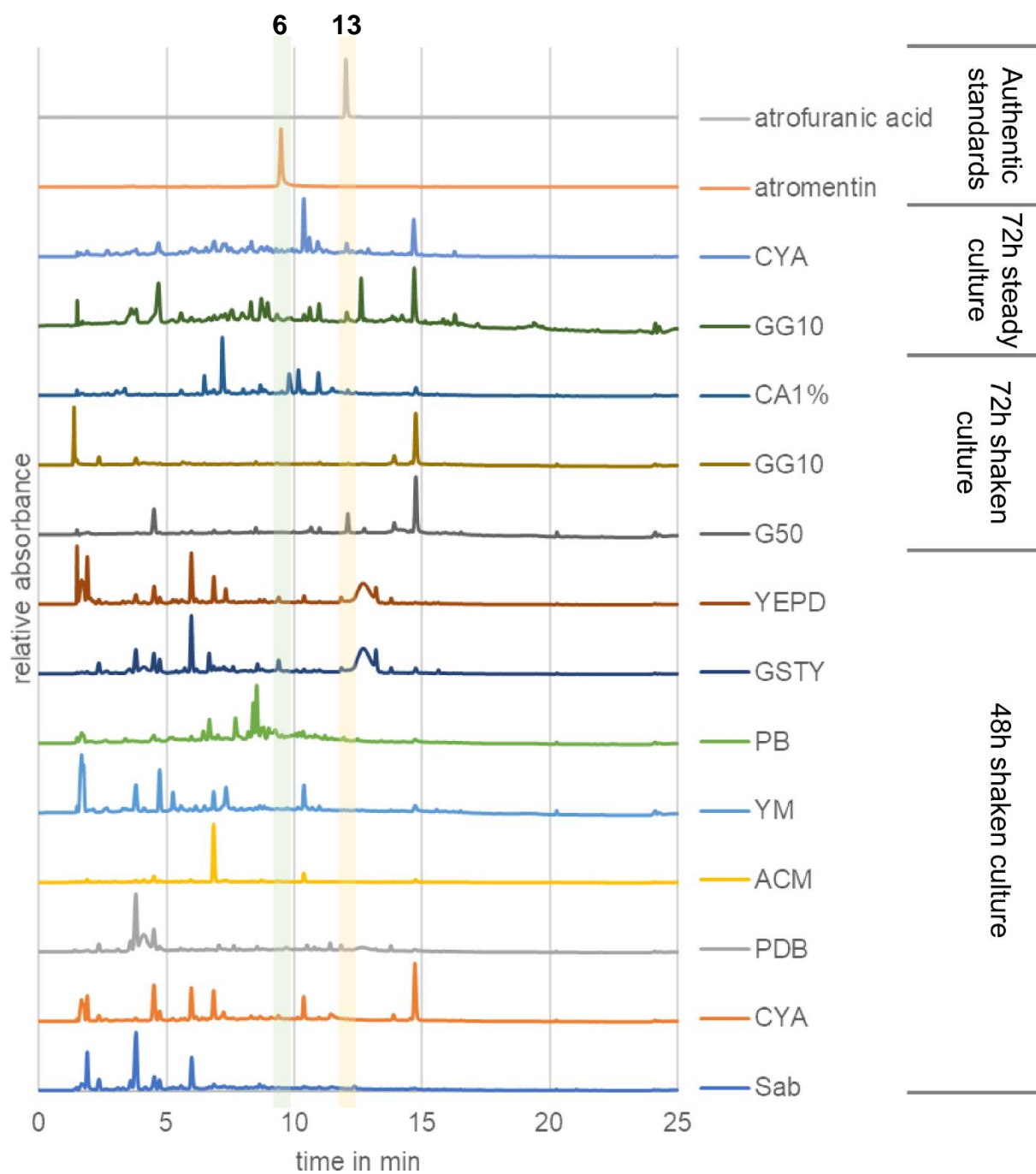
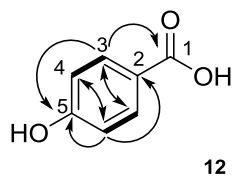


Figure S5 - Related to Figure 4: Culture filtrate extracts of *A. brasiliensis* in comparison to authentic atromentin (**6**) and atrofuranic acid (**13**) standards.

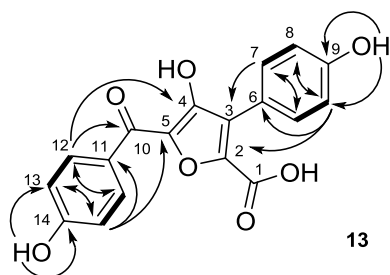
Table S1 - Related to Figure 3: NMR data for **12** in DMSO-d₆. COSY correlations are shown as bold bonds. HMBC correlations are shown as arrows.



Position	δ_C , type	δ_H , M (J in Hz)	COSY ^a	HMBC ^b
1	167.2, C			
2	121.3, C			
3	131.5, CH	7.77, d (8.7)	4	1, 3, 5
4	115.1, CH	6.81, d (8.7)	3	2, 4, 5
5	161.6, C			

^a COSY correlations are from proton(s) stated to the indicated proton. ^b HMBC correlations, optimized for 7.7 Hz, are from proton(s) stated to the indicated carbon.

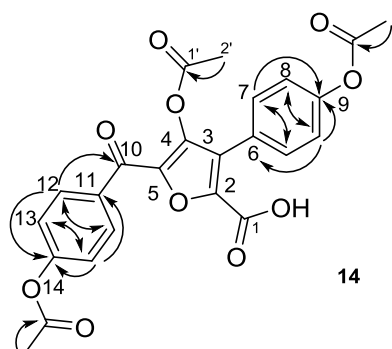
Table S2 - Related to Figure 3: NMR data for **13** in DMSO-d₆. COSY correlations are shown as bold bonds. Key HMBC correlations are shown as arrows.



Position	δ_C , type	δ_H , M (J in Hz)	COSY ^a	HMBC ^b
1	166.8, C ^c			
2	153.8, C / 139.9, C ^d			
3	124.5, C			
4	180.6, C			
5	159.6, C / 135.7, C ^d			
6	118.5, C			
7	131.4, CH ^e	7.35, d (8.6)	8	2, 3, 7, 8, 9
8	114.6, CH ^e	6.81, d (8.6)	7	2, 6, 7, 8, 9
9	157.5, C			
9-OH	-	9.67, s ^c		8, 9
10	180.6, C			
11	126.7, C			
12	131.9, CH ^e	8.12, d (8.8)	13	10, 12, 13, 14
13	115.6, CH ^e	6.95, d (8.8)	12	5, 11, 12, 13, 14
14	162.5, C			
14-OH	-	10.58, s ^c		13, 14

^a COSY correlations are from proton(s) stated to the indicated proton. ^b HMBC correlations, optimized for 7.7 Hz, are from proton(s) stated to the indicated carbon. ^c Chemical shifts were deduced from the NMR spectra of the labelled compound. ^d The different chemical shifts correspond to isomers of the compound. ^e Signal refers to two magnetically equivalent carbons.

Table S3 - Related to Figure 3: NMR data for **14** in DMSO-d₆. Key HMBC correlations are shown as arrows.



Position	δ_C , type	δ_H , M (<i>J</i> in Hz)	HMBC ^a
1	n.d.		
2	142.1, C		
3	126.7, C		
4	158.8, C		
5	n.d.		
6	125.0, C		
7	130.8, CH ^b	7.47, d (8.6)	7, 9
8	121.6, CH ^b	7.22, d (8.6)	6, 8, 9
9	150.7, C		
10	180.2, C		
11	133.4, C		
12	130.9, CH ^b	8.05, d (8.7)	10, 12, 14
13	122.3, CH ^b	7.38, d (8.7)	11, 13, 14
14	154.3, C		
1'	167.5, C		
2'	20.0, CH ₃	2.10, s	1'
1''	168.9, C		
2''	20.9, CH ₃	2.31, s	1''
1'''	169.1, C		
2'''	20.9, CH ₃	2.29, s	1'''

^a HMBC correlations, optimized for 7.7 Hz, are from proton(s) stated to the indicated carbon.

^b Signal refers to two magnetically equivalent carbons.

Table S4 - Related to STAR methods: Oligonucleotides used in this study.

primer#	Sequence (5' – 3')	construct
1	CAGGCGGAGAAACGTGTGG	<i>A. ory pyrG</i>
2	GAGCACCAAATGGTGGCTAG	<i>A. ory pyrG</i>
3	GTGAATTCGAGCTCGGTACCCCTGCAGCTCTGTCATTGC	<i>A. nig ΔpyrG</i>
4	GTATAATACGCGGCCGCGTGTGATGGAGGGGTTAATG	<i>A. nig ΔpyrG</i>
5	CGTAATCAAGCGGCCGCGGAGGATCGAAGTTCTGATGG	<i>A. nig ΔpyrG</i>
6	CTAGAGGATCCCCGGGTACCGCTGTCCCCTTAAAGAGGC	<i>A. nig ΔpyrG</i>
7	CTCGGTACCCGCGGCCGCGCAGATTGTTGGCACCATC	<i>URA blaster</i>
8	CAGGTTGTCGAGCTTCTCTTC	<i>URA blaster</i>
9	GCAGATTGTTGGCACCATC	<i>URA blaster</i>
10	GAGGATCCCCGCGGCCGCGCAGGTTGTCGAGCTTCTCTTC	<i>URA blaster</i>
11	GAAGCTCGACAACCTGCATGGTGTCTCTCGTCCGC	<i>URA blaster</i>
12	GTGCCAACAACTCTGCGGAACCTGACTACTACAATGTTG	<i>URA blaster</i>
13	CATCACAGCACCATGCATCACCATCACCATCACCAACCAAGCCTTATCCCTC	<i>melA_C→S</i>
14	CAAACGCCAACATCGACCCATAGGAATAGCC	<i>melA_C→S</i>
15	ACGGACCATACGCTCTCGCCGGCTATTCCTATGGG	<i>melA_C→S</i>
16	ATCACTGCTGCCATGGTTACATGCCCTCTCAGCAAG	<i>melA_C→S</i>
17	GAGGTAGATCGAAAGACCCGAC	<i>melA_N→D</i>
18	GTCGGGTCTTTCGATCTACCTC	<i>melA_N→D</i>
19	TGAAATCACTGCTGCTTACATGCCCTCTCAGCAAG	<i>melA_N→D</i>
20	GGAGAGCTTACCCAGGGTCG	<i>melA:invA5</i>
21	CTGGGTAAGCTCTCCAGGGCTCGTCTC	<i>melA:invA5</i>
22	ATCACTGCTGCCATGGTTACAGACCACGAGCTTCGAG	<i>invA5</i>
23	CATCACAGCACCATGGGCAGCAGCCATCATCATCATC	<i>invA5</i>
24	CATCACCATCACCATGGATCTTTCAAGAACCTCCAACAGC	<i>atrA_{At}</i>
25	CTGCTGTTATCCATGGCTAAATTCCTTCCAAAC	<i>atrA_{At}</i>
26	CATCACCATCACCATGGACAACCAAGCCTTATCCCTC	<i>melA</i>
27	CCGGGAGAGCTTACCCAG	<i>melA C1</i>
28	GGTAAGCTCTCCGGTCTAGTATCAAGGCAAGCTACG	<i>atrA C1</i>
29	CTCGGAACCGTGGTGTTC	<i>melA C2</i>
30	CACCACGGTTCGCGAGCTCAGCGCCGCGCTGCA	<i>atrA C2</i>
31	CATCACCATCACCATGGATCATTTGCCAATCTTACTGTATTC	<i>abrA</i>
32	AATCACTGCTGTTATCCATGGTCAAATTCCTTGCATCTAGTG	<i>abrA</i>
33	GAGGTTTAGAGCAAGCTTCCTTATTCGTTGACCTAGC	<i>AnPgpDA</i>
34	AAATGACATTGTGATGTCTGCTCAAGC	<i>AnPgpDA</i>
35	GACATACAATGTCATTTGCCAATCTTACTG	<i>abrA</i>
36	CTCAGTTTCCTGAAGCTTCTCTACGGTATGCGAGGAAC	<i>abrA</i>
37	CCTCCAAGAGAGATCCAGAC	<i>PterA</i>
38	GAATTTTACCAGTGGCCTAGG	<i>TtrpC</i>
39	CCTGGATAGAACTCTTCTGC	<i>abrA</i>
40	TTCGCGGACCGTGGTGTTC	<i>atrA_{At} (A+T)</i>
41	ACCACGGTCCGCGAACTTGCCGCTGCACTGGAC	<i>melA (TE)</i>
42	CTGCTGTTATCCATGGTTACATGCCCTCTCAGCAAG	<i>melA (TE)</i>

Table S5 - Related to STAR methods: Media used in this study.

Minimal media	
AMM(-N)	0.52 g/l KCl, 0.52 g/l MgSO ₄ × 7 H ₂ O, 1.52 g/l KH ₂ PO ₄ ; 1 ml/l 1000× Hutner's trace elements; pH 6.5
G50Gln10	50 mM glucose and 10 mM glutamine
G50Gln10S1.2	50 mM glucose, 10 mM glutamine and 1.2 M sorbitol
G100Gln20	100 mM glucose and 20 mM glutamine
Starch2%Gln20	2% soluble starch and 20 mM glutamine
Starch2%Gln20Talc	2% soluble starch and 20 mM glutamine, 10 g/l talc
CA1%	1% casamino acids
AMM(-N)	6 g/l NaNO ₃ , 0.52 g/l KCl, 0.52 g/l MgSO ₄ × 7 H ₂ O, 1.52 g/l KH ₂ PO ₄ ; 1 ml/l 1000× Hutner's trace elements; pH 6.5
G50	
Complex media	
YEPD	20 g/l peptone, 10 g/l yeast extract, 5 g/l glucose
YM	3 g/l yeast extract, 3 g/l malt extract, 5 g/l meat peptone; pH 6.6
GSTY	30 g/l glucose, 2.5 g/l soytone, 0.5 g/l yeast extract, 1 g/l KH ₂ PO ₄ , 1 g/l MgSO ₄ × 7 H ₂ O, 0.5 g/l NaCl, 0.5 g/l CaCl ₂ × 2 H ₂ O, 2 mg/l FeCl ₃ × 2 H ₂ O, 2 mg/l ZnSO ₄ × 7 H ₂ O; pH 5.5
PB	20 g/l potato broth; pH 6.5
CYA	3 g/l NaNO ₃ , 5 g/l yeast extract, 30 g/l sucrose, 1.3 g/l K ₂ HPO ₄ × 3 H ₂ O, 0.5 g/l MgSO ₄ × 7 H ₂ O, 0.5 g/l KCl, 10 mg/l FeSO ₄ × 7 H ₂ O, 5 mg/l CuSO ₄ × 5 H ₂ O, 5 mg/l ZnSO ₄ × 7 H ₂ O; pH 6.5
Sab	10 g/l peptone, 20 g/l glucose; pH 6.5
ACM	10 g/l glucose, 1 g/l yeast extract, 2 g/l peptone, 1 g/l casamino acids, 0.075 g/l adenine, 10 ml/l vitamin solution (400 mg/l <i>p</i> -aminobenzoic acid, 50 mg/l thiamine HCl, 2 mg/l biotin, 100 mg/l nicotinic acid, 250 mg/l pyridoxine HCl, 1.4 g/l choline chloride, 100 mg/l riboflavin), 20 ml/l salt solution (26 g/l KCl, 26 g/l MgSO ₄ × 7 H ₂ O, 76 g/l KH ₂ PO ₄), 200 µl/l trace element solution (40 mg/l Na ₂ B ₄ O ₇ × 10 H ₂ O, 800 mg/l CuSO ₄ × 5 H ₂ O, 800 mg/l FePO ₄ × H ₂ O, 800 mg/l MnSO ₄ × 4 H ₂ O, 800 mg/l NaMoO ₄ × 2 H ₂ O, 8 g/l ZnSO ₄); pH 6.5

Supplementary item titles

Figure S1 - Related to Figure 3: Time dependent extraction of (A) culture filtrates and (B) mycelium from heterologous *invA5* and *abrA* expression in the *A. niger* NP4 strain and *abrA* expression in *A. niger* ATNT16 strain. (C) *In vitro* assay with cell-free extract of an *invA5* expressing *A. niger* strain and 4-hydroxyphenylpyruvate as substrate. Minor amounts of atrofuranic acid (13) derive from the cell extract. Atromentin (6) is produced as the dominating metabolite. (D) *In vitro* assay with purified *AbrA* protein resulting in the production of atromentin (6). HPLC files were recorded with COR_ESIa method at 254 nm.

Figure S2 - Related to Figure 3: ^1H NMR spectrum of **13** (A), ^{13}C -labelled **13** (B) and **14** (C) in $\text{DMSO-}d_6$. D: ^1H , ^1H COSY NMR spectrum of **13** in $\text{DMSO-}d_6$

Figure S3 - Related to Figure 3: ^1H decoupled ^{13}C NMR spectrum of **13** (A), ^{13}C -labelled **13** (B) and **14** (C) in $\text{DMSO-}d_6$

Figure S4 - Related to Figure 3: ^1H , ^{13}C HSQC (red) and HMBC (blue) NMR spectrum of **13** (A), ^{13}C -labelled **13** (B) and **14** (= acetylated **13**) (C) in $\text{DMSO-}d_6$.

Figure S5 - Related to Figure 4: Culture filtrate extracts of *A. brasiliensis* in comparison to authentic atromentin and atrofuranic acid standards

Table S1 - Related to Figure 3: NMR data for **12** in $\text{DMSO-}d_6$. COSY correlations are shown as bold bonds. HMBC correlations are shown as arrows.

Table S2 - Related to Figure 3: NMR data for **13** in $\text{DMSO-}d_6$. COSY correlations are shown as bold bonds. Key HMBC correlations are shown as arrows.

Table S3 - Related to Figure 3: NMR data for **14** in $\text{DMSO-}d_6$. Key HMBC correlations are shown as arrows.

Table S4 - Related to STAR methods: Oligonucleotides used in this study.

Table S5 - Related to STAR methods: Media used in this study.

Genomic and metabolic diversity in *Aspergillus* section *Terrei*

Sebastian Theobald, Tammi C. Vesth, **Elena Geib**, Jane L. Nybo, Jens C. Frisvad, Thomas O. Larsen, Asaf Salamov, Robert Riley, Ellen K. Lyhne, Martin E. Kogle, Kerrie Barry, Alicia Clum, Cindy Chen, Matt Nolan, Laura Sandor, Alan Kuo, Anna Lipzen, Jon K. Magnuson, Blake A. Simmons, Uffe H. Mortensen, Igor V. Grigoriev, Matthias Brock, Scott E. Baker and Mikael R. Andersen

In preparation.

Summary of the manuscript: *Aspergillus terreus* has been in focus of research, as it is a human pathogen and known to produce high-value secondary metabolites such as lovastatin. Recently, other closely related species from section *Terrei* have drawn attention due to their emergence as pathogenic isolates or their ability to produce a broad range of natural products. In this work six *Aspergillus* members from section *Terrei* have been sequenced. Whole genome analyses were used to construct a phylogenetic tree and assess the genomes for secondary metabolite biosynthesis gene clusters (BCGs). As expected, the genomes are strongly enriched with all types of secondary metabolite producing genes. Dereplication allowed the sorting of gene clusters into distinct families. Previous studies had identified a unique type of melanin in *A. terreus* conidia and a putative family of aspulvinone E synthetases was identified that might contribute to Asp-melanin biosynthesis. This enzyme was present in most, but not all sequenced species, whereas the dihydroxynaphthalene (DHN)-melanin pathway was only present in more distantly related species. This indicates that the DHN-melanin pathway common to other *Aspergillus* species was lost during evolution and the novel type of Asp-melanin had evolved.

Contribution: 25% of practical work (in current status), significant contribution to manuscript preparation

Amplification of genes encoding NRPS-like enzymes homologous to the aspulvinone E synthetase MelA and encoding polyketide synthases homologous to the naphthopyrone synthase PksP. Cloning of genes into the SM-Xpress_URA plasmid, fungal transformation, colony screening, metabolite extraction and analytical HPLC.

1 **Genomic and metabolic diversity in**
2 ***Aspergillus section Terrei***
3

4 Sebastian Theobald (1), Tammi C. Vesth (1), Elena Geib (2), Jane L. Nybo (1), Jens C. Frisvad (1),
5 Thomas O. Larsen (1), Asaf Salamov (3), Robert Riley (3), Ellen K. Lyhne (1), Martin E. Kogle
6 (1), Kerrie Barry (3), Alicia Clum (3), Cindy Chen (3), Matt Nolan (3), Laura Sandor (3), Alan Kuo
7 (3), Anna Lipzen (3), Jon K. Magnuson (4,5), Blake A. Simmons (4,6), Uffe H. Mortensen (1), Igor
8 V. Grigoriev (3), Matthias Brock (2), Scott E. Baker (4,5)*, Mikael R. Andersen (1)*.

9

10 1) Department of Biotechnology and Bioengineering, Technical University of Denmark, Kgs.

11 Lyngby, Denmark

12 2) Fungal Genetics and Biology, School of Life Sciences, University of Nottingham, University Park,

13 NG7 2RD Nottingham, UK

14 3) US Department of Energy Joint Genome Institute, Walnut Creek, CA, USA

15 4) US Department of Energy Joint Bioenergy Institute, Berkeley, CA, USA

16 5) Pacific Northwest National Laboratory, Richland, WA, USA

17 6) Lawrence Berkeley National Laboratory, Berkeley, CA, USA

18 *Corresponding authors

19

20 **Abstract**

21 *Aspergillus terreus* has attracted interest due to its application in industrial biotechnology, particularly
22 for production of bioactive secondary metabolites. As related species also seem to possess a
23 prosperous secondary metabolism they are of high interest for genome mining and exploitation. Here,
24 we present draft genome sequences for six species from *Aspergillus* section *Terrei* and one species
25 from *Aspergillus* section *Nidulantes*. Whole-genome phylogeny revealed a clear separation of the
26 individual species in section *Terrei* and confirmed that the section is monophyletic. Genome analyses
27 approved the assumption that species from section *Terrei* are very rich in secondary metabolism
28 genes. About 70–108 secondary metabolite producing key genes (backbone synth(et)ases) were
29 identified in each of the genomes, the highest number per species found in the genus *Aspergillus* so
30 far. Comparative analyses allowed to sort the respective enzymes into 162 distinct families with most
31 of them corresponding to potentially unique compounds or compound families. Moreover, 43% of
32 the families were only found in a single species, which supports the suitability of species from section
33 *Terrei* for further exploitation. Genetic dereplication of secondary metabolite biosynthesis families
34 allowed us to identify 17 families linked to characterized compounds and gene clusters. Intriguingly,
35 this analysis combined with heterologous gene expression and metabolite identification suggested
36 that species from section *Terrei* use a strategy for UV protection different to other species from the
37 genus *Aspergillus*. Depending on the position in a genome-wide phylogenetic tree, species from
38 section *Terrei* lost dihydroxynaphtalene-melanin biosynthesis and evolved the Asp-melanin pathway
39 for protection of conidia.

40

41 **Keywords**

42 Genomics; Fungi; *Aspergillus*; *Terrei*; *Aspergillus terreus*; Secondary metabolism

43

44 **Introduction**

45 The fungal genus *Aspergillus* is of broad interest as it contains species that are used in various
46 industrial and pharmaceutical applications, but also contains species capable of infecting humans and
47 causing food and feed spoilage by mycotoxin production. Thereby, most *Aspergillus* species are
48 assumed to synthesise more than 50 different secondary metabolites. An excellent example for all
49 these traits is *Aspergillus terreus*. Primarily, *A. terreus* has attracted attention as an opportunistic
50 human pathogen (Lass-Flörl *et al.*, 2005), but is also of interest through its biosynthesis of
51 biotechnologically and pharmaceutically important products, in particular itaconic acid (Tevz,
52 Bencina and Legisa, 2010; Okabe *et al.*, 2009) and lovastatin/mevinolin, a secondary metabolite
53 capable of lowering blood cholesterol levels (Alberts *et al.*, 1980). Such statins are marketed and sold
54 for treatment of lifestyle diseases at an annual turnover of multibillion USD (Boruta and Bizukojc,
55 2017). Genome sequences already exist for several *A. terreus* strains (Savitha, Bhargavi and Praveen,
56 2016; whole genome accession number for *A. terreus* NIH2624: AAJN01000001-AAJN01000268),
57 which has accelerated research on the species and sparked multiple genome mining approaches to tap
58 into the genomic wealth of *A. terreus* (Guo and Wang, 2014b). Analysis of natural products produced
59 by *A. terreus* has shown its capability of producing secondary metabolites with diverse activities,
60 such as antiviral compounds (Miller *et al.*, 1968; Kamata, Sakai and Hirota, 1983), antitumor
61 metabolites (Arakawa *et al.*, 2008; Kaji *et al.*, 1998; Calton, Ranieri and Espenshade, 1978), and a
62 wide range of mycotoxins, including patulin (Draughon and Ayres, 1980), citrinin (Sankawa *et al.*,
63 1983), and geodin (Kiryama *et al.*, 1977; Fujii, Ebizuka and Sankawa, 1982). *A. terreus* also
64 produces the phytotoxic, antifungal and iron reducing compound terrein (Gressler *et al.*, 2015b). Due
65 to the large quantities of terrein produced, regulatory elements from the *A. terreus* terrein biosynthesis
66 gene cluster have been used to develop a heterologous expression system in *Aspergillus niger* suitable
67 for the production and characterisation of fungal secondary metabolites (Gressler *et al.*, 2015a; Geib
68 and Brock, 2017). This expression system also supported the identification of a novel type of
69 aspulvinone E-derived Asp-melanin, which protects asexual conidia of *A. terreus* (Geib *et al.*, 2016).

70 This Asp-melanin seems to discriminate *A. terreus* from other *Aspergillus* sections, in which a
71 hydroxynaphthalene-melanin protects conidia from UV and oxidative stress (Varga and Samson,
72 2008).

73 However, *A. terreus* is not the sole species member of this group, and closely related species are
74 interesting candidates for genome analyses and mining. The *Aspergillus* section *Terrei* has been
75 defined since 1985 (Gams *et al.*, 1986; Samson *et al.*, 2011), and at least 14 species (including *A.*
76 *terreus*) have been assigned to this group (Balajee, 2009b; Samson *et al.*, 2011). Consistent with the
77 name “*Terrei*”, nearly all species grouped into this section have been isolated from soil samples
78 around the world (Samson *et al.*, 2011). However, while among these species *A. terreus* remained the
79 only species with its genome sequenced, other species such as *A. alabamensis* and *A. allahabadii* are
80 of particular interest. Both species have been identified as cause of invasive aspergillosis (Balajee *et*
81 *al.*, 2009a; Lim *et al.*, 2016) and *A. alabamensis* has been identified as producer of tremorgenic
82 compounds (Samson *et al.*, 2011). Additionally, other species of the section *Terrei* show production
83 of a large number and diversity of secondary metabolites (Samson *et al.*, 2011) and it is thus of interest
84 to examine the genetic and chemical diversity in this section. In this study, we provide genome
85 sequences of *A. alabamensis* (Balajee *et al.*, 2009a), *A. allahabadii* (Lim *et al.*, 2016), *A. ambiguus*,
86 *A. aureoterreus*, *A. floccosus* and *A. neoindicus* (Samson *et al.*, 2011) and examine the potential for
87 chemical diversity in these species, as defined by predicted gene clusters for secondary metabolite
88 production. Furthermore, based on its genome sequence, a re-classification of a strain previously
89 attributed to section *Terrei* was performed.

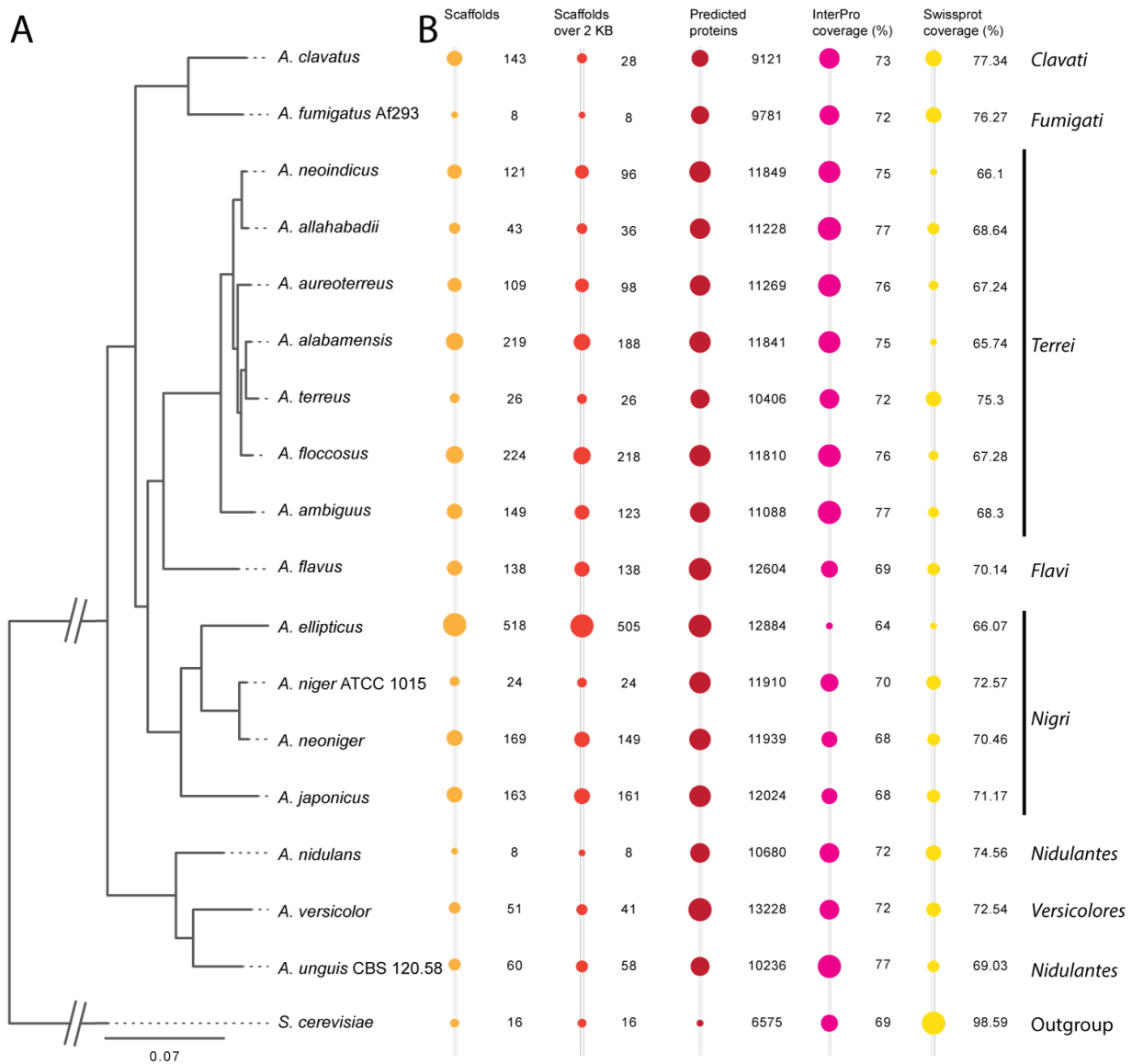
90

91 **Results and Discussion**

92 **Genome Sequencing and Genome Statistics**

93 We prepared genomic DNA from seven fungal species that were assumed to belong to section *Terrei*:
94 *A. alabamensis*, *A. allahabadii*, *A. ambiguus*, *A. aureoterreus*, *A. floccosus*, *A. microcysticus* CBS
95 126.58 (later re-annotated as *A. unguis*) and *A. neoindicus*. All genomes were Illumina-sequenced

96 and assembled and annotated using the JGI fungal genome pipeline (Grigoriev *et al.*, 2014; Grigoriev,
 97 Martinez and Salamov, 2006). All genomes are available from NCBI and the JGI genome portals and
 98 MycoCosm (Grigoriev *et al.*, 2014). Full statistics of the sequenced genomes and further genomes
 99 used for the comparative analysis are available in Suppl. Table 1. An overview on the most important
 100 statistics across 18 fungal species is provided in Figure 1.



101
 102 **Figure 1:** Dendrogram and bubble plots illustrating phylogenetic distances among seven genomes from section
 103 *Terrei* relative to reference species from genus *Aspergillus* and *S. cerevisiae* used as an outgroup. A -
 104 Phylogenetic tree created using RAxML (Stamatakis, 2014), MAFFT (Katoh and Standley, 2013), and
 105 Gblocks (Talavera and Castresana, 2007) based on 200 conserved genes found as single copy in each of the
 106 genomes (monocore genes). B - Bubble plots illustrating relative values of key genome statistics. The bubble

107 sizes are scaled within the categories and are not comparable across categories. Additional information on the
108 genomes is available in Suppl Table 1.

109

110 Unexpectedly, *A. microcysticus* CBS 126.58 had previously been described as member of the section
111 *Terrei* (Samson *et al.*, 2011), but closer examination of the genome revealed that it represents *A.*
112 *unguis* of section *Nidulantes*. Therefore, it was kept as a reference in Figure 1, but its genome was
113 not included into comparisons among the six new *Terrei* genomes. Overall, the quality-related
114 genome statistics (Figure 1, Suppl. Table 1) revealed a high quality of the new genome drafts.
115 Scaffold numbers are between 43 and 224, and scaffold *N50* were generally between 11 and 16, with
116 exception of *A. floccosus* where *N50* = 39. This indicates an excellent assembly of the genomes,
117 which is comparable to or even better than other published fungal genomes. When compared to
118 genomes from *A. flavus* and *A. clavatus*, there is a similar number of scaffolds (Figure 1C) and
119 average scaffold length, but the median scaffold length is 50-100 times higher for these new genomes
120 (Suppl Table 1). It was furthermore possible to assign InterPro predictions of function to >75% of
121 predicted proteins, which is similar or better than possible for previously sequenced *Aspergillus*
122 genomes (Figure 1, Suppl. Table 1).

123 When examining the content and characteristics of the genomes of species from section *Terrei*, the
124 genomes appear clearly quite homogenous. The genome sizes are typically around 30 Mb, whereby
125 the genome size from *A. alabamensis* is slightly expanded with 32 Mb. All new genomes have a
126 similar number of predicted proteins (within a range of 761 proteins), whereby the number for the *A.*
127 *terreus* genome is slightly lower. However, the genome of *A. terreus* was sequenced and annotated
128 by using different bioinformatic pipelines as applied in this study (Figure 1B, Suppl. Table 1). All
129 genes from species of section *Terrei* also have a common average number of 3.2 exons per gene. In
130 summary, these genome analyses indicate that the section *Terrei* comprises a very homogeneous
131 section, particularly when compared to section *Nigri*, for which we previously described a
132 substantially larger diversity (Vesth *et al.*, 2018, accepted pending revisions).

133

134 **Species Phylogeny**

135 Based on the predicted proteins, we were interested in examining the species diversity and examine
136 the phylogenetic relationship of the species at the genome level. Particularly, given that the genome
137 statistics are similar for the new genomes, it was interesting to see whether the proposed species are
138 more diverse at the sequence level. To achieve this, we built a whole-genome based phylogeny of a
139 total of 18 species across the *Aspergilli* (Figure 1A) that based on 200 genes from which exactly one
140 ortholog was found in each species (also known as monocore genes). The resulting tree is in
141 accordance with a calmodulin-based tree presented in a previous study (Samson *et al.*, 2011) and in
142 phylogenetic analysis of some section *Terrei* isolates by Varga *et al.* (Varga *et al.*, 2005). It
143 additionally supports the proposition that *A. ambiguus*, *A. aureoterreus*, *A. floccosus*, and *A.*
144 *neoindicus* should indeed be recognized as separate species, as there is a clear separation of these
145 species in the phylogram. This analysis further revealed that, despite having genome statistics similar
146 to the other section *Terrei* species from this study, *A. ambiguus* is the most separate species within
147 this group. In total, the analysis shows that despite similar genome statistics, phylogenetically the
148 isolates are quite different.

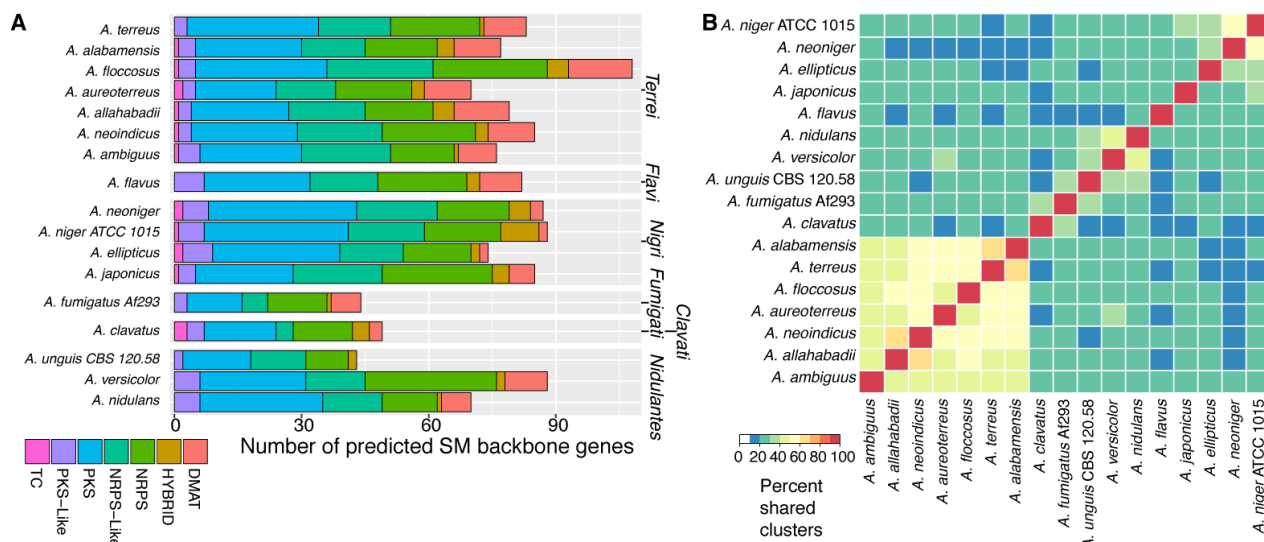
149

150 **Species in Section *Terrei* Are Particularly Rich in Genes Coding for Secondary Metabolites**

151 Analyses of secondary metabolism of *A. terreus* already showed a high diversity in the products
152 formed (Samson *et al.*, 2011). Therefore, we were interested in mapping genes responsible for the
153 diversity of secondary metabolism in section *Terrei* relative to *A. terreus* and other sections of
154 *Aspergilli*. Secondary metabolite gene clusters were predicted based on a SMURF-like prediction
155 method (Khaldi *et al.*, 2010). In total, we predicted 3275 genes in the six new genomes potentially
156 involved in secondary metabolism (Suppl. Table 2). So-called backbone genes including synthases,
157 synthetases, and cyclases that are involved in producing the backbone compound to be modified by
158 other cluster encoded enzymes were counted and sorted into categories based on predicted functions
159 (Figure 2A). In total, we found 495 backbone genes in the new genomes, which indicates that species

160 of section *Terrei* are as rich in secondary metabolism as the secondary metabolism-rich section *Nigri*
 161 (Figure 2A). In particular, *A. floccosus* revealed 108 backbone genes across 88 predicted clusters. As
 162 far as we are aware, this is the highest number of genes found for secondary metabolite production in
 163 a single *Aspergillus* species. Intriguingly, this enriched number comes from an expansion of nearly
 164 all classes of secondary metabolite backbones, whereby the genome itself is not particularly expanded
 165 as seems to be the case for genomes of species from section *Nigri*. Since *A. floccosus* has not been
 166 reported to produce a large number of known secondary metabolites (Samson *et al.*, 2011), our
 167 analyses suggest that several of these genes and gene clusters may be responsible for the production
 168 of new compounds.

169



170

171 **Figure 2: Summary of secondary metabolism-related genes and gene clusters in section *Terrei* and**
 172 **reference species. A - Total SMGC family profile of Aspergilli classified by backbone enzyme type. B - The**
 173 **heatmap is clustered horizontally and vertically according to the percentage of shared gene clusters. Note that**
 174 **the clustering generally follows the phylogeny of Figure 1. DMAT: Dimethylallyltransferase (Prenyl**
 175 **transferases), HYBRID: Gene containing domains from NRPS and PKS backbones in any order, NRPS: Non-**
 176 **ribosomal peptide synthetase, NRPS-like: Non-ribosomal peptide synthetase like containing an adenylation**
 177 **and condensation domain and either a C-terminal thioesterase or reductase domain, PKS: Polyketide synthase,**
 178 **PKS-like: Polyketide synthase like, containing at least two PKS specific domains and another domain, TC:**
 179 **Terpene cyclase.**

180 We further analysed how many of the gene clusters are shared among species – either within section
181 *Terrei* or with other *Aspergilli*. All predicted clusters in the set (1058) were compared to each other
182 and we calculated how many are shared in either direction in all two-way comparisons (Figure 2B).
183 In this comparison, it became apparent that only 50–80% of gene clusters are shared between any two
184 compared species in section *Terrei*, showing unique SM production potential in all of the *Terrei*
185 species included here. However, the internal similarity in section *Terrei* is more homogeneous than
186 that within the four members of section *Nigri*, which only share 35-60% of their SM capacity.
187 Furthermore, Figure 2B demonstrates that only 10-30 % of the secondary metabolite gene clusters
188 (SMGCs) are shared with other *Aspergillus* species included as references. In combination, this
189 further supports a very high metabolic diversity within the genome-sequenced species of section
190 *Terrei*.

191

192 **Secondary Metabolite Clusters in new *Terrei* genomes Can Be Sorted Into 162 Families**

193 As the genomes of species from section *Terrei* appear to be rich in secondary metabolite genes, we
194 wanted to see how much of the diversity was replicated between species. In a first step, it was
195 determined which of the gene clusters across genomes are variations of each other. Based on a
196 previously developed method (Theobald *et al.*, 2018, submitted), gene clusters were identified that
197 possess homologous genes for backbone enzymes and contain homologous genes for tailoring
198 enzymes. This strategy followed the hypothesis that highly similar clusters are expected to produce
199 related compounds. Including this assumption provides a more accurate measure of the chemical
200 diversity of the isolates. The output of this analysis is available in Suppl. Table 2. In total, the 495
201 SM biosynthetic genes in the seven section *Terrei* genomes, can be collapsed into 162 families, thus
202 suggesting that at least 162 different chemical moieties can be produced by the seven species. Of
203 these families, 71 are only found in a single genome, with each new genome containing 9-16 SMGCs
204 that are not found in any of the other genomes in the comparative analysis (Suppl. Figure 1). The 43%

205 (71/162) of clusters only found in single genomes indicate a potential for high chemical diversity and
206 unique chemistry in the section *Terrei*.

207

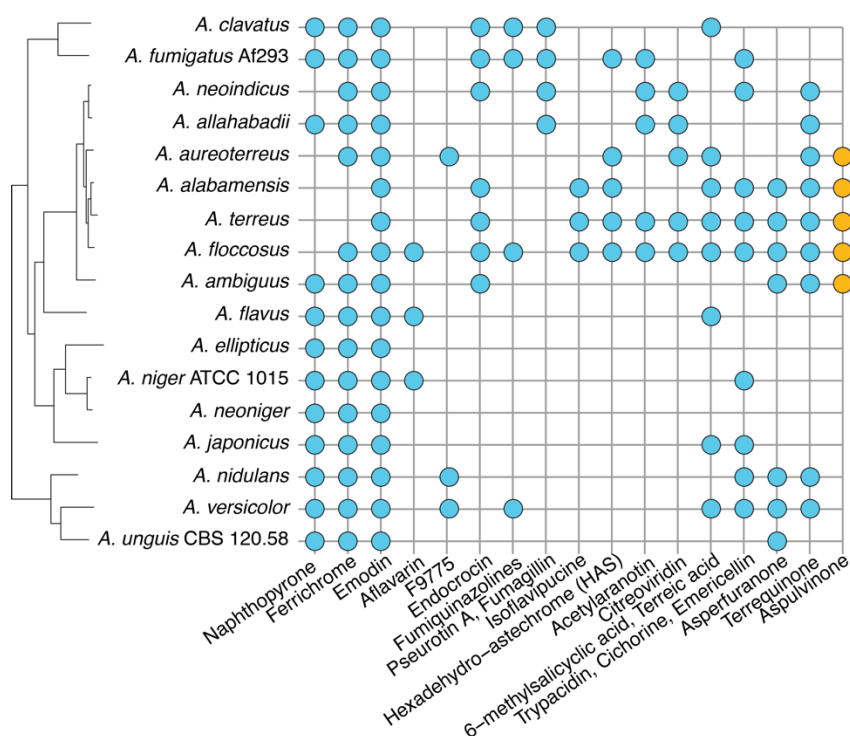
208 **Genetic Dereplication of the *Terrei* SM Gene Clusters by Comparison with the MIBiG Database**

209 The analysis of the SMGC families above led to the hypothesis that the SMGCs of section *Terrei*
210 primarily contain unknown clusters, which was specifically supported by the finding of many unique
211 clusters and only a few clusters shared between many species (Suppl. Figure 1). We thus performed
212 what can be called "genetic dereplication" of the gene clusters (Theobald *et al.*, 2018, submitted), in
213 which the families of SMGC from section *Terrei* were compared to the characterized gene clusters
214 available in the MIBiG database (Medema *et al.*, 2015).

215 We dereplicated all clusters across the full dataset of 18 species and extracted the information
216 regarding cluster families from section *Terrei*. An overview of this analysis is shown in Figure 3 (see
217 Suppl. Table 2 for details on the association of all clusters to compounds in the complete dataset).

218 This analysis confirmed our hypothesis that section *Terrei* contains a high potential for unique natural
219 product chemistry; out of the 162 identified SMGC families, only 17 (10%) could be connected to
220 characterized clusters (Figure 3, Suppl. Table 2). Some interesting observations were made during
221 this analysis: Both terreic acid and 6-methylsalicylic acid (6-MSA) are found in the same family. This
222 supports the composition of SMGC families, as terreic acid is known to be produced from 6-MSA
223 (Guo *et al.*, 2014a; Sheehan, Lawson and Gaul, 1958). Furthermore, all *Terrei* species have an SMGC
224 that is homologous to the terrequinone cluster described from *A. nidulans* (Bouhired *et al.*, 2007). A
225 previous study (Samson *et al.*, 2011) identified terrequinones in several species from section *Terrei*
226 with the exception of *A. floccosus*, *A. allahabadii* and *A. neoindicus*. The genome analysis, however,
227 suggests that these species may also be capable of producing terrequinone derivatives, but production
228 seems to be induced under yet unknown conditions. Finally, we were interested in the formation of
229 melanins protecting *Aspergillus* conidia from different environmental stressors. While a
230 naphthopyrone-derived dihydroxynaphthalene (DHN)-melanin appears common to species from

231 various *Aspergillus* sections (Tsai *et al.*, 1999; Klejnstrup *et al.*, 2012; Chiang *et al.*, 2011), previous
 232 studies revealed that *A. terreus* produces a novel type of melanin. This Asp-melanin derives from
 233 aspulvinone E, which is produced by the NRPS-like enzyme MelA and subsequently polymerised by
 234 a tyrosinase (Geib *et al.*, 2016). On the contrary, at least in *A. terreus*, no homologue for a
 235 naphthopyrone synthase such as WA from *A. nidulans* or PksP from *A. fumigatus* had been detected
 236 in *A. terreus* (Geib *et al.*, 2016; Slesiona *et al.*, 2012). Therefore, we had a closer look at PksP and
 237 MelA homologues in species from section *Terrei*.

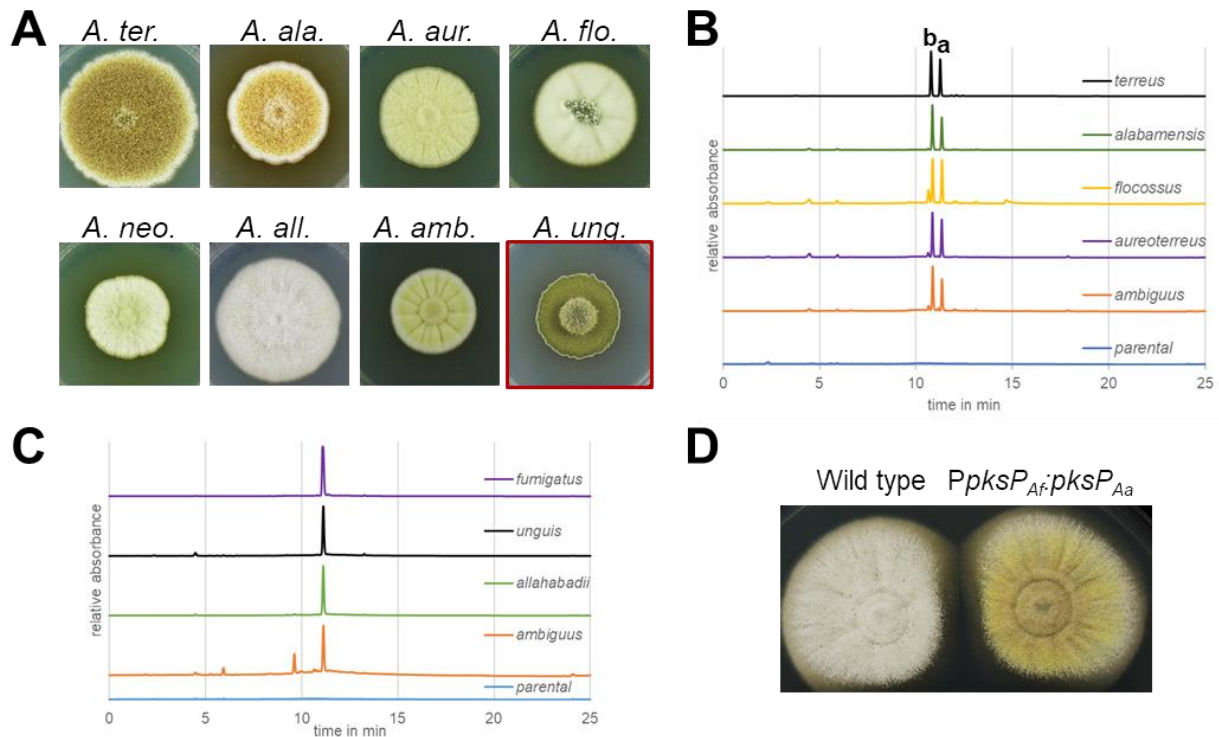


238
 239 **Figure 3: Association of gene clusters from section *Terrei* to previously assigned and**
 240 **characterized orthologous gene clusters.** All gene families were compared to the MIBiG database
 241 to identify clusters homologous to characterized gene clusters. Gene cluster families with an
 242 associated characterized cluster are marked with a dot for all species containing a member of the gene
 243 cluster family, and, thus, presumably also a proposed compound. The family associated with Asp-
 244 melanin production from aspulvinone E (orange) was added manually through searching for the *A.*
 245 *terreus* aspulvinone E synthetase MelA (see main text).

246

247 **Pigments in conidia from section *Terrei***

248 To elucidate whether Asp-melanin is specific only for *A. terreus* or common to the section *Terrei*, we
249 searched genomes for homologues of the *A. terreus* aspulvinone E synthetase *MelA* as well as for the
250 naphthopyrone synthase *PksP* from *Aspergillus fumigatus*. The genomes of *A. alabamensis*, *A.*
251 *aureoterreus*, *A. floccosus* and *A. ambiguus* indeed contained a *MelA* homologue (Figure 3), whereby
252 a *PksP* homologue was additionally detected in the *A. ambiguus* genome. *A. allahabadii* exclusively
253 revealed a *PksP* homologue. Neither of both genes was detected in *A. neoindicus*. In agreement,
254 species containing the *mela* homologue mostly produced yellow to brown pigmented conidia (Figure
255 4A), whereas *A. unguis* (as belonging to section *Nidulantes* and carrying a *PksP* homologue) produced
256 green and *A. neoindicus* white conidia. Unexpectedly, despite the presence of a *pksP* homologue in
257 *A. allahabadii*, conidia also appeared non-melanised. To verify our pigment biosynthesis predictions
258 from *in silico* analyses, the respective *mela* and *pksP* homologues were amplified from genomic DNA
259 and cloned into an *Aspergillus niger* expression platform strain ATNT16 for heterologous metabolite
260 biosynthesis (Gressler *et al.*, 2015a; Geib and Brock, 2017). Metabolite analyses confirmed that all
261 *mela* homologues produced aspulvinone E and its UV-interconvertible *cis*-isomer isoaspulvinone E
262 (Figure 4B). In addition, by taking the *PksP* product from *A. fumigatus* as reference, all *pksP*
263 homologues revealed the production of YWA1 (Figure 4C). However, all transformants producing
264 the *PksP* homologue from *A. ambiguus* revealed low product yields suggesting a comparably low
265 activity of this enzyme. As *A. ambiguus* also contains a *mela* homologue and conidia appear
266 brownish, the production of Asp-melanin may be dominating in this fungus.



267

268 **Figure 4: Analysis of conidia pigmentation in section *Terrei*.** **A** - Phenotype of colonies of species
 269 from section *Terrei* and of *A. unguis* from section *Nidulantes* on complete *Aspergillus* medium. *A.*
 270 *ter.* = *A. terreus*, *A. ala* = *A. alabamensis*, *A. aur.* = *A. aureoterreus*, *A. flo.* = *A. floccosus*, *A. neo.* =
 271 *A. neoindicus*, *A. all* = *A. allahabadii*, *A. amb.* = *A. ambiguus*, *A. ung.* = *A. unguis*. **B** – HPLC analysis
 272 of products formed from the heterologous expression of *mela* homologues from section *Terrei* in the
 273 *A. niger* expression platform ATNT16 (parental). a – aspulvinone E, b – isoaspulvinone E. **C** – HPLC
 274 analysis of products formed from the heterologous expression of *pksP* homologues from section
 275 *Terrei* and from *A. unguis* and *A. fumigatus* in *A. niger* ATNT16 (parental). **D** – *A. allahabadii* wild
 276 type and transformant with a fusion of the *A. fumigatus pksP* promoter with the *A. allahabadii pksP*
 277 gene (*PpksPAf:pksPAa*).

278

279 Unexpectedly, while conidia from *A. allahabadii* appeared unpigmented, its PksP homologue
 280 produced YWA1 (Figure 4C). Therefore, it appeared likely that the *pksP* gene is not expressed in *A.*
 281 *allahabadii* under conidia-forming conditions. To confirm this assumption, we aimed in an induced
 282 expression of the *pksP* homologue in *A. allahabadii* by replacing its native promoter with the *pksP*
 283 promoter from *A. fumigatus*. Indeed, in agreement with a yellow colour of compound YWA1, *A.*

284 *allahabadii* transformants produced yellow conidia with some green sectors (Figure 4D). This
285 indicates that the native *pksP* promoter from *A. allahabadii* is not induced during conidiation on the
286 examined media, but downstream genes required for the formation of DHN-melanin seem to be
287 active.

288 Interestingly, the production of different melanin pigments follows the phylogenetic tree shown in
289 Figure 1. *A. ambiguus*, the species most distantly related to *A. terreus* seems to produce DHN-melanin
290 and Asp-melanin in parallel. In contrast *A. allahabadii* and *A. neoindicus* produce white conidia
291 despite the presence of a DHN-melanin biosynthesis pathway in *A. allahabadii*. All other species
292 from section *Terrei* lack a PksP homologue but gained or evolved a MelA protein. This indicates a
293 complete loss of the DHN-melanin biosynthesis pathway in core species from section *Terrei*. As
294 DHN-melanin inhibits acidification of phagolysosomes in macrophages and amoeba (Slesiona *et al.*,
295 2012; Geib *et al.*, 2016), these properties appear unfavourable for species from section *Terrei*.
296 However, as a complete loss of conidia pigmentation causes increases sensitivity against oxidative
297 and UV-stress, Asp-melanin has evolved as alternative protective mechanism. Therefore, these
298 analyses indicate that Asp-melanin is a feature that can be specifically attributed to species from this
299 section.

300

301 **Materials and Methods**

302 **Fungal strains**

303 In this study, we sequenced *A. alabamensis* IBT 12702, *A. allahabadii* CBS 164.63, *A. ambiguus*
304 CBS 117.58, *A. aureoterreus* CBS 503.65, *A. floccosus* CBS 116.37 and *A. neoindicus* CBS 444.75
305 as described by Samson *et al.* (Samson *et al.*, 2011). We further sequenced CBS 120.58 in the belief
306 that it would be the species described as *A. microcysticus*, but sequencing revealed it to be an *A.*
307 *unguis*. We further compared the genome sequences to published genomes from *A. clavatus* (Arnaud
308 *et al.*, 2012), *A. fumigatus* Af293 (Nierman *et al.*, 2005), *A. terreus*
309 (<https://genome.jgi.doe.gov/Aspte1/Aspte1.home.html>), *A. flavus* (Payne *et al.*, 2006; Nierman *et al.*,

310 2015), *A. ellipticus* (Vesth *et al.*, 2018, accepted pending revisions), *A. neoniger* (Vesth *et al.*, 2018,
311 accepted pending revisions), *A. japonicus* (Vesth *et al.*, 2018, accepted pending revisions), *A.*
312 *nidulans* (Galagan *et al.*, 2005), *A. niger* ATCC 1015 (Andersen *et al.*, 2011) and *A. versicolor* (de
313 Vries *et al.*, 2017). All sequences were downloaded from the JGI web portal.

314 **Purification of DNA**

315 For all sequences generated in this study, conidia stored at -80°C were used to inoculate solid CYA
316 medium. Fresh conidia were harvested after 7-10 days and suspended in a 0.1% Tween solution. For
317 generation of biomass, liquid CYA medium was inoculated and cultivated for 5-10 days at 30°C.
318 Mycelium was isolated by filtering through Miracloth (Millipore, 475855-1R), freeze dried and stored
319 at -80°C until further use. DNA isolation was performed using a modified version of standard phenol
320 extraction (Kjærboelling *et al.*, 2018) and checked for quality and concentration using a NanoDrop
321 (BioNordika, DK)

322 **DNA sequencing and assembly**

323 All genomes in this study were sequenced with Illumina technologies. For all genomic Illumina
324 libraries, 100 ng of DNA was sheared to 270 bp fragments using the Covaris LE220 (Covaris) and
325 size selected using SPRI beads (Beckman Coulter). The fragments were treated with end-repair, A-
326 tailing, and ligated to Illumina compatible adapters (IDT, Inc) using the KAPA-Illumina library
327 creation kit (KAPA biosystems). The prepared libraries were quantified using KAPA Biosystem's
328 next-generation sequencing library qPCR kit and run on a Roche LightCycler 480 real-time PCR
329 instrument. The quantified libraries were then multiplexed with other libraries, and library pools were
330 prepared for sequencing on the Illumina HiSeq sequencing platform utilizing a TruSeq paired-end
331 cluster kit, v3, and Illumina's cBot instrument to generate clustered flow cells for sequencing.
332 Sequencing of the flow cells was performed on the Illumina HiSeq2000 sequencer using a TruSeq
333 SBS sequencing kit, v3, following a 2x150 indexed run recipe. After sequencing, the genomic fastq
334 files were QC filtered to remove artefacts/process contamination and assembled using Velvet

335 (Zerbino and Birney, 2008). The resulting assemblies were used to create *in silico* long mate-pair
336 libraries with inserts of 3000 +/- 90 bp that were then assembled with the target fastq using
337 AllPathsLG release version R47710 (Gnerre *et al.*, 2011). All genomes were annotated using the JGI
338 annotation Pipeline (Grigoriev *et al.*, 2014). Genome assembly and annotations are available at the
339 JGI fungal genome portal MycoCosm (Grigoriev *et al.*, 2014; <http://jgi.doe.gov/fungi>).

340 **Whole-genome phylogeny**

341 Protein sequences of all organisms were compared using BLASTp (e-value cut-off 1e-05).
342 Orthologous groups of sequences were constructed based on best bidirectional hits (BBH). Two
343 hundred groups with a member from each species were selected and the sequences of each organism
344 was concatenated into one long protein sequence. Concatenated sequences are aligned using MAFFT
345 (thread 16) and well-aligned regions were extracted using Gblocks (-t = p -b4=5 -b5 = h). Trees were
346 then constructed using multi-threaded RAxML, the PROTGAMMAWAG model and 100 bootstrap
347 replicates.

348 **Prediction of Secondary Metabolite Biosynthesis Gene Clusters**

349 For the prediction of secondary metabolite (SM) biosynthesis gene clusters, we developed a
350 command-line Python script roughly following the SMURF algorithm (Khaldi *et al.*, 2010). As input,
351 the program takes genomic coordinates and the annotated PFAM domains of the predicted genes.
352 Based on the multi-domain PFAM composition of identified 'backbone' genes, it can predict seven
353 types of SM clusters: 1) Polyketide synthases (PKSs), 2) PKS-like, 3) nonribosomal peptide-
354 synthetases (NRPSs) 4) NRPS-like, 5) hybrid PKS-NRPS, 6) prenyltransferases (DMATS), and 7)
355 terpene cyclases (TCs). Besides backbone genes, PFAM domains, which are enriched in
356 experimentally identified SM clusters (SM-specific PFAMs) were used in determining the borders of
357 gene clusters. The maximum allowed size of intergenic regions in a cluster was set to 3 kb and each
358 predicted cluster was allowed to have up to 6 genes without SM-specific domains.

359

360 **Generation of SMGC families**

361 Proteins of the resulting secondary metabolism gene clusters (SMGCs) were compared among each
362 other by alignment using BLASTP (BLAST+ suite version 2.2.27, e-value $\leq 1^{-10}$). Subsequently, a
363 score based on BLASTp identity and shared proteins was created to determine the similarity between
364 gene clusters: To create a cluster similarity score, a combined score of tailoring and backbone
365 enzymes was created. The sum of the BLASTp percent identity (pident) of all hits for tailoring
366 enzymes between two clusters was divided by the maximum amount of tailoring enzymes (nmax)
367 and multiplied by 0.3 (eq. 1).

$$368 \text{ pident}_{tailoring} = \text{ptailoring} * \frac{\text{ntailoring}}{\text{ttailoring}} \quad (1)$$

369 Then the score for the backbone enzymes was calculated in the same manner but multiplied by 0.7 to
370 give more weight to the backbone enzymes (eq. 2).

$$371 \text{ pident}_{backbones} = \frac{\text{nbackbone}}{\text{tbackbone}} \quad (2)$$

372 The scores were added to create an overall cluster similarity score (eq. 3).

$$373 \text{ Similarity score} = \frac{\text{sum}(\text{pident}_{tailoring})}{\text{nx}_{tailoring}} * 0.3 + \frac{\text{sum}(\text{pident}_{backbones})}{\text{nmax}_{backbones}} * 0.7 \quad (3)$$

374

375 Using these scores, we created a weighted network of SMGC clusters and used a random walk
376 community detection algorithm (R version 3.3.2, igraph_1.0.1 (Csardi and Nepusz, 2006) to
377 determine families of SMGCs. Finally, we ran another round of random walk clustering on the
378 communities which contained more members than species in the analysis. YWA and emodin gene
379 clusters from MIBiG were identified inside the families using BLASTP and their members were
380 labelled as gene clusters producing similar compounds.

381

382 **Genetic dereplication**

383 MIBiG (Medema *et al.*, 2015) genbank files were downloaded, parsed using Biopython (Cock *et al.*,
384 2009) and SMGC entries of *Aspergillus* and *Penicillium* species were searched against a database of

385 all SMURF annotated proteins of the dataset using protein BLAST (Camacho *et al.*, 2009). BLAST
386 hits with over 95 % identity were annotated with their respective MIBiG query sequence. All SMGCs
387 inside a family of the hit were annotated as related to the MIBiG query.

388

389 **Heterologous Expression of Pigment Biosynthesis Genes**

390 To heterologously express *mela* or *pksP* homologous genes in *A. niger* ATNT16, the respective genes
391 were amplified with Phusion high-fidelity DNA polymerase (ThermoFisher Scientific) from genomic
392 DNA. Oligonucleotides 1-16 (supplementary table 3) were designed containing 15 bp overhangs to
393 the *NcoI* site of the SM-Xpress_URA plasmid to allow site-specific assembly *via in vitro*
394 recombination using the In-Fusion HD cloning kit (Takara/Clontech). Plasmids were propagated in
395 *Escherichia coli* DH5 α and isolated using the NucleoSpin Plasmid kit (Macherey-Nagel). Circular
396 plasmids were used for transformation of *A. niger* ATNT16 Δ *pyrG* following the transformation
397 protocol as described previously (Geib and Brock, 2017). Regeneration and selection of positive
398 transformants was achieved on *Aspergillus* minimal medium (AMM) agar with osmotic stabilisation
399 by 1.2 M sorbitol and without uridine supplementation. Transformants were checked for integration
400 of expression constructs by diagnostic PCR. A gene specific oligonucleotide (oligos 21-24 for *mela*
401 homologues and 25-28 for *pksP* homologues) and oligonucleotide 29 (Supplementary table 3) were
402 used for amplification of the entire expression cassette with Phire Green Hot Start II DNA polymerase
403 (ThermoFisher Scientific). An *A. terreus mela* expressing ATNT16 transformant was generated in a
404 previous study (Geib and Brock, 2017).

405

406 **Promoter Exchange in *A. allahabadii***

407 To express the *A. allahabadii pksP* homologue under the control of the *A. fumigatus pksP* promoter,
408 two PCR products were generated using the Phusion high-fidelity DNA polymerase (ThermoFisher
409 Scientific): 1000 bp *PpksP* from genomic DNA of *A. fumigatus* Af293 with oligonucleotides 17+18,
410 *pksP* from *A. allahabadii* including the *A. nidulans trpC* terminator from the heterologous expression

411 plasmid with oligonucleotides 19+20 (supplementary table 3). PCR products were mixed with a
412 *Hind*III digested *ptrA*_pUC19 plasmid (Fleck and Brock, 2010) and assembled by the In-Fusion HD
413 cloning kit (Takara/Clontech). Plasmid amplification in *E. coli* and fungal transformation were
414 carried out as described for heterologous expression of pigment biosynthesis genes in *A. niger* except
415 that 0.1 µg/ml pyrithiamine was used as selection marker. Transformants were streaked three times
416 on pyrithiamine containing AMM agar and checked for construct integration with oligonucleotides
417 30+31 using Phire Green Hot Start II DNA polymerase (ThermoFisher Scientific).

418

419 **Chromatographic Analysis of Transformants**

420 Selected transformants were grown for 26 h to 46 h in AMM(-N) medium containing 50 mM glucose,
421 10 mM glutamine and 10 µg/ml doxycycline (Geib and Brock, 2017). Mycelium was removed by
422 filtration over Miracloth filter gauze (Merck Millipore) and culture filtrates were extracted with an
423 equal volume of ethyl acetate. The organic phase was collected and dried over sodium sulphate. After
424 evaporation of the solvent under reduced pressure, the residue was solved in 1 ml methanol. HPLC
425 analysis was carried out as described previously using a Dionex UltiMate3000 (ThermoFisher
426 Scientific) and an Eclipse XDB-C18 column, 5 µm, 4.6 × 150 mm (Agilent) that was kept at 40 °C.
427 (Geib and Brock, 2017).

428

429 **Acknowledgements**

430 TCV, JLN, ST, and MRA acknowledge funding from The Villum Foundation, grant VKR023437.
431 MRA and TCV acknowledge funding from the Danish National Research Foundation (DNRF137)
432 for the Center for Microbial Secondary Metabolites. MB acknowledges a scholarship towards EG
433 from the University of Nottingham. JCF acknowledge funding from the Novo Nordisk Foundation,
434 grant NNF13OC0005201. The work conducted by the U.S. Department of Energy Joint Genome
435 Institute, a DOE Office of Science User Facility, is supported by the Office of Science of the U.S.
436 Department of Energy under Contract No. DE-AC02-05CH11231.

437 **References**

- 438 Alberts, A.W., Chen, J., Kuron, G., Hunt, V., Huff, J., Hoffman, C., Rothrock, J., Lopez, M.,
439 Joshua, H., Harris, E. *et al.* (1980). Mevinolin: a highly potent competitive inhibitor of
440 hydroxymethylglutaryl-coenzyme A reductase and a cholesterol-lowering agent. *P. Natl. Acad.*
441 *Sci.* 77, 3957-61
- 442 Andersen, M.R., Salazar, M.P., Schaap, P.J., van de Vondervoort, P.J.I., Culley, D., Thykaer, J.,
443 Frisvad, J.C., Nielsen, K.F., Albang, R., Albermann, K. *et al.* (2011). Comparative genomics of
444 citric-acid-producing *Aspergillus niger* ATCC 1015 *versus* enzyme-producing CBS 513.88.
445 *Genome Res.* 21, 885-97
- 446 Arakawa, M., Someno, T., Kawada, M., and Ikeda, D. (2008). A new terrein glucoside, a novel
447 inhibitor of angiogenin secretion in tumor angiogenesis. *J. Antibiot.* 61, 442-8
- 448 Arnaud, M.B., Cerqueira, G.C., Inglis, D.O., Skrzypek, M.S., Binkley, J., Chibucos, M.C.,
449 Crabtree, J., Howarth, C., Orvis, J., Shah, P. *et al.* (2012). The *Aspergillus* Genome Database
450 (AspGD): recent developments in comprehensive multispecies curation, comparative genomics
451 and community resources. *Nucleic Acids Res.* 40, D653-9
- 452 Balajee, S.A., Baddley, J.W., Peterson, S.W., Nickle, D., Varga, J., Boey, A., Lass-Flörl, C.,
453 Frisvad, J.C., Samson, R.A., and ISHAM Working Group on *A. terreus* (2009a). *Aspergillus*
454 *alabamensis*, a new clinically relevant species in the section *Terrei*. *Eukaryot. Cell* 8, 713-22
- 455 Balajee, S.A. (2009b). *Aspergillus terreus* complex. *Med. Mycol.* 47 Suppl 1, S42-6
- 456 Boruta, T., and Bizukojc, M. (2017). Production of lovastatin and itaconic acid by *Aspergillus*
457 *terreus*: a comparative perspective. *World J. Microb. Biot.* 33, 34
- 458 Bouhired, S., Weber, M., Kempf-Sontag, A., Keller, N.P., and Hoffmeister, D. (2007). Accurate
459 prediction of the *Aspergillus nidulans* terrequinone gene cluster boundaries using the
460 transcriptional regulator LaeA. *Fungal Genet. Biol.* 44, 1134-45
- 461 Calton, G.J., Ranieri, R.L., and Espenshade, M.A. (1978). Quadrone, a new antitumor substance
462 produced by *Aspergillus terreus*. Production, isolation and properties. *J. Antibiot.* 31, 38-42

463 Camacho, C., Coulouris, G., Avagyan, V., Ma, N., Papadopoulos, J., Bealer, K., and Madden, T.L.
464 (2009). BLAST+: architecture and applications. BMC Bioinformatics 10, 421

465 Chiang, Y., Meyer, K.M., Praseuth, M., Baker, S.E., Bruno, K.S., and Wang, C.C.C. (2011).
466 Characterization of a polyketide synthase in *Aspergillus niger* whose product is a precursor for
467 both dihydroxynaphthalene (DHN) melanin and naphtho- γ -pyrone. Fungal Genet. Biol. 48, 430-
468 7

469 Cock, P.J.A., Antao, T., Chang, J.T., Chapman, B.A., Cox, C.J., Dalke, A., Friedberg, I.,
470 Hamelryck, T., Kauff, F., Wilczynski, B. *et al.* (2009). Biopython: freely available Python tools
471 for computational molecular biology and bioinformatics. Bioinformatics 25, 1422-3

472 Csardi, G., and Nepusz, T. (2006). The igraph software package for complex network research.
473 InterJournal, Complex Systems, 1695

474 Draughon, F.A., and Ayres, J.C. (1980). Insecticide inhibition of growth and patulin production in
475 *Penicillium expansum*, *Penicillium urticae*, *Aspergillus clavatus*, *Aspergillus terreus*, and
476 *Byssoschlamys nivea*. J. Agr. Food Chem. 28, 1115-7

477 Fleck, C.B., and Brock, M. (2010). *Aspergillus fumigatus* catalytic glucokinase and hexokinase:
478 expression analysis and importance for germination, growth, and conidiation. Eukaryot. Cell 9,
479 1120-35

480 Fujii, I., Ebizuka, Y., and Sankawa, U. (1982). Partial purification and some properties of emodin-
481 O-methyltransferase from (+)-geodin producing strain of *Aspergillus terreus*. Chem. Pharm.
482 Bull. 30, 2283-6

483 Galagan, J.E., Calvo, S.E., Cuomo, C., Ma, L., Wortman, J.R., Batzoglou, S., Lee, S., Baştürkmen,
484 M., Spevak, C.C., Clutterbuck, J. *et al.* (2005). Sequencing of *Aspergillus nidulans* and
485 comparative analysis with *A. fumigatus* and *A. oryzae*. Nature 438, 1105-15

486 Gams, W., Christensen, M., Onions, A.H., Pitt, J.I., and Samson, R.A. (1986). Infrageneric Taxa of
487 *Aspergillus*. In Advances in *Penicillium* and *Aspergillus* Systematics (Springer US), pp. 55–62.

488 Geib, E., Gressler, M., Viediarnikova, I., Hillmann, F., Jacobsen, I.D., Nietzsche, S., Hertweck, C.,
489 and Brock, M. (2016). A non-canonical melanin biosynthesis pathway protects *Aspergillus*
490 *terreus* conidia from environmental stress. *Cell Chem. Biol.* 23, 587-97

491 Geib, E., and Brock, M. (2017). ATNT: an enhanced system for expression of polycistronic
492 secondary metabolite gene clusters in *Aspergillus niger*. *Fungal Biol. Biotechnol.* 4, 13

493 Gnerre, S., Maccallum, I., Przybylski, D., Ribeiro, F.J., Burton, J.N., Walker, B.J., Sharpe, T., Hall,
494 G., Shea, T.P., Sykes, S. *et al.* (2011). High-quality draft assemblies of mammalian genomes
495 from massively parallel sequence data. *P. Natl. Acad. Sci.* 108, 1513-8

496 Gressler, M., Hortschansky, P., Geib, E., and Brock, M. (2015a). A new high-performance
497 heterologous fungal expression system based on regulatory elements from the *Aspergillus*
498 *terreus* terrein gene cluster. *Front Microbiol.* 6, 184

499 Gressler, M., Meyer, F., Heine, D., Hortschansky, P., Hertweck, C., and Brock, M. (2015b).
500 Phytotoxin production in *Aspergillus terreus* is regulated by independent environmental signals.
501 *eLife* 4

502 Grigoriev, I.V., Martinez, D.A., and Salamov, A.A. (2006). Fungal genomic annotation. In *Applied*
503 *mycology and biotechnology* (Elsevier), pp. 123–142.

504 Grigoriev, I.V., Nikitin, R., Haridas, S., Kuo, A., Ohm, R., Otilar, R., Riley, R., Salamov, A., Zhao,
505 X., Korzeniewski, F. *et al.* (2014). MycoCosm portal: gearing up for 1000 fungal genomes.
506 *Nucleic Acids Res.* 42, D699-704

507 Guo, C., Sun, W., Bruno, K.S., and Wang, C.C.C. (2014a). Molecular genetic characterization of
508 terreic acid pathway in *Aspergillus terreus*. *Org. Lett.* 16, 5250-3

509 Guo, C., and Wang, C.C.C. (2014b). Recent advances in genome mining of secondary metabolites
510 in *Aspergillus terreus*. *Front Microbiol.* 5, 717

511 Kaji, A., Saito, R., Nomura, M., Miyamoto, K., and Kiriyama, N. (1998). Relationship between the
512 structure and cytotoxic activity of asterriquinone, an antitumor metabolite of *Aspergillus terreus*,
513 and its alkyl ether derivatives. *Biol. Pharm. Bull.* 21, 945-9

514 Kamata, S., Sakai, H., and Hirota, A. (1983). Isolation of acetylaranotin, bisdethiodi(methylthio)-
515 acetylaranotin and terrein as plant growth inhibitors from a strain of *Aspergillus terreus*. *Agr.*
516 *Biol. Chem.* 47, 2637-8

517 Katoh, K., and Standley, D.M. (2013). MAFFT multiple sequence alignment software version 7:
518 improvements in performance and usability. *Mol. Biol. Evol.* 30, 772-80

519 Khaldi, N., Seifuddin, F.T., Turner, G., Haft, D., Nierman, W.C., Wolfe, K.H., and Fedorova, N.D.
520 (2010). SMURF: Genomic mapping of fungal secondary metabolite clusters. *Fungal Genet. Biol.*
521 47, 736-41

522 Kiriyama, N., Nitta, K., Sakaguchi, Y., Taguchi, Y., and Yamamoto, Y. (1977). Studies on the
523 metabolic products of *Aspergillus terreus*. III. Metabolites of the strain IFO 8835. 1. *Chem.*
524 *Pharm. Bull.* 25, 2593-601

525 Kjærboelling, I., Vesth, T.C., Frisvad, J.C., Nybo, J.L., Theobald, S., Kuo, A., Bowyer, P., Matsuda,
526 Y., Mondo, S., Lyhne, E.K. *et al.* (2018). *Aspergillus* species. *P. Natl. Acad. Sci.* 115, E753-
527 E761

528 Klejnstrup, M.L., Frandsen, R.J.N., Holm, D.K., Nielsen, M.T., Mortensen, U.H., Larsen, T.O., and
529 Nielsen, J.B. (2012). Genetics of polyketide metabolism in *Aspergillus nidulans*. *Metabolites* 2,
530 100-33

531 Lass-Flörl, C., Griff, K., Mayr, A., Petzer, A., Gastl, G., Bonatti, H., Freund, M., Kropshofer, G.,
532 Dierich, M.P., and Nachbaur, D. (2005). Epidemiology and outcome of infections due to
533 *Aspergillus terreus*: 10-year single centre experience. *Brit. J. Haematol.* 131, 201-7

534 Lim, S.Y., Kano, R., Ooya, K., Kimura, S., Yanai, T., Hasegawa, A., and Kamata, H. (2016). The
535 first Isolation of *Aspergillus allahabadii* from a cormorant with pulmonary aspergillosis. *Med.*
536 *Mycol. J.* 57, E77-E79

537 Medema, M.H., Kottmann, R., Yilmaz, P., Cummings, M., Biggins, J.B., Blin, K., de Bruijn, I.,
538 Chooi, Y.H., Claesen, J., Coates, R.C. *et al.* (2015). Minimum information about a biosynthetic
539 gene cluster. *Nat. Chem. Biol.* 11, 625-31

540 Miller, P.A., Trown, P.W., Fulmor, W., Morton, G.O., and Karlner, J. (1968). An
541 epidithiapiperazinedione antiviral agent from *Aspergillus terreus*. Biochem. Bioph. Res. Co. 33,
542 219-21

543 Nierman, W.C., Pain, A., Anderson, M.J., Wortman, J.R., Kim, H.S., Arroyo, J., Berriman, M.,
544 Abe, K., Archer, D.B., Bermejo, C. *et al.* (2005). Genomic sequence of the pathogenic and
545 allergenic filamentous fungus *Aspergillus fumigatus*. Nature 438, 1151-6

546 Nierman, W.C., Yu, J., Fedorova-Abrams, N.D., Losada, L., Cleveland, T.E., Bhatnagar, D.,
547 Bennett, J.W., Dean, R., and Payne, G.A. (2015). Genome Sequence of *Aspergillus flavus* NRRL
548 3357, a strain that causes aflatoxin contamination of food and feed. Genome Announcements 3,
549 e00168-15

550 Okabe, M., Lies, D., Kanamasa, S., and Park, E.Y. (2009). Biotechnological production of itaconic
551 acid and its biosynthesis in *Aspergillus terreus*. Appl. Microbiol. Biot. 84, 597-606

552 Payne, G.A., Nierman, W.C., Wortman, J.R., Pritchard, B.L., Brown, D., Dean, R.A., Bhatnagar,
553 D., Cleveland, T.E., Machida, M., and Yu, J. (2006). Whole genome comparison of *Aspergillus*
554 *flavus* and *A. oryzae*. Med. Mycol. 44, 9–11

555 Samson, R.A., Peterson, S.W., Frisvad, J.C., and Varga, J. (2011). New species in *Aspergillus*
556 section *Terrei*. Stud. Mycol. 69, 39-55

557 Sankawa, U., Ebizuka, Y., Noguchi, H., Isikawa, Y., Kitagawa, S., Yamamoto, Y., Kobayashi, T.,
558 Iitak, Y., and Seto, H. (1983). Biosynthesis of citrinin in *Aspergillus terreus*. Tetrahedron 39,
559 3583-91

560 Savitha, J., Bhargavi, S.D., and Praveen, V.K. (2016). Complete genome sequence of soil fungus
561 *Aspergillus terreus* (KM017963), a potent lovastatin producer. Genome Announcements 4,
562 e00491-16

563 Sheehan, J.C., Lawson, W.B., and Gaul, R.J. (1958). The Structure of terreic acid. J. Am. Chem.
564 Soc. 80, 5536-8

565 Slesiona, S., Gressler, M., Mihlan, M., Zaehle, C., Schaller, M., Barz, D., Hube, B., Jacobsen, I.D.,
566 and Brock, M. (2012). Persistence versus escape: *Aspergillus terreus* and *Aspergillus fumigatus*
567 employ different strategies during interactions with macrophages. *Plos One* 7, e31223

568 Stamatakis, A. (2014). RAxML version 8: a tool for phylogenetic analysis and post-analysis of
569 large phylogenies. *Bioinformatics* 30, 1312-3

570 Talavera, G., and Castresana, J. (2007). Improvement of phylogenies after removing divergent and
571 ambiguously aligned blocks from protein sequence alignments. *Systematic Biol.* 56, 564-77

572 Tevz, G., Bencina, M., and Legisa, M. (2010). Enhancing itaconic acid production by *Aspergillus*
573 *terreus*. *Appl. Microbiol. Biot.* 87, 1657-64

574 Theobald *et al.* (2018), in review with PLOS Genetics

575 Tsai, H.F., Wheeler, M.H., Chang, Y.C., and Kwon-Chung, K.J. (1999). A developmentally
576 regulated gene cluster involved in conidial pigment biosynthesis in *Aspergillus fumigatus*. *J.*
577 *Bacteriol.* 181, 6469-77

578 Varga, J., Tóth, B., Kocsubé, S., Farkas, B., Szakács, G., Téren, J., and Kozakiewicz, Z. (2005).
579 Evolutionary relationships among *Aspergillus terreus* isolates and their relatives. *Antonie van*
580 *Leeuwenhoek* 88, 141-50

581 Varga, J., and Samson, R.A. (2008). *Aspergillus* in the genomic era (Wageningen Academic
582 Publishers), pp. 73-82

583 Vesth, T.C., Nybo, J.L., Theobald, S., Frisvad, J.C., Larsen, T.O., Nielsen, K.F., Hoof, J.B., Brandl,
584 J., Salamov, A., Riley, R. *et al.* (2018). Section-level genome sequencing of *Aspergillus* section
585 *Nigri* shows inter- and intra-species-level variation. *Nat. Genet.* accepted pending revisions

586 de Vries, R.P., Riley, R., Wiebenga, A., Aguilar-Osorio, G., Amillis, S., Uchima, C.A., Anderluh,
587 G., Asadollahi, M., Askin, M., Barry, K. *et al.* (2017). Comparative genomics reveals high
588 biological diversity and specific adaptations in the industrially and medically important fungal
589 genus *Aspergillus*. *Genome Biol.* 18, 28

590 Zerbino, D.R., and Birney, E. (2008). Velvet: algorithms for *de novo* short read assembly using de
591 Bruijn graphs. *Genome Res.* 18, 821-9
592

593 **Supplementary information**

594 **Suppl. Table 1 - Genome statistics of sequencing and annotation for 18 genomes used in the**
595 **analysis.** All genomes from section *Terrei* except *A. terreus* are from this study.

596

597 **Suppl. Table 2 - Overview of predicted secondary metabolite gene clusters.** Contains data for all
598 18 genomes of the study (See Suppl. Table 1). The Cluster Family column denotes the generated
599 families of gene clusters. Genes with the same number belong to the same family of gene clusters.

600 **You can find supplementary table 2 in the appendix of this thesis.**

601

602 **Suppl. Table 3 – Oligonucleotides used in this study.**

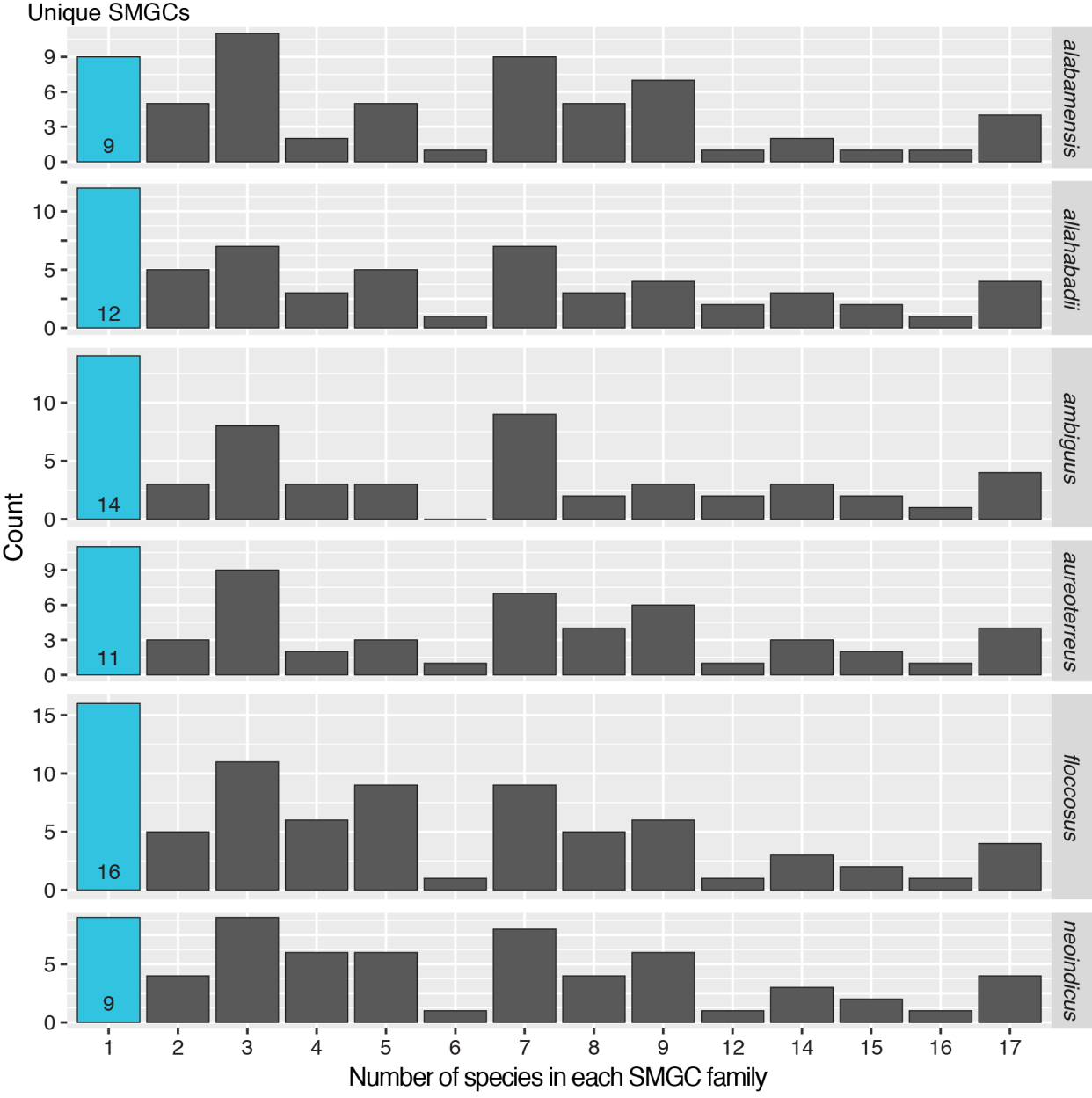
603

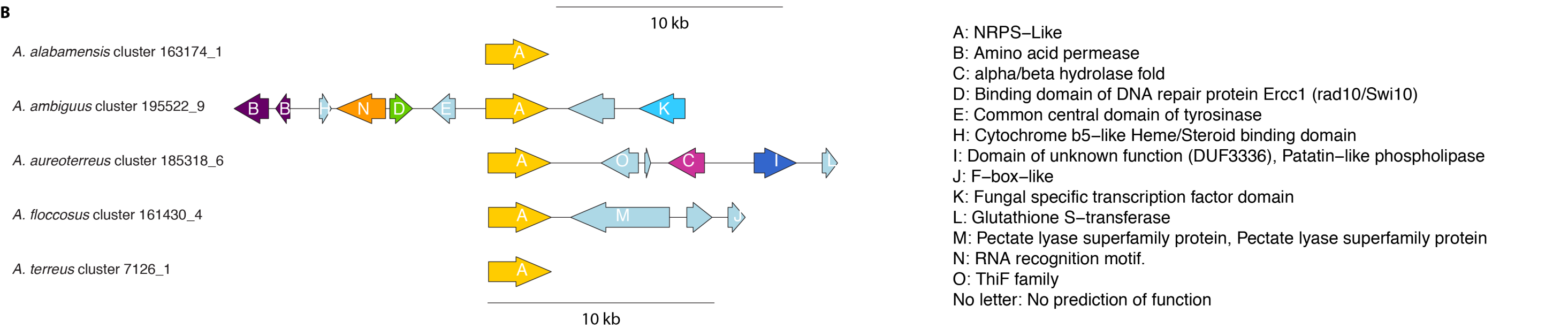
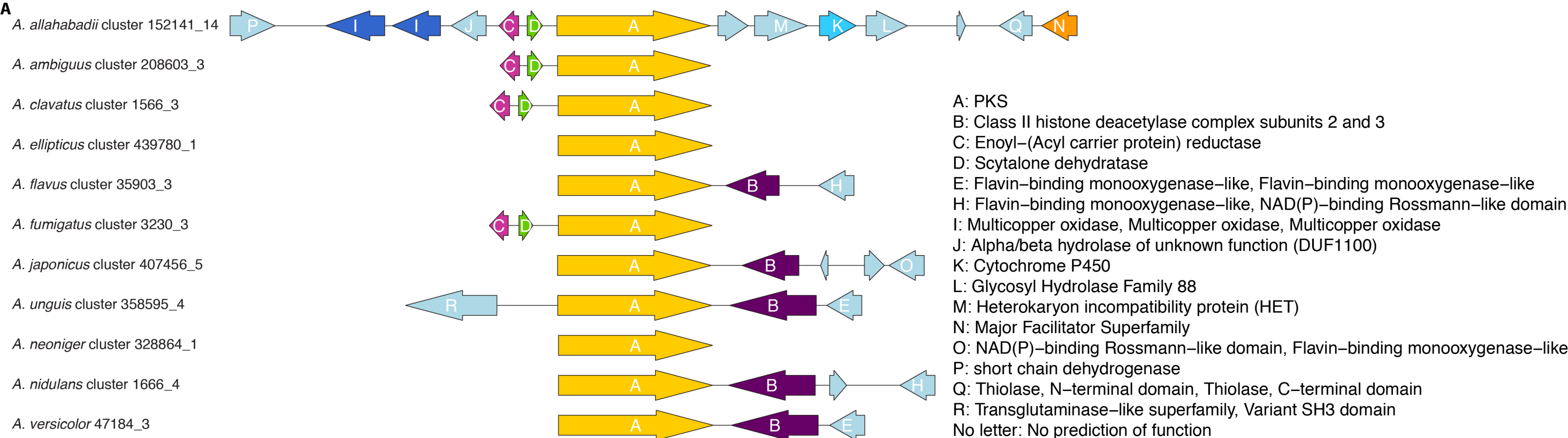
604 **Suppl. Figure 1 - Overview of SMGC family size from all species in section *Terrei*.** Each column
605 shows the number of SMGCs from the species found in families with members from X species, where
606 X is the horizontal axis.

607

608 **Suppl. Figure 2 - Synteny maps of SMGC families for pigment clusters. A - Clusters predicted**
609 **with homology to the *A. nidulans* *wA* and *A. fumigatus* *pksP* gene. B - Clusters predicted with**
610 **homology to the Asp-melanin biosynthesis pathway including the aspulvinone E synthase gene *melA***
611 **from *A. terreus*. Note that the clusters presented are the raw predictions. Cluster names refer to their**
612 **naming in Suppl. Table 2.**

613





Genome	JGI organism code	Section	Protein Count [#]	IPR Coverage [%]	GO Coverage [%]	Average number of exons [#]	Number of scaffolds [#]	Scaffolds ove	Genome Size	GC [%]	Average scaff	Median Scaff	Longest scaff	Shortest scaff	Scaffold N50	Scaffold L50 [
Aspergillus alabamensis	Aspala1	Terrei	11841	75	53	3.2	219	188	32	52%	146095	21827	1660550	1003	14	647419
Aspergillus allahabadii	Aspall1	Terrei	11228	77	55	3.2	43	36	29.8	53%	692632	419452	4076947	1156	7	1453672
Aspergillus ambiguus	Aspamb1	Terrei	11088	77	55	3.2	149	123	29.4	52%	197147	42961	1932825	1023	16	550646
Aspergillus aureoterreus	Aspaur1	Terrei	11269	76	7	3.2	109	98	29.5	54%	270791	71620	1931989	1043	15	763182
Aspergillus floccosus	Aspflo1	Terrei	11810	76	54	3.2	224	218	30.6	52%	136394	92434	736066	1017	39	249808
Aspergillus neoindicus	Aspneo1	Terrei	11849	75	53	3.2	121	96	30.9	52%	255352	20589	2418121	1007	11	910252
Aspergillus terreus	Aspte1	Terrei	10406	72	60	3.2	26	26	29.3	53%	1128123	1388580	2751824	12095	7	1912493
Saccharomyces cerevisiae	Sacce1	Saccharomyc	6575	69	56	1	16	16	12.1	38%	754431	765038	1531919	230208	6	924429
Aspergillus ellipticus	Aspell1	Nigri	12884	64	52	3.1	518	505	42.9	45%	82753	48043	684843	1067	84	158998
Aspergillus japonicus	Aspjap1	Nigri	12024	68	56	3.2	163	161	36.1	51%	221472	122459	1444553	1324	25	412690
Aspergillus neoniger	Aspneo1	Nigri	11939	68	56	3.3	169	149	35.4	49%	209565	37197	1664060	1025	18	707186
Aspergillus niger ATCC 1015	Aspni7	Nigri	11910	70	57	3.4	24	24	34.9	50%	1452220	1610718	3774411	14100	6	1937564
Aspergillus unguis CBS 120.58	Aspmic1	Nidulantes	10236	77	55	3.2	60	58	25.9	50%	431899	176653	2796312	1001	8	1152650
Aspergillus nidulans	Aspnid1	Nidulantes	10680	72	59	3.3	8	8	30.5	49%	3810499	3615053	4934093	2887738	4	3759208
Aspergillus versicolor	Aspve1	Nidulantes	13228	72	59	3.2	51	41	33.1	50%	649545	11331	5023850	1241	5	2487993
Aspergillus fumigatus Af293	Aspfu1	Fumigati	9781	72	59	2.9	8	8	29.4	49%	3673547	3937833	4918979	1833124	4	3948441
Aspergillus flavus	Aspf1	Flavi	12604	69	56	3.3	138	138	36.8	48%	266596	2301	4469204	2004	6	2388123
Aspergillus clavatus	Aspcl1	Clavati	9121	73	59	3.1	143	28	27.9	49%	194821	1387	4489098	1002	5	2493640

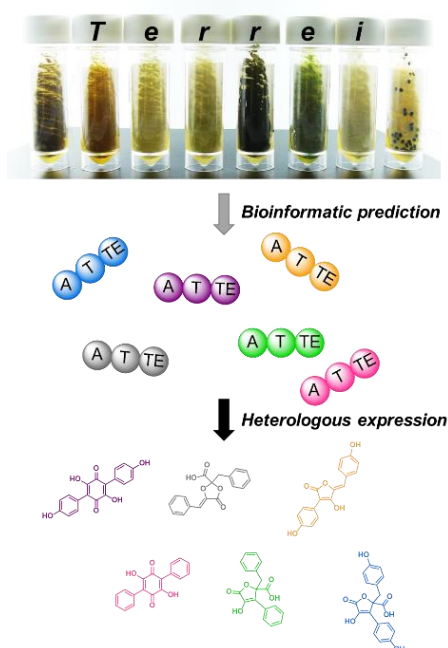
Supplementary Table 3 – Oligonucleotides Used in this Study

#	sequence	construct
1	catcaccatcaccatggacaaccaggccaagtcttattc	<i>A.alabamensis melA</i>
2	ctgctgttatccatggttacatgccctctcagtaag	<i>A.alabamensis melA</i>
3	catcaccatcaccatggacaaccaagccttattccctc	<i>A. aureoterreus melA</i>
4	ctgctgttatccatggttacatacccctctcagcaag	<i>A. aureoterreus melA</i>
5	catcaccatcaccatggatccacactgttcacacgctc	<i>A. ambiguus melA</i>
6	ctgctgttatccatggtcacatgcccttcatcaag	<i>A. ambiguus melA</i>
7	catcaccatcaccatggacaacaagcttattccctctc	<i>A. floccosus melA</i>
8	ctgctgttatccatggtcacatacccctctcagcaag	<i>A. floccosus melA</i>
9	catcacagcaccatggaaggaggcaacaagtc	<i>A. allahabadii pksP</i>
10	atcactgctgcatggctaggatgacatccactcc	<i>A. allahabadii pksP</i>
11	catcacagcaccatggagaactcccagcagg	<i>A. ambiguus pksP</i>
12	atcactgctgcatggctaagaagccattgcttggc	<i>A. ambiguus pksP</i>
13	catcacagcaccatggaggactcataccatgctc	<i>A. unguis pksP</i>
14	atcactgctgcatggtaagcgcccagagcattcg	<i>A. unguis pksP</i>
15	catcacagcaccatggaggatctccatcgctc	<i>A. fumigatus pksP</i>
16	atcactgctgcatggctaggactcatggccgtg	<i>A. fumigatus pksP</i>
17	tgcaggcatgcaagcttgcggggaaatcaaagcatg	Promoter exchange: P <i>pksP A. fumigatus</i>
18	ttgacctctccatggcgagtggttgcgcg	Promoter exchange: P <i>pksP A. fumigatus</i>
19	atggaaggaggcaacaagtc	Promoter exchange: <i>pksP A. allahabadii</i> + T
20	atgattacgccaagcttgagtgaggggtgagtacgag	Promoter exchange: <i>pksP A. allahabadii</i> + T
21	cagaccgacctgtgtatgc	<i>A.alabamensis melA</i> control
22	cacggaccatacgctctcg	<i>A.aureoterreus melA</i> control
23	ccgatcgacctgtctacg	<i>A.ambiguus melA</i> control
24	cgacctgtgtatgctctacg	<i>A.floccosus melA</i> control
25	ccagagaagctgaaatgtagc	<i>A.allahabadii pksP</i> control
26	ctaccatcccactccttgg	<i>A.ambiguus pksP</i> control
27	catctctccatccgtctgc	<i>A.unguis pksP</i> control
28	caattgcccttacatgaagacg	<i>A.fumigatus pksP</i> control
29	gaattttaccagtgccctagg	SM-Xpress plasmid control
30	CCTGCGATGCTTTAGGAGG	P <i>pksP (A. fumigatus)</i> control
31	GATGTCCAGGCTCATCTCG	<i>pksP (A. allhabadii)</i> control

Recombinant expression and characterisation of NRPS-like enzymes from *Aspergillus* species section *Terrei*

Elena Geib, Sebastian Theobald, Mikael R. Andersen and Matthias Brock

In preparation.



Summary of the manuscript: Analyses of genomes from *Aspergillus* species from section *Terrei* indicated an enrichment of NRPS-like enzymes. Here, we aimed in sorting these NRPS-like enzymes into families with the assumption that a specific family produces a single class of metabolites. Wet-lab experiments partially confirmed this hypothesis, but it became evident that prediction tools need to be refined. Multiple asp vulvinone E and butyrolactone IIa synthetases were identified and correctly grouped into families. However, within individual families NRPS-like enzymes possibly producing polyporic acid and phenylbutyrolactone IIa were identified, but final confirmation of the metabolite structures is currently pending. These products have not

previously been described as natural occurring metabolites from aspergilli. The identification and characterisation of additional and partially novel NRPS-like enzymes contributes towards the understanding of sequence patterns required for product prediction from NRPS-like enzymes. However, more synthetases need to be characterised, especially outside the genus *Aspergillus*, to collect more data for training of bioinformatic programs.

Contribution: 90% of practical work, major contribution to manuscript preparation

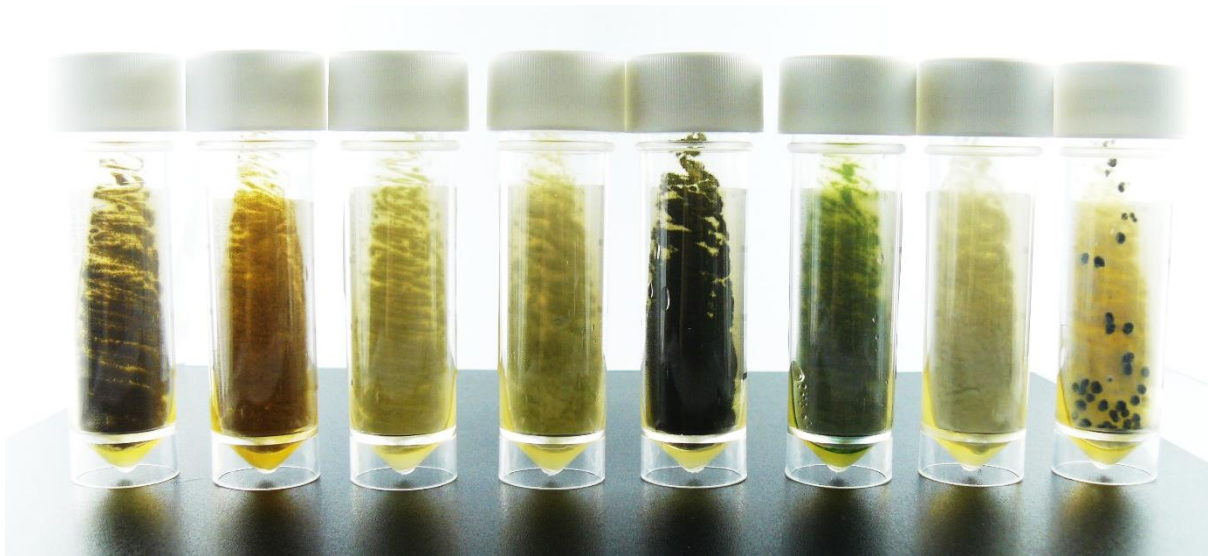
Cloning of 20 NRPS-like genes, thereof 14 previously uncharacterised, into SM-Xpress_URA plasmids. Transformation of *A. niger* ATNT16 Δ pyrG and *A. oryzae* OP12 pyrG⁻, selection, purification and testing of transformants. Extraction and analysis of secondary metabolites from selected transformants by HPLC and HR-ESI-MS. Alignment of full-length protein and thioesterase-domain sequences after sequence correction (intron-removal) for construction of phylogenetic trees.

Recombinant expression and characterisation of NRPS-like enzymes from *Aspergillus* species section *Terrei*

Elena Geib¹, Sebastian Theobald², Mikael Rørdam Andersen², Matthias Brock¹

¹ Fungal Genetics and Biology, School of Life Sciences, University of Nottingham, University Park, NG7 2RD Nottingham, UK

² Department of Biotechnology and Bioengineering, Technical University of Denmark, Kgs. Lyngby, Denmark



Abstract

Non-ribosomal peptide synthetase-like (NRPS-like) proteins are monomodular enzymes producing secondary metabolites. Although only a limited number of NRPS-like enzymes has been characterised, these enzymes produce a wide variety of different metabolites with interesting pharmacological characteristics. To obtain an overview on NRPS-like-derived metabolites in *Aspergilli* from section *Terrei*, we selected candidates for heterologous expression. Bioinformatics tools sorted enzymes into distinct families, hypothesising that enzymes from the same family produce the identical metabolite. This was indeed the case for some families such as that containing a putative phenylbutyrolactone IIa and butyrolactone IIa synthetases. However, other families showed a broader variation. The family containing the aspulvinone E synthetase ApvA from *Aspergillus terreus* also contained phenguignardic acid, atromentin and polyporic acid synthetases. Polyporic acid had previously only been known as metabolite from basidiomycetes, but it appears also present in ascomycetes. Closer analysis of phylogenetic trees revealed that phylogenetic relationship and product formation matched, but only when enzymes derived from the same fungal genus. In contrast, atromentin synthetases from basidio- and ascomycetes formed well-separated branches. This indicates that phylogenetic relationship of the species weights more than the metabolite produced. Therefore, determination of specific sequence patterns that predict the chemistry of a given NRPS-like enzyme will require the characterisation of additional enzymes not only from asco-, but especially from basidiomycetes. However, besides the limitations in defining sequence motives for the prediction of metabolites produced by NRPS-like enzymes, this study confirms the great variety of NRPS-like-derived metabolites produced from species of section *Terrei*.

Introduction

Non-ribosomal peptide synthetase-like (NRPS-like) proteins are a class of monomolecular enzymes producing secondary metabolites. They are further discriminated in enzymes containing a C-terminal reductase or thioesterase domain. While enzymes that contain a reductase domain mainly reduce carboxyl groups of metabolites into aldehydes (Wang, Beissner and Zhao, 2014), especially NRPS-like enzymes with a C-terminal thioesterase domain produce a fascinating diversity of chemical structures. Even more, these compounds have a broad diversity of potential pharmacological activities, making NRPS-like enzyme products a valuable source of small-molecule drug lead structures (Schneider *et al.*, 2007). NRPS-like enzymes are rather small proteins compared to multimodule non-ribosomal peptide synthetases (NRPS) or other mega-synthases described to be involved in secondary metabolite biosynthesis (Weissman, 2015). Lacking the condensation domain of canonical NRPS, no peptide bond formation can be catalysed. Instead, NRPS-like enzymes utilise α -keto acids, which is only observed in exceptional cases for NRPS that generally use L- or D- or other unusual amino acids. So far it seems that NRPS-like enzymes have a strong preference for α -keto acids deriving from aromatic amino acids such as phenylpyruvate, *p*-hydroxyphenylpyruvate or indole pyruvate. Product formation is generally described as the condensation of two identical α -keto acids (Schneider *et al.*, 2007). An exception might be depicted by biosynthesis of guignardic and alaguignardic acid from *Guignardia bidwellii*, which are compounds structurally related to phenguignardic acid, which is a condensation product of two phenylpyruvate molecules (Buckel *et al.*, 2013). In *Aspergillus terreus* formation of phenguignardic acid has been confirmed to be catalysed by an NRPS-like enzyme (Sun, Guo and Wang, 2016), but the biosynthetic origin of the three so-called dioxolanones produced in *Guignardia bidwellii* remains mostly elusive. However, at least the incorporation of labelled phenylalanine had been confirmed for all three products in *G. bidwellii*, whereby for production of guignardic acid a condensation with 2-oxo-3-methyl-butanoate and for alaguignardic acid a condensation with pyruvate is required (Buckel *et al.*, 2017). It appears likely that the genome of *Guignardia bidwellii* encodes NRPS-like enzymes involved in biosynthesis of these dioxolanones, but genome sequences are not yet publicly available. Therefore, it remains speculative whether a single enzyme with an unusual adenylation domain selects different substrates or if more than one enzyme is involved in biosynthesis of the different products.

Despite the limited set of enzymatic reactions carried out by NRPS-like enzymes, which is the condensation of two identical α -keto acids, the product diversity is remarkable. One of the criteria discriminating different products is their classification by the core structure formed. By now, three main core structures deriving from the biosynthesis of NRPS-like enzymes have been described: quinones, dioxolanones and furanones. The diversity within the furanone core structures is furthermore enhanced by different substitution patterns (Figure 1). Combined with

the use of the different aromatic α -keto acids, a broad range of different metabolites can be produced. Diversity is further increased by the observation that fungal NRPS-like enzymes are frequently embedded within biosynthesis gene cluster. Thereby, tailoring enzymes modify the product by prenylation, hydroxylation or other modifications (Balibar, Howard-Jones and Walsh, 2007).

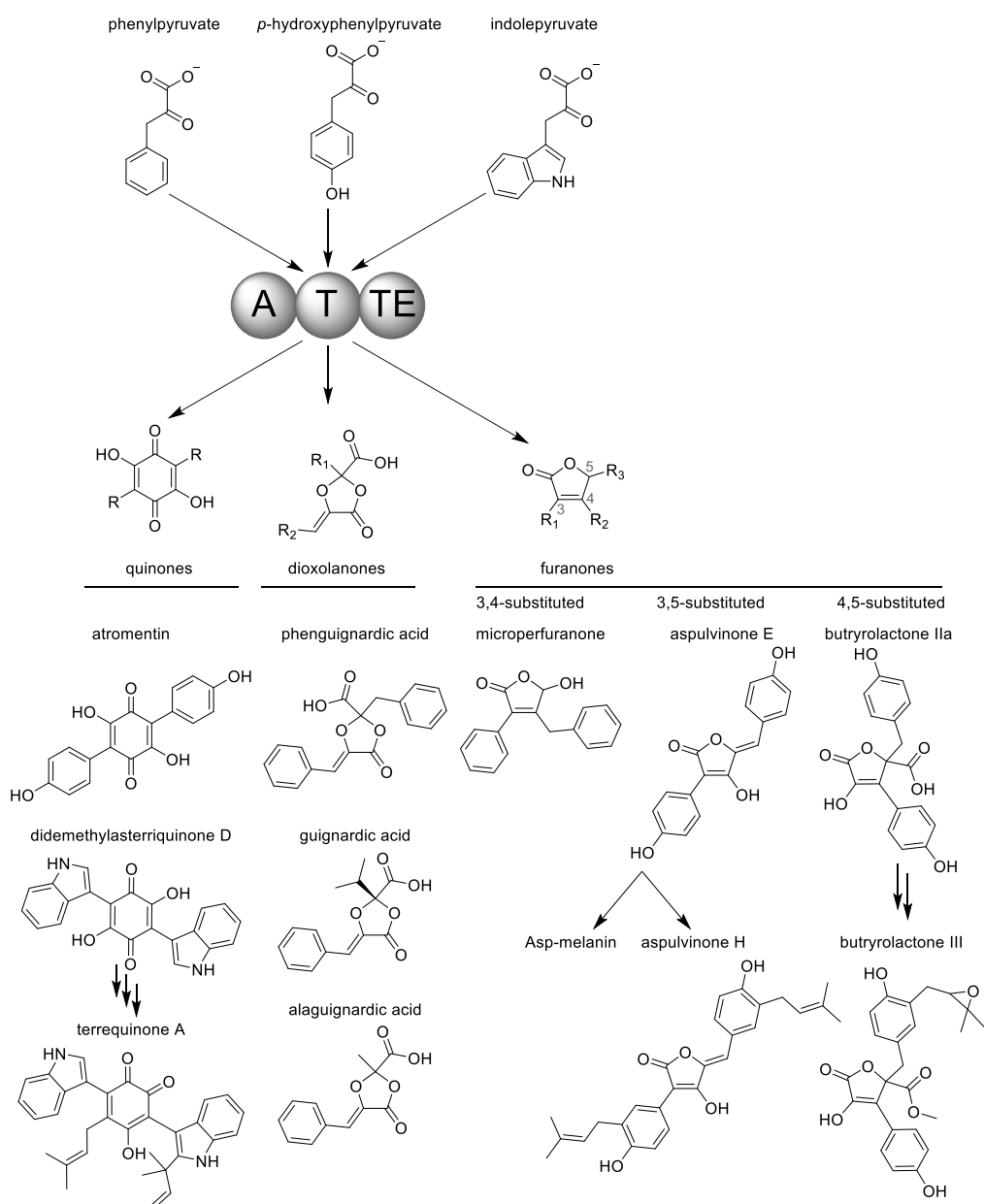


Figure 1: Examples for the complexity of NRPS-like enzyme derived metabolites. Most NRPS-like enzymes with a domain architecture of adenylation (A)-, thiolation (T)- and thioesterase (TE)-domain activate and condensate two identical aromatic α -keto acids. The resulting core structures can be classified into quinones, dioxolanones or furanones. Examples for each type of core structures are shown. Guignardic and alaguignardic acid are unusual examples for dioxolanones as different α -keto acids seem to be used as substrates. Furanone core structures produced by NRPS-like enzymes can be subdivided by their substitution

pattern. Furthermore, when embedded in biosynthesis gene clusters tailoring enzymes catalyse additional modifications of the primary metabolites as for didemethylasterriquinone D, which is transformed into terrequinone A.

Products of NRPS-like enzymes have been of great interest in several pharmaceutical studies. Many compounds show bioactivity possibly exploitable for human use. So far bis-indolylquinones have been attributed to three major areas of potential pharmaceutical exploitation: Cytotoxic anti-cancer effects have been described for asterriquinone derivatives, whereby the molecule intercalates with DNA leading to inter-strand cross-linking (Kaji *et al.*, 1998) and G1 cell cycle arrest (Kaji *et al.*, 1997). Moreover, binding to the Gbr2 adapter protein inhibits the p21^{ras} signal transduction pathway (Alvi *et al.*, 1999). Anti-diabetic properties have been described for didemethylasterriquinone B1 as it acts as antagonist for the insulin receptor (Zhang *et al.*, 1999; Velliquette *et al.*, 2005). Finally, antiretroviral effects including targeting of HIV have been attributed to didemethylasterriquinone, isocochliodinol, semicochliodinol A and B and hinnuliquinone (Fredenhagen *et al.*, 1997; Singh *et al.*, 2004). However, not only bis-indolylquinones exhibit anti-viral effects, but also the furanone core containing isoaspulvinone E, which has been shown to possess moderate activity against H1N1 neuraminidase (Gao *et al.*, 2013). Additionally, multiple hydroxylated terphenylquinones have been found to inhibit human Src protein tyrosine kinases, which are associated with metastatic tumour types in humans and might also be of use for cerebral protection after a stroke and prevention and treatment of osteoporosis (Puder *et al.*, 2005). Therefore, investigation of biosynthesis of NRPS-like enzymes can increase the portfolio of metabolites with interesting biological activities for further exploitation.

In the post-genomic era the availability of fungal genomes is constantly growing. This offers new prospects to mine genomes for NRPS-like encoding genes and to identify and characterise more of those highly valuable products. Since genomes may contain more than 15 NRPS-like encoding genes with a C-terminal TE-domain, a preselection of candidates encoding similar enzymes appears necessary to increase the likelihood to identify novel yet uncharacterised metabolites. However, the number of NRPS-like enzymes characterised so far is too small to make reliable bioinformatic predictions on product formation. This is especially due to the fact that the current knowledge on reaction mechanisms carried out by these enzymes is limited. A couple of atromentin synthetases from basidiomycetes have been investigated and, as a result, Braesel *et al.* (Braesel *et al.*, 2015) proposed fingerprint motifs to predict the type of product formed. It had been suggested that enzymes containing an NxPP motif in the thioesterase domain form quinones, whereas a DxPP motif indicates the formation of a furanone. Unfortunately, this prediction proved not sufficiently reliable as subsequent studies on NRPS-like enzymes mainly from ascomycetes revealed contradictory results. While the MelA protein encoding an aspulvinone E synthetase contained an NxPP motif it produces a furanone core

(Geib *et al.*, 2016). Therefore, additional analyses are required for a more reliable prediction of the core motif formed by NRPS-like enzymes.

In this respect, especially ascomycetes of the genus *Aspergillus* appear as valuable source for identifying and characterising NRPS-like enzymes as a large number of genomes is currently in the pipeline for sequencing. Furthermore, some *Aspergilli* have been established as model organisms and research on NRPS-like enzymes has already been carried out on the well-studied organism *A. nidulans* and the opportunistic human pathogen *Aspergillus terreus* (Table 1). In this respect, all five NRPS-like enzymes from *A. terreus* containing a TE-domain have been characterised by knock-out studies, heterologous expression or a combination thereof.

Table 1: NRPS-like enzymes and metabolites characterised from the genus *Aspergillus*.

	organism	Primary metabolite	Final metabolite	Reference
MelA	<i>A. terreus</i>	Aspulvinone E	Asp-melanin	(Geib <i>et al.</i> , 2016)
ApvA	<i>A. terreus</i>	Aspulvinone E	Aspulvinone H & B1	(Guo <i>et al.</i> , 2013)
BtyA	<i>A. terreus</i>	Butyrolactone IIa	Butyrolactone I & III	(Guo <i>et al.</i> , 2013; van Dijk, Guo and Wang, 2016)
PgnA	<i>A. terreus</i>	Phenguignardic acid		(Sun, Guo and Wang, 2016)
AtqA	<i>A. terreus</i>		Asterriquinone CT5	(Guo <i>et al.</i> , 2013)
AtrA _{At}	<i>A. terreus</i>	Atromentin		(Hühner <i>et al.</i> , 2018)
TdiA	<i>A. nidulans</i>	Didemethylasterriquinone	Terrequinone A	(Balibar, Howard-Jones and Walsh, 2007)
MicA	<i>A. nidulans</i>	Microperfuranone		(Yeh <i>et al.</i> , 2012)

While *A. terreus* is the best-known member of *Aspergilli* from section *Terrei* other members of this section have gained interest either as emerging pathogens or by the production of secondary metabolites (Balajee *et al.*, 2009; Samson *et al.*, 2011). As genomes of species from this section are currently sequenced, aim of this study was to express and characterise known and novel NRPS-like enzymes focussing on enzymes from species of section *Terrei*. Identification of compounds will help to refine sequence motifs of TE-domains to predict product formation from other yet uncharacterised enzymes.

Results

Cross-chemistry on indolylquinone-forming NRPS-like enzymes

Previous studies have shown that heterologous expression of NRPS-like enzymes may lead to unexpected product formation depending on the expression platform used. *A. niger* is an excellent host for heterologous secondary metabolite production and produces remarkably high product yields especially when used in combination with a TetOn-controlled coupled TerR/*PterA* expression system in the *A. niger* ATNT16 strain (Geib and Brock, 2017). However, when used for the recombinant expression of atromentin synthetases from various fungal sources, atrofuranic acid with a furanic acid core rather than the benzoquinone core containing atromentin was produced. In contrast, when atromentin synthetases were purified from *A. niger* expression hosts atromentin was produced under *in vitro* conditions (Geib *et al.*, 2018, manuscript submitted). Furthermore, when atromentin synthetases were expressed in the *A. oryzae* expression platform strain OP12, atromentin was the sole product formed (Geib *et al.*, 2018, manuscript submitted). This indicates a cross-specificity and cross-chemistry occurring in *A. niger* that modifies at least terphenylquinone core structures, whereas furanone core containing products were successfully produced in both expression platform strains (Geib *et al.*, 2018, manuscript submitted). Therefore, we investigated whether cross-chemistry effects are specific to terphenylquinone cores or observed on all quinone structures and selected the *tdiA* and *atqA* genes for further studies. TdiA and AtqA are known to produce the bis-indolylquinone didemethylasterriquinone D in *A. nidulans* (Schneider *et al.*, 2007) and *A. terreus* (Guo *et al.*, 2013), respectively. When *tdiA* or *atqA* were expressed as individual genes, no significant metabolite production was observed in either of both expression platforms (Figure 2). This led to the assumption that availability of the substrate indole pyruvate may be too limited for efficient product formation. Accordingly, the terrequinone A biosynthesis gene cluster from *A. nidulans* contains the tryptophan aminotransferase encoding gene *tdiD* (Schneider *et al.*, 2007), which is required for indole pyruvate formation from tryptophan. Therefore, *tdiD* was co-expressed with *tdiA* by assembling a pseudo-polycistronic expression construct (*tdiAD*) in which both genes were connected by a self-splicing viral 2A peptide sequence (P2A) (Geib and Brock, 2017). While product formation remained at very low level in *A. oryzae* OP12, *A. niger* ATNT16 transformants carrying this construct produced a large variety of different products. None of these metabolites showed the molecular mass of didemethylasterriquinone, which indicates that cross-chemistry directs the formation of products different from the indolylquinone. Further purification of individual metabolites and structure elucidations will be required to solve the structure of the metabolites formed. However, these analyses indicate that cross-chemistry is likely to occur on different quinone cores in *A. niger*. In addition, formation of indolylquinones appears less well supported in *A. oryzae*.

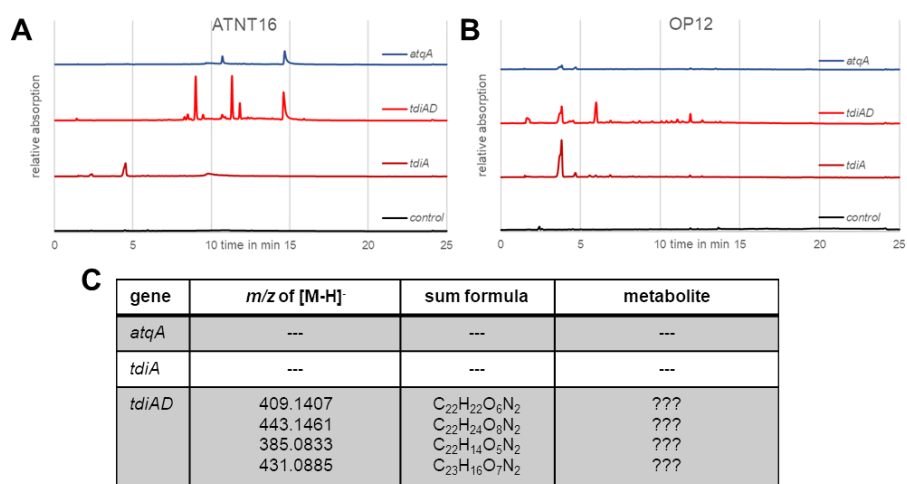


Figure 2:Analyses of culture extracts from heterologous expression of *atqA*, *tdiA* and *tdiAD* in ATNT16 and OP12. (A) HPLC profiles of genes expressed in ATNT16. (B) HPLC profiles of genes expressed in OP12. (C) HR-ESI-MS data.

Bioinformatics prediction of NRPS-like containing gene cluster in *Aspergilli* section *Terrei*

Despite difficulties in obtaining products from NRPS-like enzymes producing bis-indolylquinones, we aimed in the characterisation of NRPS-like enzymes from species from *Aspergillus* section *Terrei*. As the overall number of NRPS-like enzymes in this section is too large to be analysed (Theobald *et al.*, 2018, in preparation), a pre-selection of candidates by bioinformatics analyses was required. In first instance, we only focussed on NRPS-like enzymes containing a putative C-terminal thioesterase rather than a reductase domain. In the next step, we grouped NRPS-like enzymes into families. For this purpose, all NRPS-like enzymes were cross-aligned. Furthermore, besides only using these identity scores, information from the surrounding genes were used to generate a cluster similarity score. Thus, for finally generating the gene families the identity score from the NRPS-like sequences accounted for 75% of the final score, whereas tailoring enzymes contributed by 25% to the score. A community detection algorithm was applied to the network of all enzymes to generate the respective families (Figure 3). Furthermore, besides grouping yet uncharacterised NRPS-like enzymes, other characterised NRPS-like biosynthesis genes and gene clusters as listed in the MIBiG database (Medema *et al.*, 2015) or extracted from primary literature were added. These included biosynthesis gene clusters (BGC) from *A. terreus* for Asp-Melanin (Geib *et al.*, 2016), aspulvinone H (Guo *et al.*, 2013), asterolinone CT5 (Guo *et al.*, 2013) and butyrolactone I (Guo *et al.*, 2013) and the Tdi BGC from *A. nidulans* (Balibar, Howard-Jones and Walsh, 2007).

gene annotation in the sequenced genomes. However, in some cases, sequences appeared either too short or too long, which raised concerns on the correct prediction of the open reading frames. Therefore, such genes were excluded from further analysis in this study. In total 18 new and 6 already characterised (*apvA*, *pgnA*, *mela*, *atqA*, *bytA* and the recently discovered *atrA_{At}* gene that had not been attributed to a family in this study) NRPS-like encoding genes were selected (Table 2). While we hypothesised that enzymes belonging to the same family may produce identical compounds, this assumption was questioned by the fact that *apvA* and *pgnA* were both attributed to family 12, whereby *apvA* had been identified as aspulvinone E synthetase (Guo *et al.*, 2013) and *pgnA* as phenguignardic acid synthetase (Sun, Guo and Wang, 2016).

Table 2: Overview of genes coding for NRPS-like enzymes selected in this study. Bold genes have already been characterised for their corresponding metabolites and were used as reference genes for individual families.

family	genes selected
11	<i>all99</i>
12	<i>apvA</i>, <i>pgnA</i> <i>ala43</i> , <i>all66</i> , <i>neo72</i> , <i>aur68</i> , <i>flo14</i> , <i>flo72</i> , <i>flo91</i>
13	<i>mela</i> <i>ala74</i> , <i>aur18</i> , <i>amb22</i> , <i>flo30</i>
19	<i>all40</i> , <i>neo86</i>
37	<i>all32</i> , <i>amb61</i> , <i>amb92</i> , <i>flo34</i>
114	<i>atqA</i>
596	<i>btyA</i>

As data used in this study derived from *de novo* sequencing of fungal genomes, each gene had received a corresponding protein identification number, which consists of a species abbreviation and a protein identifier from the version of genome annotation. As an example, an NRPS-like enzyme from family 12 has the ID Aspflo1_186314_5 (**Figure 1**Figure 3), which specifies the *Aspergillus floccosus* protein 186314_5 from genome annotation 1. To simplify the gene annotation in this study, the first three letters of the species name combined with the last two numbers of the main protein ID were used. For Aspflo1_186314_5 this results in the simplified protein ID Flo14.

The selected genes were expressed by using the TerR/*PterA* expression system using both, the doxycycline inducible *A. niger* ATNT16 expression platform (Gressler *et al.*, 2015) and the sugar inducible *A. oryzae* OP12 expression platform (Geib *et al.*, 2018, manuscript submitted). Based on the above experiments, we expected a difference in product formation if metabolites produce a quinone core structure.

Heterologous expression of previously characterised NRPS-like enzymes

We first expressed the already characterised genes *apvA*, *pgnA* and *btyA* to confirm their products and to obtain reference standards for yet uncharacterised genes. The *mela* and *atrA_{At}* expressing strains had been generated in previous studies (Geib and Brock, 2017; Geib *et al.*, 2018, manuscript submitted) and were used as a reference for aspulvinone E, atrofuranic acid and atromentin formation. As expected, expression of both, *mela* and *apvA* in ATNT16 and OP12 resulted in aspulvinone E and its UV-convertible isomer isoaspulvinone E (Figure 4). Both isomers had an $m/z = 295.0611$ [M-H]⁻. *BtyA* had been characterised as butyrolactone synthetase by knock-out studies in *A. terreus* (Guo *et al.*, 2013) and by heterologous expression in *A. nidulans* (van Dijk, Guo and Wang, 2016). In agreement, a single compound (Figure 4) with the $m/z = 341.0667$ [M-H]⁻ and a calculated chemical formula of C₁₈H₁₄O₇ was produced in both expression platforms, which is in perfect agreement with the production of butyrolactone IIa. The *pgnA* gene had previously been homologously overexpressed in *A. terreus* (Sun, Guo and Wang, 2016) and heterologously in *Saccharomyces cerevisiae* (Hühner *et al.*, 2018). Despite low product yields the resulting metabolite had been identified as phenguignardic acid. Large quantities of a metabolite were detected from heterologous expression in ATNT16 and OP12 (Figure 4) and a compound with an $m/z = 309.0770$ [M-H]⁻ and a calculated sum formula of C₁₈H₁₄O₅ was identified. These data are also in perfect agreement with phenguignardic acid. Finally, expression of the *atrA_{At}* gene had been performed in both, *A. niger* and *A. oryzae* with the production of atrofuranic acid in *A. niger* and atromentin in *A. oryzae* (Figure 4).

These analyses not only confirmed the correct characterisation of NRPS-like enzymes, but also showed that *A. niger* and *A. oryzae* are suitable expression platforms for a wide variety of metabolites produced from NRPS-like enzymes.

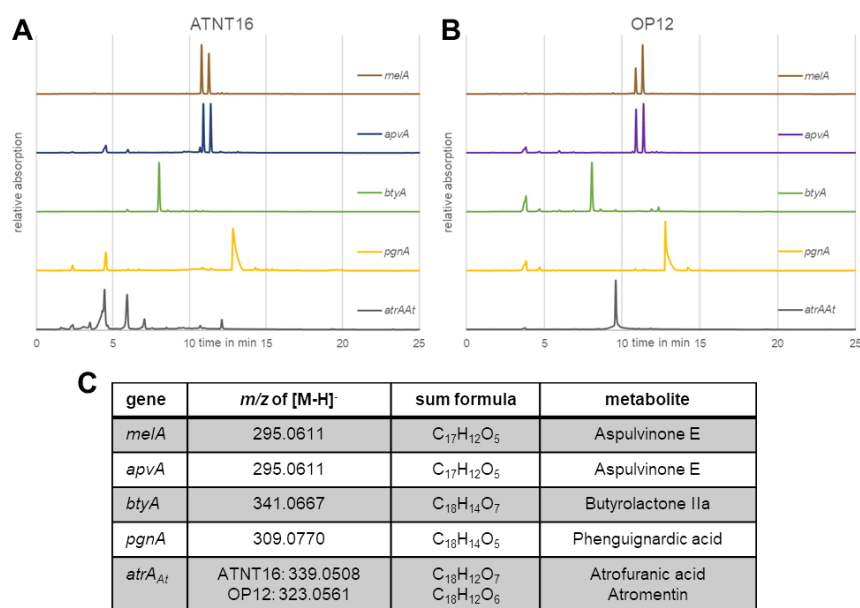


Figure 4: Analyses of products formed in ATNT16 and OP12 from previously characterised NRPS-like enzymes. (A) HPLC profiles of genes expressed in ATNT16. (B) HPLC profiles of genes expressed in OP12. (C) HR-ESI-MS data.

Identification of metabolites produced from yet uncharacterised NRPS-like enzymes

Like the already characterised genes coding for NRPS-like enzymes, we expressed all other selected genes in both expression platforms, checked integration of the complete expression construct by diagnostic PCR and cultivated selected transformants (generally three independent transformants) under inducing conditions and extracted cultures with ethyl acetate for identification of metabolites by analytical HPLC and high-resolution mass spectrometry. In the following sections results were grouped by metabolites rather than gene families as we discovered that the predicted product did not necessarily correlated with the originating family.

Identification of butyrolactone IIa synthetases

The genes *flo34* and *all32* were attributed to family 37, which did not contain a previously characterised family member. Extracts of transformants revealed an individual metabolite peak with identical retention time as observed from *btyA* expression. Furthermore, metabolites from both strains showed identical UV spectra as butyrolactone IIa, which indicates that both members from family 37 characterised here are new butyrolactone IIa synthetases. (Figure 5A). However, butyrolactone IIa appears to be labile under acidic conditions as prolonged incubation in the presence of acidic solvents increased the yield of metabolite, but led to emergence of degradation products.

Aspulvinone E synthetases from family 12

Heterologous expression of *ala43*, *all66* and *neo72* in *A. niger* ATNT16 and *A. oryzae* OP12 revealed the production of aspulvinone E and its UV-interconvertible isomer isoaspulvinone E (Figure 5B). In all transformants from both expression platforms the metabolite peaks matched those of the authentic standards from *mela* and *apvA* expressing strains. As *ala43*, *all66*, *neo72* belong to NRPS-like family 12 and are therefore regarded to be related to *apvA*, this result matched the prediction. However, as *MelA* from family 13 also produces aspulvinone E, but is required for conidia pigmentation by Asp-melanin formation, further studies need to analyse whether a prenyltransferase is encoded in close proximity and acts on products from *Ala43*, *All66*, and *Neo72* as it is the case with aspulvinone E formed by *ApvA*.

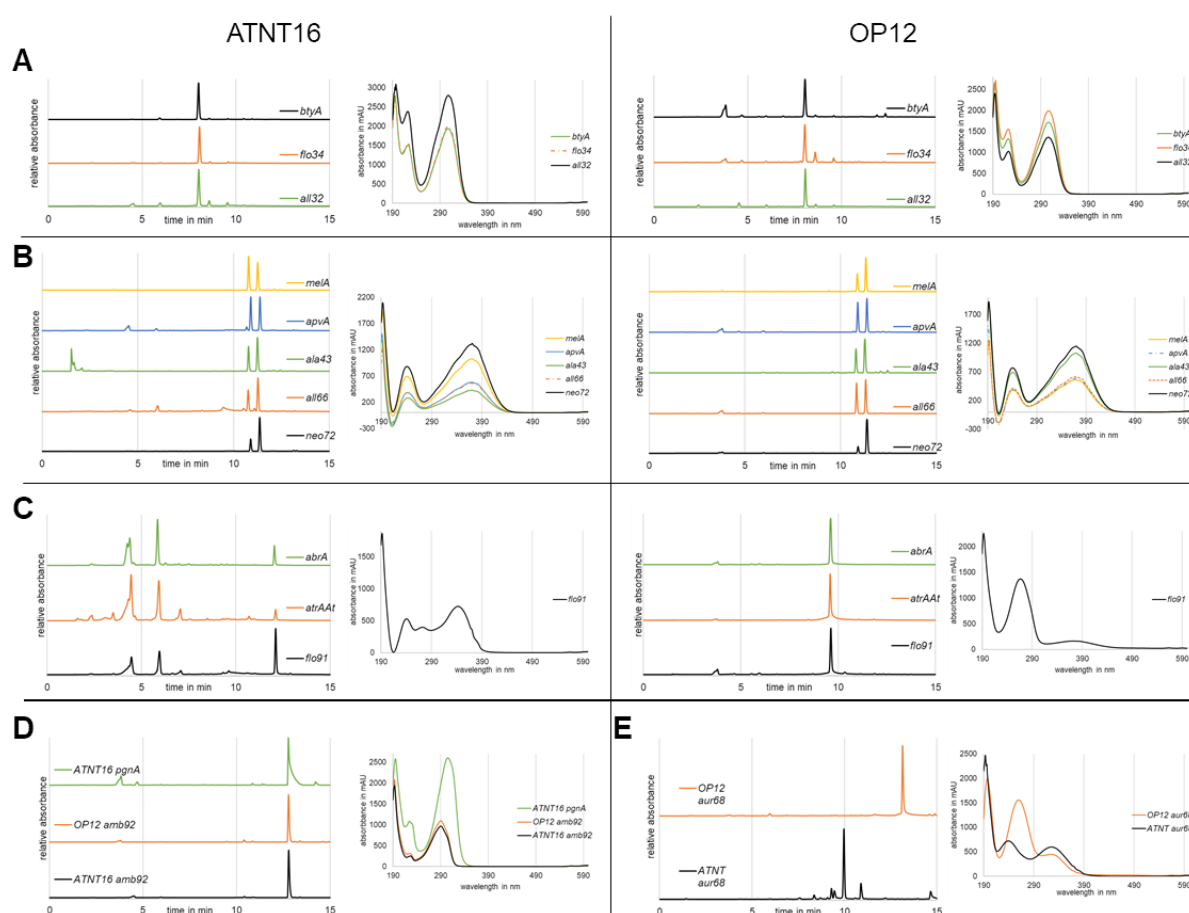


Figure 5: HPLC profiles and UV spectra of the main metabolites from culture extracts of transformants expressing uncharacterised NRPS-like genes from section *Terrei*. Metabolite production in *A. niger* ATNT16 and *A. oryzae* OP12 is shown for all genes. If available, authentic standards from reference strains are included. Reference in (A): butyrolactone IIa. Reference standard in (B): aspulvinone E and isoaspulvinone E. Reference standards in (C): atrofuranic acid from expression of *abrA* or *atrAAI* in *A. niger* or atromentin when expressed in *A. oryzae*. Reference in (D): Phenguignardic acid (note that UV profiles of samples do not match). No reference standard available for (E).

Flo91 is an atromentin synthetase

While some members of family 12 indeed matched the prediction to act as aspulvinone E synthetases, this was not the case for all members attributed to this family. The gene *flo91* from *A. floccosus* did not show the expected two peaks for aspulvinone E and isoaspulvinone E. Furthermore, *flo91* expression resulted in different metabolites depending on the expression platform strain used (Figure 5C). Thereby, OP12 transformants showed a striking purple colour during regeneration on sugar containing agar, whereas ATNT16 transformants secreted a yellow compound when grown in the presence of the expression inducer doxycycline. These characteristics pointed towards the identification of an atromentin synthetase. This was further confirmed by more detailed analysis of the metabolites produced. High resolution electrospray ionisation mass spectrometry (HR-ESI-MS) revealed an $m/z = 323.0562$ [M-H]⁻ resulting in a calculated sum formula of C₁₈H₁₂O₆ for the purple compound extracted from *A. oryzae flo91* cultures, which is in perfect agreement with the reference standards of the atromentin synthetases AbrA and Atr_{At}. Therefore, atromentin was produced in *A. oryzae*. On the contrary, an $m/z = 339.0514$ [M-H]⁻ and a calculated chemical formula of C₁₈H₁₂O₇ was obtained for the yellow compound extracted from *A. niger flo91* cultures, which is in agreement with atrofuranic acid production in *A. niger* as a result of cross-chemistry on atromentin production in this expression host (Geib *et al.*, 2018, manuscript submitted). These results confirmed that Flo91 is an atromentin synthetases and cross-chemistry in *A. niger* occurs independent from the source of the atromentin synthetase heterologously expressed. However, without homologous expression of *flo91* in *A. floccosus* it remains speculative, whether atromentin or atrofuranic acid is produced in the original host. Since Flo91 did not produce aspulvinone E, the prediction of products formed from members of family 12 appears less valid.

The product from Amb92 indicates 4,5-substituted furanone formation in family 37

Heterologous expression of *amb92* from family 37 resulted in transformants with production of the identical metabolite in both expression platform strains (Figure 5D). When a culture extract was subjected to HR-ESI-MS, the dominant metabolite peak showed an $m/z = 309.0769$ [M-H]⁻ with a calculated sum formula of C₁₈H₁₄O₅. A quinone core structure for the Amb92 metabolite appeared unlikely since the same metabolite was produced in both expression platforms and the sum formula did not support a symmetrical molecule structure as typical for quinone-core condensation products of identical α -keto acids. Under the assumption that two identical building blocks are used and the molecule features one of the previously described core structures, two alternative structures are possible: phenguignardic acid and phenylbutyrolactone IIa. The heterologous expression of *pgnA* provided an authentic standard for phenguignardic acid, which elutes at 12.77 min with a tailing end (Figure 4), which is most likely due to phenguignardic acid isomers. The prominent peak obtained from *amb92*

expression showed a similar retention time with 12.79 min but lacked the typical tailing in the HPLC profile (Figure 5D). Furthermore, in HR-ESI-MS-HPLC analyses retention times were significantly different with 8.17 min for phenguignardic acid and 7.41 min for the new metabolite. Finally, the UV profile of the metabolite produced from Amb92 in either ATNT16 or OP12 was similar to, but not identical with phenguignardic acid (Figure 5D). In summary, it is unlikely that Amb92 produces phenguignardic acid. The alternative was phenylbutyrolactone IIa, which has been described in the literature but has only been obtained as a product from the chimeric protein assembly of the A-domain of PgnA and the TE-domain of BtyA, whereby the thiolation domain from either enzyme did not add to specificity of the product formed (van Dijk, Guo and Wang, 2016). The UV spectroscopic measurements were in good agreement with published data. However, due to a characteristic and dominating UV-profile from the phenylpyruvate moieties, an authentic standard is required to discriminate metabolites. Therefore, the UV profile cannot be taken as an unambiguous proof and NMR analyses will be required to confirm the production and structure of phenylbutyrolactone IIa. However, as Amb92 was attributed to family 37 from which the two novel butyrolactone IIa enzymes Flo34 and All32 were identified (Figure 5A), it is well conceivable that Amb92 also produces such a 4,5-substituted furanone core structure. Therefore, these results indicate a consistency in product formation in family 37 and provide a first hint for a naturally occurring phenylbutyrolactone IIa synthetase.

Aur68 produces an unexpected metabolite

Expression of *aur68* from family 12 in *A. oryzae* OP12 resulted in pink culture extracts and HPLC analysis revealed a single metabolite with a retention time of 13.15 min. In contrast, when *aur68* was expressed in *A. niger* ATNT16 extracts showed a yellow colouration and one major metabolite at a retention time of 9.97 min accompanied by some minor metabolite peaks were detected. Additionally, the UV absorption profiles of the major metabolites from *A. oryzae* and *A. niger* significantly differed, which confirmed that different compounds were formed in the two expression platform strains (Figure 5E). This result pointed towards a quinone core structure of the metabolite when produced in *A. oryzae*, which undergoes cross-chemistry in *A. niger*. HR-ESI-MS measurement of the OP12 *aur68* extract revealed an $m/z = 291.0664$ [M-H]⁻ with a calculated sum formula of C₁₈H₁₂O₄. Considering these data, polyporic acid can be assumed as a product from *aur68* in *A. oryzae*. This condensation product of two phenylpyruvate molecules features a quinone core moiety and is known as mycotoxin of basidiomycetes. The lighter colour of the phenylpyruvate-derived polyporic acid (pink) compared to the *p*-hydroxyphenylpyruvate-derived atromentin (purple) is in agreement with the lack of the hydroxyl group at the aromatic moieties, which exhibit an -I- and +M-effect and thus, lead to a bathochromic colour shift in atromentin. Only minor traces of polyporic acid were detected from *aur68* expression in *A. niger* and the major metabolite from ATNT16

showed an $m/z = 309.0771$ $[M-H]^-$ and a calculated sum formula of $C_{18}H_{12}O_5$. As mentioned, this metabolite most likely results from cross-chemistry events taking place at NRPS-like enzymes in the chemical environment of *A. niger* cells. A literature search did not result in the identification of a natural product with a plausible structure, which indicates the production of a novel secondary metabolite from cross-chemistry effects. Whether the resulting structure is similar to atrofuranic acid, which is the cross-chemistry product from expression of atromentin synthetases in *A. niger*, requires further investigation. However, our results provide evidence that Aur68 from NRPS-like family 12 does not depict an aspulvinone E synthetase rather than a polyporic acid synthetase, which would describe the first characterised NRPS-like enzyme producing this metabolite.

NRPS-like enzymes without metabolite production

Heterologous expression of some of the selected genes did not result in any detectable secondary metabolite. This was true for the two selected members from family 19, which are *all40* and *neo86* and for the single selected member from family 11, namely *all99*. However, also *flo14* and *flo72* from family 12 and *amb61* from family 37 did not produce any detectable metabolite (data not shown). This could be due to several reasons: (i) enzymes that never gained or lost their function, (ii) lack of sufficient substrate, as observed for *atqA* or *tdiA* expression in the absence of *tdiD* or (iii) metabolites were not extracted or detected by the selected methods (HPLC coupled to a diode array detector).

At least for Flo72 the first option appears likely. The annotated *flo72* gene was notably shorter than expected. Indeed, no continuous open reading frame (ORF) was detected and the enzyme had been annotated as two partial proteins whereby the A-domain counted as an individual protein. As an incorrect annotation could not be excluded, we handled the entire sequence as one protein and expressed it as such. However, since no metabolite was detected it is possible that the gene is indeed separated into two ORFs, which would require an additional promoter or a fusion by introducing a P2A peptide sequence to produce functional proteins. However, it is also likely that *flo72* results from an unsuccessful recombination event of two NRPS-like coding genes and resembles genetic junk. The latter may also be true for Flo14, as all other proteins from family 12 produced a metabolite. In this respect it needs to be mentioned that whole genome analyses revealed an extremely large number of secondary metabolite biosynthesis genes in *A. floccosus* (Theobald *et al.*, 2018, in preparation) and our analyses indicate that not all genes may produce functional proteins.

While other members of family 37 produced 4,5-substituted furanone core structures, a lack of function for Amb61 is very likely when analysing the active site of the thioesterase domain. The activity of thioesterase domains from NRSP-like enzymes requires an intact Gx(S/C)xG motif. Alignments of all heterologously produced NRPS-like enzymes revealed that Amb61

carries a mutation at this position. Instead of serine or cysteine, Amb61 contains an alanine at position 726 (Figure 8). It will be interesting to see, whether a site directed mutagenesis allows restoring the activity of this enzyme.

Finally, for members of family 11 and 19 no other enzyme had previously been characterised. Interestingly, All40 and Neo86 showed several sequence stretches when aligned to other NRPS-like enzymes (Figure 8). This could indicate the use of unusual bulkier substrates, which might not be available in a heterologous host. The reason for a lack of product formation for *all99* from family 11 remains unclear.

Discussion

Analyses in this study clearly visualised the difficulties in attributing NRPS-like enzymes to specific families without a broader knowledge on the metabolites produced by individual members of the families. This becomes easily visible when a new version of the NRPS-like enzyme network plot with all identified products is considered (Figure 6). However, the inclusion of biosynthesis gene cluster information in family predictions supported the identification of aspulvinone E synthetases possibly involved in Asp-melanin biosynthesis in section *Terrei*. All genes attributed to family 13 were shown in a previous study to produce aspulvinone E, indicating that Asp-melanin is a typical feature of species from section *Terrei* (Theobald *et al.*, 2018, in preparation). In contrast, the large family 12 contained a very diverse set of different NRPS-like enzymes, indicating that the prediction in this family was less reliable (see Table 3 for a summary of metabolites identified in this study).

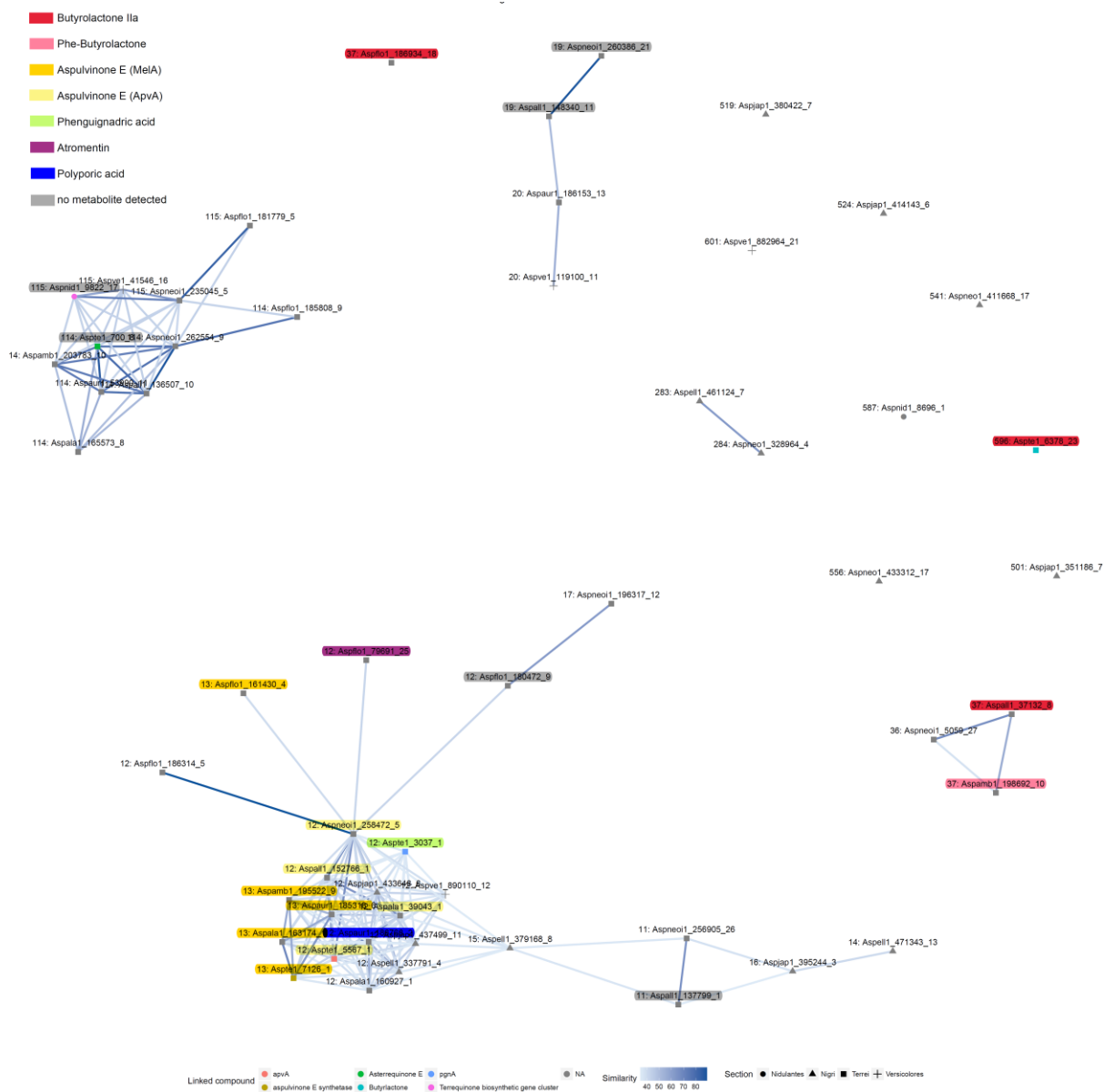


Figure 6: Similarity plot of NRPS-like containing gene cluster families with identified metabolites from this study. Phe-Butyrolactone – phenylbutyrolactone IIa.

Therefore, we generated a phylogenetic tree that based on sequence information of NRPS-like proteins and compared trees generated from full-length proteins and from the thioesterase domains only. Thereby, we included all genes from this study and NRPS-like enzymes for which the product had already been characterised (Figure 7). With the knowledge on metabolites produced, these trees indeed reliably grouped enzymes from different species that produced the same metabolite, but only when the producing organism derived from the same genus. The atromentin synthetases InvA5, AtrA and GreA from basidiomycetes formed an individual group that was only very distantly related with atromentin synthetases from *Aspergillus* species. This agrees with our previous approach in which the generation of a hybrid

between *A. terreus* MelA and *Paxillus involutus* InvA5 failed to produce a functional protein, whereas the fusion between MelA and AtrA_{At} from *A. terreus* was successful (Geib *et al.*, 2018, manuscript submitted). However, within a genus, the tree nicely reflected the products formed.

Table 3: Identified metabolites from NRPS-like enzymes. * Confirmation of metabolite structure by NMR still pending. Family 13 was investigated in a previous study (Theobald *et al.*, 2018, in preparation).

family	gene	product
11	<i>all99</i>	-----
12	<i>apvA</i>	Aspulvinone E
	<i>all66</i>	Aspulvinone E
	<i>neo72</i>	Aspulvinone E
	<i>ala43</i>	Aspulvinone E
	<i>aur68</i>	Polyporic acid *
	<i>pgnA</i>	Phenguignardic acid
	<i>flo14</i>	-----
	<i>flo72</i>	-----
	<i>flo91</i>	Atromentin
13	<i>mela</i>	Aspulvinone E
	<i>ala74</i>	Aspulvinone E
	<i>aur18</i>	Aspulvinone E
	<i>amb22</i>	Aspulvinone E
	<i>flo30</i>	Aspulvinone E
19	<i>all40</i>	-----
	<i>neo86</i>	-----
37	<i>all32</i>	Butyrolactone IIa
	<i>amb61</i>	-----
	<i>amb92</i>	Phenylbutyrolactone IIa *
	<i>flo34</i>	Butyrolactone IIa
596	<i>btyA</i>	Butyrolactone IIa
114	<i>atqA</i>	-----

Within the cluster of atromentin synthetases from *Aspergillus* species the putative polyporic acid synthetase was located, which agrees with the formation of a benzoquinone core structure in atromentin and polyporic acid. However, as both products require a different substrate, the polyporic acid synthetase showed some phylogenetic distance. The discovery of polyporic acid production is of special interest, as this metabolite was previously only found in basidiomycetes, where it can make up a significant proportion of the dry weight of fruiting bodies and has been characterised as an inhibitor of the dihydroorotate dehydrogenase (Stahlschmidt, 1877; Kraft *et al.*, 1998). This study shows that besides atromentin synthetases, which were discovered first in basidiomycetes, also polyporic acid synthetases are found in

ascomycetes. However, as no sequence of a polyporic acid synthetase from basidiomycetes has been described yet, a phylogenetic relationship between enzymes from basidio- and ascomycetes cannot be determined.

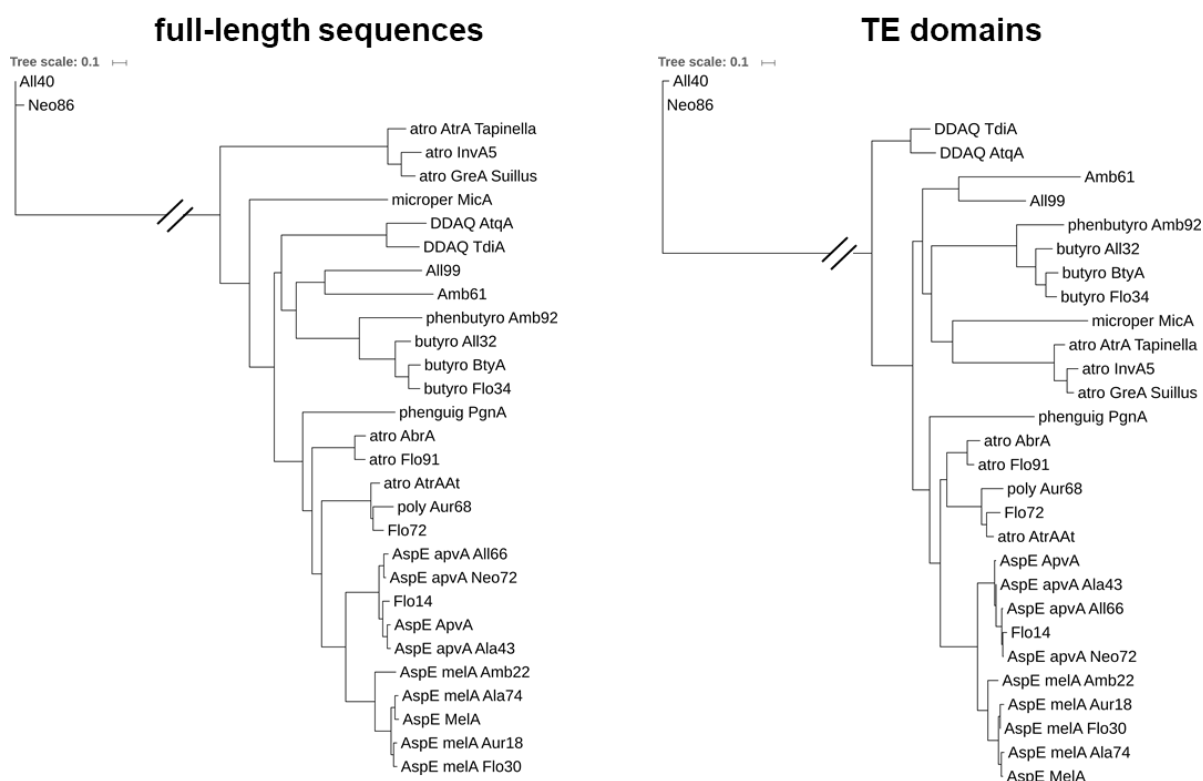


Figure 7: Phylogenetic tree of characterised NRPS-like enzymes. (A) The complete sequence or (B) the sequence of the thioesterase domains was used to create phylogenetic trees with IQ-TREE (Nguyen *et al.*, 2015). Identified products are given in abbreviated form: atro – atromentin, microper – micorperfuranone, DDAQ – didemethylasterriquinone D, phenbutyro-phenylbutyrolactone IIa, butyro – butyrolactone IIa, poly – polyporic acid, AspE – (iso)aspulvinone E.

The dioxolanone producing phenguignardic acid synthetase PgnA (Sun, Guo and Wang, 2016) was only distantly related with the family of quinone and 3,5-substituted furanone synthetases, which is in agreement with a different chemistry in dioxolanone biosynthesis compared to that from quinone or furanone formation. However, it will be interesting to compare the phylogenetic relationship of PgnA with the enzyme from *Guignardia bidwellii* that produces phenguignardic acid (Molitor *et al.*, 2012). At current, this is not possible as neither the gene nor the genome sequence of this fungus has been published.

All aspulvinone E synthetases showed a close phylogenetic relationship but were clearly discriminated between members belonging either to the ApvA or MelA family. Neo72, All66 and Ala43 all produced aspulvinone E and grouped with ApvA. The close phylogenetic relationship of Flo14 indicates that this enzyme might be expected to produce aspulvinone E, but it seems to have lost its function. Flo30, Aur18 and Ala74 are closely related to MelA and assumed to be involved in the production of Asp-melanin in their originating species (Theobald

et al., 2018, in preparation). Interestingly, the enzyme Amb22 from *A. ambiguus* is more distantly related to MelA. *A. ambiguus* additionally contains a naphthopyrone synthase required for dihydroxynaphthalene melanin biosynthesis and it cannot be excluded that a mixture of Asp- and DHN-melanin is formed in this species (Theobald *et al.*, 2018, in preparation).

Another group was formed by the butyrolactone forming enzymes. The putative phenylbutyrolactone IIa synthetase Amb92 grouped with the butyrolactone IIa producing enzymes All32, BtyA and Flo34, but with a larger phylogenetic distance. In this respect, the previous attribution to specific families placed BtyA as a sole member in family 596, whereas the other three enzymes were grouped in family 37. This different grouping is not justified from the results obtained in this study. Most strikingly, while a synthetic version of a phenylbutyrolactone IIa synthetase had been generated by fusion of the BtyA thioesterase domain with the adenylation and thiolation domains of PgnA (van Dijk, Guo and Wang, 2016), the characterisation of Amb92 is the first report on a natural occurring phenylbutyrolactone IIa synthetase. This provides further hints that recombination events of individual NRPS-like coding genes can easily lead to NRPS-like enzymes with new substrate spectrum or producing different connecting core structures.

Amb61 and All 99 as well as All40 and Neo86 formed individual groups. However, no metabolites were detected for any of these enzymes. At least for Amb61 this seems due to the mutation of an active site cysteine or serine residue into an alanine (Figure 8). Reactivation studies by site-directed mutagenesis might provide further details on the product initially formed by this enzyme. For All40 and Neo86, we assume that a bulkier substrate may be accepted by these enzymes, which is absent or limited from the heterologous production strains. This is supported by sequence stretches between all three domains that may provide more space for a bulkier substrate than required for the standard aromatic α -keto acids (Figure 8). Examination of surrounding genes might give further insights into the respective building blocks as enzymes required for their synthesis might be encoded in close proximity.

Finally, TdiA and AtqA formed an individual group. Both are assumed to produce didemethylasterriquinone D (DDAQ D), which requires indole pyruvate as substrate. This can be assumed to require a different structure of all domains compared to *p*-hydroxyphenylpyruvate or phenylpyruvate accepting enzymes. However, their distinction from other groups was more pronounced in the tree generated from thioesterase domains. Unfortunately, no product was obtained from heterologous expression of *atqA* in either ATNT16 or OP12. Similarly, when *tdiA* was expressed without *tdiD*, no product was formed. This indicates a substrate limitation in the expression hosts. However, while the *tdiAD* expression in *A. niger* resulted in the formation of several products that are most likely a result from cross-chemistry directing the formation of a compound different to the assumed product DDAQ D, no significant product formation was obtained from *A. oryzae* OP12 in this co-

expression approach. In this respect, it should be mentioned that the assumed product DDAQ D has never been produced from a heterologous expression approach. AtqA had been characterised from knock-out studies in *A. terreus*, in which the production of asterriquinone CT5 had been abolished (Guo *et al.*, 2013). Furthermore, in a recent manuscript on the heterologous production of NRPS-like enzymes from *A. terreus* in *S. cerevisiae* (Hühner *et al.*, 2018), no result or approach on *atqA* expression had been mentioned. This indicates that production of AtqA was either not approached or failed. Therefore, additional efforts are required to investigate enzymes that utilise indole pyruvate as substrate.

Phylogenetic analysis within the *Aspergillus* species provided a good indication, which type of core structure is formed. However, sequence variations among enzymes from basidio- and ascomycetes were too large to cluster on the basis of the products formed. Furthermore, the sequence patterns proposed by Braesel *et al.* (Braesel *et al.*, 2015) was not sufficient to reliably predict the core structures formed by NRPS-like enzymes from asco- and basidiomycetes. However, a closer examination of the sequence alignment used to generate the phylogenetic tree revealed a single amino acid at Position 671 in respect to *A. terreus* MelA which may be a suitable addition to predict a sequence pattern (Figure 8 – green box).

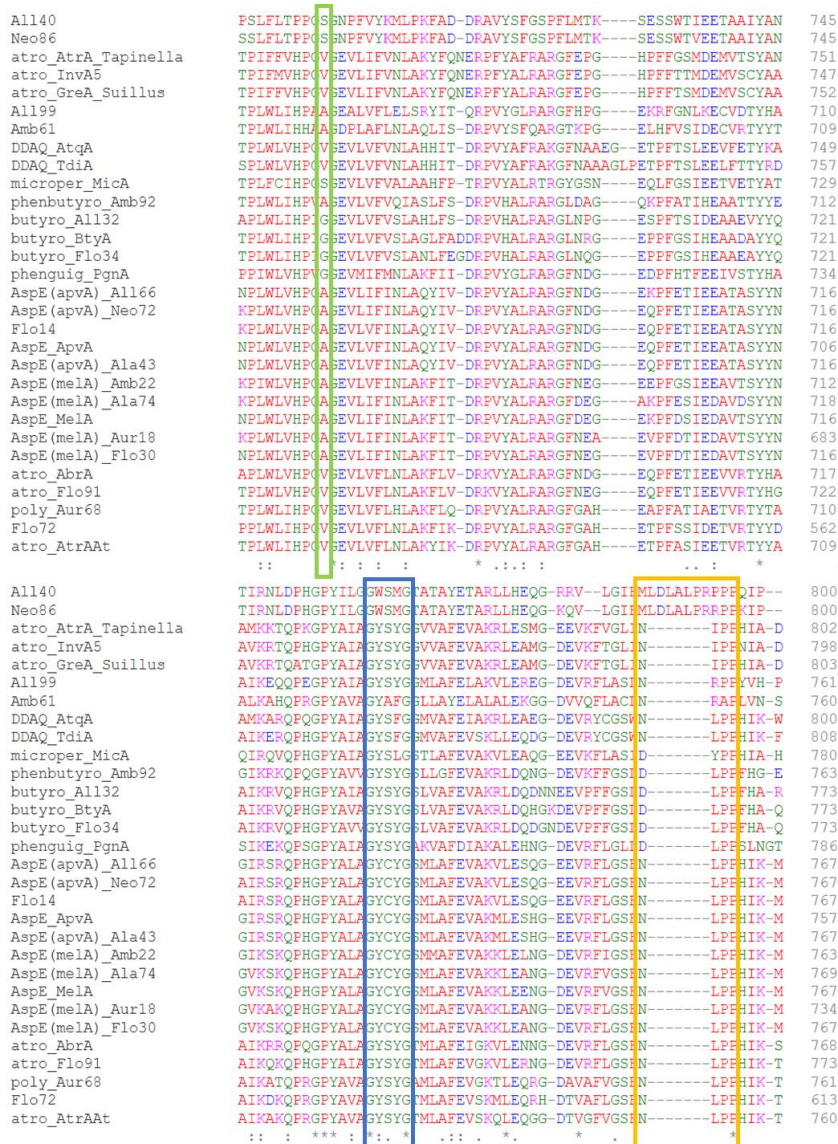


Figure 8: Alignment of all characterised NRPS-like enzymes from this study and known from literature. A section from the thioesterase domain is shown. Green box –fingerprint amino acid for core formation as proposed in this study. Blue box – Catalytic motif of thioesterase domain. Orange box – Fingerprint motif for core formation as proposed by Braesel et al. (Braesel *et al.*, 2015).

Although a single amino acid is unlikely to be sufficient to direct the massive changes required in the chemistry of the thioesterase domains, consistency was found between enzymes from basidio- and ascomycetes. NRPS-like enzymes catalysing the formation of quinones always displayed a valine at the indicated position. Furanones can be subdivided by their substitution pattern, whereby NRPS-like enzymes forming 3,5-substituted furanones display an alanine, whereas 3,4-substituted furanones possess a serine. The discrimination of 4,5-substituted furanone and dioxolanone forming enzymes is not possible, since both show a glycine at this position, which might reflect an identical first step of product dimerization that is followed by a ring closure involving a different position in the thioesterase domain. The only exception from these rules derives from phenylbutyrolactone IIa-forming (a 4,5-substituted furanone)

Amb92 protein. This particular enzyme has an alanine at the indicated position and should thereby produce a 3,5-substituted furanone (Figure 9). However, as the confirmation of the structure of the metabolite from Amb92 is still pending a final conclusion cannot be drawn. Furthermore, the number of NRPS-like enzymes from ascomycetes outside the genus *Aspergillus* and especially from basidiomycetes is currently too small to validate this enzyme position for its predictive power. Therefore, additional studies are needed to support bioinformatics predictions to a level of the Stachelhaus code that is suitable to predict substrates accepted by A-domains from non-ribosomal peptide synthetases (Stachelhaus, Mootz and Marahiel, 1999).

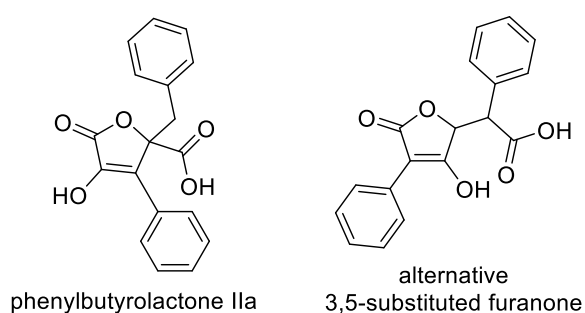


Figure 9: Alternative products possibly formed by Amb92.

In summary, this study confirmed a great variety of NRPS-like enzymes in species from section *Terrei*. As only a selection of genes had been analysed in this study, it is likely that other previously unknown metabolites can be detected. Thereby, especially the cross-chemistry occurring in *A. niger* on quinone-forming enzymes may significantly enhance the portfolio of metabolites. One promising candidate for a novel product is the metabolite produced in *A. niger* during the expression of the polyporic acid synthetase Aur68, but also metabolites produced in *A. niger* from *tdiAD* expression pend further investigation. The discovery of polyporic acid from *Aspergillus aureoterreus* (Aur68) additionally provides an example that products of NRPS-like enzymes known from basidiomycetes are likely to be present also in ascomycetes. However, from a phylogenetic point of view, enzymes may have evolved independent as atromentin synthetases from asco- and basidiomycetes did not cluster in the phylogenetic tree. This observation also shows that prediction of product formation from sequence alignments outside from genus borders may have limited success. More efforts will be needed to identify sequence patterns within individual thioesterase domains that are responsible for a specific chemistry within these domains.

Material and Methods

Cultivation of fungal strains

All strains and transformants used in this study (Table 4) were routinely cultivated at 28 °C. Conidia were generated on slopes of AMM(-N)G50Gln10 medium (Table 7) solidified with 2% agar. After 4 to 7 days cultures were overlaid PBS + 0.01% Tween 20 and conidia were scraped with sterile cotton swap. Resulting conidia suspensions were used for inoculation of liquid cultures. For protoplast formation or preparation of genomic DNA (gDNA), fungi were grown in liquid YEPD medium on an orbital shaker at 150 rpm.

Table 4: Strains used in this study.

Relevant genotype in ATNT16 Δ <i>pyrG</i>	(Geib and Brock, 2017)	Relevant genotype in OP12 <i>pyrG</i> ⁻	(Geib <i>et al.</i> , 2018, manuscript submitted)
<i>PterA: all99:TtrpC_URA</i>	This study	<i>PterA: all99:TtrpC_URA</i>	This study
<i>PterA: apvA:TtrpC_URA</i>	This study	<i>PterA: apvA:TtrpC_URA</i>	This study
<i>PterA: all66:TtrpC_URA</i>	This study	<i>PterA: all66:TtrpC_URA</i>	This study
<i>PterA: neo72:TtrpC_URA</i>	This study	<i>PterA: neo72:TtrpC_URA</i>	This study
<i>PterA: ala43:TtrpC_URA</i>	This study	<i>PterA: ala43:TtrpC_URA</i>	This study
<i>PterA: aur68:TtrpC_URA</i>	This study	<i>PterA: aur68:TtrpC_URA</i>	This study
<i>PterA: pgnA:TtrpC_URA</i>	This study	<i>PterA: pgnA:TtrpC_URA</i>	This study
<i>PterA: flo14:TtrpC_URA</i>	This study	<i>PterA: flo14:TtrpC_URA</i>	This study
<i>PterA: flo72:TtrpC_URA</i>	This study	<i>PterA: flo72:TtrpC_URA</i>	This study
<i>PterA: flo91:TtrpC_URA</i>	This study	<i>PterA: flo91:TtrpC_URA</i>	This study
<i>PterA: all40:TtrpC_URA</i>	This study	<i>PterA: all40:TtrpC_URA</i>	This study
<i>PterA: neo86:TtrpC_URA</i>	This study	<i>PterA: neo86:TtrpC_URA</i>	This study
<i>PterA: all32:TtrpC_URA</i>	This study	<i>PterA: all32:TtrpC_URA</i>	This study
<i>PterA: amb61:TtrpC_URA</i>	This study	<i>PterA: amb61:TtrpC_URA</i>	This study
<i>PterA: amb92:TtrpC_URA</i>	This study	<i>PterA: amb92:TtrpC_URA</i>	This study
<i>PterA: flo34:TtrpC_URA</i>	This study	<i>PterA: flo34:TtrpC_URA</i>	This study
<i>PterA: btyA:TtrpC_URA</i>	This study	<i>PterA: btyA:TtrpC_URA</i>	This study
<i>PterA: atqA:TtrpC_URA</i>	This study	<i>PterA: atqA:TtrpC_URA</i>	This study
<i>PterA: tdiA:TtrpC_URA</i>	This study	<i>PterA: tdiA:TtrpC_URA</i>	This study
<i>PterA: tdiA:P2A:tdiD:TtrpC_URA</i>	This study	<i>PterA: tdiA:P2A:tdiD:TtrpC_URA</i>	This study
<i>PterA: atrA_{At}:TtrpC_URA</i>	(Geib <i>et al.</i> , 2018, manuscript submitted)	<i>PterA: atrA_{At}:TtrpC_URA</i>	(Geib <i>et al.</i> , 2018, manuscript submitted)
<i>PterA: melA:TtrpC_URA</i>	(Geib and Brock, 2017)		

Generation of heterologous expression strains

Expression constructs were assembled using the *Nco*I digested SM-Xpress_URA vector as a backbone for introducing genes of interest (Geib *et al.*, 2018, manuscript submitted). Individual NRPS-like genes were amplified from genomic DNA from the respective donor strains using Phusion High-Fidelity DNA polymerase (ThermoFisher Scientific) and oligonucleotides (see Table 5) carrying a 15 bp overlap to the plasmid. See Table 6 for oligonucleotide sequences. For the *tdiAD* expression plasmid, the two genes *tdiA* and *tdiD* were individually amplified from gDNA of *A. nidulans* FGSC A4 whereby the sequence for the self-splicing peptide P2A was introduced as overlapping sequence at the *tdiA* reverse and the *tdiD* forward primer. All PCRs were carried out in a SpeedCycler² (Analytik Jena). After purification from agarose gels using the Monarch DNA gel extraction kit (NEB), amplicons and vector backbone were combined with the reaction mixture from the In-Fusion HD cloning kit (Takara/Clontech). After incubation for 20 min at 50°C, competent *Escherichia coli* DH5 α (Mix&Go! buffer kit, Zymo Research) were transformed with aliquots of the *in vitro* assemblies of the expression plasmids. Plasmids were isolated using NucleoSpin Plasmid miniprep kit (Macherey-Nagel) and used for fungal transformation as described previously (Geib and Brock, 2017). In brief, for protoplast generation mycelium from the recipient *A. niger* strain ATNT16 Δ *pyrG* and the *A. oryzae* OP12 *pyrG*⁻ strain was harvested from 24 to 30 h cultures in YEPD medium (Table 7) supplemented with 7.5 mM uridine. Mycelium was washed and soaked in 0.1 M citrate-phosphate buffer pH 7.3 with 10 mM dithiothreitol and incubated for 1 h to reduce cell-wall proteins. The buffer was exchanged with osmotic solution containing 1.3 g VinoTaste Pro (Novozymes) and 0.1 g lysing enzyme from *Trichoderma harzianum* (Sigma-Aldrich). Protoplasts were harvested over sterile Miracloth filter gauze (Merck-Millipore), washed, mixed with the respective plasmid and PEG solution (25% PEG8000, 50 mM CaCl₂, 10 mM Tris/HCl pH 7.5) and incubated for 30 min on ice. Different aliquot sizes were mixed with liquid top agar and transformants were selected and regenerated on uridine-free AMM(-N)G50Gln10S1.2 (Table 7) with 2% agar.

Table 5: Overview of PCRs for cloning of NRPS-like genes.

template	identifier	P#	size [bp]
<i>A. alabamensis</i>	<i>ala43</i>	1+2	2809
<i>A. allahabadii</i>	<i>all66</i>	1+3	2809
<i>A. allahabadii</i>	<i>all32</i>	18+19	2824
<i>A. allahabadii</i>	<i>all40</i>	20+21	3002
<i>A. neoindicus</i>	<i>neo72</i>	1+11	2809
<i>A. neoindicus</i>	<i>neo86</i>	22+23	3004
<i>A. aureoterreus</i>	<i>aur68</i>	4+5	2797
<i>A. ambiguus</i>	<i>amb61</i>	14+15	2785
<i>A. ambiguus</i>	<i>amb92</i>	16+17	2794
<i>A. terreus</i>	<i>apvA</i>	24+2	2810
<i>A. terreus</i>	<i>pgnA</i>	25+26	2872
<i>A. terreus</i>	<i>btyA</i>	27+28	2945
<i>A. terreus</i>	<i>atqA</i>	29+30	2920
<i>A. floccosus</i>	<i>flo14</i>	1+6	2809
<i>A. floccosus</i>	<i>flo72</i>	7+8	2793
<i>A. floccosus</i>	<i>flo91</i>	9+10	2827
<i>A. floccosus</i>	<i>flo34</i>	12+13	2824
<i>A. allahabadii</i>	<i>all99</i>	31+32	2788
<i>A. nidulans</i>	<i>tdiA</i>	34+33	2942
<i>A. nidulans</i>	<i>tdiA_P2A</i>	34+35	2963
<i>A. nidulans</i>	<i>P2A_tdiD</i>	36+37	1731

Table 6: Oligonucleotide sequences used in this study.

P#	sequence
1	CATCACCATCACCATGGAACCTTGAACAACCTACAGGCAC
2	CTGCTGTTATCCATGGTCACATTCCTCGCTCATCCAG
3	CTGCTGTTATCCATGGTCACATGCCTCGATCATCCAG
4	CATCACCATCACCATGGATCTTTCAAGAACCTCCAACATC
5	CTGTTATCCATGGCTACACCCCCGTGCATCCAG
6	CTGCTGTTATCCATGGTCACATCCCTCGATCATCCAG
7	catcaccatcaccatggactttcaagaacctccaacagc
8	CTGCTGTTATCCATGGCTAAATCCCCCGTGCTTCC
9	CATCACCATCACCATGGATCATTCGCCAATCTTACCGTC
10	CTGCTGTTATCCATGGTCAAATCCCCCTTGCATCTAG
11	CTGCTGTTATCCATGGTCACATGCCTCGATCATCCAAC
12	CATCACCATCACCATGGAACCAAACTCATTGATCGATctc
13	CTGCTGTTATCCATGGTTACACCCCCGAGCAGC
14	CATCACCATCACCATGGAACGTTGCAAATCTTGTCGATctc
15	CTGCTGTTATCCATGGTTAAAGCCCTCGTGCGATTAATG
16	CATCACCATCACCATGGACATCACCTCACCTATCTCCTG
17	CTGCTGTTATCCATGGTTATACTCCCCGTGCAGCC
18	CATCACCATCACCATGGAACCAAACTCATTGACAGATATCC
19	CTGCTGTTATCCATGGTTACAACCCCCGTCCGTGC
20	CATCACCATCACCATGGAATGTCCCCATCGAACTACATG
21	CTGCTGTTATCCATGGTTAACTTGAACCGTTGGATTTGAG
22	CATCACCATCACCATGGAATGACCCCCATTGAACTACATG
23	CTGCTGTTATCCATGGTTATATTGAACCGTTCTGACTTGAG
24	catcaccatcaccatggaacttgaacaacctacaggcac
25	catcaccatcaccatgaaataagaagctcaagctttctctatg
26	ctgctgttatccatggtagattccacggtcattcagc
27	catcaccatcaccatggaacaaaattgattgattaacctcc
28	ctgctgttatccatggtagagatagagagagacag
29	catcaccatcaccatggaactcgcacggagatcctc
30	ctgctgttatccatggctacaccctcgctccc
31	CATCACCATCACCATGGAGGACCAAAATCAATCAGAGACC
32	CTGCTGTTATCCATGGCTATAATGCTCTGTCTGGATAGTG
33	CTGCTGTTATCCATGGCTACAGGCCCCCGTCCC
34	tcaccatcaccatggagcaccaagcaagaccgagatc
35	cggcttgctcaggaggetgaaattgtagcgcgctgccaggccccgctcctcag
36	tctgaagcaagccggatgtggaggaaaacctggcctatgggctcaataggggcc
37	actgctgttatccatggtagaatggcaagcacatcg
38	cctccaagagatccagac
39	gaattttaccagtggcctagg

gDNA extraction and diagnostic PCR

Genomic DNA was isolated from selected transformants using a modified version of a protocol by Dellaporta *et al.* (Dellaporta, Wood and Hicks, 1983). In brief, frozen mycelium was powdered under liquid nitrogen and incubated in extraction buffer (100 mM Tris/HCl, pH 8, 50 mM EDTA, pH 8, 500 mM NaCl, 1% SDS) containing 2 µl RNase (10 mg/ml, Sigma Aldrich) at 65 °C. Cell debris and proteins were precipitated with potassium acetate (5 M) and removed by centrifugation. DNA was precipitated from supernatant with isopropanol, solved in TE buffer with ammonium acetate and precipitated a second time with isopropanol. The DNA pellet was washed with 70% ethanol. Finally, DNA was dissolved in TE buffer (50 mM Tris/HCl pH 8, 1 mM EDTA) and a dilution was used as template for PCR.

To confirm the genomic integration of the NRPS-like genes, the complete expression cassette was amplified using primer P38+P39 using Phire Hot Start II DNA polymerase (ThermoFisher Scientific) (Table 6).

Secondary metabolite extraction and HPLC analysis

Positive transformants from the ATNT16 strain were grown in AMM(-N)G50Gln10 (Table 7) supplemented with 10 µg/ml doxycycline for 36 to 48 h at 150 rpm. OP12 transformants were cultivated in AMM(-N)Starch2%Gln20 medium (Table 7) for 30 to 44 h at 150 rpm. Culture filtrate and mycelium was separated by filtration over Miracloth and extracted separately with ethyl acetate. The organic layer was collected, dried over anhydrous sodium sulphate and the solvent removed under reduced pressure. Residues were solved in methanol and used for HPLC analysis as mentioned previously (Geib and Brock, 2017). Selected extracts were analysed by high-resolution-electrospray ionisation-HPLC as described (Geib *et al.*, 2016).

Phylogenetic analysis

To construct phylogenetic trees, either full-length protein sequences or thioesterase domain sequences were used. For identification of individual domains protein sequences were analysed by InterPro (Finn *et al.*, 2017) and sequences for the alpha/beta hydrolase fold (SSF53474) were extracted as thioesterase sequences. Sequence alignments were assembled using Clustal Omega (Sievers and Higgins, 2018) and were used as basis for tree calculations with IQ-Tree. In this programme, the optimal tree building algorithm is identified before the actual tree is calculated, which ensures application of the model that results in the highest likelihood. The results were plotted by using iTOL (Letunic and Bork, 2016).

Table 7: Media used in this study.

Minimal media	
AMM(-N)	0.52 g/l KCl, 0.52 g/l MgSO ₄ × 7 H ₂ O, 1.52 g/l KH ₂ PO ₄ ; 1 ml/l 1000 × Hutner's trace elements; pH adjusted to 6.5
G50Gln10	50 mM glucose and 10 mM glutamine
G50Gln10S1.2	50 mM glucose, 10 mM glutamine and 1.2 M sorbitol
Starch2%Gln20	2% soluble starch and 20 mM glutamine
Complex media	
YEPD	20 g/l peptone, 10 g/l yeast extract, 5 g/l glucose

References

- Alvi, K.A., Pu, H., Luche, M., Rice, A., App, H., McMahon, G., Dare, H., and Margolis, B. (1999). Asterriquinones produced by *Aspergillus candidus* inhibit binding of the Grb-2 adapter to phosphorylated EGF receptor tyrosine kinase. *J. Antibiot.* 52, 215-23
- Balajee, S.A., Baddley, J.W., Peterson, S.W., Nickle, D., Varga, J., Boey, A., Lass-Flörl, C., Frisvad, J.C., Samson, R.A., and ISHAM Working Group on *A. terreus* (2009). *Aspergillus alabamensis*, a new clinically relevant species in the section *Terrei*. *Eukaryot. Cell* 8, 713-22
- Balibar, C.J., Howard-Jones, A.R., and Walsh, C.T. (2007). Terrequinone A biosynthesis through L-tryptophan oxidation, dimerization and bisprenylation. *Nat. Chem. Biol.* 3, 584-92
- Braesel, J., Götze, S., Shah, F., Heine, D., Tauber, J., Hertweck, C., Tunlid, A., Stallforth, P., and Hoffmeister, D. (2015). Three redundant synthetases secure redox-active pigment production in the basidiomycete *Paxillus involutus*. *Chem. Biol.* 22, 1325-34
- Buckel, I., Molitor, D., Liermann, J.C., Sandjo, L.P., Berkelmann-Löhnertz, B., Opatz, T., and Thines, E. (2013). Phytotoxic dioxolanone-type secondary metabolites from *Guignardia bidwellii*. *Phytochemistry* 89, 96-103
- Buckel, I., Andernach, L., Schüffler, A., Piepenbring, M., Opatz, T., and Thines, E. (2017). Phytotoxic dioxolanones are potential virulence factors in the infection process of *Guignardia bidwellii*. *Sci. Rep.* 7, 8926
- Dellaporta, S.L., Wood, J., and Hicks, J.B. (1983). A plant DNA miniprep: Version II. *Plant Mol. Biol. Rep.* 1, 19-21
- van Dijk, J.W.A., Guo, C., and Wang, C.C.C. (2016). Engineering fungal nonribosomal peptide synthetase-like enzymes by heterologous expression and domain swapping. *Org. Lett.* 18, 6236-9
- Finn, R.D., Attwood, T.K., Babbitt, P.C., Bateman, A., Bork, P., Bridge, A.J., Chang, H., Dosztányi, Z., El-Gebali, S., Fraser, M. *et al.* (2017). InterPro in 2017-beyond protein family and domain annotations. *Nucleic Acids Res.* 45, D190-D199
- Fredenhagen, A., Petersen, F., Tintelnot-Blomley, M., Rösel, J., Mett, H., and Hug, P. (1997). Semicochliodinol A and B: inhibitors of HIV-1 protease and EGF-R protein tyrosine kinase related to asterriquinones produced by the fungus *Chrysosporium merdarium*. *J. Antibiot.* 50, 395-401
- Gao, H., Guo, W., Wang, Q., Zhang, L., Zhu, M., Zhu, T., Gu, Q., Wang, W., and Li, D. (2013). Aspulvinones from a mangrove rhizosphere soil-derived fungus *Aspergillus terreus* Gwq-48 with anti-influenza A viral (H1N1) activity. *Bioorg. Med. Chem. Lett.* 23, 1776-8
- Geib, E., Gressler, M., Viediarnikova, I., Hillmann, F., Jacobsen, I.D., Nietzsche, S., Hertweck, C., and Brock, M. (2016). A non-canonical melanin biosynthesis pathway protects *Aspergillus terreus* conidia from environmental stress. *Cell Chem. Biol.* 23, 587-97

- Geib, E., and Brock, M. (2017). ATNT: an enhanced system for expression of polycistronic secondary metabolite gene clusters in *Aspergillus niger*. *Fungal Biol. Biotechnol.* 4, 13
- Geib, E., Baldeweg, F., Nett, M., and Brock, M. (2018). Cross-chemistry leads to product diversity from atromentin synthetases in *Aspergilli* from section *Nigri*. manuscript submitted
- Gressler, M., Hortschansky, P., Geib, E., and Brock, M. (2015). A new high-performance heterologous fungal expression system based on regulatory elements from the *Aspergillus terreus* terrein gene cluster. *Front. Microbiol.* 6, 184
- Guo, C., Knox, B.P., Sanchez, J.F., Chiang, Y., Bruno, K.S., and Wang, C.C.C. (2013). Application of an efficient gene targeting system linking secondary metabolites to their biosynthetic genes in *Aspergillus terreus*. *Org. Lett.* 15, 3562-5
- Hühner, E., Backhaus, K., Kraut, R., and Li, S. (2018). Production of α -keto carboxylic acid dimers in yeast by overexpression of NRPS-like genes from *Aspergillus terreus*. *Appl. Microbiol. Biot.* 102, 1663-1672
- Kaji, A., Saito, R., Nomura, M., Miyamoto, K., and Kiriyama, N. (1997). Mechanism of the cytotoxicity of asterriquinone, a metabolite of *Aspergillus terreus*. *Anticancer Res.* 17, 3675-9
- Kaji, A., Saito, R., Nomura, M., Miyamoto, K., and Kiriyama, N. (1998). Relationship between the structure and cytotoxic activity of asterriquinone, an antitumor metabolite of *Aspergillus terreus*, and its alkyl ether derivatives. *Biol. Pharm. Bull.* 21, 945-9
- Kraft, J., Bauer, S., Keilhoff, G., Miersch, J., Wend, D., Riemann, D., Hirschelmann, R., Holzhausen, H.J., and Langner, J. (1998). Biological effects of the dihydroorotate dehydrogenase inhibitor polyporic acid, a toxic constituent of the mushroom *Hapalopilus rutilans*, in rats and humans. *Arch. Toxicol.* 72, 711-1
- Letunic, I., and Bork, P. (2016). Interactive tree of life (iTOL) v3: an online tool for the display and annotation of phylogenetic and other trees. *Nucleic Acids Res.* 44, W242-5
- Medema, M.H., Kottmann, R., Yilmaz, P., Cummings, M., Biggins, J.B., Blin, K., de Bruijn, I., Chooi, Y.H., Claesen, J., Coates, R.C. *et al.* (2015). Minimum information about a biosynthetic gene cluster. *Nat. Chem. Biol.* 11, 625-31
- Molitor, D., Liermann, J.C., Berkelmann-Löhnertz, B., Buckel, I., Opatz, T., and Thines, E. (2012). Phenguignardic acid and guignardic acid, phytotoxic secondary metabolites from *Guignardia bidwellii*. *J. Nat. Prod.* 75, 1265-9
- Nguyen, L., Schmidt, H.A., von Haeseler, A., and Minh, B.Q. (2015). IQ-TREE: a fast and effective stochastic algorithm for estimating maximum-likelihood phylogenies. *Mol. Biol. Evol.* 32, 268-74
- Puder, C., Wagner, K., Vettermann, R., Hauptmann, R., and Potterat, O. (2005). Terphenylquinone inhibitors of the src protein tyrosine kinase from *Stilbella* sp. *J. Nat. Prod.* 68, 323-6

- Samson, R.A., Peterson, S.W., Frisvad, J.C., and Varga, J. (2011). New species in *Aspergillus* section *Terrei*. *Stud. Mycol.* 69, 39-55
- Schneider, P., Weber, M., Rosenberger, K., and Hoffmeister, D. (2007). A one-pot chemoenzymatic synthesis for the universal precursor of antidiabetes and antiviral bis-indolylquinones. *Chem. Biol.* 14, 635-44
- Sievers, F., and Higgins, D.G. (2018). Clustal Omega for making accurate alignments of many protein sequences. *Protein Sci.* 27, 135-45
- Singh, S.B., Ondeyka, J.G., Tsipouras, N., Ruby, C., Sardana, V., Schulman, M., Sanchez, M., Pelaez, F., Stahlhut, M.W., Munshi, S. *et al.* (2004). Hinnuliquinone, a C2-symmetric dimeric non-peptide fungal metabolite inhibitor of HIV-1 protease. *Biochem. Bioph. Res. Co.* 324, 108-13
- Stachelhaus, T., Mootz, H.D., and Marahiel, M.A. (1999). The specificity-conferring code of adenylation domains in nonribosomal peptide synthetases. *Chem. Biol.* 6, 493-505
- Stahlschmidt, C. (1877). Über eine in der Natur vorkommende organische Säure. *Liebigs Ann. Chem.* 178, 177-97
- Sun, W., Guo, C., and Wang, C.C.C. (2016). Characterization of the product of a nonribosomal peptide synthetase-like (NRPS-like) gene using the doxycycline dependent Tet-on system in *Aspergillus terreus*. *Fungal Genet. Biol.* 89, 84-8
- Theobald, S., Vesth, T.C., Geib, E., Nybo, J.L., Frisvad, J.C., Larsen, T.O., Salamov, A., Riley, R., Lyhne, E.K., Kogle, M.E. *et al.* (2018). Genomic and metabolic diversity in *Aspergillus* section *Terrei*. in preparation
- Velliquette, R.A., Friedman, J.E., Shao, J., Zhang, B.B., and Ernsberger, P. (2005). Therapeutic actions of an insulin receptor activator and a novel peroxisome proliferator-activated receptor gamma agonist in the spontaneously hypertensive obese rat model of metabolic syndrome X. *J. Pharmacol. Exp. Ther.* 314, 422-30
- Wang, M., Beissner, M., and Zhao, H. (2014). Aryl-aldehyde formation in fungal polyketides: discovery and characterization of a distinct biosynthetic mechanism. *Chem. Biol.* 21, 257-63
- Weissman, K.J. (2015). The structural biology of biosynthetic megaenzymes. *Nat. Chem. Biol.* 11, 660-70
- Yeh, H., Chiang, Y., Entwistle, R., Ahuja, M., Lee, K., Bruno, K.S., Wu, T., Oakley, B.R., and Wang, C.C.C. (2012). Molecular genetic analysis reveals that a nonribosomal peptide synthetase-like (NRPS-like) gene in *Aspergillus nidulans* is responsible for microperfuraneone biosynthesis. *Appl. Microbiol. Biot.* 96, 739-48
- Zhang, B., Salituro, G., Szalkowski, D., Li, Z., Zhang, Y., Royo, I., Vilella, D., Díez, M.T., Pelaez, F., Ruby, C. *et al.* (1999). Discovery of a small molecule insulin mimetic with antidiabetic activity in mice. *Science (New York, NY)* 284, 974-7

Methodology

Details of all methods used in this study are listed in the published manuscripts and manuscript drafts included in this thesis. However, some methods used in these studies were of paramount importance to the success of the work described here and will be briefly discussed below.

In vitro recombination

Traditional gene cloning strategies use restriction/ligation techniques, in which individual DNA-fragments are restricted with specific restriction enzymes and ligated by using a T4-ligase to a vector linearized with compatible restriction enzymes. While this procedure has been used for decades, it makes the development of cloning strategies a very tedious work. As an example, a gene coding for a standard iterative fungal non-reducing polyketide synthase generally possesses an open reading frame of about 6000 - 8000 bp. Common restriction enzymes with a six base-pair recognition site cut a statistically composed DNA at every $4^6 = 4096$ base pairs. This means that it is likely that no compatible restriction site between plasmid and DNA fragment can be found. In this case, site directed mutagenesis is required to remove individual restriction sites before the cloning strategy can proceed.

In vitro recombination revolutionised these cloning procedures. A restriction site of choice can be used to linearize the receiving plasmid. The fragment(s) to be joined with the vector do not need to be flanked by any restriction site, allowing a seamless construct to be generated. Instead, fragments are amplified by PCR with primers that contain an overlap of at least 15 bp to the sequence surrounding the restriction site of the recipient plasmid. Recombinases in the *in vitro* recombination mixture then recognise the compatible ends and assemble the construct (Park, Throop and LaBaer, 2015), which can then be used for transformation of *Escherichia coli*, in which ends are ligated and the plasmid is amplified. This technique can also be expanded to simultaneous cloning of several fragments with respective overlapping ends in one go. Therefore, this *in vitro* recombination technique was invaluable for this work. All expression plasmids generated in this study contain unique *NcoI* and/or *NsiI* sites that can be used for plasmid linearization between the *terA* promoter and the *trpC* terminator. By this means, genes of interest can be directly cloned under control of the *terA* promoter. As expression plasmids generated here also contain a marker for fungal transformation, plasmids re-isolated from *E. coli* can directly be used for transformation of the expression platform strains. Furthermore, *in vitro* recombination allowed the assembly of polycistronic transcripts by using overlapping sequences of the P2A peptide for the fragment assembly. Therefore, without *in vitro* recombination, cloning of the large number of genes and generating of domain swapping experiments would not have been possible.

Heterologous expression in *A. niger* and *A. oryzae* and use of a TetOn system

In this study, *Aspergillus niger* and *Aspergillus oryzae* were selected as expression platform strains. The selection based on several reasons: the primary aim was to characterise secondary metabolite production from *Aspergillus terreus* and species from section *Terrei*. By using *Aspergillus* species as expression hosts it was assumed that genes were correctly transcribed and spliced in the heterologous hosts. In addition, the host strains were assumed to possess the toolbox required to activate proteins resulting from heterologous gene expression. Finally, we anticipated that substrate provision in the original host and the expression host is similar and not limiting product formation. However, the last assumption of course only holds true, if no pathway specific intermediates are produced by gene cluster specific enzymes. In this case, the respective genes also need to be transferred to the expression platform for provision of the correct substrate. In most respects, these assumptions were correct, and a wide variety of different metabolites were produced in the different expression platforms (Geib *et al.*, 2016; Geib *et al.*, 2018a, manuscript submitted). However, at least two features of the expression platforms came to a surprise, which were the cross-chemistry occurring in *A. niger* and the inability to establish the TetOn system in *A. oryzae*. In general, *A. niger* was easier to handle after transformation as it produces distinct colonies on transformation plates. In contrast, the fluffier colony appearance of *A. oryzae* complicates identification and picking of individual colonies. In addition, yields of metabolites frequently seemed higher from *A. niger* when compared to *A. oryzae*. Therefore, *A. niger* was used as preferred heterologous host. However, analyses showed that cross-chemistry occurred on quinone structures resulting in metabolites different from those anticipated to be produced (Geib *et al.*, 2018a, manuscript submitted). This provides a rationale for using *A. oryzae* in parallel. Unfortunately, the *A. oryzae* system currently only exists as a sugar inducible and constitutively active system. When the TetOn system was integrated into *A. oryzae*, gene expression under TerR/PterA control remained constitutively switched on. This means that *A. oryzae* is either able to activate the minimal *gpdA* promoter from *A. nidulans* or that the reverse transactivator binds a molecule from *A. oryzae* that allows binding to the operator sequence. Further studies will be required to answer these questions. Currently there is no fine-tunable system available for *A. oryzae*, which might hamper the production of toxic metabolites. However, in the studies presented here, both strains were valuable tools for heterologous gene expression. Since it was possible to delete the internal copy of *pyrG* fully or partially, the same expression plasmids can be used for transformation of both species (Geib *et al.*, 2018a, manuscript submitted).

URA-blaster and self-splicing viral peptides

Biosynthesis of natural products frequently involves a metabolite produced from a synth(et)ase that is subsequently modified by tailoring enzymes. In fungi all genes necessary for biosynthesis and regulation are often clustered in a biosynthesis gene cluster. Therefore, to reconstitute the biosynthesis of a natural product, several genes need to be introduced into the heterologous

expression host. This can cause severe problems as the marker for transformation of wild-type *Aspergillus* strains is limited. Therefore, two different strategies were used to circumvent this problem. One solution was the development of a URA-blaster cassette. This cassette bases on direct repeats of sequences not present in the receiving host that enclose a functional copy of a *pyrG* gene. This allows the transformation of a *pyrG*⁻ strain by using uridine/uracil prototrophy as selection marker. To re-use this marker, the intact copy of the *pyrG* gene within the URA blaster needs to be removed again. This occurs spontaneously at low frequency ($10^{-4} - 10^{-5}$) by mitotic recombination of the direct repeats, resulting in excision of the *pyrG* gene and leaving one direct repeat in the genome (Brock *et al.*, 2007). Selection for this event is performed by using 5'-fluoroorotic acid (FOA) in the presence of uridine. Strains with an intact copy of the *pyrG* gene will convert FOA acid into 5'-fluorouracil, which is toxic to the cells. In contrast, cells that lost the intact copy of the *pyrG* gene cannot convert FOA, but will use the uridine for growth, forming individual colonies on plates that are ready for the next round of transformation. In this study, direct repeats consisting of an internal fragment of the methylisocitrate lyase gene *prpB* from *E. coli* were used and, although not extensively used in this study, the cassette proved functional in some proof-of-concept studies.

A method that was applied more frequently was the use of self-splicing viral peptide sequences, in this study a sequence deriving from porcine Teschovirus-1 was used (Kim *et al.*, 2011). A specific sequence motif that can be cut down to essential sequence part N-P-G-P leads to a stalling of the ribosome during translation. Thereby, the peptide bond is not formed between the glycine and proline, but translation continues. By this means, two separate proteins are formed from a single transcript with a continuous open reading frame. This study confirmed the suitability of this system by reconstituting Asp-melanin biosynthesis in combination with a fluorescent marker from a single polycistronic transcript (Geib and Brock, 2017b). In addition, it was used for generating constructs containing an NRPS-like enzyme in combination with an aminotransferase (Geib *et al.*, 2018b, in preparation). However, whether this system works equally well in *A. niger* and *A. oryzae* requires further testing, since the system was mainly applied to heterologous expression in *A. niger*.

Purification of proteins and *in vitro* metabolite production

It is always difficult to exclude, whether a metabolite produced in a heterologous host might have undergone a host specific modification. A possibility to confirm or reject this assumption derives from *in vitro* reconstitution of metabolite biosynthesis as all factors contributing to product formation are known. However, a prerequisite is the use of purified proteins and the availability of substrates and co-factors.

For protein purification, a series of expression vectors was generated that allows the addition of an N- or C-terminal histidine tag to the protein of interest depending on the restriction enzyme used to linearize the vector. This tagging was extensively used in combination with the

production of NRPS-like proteins, in which the *N*-terminal addition of the tag did not disturb protein function. This allowed purification of the proteins by Ni-chelate chromatography, whereby the purity of the protein was dependent on the production rate. In some purification approaches an additional band at about 40 kDa was obtained, which might either derive from co-purification of the transcription factor TerR, a zinc-binding protein, which may also bind to the Ni-column or could be due to a truncated protein version. By generating a next version of expression vectors, the His-tag will be replaced by a Strep-tag and tested for its suitability in protein purification. *In vitro* assays allowed the reconstitution of the Asp-melanin pathway as well as the product formation from atromentin synthetases and different chimeric proteins (Geib *et al.*, 2016; Geib *et al.*, 2018a, manuscript submitted). This was of special importance as it confirmed cross-chemistry on atromentin synthetases exclusively under *in vivo* conditions in *A. niger*, whereas purified proteins from *A. niger* tested under *in vitro* conditions produced the expected metabolite atromentin (Geib *et al.*, 2018a, manuscript submitted).

Extraction and purification of secondary metabolites

For analysis of metabolites produced from heterologous gene expression, extraction of metabolites from culture broth and/or fungal mycelium is essential. In initial analyses extraction was always performed on both entities, which led to the discovery of atrofuranic acid mainly associating with the fungal mycelium, whereas atromentin was nearly exclusively found in the culture filtrate (Geib *et al.*, 2018a, manuscript submitted). In general, most metabolites analysed in this work generally accumulated in the culture filtrate. As a solvent for primary extraction ethyl acetate was used, which turned out as an excellent solvent for extraction of products formed by NRPS-like enzymes. Moreover, it can be easily re-used after distillation. However, it should be mentioned that extractions in ethyl acetate resemble extractions under acidic conditions. On the one hand, acidification of the culture filtrate aids to improve extraction yields. On the other hand, some metabolites may show reduced stability under these conditions. In this respect, storage of lecanoric acid under acidic conditions leads to its hydrolysis into two molecules of orsellinic acid (Leuckert, 1985). Similarly, prolonged incubation of butyrolactones in ethyl acetate seem to lead to partial degradation (Geib *et al.*, 2018a, manuscript submitted). Therefore, this solvent may not always be the best choice when thinking about scaling up the production and purification process.

Purification of metabolites is required prior to structural elucidation. A range of chromatographic methods have been applied in this work such as flash chromatography on C18 reverse phase silica gel, Sephadex columns with various solvent systems or the use of different solid phase extraction columns (e.g. Chromabond, Macherey-Nagel). Crude or fractionated extracts are then subjected to semi-preparative high-performance liquid chromatography (HPLC). The best method for metabolite purification depends on the structure and nature of the individual metabolite as well as the impurities, which need to be removed. Therefore, no general guidelines can be provided. However, as can be seen from the chromatograms of NRPS-like

metabolites produced in the heterologous expression platform strains, the amount of host-derived metabolites is very low, easing the purification by (semi-) preparative HPLC for structure elucidation by NMR.

Discussion

General achievements

The focus of this work was to study secondary metabolites produced by aspergilli from section *Terrei*. In two examples, well-known but unresolved mysteries of *Aspergillus terreus* were tackled. First, the molecular basis for biosynthesis of the major metabolite terrein was identified. Second, Asp-Melanin, a previously undescribed type of melanin was discovered, which makes *A. terreus* and some members of the section *Terrei* distinguishable from other sections of aspergilli. To characterise individual biosynthetic steps or whole biosynthesis pathways a high-performance expression system was designed and refined to overcome challenges of natural product biosynthesis in heterologous host systems. However, not only the identification and elucidation of individual natural products was of interest, but also the elucidation of the proposed biological function. From these analyses we discovered possible functions of terrein and Asp-Melanin that may support the adaptation of *A. terreus* as a soil inhabiting saprophyte.

Besides studying the contribution of natural products to environmental adaptation, possible biological functions of secondary metabolites outside from their natural context were identified by an *in silico/in vitro* screening approach that was verified by experimental data. For a proof-of-concept study atromentin, a product of NRPS-like enzymes from various asco- and basidiomycetes was selected. Atromentin, as well as aspulvinone E, which is involved in Asp-melanin formation, derive from so-called NRPS-like enzymes and these small molecules have aroused interest due to proposed exploitable pharmaceutical activities. Therefore, another focus was given to the identification of products formed by selected NRPS-like enzymes from aspergilli of section *Terrei*. Unexpectedly, during over expression of NRPS-like genes it became clear that physiology of the heterologous host might interfere with the product formation and care must be taken by choosing the heterologous system. The results from individual studies carried out in this work are briefly discussed in the following sections.

Non-reducing (NR)-PKS of SAT-KS-AT-PT-ACP-ACP-TE type in aspergilli

DHN-Melanin is an important virulence determinant in plant and human pathogenic ascomycetes. The precursor 1,8-dihydroxynaphthalene (DHN) is produced by a non-reducing polyketide synthase (NR-PKS). All these NR-PKS show the same domain structure, including a tandem ACP domain. It is believed that DHN-melanin is the predominant type of melanin in filamentous ascomycetes (Braga *et al.*, 2015). For example, *Magnaporthe oryzae* requires melanin in the cell wall of appressoria to withstand the turgor pressor generated for penetration of the rice leaf epidermis (Howard and Valent, 1996). Similar melanin rings formed by *Diplocarpon rosae* result in black spot disease of rose leaves (Gachomo, Seufferheld and Kotchoni, 2010). For human pathogenic fungi melanisation is a possibility to hide from the immune system as shown for *Aspergillus fumigatus* (Chai *et al.*, 2010) and *Penicillium*

marneffei, whereas albino mutants are associated with attenuated virulence (Tsai *et al.*, 1998; Langfelder *et al.*, 1998; Woo *et al.*, 2010). These and other examples describe the importance of the class of DHN-melanin for fungal environmental adaptation and protection.

One of the first PKS identified to produce a melanin precursor was PksP/Alb1 from *A. fumigatus* (Tsai *et al.*, 1998; Langfelder *et al.*, 1998). While genome analyses revealed that homologs of PksP are highly conserved among aspergilli, this was not the case for *Aspergillus terreus* (Slesiona *et al.*, 2012). Moreover, in contrast to *A. fumigatus*, *A. terreus* does not inhibit the acidification of phagolysosomes, which was directly linked to a lack of DHN-melanin. The heterologous expression of the naphthopyrone synthetase gene *wA* from *Aspergillus nidulans* in *A. terreus* restored the phenotype observed for other aspergilli and phagolysosomes did not acidify resulting in an enhanced virulence (Slesiona *et al.*, 2012).

These results gave rise to search and analyse the closest relatives of PksP in *A. terreus*. The gene products of ATEG_07500 and ATEG_00145 are both NR-PKS enzymes possessing a SAT-KS-AT-PT-ACP-ACP-TE architecture (Zaehle *et al.*, 2014). Phylogenetic analysis based on the ketosynthase (KS) domains of characterised fungal PKS showed that both proteins do not cluster with any of the selected naphthopyrone or melanin PKSs but form distinct branches. While a distant relationship of ATEG_07500 with naphthopyrone synthases was observed, expression studies showed that ATEG_07500 remained silent under tested conditions and gene deletion caused no altered phenotype. In contrast, while expression of ATEG_00145 was independent from conidia forming conditions and a deletion did not cause a change of the colouration of conidia, the gene was induced especially on plant derived media (Zaehle *et al.*, 2014).

Elucidation of terrein biosynthesis in *A. terreus*

To study the function of ATEG_00145 a comprehensive study using a multitude of methods was applied (Zaehle *et al.*, 2014). Semiquantitative reverse transcription (RT-) PCR revealed that ATEG_00145 is co-regulated with ten other genes forming a potential biosynthesis gene cluster (ATEG_00135-ATEG_00145). Seven of the co-expressed genes have a direct function in biosynthesis of the final secondary metabolite, two encode putative major facility transporters and one gene encodes a transcription factor. Deletion of ATEG_00145 abolished the production of terrein, the major secondary metabolite produced by *A. terreus* on potato dextrose medium but, as mentioned, had no influence on the spore colouration. Consequently, due to its essential contribution to terrein biosynthesis the NR-PKS was termed TerA. These results on NR-PKS confirmed that no PksP-type polyketide synthase is involved in melanisation of *A. terreus* conidia and implied further that the origin of the pigment in *A. terreus* is not of a DHN-melanin type. Therefore, the common view that all *Aspergillus* species produce this type of melanin in their conidia needs to be revised.

Even though TerA is not involved in pigment biosynthesis, this study revealed the biosynthetic origin of the metabolite terrein. Terrein is one of the longest-known secondary metabolite from *A. terreus* (Raistrick and Smith, 1935) and is frequently mentioned as the major metabolite produced by various *Aspergillus terreus* isolates. Despite its high production levels, establishment of a confirmed structure with absolute configuration took more than two decades (Clutterbuck, Raistrick and Reuter, 1937; Barton and Miller, 1955) and the biosynthetic origin remained unknown. Nevertheless, early labelling experiments indicated a potential polyketide pathway followed by an unusual ring contraction (Birch, Cassera and Jones, 1965; Hill, Carter and Staunton, 1981). Even though a polyketide synthase-derived mechanism had been described, the study presented here is the first molecular confirmation of a PKS being responsible for terrein biosynthesis (Zaehle *et al.*, 2014).

To identify the product produced by TerA, the *terA* gene was heterologously expressed in *A. niger*. Surprisingly, instead of a single metabolite, three products were detected, that varied in the chain length of the respective polyketides. While 4-hydroxy-6-methylpyrone and orsellinic acid describe plausible products of a PKS with the domain structure SAT-KS-AT-PT-ACP-ACP-TE, the metabolite 6,7-dihydroxymellein was identified in major quantities (Zaehle *et al.*, 2014). However, this metabolite cannot be described as a direct product from a NR-PKS and requires modifications by additional enzymes. Thereby, the expected product 2,3-dehydro-6-hydroxymellein seems to have undergone a reduction and hydroxylation at position C7. It is likely that these modifications were introduced by unspecific enzymes from the heterologous *A. niger* expression host. In this respect, it should be noted that 2,3-dehydro-6-hydroxymellein was also not detected in any of the terrein biosynthesis gene cluster deletion mutants in *A. terreus*. Instead, in *A. terreus* the reduced, but not hydroxylated form 6-hydroxymellein was found (Zaehle *et al.*, 2014). While enzymes reducing 2,3-dehydro-6-hydroxymellein in *A. niger* remained unknown, a likely candidate in *A. terreus* is TerB, which contains a dehydrogenase and ketoreductase domain. However, as this was not experimentally confirmed, a reduction by other enzymes cannot be excluded. Interestingly, when *terA* was heterologously expressed in *A. nidulans*, Chiang *et al.*, identified 2,3-dehydro-6-hydroxymellein by mass spectrometry as primary product of TerA, whereby 4-hydroxy-6-methylpyrone and orsellinic acid and a hydrolysed form of 2,3-dehydro-6-hydroxymellein were also extracted after acidification of the culture filtrate (Chiang *et al.*, 2013). Taken together, these analyses confirmed that TerA is a non-reducing polyketide synthase with a relaxed product specificity as in both expression systems, *A. niger* and *A. nidulans*, three polyketides of different chain length were detected.

The identification of 2,3-dehydro-6-hydroxymellein confirms the proposals of terrein biosynthesis made by Birch *et al.* (Birch, Cassera and Jones, 1965) and Hill *et al.* (Hill, Carter and Staunton, 1981). To determine the functions of each gene of the cluster, deletion mutants were generated. High-resolution mass spectrometry (HR-MS) and NMR analyses of purified intermediates were applied to further elucidate the terrein biosynthesis pathway. Metabolite

profiles of $\Delta terC$, $\Delta terD$, $\Delta terE$ and $\Delta terF$ differed in production rates but not in metabolite composition. Therefore, individual function of enzymes cannot be assigned. All compounds identified were either reduced isocoumarin derivatives or orsellinic acid. Thus, since no metabolites with a contracted ring structure except for terrein were isolated from *A. terreus* and secondary modifications occurred during heterologous expression, a reconstitution of the biosynthesis pathway was not possible. Nevertheless, especially from a mechanistic point of view there is still great interest in further elucidation of the function of individual enzymes (Schor and Cox, 2018). Especially the oxidative ring contraction would be a valuable addition to the understanding of natural product biosynthesis. In this respect, the multicopper oxidase TerE is a promising candidate to catalyse this unusual reaction.

Function of terrein

Terrein is a metabolite of great pharmacological interest. Several studies claim a multitude of applications, among them anticancer activity against hepatoma cells (Zhang *et al.*, 2015), epithelial ovarian cancer cells (Chen *et al.*, 2014), cervical carcinoma cells (Porameesanaporn *et al.*, 2013) and multi-drug resistant breast cancer cells (Liao *et al.*, 2012). Also, a reduction of migration of breast cancer cells has been described (Kasorn *et al.*, 2018). Moreover, terrein has drawn attention as a hypo-pigmenting agent (Park *et al.*, 2004; Park *et al.*, 2009) and antioxidant, and shows activity as an enhancer of osteoblast biocompatibility on titanium surfaces (Lee *et al.*, 2010). However, whether terrein will indeed make it to the market as a panacea, only time will show.

Despite these interesting pharmacological activities, another puzzling question arose during investigation of the terrein biosynthesis pathway: Why is *A. terreus* producing such vast quantities of terrein under certain conditions as hardly any of the identified biological activities from above seem to be valuable for *A. terreus* in its ecological niche? First experiments showed that terrein can reduce seed germination and root elongation and damages the surfaces of different fruits, especially of bananas (Zaehle *et al.*, 2014). These findings indicated an adaptation to plant material by either growing as saprophyte or as a plant pathogen. A follow-up study focussed on the gene cluster activation under conditions that *A. terreus* might face in its natural ecological niches (Gressler *et al.*, 2015b). Indeed, natural inducers such as iron and nitrogen limitation, which are common in the rhizosphere, were identified as trigger for terrein production. In agreement, to counteract iron starvation, terrein can reduce ferric iron to the bioavailable ferrous iron. Furthermore, terrein production triggered by nitrogen starvation can mobilise nutrients as result of surface damage (Gressler *et al.*, 2015b). Additionally, terrein revealed a mild antifungal effect that might provide advantages against competitors. Therefore, terrein production might indeed support competitiveness of *A. terreus* in its natural environment and *A. terreus* appears well adapted to act as a saprophyte or plant pathogen (Louis, 2013; Lass-Flörl *et al.*, 2005). Whether or not terrein also contributes to pathogenic growth in humans needs

to be identified. However, as host cells restrict the availability of iron, it can be assumed that terrein production is also induced during invasive growth in humans.

Utilisation of TerR to drive heterologous gene expression in *A. niger*

The amount of terrein produced by *A. terreus* on plant-derived medium yielded more than 1.1 g/l without further optimisation of fermentation conditions and the production rate was even higher using optimised media and cultivation techniques (Yin *et al.*, 2013). These enormous quantities of terrein rely on a transcription factor present in the terrein biosynthesis gene cluster that specifically recognises and activates the cluster specific genes. This led to the idea of using the transcription factor TerR in combination with one of its target promoters to construct a heterologous expression system. From phylogenetic analysis of TerA it seemed that the terrein gene cluster is unique to *A. terreus* (Zaehle *et al.*, 2014). This implied further that TerR might not recognise and activate promoters in other *Aspergillus* species. If that holds true, no cross-talk with other secondary metabolite gene clusters is expected, which is important for the exploitation of TerR and its target promoters for heterologous gene expression and secondary metabolite production.

Construction of a TerR-based expression system

To construct a heterologous expression system, the gene for the transcriptional activator TerR was placed under control of the *Aspergillus oryzae amyB* promoter, which is one of the most frequently used promoters in fungal biotechnology (Shoji *et al.*, 2005). This promoter is inducible by sugars, e.g. starch or maltose (Kanemori *et al.*, 1999), but also shows high transcriptional activity in the presence of glucose. As target promoter element for TerR binding the bidirectional promoter region between *terA* and *terB* from the terrein biosynthesis gene cluster (Zaehle *et al.*, 2014) was tested by reporter studies for its suitability to induce genes of interest. Interestingly the transcriptional strength in *terA* direction was 8-14 times higher than in *terB* direction. For better understanding of TerR-DNA binding, recognition motifs were investigated. A consensus high-affinity binding motif was identified, and studies indicated that the *PterA/PterB* promoter region contains three medium affinity binding sites (Gressler *et al.*, 2015a). As two different very high-affinity binding motifs were detected in other terrein biosynthesis gene cluster promoters, it can be speculated that exchanges or insertions of binding sites in the *PterA/PterB* or the use of other promoter regions might result in even higher expression levels as currently observed.

Further investigation of reporter strains revealed that the use of the coupled system of *PamyB:terR* on *PterA:GoI* (*gene of interest*) resulted in a signal amplification by about three times compared to direct expression of a *GoI* under control of *PamyB* (Gressler *et al.*, 2015a). Such high expression rates allow high-level protein production and, thereof, secondary metabolite production even when using fungal transformants containing single or low copy

number integrations. This is assumed to bypass possible negative side effects as frequently observed when using strains with multiple integrations of expression constructs.

Besides the high expression rates obtained from the coupled expression system, no other secondary metabolite gene clusters were non-specifically induced when TerR was expressed in *A. niger* since secondary metabolite profiles of wild type and a *terR* expressing transformant (P2) showed no difference (Gressler *et al.*, 2015a). Therefore, when *A. niger* P2 was cultivated in minimal media with sufficient glucose and nitrogen supply, no significant production of secondary metabolites was detected in extracts from 48 h shake-flask cultures. This makes the system perfectly suited for the heterologous expression of genes encoding proteins for secondary metabolite production as it allows to identify novel metabolites easily.

In a proof-of-concept study, this coupled system was used to test secondary metabolite production from the fungal polyketide synthase OrsA from *A. nidulans*. A previous study from the Brakhage and Hertweck labs characterised OrsA as orsellinic acid synthase (Schroeckh *et al.*, 2009). Structural elucidation of the corresponding compound required extraction of 14 l of medium from a co-cultivation of *A. nidulans* with *Streptomyces hygroscopicus*. Using the coupled expression system in *A. niger*, a 100 ml culture incubated for 36 h as simple shake-flask culture was sufficient to show that OrsA predominantly produces lecanoric acid (Gressler *et al.*, 2015a). Lecanoric acid is a depside made from two orsellinic acid molecules and which is frequently found as a lichen-derived metabolite (Stocker-Wörgötter, 2008). Minor amounts of orsellinic acid can be identified as hydrolysis products of lecanoric acid (Leuckert, 1985). Huge quantities of culture medium needed to be extracted for the original study with *A. nidulans* as producer, which was accompanied by a long time that elapsed to gain sufficient material before analysis could take place. This might have led to a partial hydrolysis of lecanoric acid implying that OrsA produces orsellinic rather than lecanoric acid. Therefore, our experiment nicely visualises the power of the heterologous expression system for fast and reliable identification of natural products produced from expression of a gene of interest.

Furthermore, the coupled expression system was used to investigate the function of thioesterase domains from polyketide synthases. In a domain exchange experiment the thioesterase domain of OrsA was replaced by the thioesterase domain from TerA, which abolished lecanoric acid in favour of orsellinic acid production. This experiment not only proved OrsA to act as lecanoric acid synthase but also showed that the expression system together with the SM-Xpress plasmid is an easy-to-use tool for such applications.

Successful application of the heterologous expression system in natural product research

The TerR/*PterA*-based expression system was subsequently used by us and by other research groups to express a broad range of genes producing different natural products. Thereby, the expression system was not only restricted to expression of PKS coding genes from ascomycetes, but also for expression of several genes from basidiomycetes, from which intron-free gene

sequences had to be used as the large number of introns in genes from basidiomycetes may hinder correct intron splicing in the heterologous host *A. niger*. The heterologous expression of *PPSI* from the steraceous mushroom BY1 revealed that this gene codes for a PKS with an unusual double-bond shifting mechanism responsible for polyene production (Brandt *et al.*, 2017). Another example for successful use of the system is the characterisation of CsNPS2, an NRPS responsible for siderophore biosynthesis that is highly conserved among basidiomycetes but has not been characterised before (Brandenburger *et al.*, 2017). This multi-modular mega-enzyme was expressed in soluble and active form. The enzyme was subsequently purified from fungal mycelium without losing its activity, which confirms an application range for proteins of at least 274.5 kDa in size. Furthermore, this expression system was indispensable for discovery of a new type of melanin, where heterologous expression of the NRPS-like enzyme MelA and the glycosylated tyrosinase TyrP helped to identify reaction intermediates to reconstitute the biosynthesis pathway of Asp-melanin (Geib *et al.*, 2016). This study will be discussed in more depth further below.

Even though the expression system already proved its applicability on various asco- and basidiomycetes secondary metabolite biosynthesis genes, it might be advantageous to transfer the *PamyB:terR* system to other industrial important and genetically amenable fungi, including basidiomycetes such as *Ustilago maydis*. Also, the use in ascomycetous yeasts such as *Saccharomyces cerevisiae* or the less conventional yeast *Yarrowia lipolytica* (Barth and Gaillardin, 1997) might be considered, as yeasts have advantages for cultivation in fermenters. The latter species is additionally of interest as it can utilise unusual substrates such as hydrocarbons for growth (Flores and Gancedo, 2005)

Asp-Melanin: a novel type of melanin produced by *A. terreus*

With identification and elucidation of the terrein biosynthesis pathway, the melanin of *A. terreus* conidia remained cryptic. Previous studies showed that *A. terreus* neither possesses a highly conserved NR-PKS homologue to PksP (Slesiona *et al.*, 2012), nor does any of the encoded polyketide synthases produce a naphthopyrone (Zaehle *et al.*, 2014; Gressler *et al.*, 2015b). Taken together it appeared that *A. terreus* conidia are protected by an unusual type of pigment.

Identification of genes involved in melanin production in *A. terreus*

RT-PCR analyses on conidiating and non-conidiating conditions revealed a locus that was transcribed exclusively during production of asexual spores (Geib *et al.*, 2016). In parallel, it had been published that the deletion of an NRPS-like gene resulted in an albino phenotype of *A. terreus* (Guo *et al.*, 2013a). However, no further insight was provided whether the potential metabolite was of regulatory nature or was directly involved in the production of a melanin pigment.

In the study presented here, a combined approach of deletion analyses and heterologous expression studies unequivocally confirmed that the conidial pigment of *A. terreus* depicts a novel type of melanin, which we termed Asp-melanin (Geib *et al.*, 2016). In its biosynthesis pathway the NRPS-like enzyme MelA catalyses the condensation of two *p*-hydroxyphenylpyruvate molecules into aspulvinone E, which acts as substrate for the tyrosinase TyrP. Tyrosinases are bifunctional enzymes which hydroxylate and oxidise their substrates (Ramsden and Riley, 2014). In case of the tyrosinase TyrP, aspulvinone E is hydroxylated *in ortho* position of both *p*-hydroxyphenyl rings and further oxidised to a highly reactive delocalised hydroxyquinone methide anion (Geib *et al.*, 2016). After this activation the polymerisation can spontaneously take place.

Asp- Melanin - A novel type of melanin?

Asp-melanin fulfils the definition of a classic melanin as it derives from a polyphenolic precursor which is polymerised by a copper-dependent enzyme (Eisenman and Casadevall, 2012). Moreover, it is dark in colour and insoluble in solvents and acids. Remarkably, it does not belong to any of the previously described types of melanin. The two predominant types of melanin in the fungal kingdom are DHN-melanin, as found in various ascomycetes like *A. fumigatus* and *Magnaporthe oryzae*, and DOPA-melanin, which is produced by several human pathogenic basidiomycetes such as *Cryptococcus neoformans* or *Paracoccidioides brasiliensis* (Figure 1) (Wang, Aisen and Casadevall, 1995; Tabora *et al.*, 2008). Even though Asp-melanin was speculated to belong to the L-DOPA-melanin type (Palonen *et al.*, 2017), it is clearly distinguishable since (i) no external supply of L-DOPA or other diphenolic compounds is needed, (ii) the precursor and consequently the structure of Asp-melanin is free from nitrogen and (iii) inhibitors of the L-DOPA melanin pathway do not affect conidia colouration in *A. terreus* (Geib and Brock, 2017a). However, the similarities are that L-tyrosine acts as a precursor for generation of *p*-hydroxyphenylpyruvate (*p*-HPPA) and a tyrosinase is involved in melanin polymerisation (Figure 1). On the other hand, Asp-melanin is without a doubt not of the DHN-melanin type, due to the simple fact that 1,8-dihydroxynaphthalene is not a building block of Asp-melanin and no PKS is involved in precursor generation (Geib *et al.*, 2016). In contrast, aspulvinone E derives from a different class of fungal secondary metabolites, which has not been associated with melanin pigment formation before. Due to the extensive studies on Asp-melanin formation including several *in vivo* and *in vitro* approaches, it was confirmed that Asp-melanin is the only melanin type present in *A. terreus* conidia.

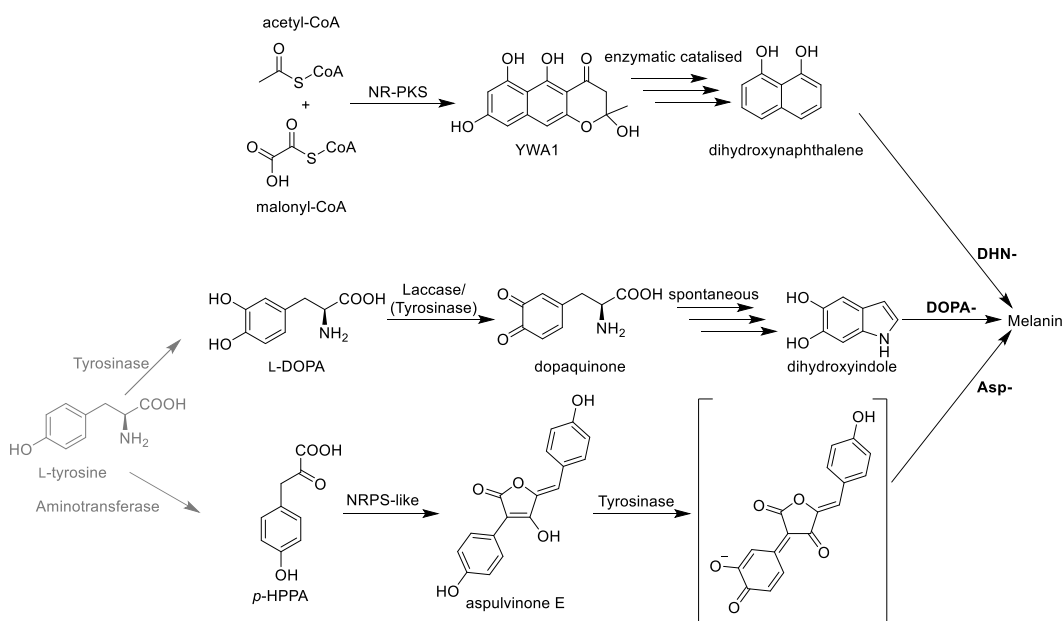


Figure 1: Different types of fungal melanins and their biosynthesis.

Melanin as virulence determinant

In *A. fumigatus* the conidia of albino mutants show an attenuated virulence (Tsai *et al.*, 1998) and have a different surface structure compared to wild-type conidia (Sugareva *et al.*, 2006). This change in surface structure is due to the lack of the rough outer layer formed by proteins, mainly hydrophobins that cannot be properly retained. This suggests that DHN-melanin is involved in the conidia cell-wall integrity and its assembly (Pihet *et al.*, 2009). On the contrary, the deletion of any of the two genes essential for melanin formation in *A. terreus* did not change the outer surface structure of conidia except for an electron-dense layer, most likely deriving from Asp-melanin in the wild type (Geib *et al.*, 2016). Transmission electron microscopy showed that this layer was more diffuse in $\Delta tyrP$ mutants and absent in $\Delta melA$ mutants. In agreement with this unaltered surface structure accompanied by a strongly attached hydrophobin layer on the surface of *A. terreus* conidia, the virulence of the melanised strain and colour mutants did not differ significantly when tested in an embryonated chicken egg infection model.

Another function of known types of melanin conferring virulence is their ability to bind drugs. It is known that some types of melanins can adsorb diverse chemical compounds, including members of major antifungals such as caspofungin or amphotericin B (Nosanchuk and Casadevall, 2006). *A. terreus* possesses an intrinsic amphotericin B resistance (Blum *et al.*, 2013), but its origin remained unclear. However, this study can also exclude that Asp-melanin increases amphotericin B resistance since As-melanin mutants showed the same susceptibility against amphotericin B as the wild type (data not shown).

However, Asp-melanin exhibits some classical protective properties as described for DHN- or DOPA-melanin. It protects against UV radiation and soil predators as fungivore amoeba, which increases the overall environmental fitness and contributes to adaptation of *A. terreus* to the rhizosphere as its natural ecological niche. Due to its unique biosynthetic origin, it was of further interest to study the distribution of Asp-melanin. Thereby, the question was asked whether Asp-melanin is a special feature of *A. terreus* or more widely distributed in aspergilli from the section *Terrei*.

Distribution of Aps-Melanin in aspergilli from section *Terrei*

Since Asp-melanin depicts a previously undescribed type of melanin, it was of scientific interest to elucidate the distribution of Asp-melanin in related species. Some species of section *Terrei* have been identified as human pathogens (Balajee *et al.*, 2009; Lim *et al.*, 2016) and, as discussed before, melanins are considered as virulence determinants. Therefore, a bioinformatic approach on six newly sequenced aspergilli from section *Terrei* was undertaken. Apparently, species phylogenetically most closely related to *A. terreus* carry the genetic prerequisite for Asp-melanin biosynthesis, for example *Aspergillus alabamensis* and *Aspergillus aureoterreus*. More distantly related species, like *Aspergillus neoindicus* or *Aspergillus allahabadii*, do not possess a MelaA homologue. Remarkably, *Aspergillus ambiguus* and *Aspergillus allahabadii* revealed BGCs for naphthopyrone/DHN-melanin synthesis, whereby *A. ambiguus* also possessed an enzymatically active MelaA homologue (Theobald *et al.*, 2018, in preparation).

To verify on a molecular level if the NRPS-like enzymes identified from a bioinformatics approach indeed act as aspulvinone E synthetase and to analyse, whether the polyketide synthases homologous to PksP are able to produce the naphthopyrone YWA1, all genes were heterologously overexpressed in *A. niger* ATNT16. Additionally, the *pksP* genes from *A. fumigatus* and *Aspergillus unguis*, which was first believed to be *Aspergillus microcysticus* from section *Terrei*, were used as references. Extracts of *melaA*-, respectively *melaA* homologue-expressing strains, led to the identification of four novel aspulvinone E synthetases. On the other hand, all *pksP* and its homologues expressing strains produced an identical compound, which was identified as YWA1 (Theobald *et al.*, 2018, in preparation). Interestingly, although the genome of *A. allahabadii* contains a functional copy of *pksP*, the conidia are of white colour and heterologous expression strains showed reduced yields of YWA1 when compared to other PksP homologues. However, a replacement of the promoter of the polyketide synthase in *A. allahabadii* showed that yellow to greenish conidia can be produced, indicating a loss of function of the native promoter to avoid the production of DHN-melanin in this species (Theobald *et al.*, 2018, in preparation).

These analyses indicate that aspergilli from section *Terrei* lost the ability to produce DHN-melanin during evolution but acquired a different strategy to protect their spores from UV radiation and other stressors. In this respect, Asp-melanin is a special characteristic of members

from section *Terrei* but is no premise to be classified into this section as *A. neoindicus* possessed no pigment biosynthesis at all, *A. ambiguus* contained both pathways and *A. allahabadi* showed a DHN-melanin biosynthesis pathway that lost its function. In conclusion, to answer the question of Asp-melanin distribution in aspergilli from section *Terrei*, a set of wet lab experiments were combined with bioinformatics predictions. Thereby, this study showed that it is of essential importance to confirm *in silico* predictions by wet-lab experiments for deeper understanding and interpretation of data as shown for the analysis of *A. allahabadii*. On the other hand, elaborated bioinformatics methods are indispensable to identify BGCs containing NRPS-like genes, since NRPS-like enzymes are composed of identical domain structures and show a high degree of similarity in their amino acid sequence (Geib *et al.*, 2018a, manuscript submitted).

Genome analyses of species from section *Terrei* furthermore indicated a vast biosynthetic potential of species from this section, which largely exceeds the number of metabolites reported from these species so far (Samson *et al.*, 2011). In future studies, unique and common BGC that may produce more than 162 different core moieties can be investigated alone from those seven *Aspergillus* species analysed in this study. Some of the NRPS-like enzymes of the A-T-TE-type have already been heterologously expressed and results are discussed further below.

Cross-Chemistry in heterologous secondary metabolite production

For the heterologous production of secondary metabolites, a range of fungal host organism have been described in the literature. For simple metabolites yeast strains such as *Saccharomyces cerevisiae* have been successfully used as production platforms (Siddiqui *et al.*, 2012), but due to a possible lack of substrate availability and the need for the co-expression of priming enzymes such as 4'-phosphopantetheinyl transferases, lower eukaryotic systems are not always perfectly suited for this task (Wattanachaisaereekul *et al.*, 2007).

Aspergilli as heterologous hosts

Since more than 30 years many members of the genus *Aspergillus* have been used as expression and production platforms. In a comparative study presented in this work two strains of *Aspergillus niger* (A1144 and N402) and one strain of *Aspergillus oryzae* (RIB40) have been used in parallel as heterologous expression platforms (Geib *et al.*, 2018a, manuscript submitted). *A. niger* N402 and *A. oryzae* RIB40 are industrially important strains that have been used for citric acid, food or enzyme production (Yang, Lübeck and Lübeck, 2017; Liu *et al.*, 2014). Both *Aspergillus* species have in common that they have also been used in many research studies as heterologous hosts for secondary metabolite production and are generally regarded as safe (GRAS) (Lazarus, Williams and Bailey, 2014). However, it should be mentioned that secondary metabolism of the expression host might unspecifically modify the heterologously produced natural products, which might lead to confusion on the primary product produced from the gene of interest. Often these modifications include hydroxylations or reductions. An

example for such a modification occurred during investigation of terrein biosynthesis. The heterologous expression of *terA* in *A. niger* unexpectedly yielded, besides 4-hydroxy-6-methylpyrone and orsellinic acid, the metabolite 6,7-dihydroxymellein (Zaehle *et al.*, 2014). As explained above, the hydroxylation at position C7 of 6,7-dihydroxymellein cannot be introduced by the PKS TerA but must be added by an unspecific enzyme from host metabolism. As a result, extracts of *A. niger* expressing *terA* were unable to restore terrein biosynthesis in *A. terreus* Δ *terA* mutants. Similarly, *A. oryzae* unexpectedly reduced a PKS-derived pathway intermediate during heterologous expression of the betaenone biosynthesis gene cluster (Ugai *et al.*, 2015). However, these examples are only case reports and were not considered as general problem. Overall, *A. niger* and *A. oryzae* strains are regarded as suitable expression hosts representing a larger number of benefits (He *et al.*, 2018) than drawbacks.

Cross-chemistry during atromentin production and general implications

Unspecific modification of secondary metabolites by the heterologous expression host was mainly described for the modification of products from polyketide synthases. However, our analyses show that unspecific modifications may also occur on metabolites produced from NRPS-like enzymes. Heterologous expression of atromentin synthetases in *A. niger* strains failed to result in atromentin production (Geib *et al.*, 2018a, manuscript submitted). Instead, a range of different metabolites was produced. Some of these metabolites such as gyroporin have previously described in the literature (Besl *et al.*, 1973). Other metabolites appear novel to nature and have been isolated and elucidated for the first time during this study. Depending on the time point of extraction the metabolite composition changed dramatically, whereby the novel metabolite atrofuranic acid appeared as the dominating metabolite under all applied cultivation conditions (Geib *et al.*, 2018a, manuscript submitted).

Unfortunately, this result indicated that during heterologous expression of an uncharacterised gene, the resulting metabolite might incorrectly be considered as the true product produced by the corresponding protein. Atromentin production that resulted in atrofuranic acid might be an extreme example and exception of host physiology modifying a secondary metabolite, but it cannot generally be ruled out that such modifications occur, and interpretation of heterologous expression data must be taken with care. Therefore, further studies may be required to proof the accuracy of chemical structures derived from other heterologous expression experiments. In tribute to the complexity of this problem different approaches are possible: (i) deletion studies in the original organism, (ii) *in vitro* assays with purified enzymes or (iii), as presented in our study, the parallel use of different expression hosts. At a time at which large number of genomes become readily available, e.g. the 1000 fungal genomes project (Grigoriev *et al.*, 2014), a huge number of novel genes and gene clusters have been identified as interesting candidates for heterologous expression. This is of special importance when the originating organisms are not amenable for genetic modification or no protocol for modification has been established. Even more, some species have extremely slow generation times or are difficult to cultivate under

laboratory conditions. Costs might also negatively impact the selection of the experimental set-up: *in vitro* assays can become expensive or not feasible due to the lack of substrate availability. Reconstitution of reaction cascades with several enzymes might also be difficult because of the requirement of different chemical parameters or need for unknown and expensive co-factors. If paralleled expression in different host systems is intended to elucidate or exclude possible cross-chemistry effects, preparation of universally usable expression constructs and generation of compatible host strains is necessary. In our case, for applying a parallel expression of *invA5* in *A. niger* and *A. oryzae*, the expression system had to be transferred into the new host strain *A. oryzae*. However, as the *A. oryzae* OP12 strain is now available as alternative to *A. niger*, it provides a useful addition of the toolbox of the TerR/*PterA* expression system (Figure 2).

Interestingly, the use of *A. niger* in biotechnological processes has been discussed controversially in the context of product safety. Many strains, which received a GRAS status for historic reasons showed significant production titres of fumonisin and ochratoxin. Related black aspergilli, such as *Aspergillus brasiliensis* or *Aspergillus acidus* were suggested as alternatives (Frisvad *et al.*, 2011). Remarkably, in the context of cross-chemistry, we identified a NRPS-like enzyme in the genome of *A. brasiliensis*, which produced atromentin under *in vitro* conditions. However, when the corresponding gene was homologously overexpressed, no atromentin but the same four cross-chemistry metabolites as described for *invA5* expression in *A. niger* were detected (Geib *et al.*, 2018a, manuscript submitted). Therefore, *A. brasiliensis* does not appear as a suitable replacement for *A. niger* to study the products formed from NRPS-like gene expression. However, it implies that cross-chemistry on benzoquinone structures appears common to the physiology of aspergilli from section *Nigri* and, moreover, indicates that atrofuranic acid may be the product formed in *A. brasiliensis* under natural inducing conditions of its intrinsic atromentin synthetase.

Besides problems in identifying the true nature of a metabolite due to a possible cross-chemistry event, there are also prospects arising from these events. Novel metabolites might be produced even from already characterised enzymes. Atrofuranic acid for example features a new core structure (Geib *et al.*, 2018a, manuscript submitted), which has not been previously described and might have interesting properties for pharmaceutical use.

Yet unpublished experiments further indicate that cross-chemistry effects are not limited to the atromentin synthetase InvA. Another quinone synthetase, TdiA, catalysing the second step in terrequinone A biosynthesis (Balibar, Howard-Jones and Walsh, 2007), also failed to produce its known primary compound of didemethylasterrequinone D when the *tdiA* gene was co-expressed with the gene of the aminotransferase *tdiD* heterologously in *A. niger* (Geib *et al.*, 2018b, in preparation). Again, several different compounds were extracted, but their structures have not been elucidated yet. Unfortunately, when the same expression construct was transferred to the *A. oryzae* expression platform, for yet unknown reasons no product was formed (Geib *et al.*, 2018b, in preparation). This indicates that *A. oryzae* might be limited in the

supply of indole pyruvate precursors required for biosynthesis of didemethylsterrequinone, but further studies are required on this aspect. However, as the *tdi*-gene cluster is well studied, it was possible to transfer the complete biosynthesis cluster in two steps as pseudo-polycistronic constructs into *A. niger*. The new metabolites that were produced from cross-chemistry events became partially prenylated by the DMATS TdiB (Schneider, Weber and Hoffmeister, 2008), which is highly interesting and needs further investigation as it implies that even cross-chemistry products can be taken as substrates in downstream modifications of a biosynthesis gene cluster (unpublished data). One gene of the cluster, *tdiE*, was reported to be non-essential, but its presence dramatically increased the terrequinone yield in the original host *A. nidulans*. So far, no function had been attributed to the gene product (Balibar, Howard-Jones and Walsh, 2007). Therefore, for the heterologous expression approach two different constructs *tdiC_tdiB_tdiE* and *tdiC_tdiB* had been assembled. Surprisingly only when the construct without *tdiE* was co-expressed in a *tdiA_tdiD* expression strain, the metabolites were modified (unpublished data). Constructs with *tdiE* did not alter the metabolite profile compare to the *tdiA_tdiD* expression alone, so that TdiE might act as quality control protein recognising and rejecting the incorrect substrate in TdiB and/ or TdiC (unpublished data).

Characterisation of NRPS-like enzymes from aspergilli section *Terrei*

The collaboration with Mikael Andersen (DTU Denmark) provided the unique opportunity to get access to genome data from species of section *Terrei*. Since most of this work specifically focussed on *A. terreus* combined with the discovery of the Asp-melanin pathway involving an NRPS-like enzyme, we had a special interest in analysing the spectrum of NRPS-like enzymes present in this section. Bioinformatics analysis of section *Terrei* genome sequences revealed that NRPS-like enzymes with a A-T-TE-domain structure are very common to this section. While these enzymes show a limited structural composition, a large variety of diverse products can be formed (Hühner *et al.*, 2018). To obtain an overview on the metabolites produced in section *Terrei*, we aimed in the heterologous expression of selected candidates of NRPS-like encoding genes. However, the first challenge was the selection of suitable candidates itself as the current knowledge on NRPS-like enzymes did not allow a prediction of the metabolite produced. Therefore, bioinformatics tools were applied to sort enzymes into distinct families with the hypothesis that enzymes from a specific family might produce the same product as shown for analysis of aspulvinone E synthetases from section *Terrei* (Theobald *et al.*, 2018, in preparation).

While the attribution to specific families showed value for some enzymes, such as butyrolactone IIa synthetases, especially the large family 12, which was assumed to contain members of the ApvA-type aspulvinone E synthetases, showed that the sorting approach was too crude. Besides aspulvinone E synthetases, this family contained atromentin, polyporic acid and phenguignardic acid synthetases. A more detailed look at the phylogenetic tree on these enzymes showed that a discrimination between the different enzymes into distinct families

might be possible, but a definition of the cut-off value may be difficult especially when there is no prior knowledge on the product formed (Geib *et al.*, 2018b, in preparation). Moreover, by including atromentin synthetases from basidiomycetes in the phylogenetic tree, a close relationship to atromentin synthetases from ascomycetes was neither observed from a tree that included the complete protein sequence nor from a tree solely based on the TE-domains. This has a striking consequence for the ability to predict products produced from NRPS-like enzymes. Genus borders seem to have a greater impact on the alignment than the product produced. Therefore, future studies will have to characterise NRPS-like enzymes from various fungal sources to search for specific sequence patterns within TE-domains that can be consistently attributed to the formation of a specific product. As the work here mainly focussed on aspergilli and more specifically on the section *Terrei*, performing such analyses is currently not possible (Geib *et al.*, 2018b, in preparation).

However, the identification of a putative polyporic acid synthetase is the first example of such an enzyme from ascomycetes. Since different products were obtained depending on the expression platform, this study confirmed that cross-chemistry occurs in *A. niger* on all quinone core structures deriving from NRPS-like enzymes (Geib *et al.*, 2018a, manuscript submitted). The identification of the specific metabolite produced is still pending, but it can be speculated that a furanic acid core might be produced. Besides that, polyporic acid, an inhibitor of the dihydroorotate dehydrogenase, has previously only been characterised from basidiomycetes (Stahlschmidt, 1877; Kraft *et al.*, 1998). Unfortunately, no reference polyporic acid synthetase from a basidiomycete has been identified yet, which would be important to support the speculation that genus borders give rise to a larger phylogenetic distance than a difference in the metabolite produced. One might speculate that a polyporic acid synthetase from a basidiomycete might show a closer phylogenetic relationship to an atromentin synthetase from basidiomycetes rather than to polyporic acid synthetases from ascomycetes.

Additionally, in the family of the butyrolactone IIa synthetases we identified a synthetase that produced the identical core structure but used phenylpyruvate rather than 4-hydroxyphenylpyruvate as substrate, which leads to the production of phenylbutyrolactone IIa. However, we must admit that NMR analyses are still pending to confirm this structure. However, if this prediction is correct, this study provides the first report of such an enzyme occurring naturally, although such an enzyme had previously generated by domain swapping experiments (van Dijk, Guo and Wang, 2016). Whether phenylbutyrolactone IIa has the same biological function as a quorum sensing molecule as identified for butyrolactone I in *A. terreus* (Schimmel, Coffman and Parsons, 1998) needs to be identified. Nevertheless, it can be assumed that naturally occurring domain swapping contributed to the large expansion of the number of NRPS-like enzymes in fungi.

In summary, this analysis provided a first insight on the large variety of different metabolites produced from NRPS-like enzymes in section *Terrei*. Sorting these enzymes in specific families

in respect to the products formed will require the knowledge from additionally characterised enzymes and especially those from basidiomycetes. Some of the enzymes heterologously expressed did not result in product formation, which may be either due to lack of the correct substrate or be due to non-functional proteins, which requires further analysis. However, overall, the heterologous expression systems in *A. niger* and *A. oryzae* proved highly valuable for this approach and should be considered when analysing additional NRPS-like enzymes.

Refinement of the TerR/*PterA* expression system toolbox

The TerR/*PterA* expression system was successfully constructed and proved as a valuable tool during different research projects described in this study. However, a system is never perfect and can be further developed to suit a multitude of applications.

Strain refinement

During heterologous expression of the gene coding for the aspulvinone E synthetase MelA from *A. terreus*, the enormous amounts of aspulvinone E produced by *A. niger* P2 was a burden to the fungus leading to a strongly reduced production of asexual conidia (Geib *et al.*, 2016). Since the expression was controlled by the amylase promoter, a sugar-free medium was required to reduce aspulvinone E production and to propagate the strain. However, the utilised casamino acid-based medium was not favoured by *A. niger*, resulting in strongly reduced growth rates. Therefore, the aim was to develop a more tightly controlled TerR/*PterA*-based expression system, which is independent from primary metabolism.

Different synthetic promoter systems are available for use in fungi, whereby one of the most sophisticated control system is the TetOn system (Meyer *et al.*, 2011; Helmschrott *et al.*, 2013; Wanka *et al.*, 2016). The induction of genetic elements placed under control of this inducible and fine-tuneable system relies on the addition of tetracycline or its analogues. To test if the combination of the tight control of TetOn with the strong induction of TerR/*PterA* exhibits the desired functionality, a TetOn:*terR* construct was assembled and transferred into *A. niger* A1144. The resulting strain with a single integration of the transcription factor was named ATNT16 (*A. niger* **A**1144 **T**et**O**n:*terR* transformant #16) (Figure 2) (Geib and Brock, 2017b). Indeed, the ATNT16 strain showed a tight regulation and dose-dependent induction of transcription, exceeding direct induction of genes of interest by TetOn elements by about five times as monitored by β -galactosidase activity assays. Highest induction was observed with 15 to 30 μ g/ml doxycycline (Geib and Brock, 2017b). The β -galactosidase production was at such a high level that normal growth rates were significantly reduced, which was most likely due to competition with synthesis of proteins required for normal cellular function. Therefore, these high doses of the inducer should only be used for expression of toxic metabolites after an induction-free period for the generation of biomass. For routine screenings a lower dose of doxycycline of about 10 μ g/ml or less and, therefore, lower induction levels should be favoured. In direct comparison with the first generation *PamyB:terR* expression system, induction rates

in the ATNT16 strain are not only tightly regulatable and titratable, but also exceed those of the P2 strain when more than 2 µg/ml doxycycline are used as inducer (Geib and Brock, 2017b).

Another drawback of the expression platforms P2, ATNT16 and OP12 (Figure 2) resulted from a shortage of selectable markers and low transformation efficiency. To boost number of transformants and to ease the selection and maintenance of positive transformants, the *pyrG* gene was deleted or inactivated in selected expression platform strains (Geib *et al.*, 2018a, manuscript submitted). Selection of transformants using auxotrophic markers, such as the orotidine-5'-phosphate decarboxylase PyrG is well established (He *et al.*, 2018). In *A. niger* P2 and ATNT16 a complete deletion of the intrinsic *pyrG* gene deletion was possible, whereas deletion attempts in *A. oryzae* OP12 failed. However, during cultivation in the presence of 5-fluoroorotic acid (5-FOA) a spontaneous mutation of *pyrG* was received that resulted in an inactivation of the gene product and allowed the use of uridine auxotrophy/prototrophy as selection marker in transformation approaches (Geib *et al.*, 2018a, manuscript submitted). While *pyrG*⁻ strains were successfully generated for *A. niger* and *A. oryzae* (Figure 2 – top panel), further problems occurred in *A. oryzae* when attempting to introduce a TetOn control. The TetOn regulatory system has already been successfully used in different aspergilli such as *A. niger* (Helmschrott *et al.*, 2013), *A. fumigatus* (Kalb *et al.*, 2015) and *A. terreus* (Sun, Guo and Wang, 2016), but preliminary analyses indicate that TetOn control in combination with TerR/*PterA* is not possible in *A. oryzae*, since the reverse transactivator appeared to be active even in the absence of doxycycline (data not shown).

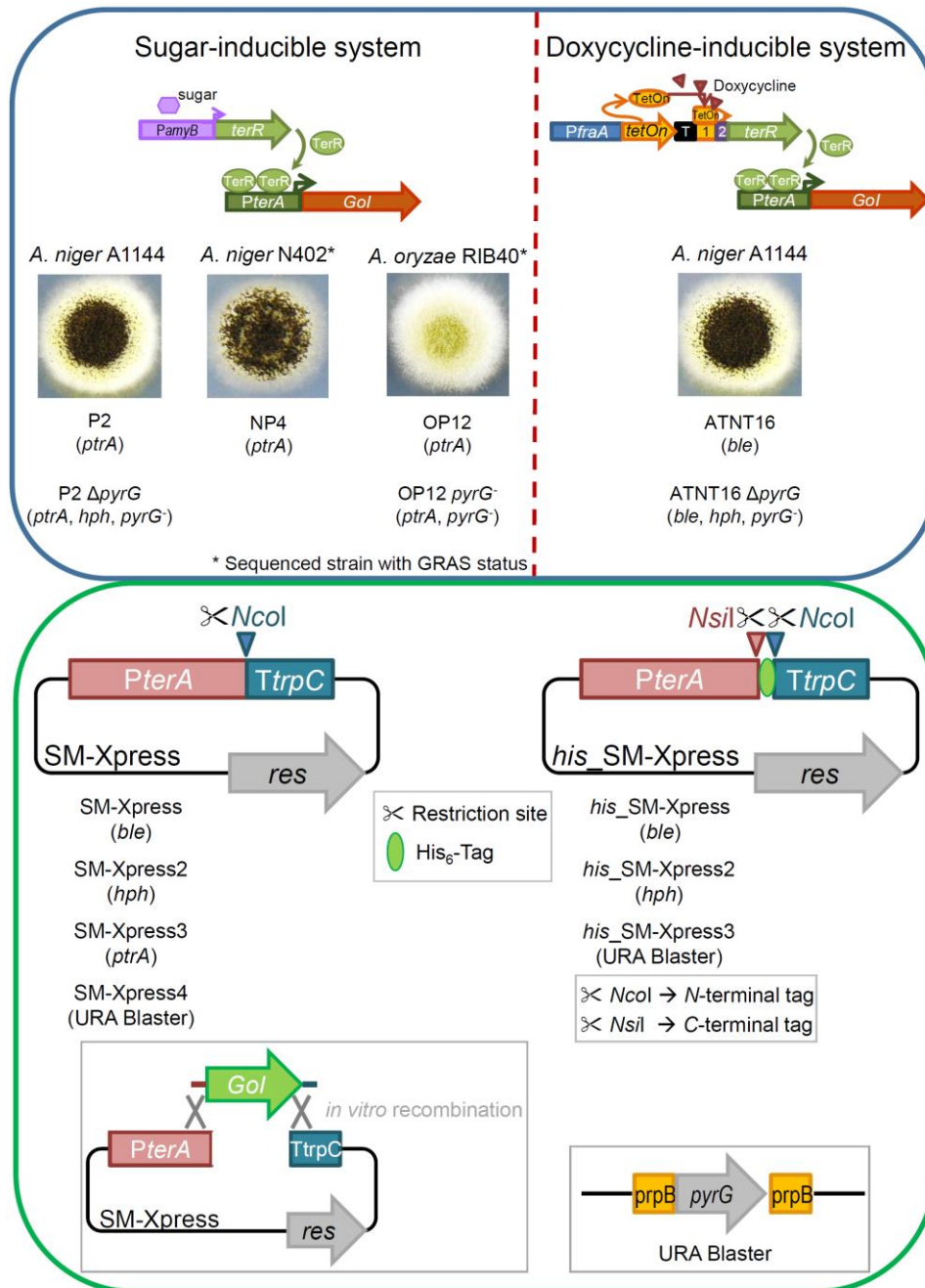


Figure 2: Current state of the TerR/PterA expression toolbox. Top panel – Available strains. On the left: sugar-inducible system. The expression of *terR* is controlled by the *A. oryzae* amylase promoter *PamyB*. Sugars in the medium will induce *terR* expression. TerR binds to the promoter of *terA* (*PterA*) with high specificity and drives expression of the gene of interest (*GoI*). On the right: doxycycline-inducible system. *PamyB* was replaced by the TetOn system. *PfraA* – constitutively active promoter of *fraA*. tetOn – reverse transactivator. T – terminator of *ergA*. 1 – tetOn responsive element. 2 – minimal *gpdA* promoter. Genes in brackets indicated selectable markers available for fungal transformation. Bottom panel – Available secondary metabolite (SM)-Xpress plasmids. *prpB* – partial sequence of the *prpB* gene in direct repeat. *ptrA* – pyrithiamine resistance gene. *hph* – hygromycin resistance gene. *ble* – phleomycin resistance gene. *pyrG* – orotidine-5'-phosphate decarboxylase gene. *res* – selection marker gene.

Not only the expression platform strains were developed and refined, but also the SM-Xpress set of plasmids. The first generation of SM-Xpress was a simple and easy-to-use plasmid: the sequence of a gene of interest is amplified with short overlapping sequences to a unique restriction site in the plasmid backbone that separates the promoter and terminator sequence. The final expression vector is then assembled by *in vitro* recombination (Figure 2 – bottom panel). Due to the unique overhangs at both ends, a directed gene cloning without further use of restriction and ligation is possible. The resulting expression plasmids are directly ready for fungal transformation since regulatory elements (*PterA*) and a selection marker (phleomycin resistance gene *ble*) were already part of SM-Xpress (Figure 2 – bottom panel). For the expression of multiple genes of interest or subsequent purification of proteins, a second generation of plasmids was required. The co-expression of both Asp-melanin pathway genes, *melaA* and *tyrP* was realised by a stepwise integration of genes into the genome of *A. niger* P2 (Geib *et al.*, 2016). For this purpose, a different selection marker for *tyrP* expression was essential. The replacement of the phleomycin resistance cassette *ble* by the hygromycin resistance gene *hph* resulted in SM-Xpress2 (Figure 2 – bottom panel). Further refinement by assembly of operon-like structures, with one promoter controlling expression of three genes separated by viral self-splicing peptide sequences, made a one-step reconstitution of the Asp-melanin pathway including a fluorescent marker possible (Geib and Brock, 2017b). To assemble this expression plasmid, the digested SM-Xpress vector was simultaneously incubated with the three inserts of the *melaA*, *tyrP* and *tdTomato* gene that contained individual overhangs for directed gene cloning and assembly.

For purification of heterologously produced proteins it is favourable to add a tag to the protein. In bacterial gene expression plasmids tag-sequences are readily available (for example Novagen pET-48, Merck Millipore) and are convenient since no additional tag-element needs to be added to the oligonucleotide during gene amplification. This was the inspiration for *his*_SM-Xpress, which encodes an *N*- or *C*-terminal His₆-tag (Geib *et al.*, 2016). The terminus at which the tag is added only depends on the restriction enzymes used to linearize the plasmid (*NcoI* for *N*-terminal tag or *NsiI* for *C*-terminal tag) (Figure 2 – bottom panel). Like the first and second-generation of SM-Xpress plasmids, this vector is available as a set with different selection markers.

Inactivation of *pyrG* in some of the expression approaches was a prerequisite for transformation using a *pyrG* containing URA-blaster cassette, which allows selection on uridine prototrophy in uridine-free medium. Additionally, it allowed the use of a marker recycling technique. As described in literature for gene deletions and disruptions a URA-blaster makes marker rescue events possible (Brock *et al.*, None). For marker recycling, a homologous recombination event is necessary. This is generally achieved by flanking a functional copy of *pyrG* with direct sequence repeats (Figure 2 – bottom panel). During cultivation on 5'-fluoroorotic acid (5-FOA)

containing medium, only individual strains that lost the *pyrG* gene are able to grow. As a result, colonies are *pyrG* negative but still carry the desired expression construct and are ready for another round of transformation. While the URA-blaster developed here provides an exquisite alternative for other resistance cassettes, it can only be used in *pyrG*⁻ strains.

Identification of biological targets of fungal secondary metabolites

Knowledge on the biological activity of fungal secondary metabolites is of high interest as it is a prerequisite for further exploitation of natural products and may explain why a specific compound is produced by the natural host. Natural product biosynthesis consumes a remarkable amount of energy and resources so that metabolites produced need to contribute to the overall fitness of the producer (Hartmann, 2008). Examples are the protection against biotic and abiotic stresses or acquisition of nutrients that are essential for survival and competitiveness in a hostile environment (Spiteller, 2008). However, while many research groups dealing with secondary metabolite biosynthesis put lots of efforts in isolation and elucidation of structures of novel secondary metabolites, reports on naturally inducing conditions of biosynthesis gene cluster or bioactivities of metabolites in the ecological context of the fungus remain rare (Spiteller, 2015a).

As presented in this work, terrein is produced by *A. terreus* in high quantities and possesses phytotoxic, iron reducing and anti-fungal properties, which perfectly suits its lifestyle as a saprophyte in the rhizosphere (Zaehle *et al.*, 2014; Gressler *et al.*, 2015b). Furthermore, the work on Asp-melanin in *A. terreus* conidia showed that it confers UV protection and reduces the attraction for predatory soil amoeba to engulf conidia (Geib *et al.*, 2016). The use of the heterologous expression system contributed to the understanding of an induced defence mechanism of the higher fungus BY1. In this study, it was only possible through production of the previously uncharacterised wound-activated PKS PPS1 from the fungus BY1 in *A. niger* P2 to isolate and understand the function of two novel polyketides (Brandt *et al.*, 2017).

However, metabolites are also a valuable treasure chest outside their biological context. For example, the depsipeptide cyclosporine A did not get famous because of its insecticidal properties, but for its immune modulatory effects in humans (Spiteller, 2015a). The use of this agent after organ transplantation revolutionised medicine (Venuta and Van Raemdonck, 2017). Furthermore, the beneficial effects of fungal natural products on humans were already recognised in ancient times; the ice mummy Ötzi carried fruiting bodies of *Piptoporus betulinus* (Capasso, 1998). It has now been (re-)discovered that secondary metabolites of this fungus have antibiotic and purgative effects. In Ötzi's time finding cures and remedies from natural sources was a trial and error study as laboratory experiments were not developed. Nowadays, the search for bioactive compounds is more systematic and high-throughput screening methods are applied (Schmid *et al.*, 1999). However, the interest by pharmaceutical companies for such screenings is declining due to high costs for evaluating compounds (Camp *et al.*, 2012). Therefore, a

targeted approach is necessary to stimulate the interest in the identification of compounds for pharmacological exploitation.

In a collaborative study an *in silico* modelling of potential targets of atromentin, one of the fungal NRPS-like products described in this work, revealed two cellular targets (Dellafiora *et al.*, 2018, in revision). One target derived from estrogen receptors, for which a weak inhibitory activity was predicted. Indeed, *in vitro* testing confirmed this weak estrogenic activity, which indicates the suitability of these model calculations. The second target identified in this study was the 17- β -hydroxysteroid dehydrogenase for which efficient binding was predicted (Dellafiora *et al.*, 2018, in revision). Unfortunately, the respective enzyme was not amenable to *in vitro* testing and therefore inhibitory effects were not confirmed in wet-lab experiments. However, it appears that the combination of *in silico* and *in vitro* methods depict a powerful tool to identify cellular targets of secondary metabolites for further development as potential new pharmaceuticals.

This *in silico* approach also sounds interesting for the identification of possible applications for other natural products, including the yet hardly characterised NRPS-like-derived metabolites. For bis-indoylquinones it is known that they possess cytotoxic, anti-diabetic and antiretroviral effects (Schneider, Weber and Hoffmeister, 2008). Also, other classes of NRPS-like products, such as the furanone core structure containing isoaspulvinone E, show antiviral effects (Gao *et al.*, 2013). Highly hydroxylated terphenylquinones can inhibit signal cascades that are essential in metastatic tumour types (Puder *et al.*, 2005). All these findings mark NRPS-like products as highly active biological agents and it is likely that more targets will be identified by *in silico* modelling combined by *in vitro* testing.

Summary and outlook

In summary, in this work a heterologous expression system for the recombinant production of secondary metabolites from fungal sources was established and refined. This system allows the rapid characterization of key genes from secondary metabolism, which is of high value considering the vast number of secondary metabolite biosynthesis gene clusters identified from fungal genome sequencing projects. However, as visualized in this study, care must be taken on the interpretation of data obtained from heterologous expression approaches. As shown for the heterologous expression of atromentin synthetases in *A. niger*, cross-chemistry may lead to the production of modified compounds with different characteristics compared to the natural metabolite produced by the host organism. Therefore, it is recommended to simultaneously express genes of interest in different expression hosts and, if possible, perform a further characterization by *in vitro* assays. This was realized in this study by establishing *A. oryzae* as an alternative expression platform and by adding *N*- or *C*-terminal tags to enable the rapid purification of the proteins produced.

The heterologous expression platforms established in this research were of tremendous importance for the identification of a new type of melanin formed in aspergilli of the section *Terrei*. By expressing the genes coding for the NRPS-like enzyme MelA and the tyrosinase TyrP it was possible to reconstitute Asp-Melanin biosynthesis from *A. terreus* in the heterologous expression host *A. niger* and to reconstitute biosynthesis under *in vitro* conditions by using purified recombinant enzymes. Further characterization of colour and albino mutants from *A. terreus* revealed that Asp-Melanin has different properties compared to DHN-melanin, which is generally present in conidia of *Aspergillus* species outside the section *Terrei*. While the protective properties of Asp-Melanin seem to be less pronounced than those from DHN-melanin, the reduced phagocytosis by amoeba mediated by Asp-Melanin might be an advantageous property that directed the evolution towards this different type of melanin. Our studies further indicate that Asp-Melanin formation is common to the section *Terrei*, but species with larger phylogenetic distance to *A. terreus* either contain both types of melanin (*Aspergillus ambiguus*) or no melanin type at all (*Aspergillus neoindicus*). Therefore, one might speculate that DHN-melanin is a more ancient mechanism to protect conidia, which was lost in the section *Terrei* and replaced by Asp-Melanin as it appears more suitable to support the physiology and life style of these soil-dwelling species.

The heterologous expression system was also optimised for a fine-tuneable expression by including the TetOn system for control of *terR* expression. This will be of high value to produce metabolites that possess antifungal properties. It allows growth of the expression platform without induction of gene expression. Once biomass is formed metabolite production can be initiated. By further including viral self-cleaving peptide sequences, the system can not only be successfully used for the heterologous expression of individual genes, but also for the expression of whole biosynthesis gene clusters. This has been shown by the simultaneous expression of the two genes from Asp-Melanin production in combination with a fluorescent marker protein. Future studies will use this system to characterise additional products formed from NRPS-like enzymes and to investigate the modifications performed by enzymes from genes surrounding an NRPS-like enzyme coding gene in biosynthesis gene clusters.

A CRISPR/Cas9 system has been successfully applied to various fungi (Nødvig *et al.*, 2015) and use of such a system could complement the current version of the fungal expression platform systems described in this thesis. With the guidance of sgRNA genes of interest can easily be placed at a specific, highly transcribed locus in the genome to realise a steady gene expression. The CRISPR/Cas9 tool does not only enable gene insertions, but can also be used for gene editing to introduce mutations or even swapping of domains between individual secondary metabolism genes. This is of high interest for modification of binding site in the *PterA* promoter region as well as for targeted mutation of NRPS-like genes.

This study also investigated some additional, previously uncharacterised NRPS-like enzymes. By applying bioinformatics tools, NRPS-like enzymes were classified in families and

individual enzymes were selected to study the products formed. While for some families, such as NRPS-like enzymes involved in Asp-Melanin formation, this *in silico* prediction was valuable, in other families the predictions and the actual metabolite formed did not match. This indicates that prior knowledge is required to train computer-based algorithms with information for correct product prediction. To obtain this knowledge, more wet-lab experiments are required, and the metabolites produced and identified in this study form a first basis for the required information.

Overall, heterologous expression is of high value to identify novel compounds of potential pharmaceutical interest. The systems described here will support the identification of novel metabolites and, by cross-chemistry, may even lead to compounds that are not produced by the natural host strain, which increases the portfolio of metabolites for further exploitation. The identification and characterisation of novel products from previously neglected NRPS-like enzymes shows the high potential of these metabolites for the identification of lead structures for pharmaceutical exploitation and seems worth to be studied in future projects.

References

- Albuquerque, P., and Casadevall, A. (2012). Quorum sensing in fungi--a review. *Med. Mycol.* 50, 337-45
- Arai, K., Rawlings, B.J., Yoshizawa, Y., and Vederas, J.C. (1989). Biosyntheses of antibiotic A26771B by *Penicillium turbatum* and dehydrocurvularin by *Alternaria cinerariae*: comparison of stereochemistry of polyketide and fatty acid enoyl thiol ester reductases. *J. Am. Chem. Soc.* 111, 3391-9
- Baker, S. (2008). *Aspergillus* genomics and DHN-melanin conidial pigmentation. In *Aspergillus in the Genomic Era* (Wageningen Academic Publishers).
- Balajee, S.A., Baddley, J.W., Peterson, S.W., Nickle, D., Varga, J., Boey, A., Lass-Flörl, C., Frisvad, J.C., and and, R.A.S. (2009). *Aspergillus alabamensis*, a new clinically relevant species in the section *Terrei*. *Eukaryot. Cell* 8, 713-22
- Balibar, C.J., Howard-Jones, A.R., and Walsh, C.T. (2007). Terrequinone A biosynthesis through L-tryptophan oxidation, dimerization and bisprenylation. *Nat. Chem. Biol.* 3, 584-92
- Barth, G., and Gaillardin, C. (1997). Physiology and genetics of the dimorphic fungus *Yarrowia lipolytica*. *FEMS Microbiol. Rev.* 19, 219-37
- Barton, D.H.R., and Miller, E. (1955). The constitution and stereochemistry of terrein. *Journal of the Chemical Society (Resumed)*, 1028
- Bengtson, S., Rasmussen, B., Ivarsson, M., Muhling, J., Broman, C., Marone, F., Stampanoni, M., and Bekker, A. (2017). Fungus-like mycelial fossils in 2.4-billion-year-old vesicular basalt. *Nature Ecology & Evolution* 1, 141
- Benocci, T., Aguilar-Pontes, M.V., Zhou, M., Seiboth, B., and de Vries, R.P. (2017). Regulators of plant biomass degradation in ascomycetous fungi. *Biotechnol. Biofuels* 10, 152
- Berbee, M.L., James, T.Y., and Strullu-Derrien, C. (2017). Early Diverging Fungi: Diversity and Impact at the Dawn of Terrestrial Life. *Annu. Rev. Microbiol.* 71, 41-60
- Bergmann, S., Schümann, J., Scherlach, K., Lange, C., Brakhage, A.A., and Hertweck, C. (2007). Genomics-driven discovery of PKS-NRPS hybrid metabolites from *Aspergillus nidulans*. *Nat. Chem. Biol.* 3, 213-7
- Bergmann, S., Funk, A.N., Scherlach, K., Schroeckh, V., Shelest, E., Horn, U., Hertweck, C., and Brakhage, A.A. (2010). Activation of a silent fungal polyketide biosynthesis pathway through regulatory cross talk with a cryptic nonribosomal peptide synthetase gene cluster. *Appl. Environ. Microb.* 76, 8143-9
- Besl, H., Bresinsky, A., Steglich, W., and Zipfel, K. (1973). Pilzpigmente, XVII. Über Gyrocyanin, das blauende Prinzip des Kornblumenröhrlings (*Gyroporus cyanescens*), und eine oxidative Ringverengung des Atromentins. *Chem. Ber.* 106, 3223-9
- Birch, A.J., Cassera, A., and Jones, A.R. (1965). The biosynthesis of terrein. *Chemical Communications (London)*, 167
- Blin, K., Wolf, T., Chevrette, M.G., Lu, X., Schwalen, C.J., Kautsar, S.A., Suarez Duran, H.G., de Los Santos, E.L.C., Kim, H.U., Nave, M. *et al.* (2017). antiSMASH 4.0-improvements in chemistry prediction and gene cluster boundary identification. *Nucleic Acids Res.* 45, W36-W41
- Blum, G., Hörtnagl, C., Jukic, E., Erbeznik, T., Pümpel, T., Dietrich, H., Nagl, M., Speth, C., Rambach, G., and Lass-Flörl, C. (2013). New insight into amphotericin B resistance in *Aspergillus terreus*. *Antimicrob. Agents Ch.* 57, 1583-8

- Blumhoff, M., Steiger, M.G., Marx, H., Mattanovich, D., and Sauer, M. (2013). Six novel constitutive promoters for metabolic engineering of *Aspergillus niger*. *Appl. Microbiol. Biot.* 97, 259-67
- Bode, H.B., Bethe, B., Höfs, R., and Zeeck, A. (2002). Big effects from small changes: possible ways to explore nature's chemical diversity. *Chembiochem*, 3, 619-27
- Boettger, D., and Hertweck, C. (2013). Molecular diversity sculpted by fungal PKS-NRPS hybrids. *Chembiochem*, 14, 28-42
- Bok, J.W., and Keller, N.P. (2004). *LaeA*, a regulator of secondary metabolism in *Aspergillus* spp. *Eukaryot. Cell* 3, 527-35
- Bok, J.W., Hoffmeister, D., Maggio-Hall, L.A., Murillo, R., Glasner, J.D., and Keller, N.P. (2006). Genomic mining for *Aspergillus* natural products. *Chem. Biol.* 13, 31-7
- Bok, J.W., Ye, R., Clevenger, K.D., Mead, D., Wagner, M., Krerowicz, A., Albright, J.C., Goering, A.W., Thomas, P.M., Kelleher, N.L. *et al.* (2015). Fungal artificial chromosomes for mining of the fungal secondary metabolome. *BMC Genomics* 16, 343
- Bonfante, P., and Requena, N. (2011). Dating in the dark: how roots respond to fungal signals to establish arbuscular mycorrhizal symbiosis. *Curr. Opin. Plant Biol.* 14, 451-7
- Braga, G.U.L., Rangel, D.E.N., Fernandes, É.K.K., Flint, S.D., and Roberts, D.W. (2015). Molecular and physiological effects of environmental UV radiation on fungal conidia. *Curr. Genet.* 61, 405-25
- Brakhage, A.A. (2013). Regulation of fungal secondary metabolism. *Nat. Rev. Microbiol.* 11, 21-32
- Brandenburger, E., Gressler, M., Leonhardt, R., Lackner, G., Habel, A., Hertweck, C., Brock, M., and Hoffmeister, D. (2017). A highly conserved basidiomycete peptide synthetase produces a trimeric hydroxamate siderophore. *Appl. Environ. Microb.* 21, e01478-17
- Brandt, P., García-Altare, M., Nett, M., Hertweck, C., and Hoffmeister, D. (2017). Induced chemical defense of a mushroom by a double-bond-shifting polyene synthase. *Angew. Chem. Int. Ed.* 56, 5937-41
- Brock, M., Gehrke, A., Sugareva, V., and Brakhage, A.A. (2007). Promoter Analysis and Generation of Knock-out Mutants in *Aspergillus fumigatus*. In *Medical Mycology* (John Wiley & Sons, Ltd), pp. 231-56.
- Bud, R. (2007). *Penicillin: triumph and tragedy* (Oxford University Press on Demand).
- Butler, M.S. (2004). The role of natural product chemistry in drug discovery. *J. Nat. Prod.* 67, 2141-53
- Camp, D., Davis, R.A., Evans-Illidge, E.A., and Quinn, R.J. (2012). Guiding principles for natural product drug discovery. *Future Med. Chem.* 4, 1067-84
- Campbell, C.D., and Vederas, J.C. (2010). Biosynthesis of lovastatin and related metabolites formed by fungal iterative PKS enzymes. *Biopolymers* 93, 755-63
- Capasso, L. (1998). 5300 years ago, the Ice Man used natural laxatives and antibiotics. *Lancet* (London, England) 352, 1864
- Chai, L.Y.A., Netea, M.G., Sugui, J., Vonk, A.G., van de Sande, W.W.J., Warris, A., Kwon-Chung, K.J., and Kullberg, B.J. (2010). *Aspergillus fumigatus* conidial melanin modulates host cytokine response. *Immunobiology* 215, 915-20
- Chen, Y., Wang, S., Shen, H., Yao, X., Zhang, F., and Lai, D. (2014). The marine-derived fungal metabolite, terrein, inhibits cell proliferation and induces cell cycle arrest in human ovarian cancer cells. *Int. J. Mol. Med.* 34, 1591-8

- Chiang, Y., Szewczyk, E., Davidson, A.D., Keller, N., Oakley, B.R., and Wang, C.C.C. (2009). A gene cluster containing two fungal polyketide synthases encodes the biosynthetic pathway for a polyketide, asperfuranone, in *Aspergillus nidulans*. *J. Am. Chem. Soc.* 131, 2965-70
- Chiang, Y., Oakley, C.E., Ahuja, M., Entwistle, R., Schultz, A., Chang, S., Sung, C.T., Wang, C.C.C., and Oakley, B.R. (2013). An efficient system for heterologous expression of secondary metabolite genes in *Aspergillus nidulans*. *J. Am. Chem. Soc.* 135, 7720-31
- Clevenger, K.D., Bok, J.W., Ye, R., Miley, G.P., Verdan, M.H., Velk, T., Chen, C., Yang, K., Robey, M.T., Gao, P. *et al.* (2017). A scalable platform to identify fungal secondary metabolites and their gene clusters. *Nat. Chem. Biol.* 13, 895-901
- Clutterbuck, P.W., Raistrick, H., and Reuter, F. (1937). Studies in the biochemistry of microorganisms: The molecular constitution of terrein, a metabolic product of *Aspergillus terreus* Thom. *Biochem. J.* 31, 987-1002
- Curran, K.A., Morse, N.J., Markham, K.A., Wagman, A.M., Gupta, A., and Alper, H.S. (2015). Short synthetic terminators for improved heterologous gene expression in yeast. *ACS Synthetic Biology* 4, 824-32
- Dean, R., Van Kan, J.A.L., Pretorius, Z.A., Hammond-Kosack, K.E., Di Pietro, A., Spanu, P.D., Rudd, J.J., Dickman, M., Kahmann, R., Ellis, J. *et al.* (2012). The Top 10 fungal pathogens in molecular plant pathology. *Mol. Plant Pathol.* 13, 414-30
- Dellafiora, L., Aichinger, G., Geib, E., Sánchez-Barrionuevo, L., Brock, M., Cánovas, D., Dall'Asta, C., and Marko, D. (2018). Hybrid *in silico/in vitro* target fishing to assign function to “orphan” compounds of food origin – the case of the fungal metabolite atromentin. *Food Chem. in revision*
- van Dijk, J.W.A., Guo, C., and Wang, C.C.C. (2016). Engineering fungal nonribosomal peptide synthetase-like enzymes by heterologous expression and domain swapping. *Org. Lett.* 18, 6236-9
- Dittmann, J., Wenger, R.M., Kleinkauf, H., and Lawen, A. (1994). Mechanism of cyclosporin A biosynthesis. Evidence for synthesis via a single linear undecapeptide precursor. *The J Biol Chem* 269, 2841-6
- Doolittle, R.F., Feng, D.F., Tsang, S., Cho, G., and Little, E. (1996). Determining divergence times of the major kingdoms of living organisms with a protein clock. *Science* 271, 470-7
- Eisenman, H.C., and Casadevall, A. (2012). Synthesis and assembly of fungal melanin. *Appl. Microbiol. Biot.* 93, 931-40
- Fleissner, A., and Dersch, P. (2010). Expression and export: recombinant protein production systems for *Aspergillus*. *Appl. Microbiol. Biot.* 87, 1255-70
- Flores, C., and Gancedo, C. (2005). *Yarrowia lipolytica* mutants devoid of pyruvate carboxylase activity show an unusual growth phenotype. *Eukaryot. Cell* 4, 356-64
- Forseth, R.R., Amaike, S., Schwenk, D., Affeldt, K.J., Hoffmeister, D., Schroeder, F.C., and Keller, N.P. (2013). Homologous NRPS-like gene clusters mediate redundant small-molecule biosynthesis in *Aspergillus flavus*. *Angew. Chem. Int. Ed.* 52, 1590-4
- Frisvad, J.C., Larsen, T.O., Thrane, U., Meijer, M., Varga, J., Samson, R.A., and Nielsen, K.F. (2011). Fumonisin and ochratoxin production in industrial *Aspergillus niger* strains. *Plos One* 6, e23496
- Fujii, I., Ono, Y., Tada, H., Gomi, K., Ebizuka, Y., and Sankawa, U. (1996). Cloning of the polyketide synthase gene atX from *Aspergillus terreus* and its identification as the 6-

- methylsalicylic acid synthase gene by heterologous expression. *Mol. Gen. Genet.* 253, 1-10
- Fujii, I., Yasuoka, Y., Tsai, H., Chang, Y.C., Kwon-Chung, K.J., and Ebizuka, Y. (2004). Hydrolytic polyketide shortening by *ayg1p*, a novel enzyme involved in fungal melanin biosynthesis. *J. Biol. Chem.* 279, 44613-20
- Gachomo, E.W., Seufferheld, M.J., and Kotchoni, S.O. (2010). Melanization of appressoria is critical for the pathogenicity of *Diplocarpon rosae*. *Mol. Biol. Rep.* 37, 3583-91
- Galanie, S., Thodey, K., Trenchard, I.J., Filsinger Interrante, M., and Smolke, C.D. (2015). Complete biosynthesis of opioids in yeast. *Science* 349, 1095-100
- Gao, H., Guo, W., Wang, Q., Zhang, L., Zhu, M., Zhu, T., Gu, Q., Wang, W., and Li, D. (2013). Aspulvinones from a mangrove rhizosphere soil-derived fungus *Aspergillus terreus* Gwq-48 with anti-influenza A viral (H1N1) activity. *Bioorg. Med. Chem. Lett.* 23, 1776-8
- Geib, E., Gressler, M., Viediernikova, I., Hillmann, F., Jacobsen, I.D., Nietzsche, S., Hertweck, C., and Brock, M. (2016). A non-canonical melanin biosynthesis pathway protects *Aspergillus terreus* conidia from environmental stress. *Cell Chemical Biology* 23, 587-97
- Geib, E., and Brock, M. (2017a). Comment on: "Melanisation of *Aspergillus terreus*-Is butyrolactone I involved in the regulation of both DOPA and DHN types of pigments in submerged culture? *Microorganisms* 2017, 5, 22". *Microorganisms* 5(2), 34
- Geib, E., and Brock, M. (2017b). ATNT: an enhanced system for expression of polycistronic secondary metabolite gene clusters in *Aspergillus niger*. *Fungal Biol. Biotechnol.* 4, 13
- Geib, E., Baldeweg, F., Nett, M., and Brock, M. (2018a). Cross-chemistry leads to product diversity from atromentin synthetases in aspergilli from section *Nigri*. manuscript submitted
- Geib, E., Theobald, S., Andersen, M.R., and Brock, M. (2018b). Recombinant expression and characterisation of NRPS-like enzymes from *Aspergillus* species section *Terrei*. in preparation
- Gerhards, N., Neubauer, L., Tudzynski, P., and Li, S. (2014). Biosynthetic pathways of ergot alkaloids. *Toxins* 6, 3281-95
- Goldman, G.H., and Osmani, S.A. (2007). The aspergilli: genomics, medical aspects, biotechnology, and research methods. (CRC press), pp. 429-39.
- Gossen, M., and Bujard, H. (1993). Anhydrotetracycline, a novel effector for tetracycline controlled gene expression systems in eukaryotic cells. *Nucleic Acids Res.* 21, 4411-2
- Gressler, M., Zaehle, C., Scherlach, K., Hertweck, C., and Brock, M. (2011). Multifactorial induction of an orphan PKS-NRPS gene cluster in *Aspergillus terreus*. *Chem. Biol.* 18, 198-209
- Gressler, M., Hortschansky, P., Geib, E., and Brock, M. (2015a). A new high-performance heterologous fungal expression system based on regulatory elements from the *Aspergillus terreus* terrein gene cluster. *Front Microbiol.* 6, 184
- Gressler, M., Meyer, F., Heine, D., Hortschansky, P., Hertweck, C., and Brock, M. (2015b). Phytotoxin production in *Aspergillus terreus* is regulated by independent environmental signals. *eLife* 4
- Grigoriev, I.V., Nikitin, R., Haridas, S., Kuo, A., Ohm, R., Otiillar, R., Riley, R., Salamov, A., Zhao, X., Korzeniewski, F. *et al.* (2014). MycoCosm portal: gearing up for 1000 fungal genomes. *Nucleic Acids Res.* 42, D699-704

- Guo, C., Knox, B.P., Chiang, Y., Lo, H., Sanchez, J.F., Lee, K., Oakley, B.R., Bruno, K.S., and Wang, C.C.C. (2012). Molecular genetic characterization of a cluster in *A. terreus* for biosynthesis of the meroterpenoid terretonin. *Org. Lett.* 14, 5684-7
- Guo, C., Knox, B.P., Sanchez, J.F., Chiang, Y., Bruno, K.S., and Wang, C.C.C. (2013). Application of an efficient gene targeting system linking secondary metabolites to their biosynthetic genes in *Aspergillus terreus*. *Org. Lett.* 15, 3562-5
- Guo, C., Yeh, H., Chiang, Y., Sanchez, J.F., Chang, S., Bruno, K.S., and Wang, C.C.C. (2013). Biosynthetic pathway for the epipolythiodioxopiperazine acetylaranotin in *Aspergillus terreus* revealed by genome-based deletion analysis. *J. Am. Chem. Soc.* 135, 7205-13
- Guo, C., Sun, W., Bruno, K.S., and Wang, C.C.C. (2014). Molecular genetic characterization of terreic acid pathway in *Aspergillus terreus*. *Org. Lett.* 16, 5250-3
- Haas, H. (2014). Fungal siderophore metabolism with a focus on *Aspergillus fumigatus*. *Nat. Prod. Rep.* 31, 1266-76
- Hamed, R.B., Gomez-Castellanos, J.R., Henry, L., Ducho, C., McDonough, M.A., and Schofield, C.J. (2013). The enzymes of β -lactam biosynthesis. *Nat. Prod. Rep.* 30, 21-107
- Hansen, B.G., Salomonsen, B., Nielsen, M.T., Nielsen, J.B., Hansen, N.B., Nielsen, K.F., Regueira, T.B., Nielsen, J., Patil, K.R., and Mortensen, U.H. (2011). Versatile enzyme expression and characterization system for *Aspergillus nidulans*, with the *Penicillium brevicompactum* polyketide synthase gene from the mycophenolic acid gene cluster as a test case. *Appl. Environ. Microb.* 77, 3044-51
- Hartmann, T. (2008). The lost origin of chemical ecology in the late 19th century. *P. Natl. Acad. Sci. Usa.* 105, 4541-6
- He, Y., Wang, B., Chen, W., Cox, R.J., He, J., and Chen, F. (2018). Recent advances in reconstructing microbial secondary metabolites biosynthesis in *Aspergillus* spp. *Biotechnol. Adv.* 36, 739-83
- van der Heijden, M.G.A., Martin, F.M., Selosse, M., and Sanders, I.R. (2015). Mycorrhizal ecology and evolution: the past, the present, and the future. *New Phytol.* 205, 1406-23
- Helfrich, E.J.N., Reiter, S., and Piel, J. (2014). Recent advances in genome-based polyketide discovery. *Curr. Opin. Biotech.* 29, 107-15
- Helmschrott, C., Sasse, A., Samantaray, S., Krappmann, S., and Wagener, J. (2013). Upgrading fungal gene expression on demand: improved systems for doxycycline-dependent silencing in *Aspergillus fumigatus*. *Appl. Environ. Microb.* 79, 1751-4
- Henrikson, J.C., Hoover, A.R., Joyner, P.M., and Cichewicz, R.H. (2009). A chemical epigenetics approach for engineering the *in situ* biosynthesis of a cryptic natural product from *Aspergillus niger*. *Org. Biomol. Chem.* 7, 435-8
- Hertweck, C. (2009). The biosynthetic logic of polyketide diversity. *Angew. Chem. Int. Ed.* 48, 4688-716
- Hill, R.A., Carter, R.H., and Staunton, J. (1981). Biosynthesis of fungal metabolites. Terrein, a metabolite of *Aspergillus terreus* Thom. *J. Chem. Soc., Perkin Trans.* 1, 2570
- Homer, C.M., Summers, D.K., Goranov, A.I., Clarke, S.C., Wiesner, D.L., Diedrich, J.K., Moresco, J.J., Toffaletti, D., Upadhyya, R., Caradonna, I. *et al.* (2016). Intracellular action of a secreted peptide required for fungal virulence. *Cell Host Microbe* 19, 849-64
- Hornby, J.M., Jensen, E.C., Lise, A.D., Tasto, J.J., Jahnke, B., Shoemaker, R., Dussault, P., and Nickerson, K.W. (2001). Quorum sensing in the dimorphic fungus *Candida albicans* is mediated by farnesol. *Appl. Environ. Microb.* 67, 2982-92

- Howard, R.J., and Valent, B. (1996). Breaking and entering: host penetration by the fungal rice blast pathogen *Magnaporthe grisea*. *Annu. Rev. Microbiol.* 50, 491-512
- Huang, X., Liang, Y., Yang, Y., and Lu, X. (2017). Single-step production of the simvastatin precursor monacolin J by engineering of an industrial strain of *Aspergillus terreus*. *Metab. Eng.* 42, 109-114
- Hur, G.H., Vickery, C.R., and Burkart, M.D. (2012). Explorations of catalytic domains in non-ribosomal peptide synthetase enzymology. *Nat. Prod. Rep.* 29, 1074-98
- Hühner, E., Backhaus, K., Kraut, R., and Li, S. (2018). Production of α -keto carboxylic acid dimers in yeast by overexpression of NRPS-like genes from *Aspergillus terreus*. *Appl. Microbiol. Biot.* 102, 1663-72
- Kalb, D., Heinekamp, T., Lackner, G., Scharf, D.H., Dahse, H., Brakhage, A.A., and Hoffmeister, D. (2015). Genetic engineering activates biosynthesis of aromatic fumaric acid amides in the human pathogen *Aspergillus fumigatus*. *Appl. Environ. Microb.* 81, 1594-600
- Kanemori, Y., Gomi, K., Kitamoto, K., Kumagai, C., and Tamura, G. (1999). Insertion analysis of putative functional elements in the promoter region of the *Aspergillus oryzae* Taka-amylase A gene (*amyB*) using a heterologous *Aspergillus nidulans amdS-lacZ* fusion gene system. *Biosci. Biotechnol. Biochem.* 63, 180-3
- Kasorn, A., Loison, F., Kangsamaksin, T., Jongrungruangchok, S., and Ponglikitmongkol, M. (2018). Terrein inhibits migration of human breast cancer cells via inhibition of the Rho and Rac signaling pathways. *Oncol. Rep.* 39, 1378-86
- Kato, J., Funai, N., Watanabe, H., Ohnishi, Y., and Horinouchi, S. (2007). Biosynthesis of γ -butyrolactone autoregulators that switch on secondary metabolism and morphological development in *Streptomyces*. *P. Natl. Acad. Sci. Usa.* 104, 2378-83
- Kealey, J.T., Liu, L., Santi, D.V., Betlach, M.C., and Barr, P.J. (1998). Production of a polyketide natural product in nonpolyketide-producing prokaryotic and eukaryotic hosts. *P. Natl. Acad. Sci. Usa.* 95, 505-9
- Keller, N.P., Turner, G., and Bennett, J.W. (2005). Fungal secondary metabolism - from biochemistry to genomics. *Nat. Rev. Microbiol.* 3, 937-47
- Kennedy, J., Auclair, K., Kendrew, S.G., Park, C., Vederas, J.C., and Hutchinson, C.R. (1999). Modulation of polyketide synthase activity by accessory proteins during lovastatin biosynthesis. *Science* 284, 1368-72
- Khalidi, N., Seifuddin, F.T., Turner, G., Haft, D., Nierman, W.C., Wolfe, K.H., and Fedorova, N.D. (2010). SMURF: Genomic mapping of fungal secondary metabolite clusters. *Fungal Genet. Biol.* 47, 736-41
- Kim, J.H., Lee, S., Li, L., Park, H., Park, J., Lee, K.Y., Kim, M., Shin, B.A., and Choi, S. (2011). High cleavage efficiency of a 2A peptide derived from porcine teschovirus-1 in human cell lines, zebrafish and mice. *Plos One* 6, e18556
- Kraft, J., Bauer, S., Keilhoff, G., Miersch, J., Wend, D., Riemann, D., Hirschelmann, R., Holzhausen, H.J., and Langner, J. (1998). Biological effects of the dihydroorotate dehydrogenase inhibitor polyporic acid, a toxic constituent of the mushroom *Haploporus rutilans*, in rats and humans. *Arch. Toxicol.* 72, 711-21
- Köhler, J.R., Casadevall, A., and Perfect, J. (2014). The spectrum of fungi that infects humans. *Cold Spring Harbor Perspectives in Medicine* 5, a019273

- Langfelder, K., Jahn, B., Gehringer, H., Schmidt, A., Wanner, G., and Brakhage, A.A. (1998). Identification of a polyketide synthase gene (*pksP*) of *Aspergillus fumigatus* involved in conidial pigment biosynthesis and virulence. *Med. Microbiol. Immun.* 187, 79-89
- Lass-Flörl, C., Griff, K., Mayr, A., Petzer, A., Gastl, G., Bonatti, H., Freund, M., Kropshofer, G., Dierich, M.P., and Nachbaur, D. (2005). Epidemiology and outcome of infections due to *Aspergillus terreus*: 10-year single centre experience. *Brit. J. Haematol.* 131, 201-7
- Latgé, J.P. (1999). *Aspergillus fumigatus* and aspergillosis. *Clin. Microbiol. Rev.* 12, 310-50
- Lazarus, C.M., Williams, K., and Bailey, A.M. (2014). Reconstructing fungal natural product biosynthetic pathways. *Nat. Prod. Rep.* 31, 1339-47
- Lee, Y., Lee, N., Bhattarai, G., Oh, Y., Yu, M., Yoo, I., Jhee, E., and Yi, H. (2010). Enhancement of osteoblast biocompatibility on titanium surface with Terrein treatment. *Cell Biochem. Funct.* 28, 678-85
- Leuckert, C. (1985). Probleme der Flechten-Chemotaxonomie — Stoffkombinationen und ihre taxonomische Wertung. *Ber. Deut. Bot. Ges.* 98, 401-408
- Li, D., Tang, Y., Lin, J., and Cai, W. (2017). Methods for genetic transformation of filamentous fungi. *Microb. Cell Fact.* 16, 168
- Liao, W., Shen, C., Lin, L., Yang, Y., Han, H., Chen, J., Kuo, S., Wu, S., and Liaw, C. (2012). Asperjinone, a nor-neolignan, and terrein, a suppressor of ABCG2-expressing breast cancer cells, from thermophilic *Aspergillus terreus*. *J. Nat. Prod.* 75, 630-5
- Lim, S.Y., Kano, R., Ooya, K., Kimura, S., Yanai, T., Hasegawa, A., and Kamata, H. (2016). The first isolation of *Aspergillus allahabadii* from a cormorant with pulmonary aspergillosis. *Med. Mycol. J.* 57, E77-E79
- Lin, T., Chiang, Y., and Wang, C.C.C. (2016). Biosynthetic pathway of the reduced polyketide product citreoviridin in *Aspergillus terreus* var. *aureus* revealed by heterologous expression in *Aspergillus nidulans*. *Org. Lett.* 18, 1366-9
- Lincke, T., Behnken, S., Ishida, K., Roth, M., and Hertweck, C. (2010). Closthioamide: an unprecedented polythioamide antibiotic from the strictly anaerobic bacterium *Clostridium cellulolyticum*. *Angew. Chem. Int. Ed.* 49, 2011-3
- Liu, X., and Walsh, C.T. (2009). Cyclopiazonic acid biosynthesis in *Aspergillus* sp.: characterization of a reductase-like R* domain in cyclopiazonate synthetase that forms and releases cyclo-acetoacetyl-L-tryptophan. *Biochemistry.* 48, 8746-57
- Liu, L., Feizi, A., Österlund, T., Hjort, C., and Nielsen, J. (2014). Genome-scale analysis of the high-efficient protein secretion system of *Aspergillus oryzae*. *BMC Syst. Biol.* 8, 73
- Louis, B. (2013). *Aspergillus terreus* Thom a new pathogen that causes foliar blight of potato. *Pl. Pathol. Quarant.* 3, 29–33
- Macheleidt, J., Mattern, D.J., Fischer, J., Netzker, T., Weber, J., Schroeckh, V., Valiante, V., and Brakhage, A.A. (2016). Regulation and role of fungal secondary metabolites. *Annu. Rev. Genet.* 50, 371-92
- Mallick, E.M., and Bennett, R.J. (2013). Sensing of the microbial neighborhood by *Candida albicans*. *Plos Pathog.* 9, e1003661
- Maruyama, J., and Kitamoto, K. (2008). Multiple gene disruptions by marker recycling with highly efficient gene-targeting background ($\Delta ligD$) in *Aspergillus oryzae*. *Biotechnol. Lett.* 30, 1811-7
- May, R.C., Stone, N.R.H., Wiesner, D.L., Bicanic, T., and Nielsen, K. (2016). *Cryptococcus*: from environmental saprophyte to global pathogen. *Nat. Rev. Microbiol.* 14, 106-17

- Mayer, F.L., Wilson, D., and Hube, B. (2013). *Candida albicans* pathogenicity mechanisms. *Virulence* 4, 119-28
- Meyer, V., Wanka, F., van Gent, J., Arentshorst, M., van den Hondel, C.A.M.J.J., and Ram, A.F.J. (2011). Fungal gene expression on demand: an inducible, tunable, and metabolism-independent expression system for *Aspergillus niger*. *Appl. Environ. Microb.* 77, 2975-83
- Michielse, C.B., Pfannmüller, A., Macios, M., Rengers, P., Dzikowska, A., and Tudzynski, B. (2014). The interplay between the GATA transcription factors AreA, the global nitrogen regulator and AreB in *Fusarium fujikuroi*. *Mol. Microbiol.* 91, 472-93
- Miersch, O., Bohlmann, H., and Wasternack, C. (1999). Jasmonates and related compounds from *Fusarium oxysporum*. *Phytochemistry* 50, 517–523
- Miller, M.B., and Bassler, B.L. (2001). Quorum sensing in bacteria. *Annu. Rev. Microbiol.* 55, 165-99
- Molitor, D., Liermann, J.C., Berkelmann-Löhnertz, B., Buckel, I., Opatz, T., and Thines, E. (2012). Phenguignardic acid and guignardic acid, phytotoxic secondary metabolites from *Guignardia bidwellii*. *J. Nat. Prod.* 75, 1265-9
- Morales, H., Sanchis, V., Rovira, A., Ramos, A.J., and Marín, S. (2007). Patulin accumulation in apples during postharvest: Effect of controlled atmosphere storage and fungicide treatments. *Food Control* 18, 1443-8
- Mosbach, K. (1969). Biosynthesis of lichen substances, products of a symbiotic association. *Angew. Chem. Int. Ed.* 8, 240-50
- Nitta, K., Fujita, N., Yoshimura, T., Arai, K., and Yamamoto, Y. (1983). Metabolic products of *Aspergillus terreus*. IX. Biosynthesis of butyrolactone derivatives isolated from strains IFO 8835 and 4100. *Chem. Pharm. Bull.* 31, 1528–1533
- Nielsen, M.T., Nielsen, J.B., Anyaogu, D.C., Anyaogu, D.C., Holm, D.K., Nielsen, K.F., Larsen, T.O., and Mortensen, U.H. (2013). Heterologous reconstitution of the intact geodin gene cluster in *Aspergillus nidulans* through a simple and versatile PCR based approach. *Plos One* 8, e72871
- Nødvig, C.S., Nielsen, J.B., Kogle, M.E., and Mortensen, U.H. (2015). A CRISPR-Cas9 system for genetic engineering of filamentous fungi. *PLoS ONE* 10(7), e0133085.
- Nosanchuk, J.D., and Casadevall, A. (2006). Impact of melanin on microbial virulence and clinical resistance to antimicrobial compounds. *Antimicrob. Agents Ch.* 50, 3519-28
- Oakley, C.E., Ahuja, M., Sun, W., Entwistle, R., Akashi, T., Yaegashi, J., Guo, C., Cerqueira, G.C., Russo Wortman, J., Wang, C.C.C. *et al.* (2017). Discovery of McrA, a master regulator of *Aspergillus* secondary metabolism. *Mol. Microbiol.* 103, 347-65
- Pachlinger, R., Mitterbauer, R., Adam, G., and Strauss, J. (2005). Metabolically independent and accurately adjustable *Aspergillus* sp. expression system. *Appl. Environ. Microb.* 71, 672-8
- Pahirulzaman, K.A.K., Williams, K., and Lazarus, C.M. (2012). A toolkit for heterologous expression of metabolic pathways in *Aspergillus oryzae*. *Methods Enzymol.* 517, 241-60
- Palonen, E.K., Raina, S., Brandt, A., Meriluoto, J., Keshavarz, T., and Soini, J.T. (2017). Melanisation of *Aspergillus terreus*-Is Butyrolactone I involved in the regulation of both DOPA and DHN types of pigments in submerged culture?. *Microorganisms* 5(2), 22
- Park, S., Kim, D., Kim, W., Ryoo, I., Lee, D., Huh, C., Youn, S., Yoo, I., and Park, K. (2004). Terrein: a new melanogenesis inhibitor and its mechanism. *CMLS* 61, 2878-85

- Park, S., Kim, D., Lee, H., Kwon, S., Lee, S., Ryoo, I., Kim, W., Yoo, I., and Park, K. (2009). Long-term suppression of tyrosinase by terrein via tyrosinase degradation and its decreased expression. *Exp. Dermatol.* 18, 562-6
- Park, J., Throop, A.L., and LaBaer, J. (2015). Site-specific recombinational cloning using gateway and in-fusion cloning schemes. *Curr. Protoc. Mol. Biol.* 110, 3.20.1-23
- Paulussen, C., Hallsworth, J.E., Álvarez-Pérez, S., Nierman, W.C., Hamill, P.G., Blain, D., Rediers, H., and Lievens, B. (2017). Ecology of aspergillosis: insights into the pathogenic potency of *Aspergillus fumigatus* and some other *Aspergillus* species. *Microb. Biotechnol.* 10, 296-322
- Pihet, M., Vandeputte, P., Tronchin, G., Renier, G., Saulnier, P., Georgeault, S., Mallet, R., Chabasse, D., Symoens, F., and Bouchara, J. (2009). Melanin is an essential component for the integrity of the cell wall of *Aspergillus fumigatus* conidia. *BMC Microbiol.* 9, 177
- Porameesanaporn, Y., Uthaisang-Tanechpongamb, W., Jarintanan, F., Jongrungruangchok, S., and Thanomsub Wongsatayanon, B. (2013). Terrein induces apoptosis in HeLa human cervical carcinoma cells through p53 and ERK regulation. *Oncol. Rep.* 29, 1600-8
- Puder, C., Wagner, K., Vettermann, R., Hauptmann, R., and Potterat, O. (2005). Terphenylquinone inhibitors of the src protein tyrosine kinase from *Stilbella* sp. *J. Nat. Prod.* 68, 323-6
- Pusztahelyi, T., Holb, I.J., and Pócsi, I. (2015). Secondary metabolites in fungus-plant interactions. *Front. Plant Sci.* 6, 573
- Raina, S., Odell, M., and Keshavarz, T. (2010). Quorum sensing as a method for improving sclerotiorin production in *Penicillium sclerotiorum*. *J. Biotechnol.* 148, 91-8
- Raistrick, H., and Smith, G. (1935). Studies in the biochemistry of micro-organisms: The metabolic products of *Aspergillus terreus* Thom. A new mould metabolic product-terrein. *The Biochemical Journal* 29, 606-11
- Raistrick, H. (1950). Bakerian Lecture: A Region of biosynthesis. *Proceedings of the Royal Society B: Biological Sciences* 136, 481-508
- Ramage, G., Saville, S.P., Wickes, B.L., and López-Ribot, J.L. (2002). Inhibition of *Candida albicans* biofilm formation by farnesol, a quorum-sensing molecule. *Appl. Environ. Microb.* 68, 5459-63
- Ramsden, C.A., and Riley, P.A. (2014). Tyrosinase: the four oxidation states of the active site and their relevance to enzymatic activation, oxidation and inactivation. *Bioorgan. Med. Chem.* 22, 2388-95
- Richter, L., Wanka, F., Boecker, S., Storm, D., Kurt, T., Vural, Ö., Süßmuth, R., and Meyer, V. (2014). *Aspergillus niger* for the production of secondary metabolites. *Fungal Biol Biotechnol.* 1, 4.
- Ro, D., Paradise, E.M., Ouellet, M., Fisher, K.J., Newman, K.L., Ndungu, J.M., Ho, K.A., Eachus, R.A., Ham, T.S., Kirby, J. *et al.* (2006). Production of the antimalarial drug precursor artemisinic acid in engineered yeast. *Nature* 440, 940-3
- Rutledge, P.J., and Challis, G.L. (2015). Discovery of microbial natural products by activation of silent biosynthetic gene clusters. *Nat. Rev. Microbiol.* 13, 509-23
- Röttig, M., Medema, M.H., Blin, K., Weber, T., Rausch, C., and Kohlbacher, O. (2011). NRPSpredictor2--a web server for predicting NRPS adenylation domain specificity. *Nucleic Acids Res.* 39, W362-7

- Samson, R.A., Peterson, S.W., Frisvad, J.C., and Varga, J. (2011). New species in *Aspergillus* section *Terrei*. *Stud. Mycol.* 69, 39-55
- Sanchez, J.F., Somoza, A.D., Keller, N.P., and Wang, C.C.C. (2012). Advances in *Aspergillus* secondary metabolite research in the post-genomic era. *Nat. Prod. Rep.* 29, 351-71
- Sarikaya-Bayram, Ö., Palmer, J.M., Keller, N., Braus, G.H., and Bayram, Ö. (2015). One Juliet and four Romeos: VeA and its methyltransferases. *Front. Microbiol.* 6, 1
- Scharf, D.H., Heinekamp, T., and Brakhage, A.A. (2014). Human and plant fungal pathogens: the role of secondary metabolites. *Plos Pathog.* 10, e1003859
- Schimmel, T.G., Coffman, A.D., and Parsons, S.J. (1998). Effect of butyrolactone I on the producing fungus, *Aspergillus terreus*. *Appl. Environ. Microb.* 64, 3707-12
- Schmid, I., Sattler, I., Grabley, S., and Thiericke, R. (1999). Natural products in high throughput screening: Automated high-quality sample preparation. *J. Biomol. Screen.* 4, 15-25
- Schmidt-Dannert, C. (2015). Biosynthesis of terpenoid natural products in fungi. *Adv. Biochem. Eng. Biotechnol.* 148, 19-61
- Schneider, P., Weber, M., Rosenberger, K., and Hoffmeister, D. (2007). A one-pot chemoenzymatic synthesis for the universal precursor of antidiabetes and antiviral bis-indolylquinones. *Chem. Biol.* 14, 635-44
- Schneider, P., Weber, M., and Hoffmeister, D. (2008). The *Aspergillus nidulans* enzyme TdiB catalyzes prenyltransfer to the precursor of bioactive asterriquinones. *Fungal Genet. Biol.* 45, 302-9
- Schor, R., and Cox, R. (2018). Classic fungal natural products in the genomic age: the molecular legacy of Harold Raistrick. *Nat. Prod. Rep.* 35, 230-56
- Schrettl, M., Bignell, E., Kragl, C., Joechl, C., Rogers, T., Arst, H.N., Haynes, K., and Haas, H. (2004). Siderophore biosynthesis but not reductive iron assimilation is essential for *Aspergillus fumigatus* virulence. *J. Ex. Med.* 200, 1213-9
- Schroeckh, V., Scherlach, K., Nützmann, H., Shelest, E., Schmidt-Heck, W., Schuemann, J., Martin, K., Hertweck, C., and Brakhage, A.A. (2009). Intimate bacterial-fungal interaction triggers biosynthesis of archetypal polyketides in *Aspergillus nidulans*. *P. Natl. Acad. Sci.* 106, 14558-63
- Shoji, J., Maruyama, J., Arioka, M., and Kitamoto, K. (2005). Development of *Aspergillus oryzae* *thiA* promoter as a tool for molecular biological studies. *FEMS Microbiol. Lett.* 244, 41-6
- Siddiqui, M.S., Thodey, K., Trenchard, I., and Smolke, C.D. (2012). Advancing secondary metabolite biosynthesis in yeast with synthetic biology tools. *FEMS Yeast Res.* 12, 144-70
- Slesiona, S., Gressler, M., Mihlan, M., Zaehle, C., Schaller, M., Barz, D., Hube, B., Jacobsen, I.D., and Brock, M. (2012). Persistence versus escape: *Aspergillus terreus* and *Aspergillus fumigatus* employ different strategies during interactions with macrophages. *Plos One* 7, e31223
- Soukup, A.A., Keller, N.P., and Wiemann, P. (2016). Enhancing nonribosomal peptide biosynthesis in filamentous fungi. *Meth. Mol. Biol.* 1401, 149-60
- Spiteller, P. (2008). Chemical defence strategies of higher fungi. *Chem. Eur. J.* 14, 9100-10
- Spiteller, P. (2015). Chemical ecology of fungi. *Nat. Prod. Rep.* 32, 971-93
- Stahlschmidt, C. (1877). Über eine in der Natur vorkommende organische Säure. *Liebigs Ann. Chem.* 178, 177-97

- Stocker-Wörgötter, E. (2008). Metabolic diversity of lichen-forming ascomycetous fungi: culturing, polyketide and shikimate metabolite production, and PKS genes. *Nat. Prod. Rep.* 25, 188-200
- Strieker, M., Tanović, A., and Marahiel, M.A. (2010). Nonribosomal peptide synthetases: structures and dynamics. *Curr. Opin. Struc. Biol.* 20, 234-40
- Sugareva, V., Härtl, A., Brock, M., Hübner, K., Rohde, M., Heinekamp, T., and Brakhage, A.A. (2006). Characterisation of the laccase-encoding gene *abr2* of the dihydroxynaphthalene-like melanin gene cluster of *Aspergillus fumigatus*. *Arch. Microbiol.* 186, 345-55
- Sugui, J.A., Pardo, J., Chang, Y.C., Zarembek, K.A., Nardone, G., Galvez, E.M., Müllbacher, A., Gallin, J.I., Simon, M.M., and Kwon-Chung, K.J. (2007). Gliotoxin is a virulence factor of *Aspergillus fumigatus*: *gliP* deletion attenuates virulence in mice immunosuppressed with hydrocortisone. *Eukaryot. Cell* 6, 1562-9
- Sun, W., Guo, C., and Wang, C.C.C. (2016). Characterization of the product of a nonribosomal peptide synthetase-like (NRPS-like) gene using the doxycycline dependent Tet-on system in *Aspergillus terreus*. *Fungal Genet. Biol.* 89, 84-8
- Süssmuth, R.D., and Mainz, A. (2017). Nonribosomal Peptide Synthesis-Principles and Prospects. *Angew. Chem. Int. Ed.* 56, 3770-821
- Sykes, R.B., and Bonner, D.P. (1985). Aztreonam: the first monobactam. *Am. J. Med.* 78, 2-10
- Taborda, C.P., da Silva, M.B., Nosanchuk, J.D., and Travassos, L.R. (2008). Melanin as a virulence factor of *Paracoccidioides brasiliensis* and other dimorphic pathogenic fungi: a minireview. *Mycopathologia* 165, 331-9
- Takano, E. (2006). γ -butyrolactones: *Streptomyces* signalling molecules regulating antibiotic production and differentiation. *Curr. Opin. Microbiol.* 9, 287-94
- Theobald, S., Vesth, T.C., Geib, E., Nybo, J.L., Frisvad, J.C., Larsen, T.O., Salamov, A., Riley, R., Lyhne, E.K., Kogle, M.E. *et al.* (2018). Genomic and metabolic diversity in *Aspergillus* section *Terrei*. in preparation
- Thines, E., Anke, H., and Weber, R.W.S. (2004). Fungal secondary metabolites as inhibitors of infection-related morphogenesis in phytopathogenic fungi. *Mycol. Res.* 108, 14-25
- Tsai, H.F., Chang, Y.C., Washburn, R.G., Wheeler, M.H., and Kwon-Chung, K.J. (1998). The developmentally regulated *alb1* gene of *Aspergillus fumigatus*: its role in modulation of conidial morphology and virulence. *J. Bacteriol.* 180, 3031-8
- Ugai, T., Minami, A., Fujii, R., Tanaka, M., Oguri, H., Gomi, K., and Oikawa, H. (2015). Heterologous expression of highly reducing polyketide synthase involved in betaenone biosynthesis. *Chem. Commun.* 51, 1878-81
- Unkles, S.E., Valiante, V., Mattern, D.J., and Brakhage, A.A. (2014). Synthetic biology tools for bioprospecting of natural products in eukaryotes. *Chem. Biol.* 21, 502-8
- van de Veerdonk, F.L., Gresnigt, M.S., Romani, L., Netea, M.G., and Latgé, J. (2017). *Aspergillus fumigatus* morphology and dynamic host interactions. *Nat. Rev. Microbiol.* 15, 661-74
- Venuta, F., and Van Raemdonck, D. (2017). History of lung transplantation. *J. Thorac. Dis.* 9, 5458-71
- Verdoes, J.C., Punt, P.J., and van den Hondel, C.A.M.J.J. (1995). Molecular genetic strain improvement for the overproduction of fungal proteins by filamentous fungi. *Appl. Microbiol. Biot.* 43, 195-205

- Vogt, K., Bhabhra, R., Rhodes, J.C., and Askew, D.S. (2005). Doxycycline-regulated gene expression in the opportunistic fungal pathogen *Aspergillus fumigatus*. *BMC Microbiol.* 5, 1
- de Vries, R.P., Riley, R., Wiebenga, A., Aguilar-Osorio, G., Amillis, S., Uchima, C.A., Anderluh, G., Asadollahi, M., Askin, M., Barry, K. *et al.* (2017). Comparative genomics reveals high biological diversity and specific adaptations in the industrially and medically important fungal genus *Aspergillus*. *Genome Biol.* 18, 28
- Walsh, C.T., O'Brien, R.V., and Khosla, C. (2013). Nonproteinogenic amino acid building blocks for nonribosomal peptide and hybrid polyketide scaffolds. *Angew. Chem. Int. Ed.* 52, 7098-124
- Wang, Y., Aisen, P., and Casadevall, A. (1995). *Cryptococcus neoformans* melanin and virulence: mechanism of action. *Infect. Immun.* 63, 3131-6
- Wang, M., Beissner, M., and Zhao, H. (2014). Aryl-aldehyde formation in fungal polyketides: discovery and characterization of a distinct biosynthetic mechanism. *Chem. Biol.* 21, 257-63
- Wanka, F., Cairns, T., Boecker, S., Berens, C., Happel, A., Zheng, X., Sun, J., Krappmann, S., and Meyer, V. (2016). Tet-on, or Tet-off, that is the question: Advanced conditional gene expression in *Aspergillus*. *Fungal Genet. Biol.* 89, 72-83
- Wasil, Z., Pahirulzaman, K.A.K., Butts, C., Simpson, T.J., Lazarus, C.M., and Cox, R.J. (2013). One pathway, many compounds: heterologous expression of a fungal biosynthetic pathway reveals its intrinsic potential for diversity. *Chem. Sci.* 4, 3845
- Watanabe, A., Fujii, I., Tsai, H., Chang, Y.C., Kwon-Chung, K.J., and Ebizuka, Y. (2000). *Aspergillus fumigatus alb1* encodes naphthopyrone synthase when expressed in *Aspergillus oryzae*. *FEMS Microbiol. Lett.* 192, 39-44
- Wattanachaisaereekul, S., Lantz, A.E., Nielsen, M.L., Andrésson, O.S., and Nielsen, J. (2007). Optimization of heterologous production of the polyketide 6-MSA in *Saccharomyces cerevisiae*. *Biotechnol. Bioeng.* 97, 893-900
- Weissman, K.J. (2015). The structural biology of biosynthetic megaenzymes. *Nat. Chem. Biol.* 11, 660-70
- Wolf, T., Shelest, V., Nath, N., and Shelest, E. (2016). CASSIS and SMIPS: promoter-based prediction of secondary metabolite gene clusters in eukaryotic genomes. *Bioinformatics* 32, 1138-43
- Woo, P.C.Y., Tam, E.W.T., Chong, K.T.K., Cai, J.J., Tung, E.T.K., Ngan, A.H.Y., Lau, S.K.P., and Yuen, K. (2010). High diversity of polyketide synthase genes and the melanin biosynthesis gene cluster in *Penicillium marneffeii*. *FEBS* 277, 3750-8
- Xu, Y., Espinosa-Artiles, P., Schubert, V., Xu, Y., Zhang, W., Lin, M., Gunatilaka, A.A.L., Süssmuth, R., and Molnár, I. (2013). Characterization of the biosynthetic genes for 10,11-dehydrocurvularin, a heat shock response-modulating anticancer fungal polyketide from *Aspergillus terreus*. *Appl. Environ. Microb.* 79, 2038-47
- Yang, L., Lübeck, M., and Lübeck, P.S. (2017). *Aspergillus* as a versatile cell factory for organic acid production. *Fungal Biol. Rev.* 31, 33-49
- Yeh, H., Chiang, Y., Entwistle, R., Ahuja, M., Lee, K., Bruno, K.S., Wu, T., Oakley, B.R., and Wang, C.C.C. (2012). Molecular genetic analysis reveals that a nonribosomal peptide synthetase-like (NRPS-like) gene in *Aspergillus nidulans* is responsible for microperforanone biosynthesis. *Appl. Microbiol. Biot.* 96, 739-48

- Yeh, H., Ahuja, M., Chiang, Y., Oakley, C.E., Moore, S., Yoon, O., Hajovsky, H., Bok, J., Keller, N.P., Wang, C.C.C. *et al.* (2016). Resistance gene-guided genome mining: serial promoter exchanges in *Aspergillus nidulans* reveal the biosynthetic pathway for fellutamide B, a proteasome inhibitor. *ACS Chem. Biol.* 11, 2275-84
- Yin, Y., Xu, B., Li, Z., and Zhang, B. (2013). Enhanced production of (+)-terrein in fed-batch cultivation of *Aspergillus terreus* strain PF26 with sodium citrate. *World J. Microb. Biot.* 29, 441-6
- Yun, C., Motoyama, T., and Osada, H. (2015). Biosynthesis of the mycotoxin tenuazonic acid by a fungal NRPS-PKS hybrid enzyme. *Nat. Commun.* 6, 8758
- Zaehle, C., Gressler, M., Shelest, E., Geib, E., Hertweck, C., and Brock, M. (2014). Terrein biosynthesis in *Aspergillus terreus* and its impact on phytotoxicity. *Chem. Biol.* 21, 719-31
- Zhang, F., Mijiti, M., Ding, W., Song, J., Yin, Y., Sun, W., and Li, Z. (2015). (+)-Terrein inhibits human hepatoma Bel-7402 proliferation through cell cycle arrest. *Oncol. Rep.* 33, 1191-200
- Zobel, S., Boecker, S., Kulke, D., Heimbach, D., Meyer, V., and Süssmuth, R.D. (2016). Reprogramming the biosynthesis of cyclodepsipeptide synthetases to obtain new enniatins and beauvericins. *Chembiochem* 17, 283-7

Conference contributions

2015 – 28th Fungal Genetics Conference (17th-22nd of March, Asilomar): Poster presentation

A new type of melanin required for pigmentation of *Aspergillus terreus* conidia

Elena Geib, Markus Gressler, Sandor Nietzsche, Christian Hertweck and Matthias Brock

2015 – SoLS PGR symposium (11th-12th of June, Nottingham): Poster presentation

A new type of melanin required for pigmentation of *Aspergillus terreus* conidia

Elena Geib, Markus Gressler, Sandor Nietzsche, Christian Hertweck and Matthias Brock

2016 – 28. Irseer Naturstofftage (24th-26th February, Irsee): Poster Presentation

Heterologous *in vivo* and *in vitro* reconstitution of the pigment synthesis from *Aspergillus terreus* conidia

Elena Geib, Markus Gressler, Christian Hertweck and Matthias Brock

2016 – VAAM Annual Conference (13th-16th of March, Jena): Poster Presentation

Heterologous *in vivo* and *in vitro* reconstitution of the pigment synthesis from *Aspergillus terreus* conidia

Elena Geib, Markus Gressler, Christian Hertweck and Matthias Brock

2016 – SoLS PGR symposium (14th-15th July, Nottingham): Oral presentation

Biosynthesis of an unusual pigment in *Aspergillus terreus* conidia or Does colour matter?

2017 – Asperfest 14 (13th-14th of March, Asilomar): Poster presentation

***Aspergillus niger* versus *Aspergillus oryzae*: Expression platforms for heterologous secondary metabolite production**

Elena Geib and Matthias Brock

2017 – 29th Fungal Genetics Conference (14th-19th of March, Asilomar): Poster presentation

***Aspergillus niger* versus *Aspergillus oryzae*: Expression platforms for heterologous secondary metabolite production**

Elena Geib and Matthias Brock

2017 – Joint BSPP-BMS Meeting (11th-13th of September, Nottingham): Oral presentation

Expression platforms for heterologous secondary metabolite production

Awards

2015 – Fungal Genetics Conference: **Poster presentation award**

2016 – Irseer Naturstofftage (natural products conference): **Poster presentation award**

2016 – SoLS PGR symposium – **Best presenter award** (oral presentation)

2016 – SoLS: **Early Researcher of Excellence Award**

2017 – SoLS: **Travel grant** for conference attendance

2017 – University of Nottingham Graduate School: **Travel prize**

2017 – Genetics Society of America: **Travel award**

2017 – Fungal Genetics Conference Satellite Meeting: **Poster presentation award**

Acknowledgement

It's been a long way. And I am grateful for all those awesome people who helped and taught me all along. First of all, I have to express my gratitude to my exceptional supervisor, Matthias Brock. You always believed in me. You challenged and supported me. You taught me more skills than I can recall. You gave me the chance to present my research to the community at all my stages of PhD. All those conferences were not only a scientific success but brought us to amazing places I will always remember. It has been an amazing time in your lab. Thank you!

I would like to express my gratitude to the School of Life Sciences who awarded me with a stipend to continue my research at the University of Nottingham. I would like to thank my examiners for assessing my work.

Thanks to all co-workers who contributed to my manuscripts or whose manuscripts I was able to contribute to. You made science the way it should be: a vivid discussion, a mixing of skills and strengths and a great collaborative approach to reach new insights.

A big thank you goes to Christoph Zähle and Markus Greßler. You have been patient with me during my first, unsteady steps in natural product chemistry and genetic modifications. From you two I picked up the best bits from two worlds: analytical chemistry and molecular biology. Without you I wouldn't have built my skill portfolio to this extent. And on top you have been the best colleagues you can hope for. Also, I had some more amazing colleagues who made working enjoyable, namely my lab house gang: Florian Meyer, Daniel Heine, Sabrina Boldt and Radon Rene 😊.

I also received a lot of technical support for which I am very grateful. First from Daniela Hildebrandt, who lovingly and tirelessly dealt with my colourful "Dear Dany" notes. Later, from Lee Shunburn and Matthew Kokolski, who tried to order all my eccentric items and fixed my particular problems. Sam Simpson, who came far too late, but learnt so quickly and was charmingly entertaining. Without you, dear Sam, we would have lost some project students as collateral damage. Heike Heinicke and Andrea Perner, who recorded the most beautiful NMR and HR-ESI-MS spectra for me. Some students I supervised left their marks. One student I will remember: Olga, you have been a great help! With your curiosity and your careful enthusiasm, it was a pleasure to work with you. I am sure that a great future awaits you.

Thank you, Knit-a-soc, for your existence. For being a place where I was able to transform my obsession into something good and make premie hats and baby blankets for charity. For the collection of unbelievable adorable and genuine people you are.

My friends and family, who tried very hard to keep me sane.

This is it, my "fifty shades of yellow" thesis.

